Large Pool LMFBR Design
Volume 3: Appendixes

EPRI

Keywords:
Breeder Reactor
Pool-Type Reactor
Nuclear Power Plant
LMFBR

EPRI NP-883
Volume 3
Project 620-26
August 1978

Prepared by
Westinghouse Electric Corporation
Madison, Pennsylvania

ELECTRIC POWER RESEARCH INSTITUTE

Large Pool LMFBR Design
Volume 3: Appendixes

NP-883
Research Project 620-26

Final Report, August 1978

Prepared by

WESTINGHOUSE ELECTRIC CORPORATION
Advanced Reactors Division
Box 158
Madison, Pennsylvania 15663

Project Manager
J. F. Wett

Prepared for

Electric Power Research Institute
3412 Hillview Avenue
Palo Alto, California 94304

EPRI Project Manager
G. D. Baston
Nuclear Power Division

VOLUME 3
APPENDICES
TABLE OF CONTENTS

APPENDIX A
STRUCTURAL ANALYSIS

A.1 SUMMARY

A stick and mass finite element model was used to evaluate the LPR vessel for seismic loading. The OBE and SSE response spectrum used were the same as for Phase A of the LPR project. All major components were modeled and all masses of the system were included. The analysis was performed for the seventy-five foot inside diameter vessel.

The purpose of the analysis was to determine the thickness required for the reactor vessel. The analysis shows that based on the response spectrum used, a three in thickness is required for the first 10 ft below the deck, a 2.5 in thickness is required for the next 7.5 ft, and a two inch thickness is required below this. The limiting factor on the above thicknesses is the ability to meet ASME limits for compressive stress for the OBE case.

Also examined in the analysis was the difference in reaction loads due to variations in the reactor support concept. The reference concept is supported at the middle elevation of the deck. This concept and concepts that are supported at the bottom of the deck are found to have similar responses due to the high horizontal stiffness of the deck. Other concepts, however, are supported by a cylinder below the deck. The flexibility of this support results in horizontal reaction loads about 25% higher than the other concepts for the same input response spectrum. The moment reactions at the support are lower for the concepts that include the cylinder since the support elevation is lower but at the top of the vessel wall the bending stresses are about 10% higher.

The evaluation of the lower head of the reactor vessel shows that, for a two inch thick shell, the 16/60 torispherical lower head adequately withstands a pressure of 50 psi when combined with the self weight of the vessel.

Because of the membrane stress intensity limit, the radius of the torus should not be less than 16 ft nor should the radius of the spherical cap be greater than 60 ft.

The results of the analysis of the lower support structure/vessel interface show that the original number of shear panels in the outer support ring of the lower support structure would be overstressed. Therefore, the outer ring configuration of the lower support structure was revised to be similar to the outer ring of the deck, i.e., contains a similar number of radial shear panels. The results also show the need for a detailed thermal and structural evaluation as high stresses can be developed due to thermal gradients in this region.

The evaluation of the upper shell of the vessel includes the effects of seismic events and the thermal gradient. The combined effect of the horizontal and vertical seismic events are used to obtain realistic stresses at the intersection of the vessel and deck. Results of the analysis are within ASME Code allowable stress values for all loading conditions considered.

The evaluation of the deck during the current phase of the pool design effort was limited to an investigation of the method of supporting the deck and reactor system. The results of the analysis show two highly stressed areas in the structure; the shear panel in the box flange, and the support cylinder for those cases where a cylinder is used. The shear stress in the shear panels is approximately proportional to the area in the panels. These shear stresses can be mitigated by increasing the thickness of the panels but other considerations may limit the increase in size.

The stresses in the support cylinder are directly related to the length and thickness of the cylinder. As the thickness increases, the moment load required to bend the cylinder to conform to the deck rotation also increases. This may generate large stresses at the lower end of the cylinder where a built-in condition exists. But the use of a simple-type support tends to eliminate this problem.

A finite element technique was used to perform a preliminary evaluation of shell mode vibration for the LPR plenum separator. The fundamental frequency was found to be 10.5 hz for eight (8) circumferential waves. The analysis shows further that the frequency can be increased by attaching a stiffening ring to the top of the plenum separator. Final tuning of the plenum separator is deferred to allow discussion of the seismic response spectrum and space requirements with the design team.

The seismic analysis also provided stress and deflection values for the upper internals structure (UIS). This part of the model was based on a 150 in diameter UIS with a 1 in wall thickness. For the reference concept, the deflection of the bottom of the UIS relative to the top of the core barrel was found to be about .77 in for the OBE and 1.32 in for SSE. The bending stress was found to be 9.0 ksi for OBE and 15.7 ksi for SSE. These bending stresses exceed the allowable stress to preclude buckling, indicating a need to reduce the load (seismic spectrum) or to increase the UIS load capability.

The scoping structural evaluation of the LPR pump support was performed to determine the ability of the support configuration to adequately withstand the imposed operating loads. The limiting loads are the operating basis earthquake (OBE) and the safe shutdown earthquake (SSE) events.

The most severe case considered is when the top of the pump is built-in. This may be overly conservative when the pump is loaded in the radial direction but is realistic when the loading corresponds to the circumferential direction. The results of the analysis for the configuration analyzed demonstrate that bolt stress limits are exceeded by the combination of tensile loads due to an overturning moment and shear loads. The tensile limits can be met by increasing the size, the number of bolts, and/or specification of high strength bolts. The shear stresses can be reduced by incorporating a shear member into the design.

At the bottom of the pump, the clearance between the pump and the pump receptacle must be enlarged to preclude bending of the pump. Also, the current clearance does not include the deflection and rotation of the lower

support structure as these have not been determined. It is recommended that the combined diametral clearance be increased from the present 0.2 in to a minimum of 0.25 in. Alternatively, the distance between the piston ring chamfers could be decreased to obtain the same effect.

A.2 INTRODUCTION

This appendix presents the structural analysis performed during the current phase of the Large Pool Reactor Study. Because of the lag between design and analysis, some of the work reported may not represent the current design.

The description is divided into seven areas that correspond to the seven components or systems investigated during this phase of the pool study. The loads applied consist of the mechanical operating loads, steady state temperatures, and the loads due to seismic events. The results of the analyses are more qualitative than quantitative and tend to identify problem areas rather than to provide a detailed description of the stress distribution throughout the system. The component configurations presented in Volumes 1 and 2 of this report may already incorporate the findings of the analyses reported herein. And appropriate action has or will be taken to resolve the implied problem areas.

A.3 VESSEL

Because of its importance with regard to the total plant, a significant portion of the structural effort during this phase of the pool study was devoted to the reactor vessel. A complete system modal/seismic analysis was performed since seismic loads were found to be the limiting case in Reference 1 and a relatively complete system mechanical/thermal stress analysis was performed to insure the adequacy of the design. Each of these system analyses and a description of the major components of the reactor vessel are provided below.

A.3.1 SYSTEM SEISMIC ANALYSIS

A stick and mass finite element model was used to evaluate the LPR vessel for seismic loading. The Operating Basis Earthquake (OBE) and Safe Shutdown Earthquake (SSE) response spectrum used were the same as for Phase A of the LPR project and are shown in Figure A-1. All major components were modeled

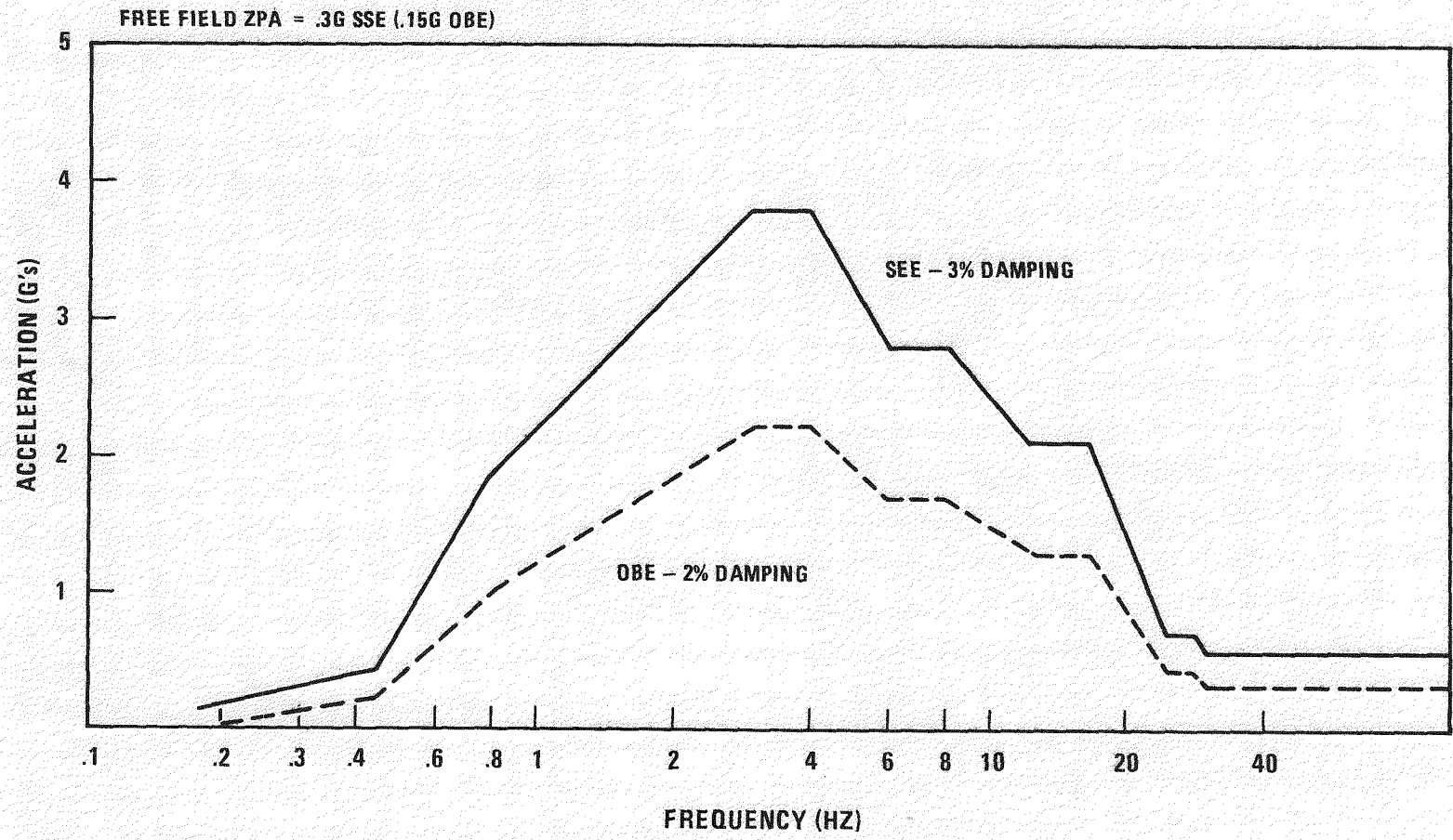

Figure A-1. PLBR Enveloped Horizontal Response Spectra

and all masses of the system were included. The analysis was performed for the seventy-five foot inside diameter vessel, based on revision 2 of the LPR design control drawing.

One objective of the analysis was to determine the thickness required for the reactor vessel. The analysis shows that based on the response spectrum used, a three inch thickness is required for the first 10 feet below the deck, a two and one half inch thickness is required for the next 7.5 feet, and a two inch thickness is required below this. The limiting factor on the above thicknesses is the ability to meet ASME limits (Reference 7) for compressive stress for the OBE case.

Also examined in the analysis was the difference in reaction loads due to variations in the reactor support concept. The reference concept is denoted as concept 5 in Figure A-2, and is characterized by supporting the deck at its middle elevation. This concept, and concepts 2 and 4 which are supported at the bottom of the deck, were found to have similar responses due to the high horizontal stiffness of the deck. Concepts 1 and 3, however, are supported by a cylinder below the deck. The flexibility of this support results in horizontal reaction loads about 25% higher than the other concepts for the same input response spectrum. The moment reactions at the support however, are lower for concepts 1 and 3 since the support elevation is lower. At the top of the vessel wall the bending stresses are about 10% higher for concepts 1 and 3 than for the other concepts.

The analysis also provides the stress and deflection values for the UIS. This part of the model was based on a 150 inch diameter UIS with a one inch wall thickness. For the reference concept, the deflection of the bottom of the UIS relative to the top of the core barrel was found to be about 0.77 inches for the OBE and 1.32 inches for SSE. The bending stress was found to be 9.0 ksi for OBE and 15.7 ksi for SSE. These bending stresses exceed the allowable stress to preclude buckling, indicating a need to reduce the load (seismic spectrum) or to increase the UIS load capability. Details of the UIS evaluation are contained in Section A.6.

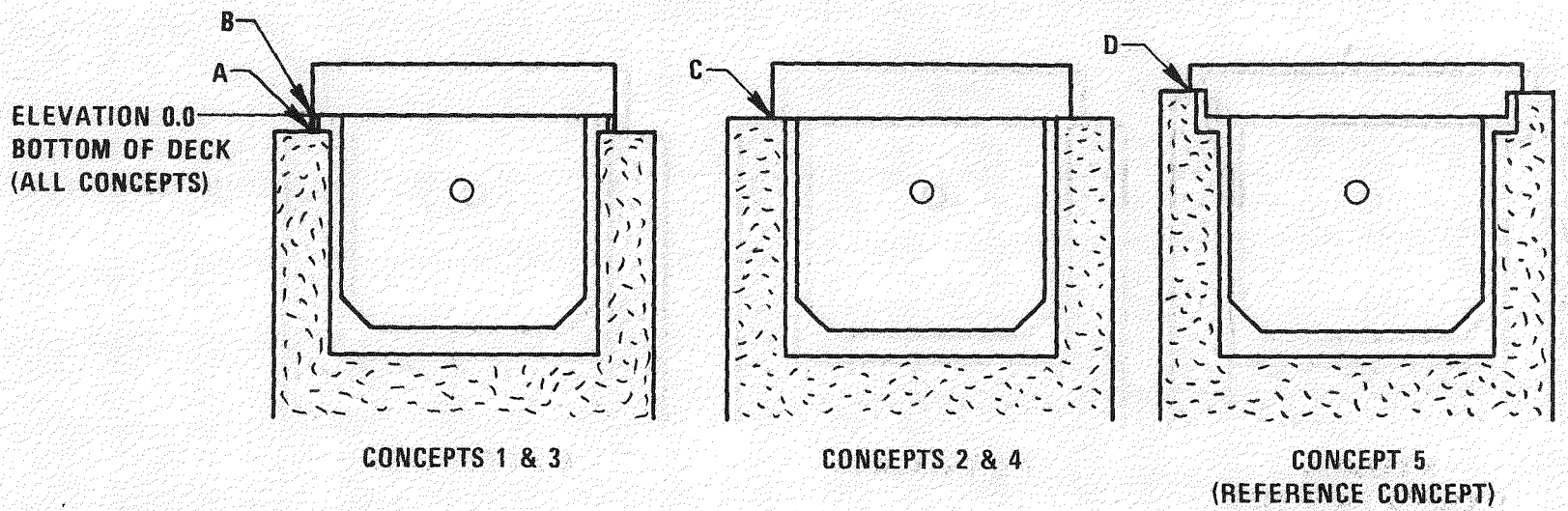

Figure A-2. Alternative Support Concepts

A.3.1.1 LOADS

The loading used in this study consisted of a 1G horizontal load case, an Operating Basis Earthquake (OBE) horizontal loading, and a Safe Shutdown Earthquake (SSE) horizontal loading. The seismic acceleration spectrum used is shown in Figure A-1.

A.3.1.2 FINITE ELEMENT MODELS

A two-dimensional stick and mass finite element model was constructed using the ANSYS general purpose finite element code Reference 3. Figures A-3 and A-4 show the models used for concepts 1 and 3, and concept 5 respectively. The model for concepts 2 and 4 was basically the same as for concept 5 but with node 1 moved to elevation +1.0 inch.

In all of the above models, the node numbers apply to the components as follows:

1-4:	Reactor Support
10-20:	Deck
100-116:	Vessel
200-210:	UIS
300-305:	Plenum Separator
400-408:	Support Cone
500-505:	Neutron Shield
600-608:	Core Barrel

A description of the modeling for each component is given in the following paragraphs and element constants and material properties are given in Table A-1.

The reactor support for concepts 1 and 3 is modeled as a cylinder of 996 inches OD and 989 inches ID using ANSYS beam elements, STIF 3, with the

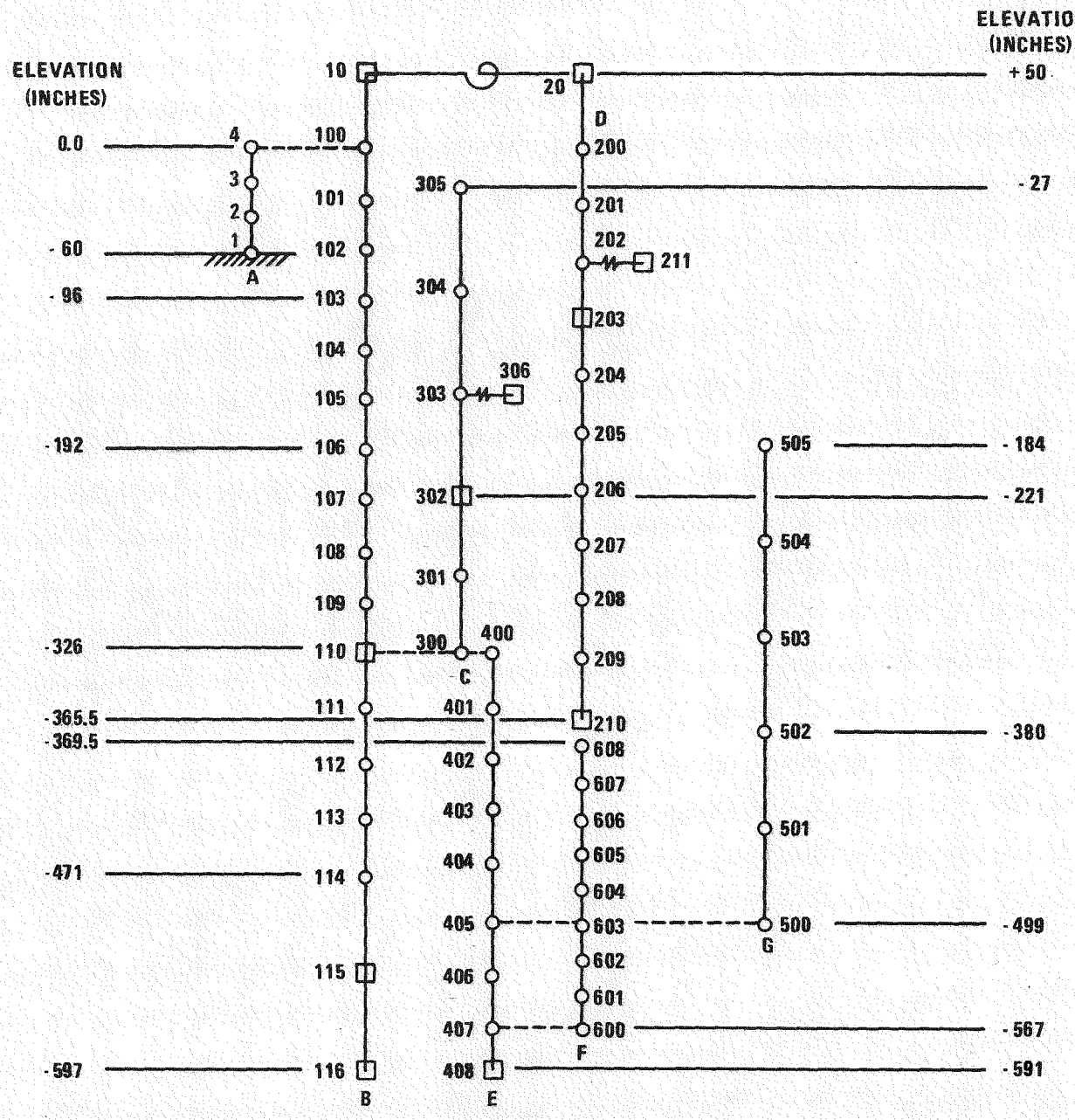

A. REACTOR SUPPORT
B. VESSEL AND BOTTOM HEAD
C. PLENUM SEPARATOR
D. UPPER INTERNALS
E. LOWER SUPPORT CONE
F. CORE BARREL AND CORE
G. NEUTRON SHIELD

NOTE: THIS MODEL IS A UNIAXIAL MODEL AND IS SHOWN WITH CENTERLINES DISPLACED FOR CLARITY. NODE ELEVATIONS ARE EVENLY SPACED BETWEEN THOSE ELEVATIONS SHOWN.

COUPLED NODE ------
BEAM ELEMENT |
SPRING —/\/\—
TORSIONAL SPRING
MASS ELEMENT □

Figure A-3. Node Numbers and Elevations for Concept 1 & 3 Vessel Seismic Model

0665-44

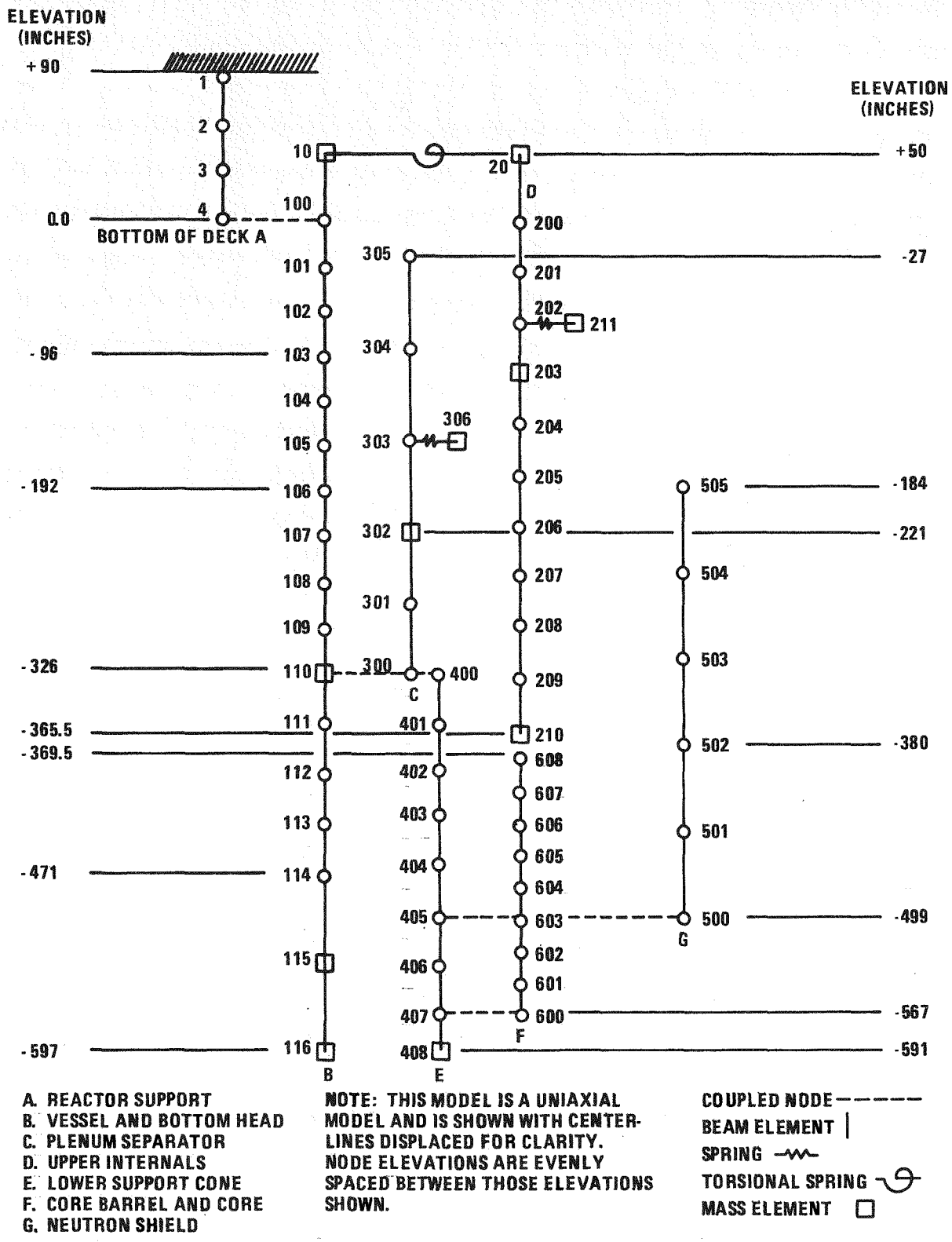

Figure A-4. Node Numbers and Elevations for Concept 5 Vessel Seismic Model

Table A-1

ELEMENT CONSTANTS AND MATERIAL PROPERTIES
IN CONCEPT 1 TO 5 MODELS

COMPONENT	CONCEPT	TYPE OF ELEMENT	NODES	AREA IN^2	AREA MOM. OF INERTIA IN^4	OUTER DIAMETER IN.	INNER DIAMETER IN.	SHEAR DEFLECTION AREA RATIO	MASS (LB_f-SEC^2/IN.)	MASS MOM. OF INERTIA (LB_f-SEC^2-IN)	ELASTIC MODULUS (LB_f/IN^2)	DENSITY	POISSON'S RATIO	SPRING CONSTANT (EXTENSION SPRING) (LB_f/In)	SPRING CONSTANT (ROTATIONAL SPRING) (IN-LB_f/RAD)
Reactor Support	1 & 3	Beam	1-4	$.109\times10^{5}$	$.134\times10^{10}$	996	989	2			27.7×10^{6}	$.733\times10^{-3}$	.30		
Reactor Support	5	Beam	1-4	$.176\times10^{6}$	$.194\times10^{11}$	996	876	2			27.7×10^{6}	$.1\times10^{-8}$	.30		
Deck & Components	1-5	Mass	10						$.227\times10^{5}$						
Deck (Horiz. Stiff.)	1-5	Beam	100-10 & 20-200	$.176\times10^{6}$	$.194\times10^{11}$	996	876	2			27.7×10^{6}	$.1\times10^{-8}$	.30		
Rotating Plugs	1-5	Mass	20						$.486\times10^{4}$	$.583\times10^{8}$					
Vessel	1-5	Beam	100-103	$.851\times10^{4}$	$.868\times10^{9}$	906	900	2			27.6×10^{6}	$.263\times10^{-2}$	.2711		
Vessel	1-5	Beam	103-106	$.710\times10^{4}$	$.724\times10^{9}$	906	901	2			26.07×10^{6}	$.30\times10^{-2}$	.2851		
Vessel	1-5	Beam	106-114	$.568\times10^{4}$	$.580\times10^{9}$	906	902	2			24.77×10^{6}	$.357\times10^{-2}$	.2931		
Vessel	1-5	Tapered Beam(Upper & Lower End Properties)	114	$.622\times10^{4}$	$.629\times10^{9}$	902	899.6	2			24.77×10^{6}	$.751\times10^{-3}$	.2931		
			115	$.586\times10^{4}$	$.527\times10^{9}$	850	845.6	2			24.77×10^{6}	$.751\times10^{-3}$	.2931		
Vessel	1-5	Tapered Beam	115	$.759\times10^{4}$	$.680\times10^{9}$	850	844.3	2			24.77×10^{6}	$.751\times10^{-3}$	.2931		
			116	$.644\times10^{4}$	$.416\times10^{9}$	722	716.3	2			24.77×10^{6}	$.751\times10^{-3}$	.2931		
Vessel & Lower Supt.	1-5	Mass	110						$.336\times10^{4}$						
Vessel Bottom Head and Sodium	1-5	Mass	115						$.286\times10^{4}$						
Vessel Bottom Head and Sodium	1-5	Mass	116						$.413\times10^{4}$	$.821\times10^{8}$					

Table A-1 (Continued)

COMPONENT	CONCEPT	TYPE OF ELEMENT	NODES	AREA IN^2	AREA MOM. OF INERTIA IN^4	OUTER DIAMETER IN.	INNER DIAMETER IN.	SHEAR DEFLECTION AREA RATIO	MASS $(\frac{LB_f\text{-}SEC^2}{IN.})$	MASS MOM. OF INERTIA $(LB_f\text{-}SEC^2\text{-}IN)$	ELASTIC MODULUS (LB_f/IN^2)	DENSITY $(\frac{LB_f/SEC^2}{IN^4})$	POISSON'S RATIO	SPRING CONSTANT (EXTENSION SPRING) (LB_f/IN)	SPRING CONSTANT (ROTATIONA SPRING) $(IN\text{-}LB_f/RAD$
Deck (Rotat. Stiff.)	1-5	Rotational Spring	10-20												$.111x10^{13}$
UIS	1-5	Beam	200-204	468.	$.130x10^{7}$	150	148	2			$22.92x10^{6}$	$.75x10^{-3}$	.3027		
UIS	1-5	Beam	204-210	468.	$.130x10^{7}$	150	148	2			$22.92x10^{6}$	$.368x10^{-3}$	.3027		
UIS Sodium	1-5	Mass	203						147.						
UIS	1-5	Mass	210						207.	$.420x10^{6}$					
UIS Sodium	1-5	Mass	211						36.2						
UIS Sodium	1-5	Spring	202-211											340.	
Plenum Separator (P.S.)	1-5	Beam	300-302	$.527x10^{4}$	$.462x10^{9}$	840	836	2			$24.77x10^{6}$	$.751x10^{-3}$	.2931		
P. S.	1-5	Beam	302-305	$.787x10^{4}$	$.686x10^{9}$	840/830*	836/828*	2			$24.77x10^{6}$	$.751x10^{-3}$	.2931		
P. S. Sodium	1-5	Mass	302						$.345x10^{4}$						
P. S. Sodium	1-5	Mass	306						$.319x10^{4}$						
P. S. Sodium	1-5	Spring	303-306											$.471x10^{4}$	
Lwr. Support Cone	1-5	Tapered Beam	400	$.152x10^{5}$	$.132x10^{10}$	879.8/789.8**	874/784**	2			$24.77x10^{6}$	$.1924x10^{-2}$	.2931		
			408	$.521x10^{4}$	$.572x10^{8}$	333.8/243.8	328/238	2			$24.77x10^{6}$	$.1924x10^{-2}$	.2931		
Lower Support	1-5	Mass	408						$.155x10^{4}$	$.108x10^{8}$					

* O.D. and I.D. are given for plenum separator outer wall and inner wall respectively.

** O.D. and I.D. are given for outer support cone and inner support cone respectively.

Table A-1 (Continued)

COMPONENT	CONCEPT	TYPE OF ELEMENT	NODES	AREA IN^2	AREA MOM. OF INERTIA IN^4	OUTER DIAMETER IN.	INNER DIAMETER IN.	SHEAR DEFLECTION AREA RATIO	MASS $\frac{(LB_f\text{-}SEC^2)}{IN.}$	MASS MOM. OF INERIIA $(LB_f\text{-}SEC^2\text{-}IN)$	ELASTIC MODULUS (LB_f/IN^2)	DENSITY	POISSON'S RATIO	SPRING CONSTANT (EXTENSION SPRING) (LB_f/IN)	SPRING CONSTANT (ROTATIONAL SPRING) $(IN\text{-}LB_f/RAD)$
Neutron Shield	1-5	Beam	500-502			464	392				$24.77x10^6$	$.392x10^{-3}$	.2931		
Neutron Shield	1-5	Beam	502-505			464	422				$24.77x10^6$	$.589x10^{-3}$	.2931		
Core Barrel and Core	1-5	Beam	600-608	$.266x10^4$	$.150x10^8$	216	208	2			$24.77x10^6$	$.738x10^{-2}$	.2931		

shear deflection option included. Material properties from the Nuclear Systems Materials Handbook (Reference 4) for medium carbon steel at 200^{o}F were used.

For concept 5, the support is located at the middle elevation of the deck (+90 inches). A beam element was used to provide a connection between node 1 at elevation +90 to node 4 at the bottom of the deck. This beam connection was made very rigid since it is expected that the deck is very rigid with respect to horizontal loading. The density value used for this beam was made very low since the mass of the ring girder and rotating plugs was already included at node points 10 and 20.

For concepts 2 and 4, the reactor support from concept 5 was shortened from 90 inches to 1 inch to give a support elevation at the bottom of the deck.

To model the effects of the deck, the mass of the rotatable plugs and shielding, based on an estimated weight of 939 tons, was added to the model at node 20. In addition, the mass moment of inertia was included based on a calculation assuming distribution of the mass in the form of a thin disc. The remainder of the deck weight and deck mounted equipment weight was estimated to be 4382 tons based on Reference 2. This included the weight of the deck, shielding, pumps and IHXs. The resistance of the deck to rotation due to a central bending moment reaction from the upper internals was estimated based on an equation for a uniform circular plate. For a 15 foot thick deck with top and bottom parallel circular plates of 1.5 inch thickness, the torsional spring constant is estimted to be 1.113 x 10^{12} in-lb/rad.

The model for the vessel consists of beam elements (ANSYS, STIF 3) with shear deflection included. The vessel is modeled with the stiffness properties of a cylinder of 900 inches ID and varying thickness. For the first 96 inches below the deck, the vessel wall thickness is 3.0 inches. For the next 96 inches, the thickness is 2.5 inches. Below this elevation the thickness is 2.0 inches. The material properties (other than density)

used for these elevations were based on 304 stainless steel at 200°F for the first 96 inches, 500°F for the next 96 inches, and 700°F below this elevation. The density for the first vessel element (between nodes 100 and 101) is based on stainless steel at 70°F and is 0.29 lb/in^3. Below this elevation the weight of the sodium associated with the vessel is included as part of the vessel wall material density as explained below.

The weight of the sodium was distributed on the components by estimating the volume and weight of sodium within each component and then increasing the material density of each component by an appropriate amount. The distribution is based on a total sodium weight of 4975 tons from Reference 2. The breakdown of this weight to each component is as follows:

Neutron Shield:	530.0 tons
Plenum Separator:	1281.5 tons
UIS:	92.5 tons
Support Cone:	610.0 tons
Vessel Bottom Head:	1103.5 tons
Vessel:	1357.5 tons

The bottom head of the vessel was modeled with two tapered beam elements (ANSYS, STIF 54) extending from elevation -471 down to -597 which is the estimated center of gravity of the bottom head. The mass and mass moment of inertia of the bottom head were estimated based on an ellispsoidal shape and were located at the center of gravity (node 116). The sodium mass in the bottom head was located in the model by including half at node 115 and half at node 116.

The UIS was modeled with the stiffness of a cylinder of 150 inches outer diameter and 148 inches inner diameter and with material properties based on 304 stainless steel at 950°F. A mass equivalent to 40 tons was added at the bottom of the UIS. The mass of the cylinder was an additional 24.8 tons for a total UIS weight of 64.8 tons. The sodium internal to the UIS was estimated at 92.5 tons. This sodium was distributed by locating 7 tons at

node 211 as an oscillating mass, 28 tons at node 203 and the remainder was distributed evenly below node 204 by increasing the material density. The spring constant for the oscillating mass and the distribution of the sodium mass were based on chapter 6 of Reference 5.

The plenum separator was modeled with the properties of the outer cylinder given in Table A-1 for the first two elements. Above these elements the element constants are based on the sum of the area and moment of inertia for the outer cylinder and the inner cylinder. The internal sodium weight was estimated to be 1281.5 tons. Of this weight, 616.5 tons were placed at node 306 as an oscillating mass and 665 tons were placed at node 302 based on methods of Reference 5.

The support cone was modeled using eight tapered beam elements (ANSYS, STIF 54). Table A-1 gives the properties at the top of the first element and at the bottom of the last element. The element properties between these are linearly related. The stiffness and area of the two cones forming the support cone are combined additively to obtain properties for the elements between nodes 400 and 408. An internal sodium weight of 610 tons is distributed on the cone by increasing the material density.

The neutron shield was modeled with pipe elements (ANSYS, STIF 23) and with material properties based on stainless steel. The model of this component is artificially rigid since the stiffness was based on a solid cylinder. However, the density is set to provide the correct total mass of the structure plus 530 tons of internal sodium.

The core barrel stiffness is based on that of a cylinder of 216 inches overall diameter and 4 inch wall thickness. The material properties are based on 304 stainless steel at 700^{o}F except for density, which is adjusted to give a total weight for the core and core barrel of 750 tons.

The weight of the IHX and pump standpipes, internal baffles, fuel transfer station, and miscellaneous structures totals to 648 tons. The mass is included at node 110 in the models.

A.3.1.3 RESULTS

A comparison of the three basic support concepts is given in this section by comparing reaction loads or stresses at key locations. A comparison of natural frequency is also included for the UIS and vessel in Table A-2.

The reactions at the support of each concept are given in Table A-3. The trend shows higher moment reaction loads as the support elevation is made higher but lower lateral reaction loads for OBE and SSE.

The UIS reactions and stresses are given in Table A-4. In all cases in this Table, the UIS stiffness was modeled based simply on a 150 inch cylinder of 1 inch wall thickness. Also, an estimate of the internal sodium mass was made. As described previously, some of this mass was included as part of the mass of the UIS wall and some as part of a spring-mass system attached to the UIS. A comparison of computer runs with and without the spring mass system showed very little difference in results. The stress values given in Table A-4 include bending stress only and, thus, do not account for shear stress or vertical stress due to veritical seismic loading. Table A-5 gives the deflection of the bottom of the UIS relative to the top of the core barrel. Since the UIS and core barrel have the potential to vibrate in opposite directions at the same time, the displacements from the spectrum analysis were added. The support deflection, however, was subtracted since it does not contribute to this relative deflection.

The plenum separator reactions and stresses are given in Table A-6 for each concept. These stress values include only the bending stress due to lateral loading.

TABLE A-2

COMPARISON OF NATURAL FREQUENCY
FOR CONCEPTS 1 THRU 5

Concept	UIS Frequency* (Hz)		Vessel Frequency (H_z)	
	f_1	f_2	f_1	f_2
1 & 3	8.34	24.19	6.86	13.70
2 & 4	8.34	24.20	7.18	13.75
5	8.34	24.20	7.15	13.74

* UIS model includes internal sodium mass.

TABLE A-3

REACTION LOADS FOR VARIOUS REACTOR SUPPORT CONCEPTS

Concept	Location (See Fig. A-2)	Lateral Reaction (10^6 Lb.)			Moment Reaction (10^9 In-Lb.)		
		1G	OBE	SSE	1G	OBE	SSE
1 & 3	a	28.43	39.46	66.57	3.55	12.28	20.82
1 & 3	b	28.24	39.41	66.48	5.25	14.34	24.34
2 & 4	c	28.24	28.87	49.00	5.25	12.87	21.85
5	d	28.24	29.70	51.76	7.79	15.58	26.83

TABLE A-4

UIS REACTION LOADS AND STRESS AT BOTTOM ELEVATION OF DECK

Concept	Lateral React. (10^6 Lb.)			Moment Reaction (10^6 In-Lb.)			Bending Stress[1,3] (ksi)		
	1G	OBE	SSE	1G[2]	OBE	SSE	1G	OBE	SSE
1 & 3	.316	.485	.817	75.24	147.2	248.1	4.34	8.50	14.33
2 & 4	.316	.519	.875	75.24	159.5	268.7	4.34	9.21	15.51
5	.316	.509	.887	75.24	156.1	271.7	4.34	9.01	15.68

Notes:

(1) Based on a 1 inch thick cylinder of 150 inches O.D.

(2) Includes reaction due to internal sodium.

(3) Vertical stress was found to cause an insignificant increase in stress ($\sim$ .3%) and was therefore excluded to simplify calculations. The above conclusion was based on a net upward load of .8G for OBE and 1.8G for SSE.

TABLE A-5

UIS DEFLECTION RELATIVE TO TOP OF CORE BARREL

Concept	Lateral UIS Deflec.* (Mils)			Lateral C.B.Deflec.* (Mils)			Relative Deflec.** (Mils) UIS to C.B.		
	1G	OBE	SSE	1G	OBE	SSE	1G	OBE	SSE
1 & 3	-197	368	619	-214	478	812	17	806	1363
2 & 4	-166	380	641	-182	388	659	16	768	1300
5	-169	372	653	-185	395	670	16	767	1323

*Deflection includes vessel and support deflections

**Support deflection is subtracted on concept 1 and is negligible on the other concepts.

TABLE A-6

REACTION LOADS AT BOTTOM OF PLENUM SEPARATOR

	Lateral Reaction (10^6 Lb.)			Moment Reaction (10^9 In-Lb)			Bending Stress* (psi)		
Concept	1G**	OBE	SSE	1G**	OBE	SSE	1G**	OBE	SSE
1 & 3	3.167	3.998	6.784	.4467	.4755	.8061	406	431	733
2 & 4	3.167	3.511	5.964	.4467	.4139	.7032	406	376	639
5	3.167	3.540	6.015	.4467	.4169	.7088	406	379	643

* Based on a 2 inch thick cylinder of 840 inches O.D.

** Includes reaction due to internal sodium

The reaction loads at the top of the vessel are given in Table A-7. Also included are bending stresses for OBE and SSE. In the case of an OBE event, the vertical seismic force used was a 1G dynamic load resulting in a zero net upward load when added to the dead weight of the vessel. For an SSE event, a 2G dynamic load was used resulting in a 1G net upward load. The resulting vertical stress was combined with the stress from a North-South and an East-West event using the square root of the sum of the squares method. The SSE vertical reactions are estimates based on computer runs using a combined horizontal and vertical model (Reference 6) to obtain OBE vertical results.

Figures A-5 and A-6 show the compressive stresses in the vessel wall for concept 5 for OBE and SSE occurrences. As described above for Table A-7 these stresses are a combination of results for two orthogonal horizontal directions and the vertical direction. The reaction moments used in calculating the stress shown in Figures A-5 and A-6 were based on the models which assume a 3.0 inch wall thickness for the first eight feet, a 2.5 inch wall for the next eight feet and a 2.0 inch wall thickness for the remainder of the vessel. These stresses do not account for an effect on frequency response due to thicknesses other than those modeled.

The limits given in Table A-8 and on Figure A-5 for OBE are based on section NB-3133.6 of Reference 7 for cylinders in uniform compression. It appears that the ASME Code does not address cylinders in bending. However, Reference 8 indicates that a factor to increase the critical buckling stress from the axial compression case to the bending case can be defined as a function of the radius to thickness ratio. A 10% increase could be justified for the radius to thickness ratios (R/T) typical of the pool reactor vessel based on experimental results given on page 4-58 of Reference 8. The limits shown on Figures A-5 and A-6 do not include this increase, however.

TABLE A-7

REACTION LOADS AND STRESS AT TOP OF VESSEL
(BOTTOM ELEVATION OF DECK)

Concept	Lateral Reaction (10^6 Lb)			Moment Reaction (10^9 In-Lb)			Bending Stress (psi)		
	1G	OBE	SSE	1G	OBE	SSE	1G	OBE*	SSE*
1 & 3	17.28	35.85	60.80	5.71	14.35	24.38	2982	7498	12883
2 & 4	17.28	31.34	53.20	5.71	12.84	21.80	2982	6705	11543
5	17.28	31.62	53.71	5.71	12.94	21.98	2982	6759	11650

* OBE and SSE stress are results of SRSS combination of equal orthogonal horizontal events and of a 1G vertical load for OBE (net 0 upward load) and 2G vertical for SSE (net 1G upward load).

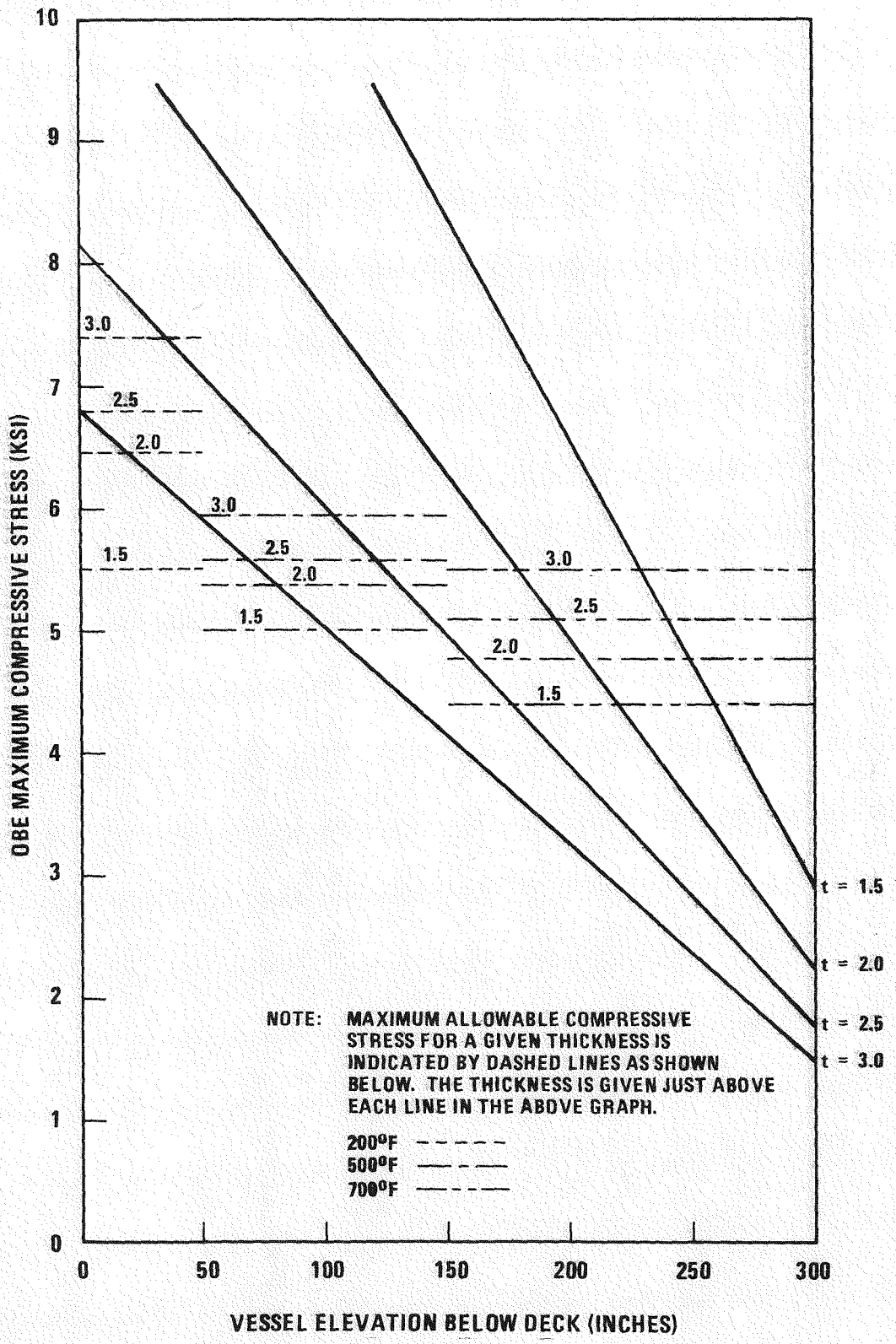

Figure A-5. OBE Compressive Stresses in Concept 5 for Various Wall Thicknesses

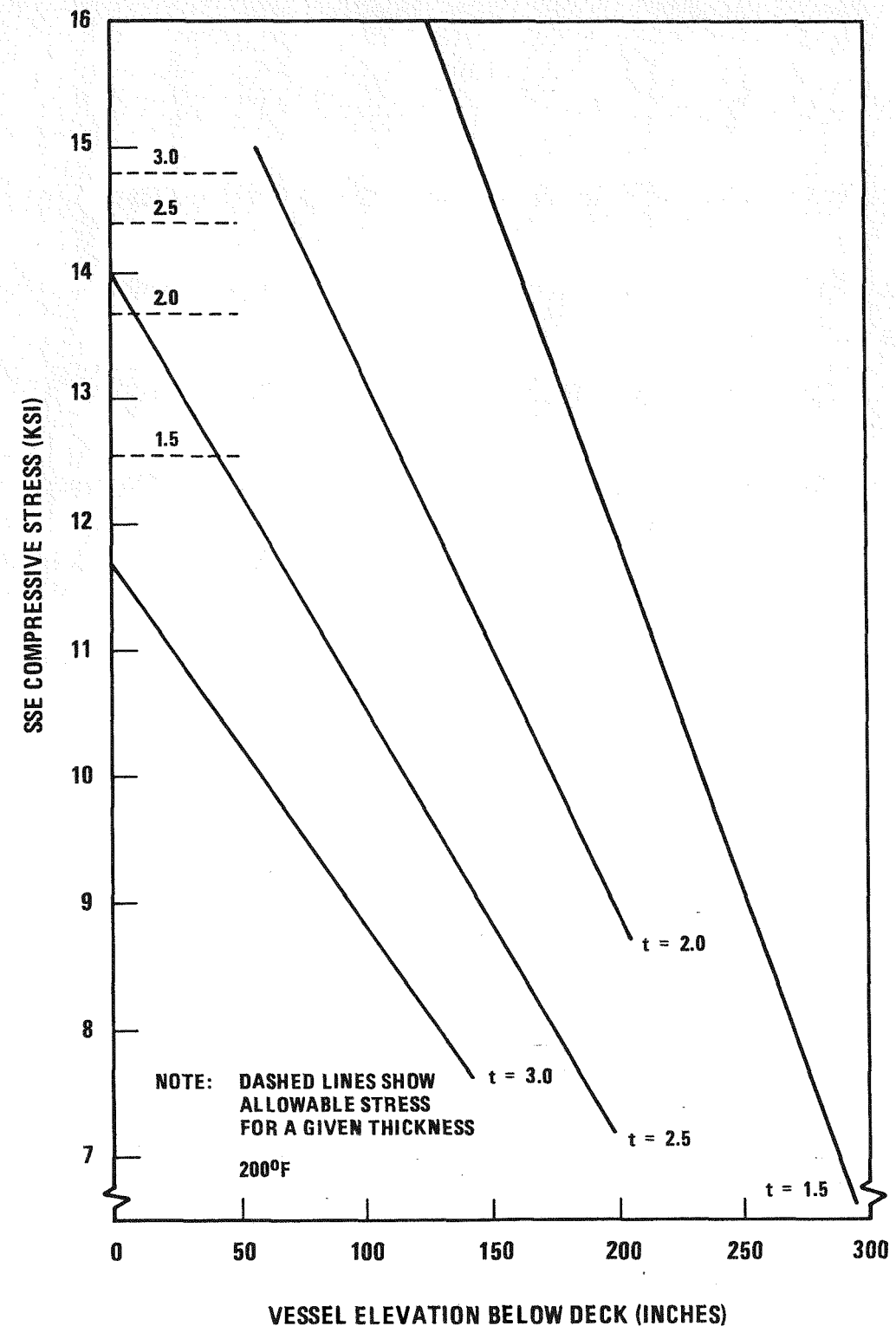

Figure A-6. SSE Compressive Stresses Concept 5 Vessel for Various Wall Thicknesses

0665-41

TABLE A-8

SUMMARY OF ASME LIMITS ON COMPRESSIVE STRESS FOR A CYLINDER
OBE CASE, EVENT LEVEL B, ASME NB-3133.6

Material Temperature °F	Vessel Wall Thickness (Inches)	Radius to Thickness Ratio (R/T)	ASME Allowable Stress (psi)	1.1 x ASME Allowable Stress (psi)
200	1.5	301	5500	6050
500	1.5	301	5000	5500
700	1.5	301	4400	4840
200	2.0	226	6500	7150
500	2.0	226	5400	5940
700	2.0	226	4800	5280
200	2.5	181	6800	7480
500	2.5	181	5600	6160
700	2.5	181	5100	5610
200	3.0	151	7400	8140
500	3.0	151	6000	6600
700	3.0	151	5500	6050

The limits for SSE allowable compressive stress given in Table A-9 and on Figure A-6 were derived by solving an elastic buckling equation and an inelastic buckling equation (see Vol. 4, p. 121 of Reference 1) as shown in Figure A-7. A lower limit line was drawn below the two curves to account for experimental data observed in that region. The critical buckling stress for a given R/T ratio was then determined based on the lower limit line. This stress was then divided by a 1.5 safety factor (consistent with ASME Code Case 1592) to obtain the values in Table A-9.

Estimated maximum temperatures over the upper length of the vessel wall are:

$T < 200^{o}F$ for 0 to 50 inches below deck
$T < 500^{o}F$ for 50 to 150 inches below deck
$T < 700^{o}F$ for 150 to 300 inches below deck

These limits were the basis for placement of the stress limit lines on Figures A-5 and A-6.

A.3.1.4 CONCLUSIONS

For the reference support concept (concept 5), the conclusion for the LPR vessel thickness is that a three inch thickness is adequate at the top. Also, due to more conservative ASME limits for a level B event, the OBE case is the limiting event rather than the SSE. Use of the ASME limits shows that a three inch wall thickness is required for the first 120 inches, and that a 2.5 inch thickness is required for the next 90 inches, below which a 2.0 inch thickness would be adequate. These distances are based on the above temperature assumptions, which are believed to be reasonable, and on the seismic spectrum of Figure A-1.

The concept 5 model was also used to obtain an estimate of UIS deflection relative to the top of the core barrel. A relative deflection of 1.3 inches was obtained. The bending stress at the top of the UIS is estimated to be 9 ksi for an OBE case and 15.7 ksi for an SSE.

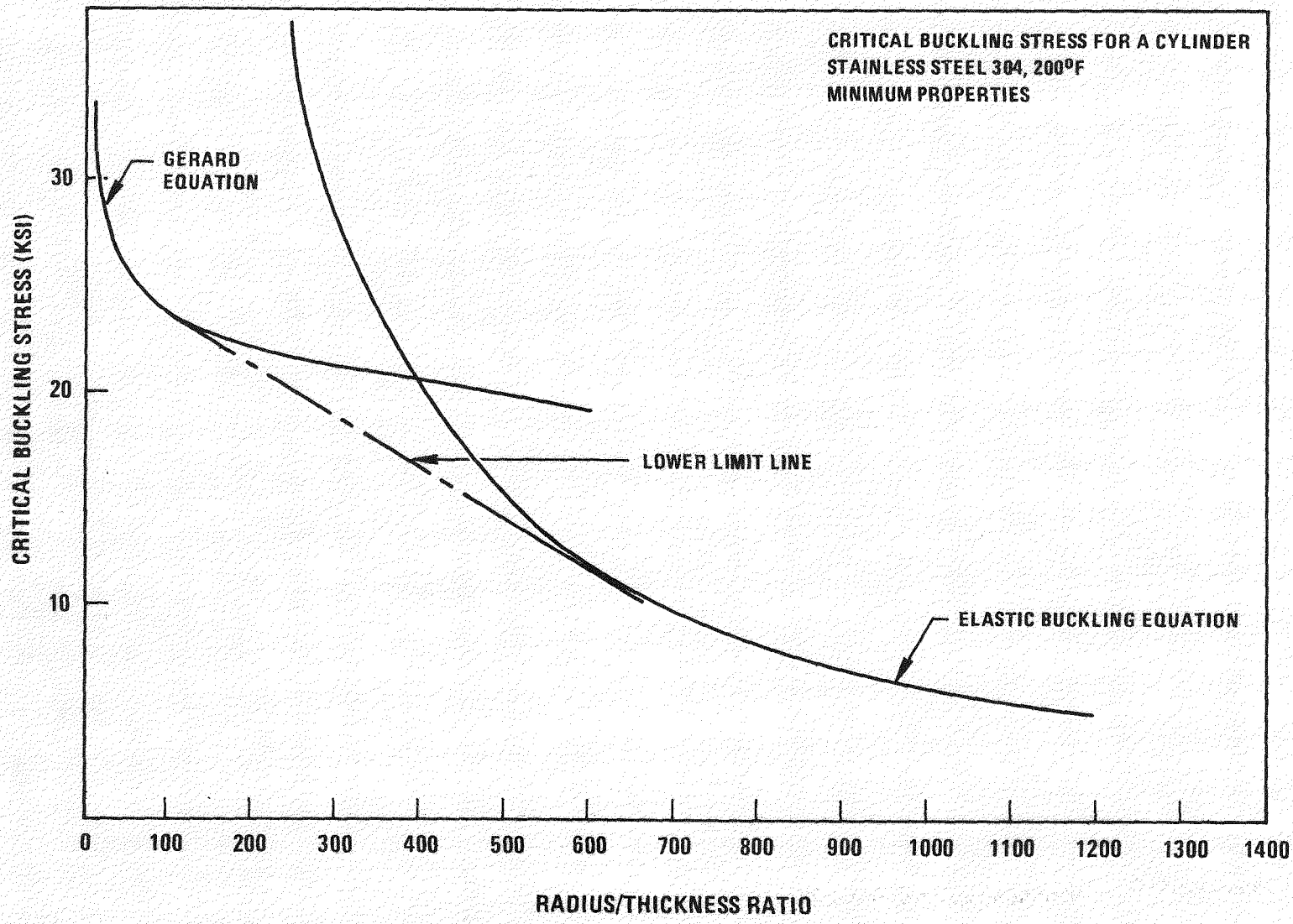

Figure A-7. Axisymetric Cylinder Buckling for 304 Stainless Steel at 200°F

TABLE A-9

LEVEL D SSE LIMITS ON COMPRESSIVE STRESS BASED ON 1.5 SAFETY FACTOR TO CRITICAL BUCKLING STRESS

Material Temperature °F	Vessel Wall Thickness (Inches)	Radius to Thickness Ratio	$\sigma_a = \frac{\sigma_{critical}}{1.5}$	$1.1\ \sigma_a$
200	1.5	301	12530	13780
200	2.0	226	13670	15040
200	2.5	181	14400	15840
200	3.0	151	14800	16280

The results given for the vessel and UIS are based on a seismic acceleration spectrum used in Reference 1. The horizontal spectrum was assumed to act equally in both the North-South and East-West directions. This represents a conservative assumption. The LPR system should be reanalyzed when an applicable seismic spectrum is developed.

One of the objectives of the analysis was to compare the results of the five vessel support concepts for an equal input response spectrum. The results show that concepts 2 and 4 give about the same response as concept 5 but that concept 1 does have significant differences. The lateral reaction load at the support is about 25% higher for concept 1 and 3 as compared to the other concepts. This is due to the additional flexibility of the support for concepts 1 and 3. For moment reaction loads, concept 5 is about 30% higher than concept 1 and concept 2 is about 5% higher than concept 1 due to the higher elevations of concepts 2, 4 and 5. For the vessel upper wall concept 1 gives about 10% higher stresses than the reference concept 5.

A.3.2 SYSTEM MECHANICAL/THERMAL ANALYSIS

The analysis of the reactor vessel system was performed using a finite element model in conjunction with the ANSYS computer code. Since only preliminary steady state loads have been specified, the evaluation was performed only for these steady state loads combined with the seismic loads of Section A.3.1.

The axisymmetric finite element model used for this evaluation is based upon revision 2 of the LPR design control drawing. Those parts of the reactor system that are continuous in the circumferential direction were modeled using the axisymmetric conical shell element, STIF 61. The shear panels that are not continuous were modeled using rectangular flat shell elements, STIF 43. A two inch thickness was used for the flat shell elements since this gives a stiffness for the entire structure that is approximately correct. Figure A-8 shows the model including the shear members and Figure A-9 shows only the axisymmetric portion of the model.

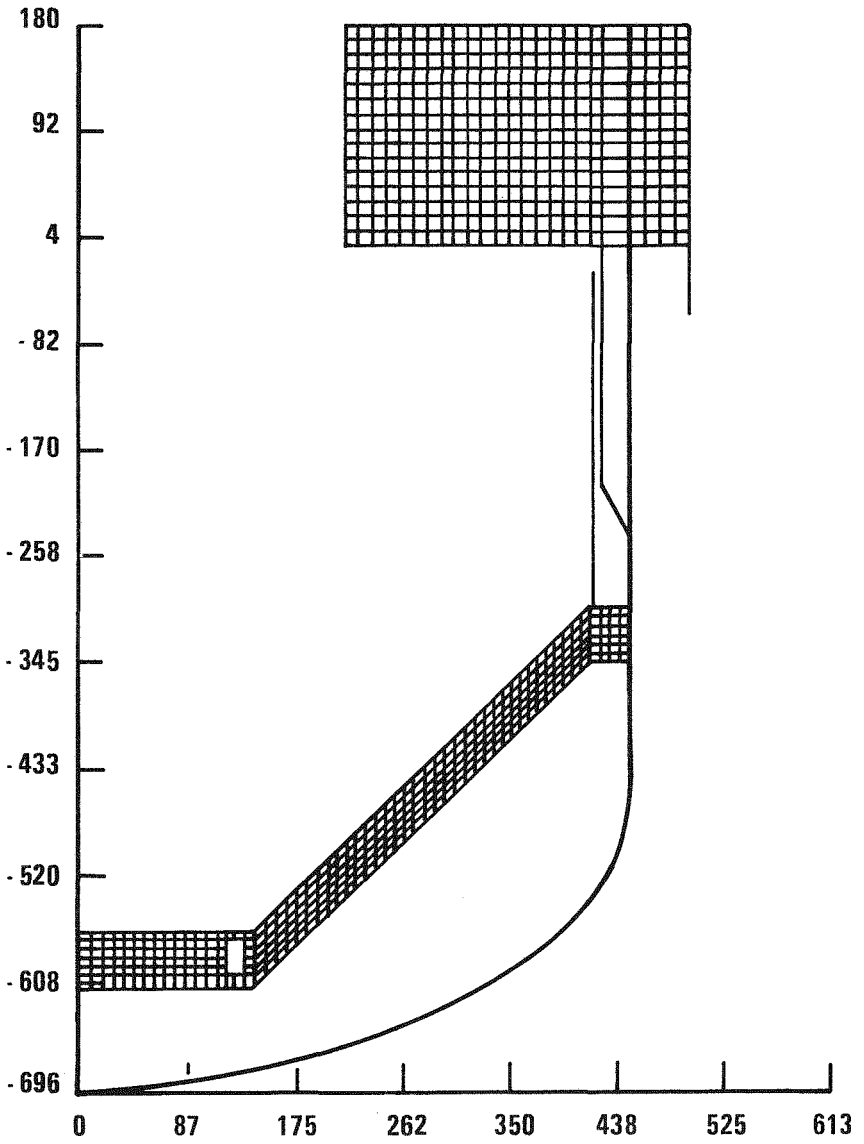

Figure A-8. Axisymmetric Model of LPR System with Shear Panels

0665-183

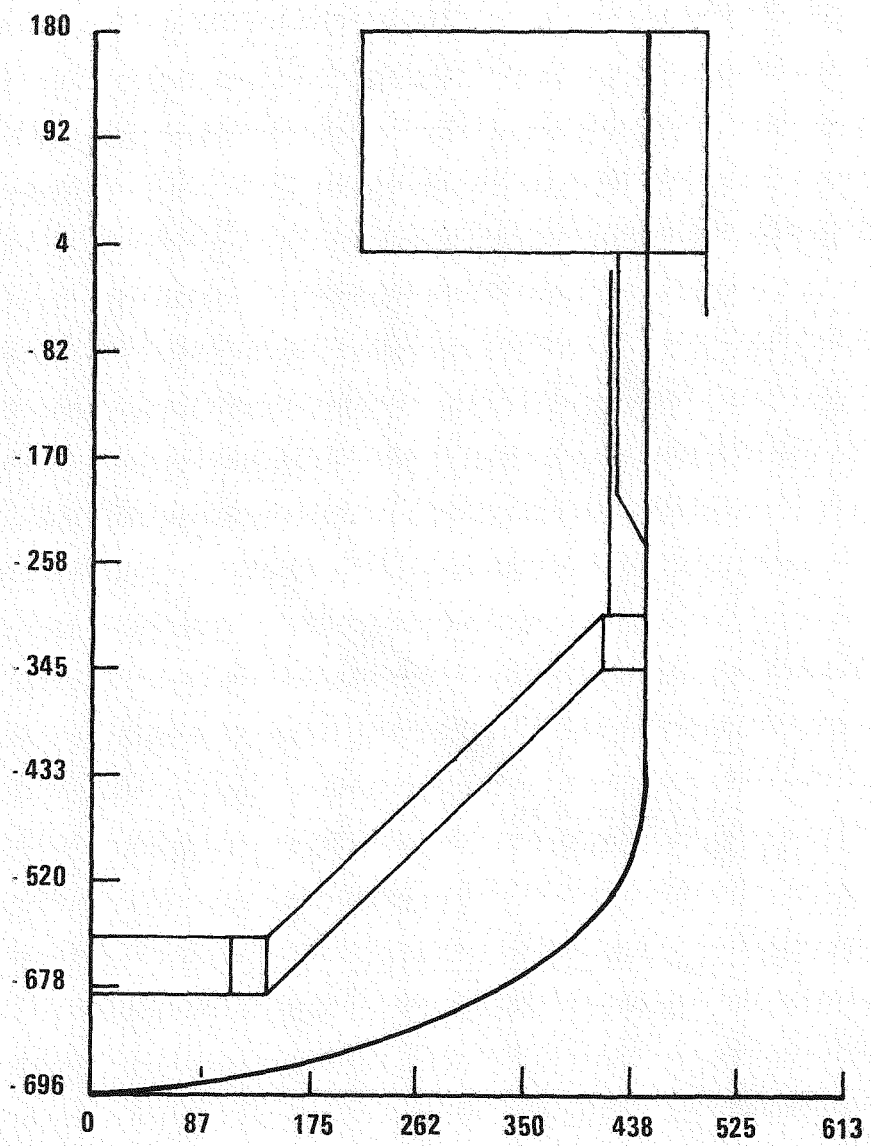

Figure A-9. Axisymmetric Model of LPR System without Shear Panels

A.3.2.1 LOWER HEAD

The equations presented in Reference 9 for the stress in a thin shell for an applied internal pressure show that the torus portion of this vessel will experience the largest stress. This stress is directly proportional to the radius of the spherical cap and inversely proportional to the radius of the torus. Reference 9 further showed that the circumferential compressive stress would be mitigated by the adjoining shells and that the actual stress intensity from the finite element analysis would be approximately two-thirds of the magnitude predicted by the equation. To gain some insight into the variation of stress intensity at the junction of the torus and the spherical cap, the expected stress intensity for a 2 inch thick shell was calculated and plotted against the radius of the torus for different spherical cap radii. The results are shown in Figure A-10.

A second criteria that would stipulate the design of the lower head is the limit pressure as specified by Reference 10. The limit pressure was also calculated and plotted against the radius of the torus for different spherical cap radii (also for a 2 inch thick shell). The results for the pressure are shown in Figure A-11.

Using the stress intensity from Figure A-10 and the limit pressure from Figure A-11, a first guess at the size of the lower head is taken as 16 feet for the torus radius and 60 feet for the spherical cap radius. This size satisfies the limit pressure requirement but does not satisfy the stress intensity limit. But as noted previously, the relaxation of the boundary conditions on the torus by the spherical cap will reduce the stress at the junction.

To evaluate the stresses in the actual vessel for the 16/60 torispherical head, a finite element model of the vessel was developed using the ANSYS computer code and the harmonically loaded axisymmetric conical shell

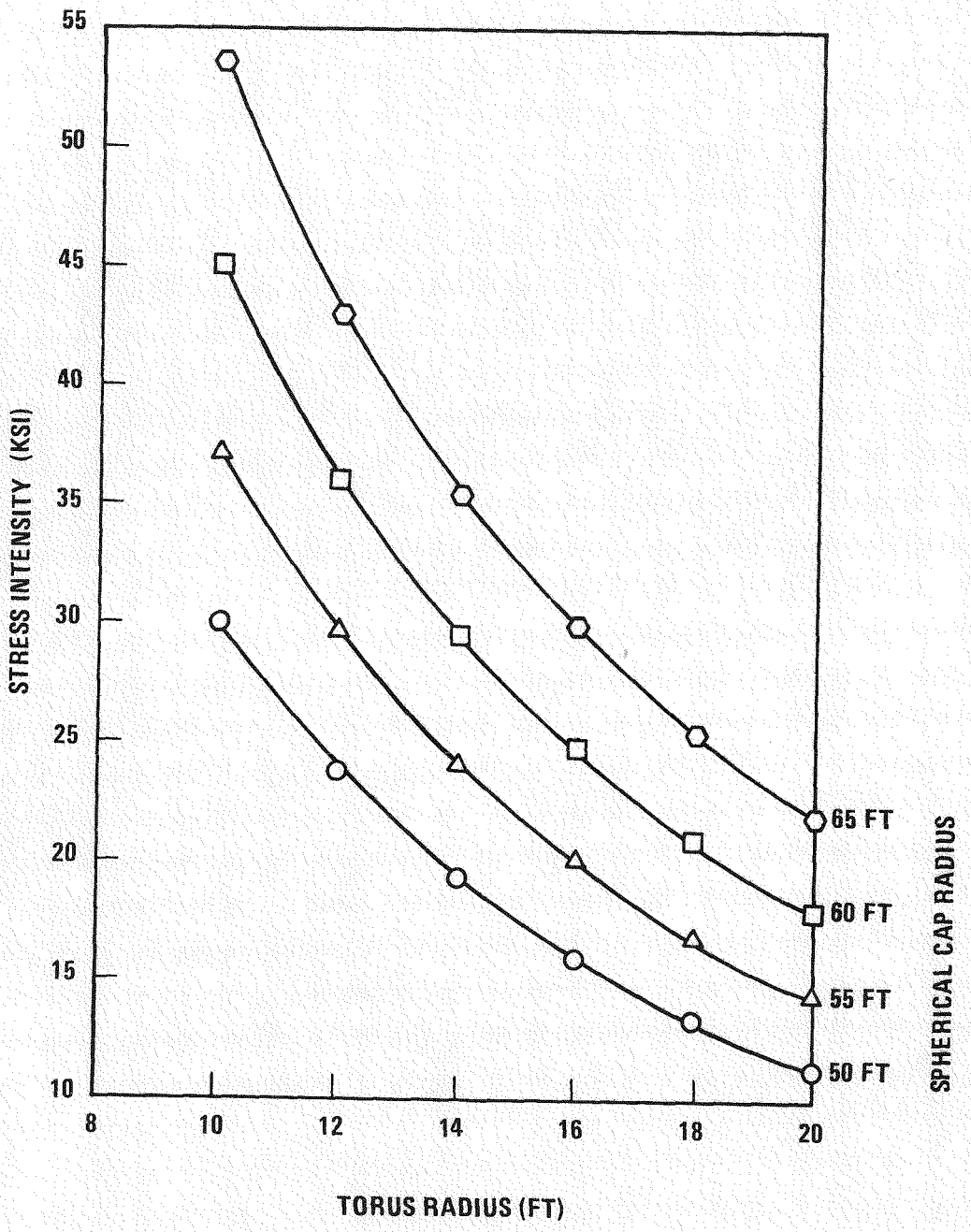

Figure A-10. Maximum Theoretical Torus Stress Intensity

0665-181

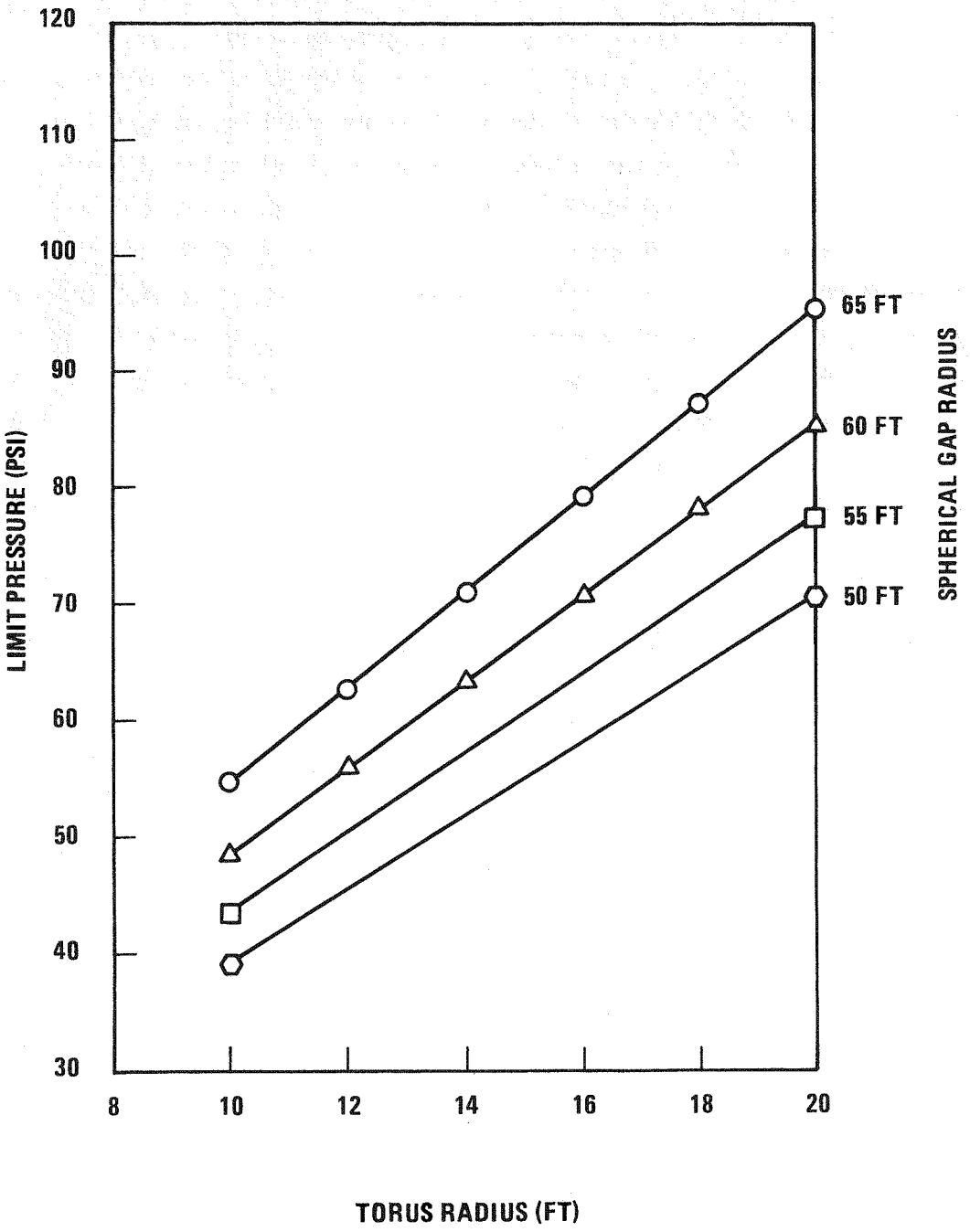

Figure A-11. Limit Pressure for Torospherical Head

element, STIF 61. The model incorporated the entire vessel from the roof to the centerline and is shown in Figure A-12. The applied loads consisted of an internal pressure of 50 psi and the dead weight of the vessel.

The results of the analysis are shown graphically in Figures A-13 through A-15. Figure A-13 shows the variation in membrane stress intensity along the length of the vessel and Figure A-14 shows the compressive circumferential stress in the region of the torus. The maximum membrane stress intensity is 15,400 psi near the junction of the torus and the spherical cap, compared to an allowable stress intensity of 15,600 psi for 304 SS at 750^{o}F. The maximum compressive stress in Figure A-14 is 7,900 psi which is less than the allowable compressive stress of 15,600 psi from Reference 9. Figure A-15 shows the membrane-plus-bending stress intensity in the vessel but the bending stresses are generally small and the membrane stress intensity limit governs the design.

As an additional check, the vessel with an 18 foot torus and a 60 foot spherical cap was also analyzed, and the results are plotted on Figures A-13 and A-14 and confirm that the larger torus radius gives small stresses.

It is concluded from this analysis that, for a 2 inch thick shell, the 16/60 torispherical lower head can adequately withstand a pressure of 50 psi when combined with the dead weight of the vessel. And because of the membrane stress intensity limit, the radius of the torus should not be less than 16 feet nor should the radius of the spherical cap be greater than 60 feet. Also, in this range, the stress in the lower head varies linearly with the thickness of the shell. But under no circumstances should the thickness be less than 2 inches since the diameter-to-thickness ratio of 500 must also be satisfied per Reference 9.

A.3.2.2 LOWER SUPPORT STRUCTURE/VESSEL INTERFACE

The loads applied to the model, Figure A-16 and A-17, for the evaluation of the LSS/vessel interface consisted of the dead weight of the structure, the weight of the core, the weight of the neutron shielding, the weight of the

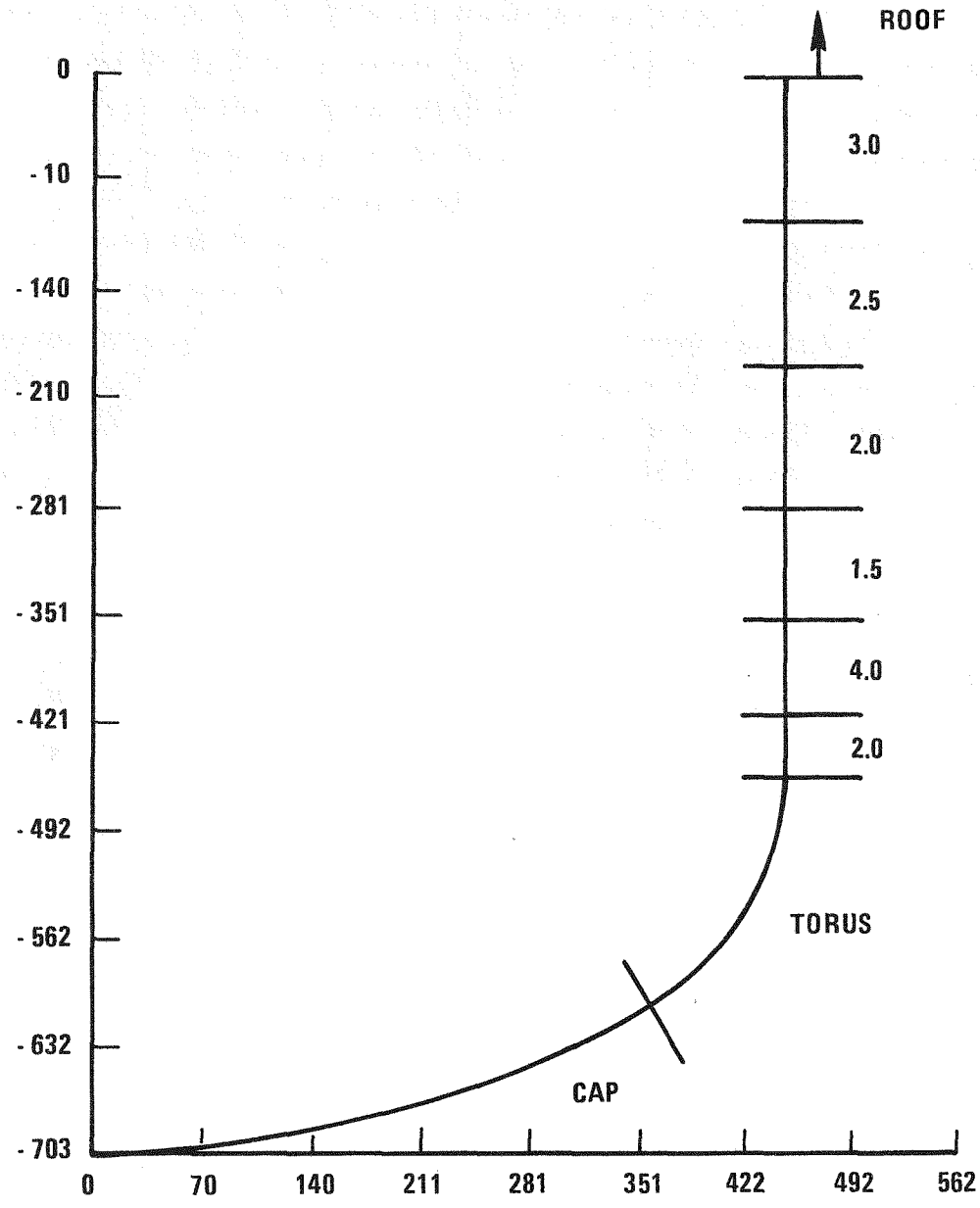

Figure A-12. Finite Element Model of LPR Vessel

0665-179

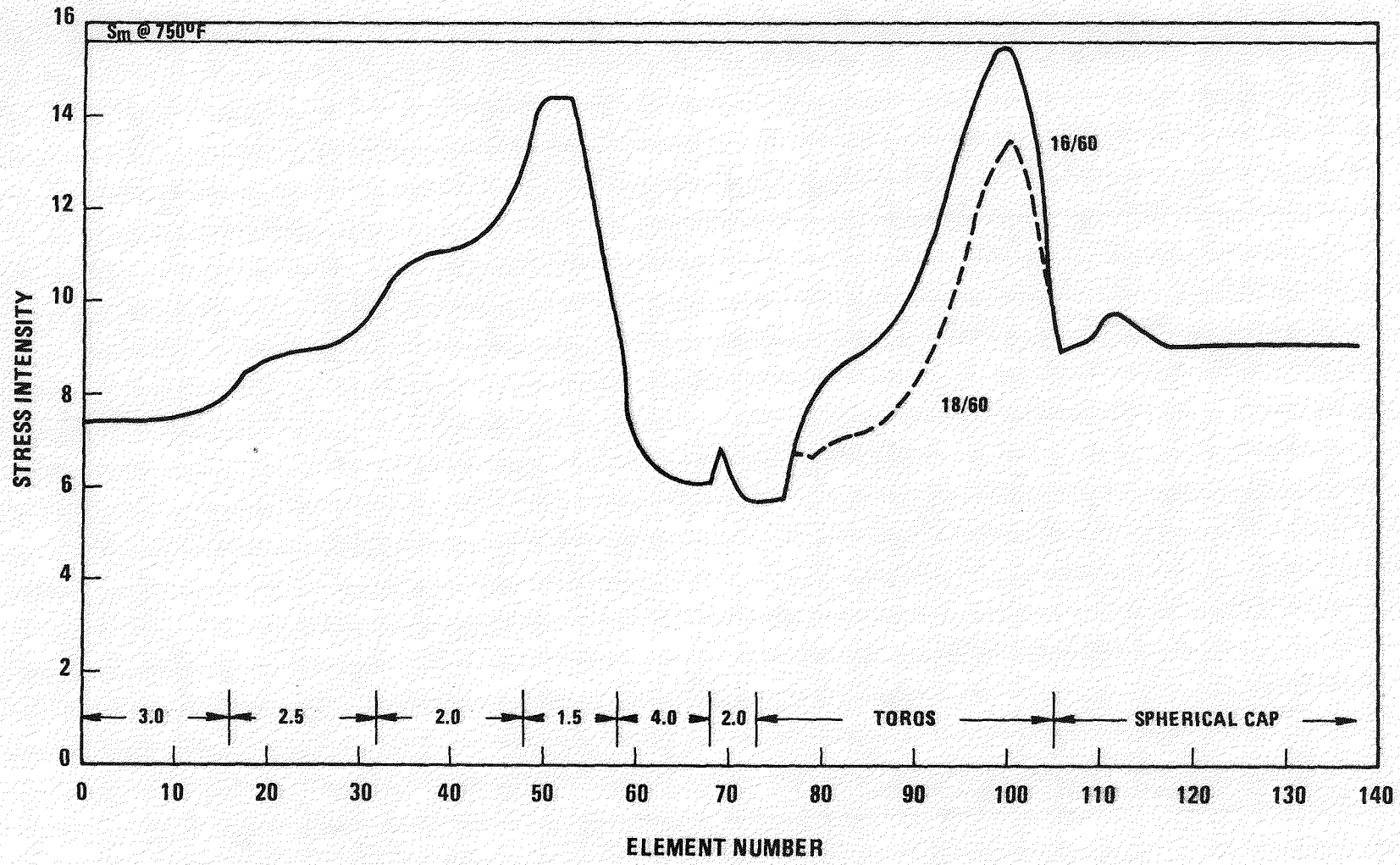

Figure A-13. Membrane Stress Intensity Along Vessel

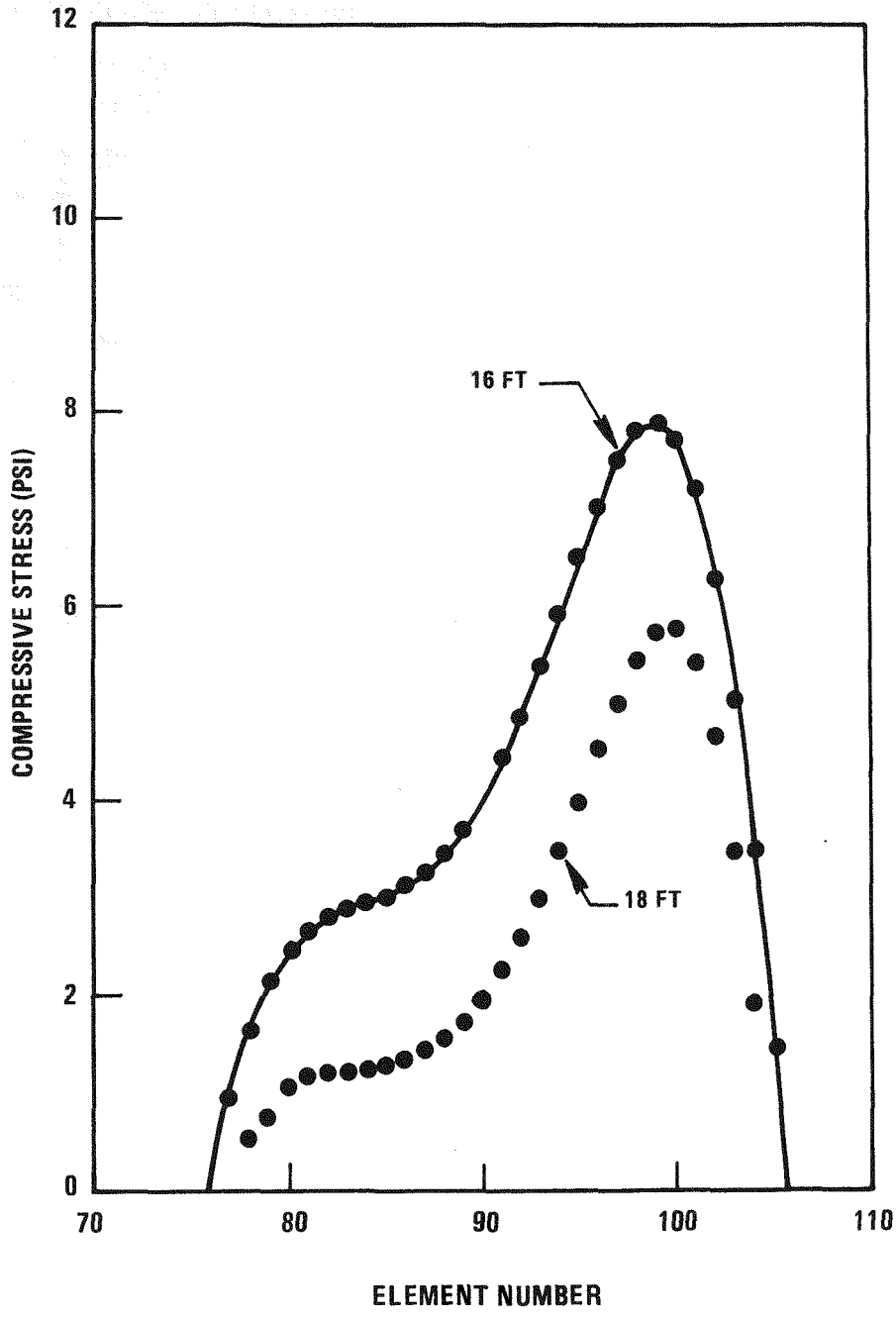

Figure A-14. Compressive Stress in Torus

0665-177

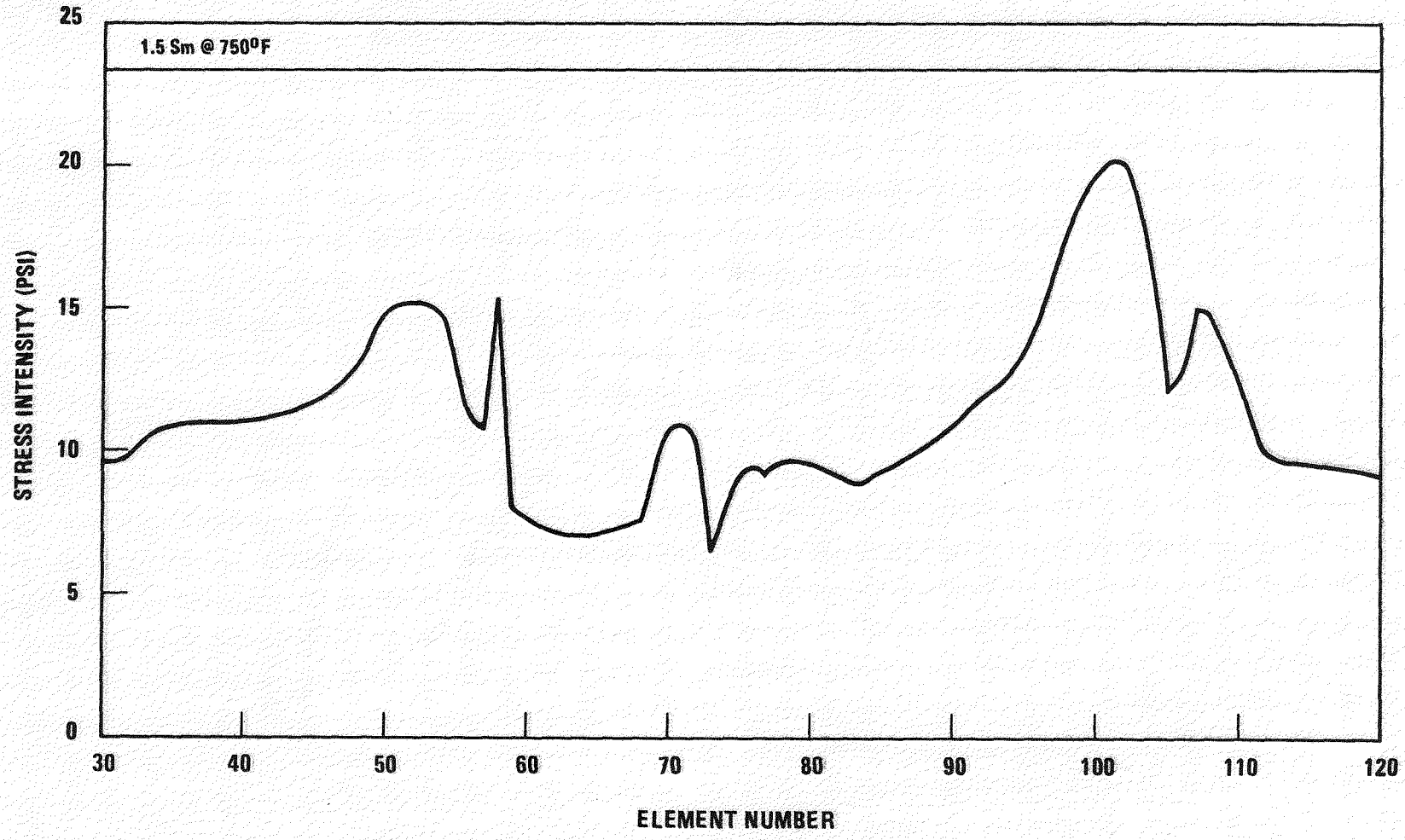

Figure A-15. Membrane Plus Bending Stress Intensity Along Vessel

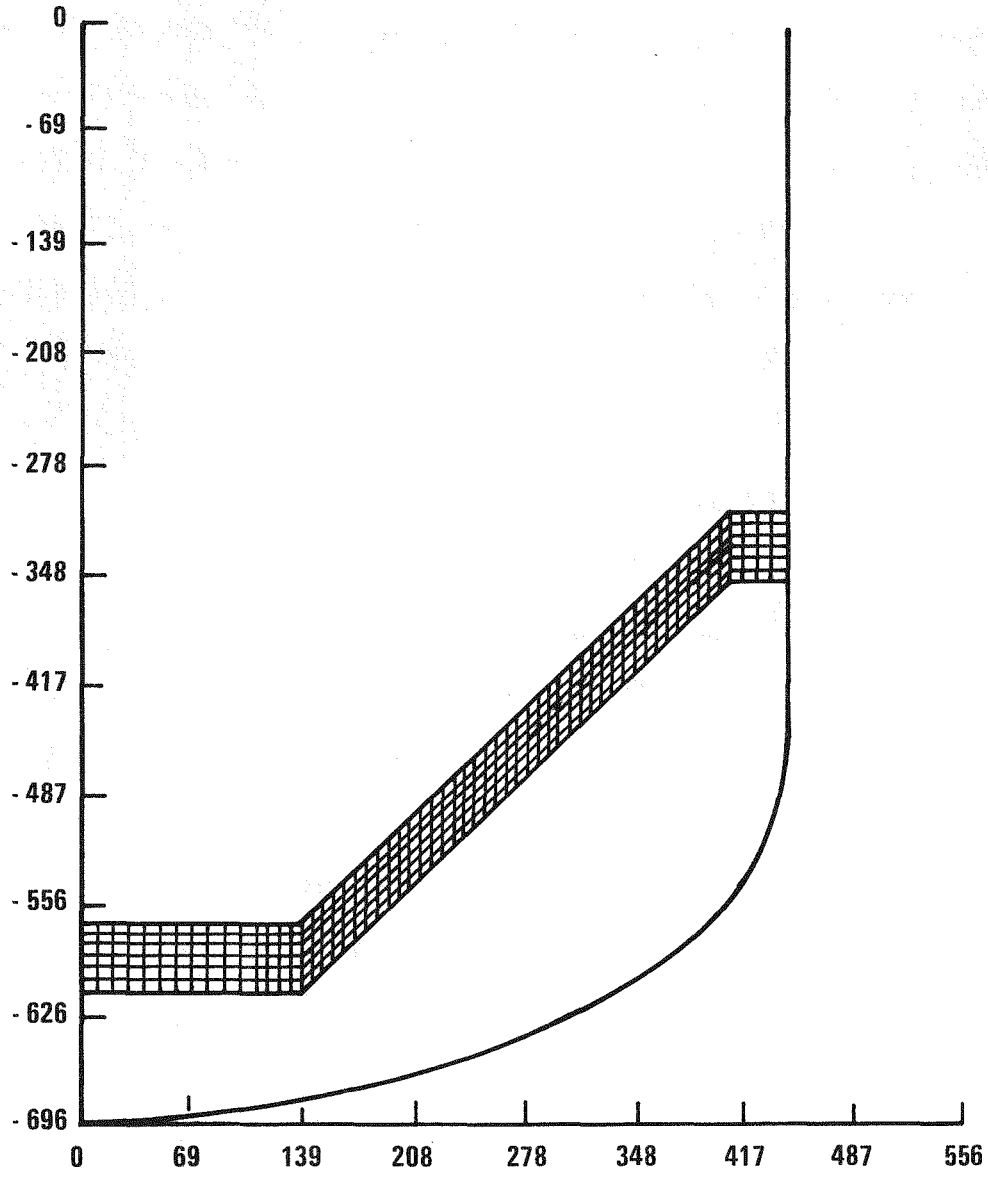

Figure A-16. Finite Element Model of Lower Support Structure

0665-175

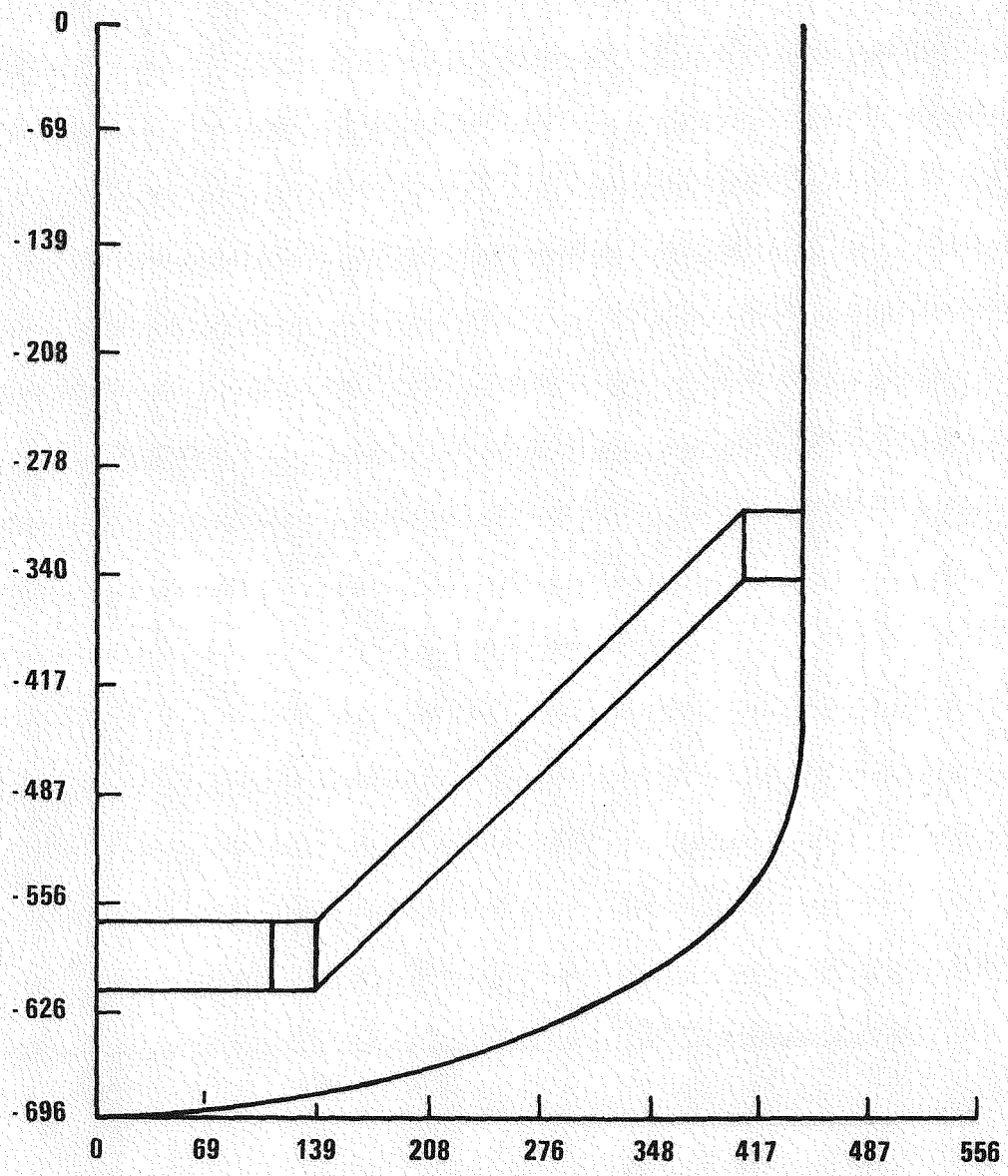

Figure A-17. Axisymmetric Portion of Lower Support Structure Finite Element Model

0665-174

pump and IHX standpipes, the differential pressure of 3 psig and the steady state temperature distribution. The various weights were taken from Reference 2. The temperatures are preliminary estimates as specified on the design control drawing.

The results of the analysis of dead weight (1g) loading of the model show that the stresses in the lower support structure are generally low except in the shear panels in the box structure at the LSS/vessel interface. Shear stresses in these members are high since they serve to retain the rectangular shape of the box. Figure A-18 shows these shear stresses at the centroid of the finite elements in the model. Under vertical seismic conditions, these shear stresses could be expected to triple in magnitude. Then if converted to a stress intensity for comparison with an allowable, the resulting stress intensity would be

$$P_m = 2 \times 3 \times 8571 = 51426 \text{ psi.}$$

That far exceeds the allowable stress intensity of 1.2 x 16300 = 19560 psi for 316 SS at 700^{o}F. If the thickness of the shear panels is increased to 6 inches, these shear stresses are reduced as shown in Figure A-19. This would correspond to increasing the number of shear panels by a factor of 3 rather than increasing the thickness of any individual panel. In this case, a plan view of the LSS/CSS would be similar to a plan view of the deck structure where a large number of shear members are present between the vessel wall and the outer wall of the deck. Although a quick calculation of the stress intensity from the values in Figure A-19 would indicate that the shear panels would still be overstressed, the results are expected to demonstrate that this region is adequate when a detailed evaluation is performed, based upon experience with a similar evaluation for the deck structure, References 1 and 11.

An alternative to increasing the number of shear panels is to modify the design by extending the conical lower support structure into the vessel. The finite element model was modified to reflect this configuration as shown

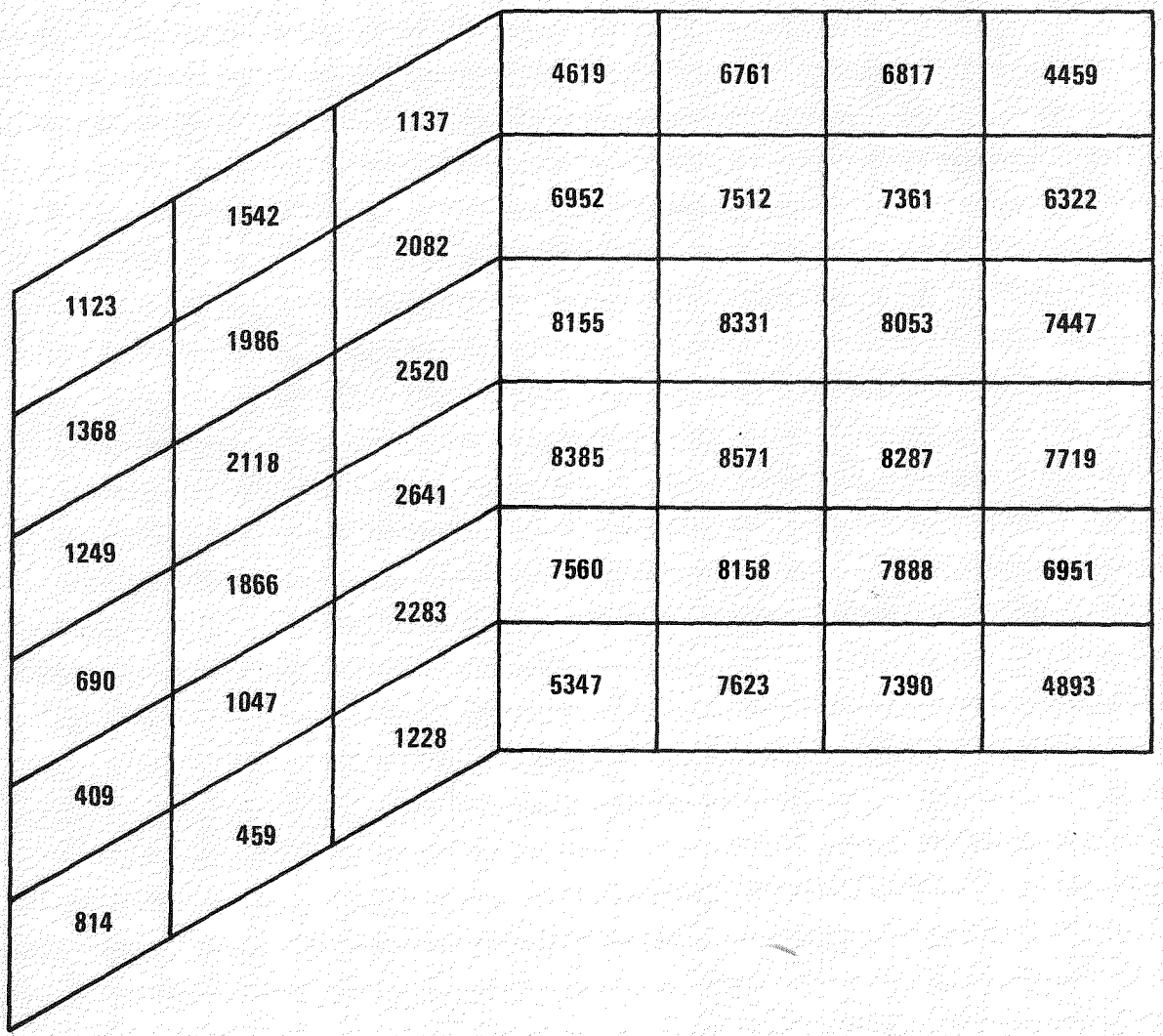

Figure A-18. Average Shear Stress in Box Structure for 2 Inch Panels

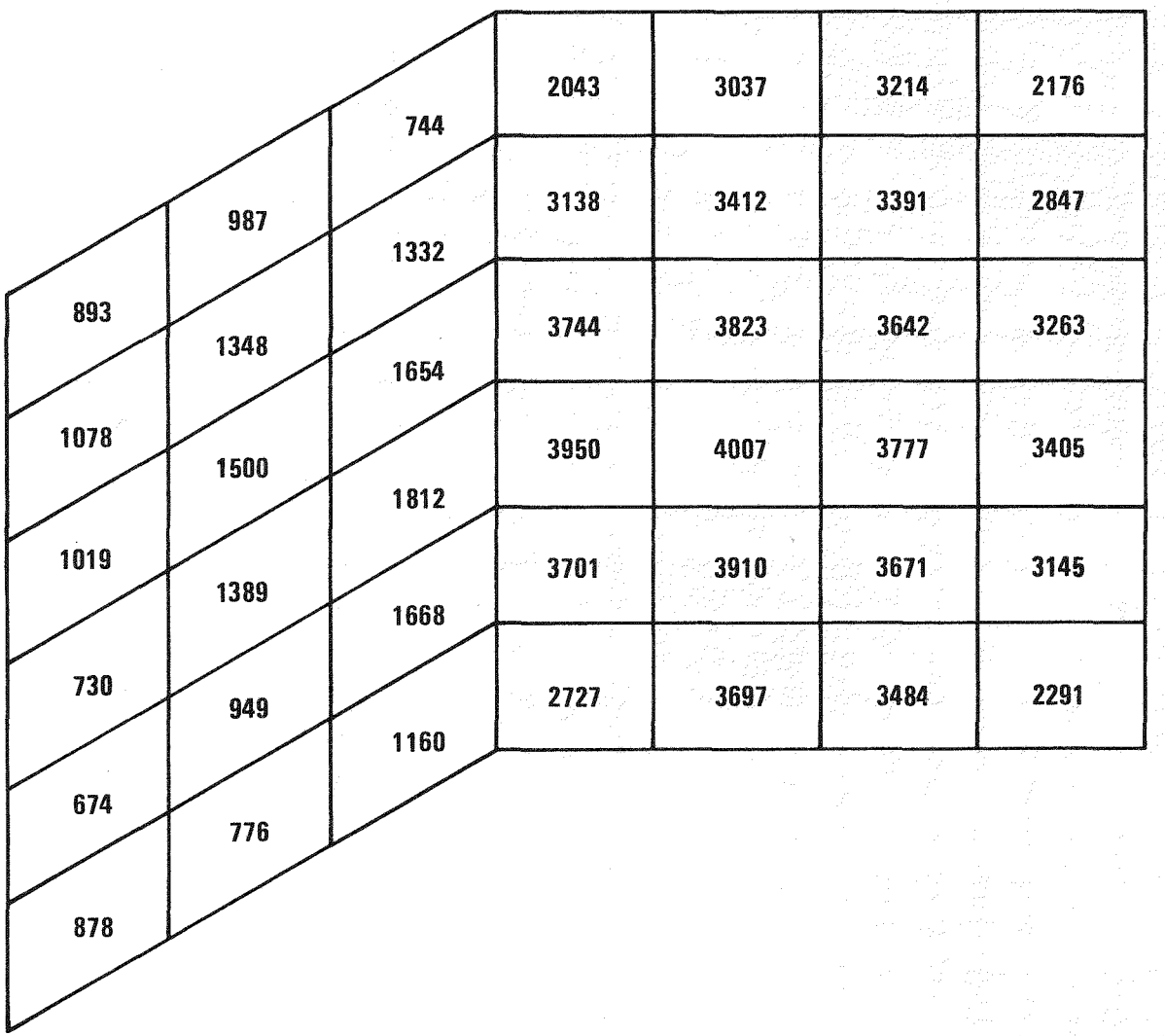

Figure A-19. Average Shear Stress in Box Structure for 6 Inch Panels

in Figures A-20 and A-21. The results show a reduction in the shear panel stresses. Figure A-22 presents the shear stress magnitudes for a 2 inch shear panel. This reduction was expected since the conical LSS stiffness is provided by hoop tension members rather than by shear panels.

In addition to stresses from the mechanical loads, thermal stresses were also investigated for this study. A best fit interpolation was applied to the defined temperatures to obtain all of the temperatures required in the finite element model. The results indicate that the thermal stresses are low except on the cone near the box structure. As shown in Figure A-23, a thermal discontinuity exists in this region where the top of the cone is significantly hotter than the bottom of the box structure. The cone will, then, be restrained from expanding by the box. Stress on the order of 30,000 psi can be expected. While this is not sufficiently high to violate the primary plus secondary stress requirements of ASME Section III, it does indicate the need for detailed thermal and structural analysis in this region.

The results of the analysis demonstrate that the design is acceptable with the modification to the outer box structure. The results also indicate the need for detailed thermal evaluation near the outer box structure so that a complete structural evaluation can be performed.

A.3.2.3 UPPER VESSEL SHELL

The upper vessel shell extends from the lower support structure to the bottom of the deck. The thickness of the shell varies from 2 inches just above the lower support structure to 3 inches at the deck due to the seismic considerations as described in Section A.2.1. The temperature of the upper shell varies from 800^{o}F above the LSS to 150^{o}F at the deck.

During normal operating conditions, the loads applied to the upper shell consist of the dead weight of the reactor vessel and vessel internals, the sodium contained within the vessel, and the steady state temperature

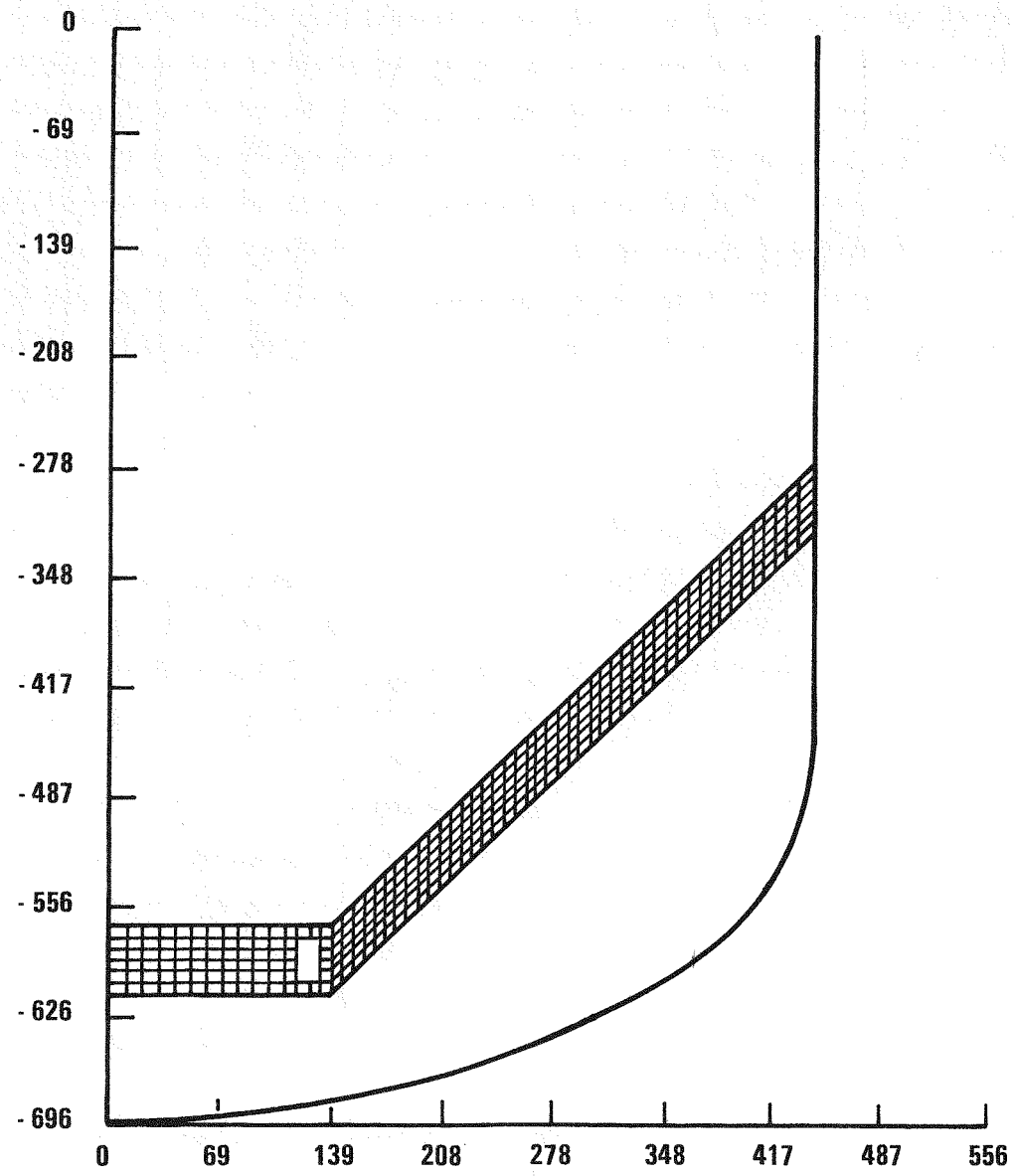

Figure A-20. Finite Element Model of Conical Lower Support Structure

0665-173

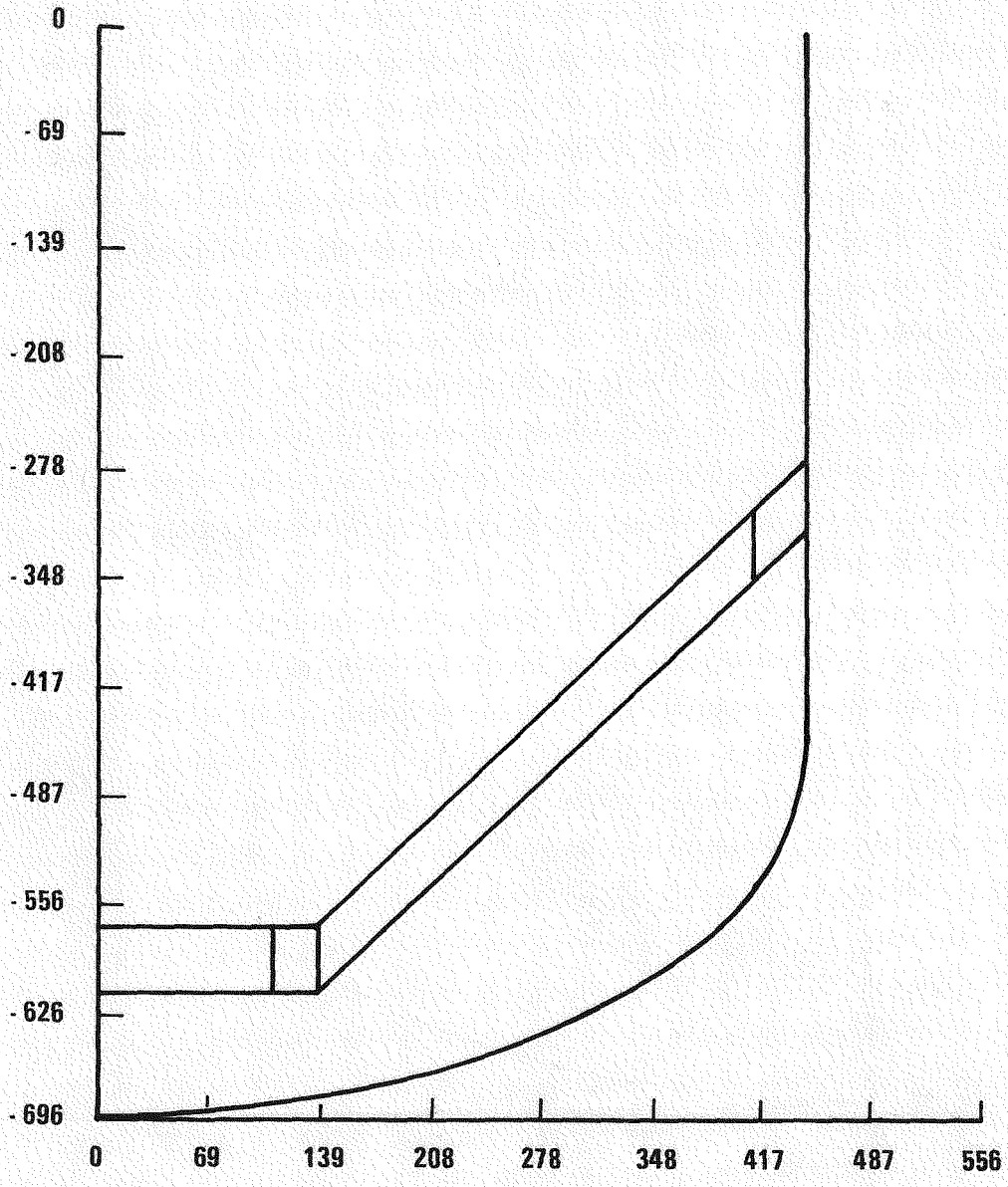

Figure A-21. Axisymmetric Portion of Conical Lower Support Structure Model

0665-172

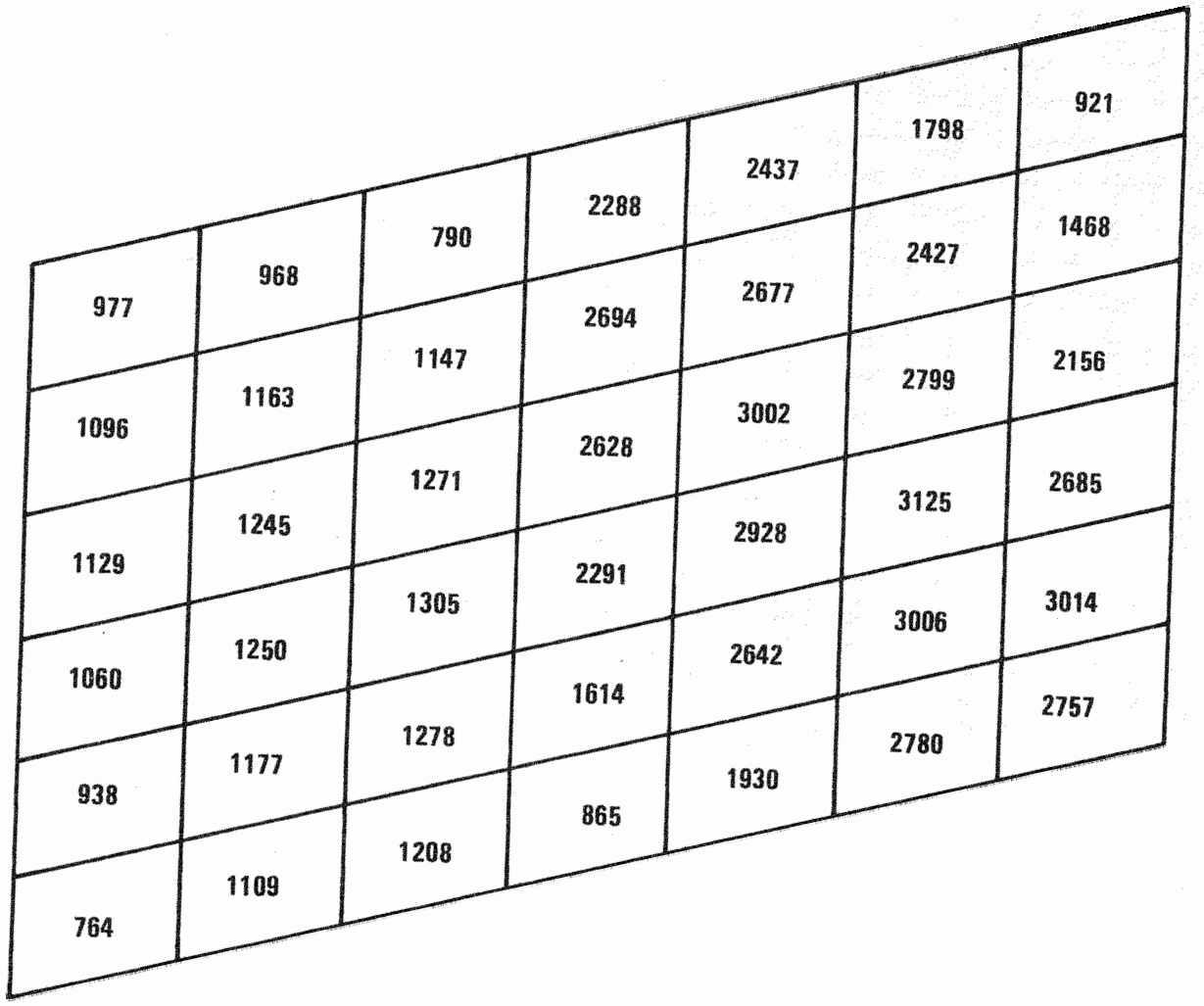

Figure A-22. Average Shear Stress in Conical Box Structure

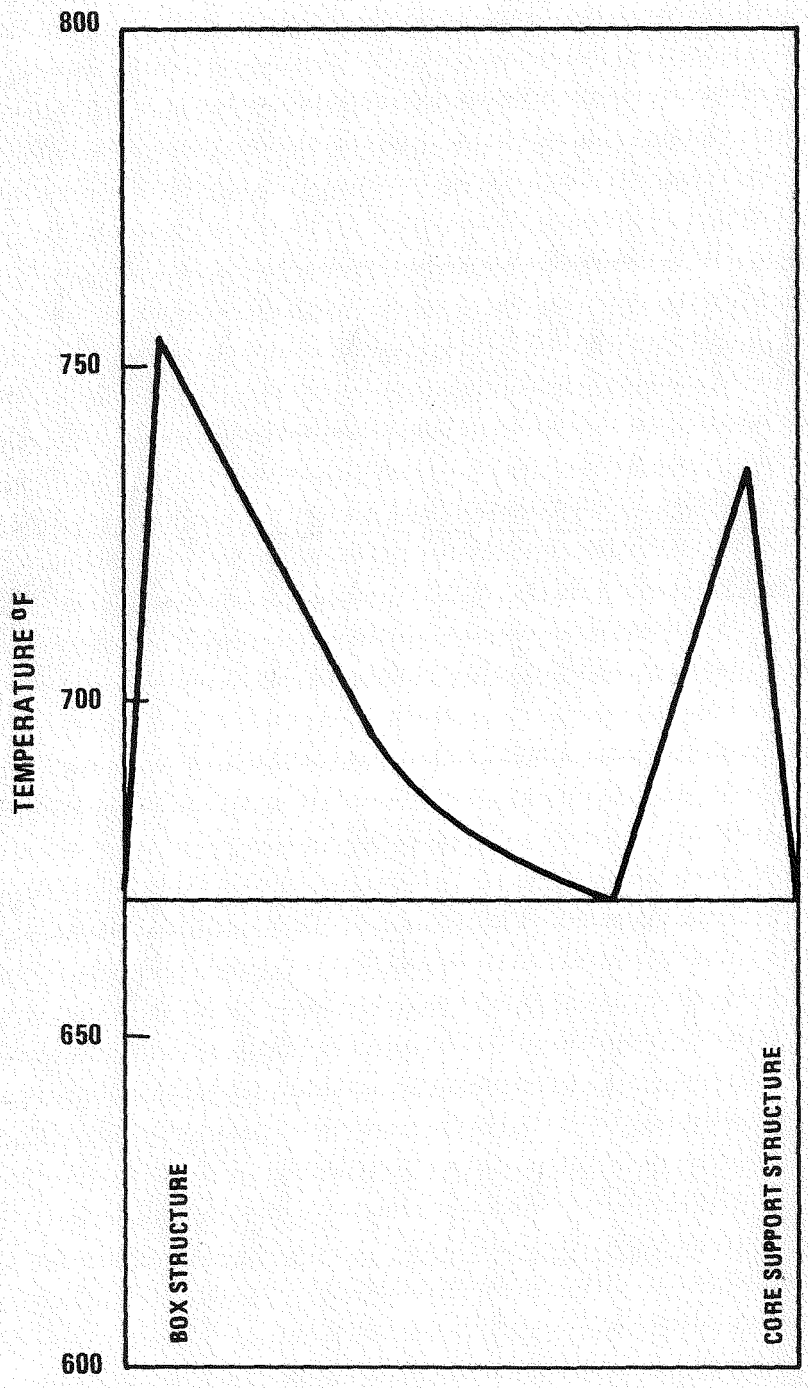

Figure A-23. Temperature Distribution Along Lower Support Structure

0665-188

distribution. During abnormal operations, the seismic loads due to the horizontal and vertical earthquake would be superimposed upon the normal operation loads. Each of these loading conditions is now described.

The mechanical loads introduce longitudinal and circumferential stresses in the shell due to the dead weight of the system and the sodium pressure inside the shell. The estimated weight supported by the upper shell is 18.85×10^6 lb (9425 tons). This dead weight introduces a stress of approximately 2500 psi in the axial direction in the shell. The hoop stress due to the sodium pressure varies along the length of the shell as the hydraulic head of the sodium decreases from bottom to top. The stresses introduced by the pressure load are small due to the small pressure. Conservatively estimating the pressure in the vessel at 10 psi on the upper shell, the stress is

$$\sigma_{HOOP} = \frac{PR}{t} = \frac{10 \times 450}{2.5} = 1800 \text{ psi}$$

The largest stress in the upper shell is the bending stress due to the deflection of the deck under dead weight conditions. Because of the thickness of the deck, in-plane rotations of the vertical members of the deck cause the bottom plate to move in the radial outward direction, as shown in Figure A-24. The vessel must then be pulled out, generating hoop tensile stresses at the top of the upper shell, and rotated back, generating "negative" bending stresses. Figure A-25 shows the longitudinal stresses in the shell and Figure A-26 shows the membrane hoop stresses.

The temperature distribution in the vessel and in the deck also introduce stresses in the upper vessel shell. The preliminary temperature distribution along the shell shows that it decreases from $670^{\circ}F$ to $68^{\circ}F$ and then increases to match the deck temperature of $138^{\circ}F$. Also, the temperature distribution in the deck tends to increase the curvature of the deck and the amount of bending required for continuity between the vessel and the deck. The combined thermal effect stresses are shown in Figure A-27

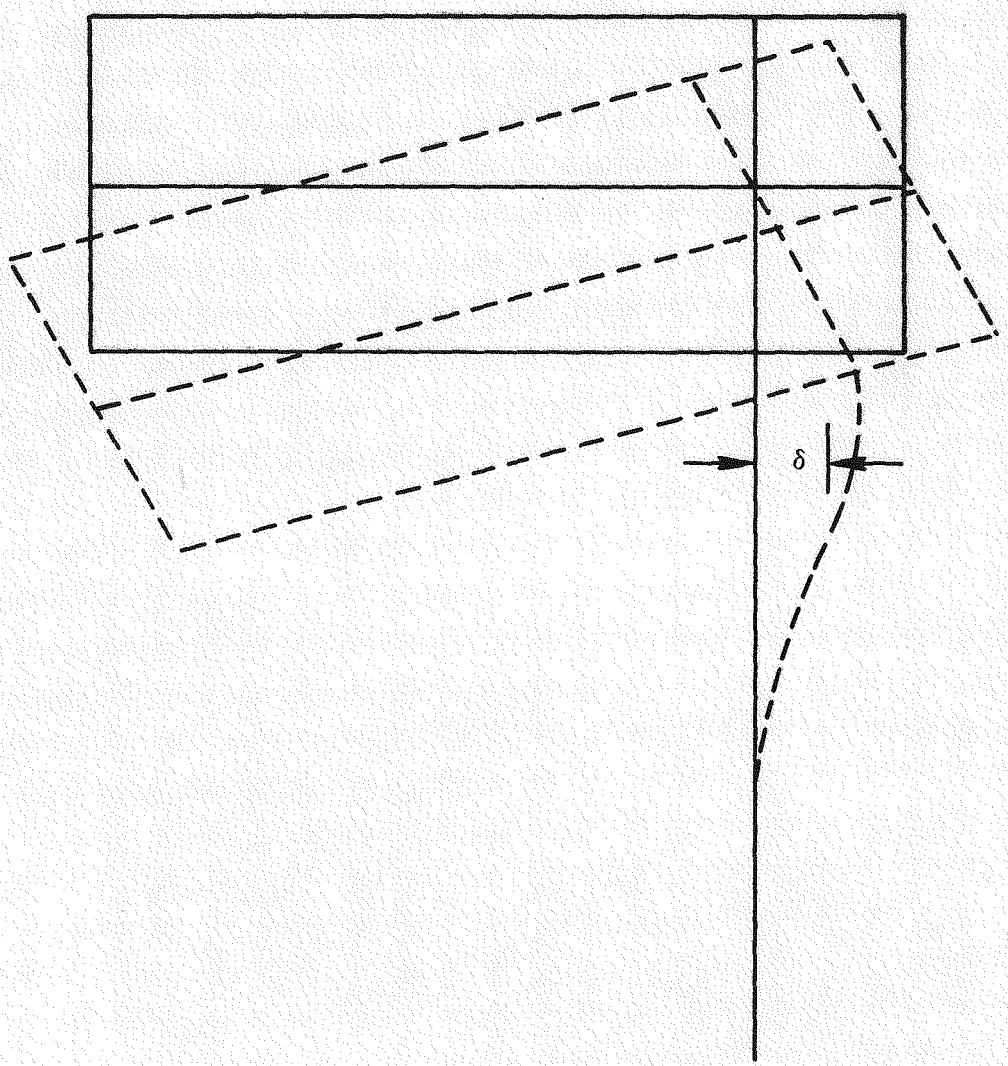

Figure A-24. Interaction of Vessel and Deck Under Dead Weight Loading

0665-189

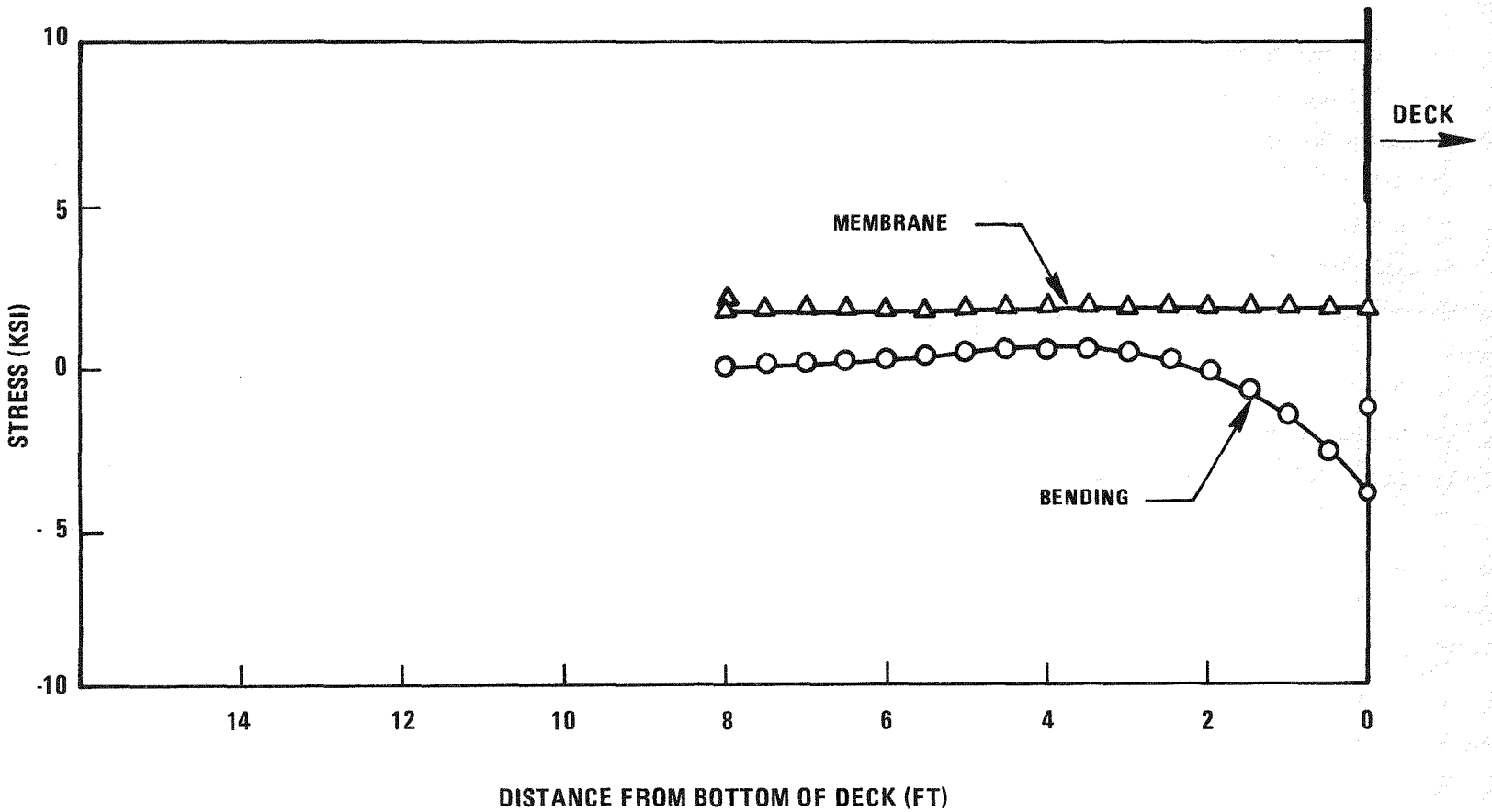

Figure A-25. Mechanical Longitudinal Stresses in Vessel Upper Shell

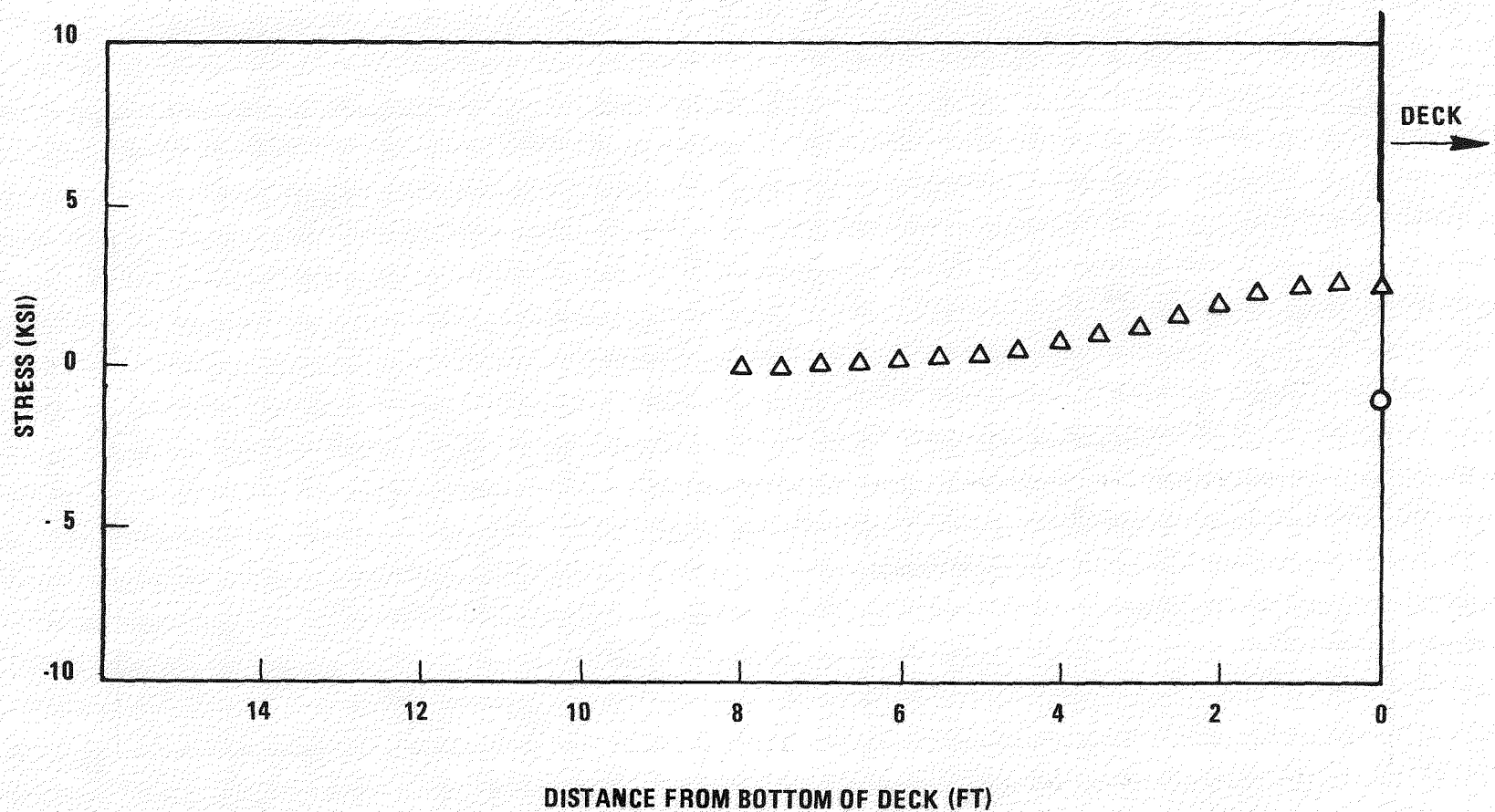

Figure A-26. Mechanical Hoop Stresses in Vessel Upper Shell

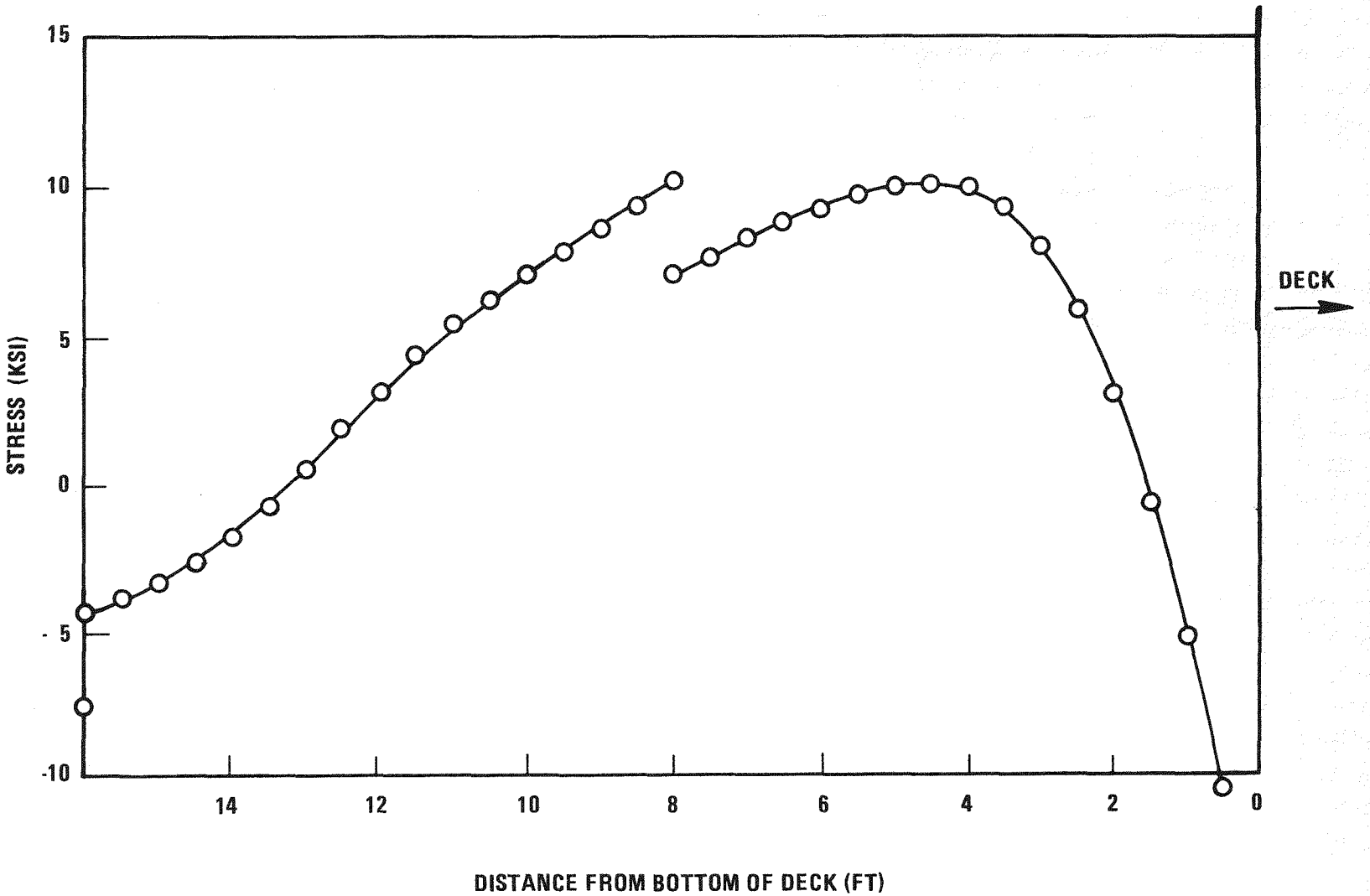

Figure A-27. Steady State Longitudinal Thermal Bending Stress in Vessel Upper Shell

and A-28 for the longitudinal and hoop stresses respectively. The discontinuity in stress at -8 feet is due to the change in thickness from 3.0 inches to 2.5 inches at that elevation.

A later revision of the temperature profile in the vessel is presented in Figure A-29. This represents a change in design from an active cooling system to a passive cooling system and is the current reference configuration. The stress distribution corresponding to this profile is shown in Figure A-30. The bending stresses change sign but the magnitude has remained approximately the same. The change in sign of the bending stress from the preliminary temperature distribution is because the upper shell previously became cooler than the deck whereas now the shell is always at least as hot as the deck.

From the above discussion it is obvious that the critical stress region occurs at the junction of the upper shell and the deck. Also, from Section A.3.1, the maximum seismic stresses occur at this location. But the seismic results of Section A.3.1 do not provide a complete picture of the stresses at the top of the vessel as deflections of the deck are not included. Since the bending stresses in the vessel are induced by the membrane loads in the vessel skirt, the total seismic effect can be found by ratioing the dead weight stresses to the seismic stresses to obtain amplification factors. The stresses on the tensile side are:

$$\sigma_{DW} = 2250 \text{ psi}$$

$$\sigma_{OBE} = 7500^2 + 2250^2 = 7830 \text{ psi}$$

$$\sigma_{SSE} = 12900^2 - 2250^2 + 4500^2 = 13475 \text{ psi}$$

and the amplification factors are

$$AMP_{OBE} = \frac{7830}{2250} = 3.5$$

$$AMP_{SSE} = \frac{13475}{2250} = 6.0$$

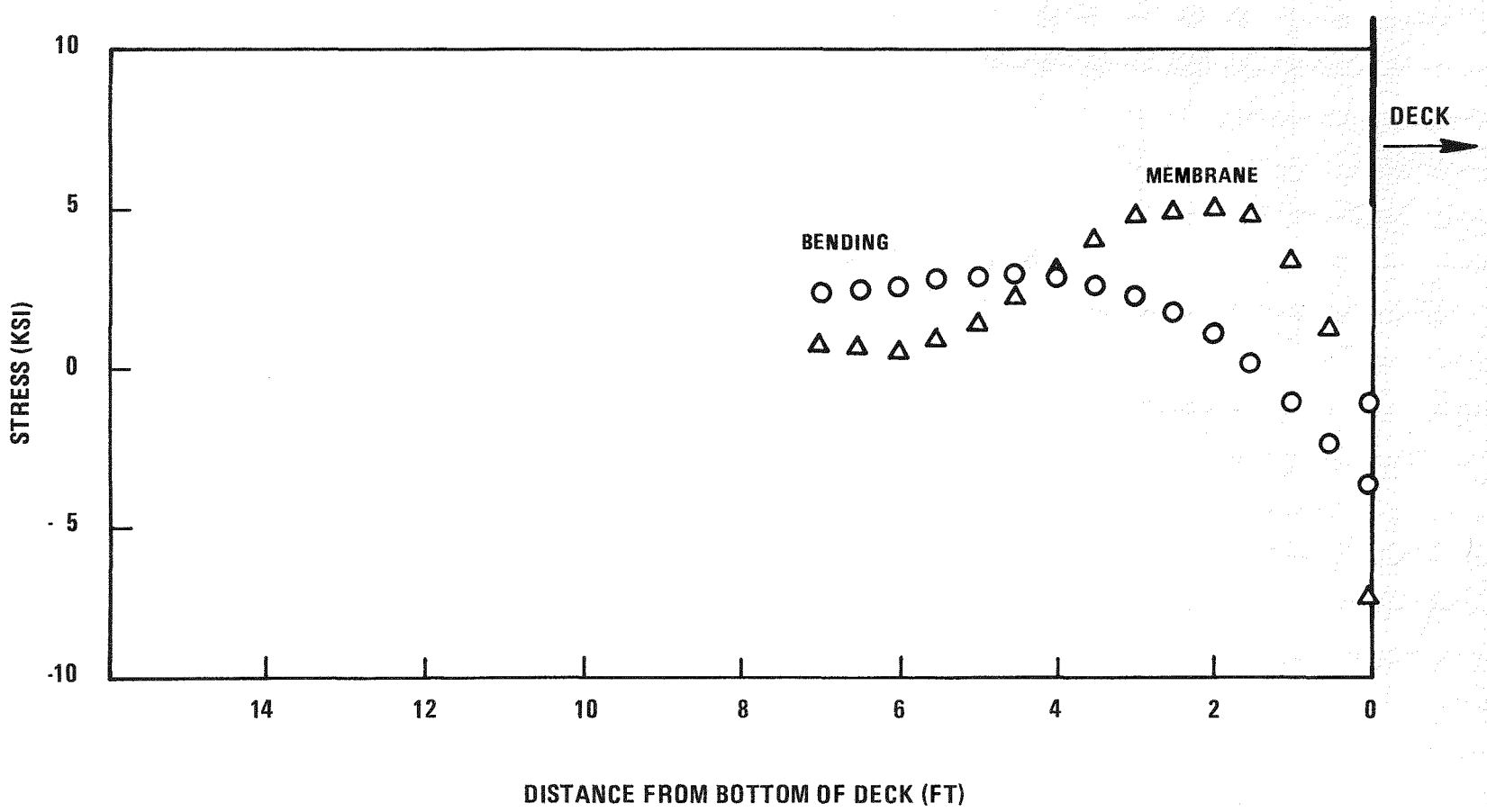

Figure A-28. Steady State Hoop Thermal Stresses in Vessel Upper Shell

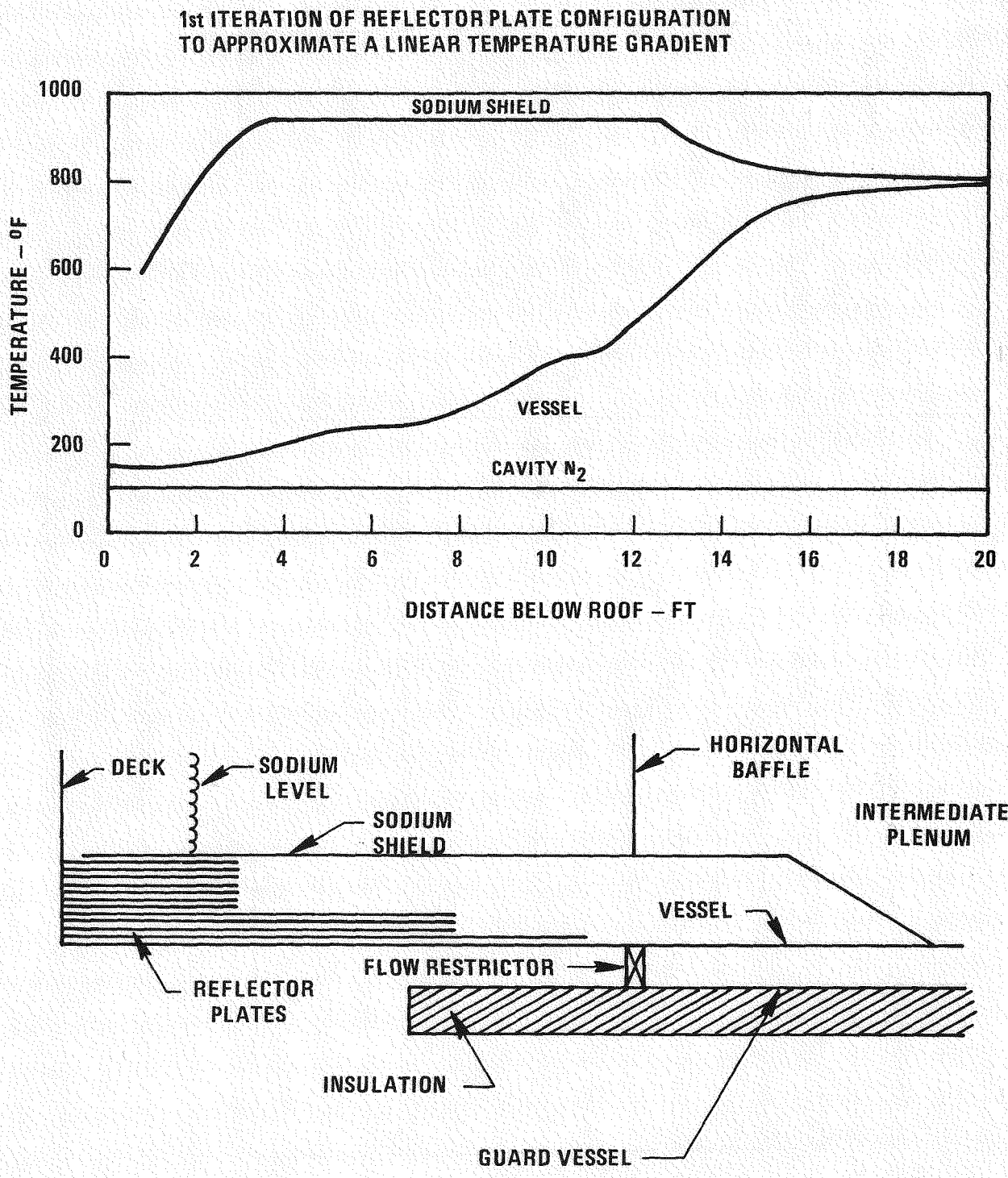

Figure A-29. Temperature Distribution in Top of Vessel

0665-167

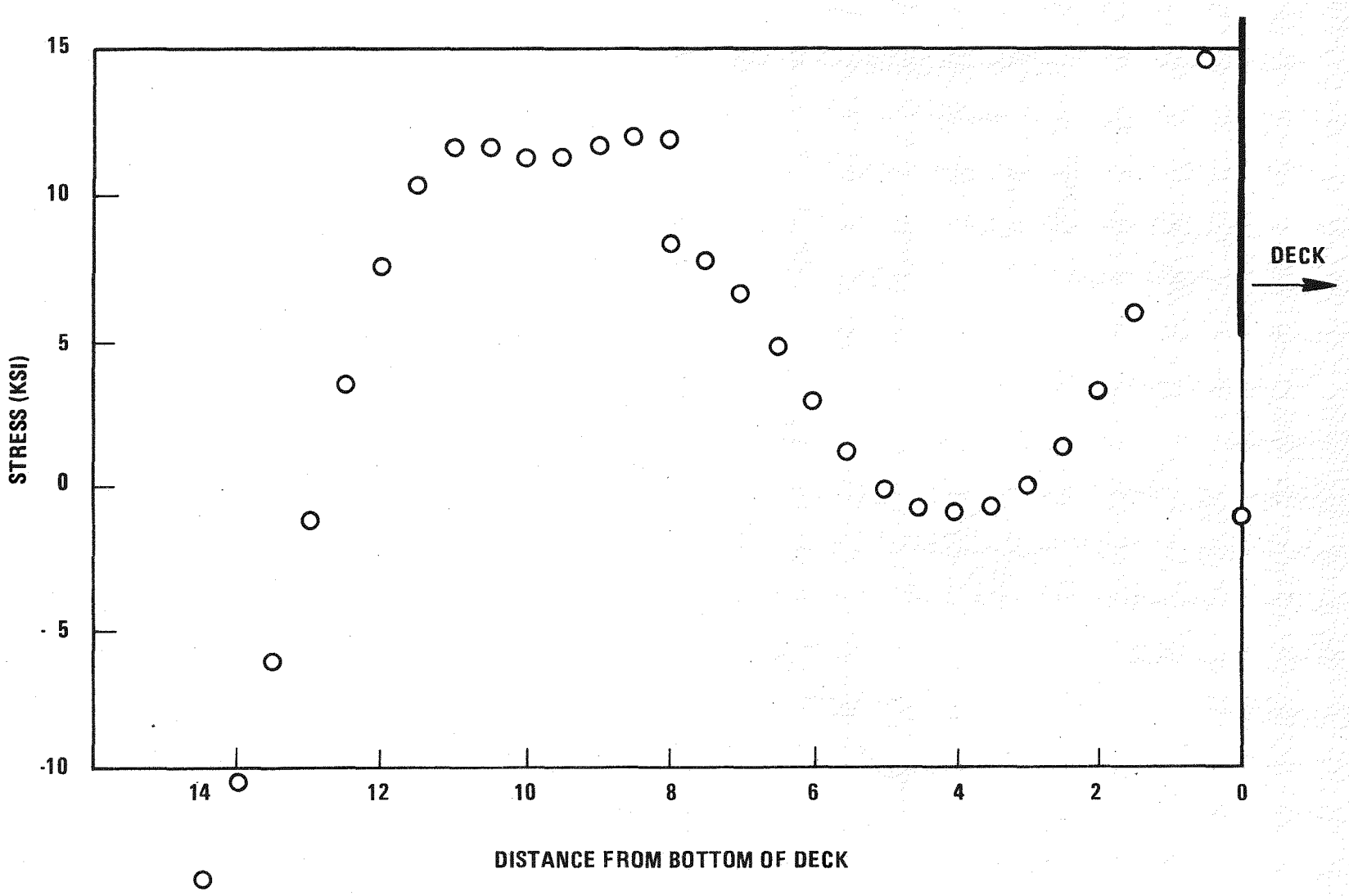

Figure A-30. Longitudinal Thermal Bending Stress in Vessel Upper Shell for Revised Gradient

The mechanical stresses at the top of the vessel are

$$\sigma_{AXIAL} = 2250 \pm 5860 \text{ psi}$$

$$\sigma_{HOOP} = 2430 \text{ psi}$$

and the thermal stresses are

$$\sigma_{AXIAL} = \pm 14300 \text{ psi}$$

$$\sigma_{HOOP} = -7450 \text{ psi}$$

The allowable stress intensity at the top of the vessel, Sm, for 304 SS at $150^{O}F$ is 20,000 psi.

For normal operating conditions, the primary membrane stresses are

$$\sigma_{L} = 2250 \text{ psi}$$

$$\sigma_{H} = 2430 \text{ psi}$$

$$\sigma_{R} = 0$$

Then $P_m = 2430 - 0 = 2430$ psi. That is less than the allowable stress intensity of 20,000 psi. The primary plus secondary stresses are

$$\sigma_{L} = 2250 + 5860 + 14300 = 22410 \text{ psi}$$

$$\sigma_{H} = 2430$$

$$\sigma_{R} = 0$$

And the $(P_L + P_B + Q)_R = 22410$ psi. That is less than the allowable stress intensity of $3\ S_m = 60000$ psi.

For upset conditions, that include the OBE, the primary membrane stresses are

$$\sigma_L = 2250 + 3.5 \times 2250 = 10125 \text{ psi}$$

$$\sigma_H = 2430 + 3.5 \times 2430 = 10935 \text{ psi}$$

$$\sigma_R = 0$$

Then $P_m = 10935 - 0 = 10935$ psi. That is less than the allowable stress intensity of 20000 psi. For the primary plus secondary stresses, the range of stress intensity must be considered due to the general bending of the vessel. On the tensile side, the stresses are

$$\sigma_L = 2250 + 5860 + 3.5 \times (2250+5860) + 14300$$

$$= 50795 \text{ psi}$$

$$\sigma_H = 2430 + 3.5 \times 2430 = 10935$$

$$\sigma_R = 0$$

and $(P_L + P_B + Q) = 50795$ psi.

On the compressive side, the stresses are

$$\sigma_L = 2250 + 5860 - 3.5 \times (2250+5860) + 14300$$

$$= - 5975 \text{ psi}$$

$$\sigma_H = 2430 - 3.5 \times 2430 = - 6075 \text{ psi}$$

$$\sigma_R = 0$$

and $(P_L + P_B + Q) = -5975$ psi. The range of the primary plus secondary stress is, then,

$$(P_L + P_B + Q)_R = 50795 + 5975 = 56770 \text{ psi.}$$

That is less than the allowable stress of $3\ S_m = 60000$ psi.

For the emergency condition, that includes the SSE, the primary membrane stresses are

$$\sigma_L = 2250 + 6 \times 2250 = 15750 \text{ psi}$$

$$\sigma_H = 2430 + 6 \times 2430 = 17010 \text{ psi}$$

$$\sigma_R = 0$$

Then $P_m = 17010$ psi. That is less than the allowable membrane stress intensity of $1.2\ S_m = 24000$ psi. There is no requirement to satisfy the secondary stresses for emergency conditions.

The results of this analysis satisfy the requirements of Reference 7 in a general sense without a detailed evaluation. It is concluded, therefore that the current design for the vessel upper shell is acceptable.

A.4 DECK

Evaluation of the deck during the current phase of the LPR study has been limited to a comparative analysis of various methods of system support. The only change in the deck from that reported in Reference 1 was to decrease the diameter to be consistent with the 75 foot vessel. The evaluation reported in Reference 1 is, therefore, conservative as applied to the current design.

Five different methods of supporting the reactor system were investigated and these are shown schematically in Figure A-31. For case 1, the system is supported by a 60 inch long cylindrical shell that extends down from the outermost diameter of the deck, and is built-in at the support ledge. Case 2 is similar to case 1 except that the deck is simply supported at the outermost diameter at an elevation corresponding to the bottom elevation of the deck. For case 5, the reactor system is supported at an elevation that corresponds to the neutral axis of the deck such that no relative horizontal motion would exist between the deck and the support ledge due to bending of the deck. In this case, the deck is supported by a 12 inch long cylinder that is built-in at the support ledge. Case 6 is similar to case 5 except that the deck is simply supported at the outermost diameter. Case 7 is similar to case 1 except that the supporting cylinder extends upward to the support ledge. The finite element models used for this analysis are shown in Figure A-32 through Figure A-36.

Table A-10 presents the results of the comparative study in the several areas of the structure defined in Figure A-37 for dead weight plus steady state temperature loading. The top number in each box is for the dead weight alone, the middle number is for the temperature alone, and the bottom numbers are for the combined loading. The results do not include any amplification due to horizontal or vertical seismic loading. A rough estimate can be obtained by using the amplification factors of Section A.3.2.

The results of the analysis show two highly stressed areas in the structure; the shear panel in the outer deck and the support cylinder for those cases where the cylinder is included. The shear stress in the shear panels is approximately proportional to the area in the panels. As the shear area decreases, as from case 1 to case 5, the shear stress increases. This effect can be mitigated by increasing the thickness of the panels but other considerations may limit the increase in size.

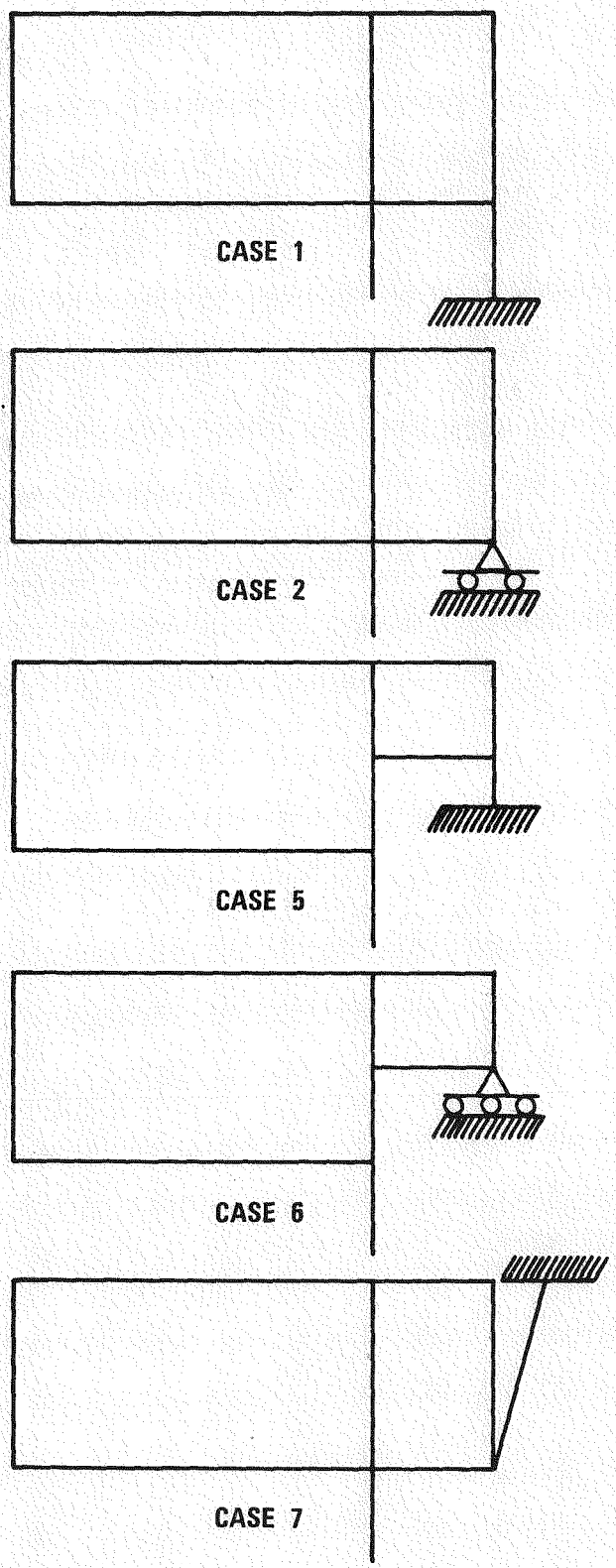

Figure A-31. Alternative Methods of Deck/System Support

0665-190

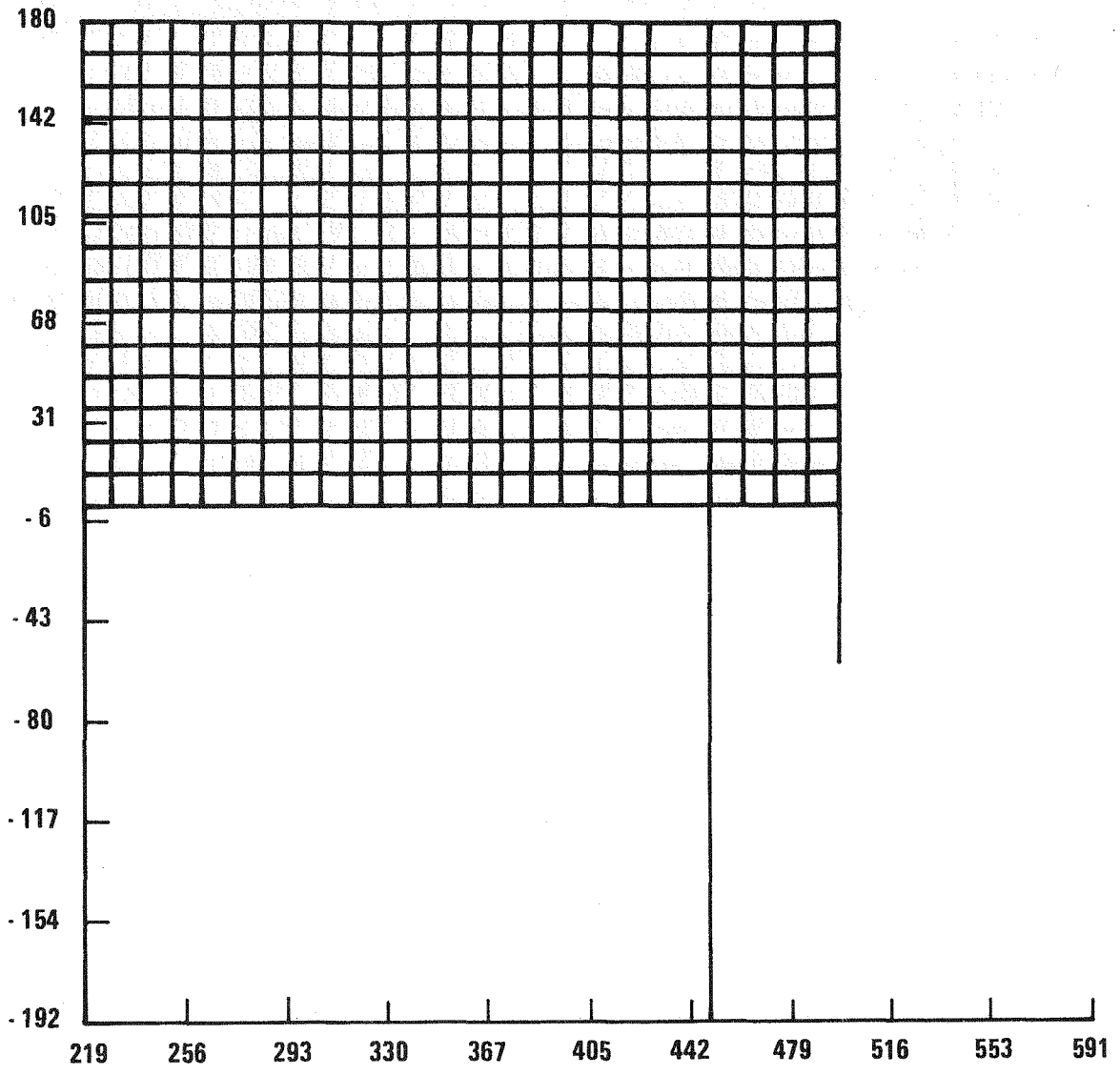

Figure A-32. Finite Element Model for System Support – Case 1

0665-165

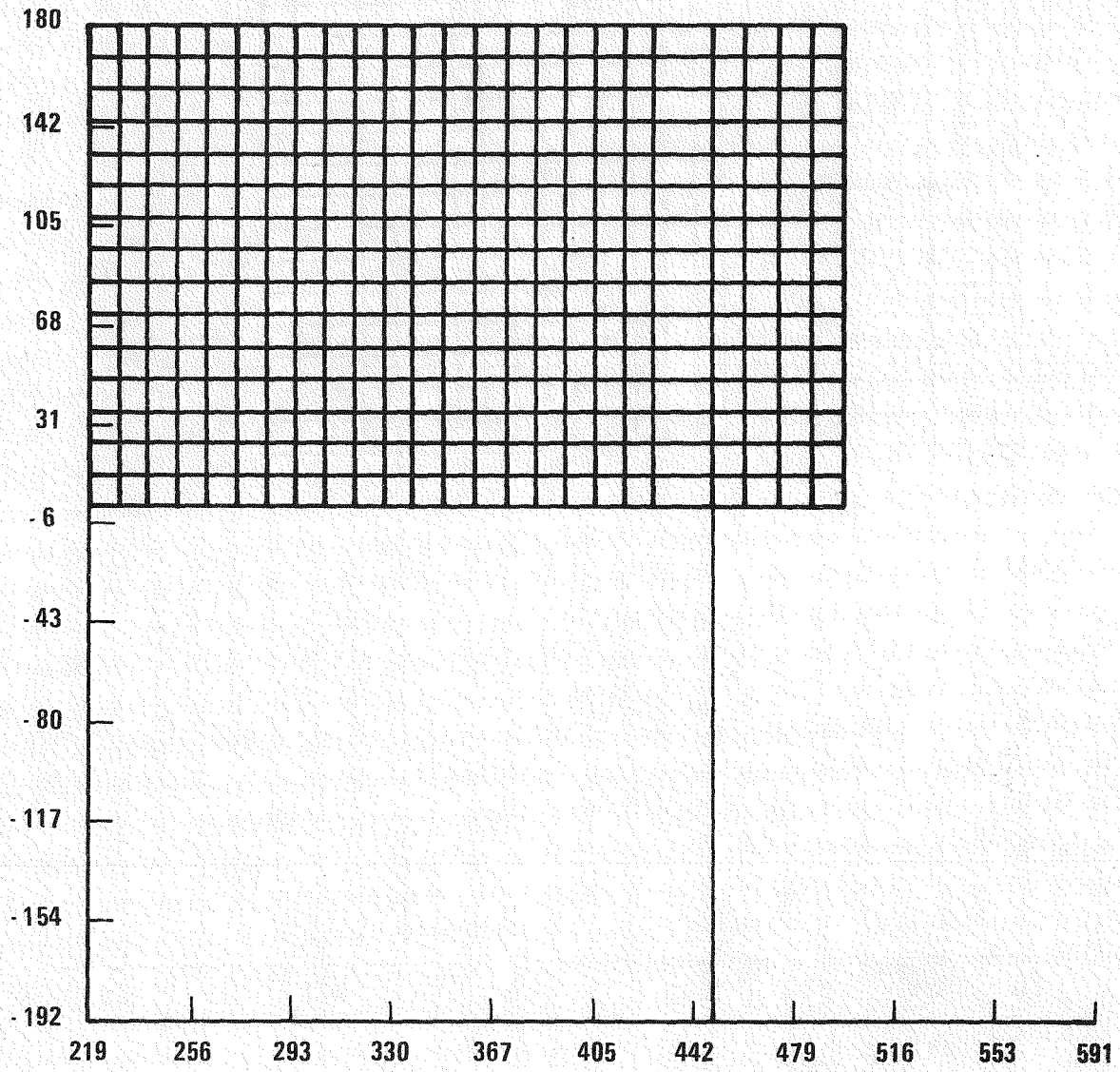

Figure A-33. Finite Element Model for System Support – Case 2

0665-164

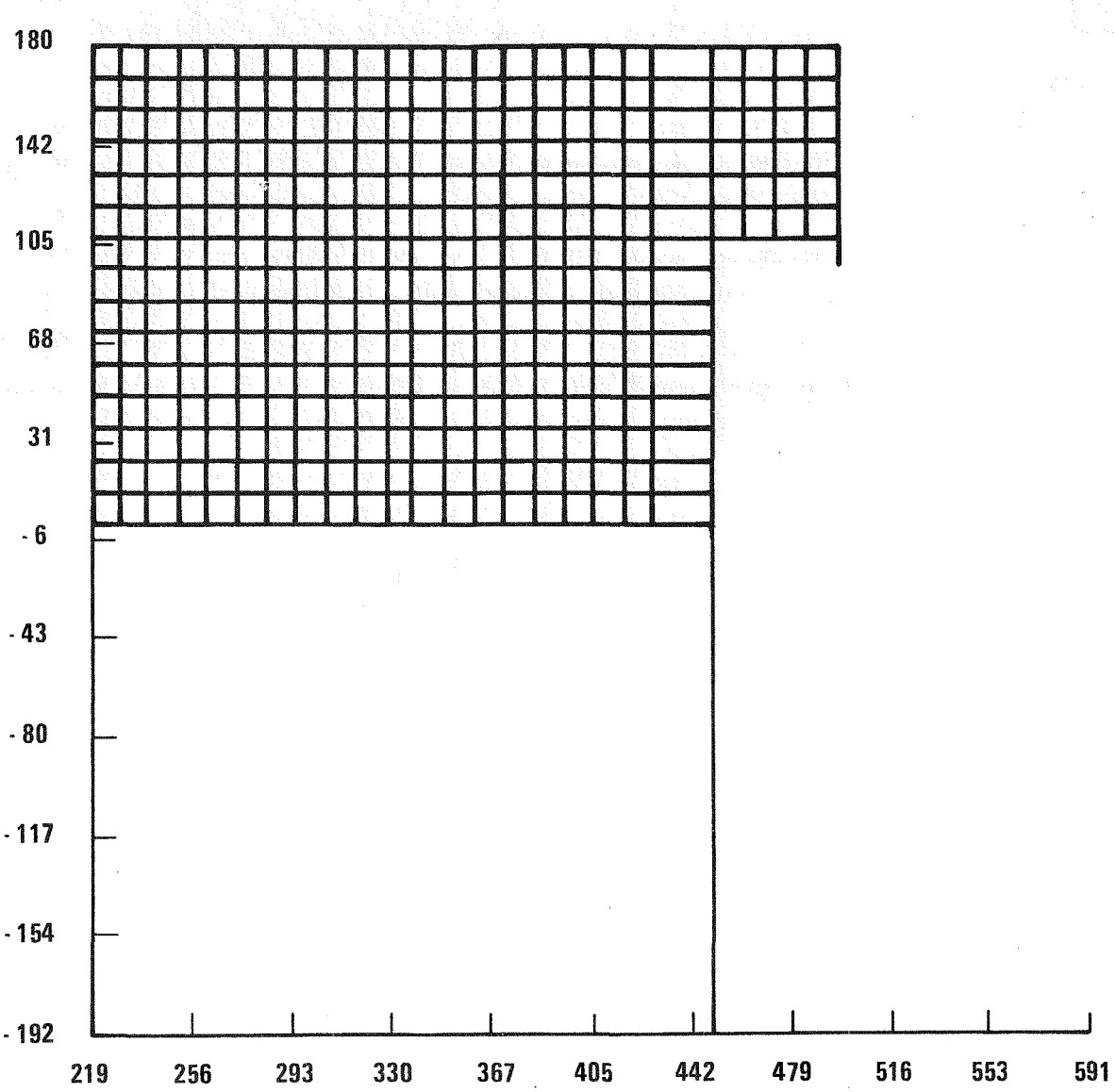

Figure A-34. Finite Element Model for System Support – Case 5

0665-163

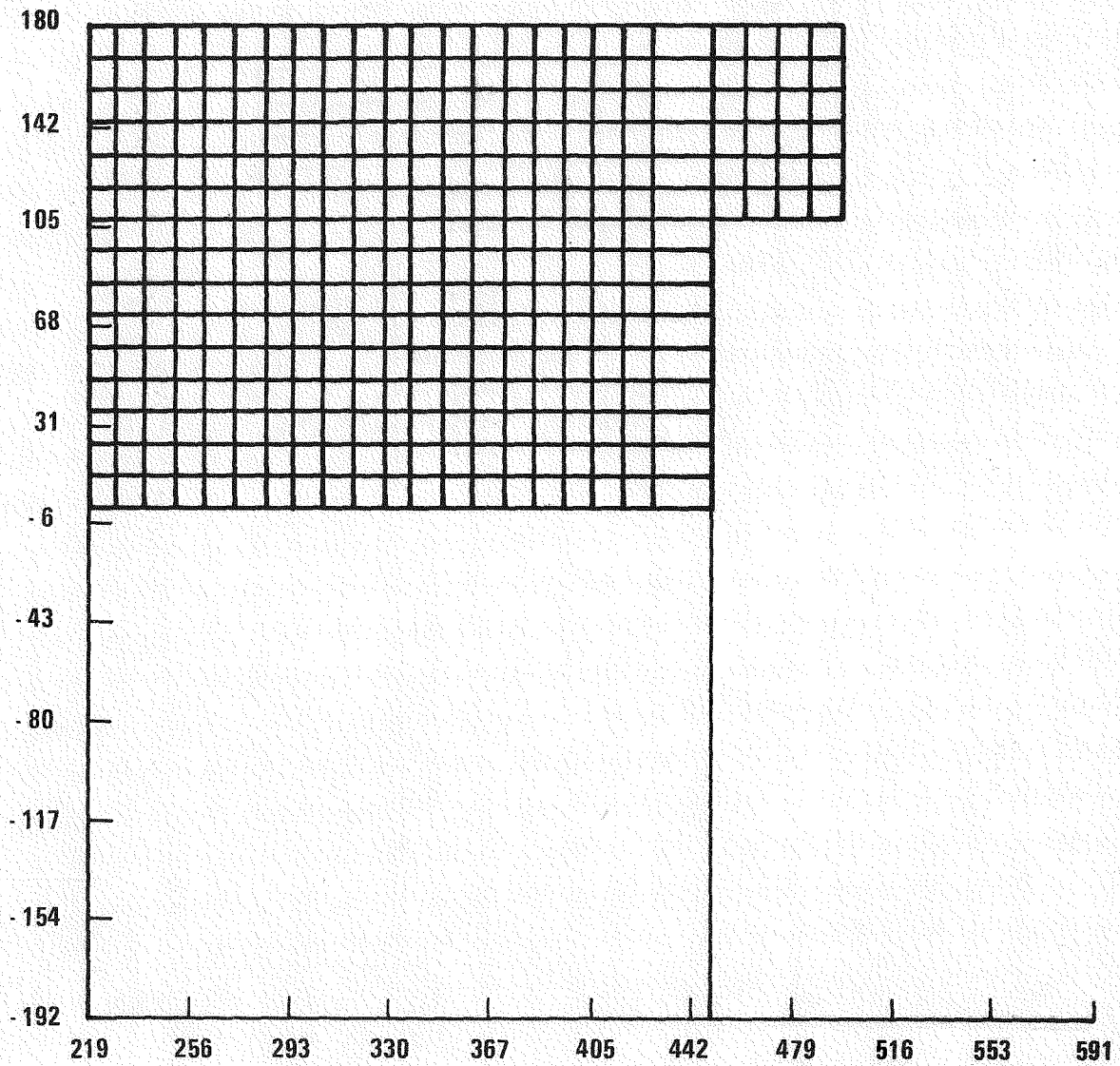

Figure A-35. Finite Element Model for System Support – Case 6

0665-162

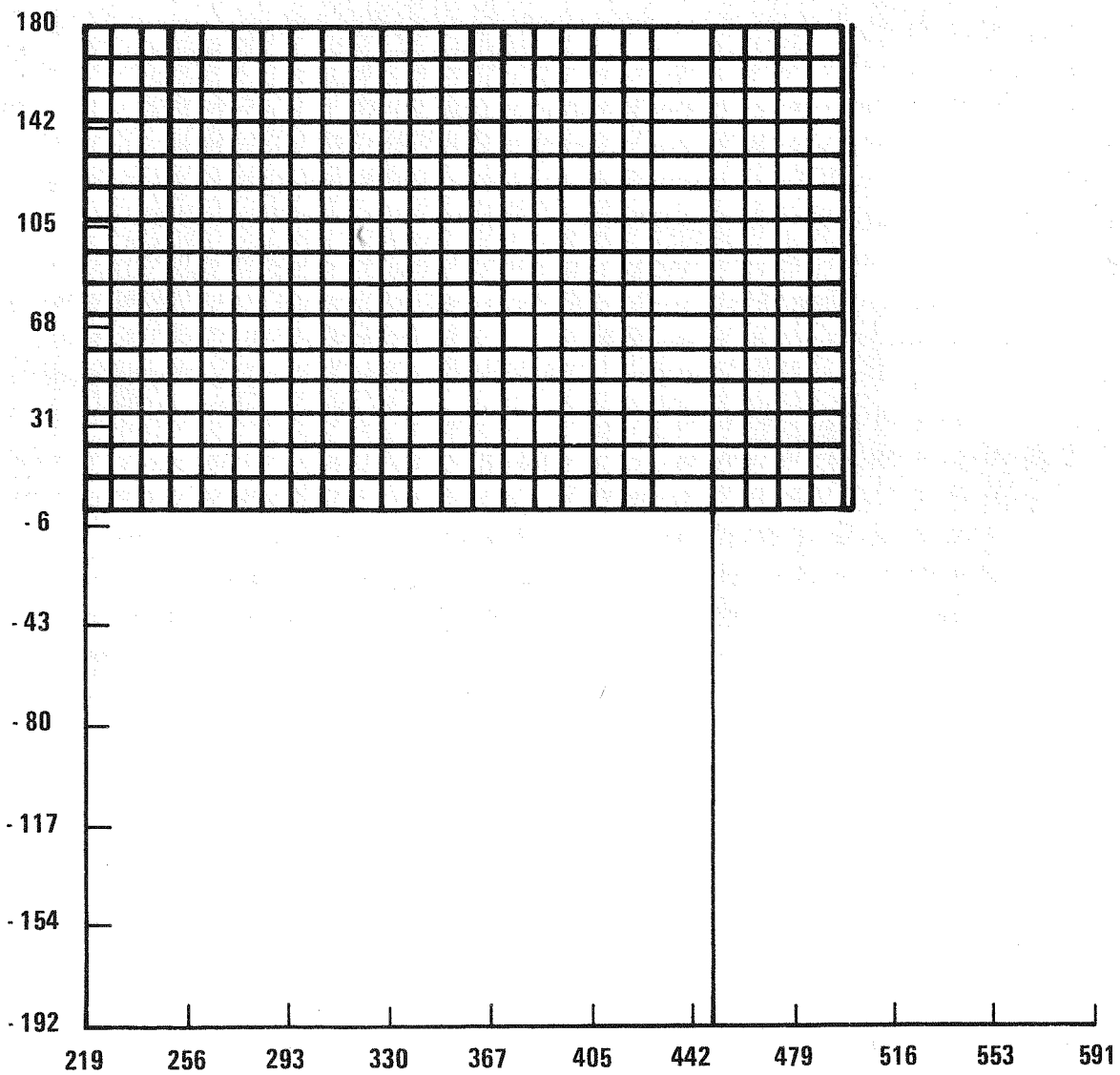

Figure A-36. Finite Element Model for System Support – Case 7

0665-161

TABLE A-10

		CASE 1	CASE 2	CASE 5	CASE 6	CASE 7
A	Vertical Deflection	.231 .103 .334	.229 .131 .360	.310 .129 .439	.340 .126 .466	.244 .220 .464
	Rotation	.051 .025 .077	.052 .027 .079	.071 .022 .093	.066 .024 .091	.052 .027 .078
	Hoop Stress	-6206 -1691 -7897	-6288 -1808 -8096	- 9397 - 892 -10290	-8546 -1263 -9809	-6263 -1743 -8006
B	Vertical Deflection	.053 .013 .066	.048 .038 .086	.113 .034 .147	.144 .030 .174	.065 .125 .191
	Horizontal Deflection	.028 .156 .184	.030 .158 .188	.021 .166 .187	.025 .165 .190	.029 .159 .188
	Stress	8108 15026 23100	8341 15237 23579	6403 15735 22102	6452 15705 22211	8153 15422 23540
C	Shear Stress	5820 4716 5967	5405 5260 6193	13915 634 13441	11714 158 11733	5527 4686 6056
D	Horizonal Deflection	.028 .176 .204	.030 .178 .208	.004 .086 .090	.056 .070 .125	.028 .180 .208
	Rotation	.023 .042 .065	.042 .081 .124	.020 .039 .059	.132 .021 .153	.050 .027 .078
	Stress	-7012 -8216 -15228		-17388 - 1254 -16511		4300 11555 12828
E	Stress	-6160 -11259 -17419		-14297 - 6624 - 7688		4371 1050 3322

Figure A-37. Critical Regions for Deck/System Support Evaluation

The stresses in the support cylinder are directly related to the length and thickness of the cylinder. As the thickness increases, the moment load required to bend the cylinder to conform to the deck rotation increases. And the wave length of the cylinder increases with thickness, such that the two ends of the cylinder may not be independent. For an 80 foot diameter cylinder that is 3.5 inches thick, the wave length of the cylinder is

$$\ell = \frac{\pi \cdot Rt}{1.2854} = 100 \text{ inches}$$

Thus, the application of a load at the top of the cylinder would have an effect on the stress state at the bottom of the cylinder.

As stated previously, the stress results in Table A-10 do not include the seismic effects. The complex nature of the interaction between the vessel and the support, when a support cylinder is involved, leads to the conclusion that an axisymmetric evaluation may not be appropriate. But if a factor of 3.5 is appropriate, as in Section A.3.2, then the primary membrane plus secondary bending stress in the support cylinder would be 39800 psi and 79500 psi for case 1 and case 5, respectively.

A.5 PLENUM SEPARATOR

The plenum separator refers to the cylindrical shell that extends upward from the lower support structure to within several inches of the deck. The function of the plenum separator is to contain the sodium in the hot pool to provide isolation from the cold pool or from other parts of the structure. In the early stage of the design, the plenum separator provided an annulus for bypass sodium flow between the hot pool and the vessel. Later the bypass flow was eliminated and the function of the plenum separator became that of a sodium shield.

The steady state operating loads consist of the dead weight, the sodium pressure and the steady-state temperature gradient. The stresses due to the mechanical loads are small and only the thermal stresses need be considered. For the plenum separator, the temperature gradient is shown in Figure A-29 (sodium shield) and the resulting stress distribution at the top of the plenum separator is shown in Figure A-38. These stresses are secondary in nature and the allowable stress intensity is $3S_m$ = 45,300 psi @ 800°F.

Another potential problem for the plenum separator is that of vibration in the shell modes. The axisymmetric shell finite element with non-axisymmetric loadings in Reference 3 can be used to describe the frequency and mode shapes for cylindrical shells. The evaluation for the plenum separator is described below.

The modal analysis for the clamped-free plenum separator shows that the fundamental frequency is 10.5 hz and occurs for one longitudinal half wave (m = 1) and eight circumferential waves (n = 8). The second mode frequency is 26.5 hz and occurs when m = 2 and n = 11. Figure A-39 shows graphically how the frequency in the plenum separator varies with respect to the number of circumferential waves. Also shown in Figure A-39 is the curve for a clamped - clamped shell whose dimensions are that of the plenum separator. The clamped - clamped shell has a frequency that is approximately 10% lower than the second mode of the plenum separator due to a slight variation in the mode shape of the plenum separator.

Since the fundamental frequency of the plenum separator is in the range where seismic excitation could occur, it is desirable to raise the frequency to some higher value. One method for raising the frequency is to attach a ring to the top of the shell. In theory, this will stiffen the top of the shell and change the fundamental mode of the separator to a higher harmonic. Several different sizes of rings were used and the results are shown in Figure A-40. It is seen that the effect of the larger rings is to shift the fundamental mode to a lower number of circumferential waves but

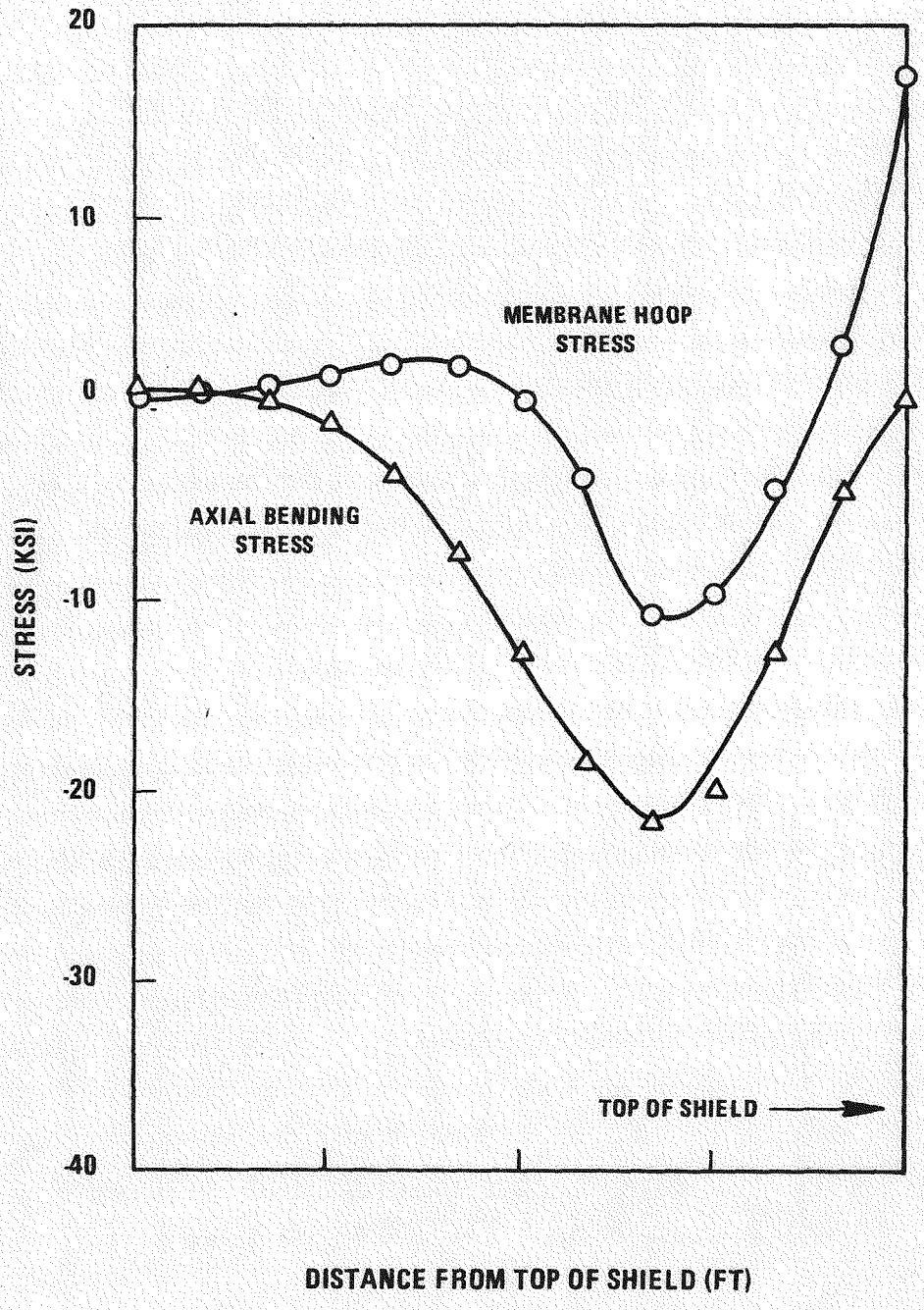

Figure A-38. Thermal Stresses in Sodium Shield

0665-160

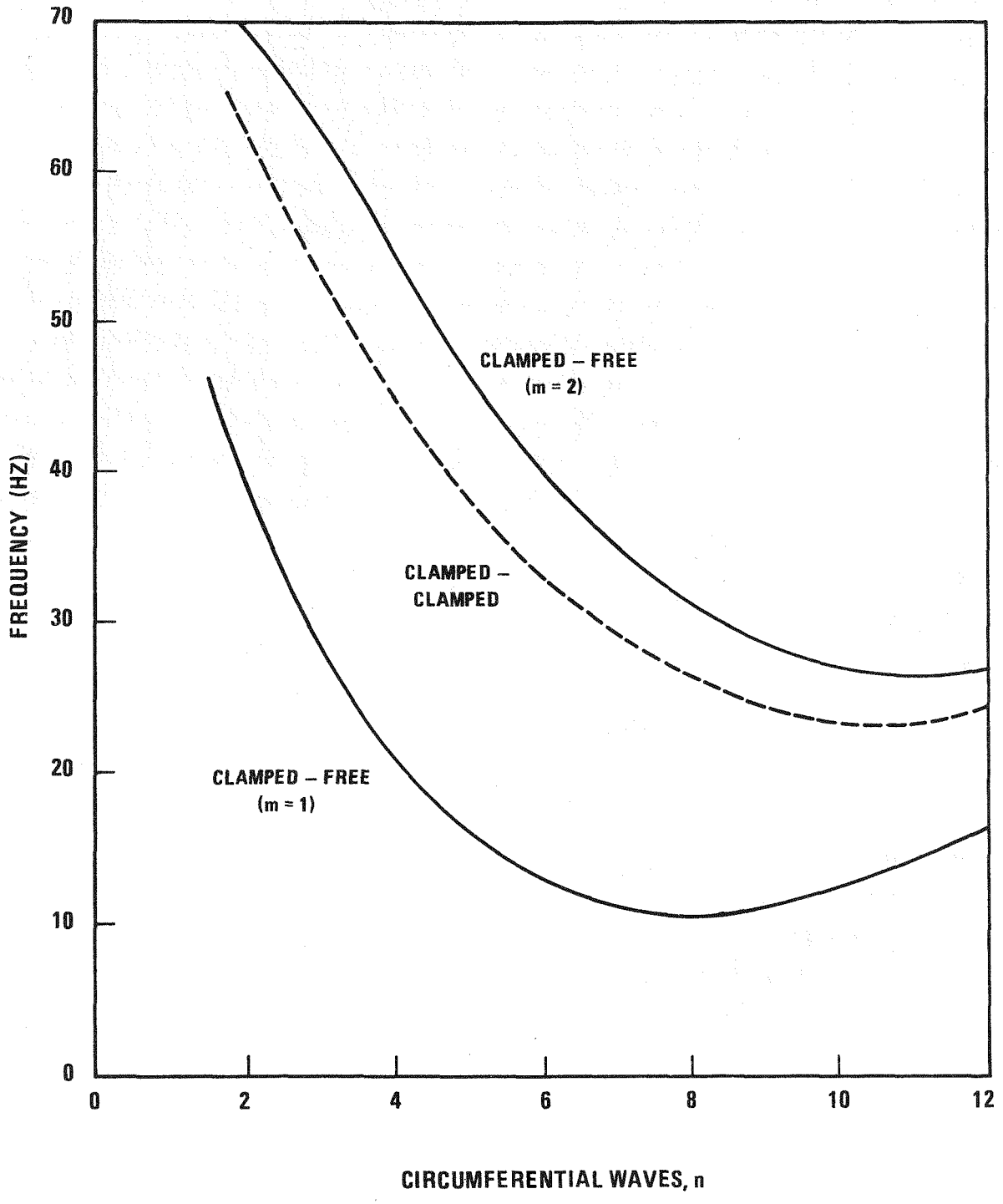

Figure A-39. Frequency Character of Plenum Separator

0665-159

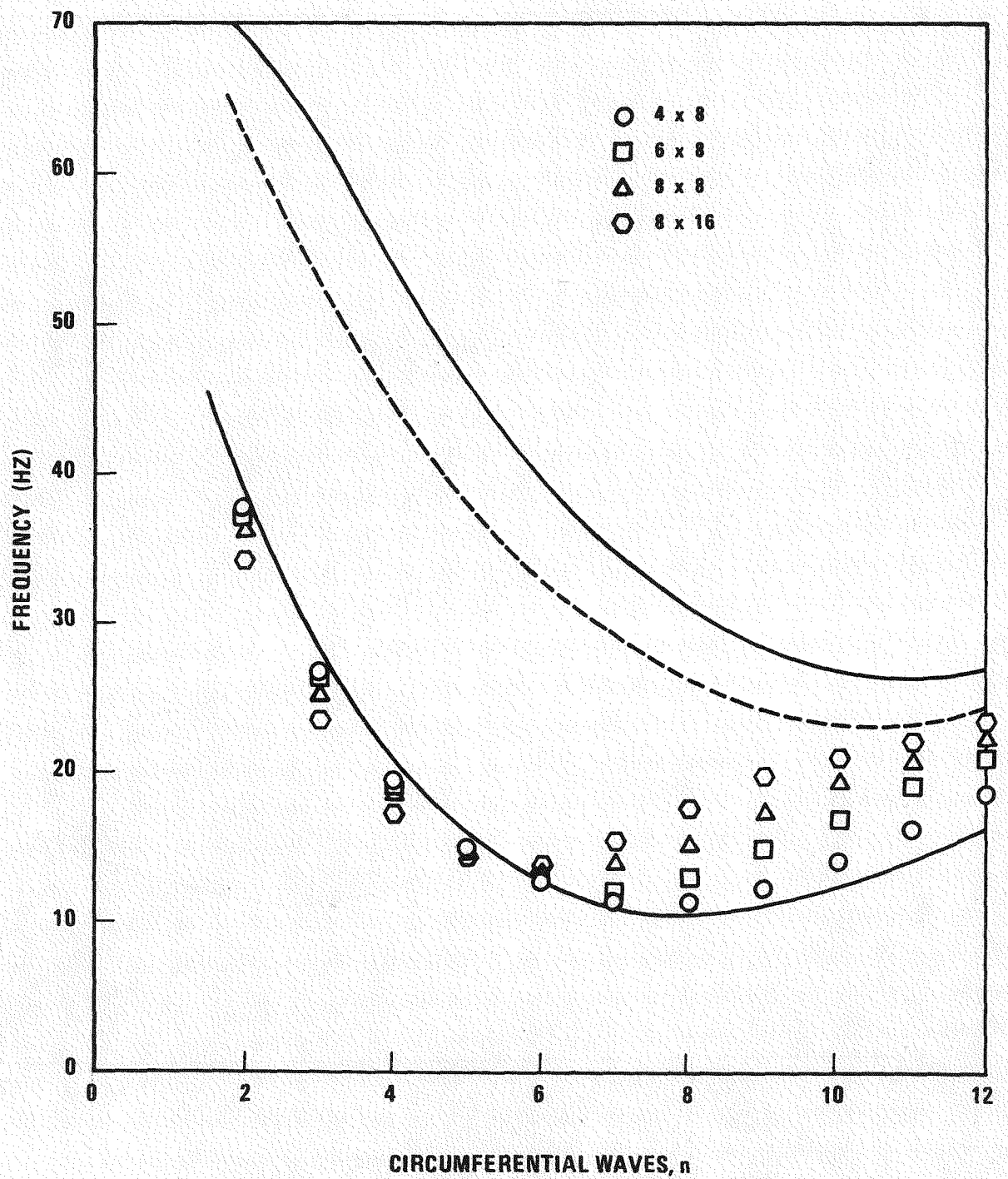

Figure A-40. Effect of Stiffening Top of Plenum Separator

0665-158

only for the high number of circumferential waves does the fundamental mode with the ring approach the second separator mode. For a small number of circumferential waves, the frequency decreases due to the added mass of the ring. The increase in the fundamental frequency is due to this shifting of the fundamental mode to a fewer number of circumferential waves rather than increasing the entire curve by an elastic boundary condition at the top.

From the above results, it would appear that it is desirable to have a ring to increase the frequency but it is equally undesirable to have the added mass of the ring. Figure A-41 shows the effect of the mass for the 8 x 16 ring. Without the mass of the ring included, the frequency over the entire range increases, but with the mass, the frequency decreases for a low number of waves but then increases later. In either case, the clamped - clamped shell is approached for a large number of circumferential waves. One method of obtaining the stiffness of a beam without the mass is to use a wide flange configuration. Figure A-42 shows the effect of using two configruations of wide-flange beam (with the mass of the beam included) on the frequency of the separator. The fundamental frequency is increased from 10.5 hz to 16 hz by use of the wide flange beam. From this case, it appears that the wide flange beam has more effect in the range of a few numbers of circumferential waves rather than for a large number.

The results of this analysis show that the fundamental frequency of the plenum separators can be raised by incorporating a stiffening ring at the top of the shell. No specific design is recommended until a response spectrum for the LPR is received. Final tuning of the separators will be done in conjunction with the design team.

A.6 UPPER INTERNALS STRUCTURE

To obtain a scoping analysis of the UIS for seismic conditions, a finite element model shown in Figure A-4 was used to determine UIS deflection, stress, and reaction loads. This model, described in detail in Section A.3.1, was developed primarily for vessel analysis but also allows

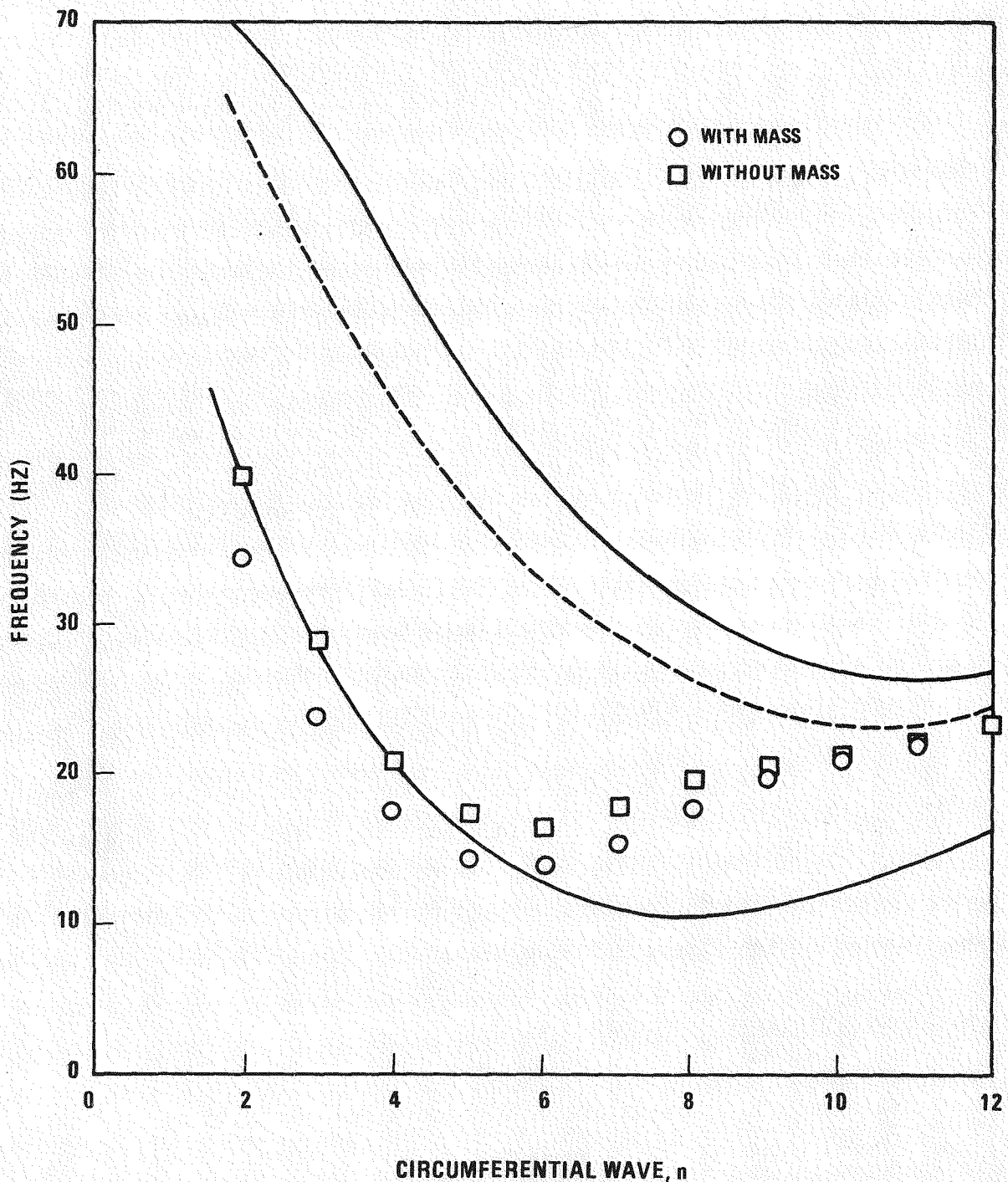

Figure A-41. Effect of Mass on 8 x 16 Stiffening Ring atop Plenum Separator

0665-157

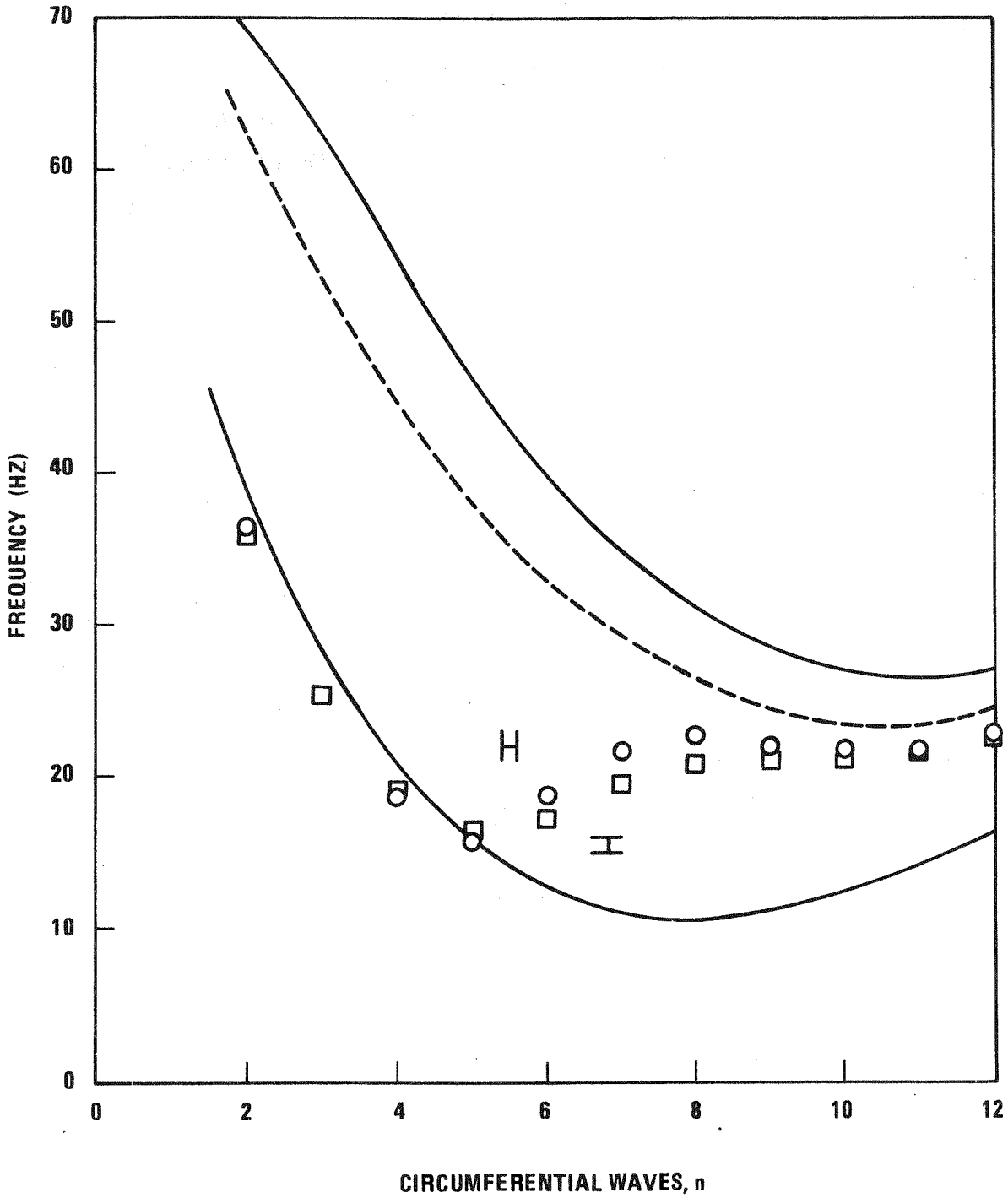

Figure A-42. Effect of Wide-Flanged Beam atop Plenum Separator

0665-156

determination of relative deflection between the bottom of the UIS and the top of the core barrel. Stress limits were determined for the UIS for an SSE event to preclude buckling at the top of the UIS. Stress values and limits were also determined for the bolts at the top of the UIS.

The results of the relative deflection analysis of the SSE show this deflection to be 1.32 inches with the present 1.0 inch UIS wall thickness. For 2-inch and 3-inch wall thicknesses, the value decreases to 1.05 and 0.99 inches respectively.

The results of the stress analysis for the outer cylinder of the UIS show SSE stresses to be most critical at an elevation 54 inches below the bottom of the deck at the top row of flow holes. The stress at this elevation is 16,350 psi as compared to a limit based on buckling considerations of 12,300 psi in the case of the 1-inch UIS wall thickness. For a 2-inch case, the predicted stress and allowable stress are respectively 7,860 and 13,800 and for a 3 inch case they are 5,470 and 14,500. The stresses at the top row of flow holes could be reduced by lowering the elevation of the holes and by having a lower number of holes in the top row. The minimum required thickness, based on SSE results, is 1.4 inches, with the flow holes being the limiting region for the present design. By minor redesign, the stress at the flow holes could be reduced and the minimum required thickness could be reduced to 1.2 inches with the limiting region being the upper end of the UIS. OBE analysis, not conducted during this preliminary study, would be expected to result in larger values for required thickness due to more conservative allowable stress levels.

The analysis for maximum bolt load and stress shows that with the use of 60 bolts, the stress levels for 1.5, 2.0, or 2.5 inch diameter bolts are respectively 64,000 psi, 36,000 psi, and 23,000 psi. Other numbers of bolts (from 10 to 80) are considered and it is clear that a satisfactory combination of bolt diameter and number of bolts can be selected to withstand the UIS overturning moment.

A.6.1 LOADS

The loading used for this study consisted of an acceleration response spectrum which was the same as that given in Section A.3.1. The SSE case was used for this scoping analysis in order to obtain upper limits on relative deflection. At the frequency of the upper internals vibration, 8.34 Hz with a 1-inch wall thickness, the acceleration from the response spectrum was 2.74 g. For a 2-inch wall thickness, with a natural frequency of 9.97 Hz the acceleration from the spectrum was 2.44 g and for a 3-inch wall thickness the corresponding frequency and acceleration were 10.58 Hz and 2.33 g. The results given in this report are combinations determined by the square root of the sum of the squares method assuming equal seismic spectra for both the north-south and east-west events.

The UIS weight for a 1-inch wall thickness was conservatively modeled with a 40 ton mass at the bottom, 25 tons distributed over the length, and with 93 tons of internal sodium. Of this 93 tons of sodium, 7 tons is considered to be sloshing at a low frequency during a seismic event. For a 2-inch wall upper internals, 50 tons of stainless steel material weight was distributed over the length and for a 3-inch wall 74 tons was distributed over the length of the UIS.

An SSE vertical load of 1.8 g upward was also placed on the UIS. This estimate was based on results using a simplified vertical model described in Reference 6.

A.6.2 DEFLECTION RESULTS

The deflection result of most importance is the relative lateral deflection between the bottom of the UIS and the top of the core barrel. The deflection at this elevation could influence control rod performance during a seismic event. These results are shown in Figure A-43 and Table A-11. Since the UIS and core barrel could be vibrating in opposite directions, the displacements are added.

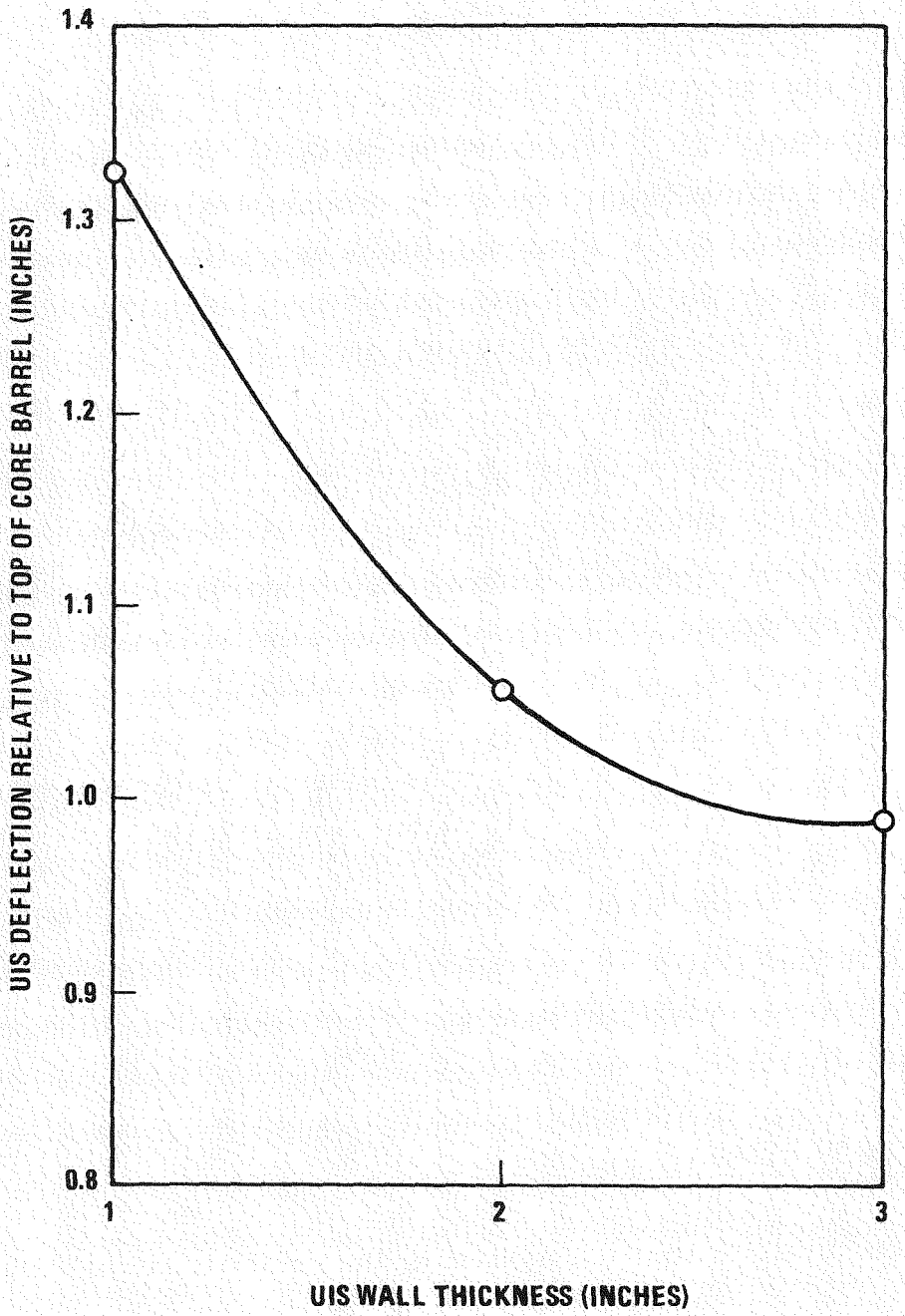

Figure A-43. SSE Relative Deflection of UIS and Core Barrel for Various UIS Wall Thicknesses

0665-155

TABLE A-11

LATERAL DEFLECTION OF UIS AND CORE BARREL - SSE

UIS Wall Thickness (Inches)	Core Barrel Deflection (Inches)	UIS Deflection (Inches)	Relative Deflection (Inches)
1	.6708	.6539	1.325
2	.6704	.3851	1.056
3	.6704	.3187	0.989

A.6.3 STRESS AND ALLOWABLE STRESS FOR UIS OUTER CYLINDER

The stress under consideration in this study is the bending of the UIS due to seismic events. It was expected that the limiting considerations would be the allowable stress to preclude buckling. Figure A-44 shows the bending moment and bending stress at the elevation of the bottom of the deck for 1G lateral acceleration and for SSE. Figure A-45 shows the bending moment for the SSE case at all elevations over the upper end of the UIS.

The bending stress at the bottom of the UIS insulation plates (elevation -20 inches in model) is of interest and is plotted in Figure A-46. A temperature of 950^{o}F was assumed to occur at this elevation whereas higher elevations would have lower temperatures and thus higher allowable stresses. Another area of interest was at elevation -54 inches where the upper row of flow holes is located. At this elevation, the cross sectional area is reduced significantly, making the cylinder more susceptible to buckling and increasing the nominal stress by 27 percent. This additional factor was determined by calculating a reduced thickness which gives the same cross sectional area as the actual thickness including the effect of 24 holes. Based on the reduced thickness, a reduced moment of inertia was calculated which gives an increase in stress. These stresses are shown in Figure A-47.

The vertical stresses resulting from an upward UIS acceleration of 1.8 g were calculated for a 1-inch thick UIS case. These were then added to the bending stress using the square root of the sum of the squares method. The resulting increase in stress was found to be negligible. To simplify the calculations, the vertical stresses were neglected for the remaining cases.

The allowable stress curve on Figure A-46 was determined by first determining the critical buckling stress from Figure A-48 at the appropriate radius to thickness ratio and then dividing by 1.5 to determine an SSE allowable. The allowable stress curve in Figure A-47 which includes effects of flow holes, was determined in the same manner as above except the

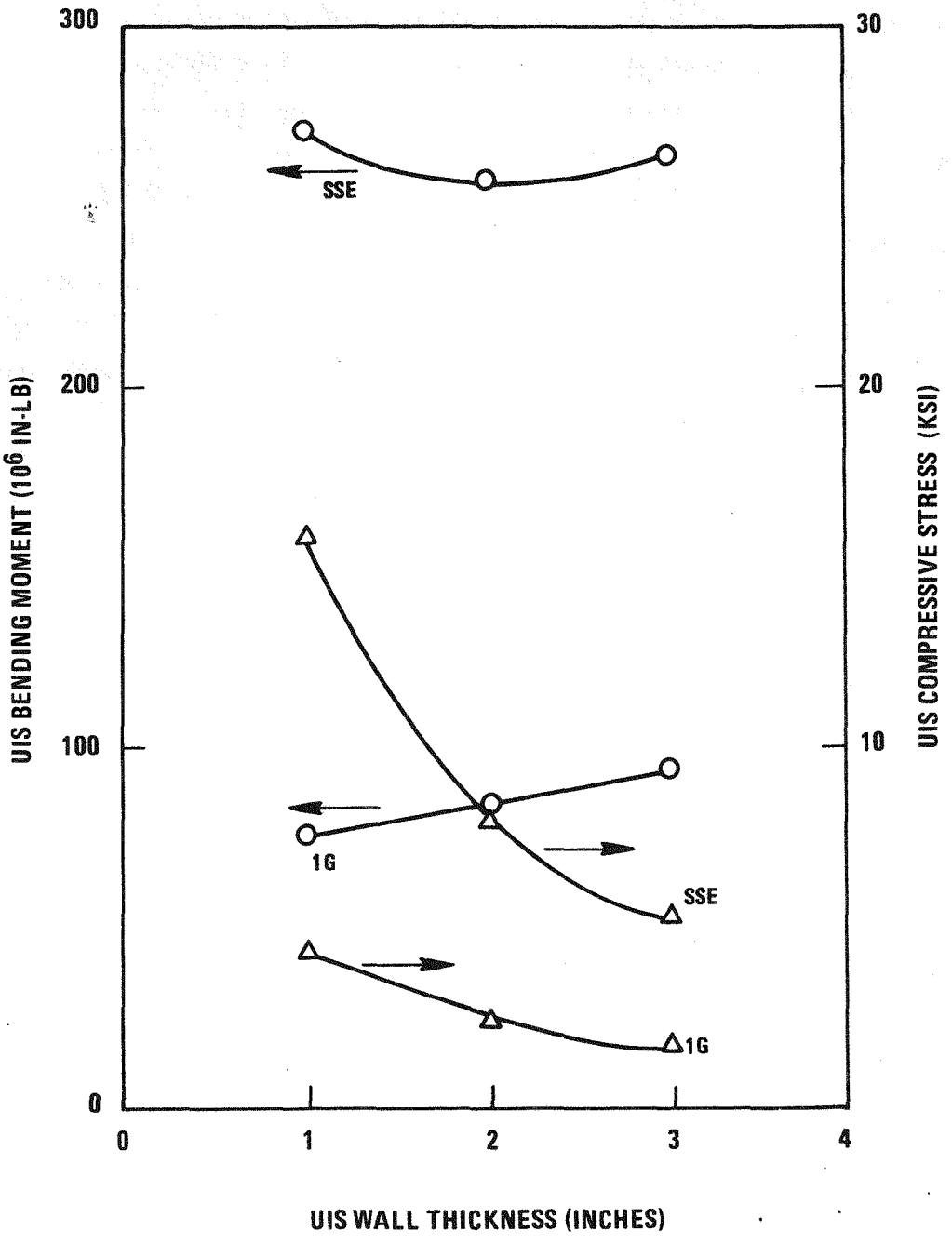

Figure A-44. UIS Bending Moment and Stress for Various UIS Wall Thickness

0665-154

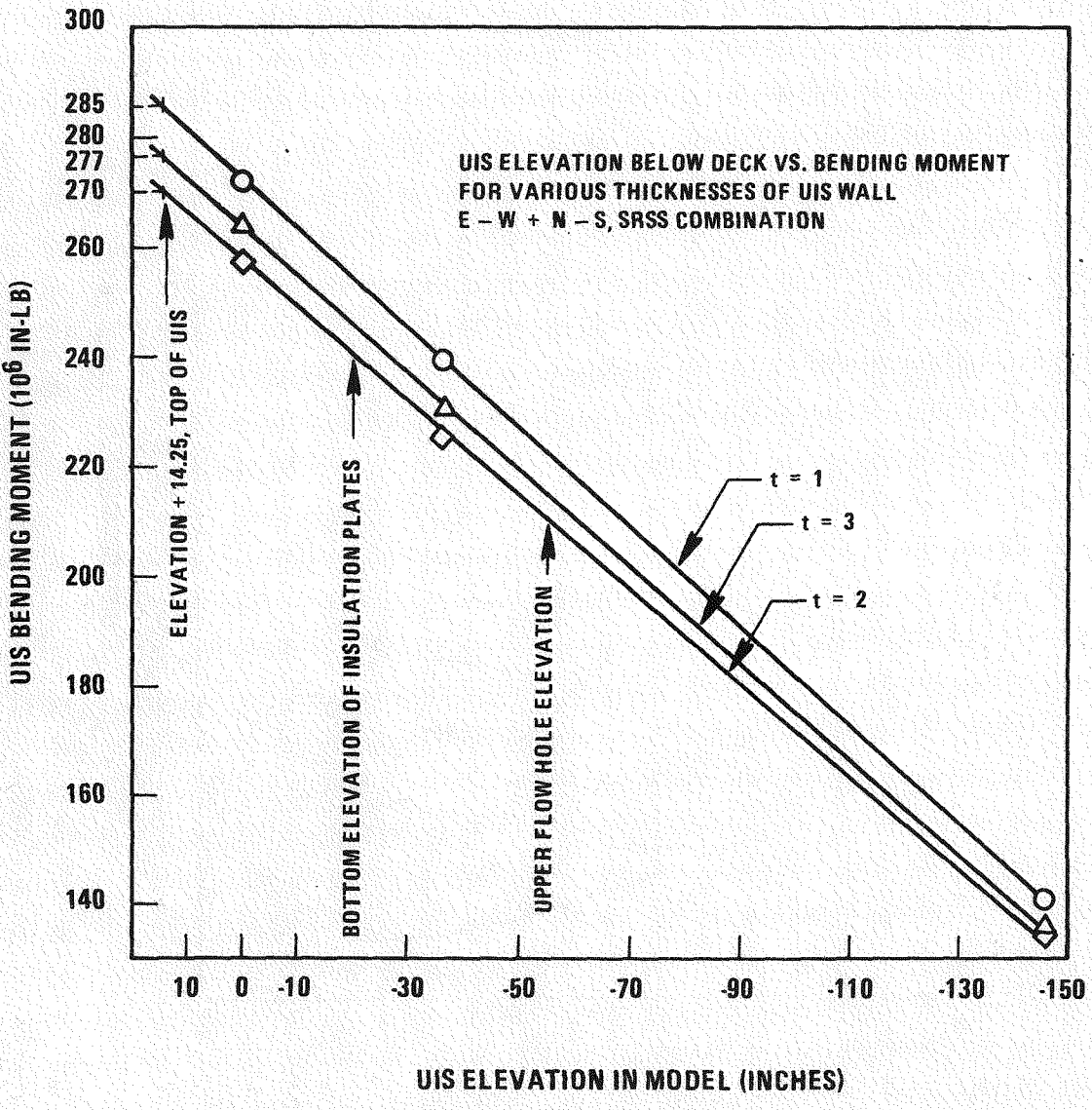

Figure A-45. Variation in SSE Bending Moment in UIS Below Deck

0665-153

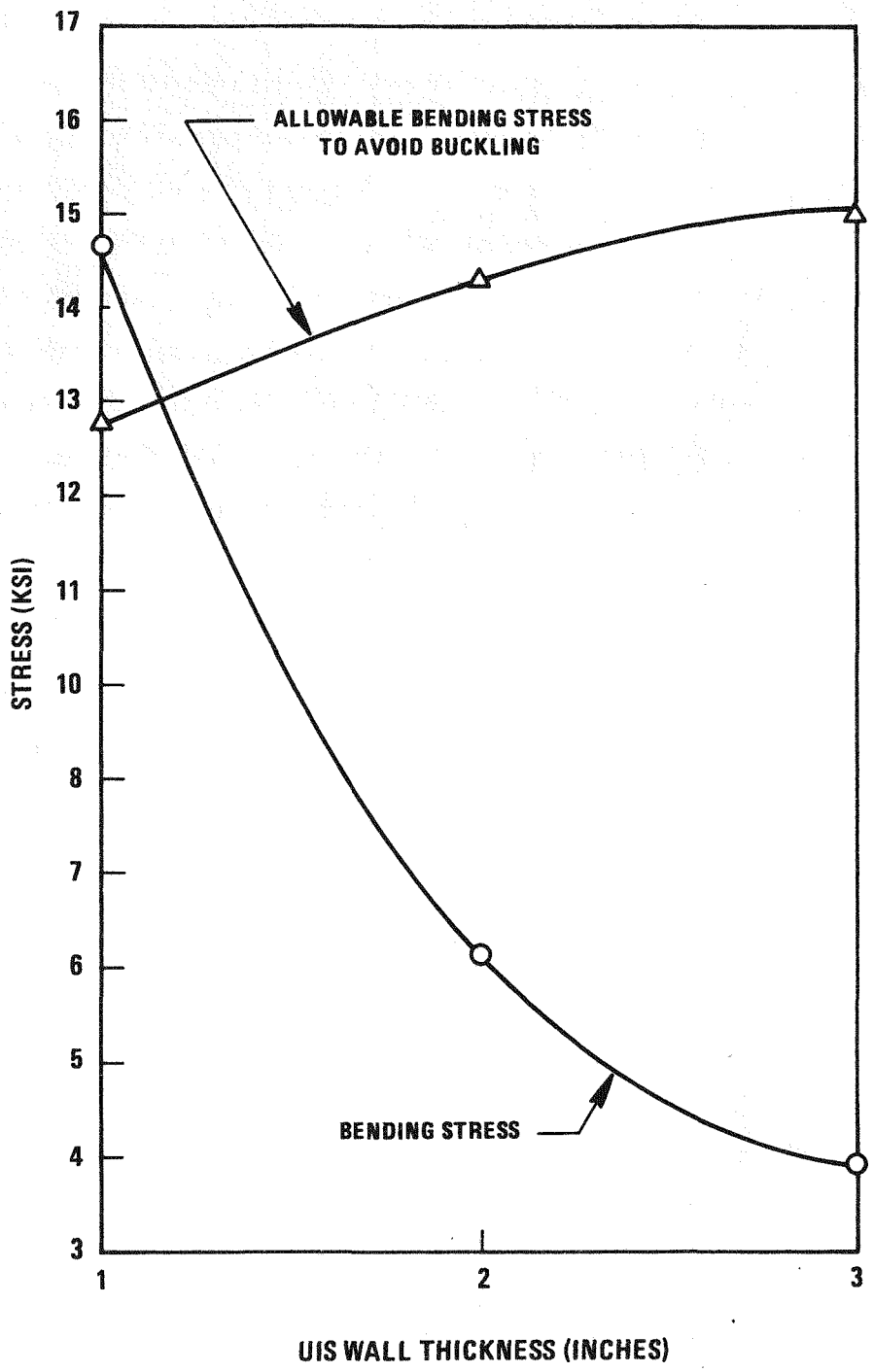

Figure A-46. Bending Stress and Allowable Bending Stress in UIS for SSE at 20 Inches Below Deck

0665-152

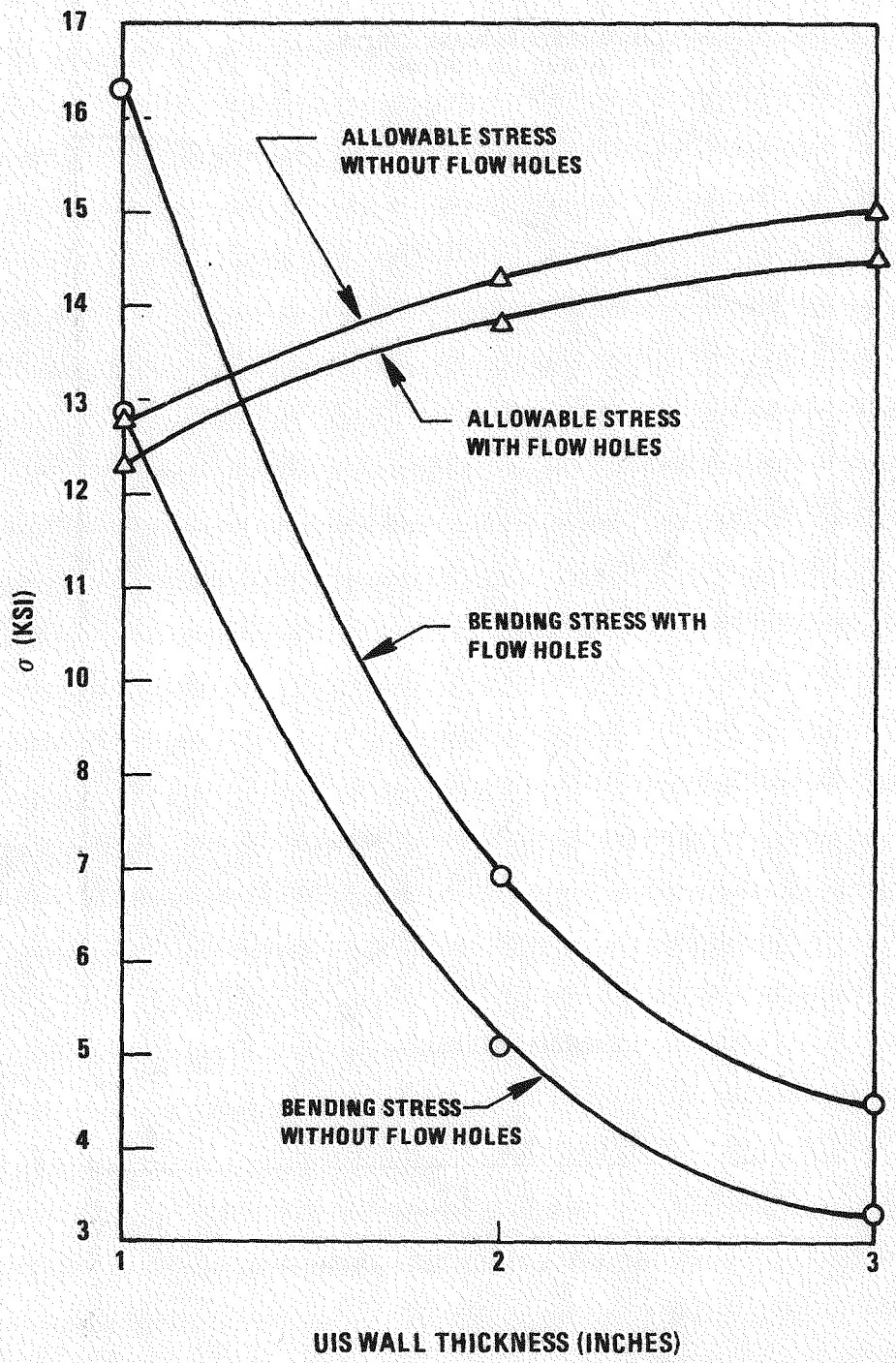

Figure A-47. Bending Stress and Allowable Bending Stress in UIS for SSE at 54 Inches Below Deck

0665-151

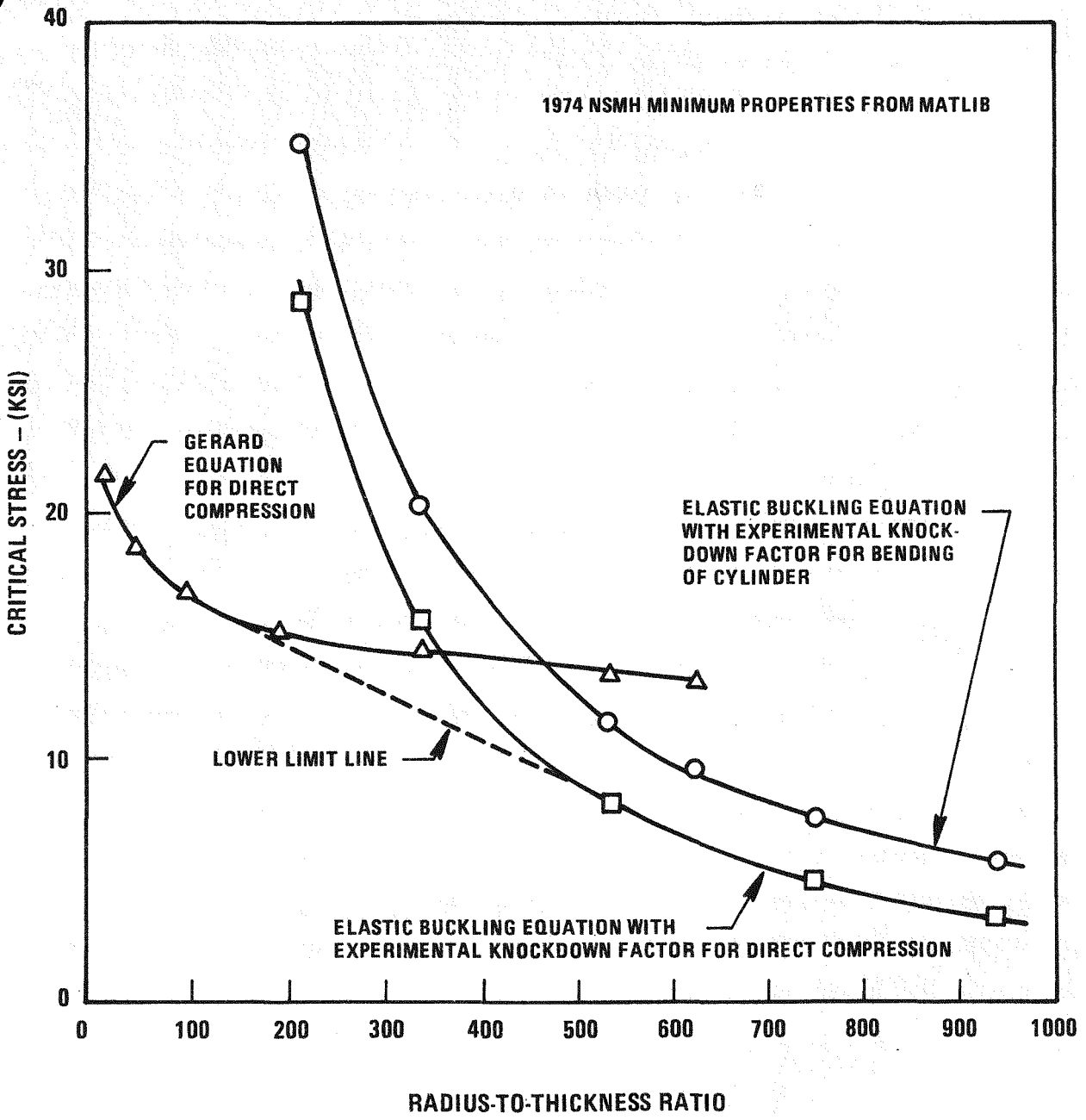

Figure A-48. Axisymmetric Cylinder Buckling Stainless Steel 316, 950°F

0665-150

thickness used was the same reduced thickness used in calculating the stress. The buckling equations used to develop Figure A-48 have been shown in References 8 and 12 to give reasonable results for the critical stress.

A comparison of Figures A-46 and A-47 shows that the stresses of Figure A-47, at the flow holes, are most limiting. Table A-12 shows this comparison where the flow holes are limiting on the basis of lower margins of stress to allowable stress.

A.6.4 STRESS IN BOLTS AT TOP OF UIS

The objective here was to examine a fairly wide range of bolt ring configurations in terms of the number and diameter of bolts needed to withstand the UIS overturning moment for an SSE. The study included consideration of 10 through 80 bolts in increments of 10 and diameters included 1.5 inch, 2.0 inch, and 2.5 inch. A proportionality constant, K_m, giving the ratio of maximum bolt load to the applied moment was determined and Figure A-49 shows the results for K_m for 1.5 inch diameter bolts. The results for 2.0 inch and 2.5 inch diameter bolts gave essentially the same results. The case shown in Figure A-49 is based on a 3-inch length for the stretched portion of the bolt. Cases were also run for a 6-inch length, but gave approximately the same results. Thus, the proportionality constant is sensitive to the number of bolts but not to the diameter or length within the range of parameters considered.

The overturning moment at the top of the UIS is 285×10^6 in-lb at elevation +14.25 as shown on Figure A-45. Using this moment and the K_m values of Figure A-49 the load and stress values shown in Table A-13 were calculated. From this table it is clear that a satisfactory combination of number and diameter of bolts can be selected to meet the allowable stress of whatever material is selected.

TABLE A-12

COMPARISON OF STRESS AND ALLOWABLE STRESS AT ELEVATIONS 20 AND 54

Elevation (Inches Below Deck)	UIS Wall Thickness (Inches)	Compressive Stress (psi)	Allowable Stress (psi)	Margin*
20 (Bottom of Insulation Plates)	1	14660	12760	-0.13
	2	7070	14300	1.02
	3	4930	15000	2.04
54 (Top Elevation of Flow Holes)	1	16350	12300	-0.25
	2	7860	13800	0.76
	3	5470	14500	1.65
*Margin = (Allowable Stress/Compressive Stress) -1				

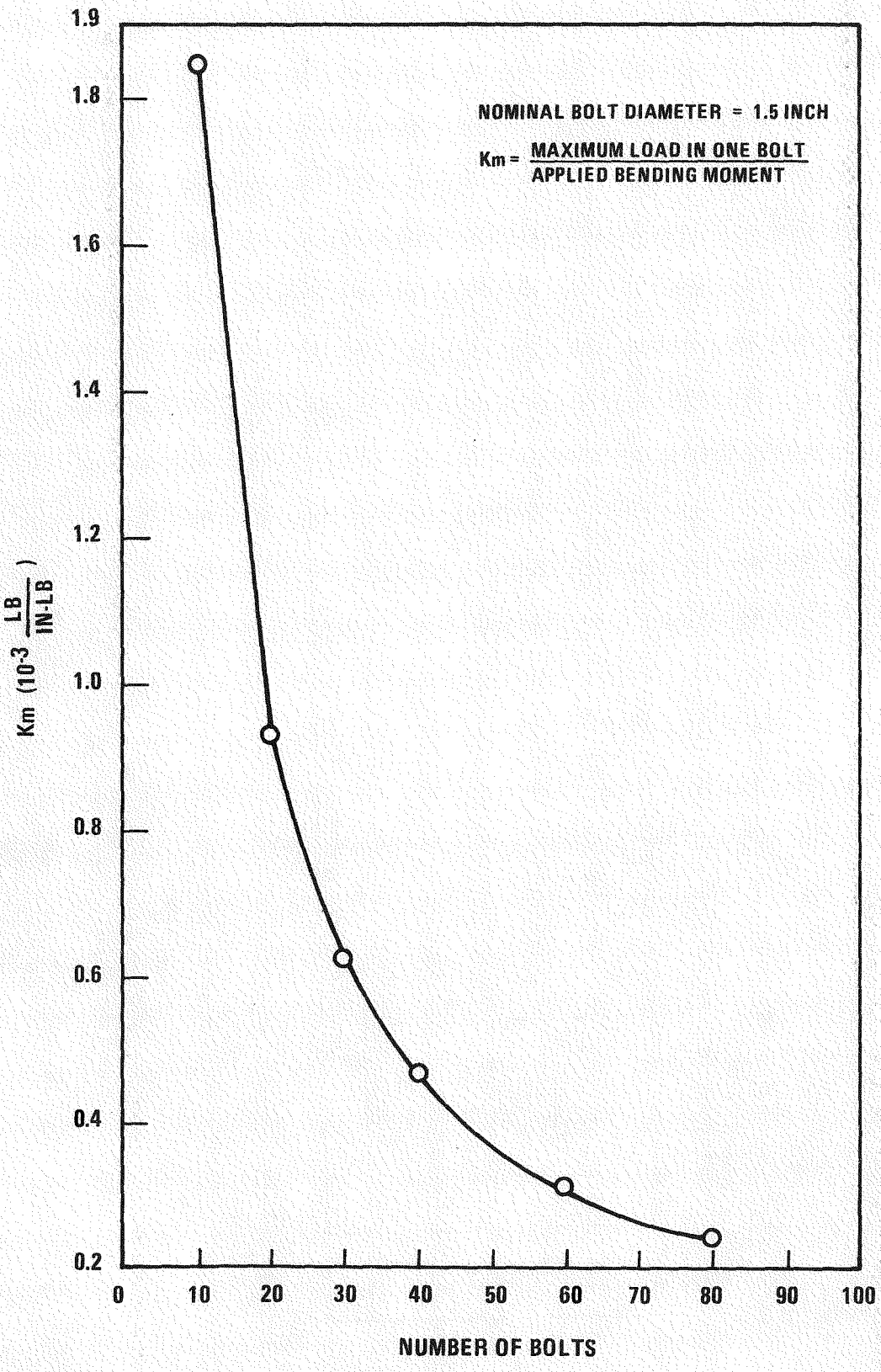

Figure A-49. Constant, Km, for Maximum Bolt Load versus Number of Bolts

0665-149

TABLE A-13

UIS BOLT LOADS AND STRESS WITH M = 285 x 10^6 IN-LB.

No. of Flange Bolts	Maximum Load in One Bolt (10^3 Lb.)	1.5 Inch Dia. Bolt Max. Stress (ksi)	2.0 Inch Dia. Bolt Max. Stress (ksi)	2.5 Inch Dia. Bolt Max. Stress (ksi)
20	265	188.7	106.0	66.0
40	134	95.6	53.7	33.5
60	90	64.3	36.1	22.6
80	68	48.5	27.3	17.0

A.6.5 CONCLUSIONS AND RECOMMENDATIONS

The deflection analysis shows that 1.3 inches of relative deflection can be expected for the reference case. Thickening the UIS results in less relative deflection, but about 1 inch is predicted even for a 3 inch thick UIS. This result is due to significant core barrel deflection. Also, the reduced UIS deflection with increasing wall thickness is most pronounced between 1 and 2 inches thickness with little reduction being achieved beyond 2 inches thickness due to added weight and less effect on stiffness.

The stress results for the UIS outer cylinder show that for the seismic loads considered, the allowable stress to preclude buckling is the limiting factor. The flow holes near the top of the UIS reduce the cross sectional area thereby increasing stress and reducing the allowable stress. These holes should be lowered as much as possible to reduce the bending moment acting on that cross section. Also, the number of holes at a single elevation should be decreased to increase the cross sectional area. The above recommendations will shift the critical stress location to the upper end of the UIS and would allow a thinner wall thickness to meet the allowable stresses. Based on SSE limits, which are less conservative than the OBE limits, the required wall thickness is 1.2 inches at the top end of the UIS. The required wall thickness at the top row of flow holes is 1.4 inches with the present design.

The bolt stress results show that a number and diameter for the bolts can be selected to meet the allowables of most bolting materials. Thus, an adequate basis for selection of the bolt material is available.

A.7 PUMP SUPPORT

The scoping structural evaluation of the LPR pump support was performed to determine the ability of the support configuration to adequately withstand the imposed operating loads. The limiting loads are the operating basis earthquake (OBE) and the safe shutdown earthquake (SSE) events. The results

of the analysis show that the support configuration is feasible with minor modifications in the design. Also, the stresses in the pump itself, while not properly a part of the current study, are expected to be low.

For the purposes of this analysis, the pump is considered to be a simple beam whose bottom end is simply supported and whose top end is elastically restrained. The elastic restraint is assumed to vary from a simple support to a built-in condition. Since most of the mass of the pump is distributed near the top of the pump, a non-uniform weight distribution is assumed. The applied loads were a lateral acceleration of 2.25 g for the OBE and 3.80 g for the SSE.

The most severe case considered is when the top of the pump is built-in. This may be overly conservative when the pump is loaded in the radial direction but is realistic when the loading corresponds to the circumferential direction. The results of the analysis for the configuration analyzed demonstrate that bolt stress limits are exceeded by the combination of tensile loads due to an overturning moment and shear loads. The tensile limits can be met by increasing the size, the number of bolts, and/or specification of high strength bolts. The shear stresses can be reduced by incorporating a shear member into the design.

At the bottom of the pump, the clearance around the plug-in feature will have to be enlarged to preclude binding at the pump inlet. Also, this clearance does not include the deflection and rotation of the lower support structure as these have not been determined. It is recommended that the combined diametral clearance be increased, if feasible, from the present 0.2 inches to a minimum of 0.25 inches. Additional diametral clearance may be required due to the motion of the LSS. Alternatively, the distance between the piston ring chamfers could be decreased to obtain the same effect.

For the hold-down lug area, the analysis indicates the need for high strength bolt material. With 2.0 inch bolts the ultimate tensile strength required would be about 140 ksi and with 2.5 inch bolts, about 100 ksi.

Table A-14 provides a summary of predicted stresses and allowable stresses for several key locations on the pump support.

A.7.1 DESIGN CONFIGURATION ANALYZED

The concept analyzed, shown in Figures A-50 and A-51, provides a top support bearing mounted on a supporting column attached to the roof penetration nozzle. An intermediate support is also provided about fifty inches below the top bearing, with a small radial clearance of 15 to 30 mils. The bottom support has a tight clearance of 30 mils radially at the plug-in feature of the lower support structure.

A.7.1.1 LOADS

The loading assumed for this study is that due to a horizontal seismic event. Peak response accelerations of 2.25 g and 3.8 g were used for OBE and SSE respectively. These are based on the response spectra of Section A.3.1 and are considered to be conservative. For this reason, no additional magnification factor was used in the simplified analysis that follows.

The weight of the pump is estimated to be 75 tons with most of the pump weight distributed near the top end of the pump. This is a good approximation when the motor, an additional 75 tons, is mounted separately. The sodium weight inside the pump is estimated at 22 tons based on sodium level and pump dimensions shown in the simplified pump geometry of Figure A-52. The loading distribution assumed is shown in Figure A-53.

A.7.2 FINITE ELEMENT MODEL

A beam element model shown in Figure A-53 was constructed using the Reference 32-dimensional beam element, (STIF 3). The purpose of this model is to determine reaction forces and deflections for various pump support methods, i.e., fixed support, simple support, and resilient support. The support and pump geometry were simplified by the use of one set of cross

TABLE A-14

SUMMARY OF STRESSES AT KEY AREAS OF PUMP SUPPORT

LOCATION & CONFIGURATION	TYPE OF LOAD CONSIDERED	ASME ALLOWABLE STRESS METHOD CALCULATED OBE	ASME ALLOWABLE STRESS METHOD CALCULATED SSE	ASME ALLOWABLE STRESS VALUE (KSI) OBE	ASME ALLOWABLE STRESS VALUE (KSI) SSE	CALCULATED STRESS OR INTENSITY (KSI) OBE	CALCULATED STRESS OR INTENSITY (KSI) SSE	MARGIN(4) OBE	MARGIN(4) SSE
1. Hold-Down Bolts:									
4, 2 in. bolts	Compressive	2 S_m	2 S_m(1)	100.0(2)	100.0	45.7	77.1	1.19	.30
4, 2.5 in. bolts	Compressive	2 S_m	2 S_m(1)	76.6(3)	76.6	28.6	48.2	1.68	.59
2. Flange Bolts at Bottom of Support Column and In Upper Part of Column (Locations C, D, & F in Fig. B-54)(7)									
40, 1 in. bolts	Tension & Shear	3 S_m(5)	3 S_m(1)	150.0(2)	150.0	111.9	189.0	.34	-.21(6)
40, 1 in. bolts	Tension Only	2 S_m	2 S_m(1)	100.0(2)	100.0	29.3	49.7	2.41	1.01
48, 1.5 in. bolts	Tension & Shear	3 S_m(5)	3 S_m(1)	114.9(3)	114.9	40.2	68.0	1.86	.69
48, 1.5 in. bolts	Tension Only	2 S_m	2 S_m(1)	76.6(3)	76.6	10.6	18.1	6.23	3.23
3. Bolts at Bottom of Bellows (Location E in Figure B-54)									
40, 1.0 in. bolts	Shear Only	.6 S_m	1.2 S_m(8)	23.0(3)	46.0	54.0	91.2	-.57(9)	-.50(9)

NOTES: 1. SSE limit was assumed to be the same as OBE limit for conservatism.

2. Assumes the use of nickel alloy 718 material, type SA-637 with S_t = 185,000 psi

3. Assumes the use of 17 Cr-4 Ni-4 Cu alloy, type SA-564 with S_t = 140,000 psi

4. Margin = $\frac{\text{Allowable Stress}}{\text{Calculated Stress}} - 1$

5. Based on NB 3232.2

6. It is recommended that this low margin of allowable to calculated stress be corrected by providing larger bolts (e.g. 48, 1.5 in. bolts) and a shear ledge of 1.375 inches depth to resist the shear loading.

7. This is a limiting case for all three locations.

8. Based on approximately 1.5 factor of safety to yield.

9. It is recommended that a 1.75 inch shear ledge be added to resist the shear loading.

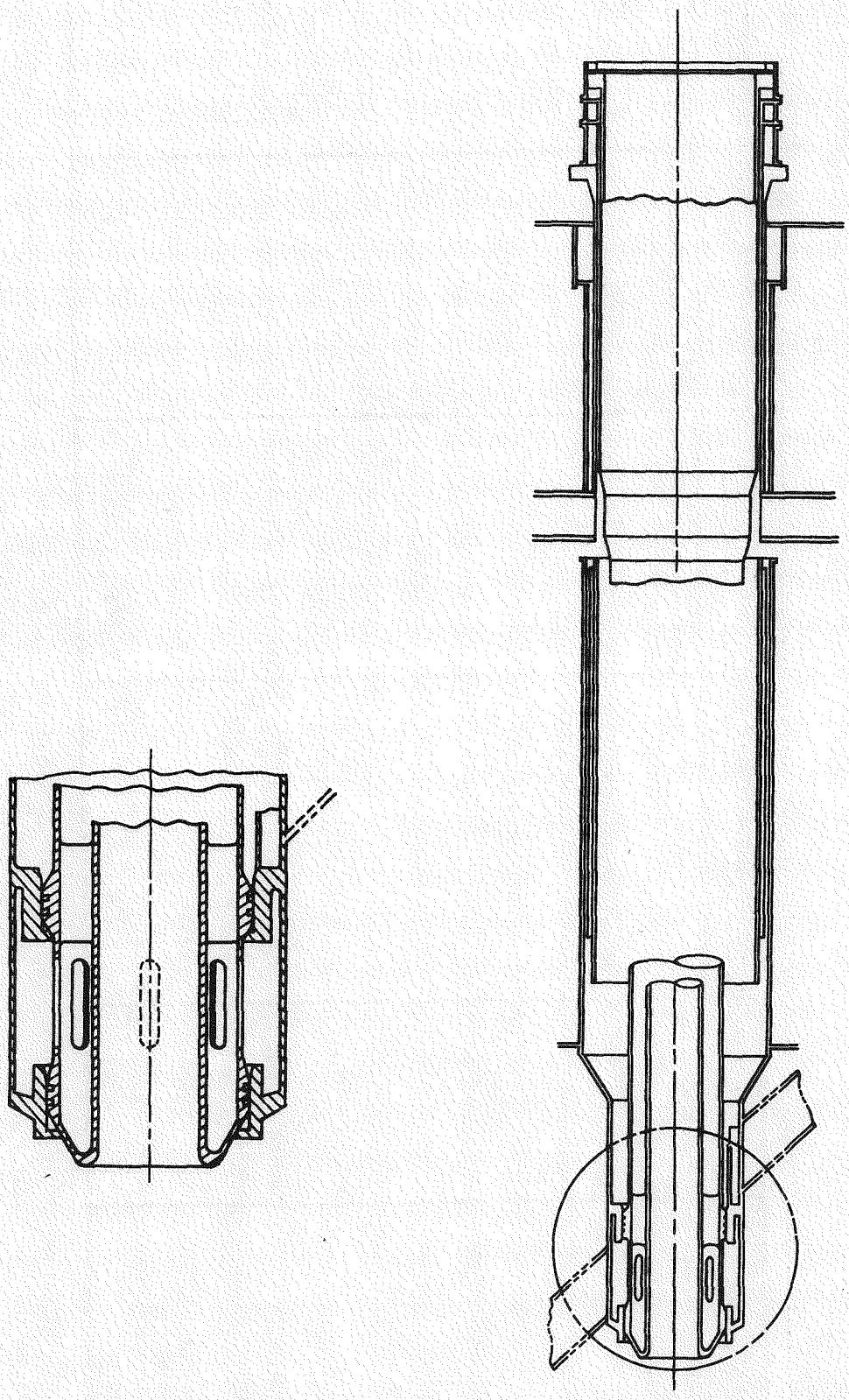

Figure A-50. LPR Pump Support

0665-148

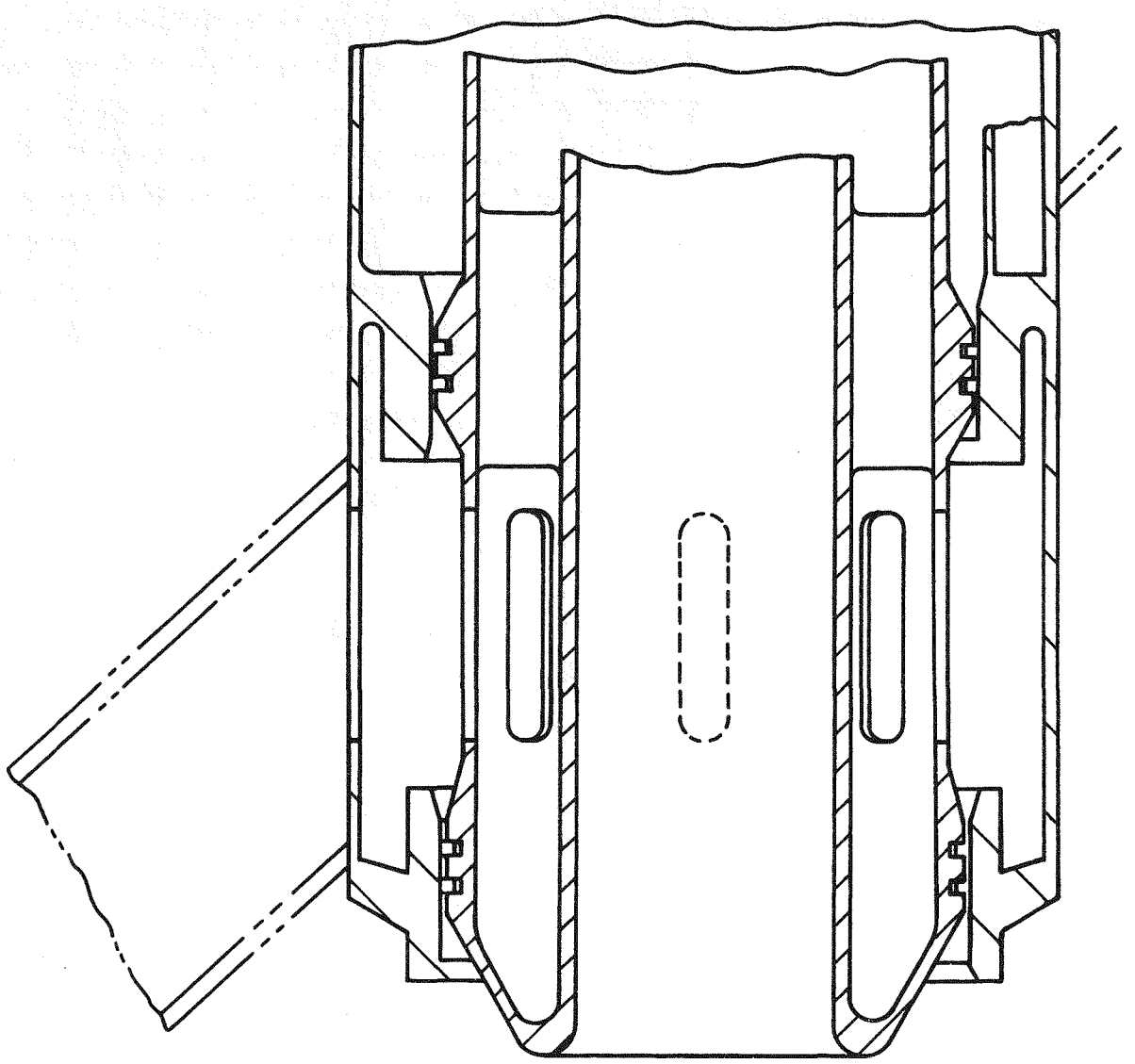

Figure A-51. Lower Support for Pump

0665-7

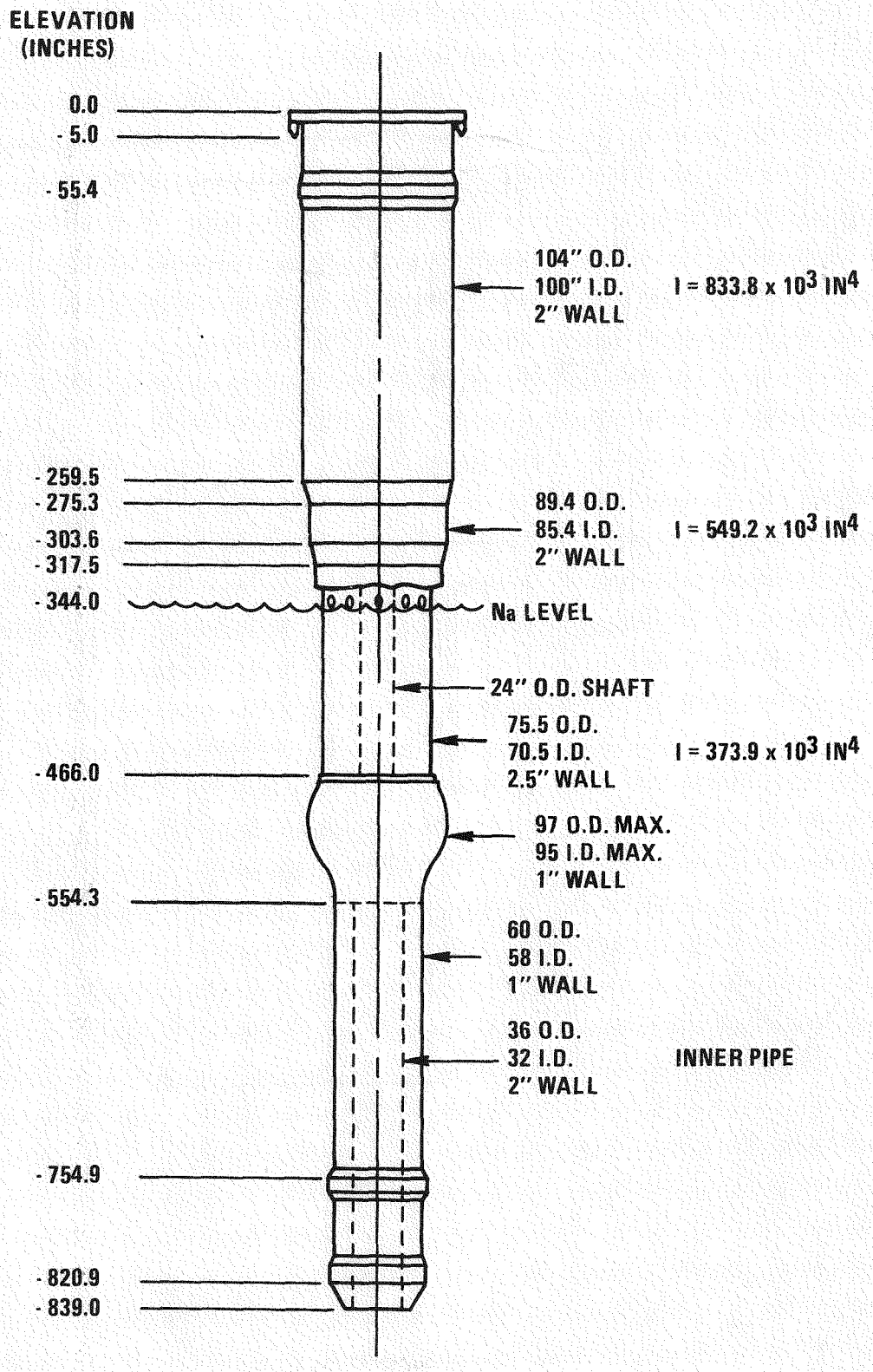

Figure A-52. LPR Pump Elevations and Geometry

0665-146

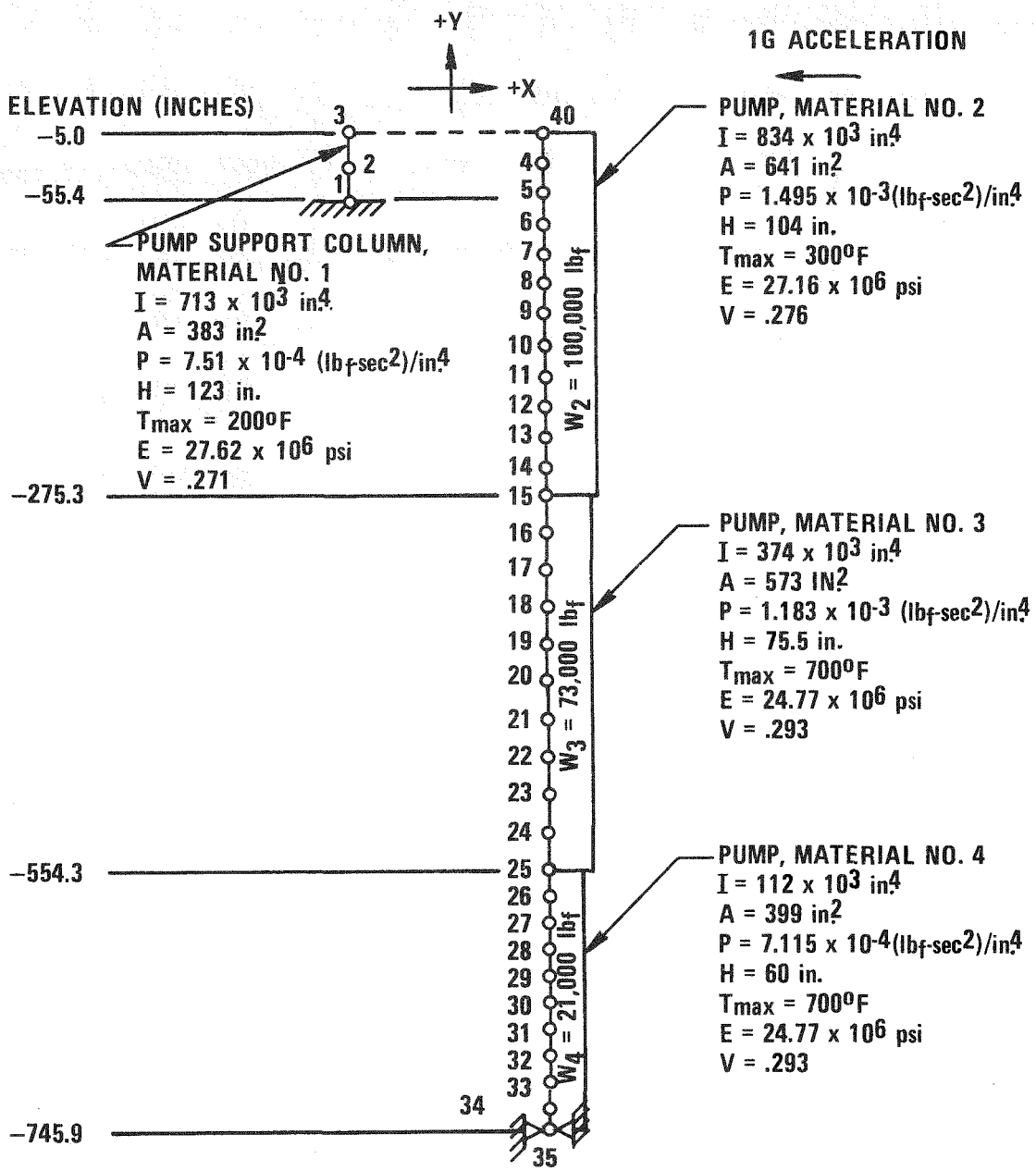

Figure A-53. Pump Support Beam Model Node Numbers and Element Constants

0665-4

sectional properties for the pump support column and three sets for the pump as shown in Figures A-52 and A-53. A verification check was made using material #3 and constant table #3 properties over the full length of the pump. The results compared well with an independent hand calculation for reaction loads and deflection. The lateral spring constant of the support column was also determined by hand calculation and found to be within 5% of the finite element model results.

A.7.3 RESULTS

A.7.3.1 UPPER SUPPORT REACTION LOADS

Several types of upper supports were examined to determine limiting values of reaction loads. These include fixed, simple, and resilient constraints at the top end of the pump. Each of these constraints is possible depending upon the direction of loading and the tolerance between adjoining parts.

For the design with an intermediate support located about fifty inches below the top support, a limiting case is given by a fixed top end in both the X and Z directions (see Figure A-50). This is possible in the X direction since the radial clearance at the intermediate support could be distributed on one side of the circumferential load pad with zero clearance on the other side. The combination of zero clearance and the top support gives a fixed end condition in that direction. In the Z direction, the same condition as mentioned above could occur and in addition, the hold-down lugs provide a fixed connection to the pump support column. For a design without an intermediate support, the applicable constraint for X direction loading is a simple support at the top bearing. For the Z direction a fixed support at the top bearing is appropriate. The actual top support will be somewhat resilient since the support column will bend and the bearing material (lubrite) may have a low spring constant.

A.7.3.2 SIMPLE UPPER SUPPORT

For the simply supported case, the most significant reaction loads occur at the spherical bearing and at the bottom of the support column. These are given in Table A-15 along with the load at the bottom support of the pump.

A.7.3.3 FIXED UPPER SUPPORT

For the fixed support case the deflection profile and reactions are as shown in Figure A-55.

Referring to Figure A-54, the critical locations for this case will be shear on the bearing at "A", shear on the bolt circle at "E", and a shear and moment loading at "F". The reactions for these locations are given in Table A-16. The reactions at location "F" are close approximations based on neglecting the weight of the support column but including all other loads.

A.7.3.4 RESILIENT UPPER SUPPORT

For the resilient support case the deflection profile and reaction loads are as shown in Figure A-56.

The free deflection and spring constant at point 1 were determined to be:

OBE: $\delta = .040$
SSE: $\delta = .067$
$K = 16.989 \times 10^6$ lb/in

Thus, the reaction force for any value of δ_1 less than the free deflection is:

OBE: $R_1 = 16.989 \times 10^6 \ (.040-\delta_1) \ (lb_f)$
SSE: $R_1 = 16.989 \times 10^6 \ (.067-\delta_1) \ (lb_f)$

TABLE A-15

REACTION LOADS - SIMPLE UPPER SUPPORT

LOCATION (see Fig. A-46)	LATERAL (SHEAR) LOAD (10^6 LBS)			MOMENT (10^6 IN-LBS)		
	1G	OBE	SSE	1G	OBE	SSE
Spherical Bearing, "B"	.117	.263	.445	----	----	----
Bottom of Support Column, "F"	.123	.277	.467	6.04	13.6	23.0
Bottom of Pump	.077	.173	.293	----	----	----

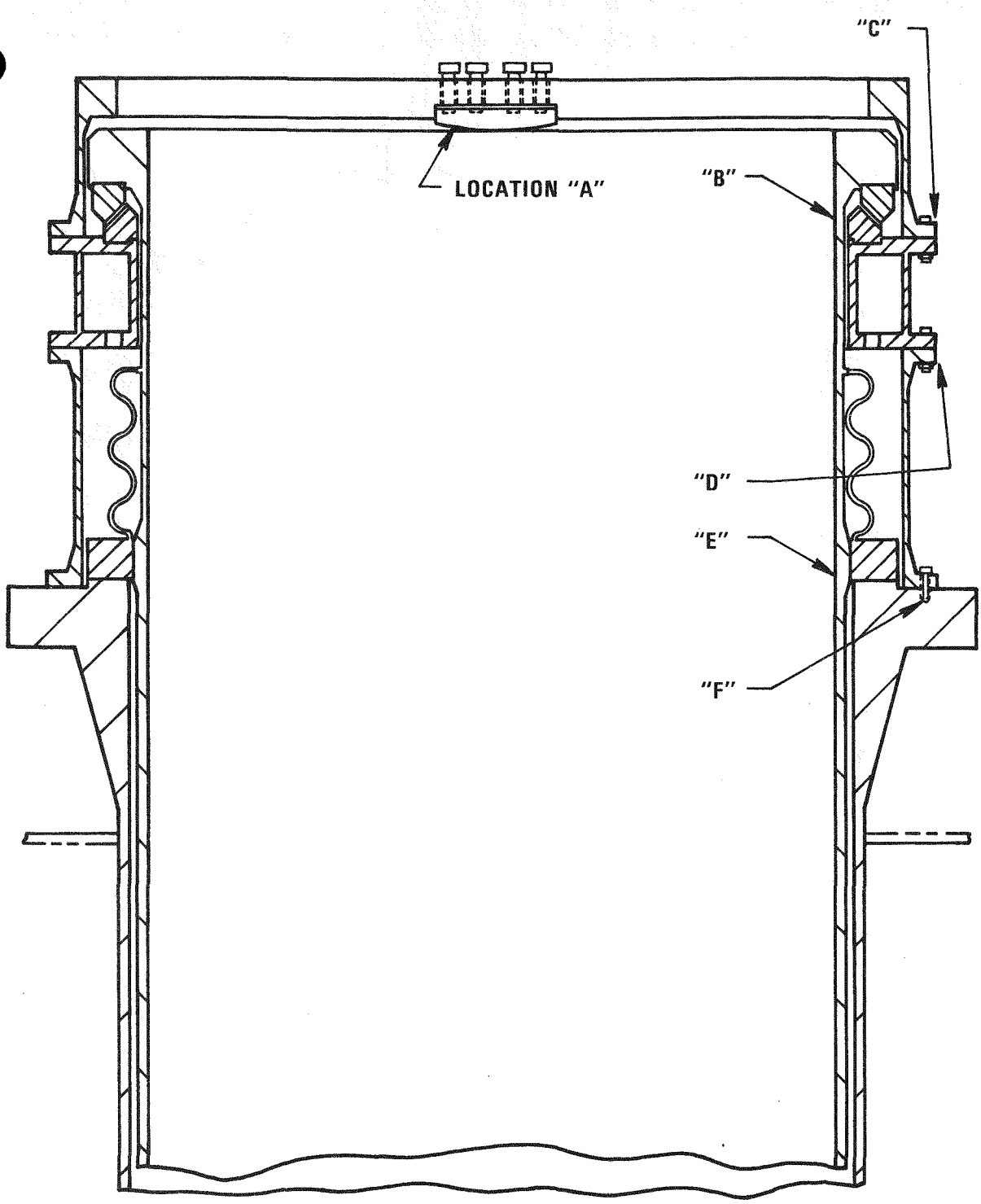

Figure A-54. Specific Locations on Upper Support for Pump

0665-6

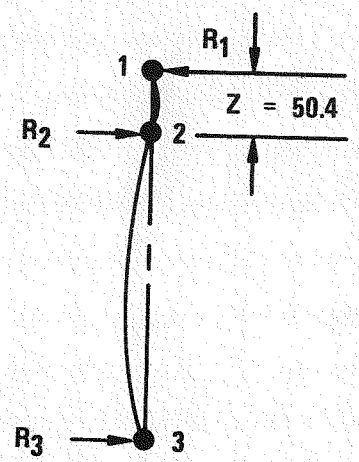

Figure A-55. Simple Support for Top End of Pump

0665-193

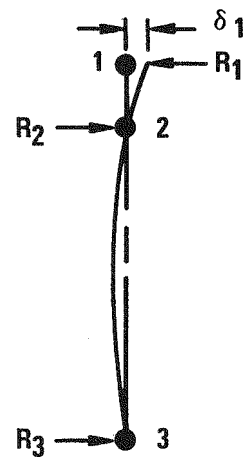

Figure A-56. Elastic Support for Top End of Pump

0665-192

TABLE A-16

REACTION LOADS - FIXED TOP SUPPORT

LOCATION (See Fig. A-46)	REACTION FORCE	SHEAR LOAD (10^6 LBS)		MOMENT (10^6 IN-LBS)	
		OBE	SSE	OBE	SSE
B	R_1	.672	1.13	----	----
E	R_2	1.00	1.69	----	----
F	R_1 & $2xR_1$	.672	1.13	33.8	57.2
Bottom of Pump		.106	.179	----	----

Once the value of R_1 is determined, the deflection of the support column and the value of R_2 can be found as follows:

δ_s = support column deflection = $(R_1/68.6 \times 10^6)$ (in)

R_2 = $(125{,}663 + 1.073\ R_1)$ (lb_f)

Thus, for an arbitrary value of δ_1, corresponding to a resilience and/or a gap at the top support bearing, the reaction forces and support column deflection can be determined by the above equations. These are tabulated in Table A-17 for the SSE case.

In Table A-17, the first entry, with δ_1 = .013 inches, represents the most reasonable case on which to base the design loads for the X direction. For the Z direction, however, lateral reaction loads R_1 and R_2 will be lower and the moment at location F could be as high as 57.2×10^6 in-lb_f from Table A-16.

A.7.3.5 BOLT STRESS DUE TO REACTION LOADS

The reaction loads determined in the previous section include shear and moment loads at several bolted flange connections, all with the same proportions and similar configurations. A proportionality constant, K_m, relating the maximum bolt force and the flange bending moment is defined as:

$$K_m = \frac{\text{Maximum Bolt Load (lb)}}{\text{Bending Moment (in-lb)}}$$

Thus, the maximum bolt loads can be determined based on the reactions from the previous section. Table A-18 gives proportionality constants for various bolt diameters and numbers and applies to flanges at locations C, D and F of Figure A-54 since these three flanges are similar in geometry.

The most highly loaded flange is at location F of Figure A-54. The moments are:

TABLE A-17

REACTION LOADS FOR SSE CASE - RESILIENT SUPPORT

Total Deflection Assumed, δ_1 (Inches)	Bearing* Deflection (Inches)	Support Col. Lateral Deflection (Inches)	Reaction Load R_1 (Locations B, D, & F In Fig. 5) (Lbs.)	Reaction Load R_2 (Location E in Fig. 5) (Lbs.)	Moment at Bottom of Support (Location F) (10^6 In-Lbs.)
.013	0	.013	912,000	1,105,000	46.0
.030	.021	.009	628,600	800,100	31.7
.040	.033	.007	458,700	617,800	23.1
.050	.046	.004	288,800	435,600	14.6
.060	.058	.002	118,900	253,600	6.0
.067	.067	0	0	125,700	0

* With zero spring constant, i.e., equivalent to gap

TABLE A-18

RATIO OF MAXIMUM BOLT LOAD TO TOTAL FLANGE MOMENT

Bolt Configuration of Flange	K_m (lb/in-lb.)
40, 1" Bolts	5.26×10^{-4}
60, 1" Bolts	3.50×10^{-4}
80, 1" Bolts	2.65×10^{-4}
48, 1.5" Bolts	4.41×10^{-4}
60, 1.5" Bolts	3.56×10^{-4}
80, 1.5" Bolts	2.68×10^{-4}

Simple Support: OBE: 13.7×10^6 in-lb
SSE: 23.1×10^6 in-lb

Fixed Support: OBE: 33.8×10^6 in-lb
SSE: 57.2×10^6 in-lb

The moments for a resilient top support will be between the above two cases. The bolt loads and stresses are given in Table A-19 based on bolt areas of 0.606 in^2 for a 1 inch bolt and 1.405 in^2 for a 1.5 inch bolt.

The bolt loads in Table A-19 do not consider preload of the flange bolts. However, due to the high stiffness of the flange relative to the bolts, the bolt loads would fluctuate very little as long as the load from Table A-19 is less than the preload force.

In some cases, the shear load may be carried by the bolts rather than by friction, shear pins, or a shear ledge. The shear load for several limiting cases from the SSE results are:

Simple Support, location F: 467,000 lb_f from Table A-15
Fixed Support, location F: 912,000 lb_f from Table A-17
Fixed Support, location E: 1,105,000 lb_f from Table A-17

In Table A-20 the maximum average shear stress for any single bolt for the above loads is:

$$\tau \text{ max } \underline{\sim} \; 2 \quad \tau \text{ average} = 2 \frac{V}{A}$$

A.7.3.6 HOLD-DOWN LUG LOADS AND STRESS

The hold-down lugs are shown in Figure A-54 at Location "A". For a seismic event in a direction parallel to a line intersecting the two lugs, there

TABLE A-19

TENSILE LOAD AND STRESS FOR MOMENT LOAD ON FLANGE "F"

Bolt Dia. Inches	No. of Flange Bolts	SIMPLE SUPPORT				FIXED SUPPORT			
		Max. Load Lbs.		Max. Stress Ksi		Max. Load Lbs.		Max. Stress Ksi	
		OBE	SSE	OBE	SSE	OBE	SSE	OBE	SSE
1.0	40	7200	12150	11.9	20.1	17800	30050	29.3	49.7
1.0	60	4800	8100	7.9	13.3	11850	20050	19.5	32.9
1.0	80	3650	6100	6.0	10.1	8950	15100	14.8	25.0
1.5	48	6050	10200	4.3	7.3	14900	25250	10.6	18.1
1.5	60	4900	8200	3.5	5.9	12050	20300	8.6	14.6
1.5	80	3700	6200	2.6	4.4	9050	15350	6.4	10.9

TABLE A-20

ESTIMATE OF SHEAR STRESS FOR SSE

Bolt Dia. Inches	No. of Flange Bolts	Total Area In^2	MAXIMUM AVERAGE SHEAR STRESS (KSI)		
			Simple Support Location F $V=467x10^3$ Lb_f	Resilient Support Location F $V=912x10^3$ Lb_f	Resilient Support Location E $V=1105x10^3$ Lb_f
1.0	40	24.24	38.6	75.2	91.2
1.0	60	36.36	25.8	50.2	60.8
1.0	80	48.48	19.2	37.6	45.6
1.5	48	67.44	13.8	27.0	32.8
1.5	60	84.30	11.0	21.6	26.2
1.5	80	112.40	8.4	16.2	19.7

will be vertical forces which these lugs must restrain. Two limiting cases can be defined: 1) no reaction force at elevation -55.4 i.e., simple support at the top, and 2) zero deflection at elevation -55.4.

Case 1 will be more severe and will be examined here. The moment loading on the top flange will be:

1G: 22.5×10^6 in-lb
OBE: 50.6×10^6 in-lb
SSE: 85.5×10^6 in-lb

The moment is resisted by the shear lugs as shown in Figure A-57:

$$F_{lug} \leq \frac{M}{2L} = \frac{M}{2(111/2)}$$

The results for force on the lug are:

1G: $F = 0.203 \times 10^6$ lb_f
OBE: $F = 0.457 \times 10^6$ lb_f
SSE: $F = 0.771 \times 10^6$ lb_f

These forces are resisted by four bolts in compression. The compressive stresses are given in Table A-21 based on the use of either a 2.0 inch or 2.5 inch nominal diameter bolt.

A.7.3.7 PUMP DEFLECTIONS

Knowledge of pump deflections during plant heat up and during seismic events is important if binding of the pump at its lower support is to be prevented. It would also be useful in providing adequate lateral clearance in the standpipes.

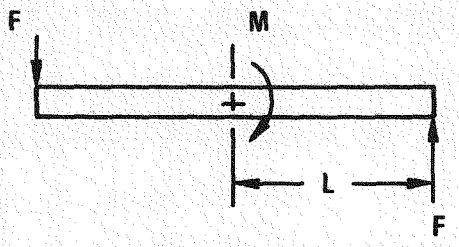

Figure A-57. Loading on Top Flange of Pump

0665-194

TABLE A-21

COMPRESSIVE STRESS FOR HOLD-DOWN LUG BOLTS

Nominal Bolt Diameter (Inch)	Maximum Stress (Ksi) OBE	Maximum Stress (Ksi) SSE
2.0	45.7	77.1
2.5	28.6	48.2

The angle of the pump deviates from true vertical due to expansion of the bottom support relative to the top support and due to static deflection of the roof. The effect of static roof deflection could be largely calibrated out and half the thermal expansion can be imposed at room temperature to help prevent binding of the lower end of the pump in its receptacle. However, dynamic deflections of the roof, the pump, and the core support structure will also influence potential binding of the pump lower end. Binding would occur in the current design when the pump angularity exceeds 1.33×10^{-3} radians. This angle of binding is based on diametral clearances of 0.060 and 0.140 inch at the upper and lower piston ring chamfers as shown in Figure A-50. The distance between these chamfers, also a parameter influencing binding, is about 75 inches. The pump length over which the angularity due to thermal expansion was calculated is 694 inches and the radius of the pump centerline used is 344 inches. Table A-22 gives the amount of angularity as a result of various factors.

The maximum lateral deflection of the pump occurs slightly below the middle of the pump and is:

1G: δ_{max} = .097 inches
OBE: δ_{max} = .181 inches
SSE: δ_{max} = .185 inches

These deflections include 0.030 inch radial clearance motions at the top and bottom of the pump.

A.7.3.8 CONCLUSIONS AND RECOMMENDATIONS

The maximum average tensile stress is 49.7 ksi in the worst case bolt due to bending about the axis of the pump. Since bolting materials are available for which this represents an acceptable stress level, it may be concluded that the reference design as shown in Figures A-50 and A-51 is a workable concept with regard to resisting an overturning moment at the top support of the pump.

TABLE A-22

ANGULAR MOTION AT LOWER END OF PUMP

Source of Angularity	$\Delta\theta$ At Lower End of Pump (Radians)
Thermal Expansion of CSS Relative to Roof: Nominal $\Delta T = 500°F$	2.6×10^{-3} ($1/2\ \Delta\theta = 1.3 \times 10^{-3}$)
Upper Limit $\Delta T = 630°F$	3.1×10^{-3} ($1/2\ \Delta\theta = 1.55 \times 10^{-3}$)
Dynamic Roof Deflection, $\delta = 0.5$ Inch at Inside Radius of Ring Girder	$.51 \times 10^{-3}$
Pump Bending, OBE	1.62×10^{-3}
SSE	2.74×10^{-3}
CSS Deflection	Not Available

For shear loading, the maximum stresses may be quite high as shown in Table A-20. It is recommended that a method of resisting the shear load other than through the bolts be developed. These high shear loads are possible in a design that provides an intermediate support below the top bearing. In such a design, the clearance could be zero on one side of the pump resulting in a fixed top support and high shear loads.

If shear pins were used at locations F, B, D and E shown in Figure A-54, the shear pin area required, assuming that only one-half of the available area is active, is shown in Table A-21. The maximum shear loads were given in Table A-15 for SSE as 912,000 lb_f at locations B, D and F and 1,105,000 lb_f at location E. For an OBE event, the corresponding loads are 540,000 lb_f at B, D and F and 654,000 at E since they are lower by the ratio of OBE to SSE acceleration. The OBE loads determine the shear area since the allowable stress is lower for an OBE case. The allowable stress will also depend on the pin material, so several different strengths of materials are considered in Table A-23.

If a shear ledge is used at these same locations, the required depth of the ledge is 1.375 inches for F, B and D and 1.75 inches at E. These are based on a ledge material having a yield strength of 30 ksi and on 1/8 of the circumference of the ledge resisting the shear load.

The hold-down lug concept appears to be a workable method of providing holddown. However, the present 2.0 inch bolts would require a very high strength bolting material (e.g., $S_t \geq 140{,}000$ psi) to be acceptable. thus, the use of 2.5 inch bolts would allow a wider choice of bolting material ($S_t \geq 100{,}000$ psi) and would also lower bearing stress on the hold-down plate. With the use of 2.0 inch bolts, the hold-down plate material should have a minimum yield strength of approximately 80 ksi and for 2.5 inch bolts, this would be about 50 ksi. The length of thread required to prevent stripping is about 2.5 inches for either size bolt.

TABLE A-23

SHEAR PIN AREA REQUIRED

Shear Pin Yield Strength (ksi)	Area Required at F, B, D (in^2) (See Fig. A-46)	Area Required at E (in^2)
30	180	220
85	65	80
150	40	45

Some modification of the lower support would be necessary to prevent binding under all conditions. Otherwise, further work would be required to determine the level of binding interference which would be acceptable. As a minimum, enough clearance should be provided to prevent binding during pump insertion and non-seismic operation. Table A-24 below gives the angle at which binding would occur if the pump moves off vertical, as a function of the clearance at the piston ring chamfers.

It is recommended that 0.25 inches of combined clearance be allowed to preclude binding under most conditions other than seismic loading. This assumes that the effects of static deflections are calibrated out and also does not include thermal distortions of the lower support structure which will be examined in a future study. An alternate method to increasing clearance would be to decrease the distance between the chamfers. This would have the same effect of increasing the binding angle.

A.8 GUARD TANK

The primary function of the guard tank is to contain the primary sodium in the event a sodium leak in the reactor vessel. The guard tank consists of a 1.5 inch shell that is supported by a 2.0 inch conical section at the top. A heavy section of approximately 6.0 inch is used to connect the shell with the conical section to mitigate the discontinuity effects in this region.

During normal operating conditions, the applied loads consist of the dead weight of the structure (without sodium) and the steady state thermal gradient. The dead weight of the sodium is not expected to be contained by the guard tank during normal operating conditions. But the sodium must be considered as a part of the design load for the tank and, for convenience, will be included as a normal operating load. The effects of a seismic event combined with a sodium leak are difficult to predict due to the interaction of the guard tank and the reactor vessel, and it seems to be unduly severe to require that the guard tank withstand the worst possible loads (the

TABLE A-24

BINDING ANGLE AS A FUNCTION OF CLEARANCE

Sum of Upper & Lower Diametral Clearance (Inches)	Angle From Vertical at Which Binding Occurs (Radians)
.20	1.33×10^{-3}
.22	1.47×10^{-3}
.24	1.60×10^{-3}
.26	1.73×10^{-3}
.28	1.87×10^{-3}

weight of all of the sodium under a seismic event) since the reactor vessel would still provide significant support for the contained sodium in the event of a leak.

To evaluate the tank vessel for dead weight conditions, a finite element model was developed using the axisymmetric conical shell element (STIF-61) from Reference 3. The model consisted of the 1.5 inch tank, the 2.0 inch conical section and the 6.0 inch transition section. This model is shown in Figure A-58. The dead weight of the tank was applied as a uniform acceleration in the vertical direction. The results show that the dead weight stresses are low and the maximum stresses occur at the top of the 1.5 inch shell with magnitudes of

$$\sigma_{AXIAL} = 200 \pm 1310 \text{ psi}$$
$$\sigma_{HOOP} = 510 \text{ psi}.$$

Then the maximum stress intensity for dead weight loading is

$$P_m = 510 \text{ psi}$$
$$P_L + P_b + Q = 1620 \text{ psi}.$$

When the dead weight of the sodium is included, these stresses increase by a factor of

$$\frac{W_{NA} + W_{ss}}{W_{ss}} = \frac{9.95 \times 10^6 + .88 \times 10^6}{.88 \times 10^6} = 12.3$$

and the stresses become

$$P_m = 12.3 \times 510 = 6270 \text{ psi}$$
$$P_L + P_b + Q = 12.3 \times 1620 = 19925 \text{ psi}$$

In each case, the stress intensities satisfy the limit for primary membrane stress intensity above.

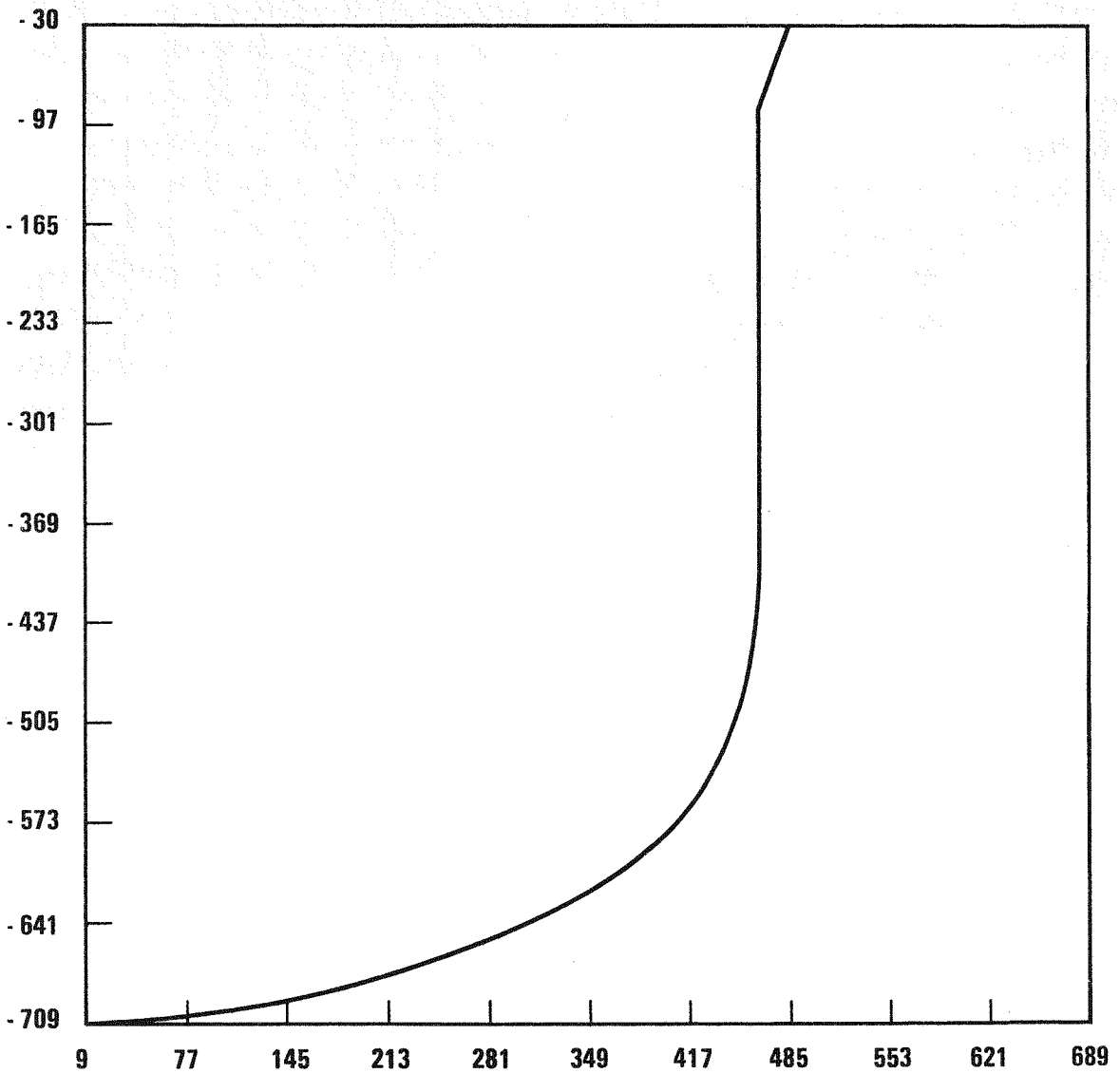

Figure A-58. Finite Element Model of the LPR Guard Tank

0665-

In addition to the dead weight loading, the steady state temperature distribution must also be considered. The top of the guard tank is at 120^{o}F and the temperature increases to 760^{o}F below the vessel shielding elevation. This temperature profile is shown in Figure A-59. The resulting longitudinal bending stress in the tank is shown in Figure A-60. The maximum thermal bending stress is 22000 psi and occurs 16 feet below the bottom of the deck. In the region, the thermal stresses are not superposed on the mechanical bending stresses so that the maximum stress intensity is 22000 psi.

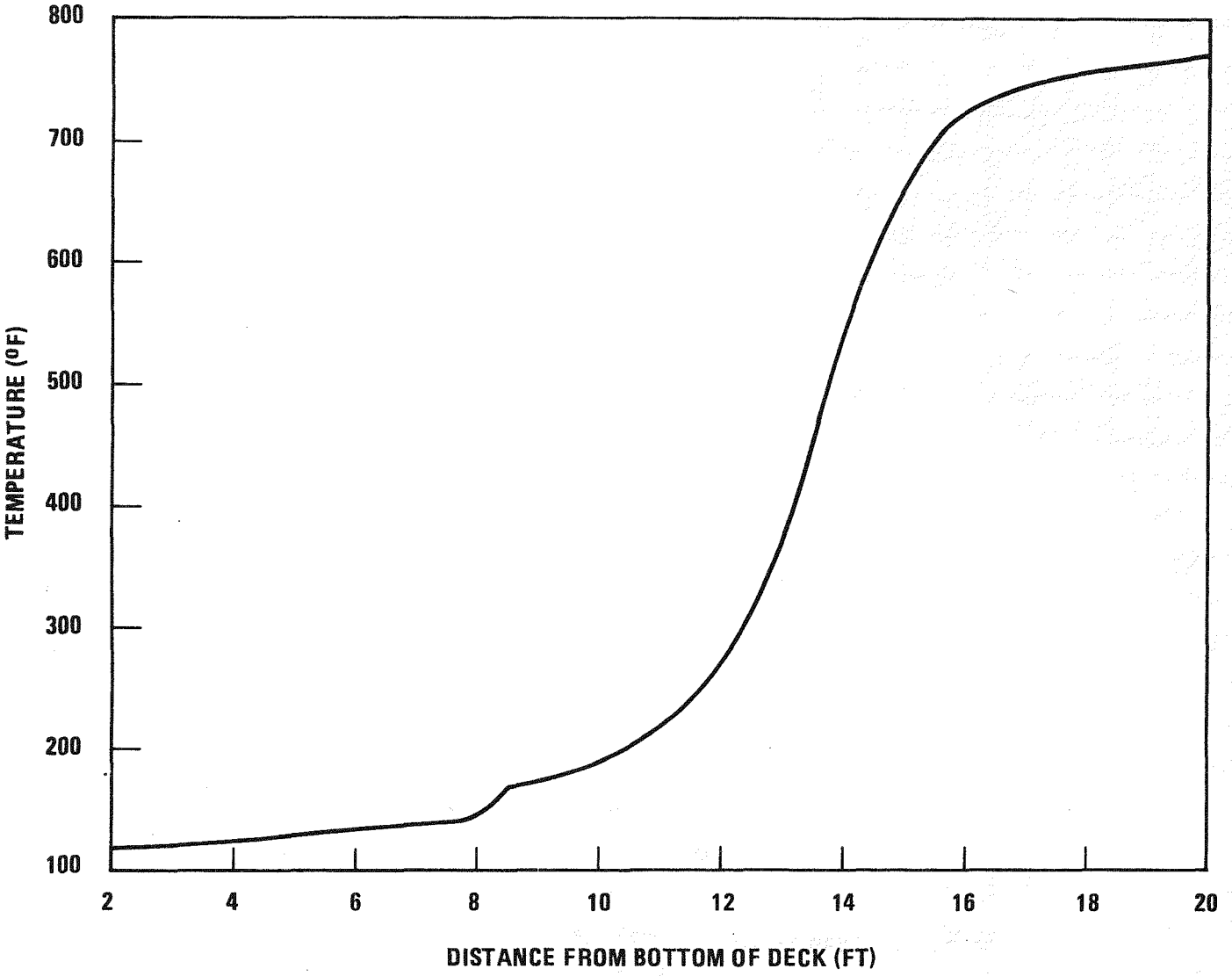

Figure A-59. Steady State Temperature Profile of LPR Guard Tank

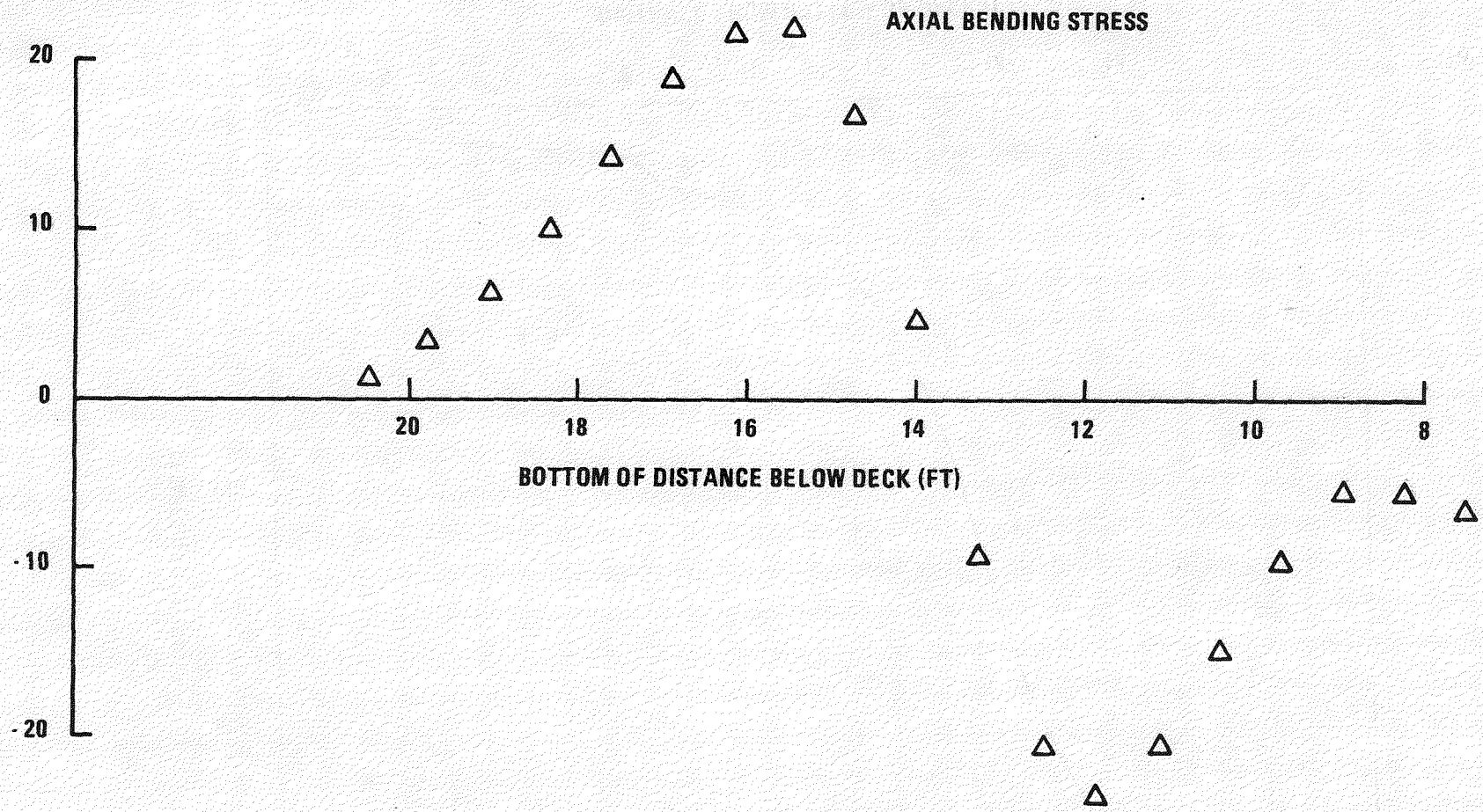

Figure A-60. Thermal Bending Stress in LPR Guard Tank

REFERENCES

1. J. F. Wett, LPR Interim Report, TR-78-30, 2/24/78.

2. J. E. Sharbaugh, LPR Design Weights, TR-78-49, 3/7/78.

3. J. A. Swanson, ANSYS Computer Program, Swanson Analysis Systems, Inc., 3/1/75.

4. Nuclear Systems Materials Handbook, TID-26666.

5. T. H. Thomas, et. al., Nuclear Reactors and Earthquakes, TID-7024, August 1963.

6. J. M. Thompson, Seismic Model of Reactor Vessel, LRS-78-255, 5/12/78.

7. American Society of Mechanical Engineers, Boiler and Pressure Vessel Code, Section III, 1977 Edition.

8. D. S. Griffin, High Temperature Structural Design Technology; Application, Quarterly Progress Report, WARD-SD-3045-1, December 1976.

9. C. S. Chang, "On the Torispherical Head Design for the Large Pool Reactor," TR-77-173, 12/12/77.

10. Shield, R. T. and Drucker, D. C., "Design of Thin-Walled Torispherical and Toriconical Pressure Vessel Heads", ASME JAM, pp. 292-299, June 1961.

11. J. M. Thompson, TR-77-169, "Preliminary Finite Element Evaluation of the Concept A Roof Structure", 12/8/77.

A. K. Dhalla, L. H. Sobel, Plastic Buckling of Axially Compressed Cylinders, WARD-SD-3045-9, November 1977.

APPENDIX B

DECK COOLING ANALYSIS

B.1 INTRODUCTION

Results of the LPR deck cooling analysis are documented in this Appendix. An active air cooling system is utilized to maintain the deck temperatures at acceptable levels. The adequacy of the deck cooling system to maintain a "cold" deck is demonstrated. At normal reactor operating conditions, the cold deck has:

- an average temperature of the deck primary boundary plate less than 150°F.
- an average temperature of the deck top plate less than 110°F.

The stationary portion of the deck and the rotatable plugs are analyzed separately. The following key items, discussed briefly below, are addressed in detail in this Appendix:

- A discussion of the deck cooling concept is presented. It consists basically of reflector plates to insulate the deck and an air cooling system to remove the heat transfered from the hot pool.
- A parametric study varying the number of thermal reflector plates used for deck insulation is conducted. A rationale is thus provided for selecting the reference design number of plates.
- Deck cooling system flow rates are defined to be compatible with the heat flux passing through the reflector plates and heating from deck mounted equipment that penetrates into the hot sodium pool.
- The cooling system plena geometry is sized, so that in conjunction with the system flow, efficient heat removal capability is provided and reasonable pressure drops are maintained.
- Verification analysis of the stationary deck is performed, using a 2-D thermal model.

- The thermal transient response of the stationary deck to a loss of air coolant accident is reported.
- The feasibility of a totally passive system, with specific application to the rotatable plugs, is presented in detail.

B.2 DECK COOLING CONCEPT

An active cooling system is utilized to maintain the temperature of both the stationary and the rotatable plug primary boundary plates below the $150^{o}F$ design temperature. Forced air is channeled through plena located directly above the deck primary boundary to remove heat flux transmitted from the pool. To mitigate this heating, thermal reflector plates are installed between the pool and the deck primary boundary plate. The cooling system is schematically illustrated in Figure B-1.

The deck cooling system is a network of parallel cooling compartments illustrated schematically in Figure B-2. Redundant suction fans draw air from the containment building through the individual stationary deck and rotatable plug discharge plena. Suction fans are used to ensure that the absolute pressure of the inert argon cover gas is greater than that of the coolant air. This prevents the possibility of air leakage into the vessel. Separate fan systems are used for the stationary portion and the rotatable plug portions of the deck.

A breakdown of the deck cooling compartments is as follows:

- 12 stationary deck cooling compartments, each segment circumferentially covering about 30^{o}, e.g., an IHX or a pump deck segment.
- 4 rotatable plug cooling compartments

A plan view of the stationary deck and rotatable plugs cooling plena is illustrated in Figure B-3. In addition, cooling is provided for the 6 IHX standpipes. A detailed description is provided in Section B.3.

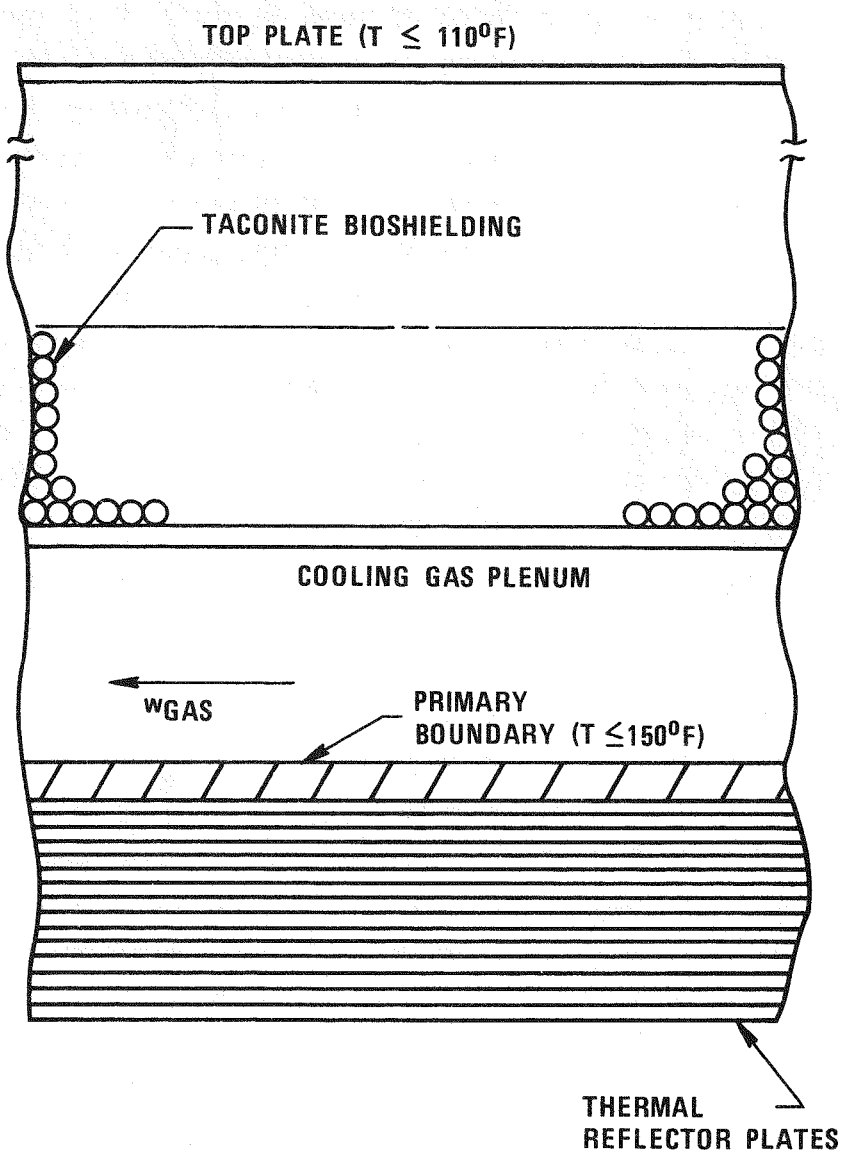

Figure B-1. LPR Deck Cooling Concept

0665-8

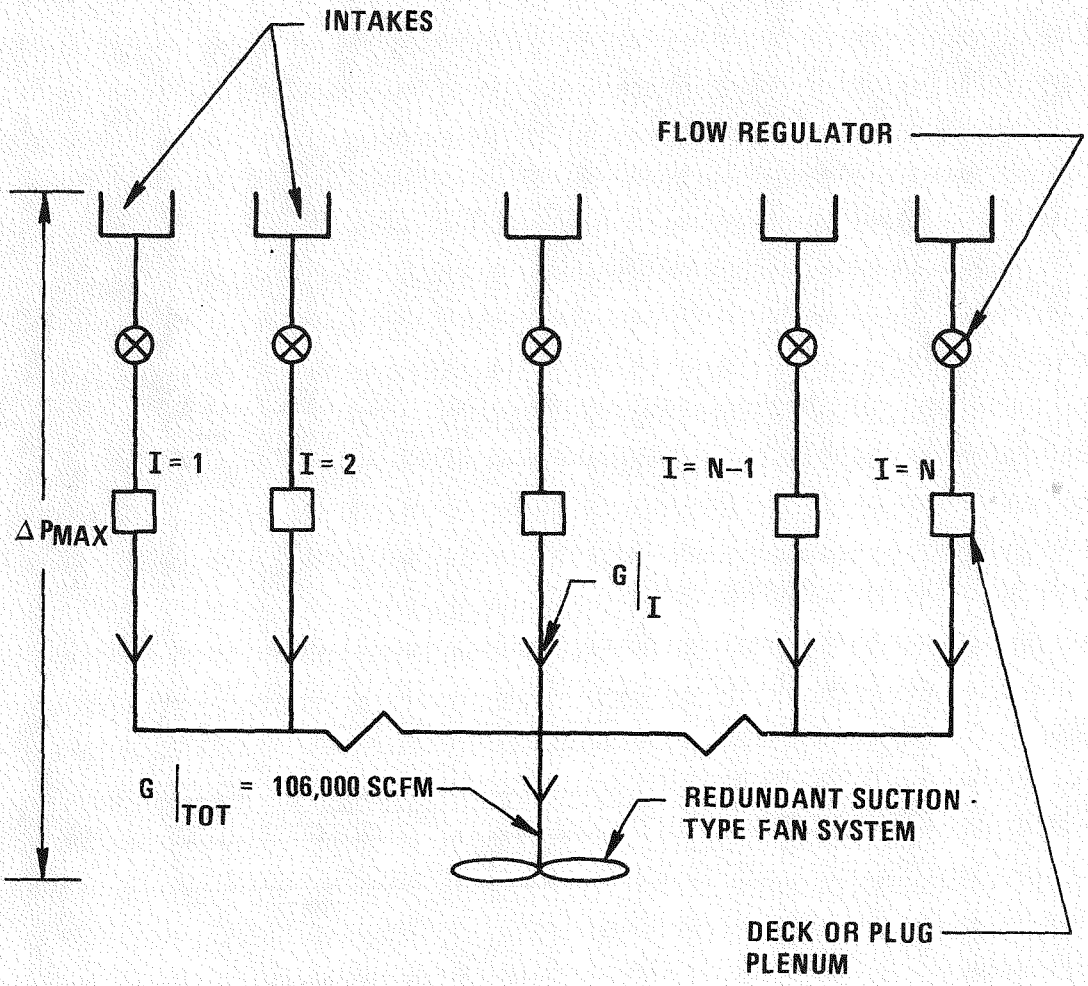

NOTE: 1) $G|_I \simeq$ 3000 - 6000 SCFM

2) ΔP_{MAX} = 27 INCHES H_2O

3) N = 22 COOLING COMPARTMENTS, TOTAL
   (a) 12 DECK COMPARTMENTS
   (b) 6 IHX STANDPIPES
   (c) 4 PLUG COMPARTMENTS

Figure B-2. Schematic of LPR Deck Cooling System

0665-9

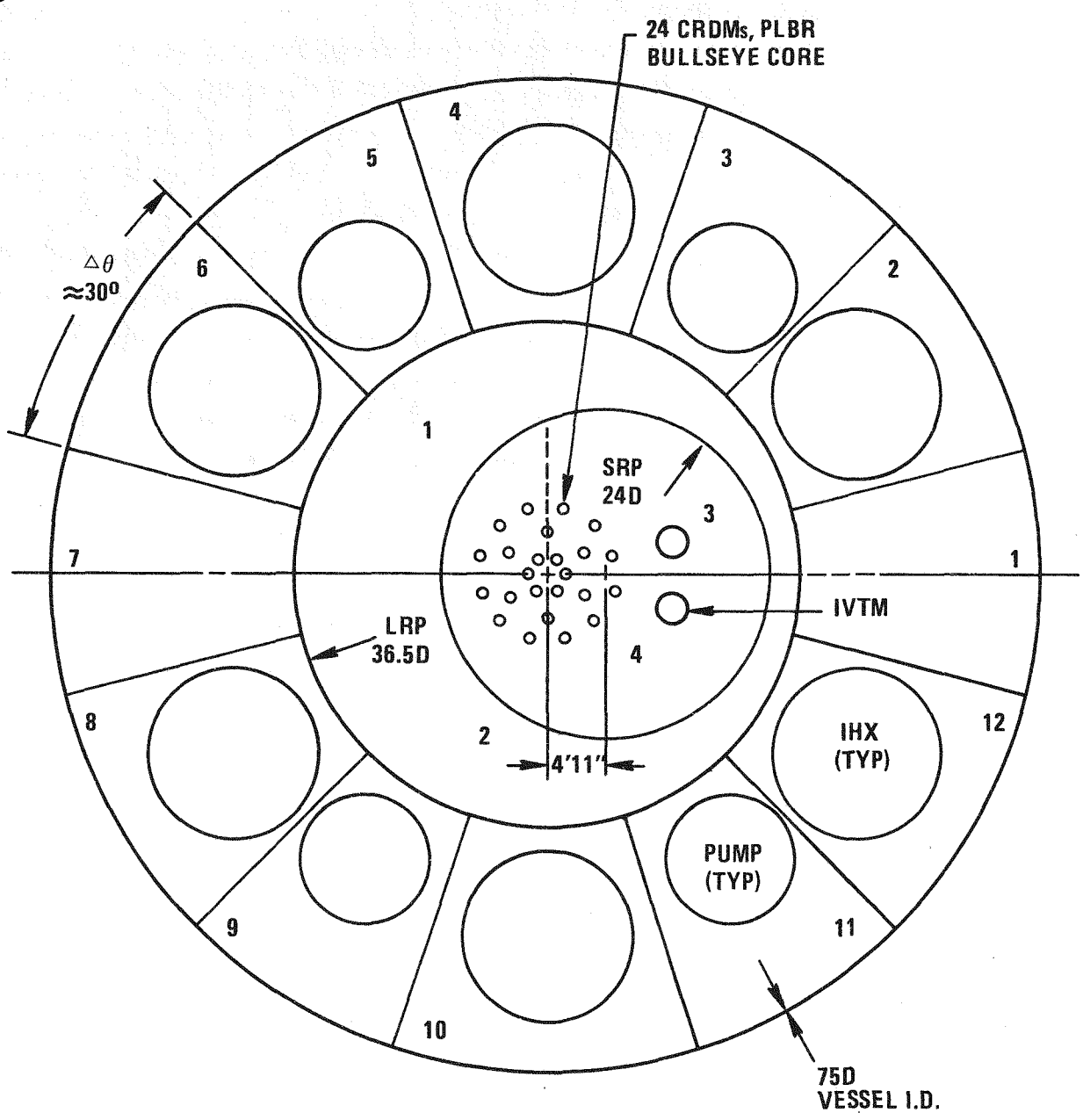

NOTE: 6 IHX STANDPIPES ARE COOLED

Figure B-3. Plan View of LPR Rotatable Plugs and Deck Cooling Plena

0665-

B.3 STATIONARY DECK ANALYSIS

Stationary deck cooling requirements are determined from the heat flux passing through the reflector plate insulation, and heating from deck mounted components that penetrate into the hot sodium pool. Nuclear heating is also factored in as a heating load. Based on the total heating, the flow requirements are determined to satisfy the deck temperature criteria. The cooling plena geometry is sized so that efficient heat removal capability is ensured. Flow velocities are sufficiently large to provide good heat transfer coefficients, but not too large so that the pressure drops are prohibitive. The effect of the air inlet temperature is evaluated.

A deck segment surrounding an IHX is selected for detailed analysis. From a standpoint of heating, an IHX segment is considered to be the most critical, since the penetration heating is more severe in this region, in contrast to the remainder of the deck. Scaling factors are then applied to obtain cooling requirements for the pumps and nominal deck segments (Figure B-3).

Verification analysis of the staionary deck is performed, utilizing a 2-D thermal model. In the same analysis, temperatures at the deck support are estimated. The transient response of the stationary deck to loss of gas coolant is evaluated.

B.3.1 STATIONARY DECK HEATING

Source heating to the deck is a result of thermal radiation from the hot pool and also of natural convection from the cover gas to the reflector plate insulation. Substantial heating from deck mounted equipment penetrating the pool such as the IHX also occurs. Nuclear heating from the activated sodium gamma rays, neutrons from the core, and cover gas radiation contribute to the deck heating. The net contribution of nuclear heating is relatively small (less than 10% of the total heating) and is considered in the analysis.

B.3.1.1 REFLECTOR PLATE HEAT FLUX PARAMETER STUDY

The stationary deck reference design includes 20 reflector plates located between the deck and the pool. To optimize the number of plates, a parametric study is conducted, allowing the number of plates to vary. A description of the reflector plates physical constants is given in Table B-1.

TABLE B-1

REFLECTOR PLATE DESCRIPTION

Material	Stainless Steel
Emissivity	0.28
Plate Thickness	0.15 inches
Nominal Center to Center Spacing*	0.9 inches
Spacer Conduction Area	2.7% of plate system area

A 1-D thermal model is utilized in the analysis, shown in Figure B-4. Effects of natural convection and radiation between the pool and the first plate are simulated. Between the plates the following modes of heat transfer are: radiation (emissivity = 0.28), Argon gas conduction and a spacer conduction based on 2.7% of the vessel surface area. Nuclear heating is included. Major equipment penetration heating is not included, but is calculated separately.

Shown in Figure B-5 is a plot of the reflector plate heat flux versus the number of reflector plates, corresponding to a primary boundary plate temperature of $150^{o}F$. At the 20 reflector plate reference design point, the heat flux is 210 $Btu/hr\text{-}ft^{2}\text{-}^{o}F$ for an emissivity equal to 0.28. No significant heat flux saving is obtained by increasing the number of

*The spacings are less for 30 and 40 plate arrays to be consistent with a 23 inch elevation constant below the deck.

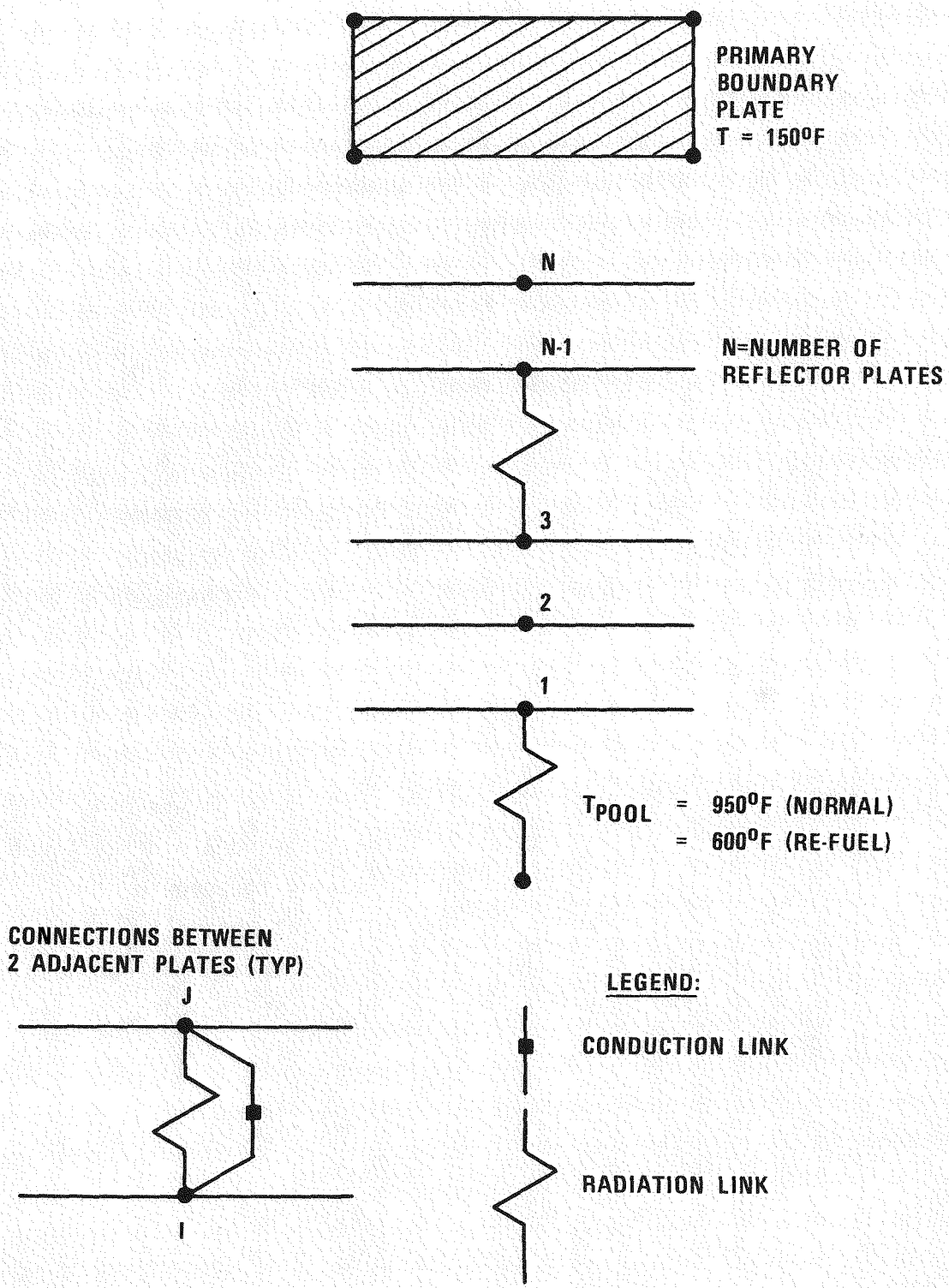

Figure B-4. 1-D Thermal Model of Reflector Plate Array

0665-11

and Emissivity = 0.28

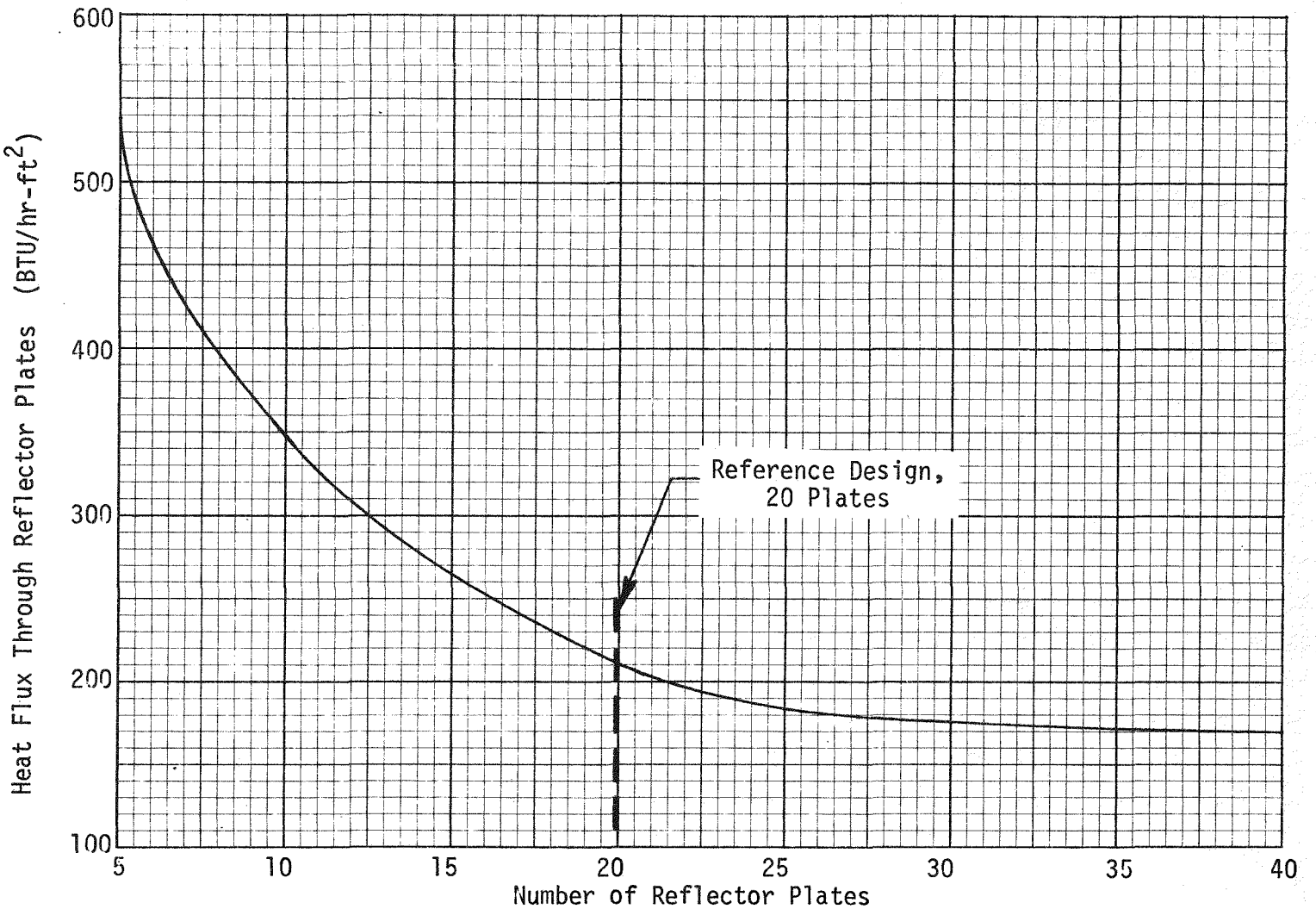

Figure B-5. Reflector Plate Heat Flux Versus Number of Reflector Plates

plates, with respect to a 23 in elevation constraint imposed.** On an integrated basis over the surface area of the deck, the reflector plate heat flux is 525,000 Btu/hr. The stationary deck area excluding the equipment penetration ports is 2500 ft.^{2}. The heat flux variation versus the number of reflector plates is summarized in Table B-2.

TABLE B-2

RESULTS OF 1-D REFLECTOR PLATE PARAMETER STUDY

Number of Reflector Plates	Heat Flux (Btu/hr-ft^2)
5	538
10	347
20	210
30	175
40	170

B.3.1.2 PENETRATION HEATING/DECK HEAT LOAD SUMMARY

All heating loads inclusive of major penetration heating are tabulated in Table B-3. IHX standpipe heating is also included, in addition to the wicking effect. This results from heat, estimated as 40 BTU/hr-ft^2, flowing radially outward from the hot core of the IHX into the deck, over the 13 ft height of the deck. The integrated heating for the 6 standpipes is 108,000 BTU/hr.

**This places a limit on the length for heat conduction through the spacers, which has been shown to be significant. It therefore is possible to achieve a greater heat flux savings with N = 30 and 40 plates by increasing the path length for spacer conduction. The 23 inch limit is required, however, for minimizing the deck thickness and still maintain the structural integrity of the stationary deck, without having to increase the reactor vessel elevation. This constraint does not exist in the center plug region.

TABLE B-3

STATIONARY DECK HEAT LOAD SUMMARY

Region	Q (Btu/hr)
Reflector Plates	525,000
6 IHXs (Penetration)	127,000
4 Pumps	31,000
2 Cold Traps	11,000
IHX Standpipes (6 Total)	108,000
Total	802,000

Effects of minor penetrations such as the low level flux monitors are neglected. The major penetration heat loads of Table B-3 are calculated in a conservative fashion.

B.3.2 STATIONARY DECK COOLING

Deck coolant flow requirements, compatible with the deck heating and a 150^{o}F deck, are defined in this section. A parameter study is conducted accounting for all of the significant variables as a function of flow. Detailed analysis is performed for an IHX deck segment. From the detailed cooling analysis of typical deck sections, the total deck cooling requirements are synthesized.

B.3.2.1 DECK COOLING PARAMETER STUDY

A parametric analysis is conducted to determine the deck cooling flow requirements. Since many variables are involved, the determination of the flow rate is not a straightforward calculation based on a simple enthalpy rise in air coolant stream. Rather, a more complex solution is required involving inter-relationships of many parameters. Among the most significant parameters are:

- o 150^{o}F deck temperature
- o variable system geometry
- o air coolant inlet temperature

- o air coolant temperature rise
- o required heat transfer coefficient
- o calculated heat transfer coefficient

The determination of the design coolant flow rate evolves from the following three procedures, whereby all significant parameters can be related directly to flow.

- o The coolant flow required to remove heat from an IHX deck segment is calculated as a function of coolant temperature rise. Of the 12 stationary deck cooling plena (see Figure B-3), the webbed segment surrounding an IHX is considered to be the most critical from a standpoint of heat flux and coolant flow, because penetration heating is more significant in this region and the large IHX tends to restrict the coolant flow, as shown in Figures B-6 and B-7. Flow requirements for the four pump segments and the two nominal segments are later conservatively calculated on the basis of appropriate scaling factors.

  Figure B-8 shows the variation of the air coolant temperature rise as a function of the flow. Including the wicking effect, the average deck heat flux in the region of an IHX is 300 BTU/hr-ft^2, and the deck area is 245 ft^2, this resulting in a heat load of 73,500 BTU/hr. The variation of the coolant temperature rise versus the flow (Figure B-8) provides the most fundamental relationship needed.

- o A correlation expressing the relationship between the required heat transfer coefficient, the air inlet temperature, and the air coolant temperature rise is given by

$$h_{REQ} = q \; / \; (T_{PB} - \overline{T}_{AIR})$$

where, on a unit area basis,

$$q = \underline{300 \text{ BTU/hr-ft}^2}$$

and T_{PB} = Specified primary boundary plate temperature

$$= \underline{150^{\circ}F}$$

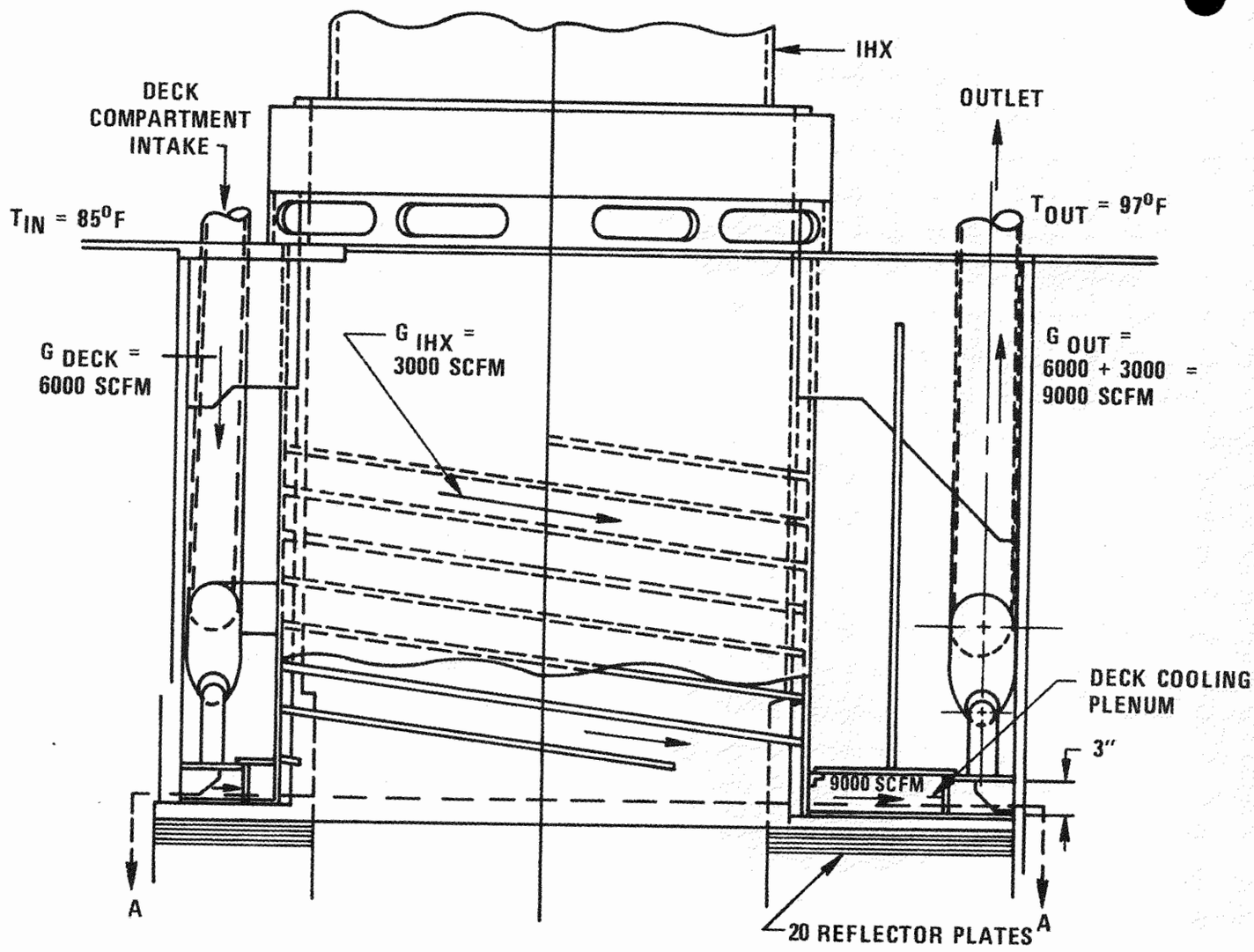

Figure B-6. Cooling Plena Schematic for Deck and IHX Stand Pipe

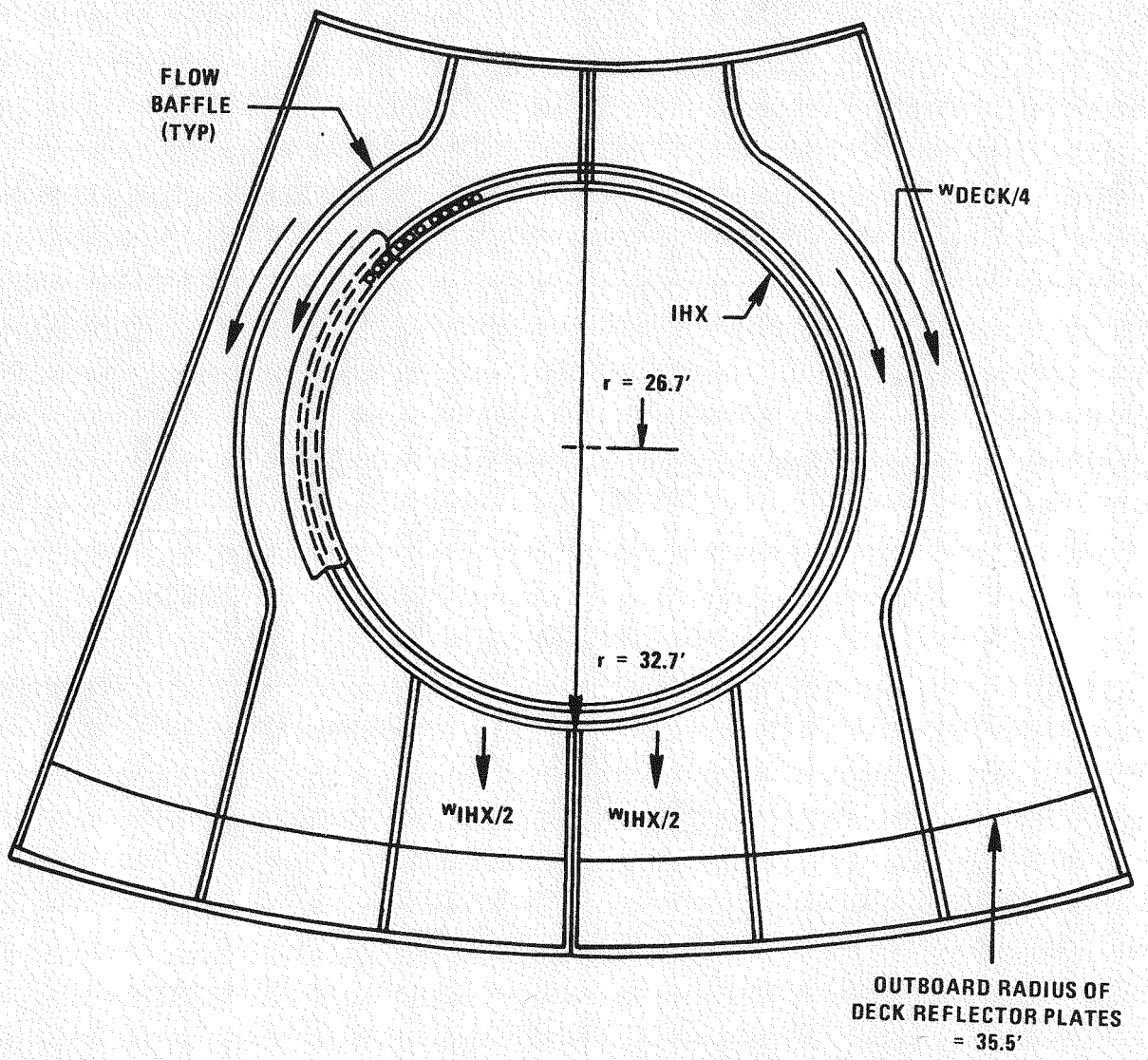

NOTE: SECTION A-A OF FIGURE B-6 SHOWN

Figure B-7. Plan View of IHX Deck Segment Cooling Plenum

0665-131

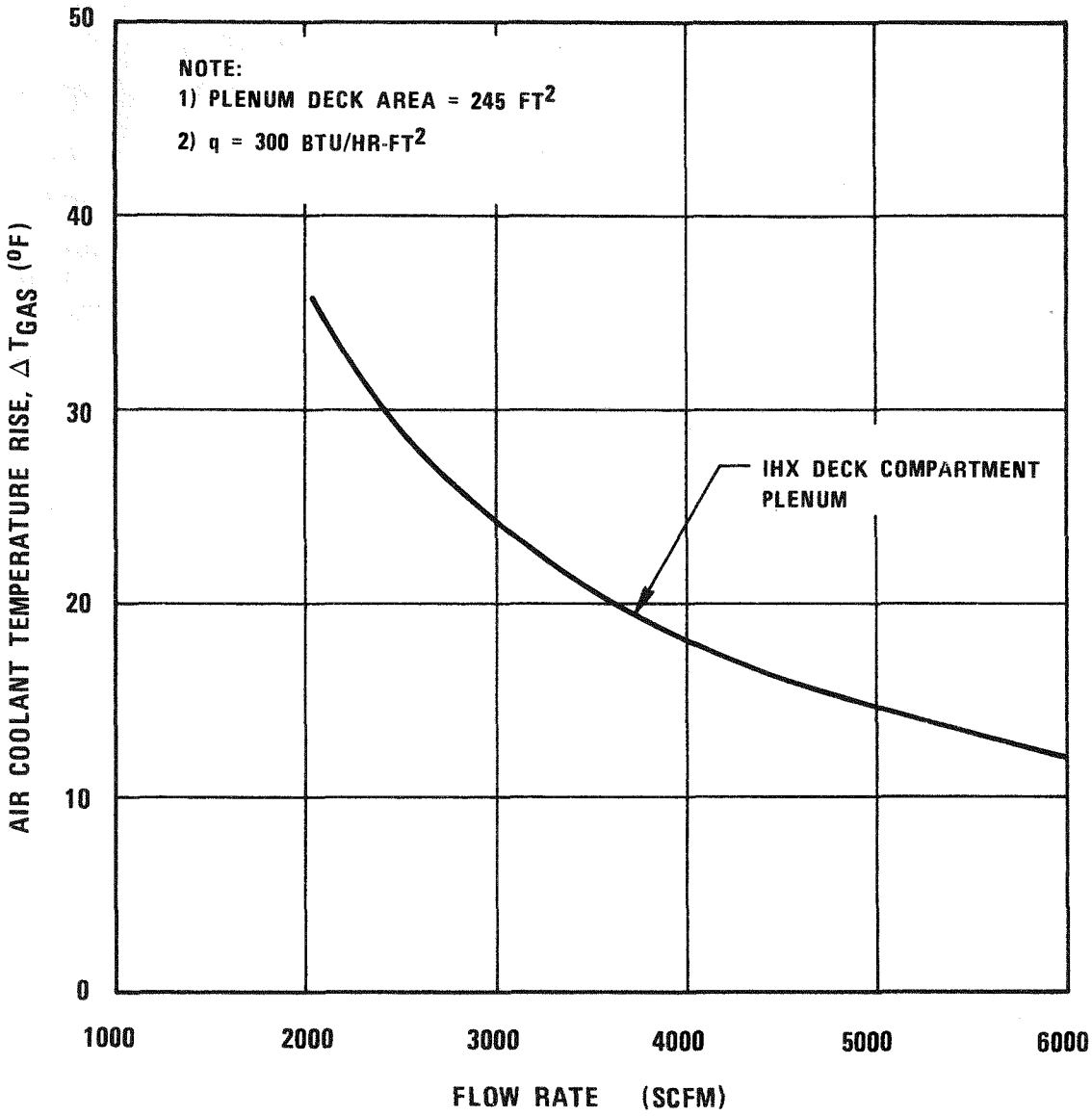

Figure B-8. Bulk Coolant Temperature Rise Versus Air Coolant Flow Rate

0665-14

$$\bar{T}_{AIR} = T_{INLET} + \Delta T_{AIR}/2$$

Applying the above definition of the required heat transfer coefficient, the variation of h_{REQ} as a function of the air coolant temperature rise, ΔT_{AIR}, is presented in Figure B-9. The air inlet temperature is varied as a parameter. Air inlet temperatures of 70^{o}, 85^{o} and $100^{o}F$ are considered. The variation of h_{REQ} versus ΔT_{AIR} provides the second needed correlation for selection of coolant flow. Since ΔT_{AIR} versus flow is known per Figure B-8, h_{REQ} versus flow is obtained indirectly.

- For efficient heat transfer, the calculated heat transfer coefficient, h_{CALC}, should be approximately equal to the required heat transfer coefficient,

$$h_{CALC} \geq h_{REQ}$$

The calculated heat transfer coefficient corresponds to the coolant flow and plenum geometry. Assuming fully developed turbulent flow through a duct, h_{CALC} is given by the standard expression

$$h_{CALC} = 0.023\, \alpha v\, c_p/Re^{0.2}Pr^{1/3}$$

where, in compatible units,

α = density
v = velocity
c_p = specific heat
Re = Reynolds Number
Pr = Prandtl Number

In terms of flow, channel cross-section area, and hydraulic diameter, the above expression can be re-arranged

$$h_{CALC} = 0.01185 \frac{w^{0.8}}{A^{0.8}} D_H^{-0.2} \quad @\ 100^{o}F \text{ Preference Properties}$$

where w = flow in SCFM
A = area, ft^2
D_H = hydraulic diameter, ft

The variation of the calculated heat transfer coefficient as a function of flow is shown in Figure B-10, at the inlet, restricted, and outlet radii of the plenum. Referring to Figure B-7, it is seen that the flow passage varies radially. This gives rise to variable flow velocities and heat transfer coefficients. At the

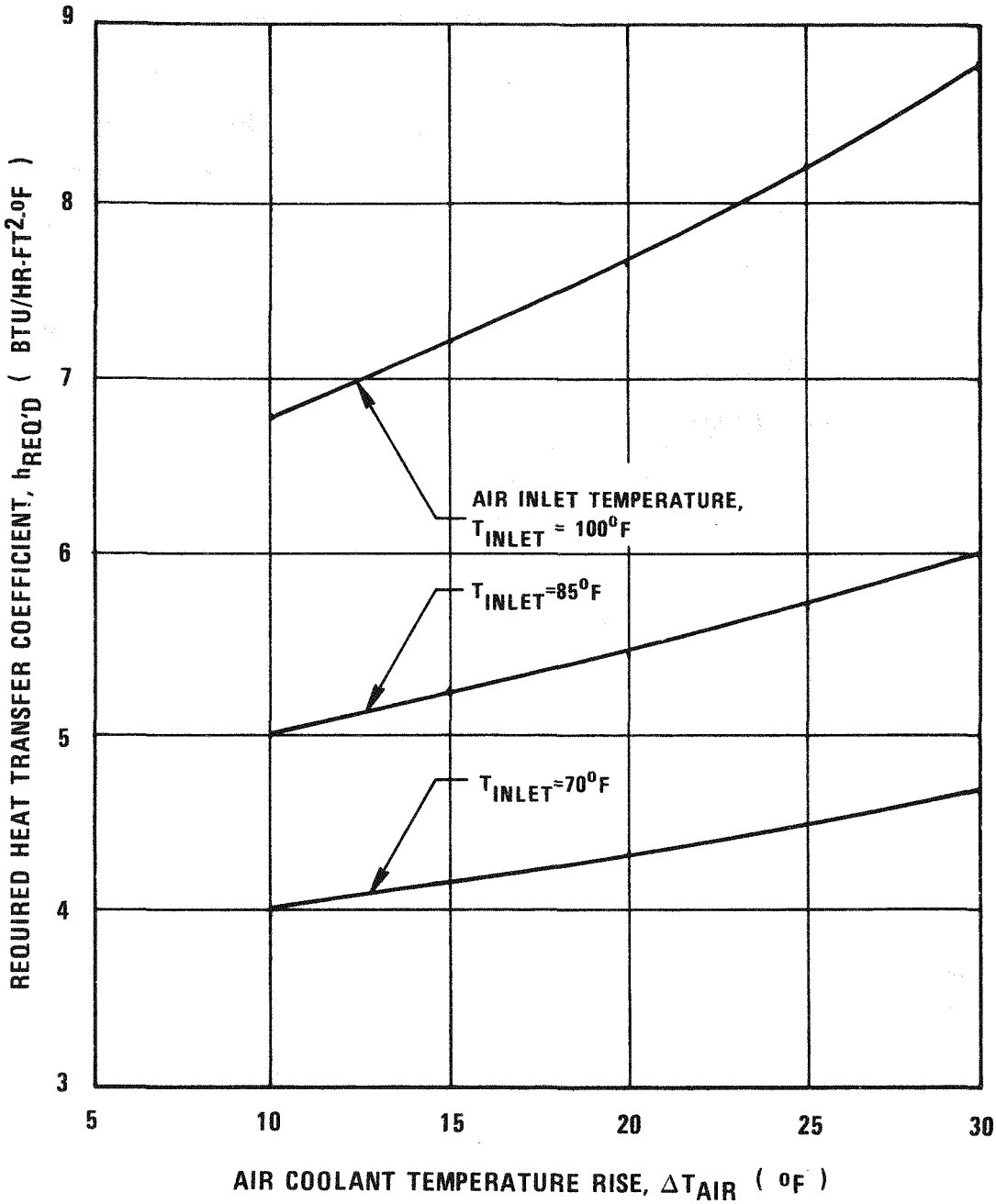

Figure B-9. LPR Deck Cooling Plena Required Heat Transfer Coefficient Versus Air Coolant Temperature Rise

0665-12

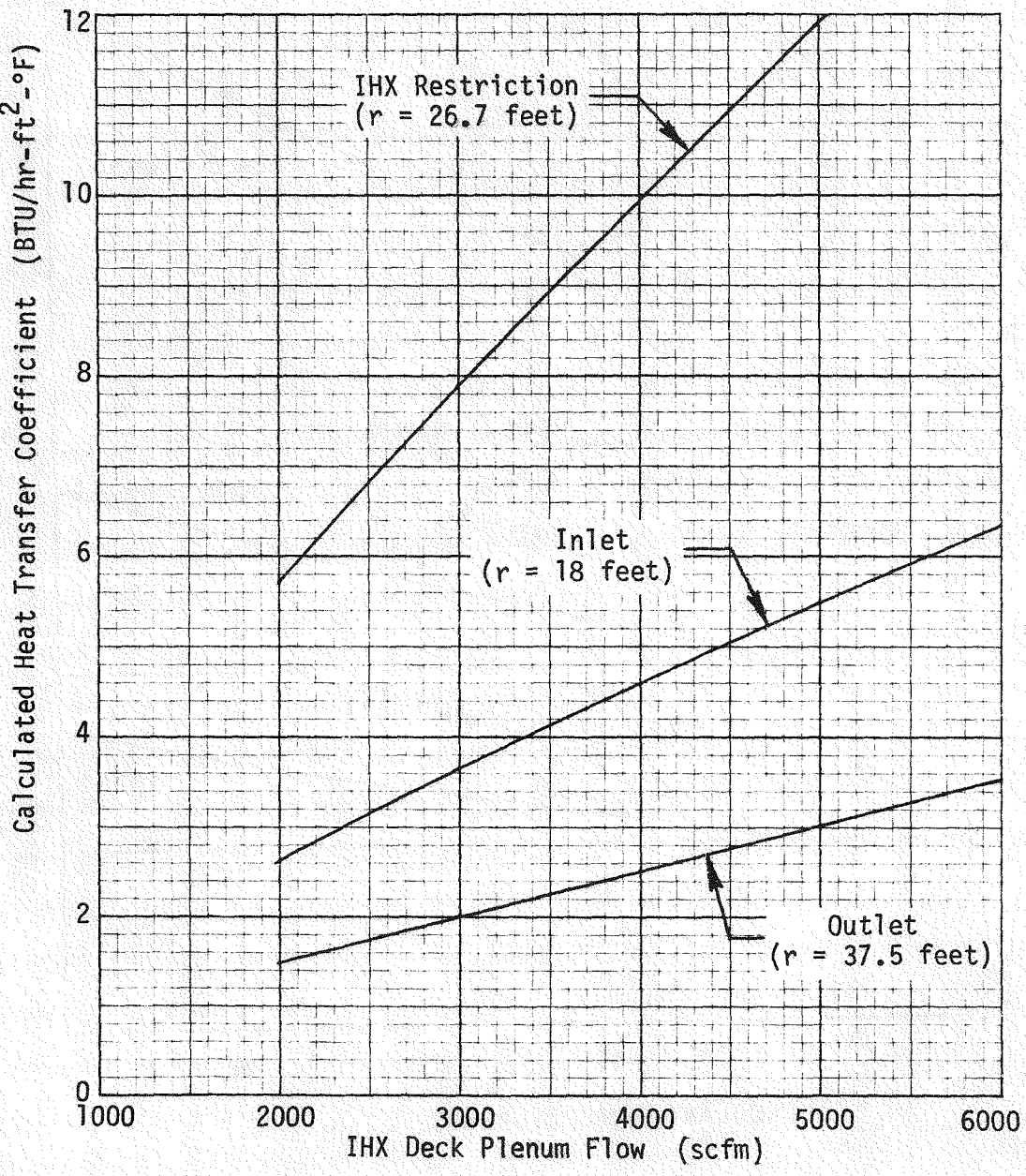

Figure B-10. IHX Deck Cooling Plenum Calculated Heat Transfer Coefficient Versus Flow

outset of the analysis, by a trial and error method, placement of a horizontal baffle at a height of 3 in above the primary boundary plate resulted in favorable flow velocities required for good heat transfer, roughly between 30 to 60 ft/sec. These velocities further do not result in prohibitive pressure drops. A summary of the channel geometry is presented below:

Region	Radius ft	Flow Channel Area (ft^2)	Hydraulic Diameter, D_H (ft)
Inlet	18	2.83	0.46
IHX Restriction	26.7	1.11	0.41
Outlet	37.5	5.89	0.47

Advantage is also taken of the IHX standpipe flow which joins the nominal deck segment flow radially outboard of the IHX proper. See Figure B-6. This topic is addressed in greater detail in Section B.3.2.3.

Figures B-8, B-9, and B-10 directly or indirectly relate all significant parameters to flow, permitting selection of the design basis flow. Calculated and required heat transfer coefficients are matched, considering effects of air inlet temperatures.

B.3.2.2 SELECTION OF DESIGN BASIS COOLANT FLOW

Shown in Tables B-4 and B-5, respectively, are summaries of required and actual plenum heat transfer coefficients, tabulated as functions of the supply gas flow rate. Table B-4 is obtained from results presented in

TABLE B-4

REQUIRED PLENUM HEAT TRANSFER COEFFICIENTS VERSUS COOLANT FLOW

Coolant Flow (SCFM)	ΔT_{air} (^oF)	$h_{required}$ (BTU/hr-ft^2-^oF*) Air Inlet Temperature, T_{in} T_{in} = 70^oF	T_{in} = 85^oF	T_{in} = 100^oF
3000	24	4.5	5.7	7.9
4000	18	4.3	5.4	7.3
5000	15	4.2	5.3	7.1
6000	12	4.0	5.1	6.8

*150^{o}F deck criterion reflected in the $h_{REQUIRED}$

Figures B-8 and B-9; results in Table B-5 are obtained from Figure B.10, at the locations identified in Figure B-7. The flow velocities of Table B-5

TABLE B-5

CALCULATED PLENUM HEAT TRANSFER COEFFICIENTS VERSUS COOLANT FLOW

Coolant Flow (SCFM)	h (BTU/hr-ft^2-^{o}F) r (feet)			V (ft/sec) r (feet)		
	18	26.7	37.5	18	26.7	37.5
2000	2.6	5.7	2.0	12	30	8
3000	3.7	7.9	2.8	18	45	13
4000	4.7	10.0	3.5	24	61	17
5000	5.4	12.0	4.2	29	76	21
6000	6.3	14.0	4.9	35	91	25

are obtained from flow continuity. Based on a comparison of heat transfer coefficients, a design flow of 6000 SCFM at a gas inlet temperature of 85^{o}F is selected for the following reasons:

- At 6000 SCFM and at an inlet temperature of 85^{o}F, the actual heat transfer coefficients (Table B-5) are, on the whole, greater than the required heat transfer coefficient of 5.1 Btu/hr-ft^2-^{o}F (Table B-4); i.e., at r = 18, 26.7 and 37.5 feet, the calculated h's are 6.3, 14.0, and 4.9 Btu/hr-ft^2-^{o}F, respectively. It is noted in Table B-5 that if the flow is decreased, the calculated h's become increasingly more marginal. See Figure B-11 for the locations of the calculated heat transfer coefficients, and corresponding flow velocities. The bulk coolant temperature rise is 12^{o}F, per Table B-4.

- At an air inlet temperature of 100^{o}F, the required h's of Table B-4 exceed the calculated h's of Table B-5 at all of the flow rates considered. Increasing the flow above 6000 SCFM to obtain higher calculated h's would incur more severe system pressure drops, and correspondingly, increased fan horsepower requirements.

- At an air inlet temperature of 70°F, the required h's are lowest, but from discussion with A-E personnel, supplying inlet air at this temperature would incur more prohibitive penalties on the containment HVAC, which processes the stationary deck and rotatable plug discharge air. An inlet temperature of 85°F is substantially more acceptable from an HVAC standpoint.

  It is noted in Table B-5 that variable heat transfer coefficients are obtained over the path length in the deck cooling compartment of Figure B-11. The non-uniform cooling could possibly result in adverse radial temperature gradients in the primary boundary and plenum structure. It is felt, however, that the potential gradients would be substantially smoothed out by lateral conduction in the 3 inch thick primary boundary plate.

B.3.2.3 TOTAL DECK COOLING

Flow requirements for the six IHX standpipes are defined in this section. Scaling factors are applied to the IHX deck segment flow to obtain flow requirements for the 4 pump segments and 2 remaining segments of the total of 12 deck segments.

B.3.2.3.1 IHX DOWNCOMER COOLING

Cooling of the IHX downcomer or standpipe serves a dual purpose:

- Remove a radial heat load of 18,000 BTU/hr from each IHX, over the elevation (≈13 ft) penetrating the deck. This heat emanates from the hot core of the IHX, which is insulated to limit the radial heat flux at the IHX shell surface to a maximum of 40 BTU/hr-ft^2.

- Provide additional flow to the IHX deck plenum at the outboard region of the deck. In addition to cooling the IHX downcomer, providing the extra flow at the wider outboard region of the deck ensures higher flow velocities required for good heat transfer, where velocities otherwise would decrease. Equally important, with the IHX flow augmenting the deck flow, a smooth overall flow field is maintained since the deck inlet flow is not required to make a full turn about the IHX, resulting in possible stagnation regions. See Figures B-6 and B-11.

  A flow of 3000 SCFM is calculated for each IHX downcomer. This flow is more than adequate to remove the radial heat load of 18,000 BTU/hr.

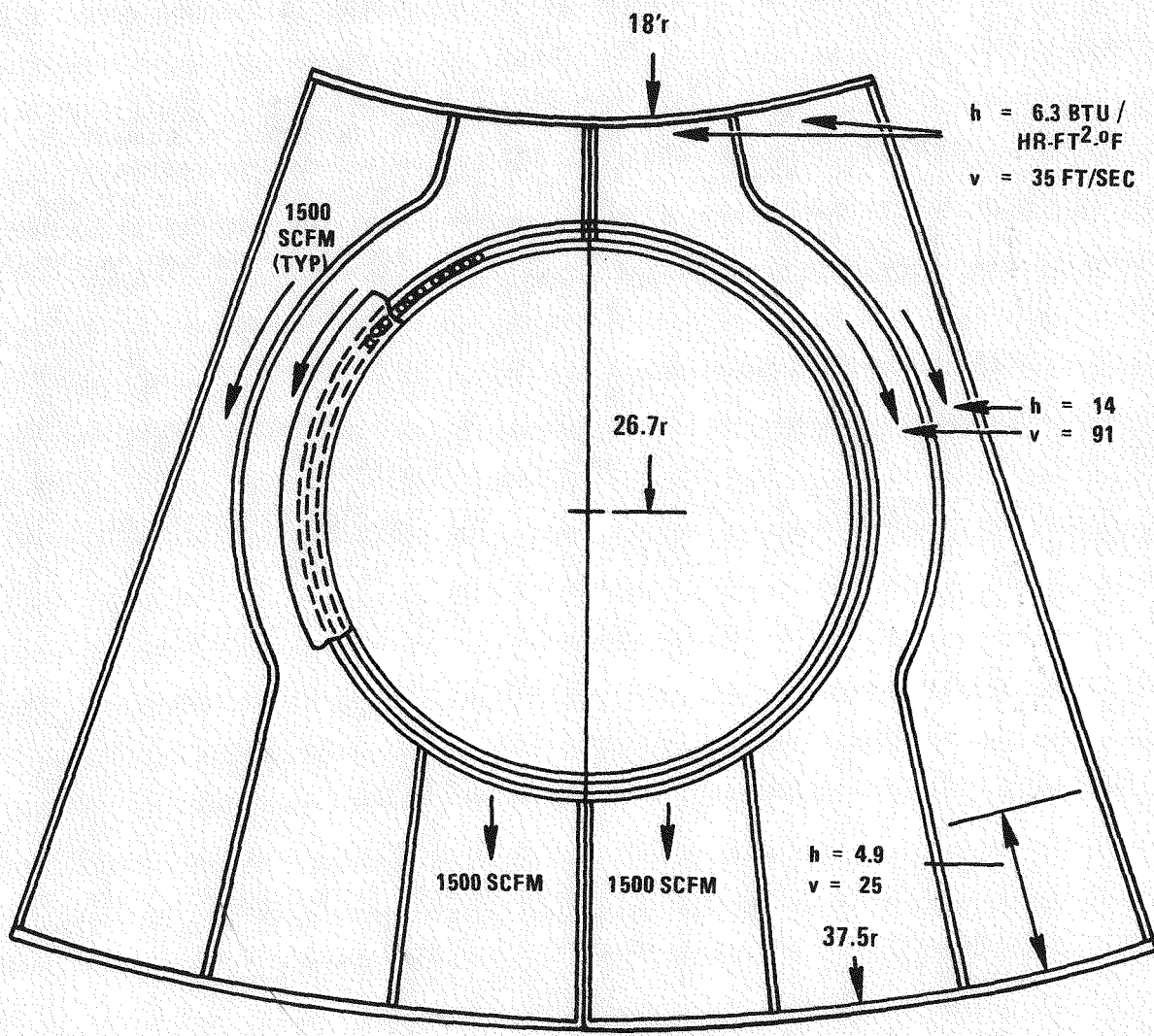

NOTE: TO MAINTAIN PRESSURE BOUNDARY PLATE AT $T \leq 150^{o}F$, $h_{REQUIRED} = 5.1$ BTU/HR-FT^{2}.^{o}F

Figure B-11. IHX Deck Segment Heat Transfer Coefficients and Velocities at Design Flow Condition

0665-132

B.3.2.3.2 DECK COOLING FLOW SUMMARY

Area scaling factors are applied to determine flows for the remaining 6 deck segments, e.g., the segments surrounding a pump. An overall deck heat flux of 300 BTU/hr-ft^2 is applied in combination with the area scaling factors to result in a coolant flow of 6000 SCFM for each of these segments. The total deck flow rate is summarized in Table B-6.

TABLE B-6

LPR STATIONARY DECK SEGMENT COOLING SUMMARY

Region	Number of Segments	Flow per Segment, SCFM	Flow, SCFM
IHX Deck	6	9000*	54000
Pumps	4	6000	24000
Nominal	2	6000	12000
		TOTAL	90000

*Includes IHX Downcomer Flow

B.3.2.4 DECK FAN SYSTEM HORSEPOWER REQUIREMENTS

A worse case pressure drop of 13.5 inches of water is determined, considering the entire deck cooling system. Since the manifolding system and flow regulation system was only conceptually defined at the time of the analysis, the ΔP is doubled to 27 inches of H_2O providing an uncertainty factor of 2.0 to the deck cooling system.

Combined with the 27 inches of water pressure drop, and with respect to the total deck flow of 90,000 SCFM, a total theoretical horsepower rating of 382 H.P. is obtained for the stationary portion of the deck. Assuming an efficiency factor of 0.7, the actual horsepower is 546 H.P.

B.3.2.5 STATIONARY DECK COOLING SYSTEM PARAMETER SUMMARY

The LPR stationary deck cooling system parameters are summarized in Table B-7.

TABLE B-7

LPR DECK COOLING SYSTEM-SYSTEM PARAMETERS

Quantity	Value
Primary Boundary Plate Design Temperature	150°F
Deck Top Plate Design Temperature	110°F
Total Stationary Deck Heat Load	800,000 BTU/hr
Design Flow Rate (Max.)	90,000 SCFM
Air Coolant Inlet Temperature	85°F
Air Coolant Temperature Rise	12°F
Maximum System Pressure Drop	27 inches H_2O
Total Fan Horsepower (70% effective)	546
System Uncertainty Factor (Reflected in Fan Horsepower)	2.0

Verification of the cooling system is made in the following section, based on a 2-D thermal analysis.

B.3.3 STATIONARY DECK COOLING VERIFICATION DURING NORMAL OPERATION

B.3.3.1 DISCUSSION

To verify the deck cooling system, a 2-D thermal analysis is performed. The purpose of the analysis is:

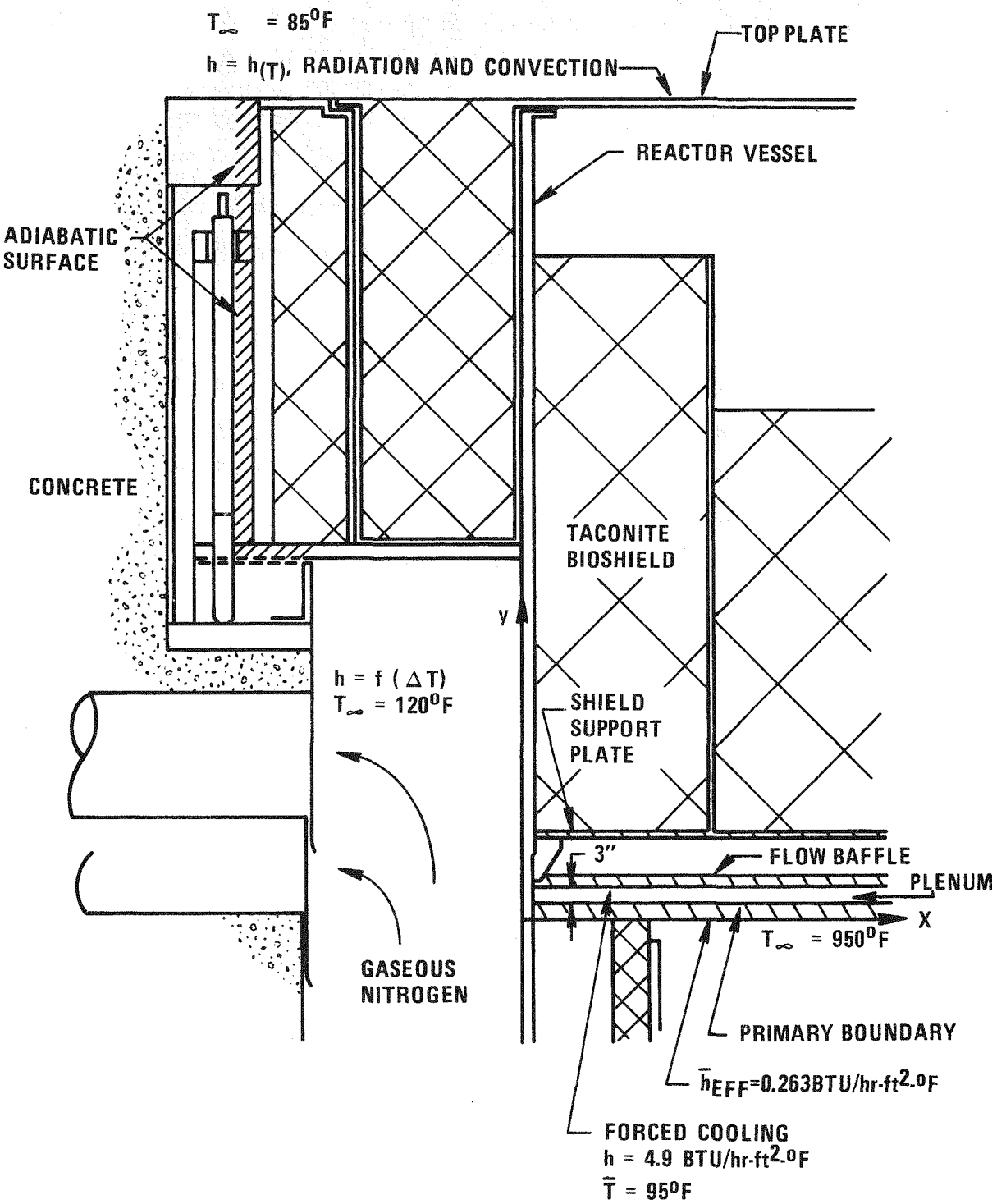

Figure B-12. LPR Stationary Deck Elevation View at Deck Support Region

0665-92

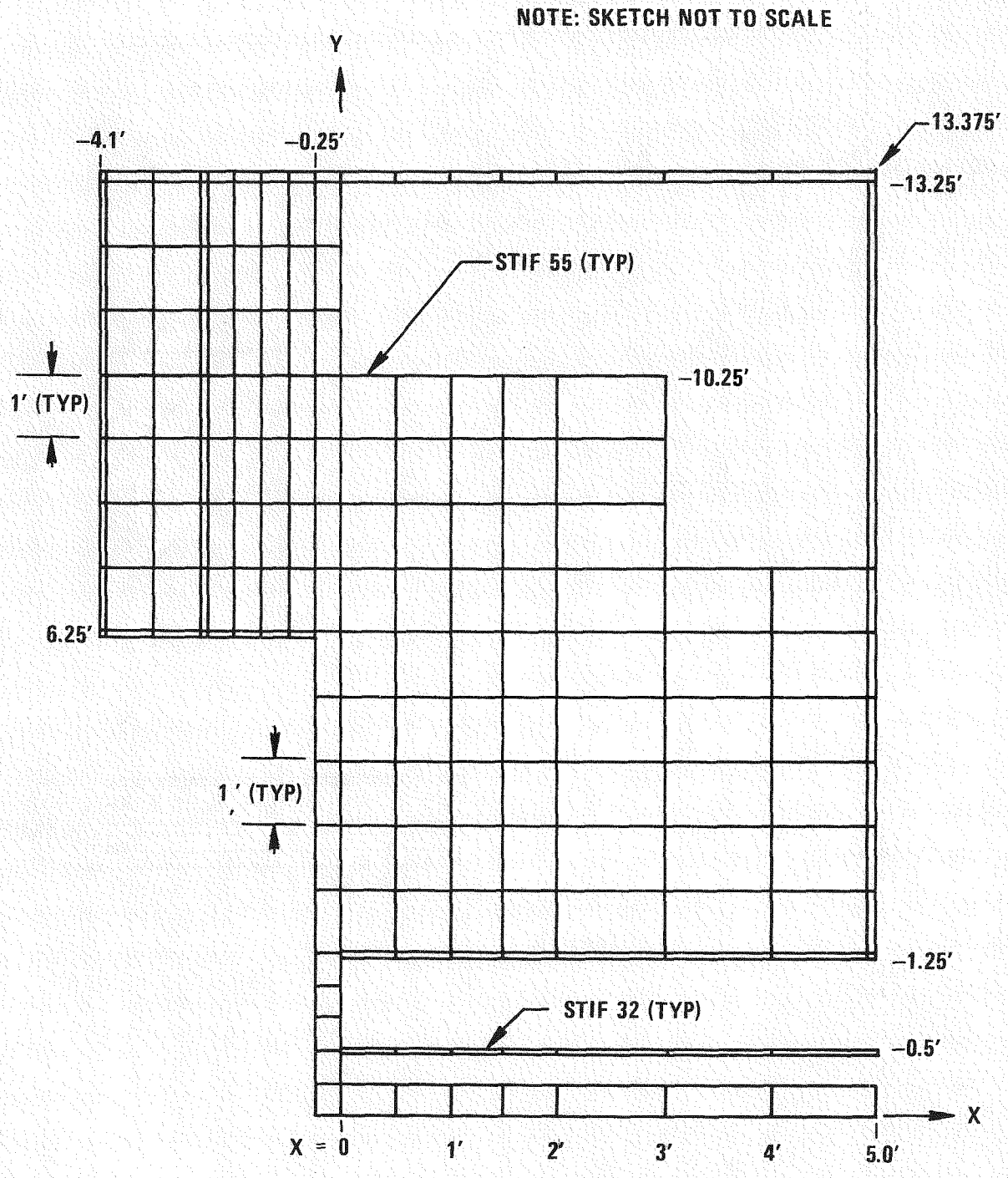

Figure B-13. ANSYS Thermal Model of LPR

0665-91

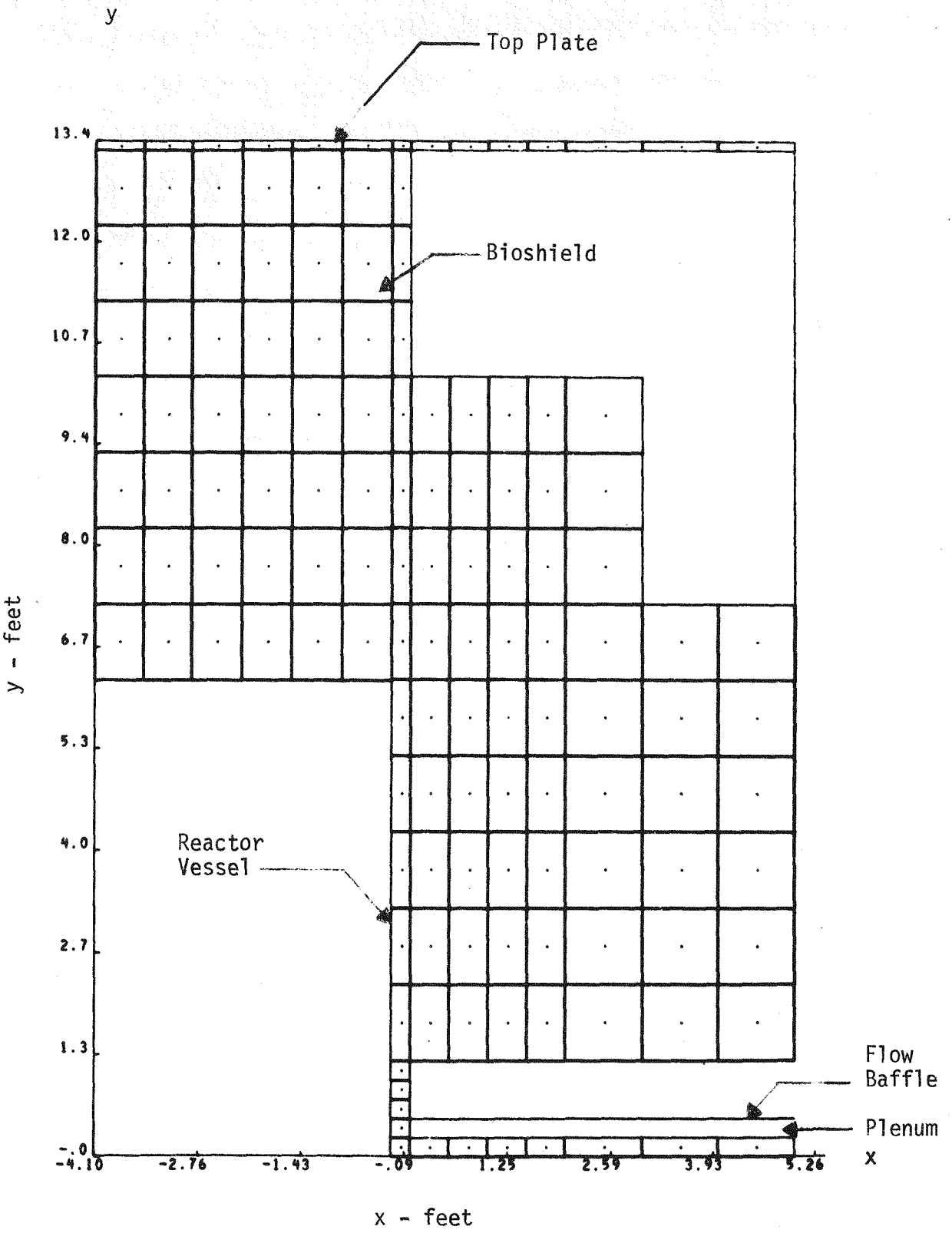

Figure B-14. ANSYS Verification Plot of LPR Stationary Deck Model

- o ensure that primary boundary plate and top plate temperatures are maintained at or below 150°F and 110°F, respectively, at simulated design basis flow conditions

- o predict temperatures in the region of the deck interface, ensuring that no potentially adverse temperatures and gradients exist that could result in structural problems.

The portion of the deck investigated is shown in Figure B-12. An ANSYS model is shown in Figure B-13, and a model verification plot is shown in Figure B-14. Natural convection and radiation surface conditions are applied on all exposed surfaces. Included are the deck top plate exposed to containment air, and the reactor vessel surface exposed to the vessel gaseous nitrogen cooling cavity. Ambient temperatures of 85°F and 120°F are assumed in the head access area above the top plate and in the nitrogen cooling cavity, respectively. The presence of the 20 reflector plates below the primary boundary plate is simulated by applying an effective heat transfer coefficient of 0.263 BTU/hr-ft^2-°F. The corresponding pool temperature is 950°F. At normal operating conditions, this results in a slight conservatism opposed to the case where the reflector plates are actually modelled. This assessment is predicated on a preliminary 1-D analysis of the deck.

Adiabatic boundary conditions are applied at the interface with the deck support, indicated in Figure B-12. An adiabatic boundary condition is also applied at the reactor vessel cutoff, (i.e., $dT/dy = 0$ at $y = 0$), based on the reactor vessel cooling analysis (Appendix C). Inspection of the axial temperature gradient near the roof interface shows that this is a reasonable assumption.

B.3.3.2 DESCRIPTION OF STEADY STATE THERMAL CASES

Steady state thermal cases are examined simulating stationary deck fan system operation at (a) full rated capacity, or 100% coolant flow and (b) 66.6% coolant capacity. Forced convection boundary conditions corresponding to these cases are obtained from Tables B-4 and B-5 of Section B.3.2.2 and are summarized below. The air inlet temperature is 85°F.

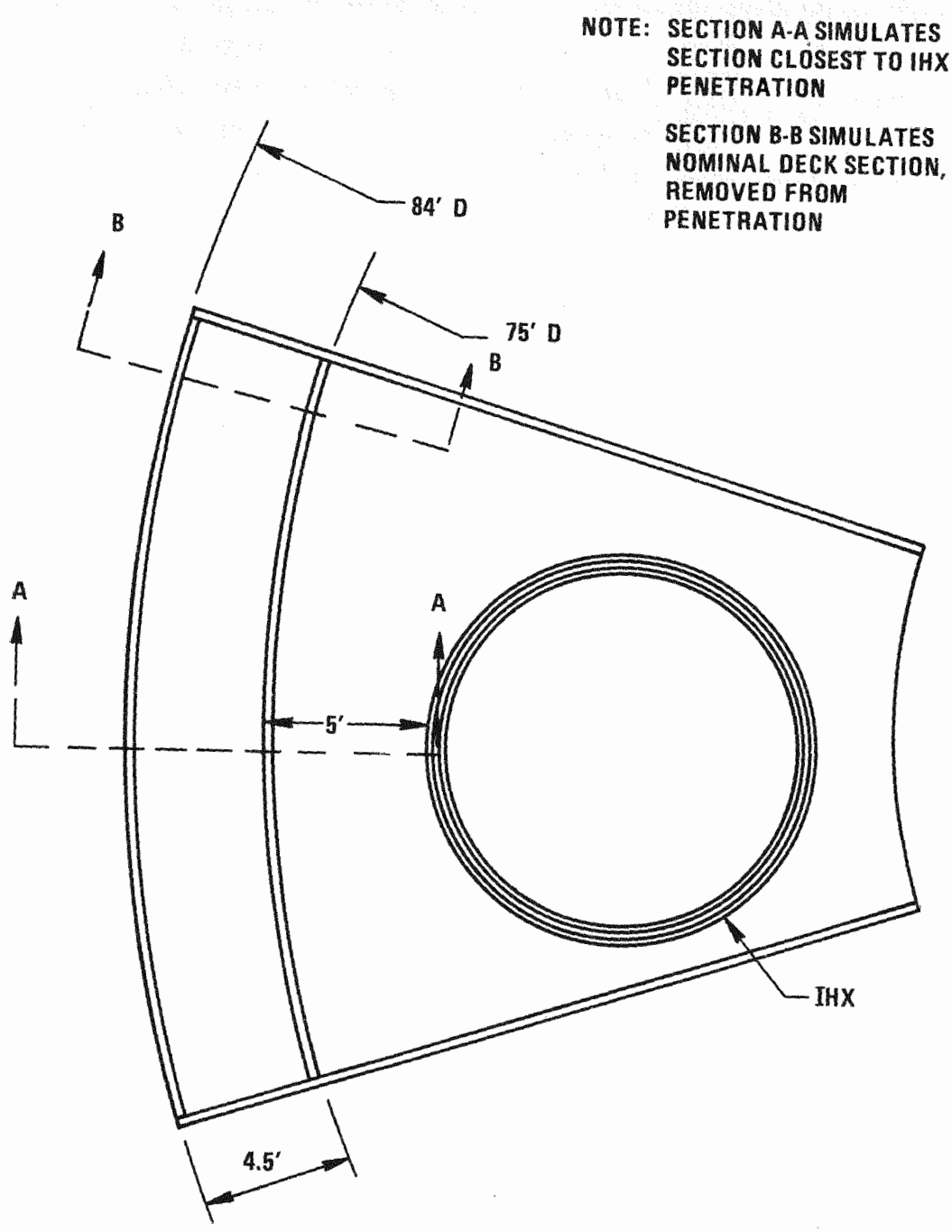

Figure B-15. Plan View of 2-D Model Section of Deck/Deck Support

0665-93

% Flow	ΔT_{air} (^oF)	h_{air} (BTU/hr-ft^2-^oF)	$\bar{T}_{air}$ (^oF)	IHX Deck Segment Flow (SCFM)
100	12	4.9	91	6000
66.6	18	3.5	94	4000

Additionally, for each case, two sub-cases are examined:

- o heating conditions for deck section closest to an IHX penetration (See Section A-A, Figure B-15), and
- o heating conditions at a nominal deck section sufficiently removed from penetrations (See Section B-B of Figure B-15)

IHX penetration heating is simulated in the first subcase, and cooling effects of the IHX standpipe are also included. For the second subcase, an adiabatic boundary condition is applied at cutoff surface at x = 5 feet (Figure B-13).

B.3.3.3 RESULTS

Temperature distributions at representative locations of the deck are presented in Figures B-16 through B-19. Significant results are tabulated in Table B-8.

From Table B-8, it is indicated that:

- o Average primary boundary plate temperatures of 132^{o}F and 144^{o}F, occurring at a nominal section removed from penetrations, are within the allowable temperature of 150^{o}F, at 100% and 66.6% cooling capacity, respectively. At a section nearest an IHX, the corresponding temperature are 143^{o}F and 164^{o}F.
- o Maximum primary boundary plate temperatures of 205 and 234^{o}F are predicted at the IHX interface, at the respective flow conditions of 100% and 66.6% capacity flow. The gradients encountered ($\lesssim$5^{o}F/in, max) should pose no serious structural problems,

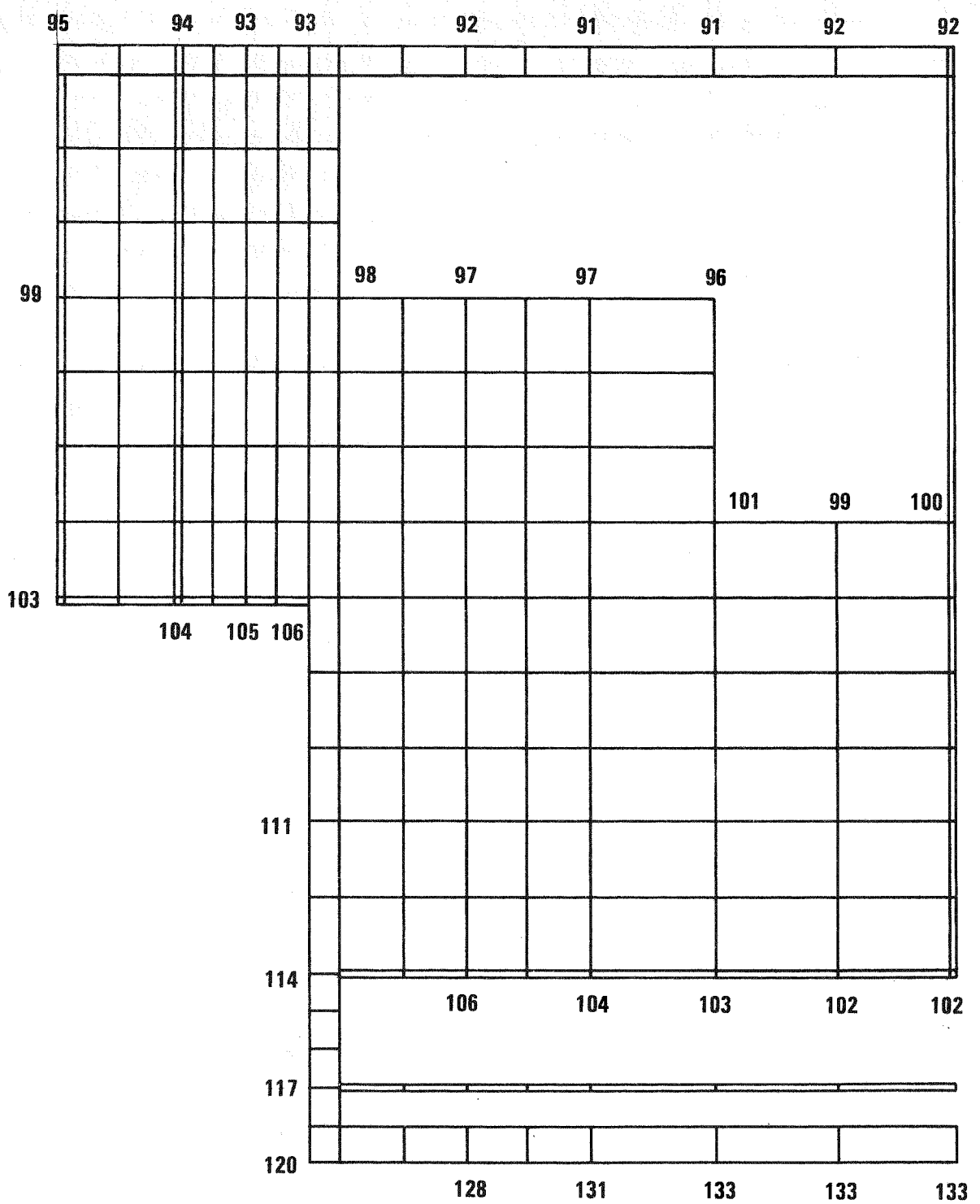

Figure B-16. Deck Temperatures at Nominal Section – 100% Coolant Capacity

0665-99

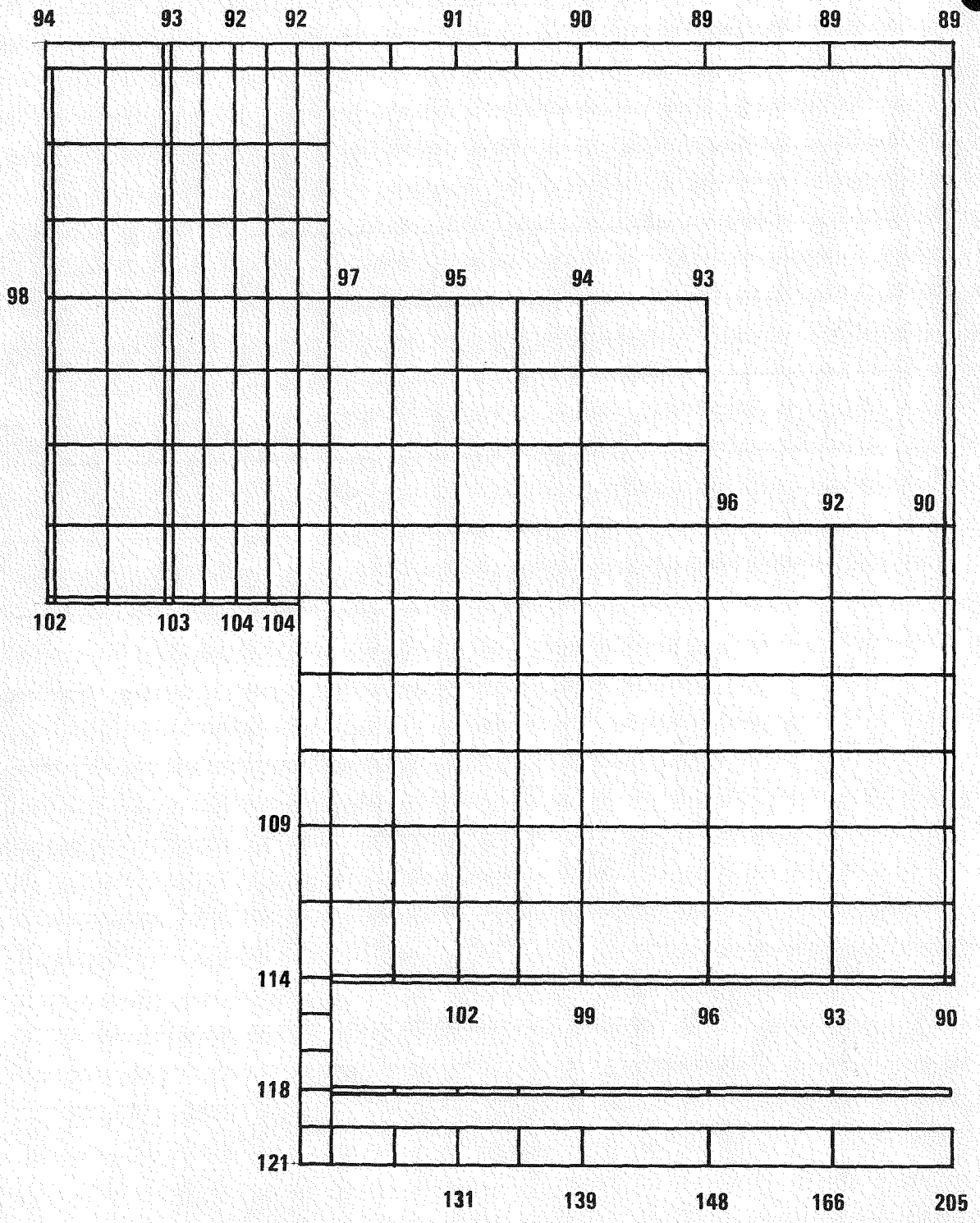

Figure B-17. Deck Temperatures at Section Nearest IHX – 100% Coolant Capacity

0665-98

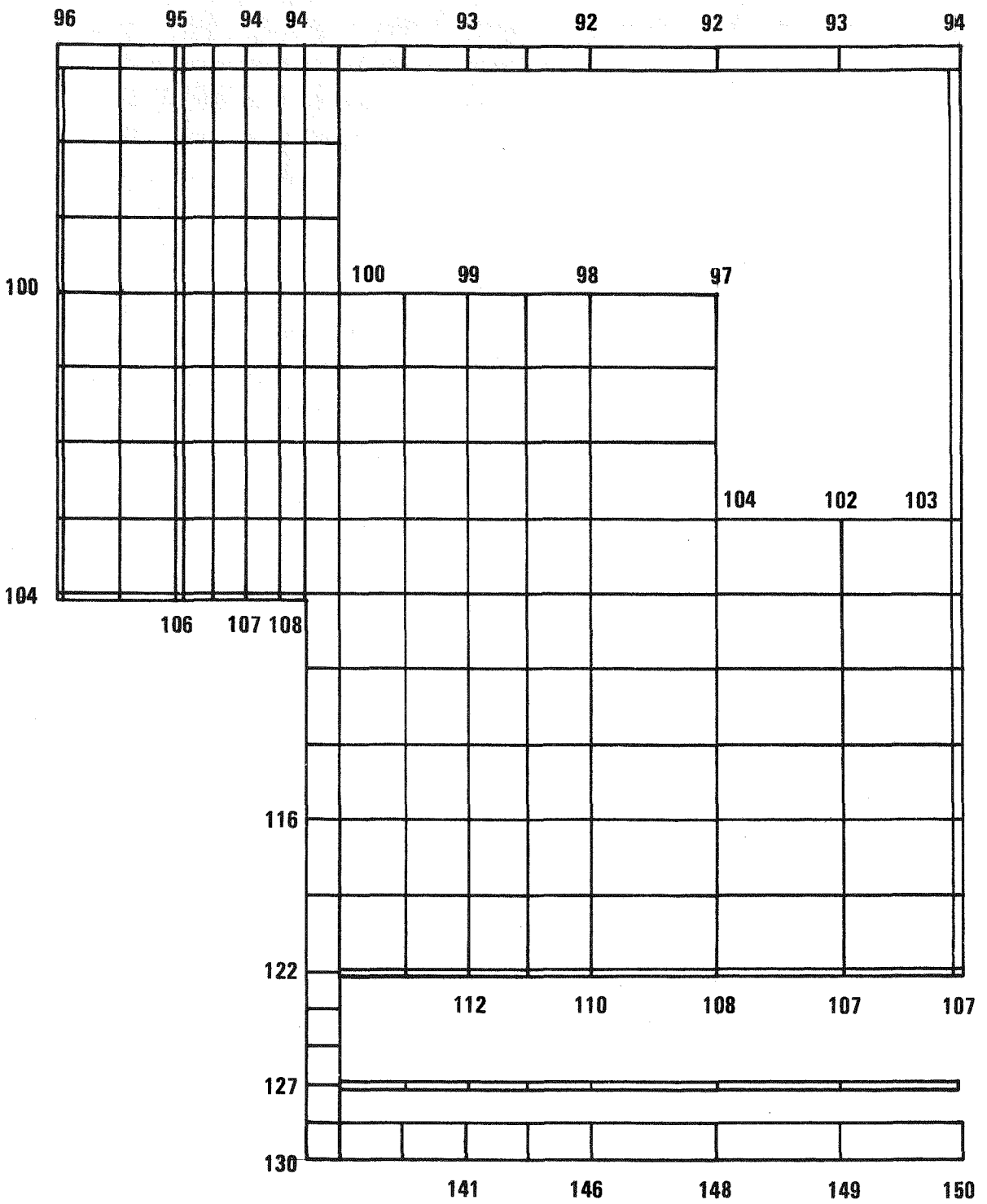

Figure B-18. Deck Temperatures at Nominal Section – 66.6% Coolant Capacity

0665-101

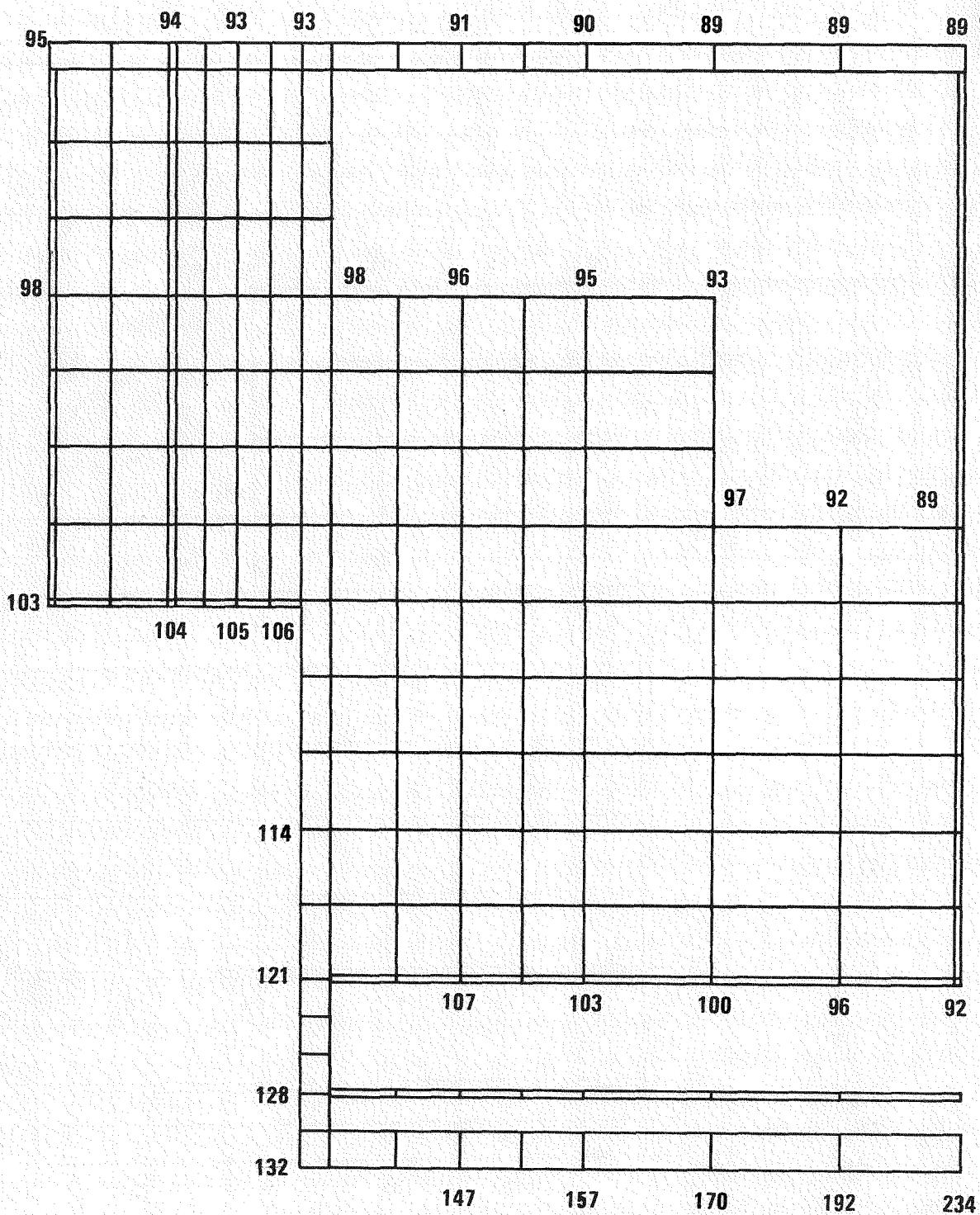

Figure B-19. Deck Temperatures at Section Nearest IHX – 66.6% Coolant Capacity

0665-100

TABLE B-8

LPR STATIONARY DECK TEMPERATURE SUMMARY

Region	Nominal Deck Section		Section Closest to IHX	
	100% Coolant Flow	66.6% Coolant Flow	100% Coolant Flow	66.6% Coolant Flow
Primary Boundary Plate	132	147	143	164
Primary Boundary Plate, $T_{Max.}$, (IHX Interface)	133	150	205	234
Shielding Support Plate	104	109	98	102
Deck Top Plate	92	93	91	91
Bottom Interface of Deck Support Beam	105	107	103	105

*Average Temperature Specified Unless Otherwise Indicated.

based on analysis done during the Phase A effort, where temperature gradients were more severe ($\mathcal{S}9^{o}F/in$).

- For all cases examined, the maximum average top plate temperature is $93^{o}F$, less than the specified allowable of $110^{o}F$.
- The maximum average temperature of the bottom of the deck supporting beam is $107^{o}F$. With respect to the top plate temperature of $93^{o}F$, the temperature difference is only $14^{o}F$ over a 7 foot depth, and should result in no structural problem.

Deck temperatures are within specified levels, both at 100% and 66.6% cooling sytem capacity. Since acceptable temperatures are obtained at the reduced coolant flow, it is concluded that the deck cooling system is adequate at steady state normal operation and that sufficient margin is provided against uncertainty. A loss of coolant flow transient is addressed in the subsequent section.

B.3.4 LOSS OF COOLANT FLOW TRANSIENT

B.3.4.1 THERMAL TRANSIENT DISCUSSION

The expected worst case thermal transient affecting the deck structure is loss of coolant air flow in the gas plenum. The heating of the deck structure must be ascertained during this transient, since the resultant thermal force vectors tend to shear out the web structure in the gas plenum, and also bow the deck, giving rise to potential misalignment problems. The objective of this analysis, then, is to determine the thermal response of the deck in the event of loss of forced air cooling.

B.3.4.2 TRANSIENT ANALYSIS

A 1-D ANSYS thermal model used in obtaining temperature histories of the deck is shown in Figure B-20. Included are 20 reflector plates and the deck proper. Equipment penetrations to the pool, (i.e., the IHX, pumps and cold traps) are also modelled, as well as the web structure between the primary boundary plate and the top plate of the deck. Effective conductances are determined on basis of area ratios of these respective components to the overall stationary deck area ($\sim$2500 square feet). On a per square foot basis, the area ratios are summarized in Table B-9.

TABLE B-9

LPR DECK PENETRATION AREAS

Component(s)	Area Ratio
6 IHXs, 4 Pumps, 2 Cold Traps	0.0168
Reflector Plate Spacers	0.027
Webs + Equipment between Primary Plate/Shield Support Plate in Plenum	0.068
Webs + Equipment above Air Coolant Plenum	0.093

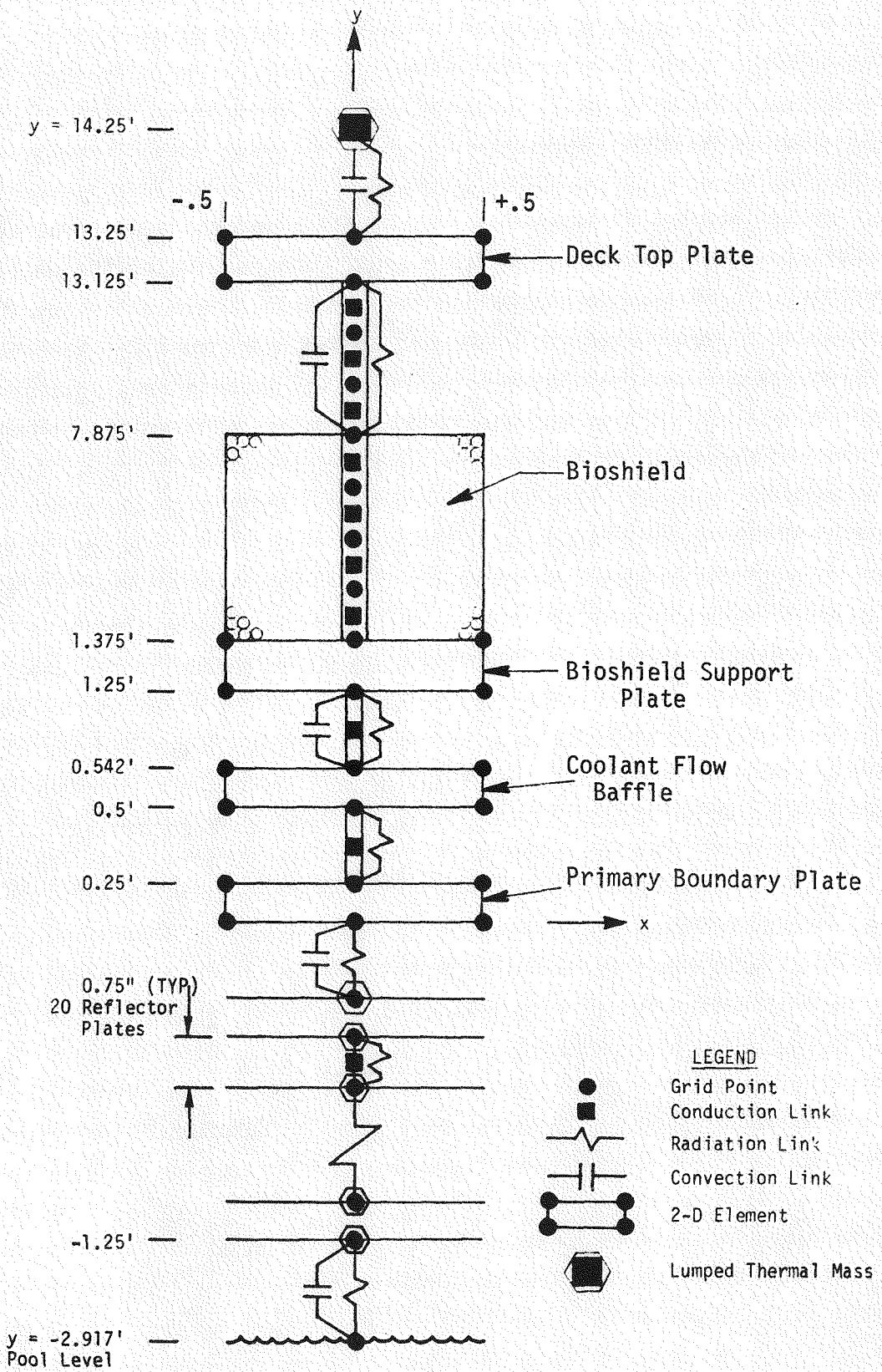

Figure B-20. LPR Deck 1-D Loss of Gas Coolant Thermal Transient Model

Radiation and natural convection boundary conditions are applied on all free surfaces, including the first reflector plate exposed to the pool, and also the deck top plate. Radiation and argon gaseous conduction is simulated between the reflector plates. The thermal capacitance of each 0.15 inch thick reflector plate is idealized as a lumped thermal mass (STIF 71 in ANSYS).

B.3.4.3 THERMAL TRANSIENT CASES

A total of three transients are investigated:

- A steady state run is made at normal operating conditions. The pool temperature is at 950°F and the head access area air temperature is at 85°F. A heat transfer coefficient of 4.9 BTU/hr-ft^2-°F is applied in the gas plenum and the bulk air coolant temperature is 90°F. The above data supplied the initial condition for the transient.

- At the inception of loss of coolant flow, or at time t = 0 hours, the gas plenum heat transfer coefficient is set equal to zero, initiating the transient. The most severe loss of coolant transient occurs if the cooling fan system power including emergency power supply is lost. In this situation, plant shutdown occurs immediately. For analytical purposes, it is conservatively assumed that the pool temperature is held constant at 950°F for a postulated, but unlikely, 180 hr transient. It is expected that cooling would be restored well before 180 hrs.

- A final steady state run is made, assuming the gas plenum cooling has not yet been restored. Based on results presented below, this unlikely situation implicitly occurs at a time much greater than 180 hours, and the final steady state temperatures represent an extreme upper limit.

An additional transient is run considering an end-of-life (E.O.L.) reflector plate emissivity of 0.8, repeating the above steps.

B.4.4.4 RESULTS

Temperature histories of the deck at key locations are presented in Figure B-21. The end-of-life transient is presented in Figure B-22. Shown are time/temperature plots of the primary boundary plate, deck top plate and the top surface of the bioshielding. Also presented is a plot of the temperature difference between the primary boundary plate and the bioshield support plate. Initial temperatures (t = 0 hours), temperatures occurring at 6, 68 and 180 hours and final steady state temperatures, assuming forced cooling has not been restored, are summarized in Table B-10. At time t = 6 hours, it is assumed that the failure which has occurred is repaired, or repair is very imminent, and the cooling system again becomes operative. Should the malfunction continue, the maximum temperature difference between the primary boundary plate and the bioshield support plate occurs at time t = 68 hours. This results in the maximum shear condition in the plenum web structure.

TABLE B-10

LPR DECK TRANSIENT TEMPERATURES - NOMINAL CONDITIONS

	Temperature ↷ °F				
Location	t=0	t=6	t=68	t=180	t >>180 hr.*
Primary Boundary Plate	123	171	298	385	530
Bioshield Support Plate	109	124	230	320	477
Top Surface of Bioshield	99	99	111	166	272
Deck Top Plate	93	94	99	129	188

*Final steady state temperatures without forced cooling restored.

NOTE: Nominal Reflector Plate Emissivity = 0.28

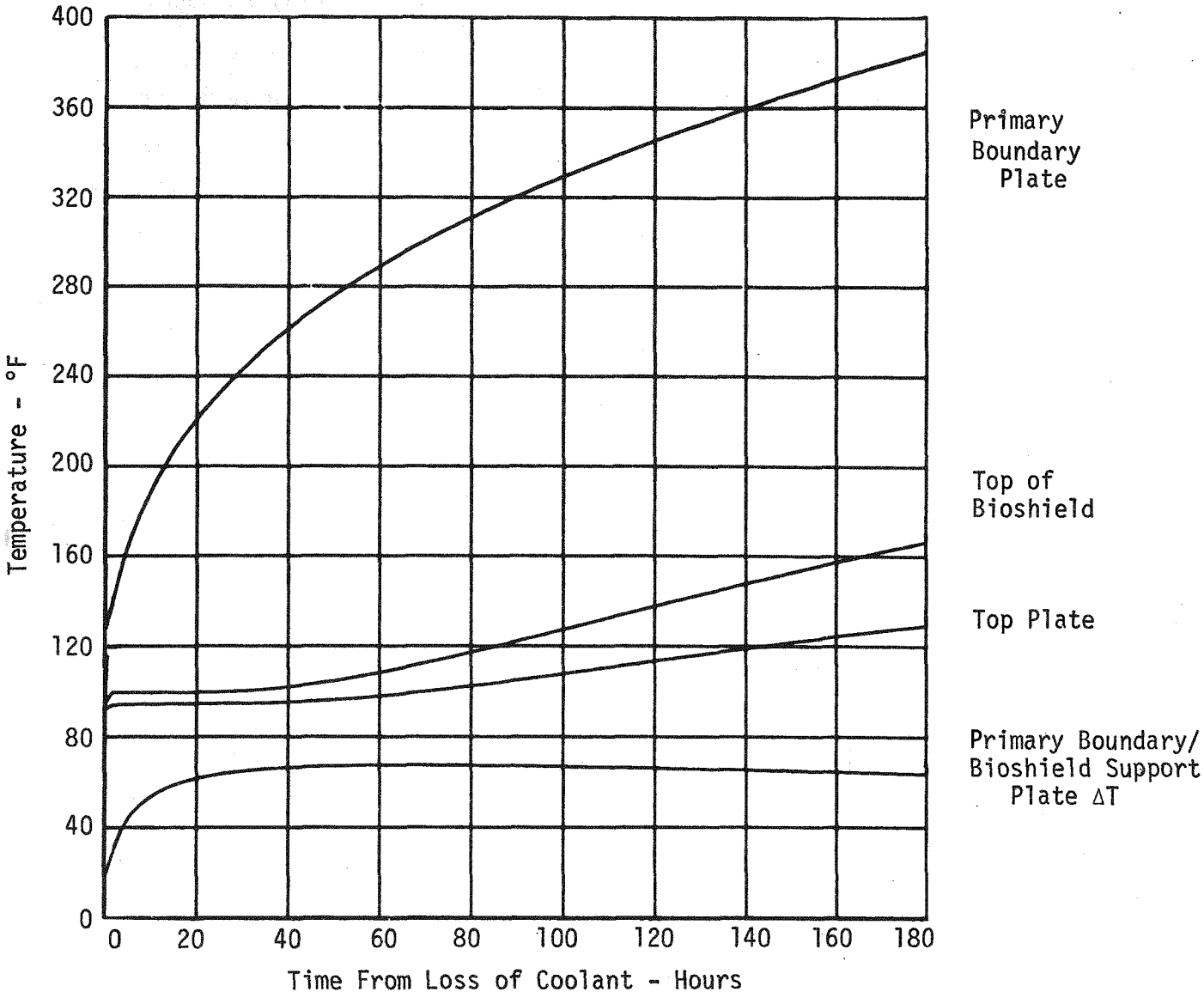

Figure B-21. LPR Deck Temperature History During Loss of Coolant Transient - Nominal Reflector Plate Emissivity

NOTE: E.O.L. Emissivity = 0.8

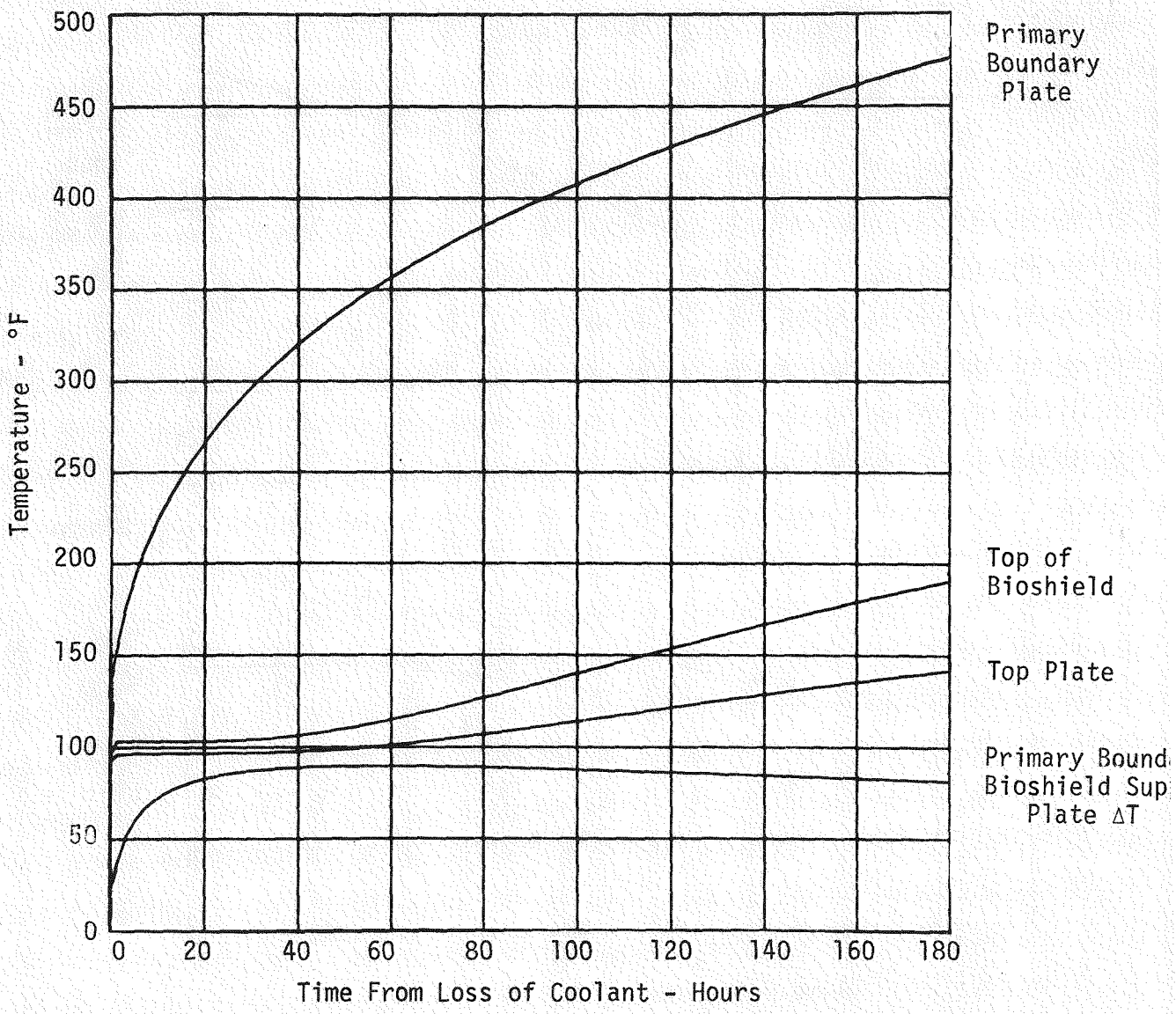

Figure B-22. LPR Deck Temperature History During Loss of Coolant Transient - End of Life Reflector Plate Emissivity

Comparison of these results and those presented in the Interim Report, (Volume 4, pp. 4-78) indicates a slower heatup and less severe gradients for the present case, (i.e., the maximum ΔT occurring between the pressure boundary plate and the bioshield support plate is $68^{o}F$ versus $110^{o}F$ for the previous case). The difference occurs for the following reasons:

- In the interim report, the thermal plates were not included, but their presence simulated in a substantially more conservative fashion than the actual modelling done herein. This is partly due to the more conservative nuclear heating applied in the interim report analysis. The latter is based on CRBRP data.

- In the present analysis, the thermal capacitance of the 20 reflector plates was included, which was previously neglected. Cumulatively, this is equivalent to placing a 3 inch thick plate below the pressure boundary plate. The net effect is a slower heatup of the latter member.

Evaluating the end-of-life transient, the maximum ΔT occurring between the pressure boundary plate and the bioshield support plate is $89^{o}F$ versus $68^{o}F$ at nominal conditions. No structural problems are anticipated.

With respect to the more severe results in the Interim Report, the deck structure was nominally shown adequate (Volume 4, pp. 4-66). It is concluded that the deck is still acceptable from a standpoint of thermal stress with respect to the present revised analysis, which resulted in less severe gradients than the previous analysis. Structural verification analyses should be performed in the future as the design evolves.

B.4 ROTATABLE PLUGS ANALYSES

An active cooling system is provided for the rotatable plugs section of the deck. Conceptually, the design is identical to the stationary deck cooling system, except that 30 plates instead of 20 thermal reflector plates are utilized, as shown in Figure B-23. The plate spacing is the same as that of the stationary deck, (i.e., the 0.15 inch thick center to center spacing is [illegible] in). As a consequence, the increased height of the primary boundary plate above the pool results in a less severe axial temperature gradient above the hot pool in the Upper Internals Structure (UIS) cylinder, which

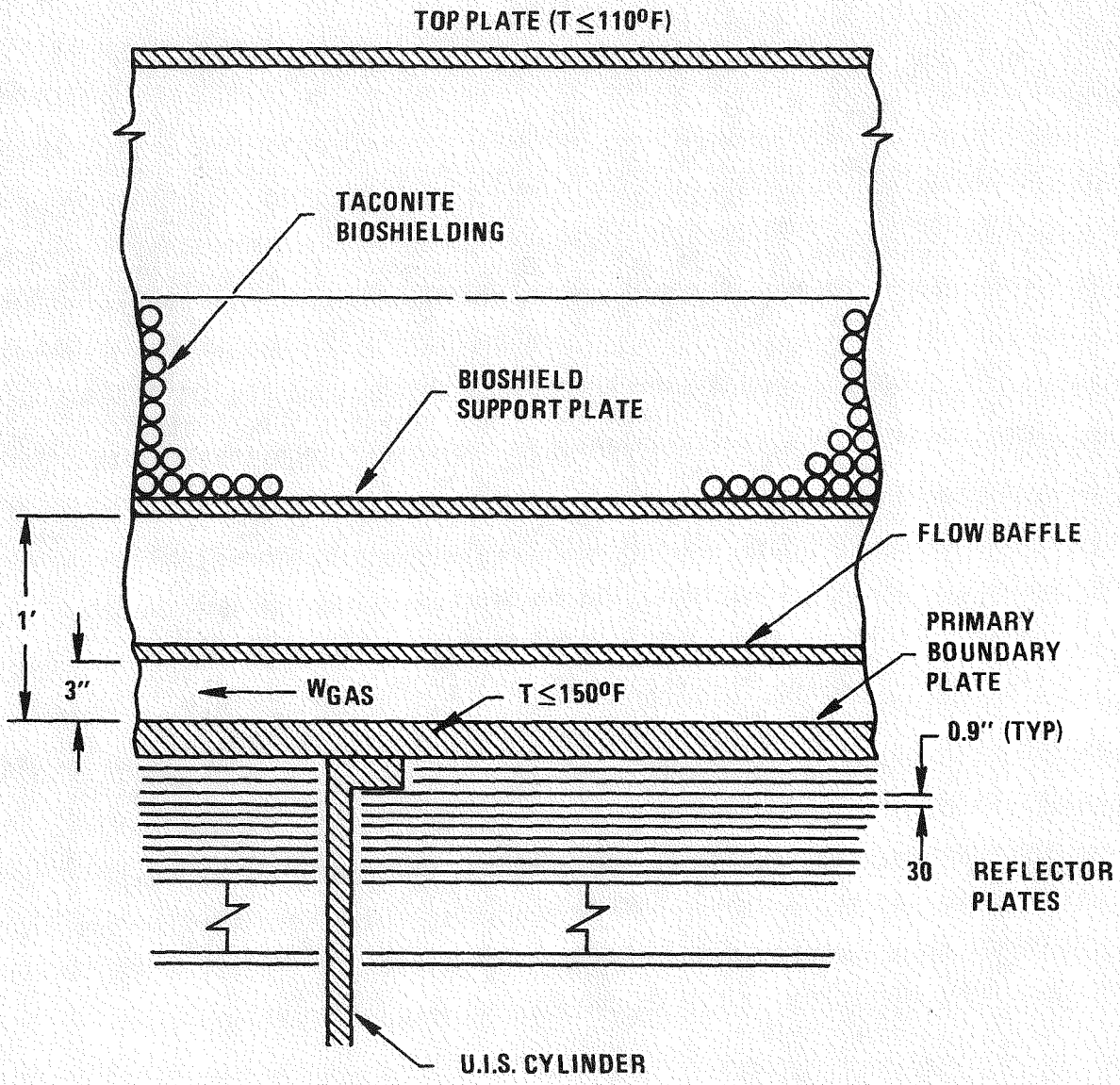

Figure B-23. LPR Deck Rotatable Plugs Cooling Concept

0665-133

interfaces with the primary boundary, shown in Figure B-23. The more severe gradient associated with an array of 20 plates was shown to result in a thermal stress problem near the attachment portion of the UIS. A moderate reduction in the reflection plate heat flux is also realized with 30 plates.

The cooling system is designed so that primary boundary plate and deck top plate temperatures of 150°F and 110°F, respectively, are maintained.

B.4.1 ACTIVE VERSUS PASSIVE COOLING

The feasibility of using passive cooling (insulation and/or reflection plates) is examined in detail, since the possibility of eliminating the more complex active cooling system is offered. Documentation to support the position that passive cooling alone is inadequate to thermally protect the rotatable plug structure, and that active cooling is required, is presented below.

B.4.1.1 INTRODUCTION

The LPR deck is an 80 foot diameter by 13.25 foot deep structure consisting of centrally located rotatable plugs surrounded by a permanent shield deck. The deck system is an open gridwork, bridge-type design as opposed to a solid steel or concrete structure. A "cold deck" design is selected for the rotatable plugs because fewer structural, thermal, and distortion problems are encountered with a deck system that operates at near ambient temperatures than with a deck system that operates nearer the temperature of the sodium pool (950°F).

A cold deck can be achieved in three ways:

- By providing enough insulation between the sodium pool and the deck structure to reduce the heat flux to a practical minimum such that no forced fooling is required (strictly passive).

- o By actively cooling the deck structure bottom plate thereby removing the heat that passes from the sodium pool into the structure (purely active).
- o A combination of the above two methods.

It is the purpose of this section to show that insulation alone (#1 above) does not provide sufficient thermal protection to maintain the primary boundary temperature below 150^{o}F and the top deck surface temperature below 110^{o}F.

B.4.1.2 THERMAL PROTECTION UTILIZING INSULATION (SIMPLIFIED MODEL)

B.4.1.2.1 DISCUSSION (SIMPLIFIED MODEL)

Figure B-24 shows a simplified one dimensional section of the rotatable plug. The primary boundary is protected by a layer of insulation which is assumed to have a conductivity of 0.1 BTU/Hr-ft ^{o}F. A three inch thick steel plate is used to support the insulation. This plate also acts as a sink for a portion of the nuclear heating, consisting primarily of γ and β radiation from the activated sodium and cover gas. On an integrated basis, the nuclear heat flux is distributed as a point source in the insulation casing as well as in the primary roof structure. Practically all of the nuclear heating is dissipated in the casing and the primary boundary plate. Above the primary boundary, the nuclear heating is negligible.

Utilizing an ANSYS model, steady-state temperature distributions are obtained at both normal operating and hot standby conditions, varying the insulation thickness as a parameter. Effects of nuclear heating as described above are considered. Grey body radiation between the pool and the three inch steel plate and between the steel shot shielding and the top plate are also accounted for. Web conduction between the top and bottom deck plates of the deck is simulated, assuming that the effective web area for conduction is 10% of the center plug roof area.

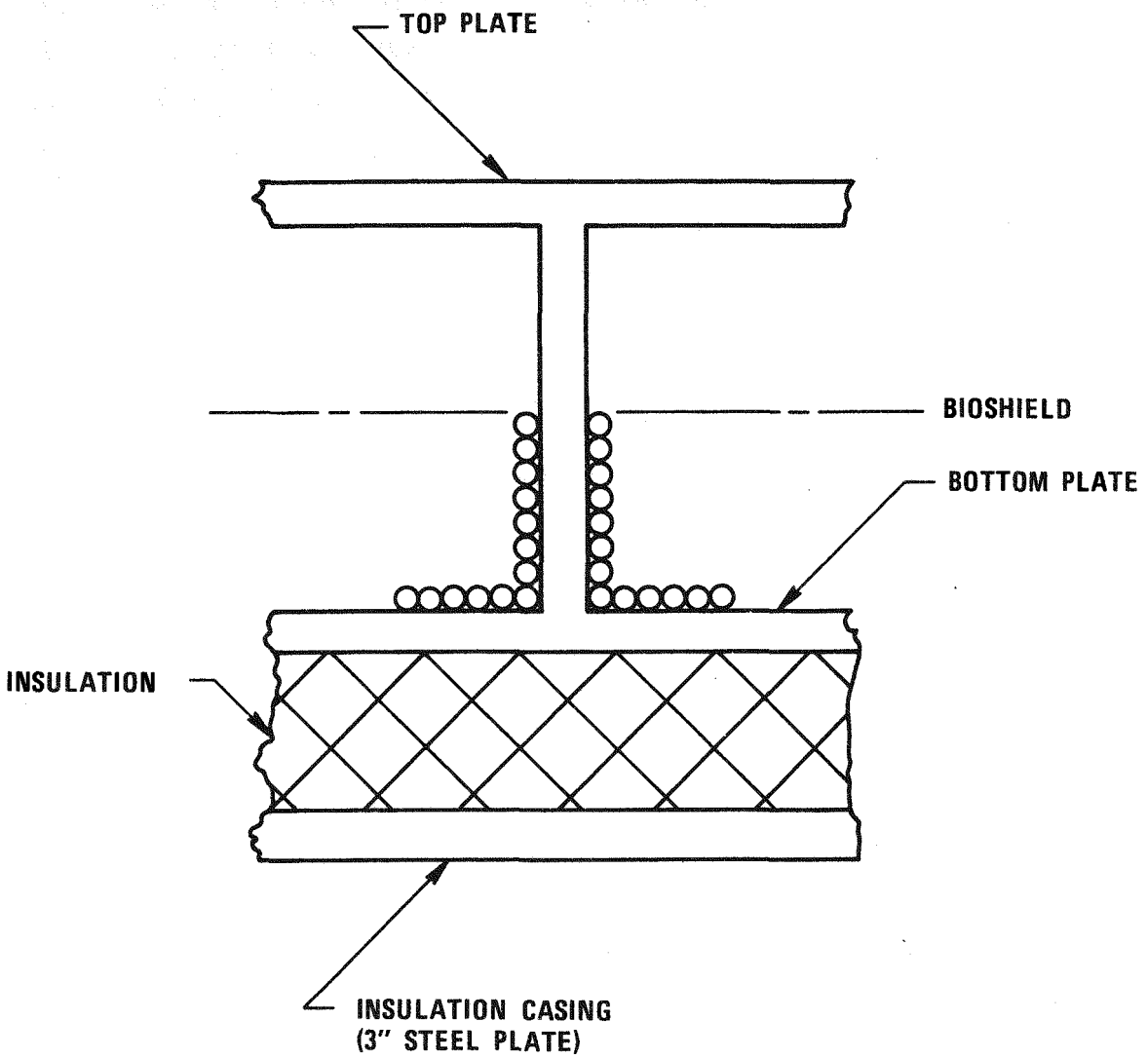

Figure B-24. Section of Center Plug – Passive Cooling with Insulation

0665-94

B.4.1.2.2 RESULTS (SIMPLIFIED MODEL)

Temperatures of the top and bottom plates as a function of the insulation thickness are presented in Figures B-25 and B-26, respectively. If 5 feet of insulation is applied, the top plate temperatures are 107^{o}F and 99^{o}F, respectively, at normal and hot standby conditions. Analogous temperatures of the bottom plate are 130^{o}F and 111^{o}F. Additionally, in all of the cases examined, the temperature of the three inch thick plate supporting the insulation does not exceed 960^{o}F.

These results provide satisfactory top and bottom deck plate temperatures. The analysis, however, is deficient in that it fails to account for thermal shorts between the sodium pool and the deck structure due to equipment such as the upper internals structure, the control rod drive lines and the In-Vessel Transfer Machine. The effect of this is addressed in the next section.

B.4.1.3 THERMAL PROTECTION UTILIZING INSULATION (COMPLEX MODEL)

B.4.1.3.1 DISCUSSION (COMPLEX MODEL)

As stated in the previous section, no account was made for major penetrations which could significantly increase the overall temperature. Therefore a more detailed analysis of the rotatable plugs inclusive of all major penetrations is performed.

Shown in Figure B-27 is the section of the deck rotatable plugs, at the circumferential station where the offset small rotatable plug is closest to the stationary deck. The basic center plug configuration consists of a box-type structure, protected by 5 feet of insulation (k = 0.1 BTU/hr-ft-^{o}F). Approximately 5 feet of taconite pellets are used for shielding. A plan view is shown in Figure B-28.

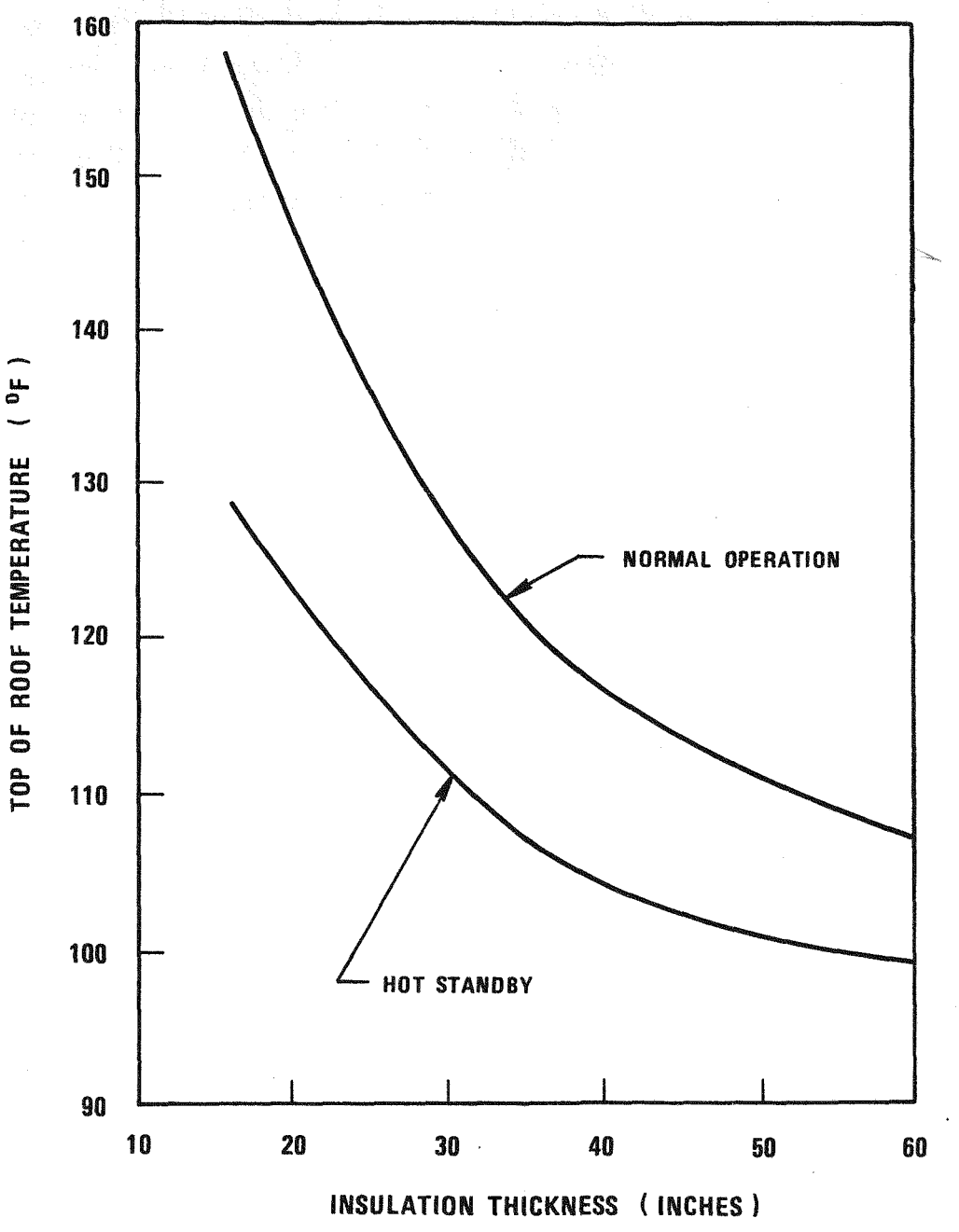

Figure B-25. Top Plate Temperature vs. Insulation Thickness

0665-95

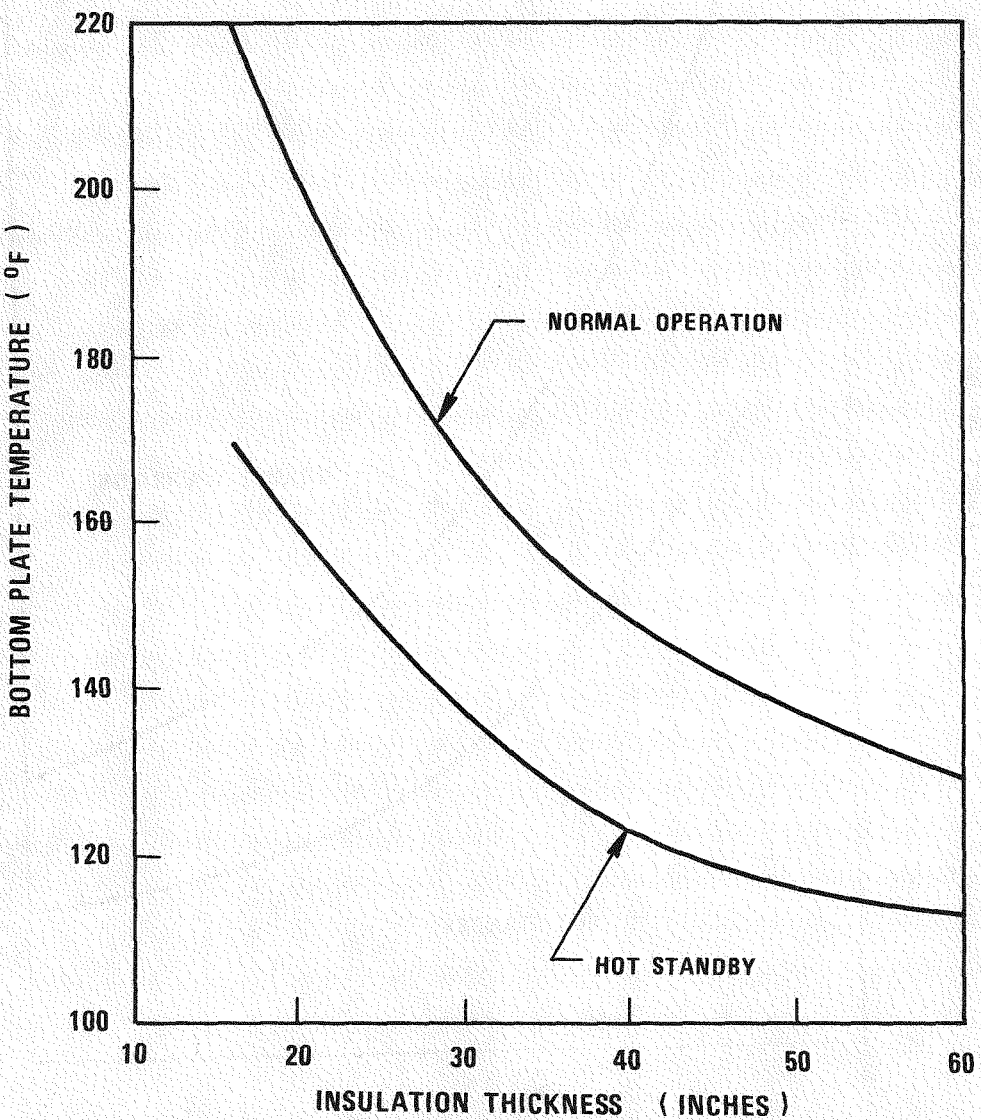

Figure B-26. Bottom Plate Temperature Versus Insulation Thickness

0665-96

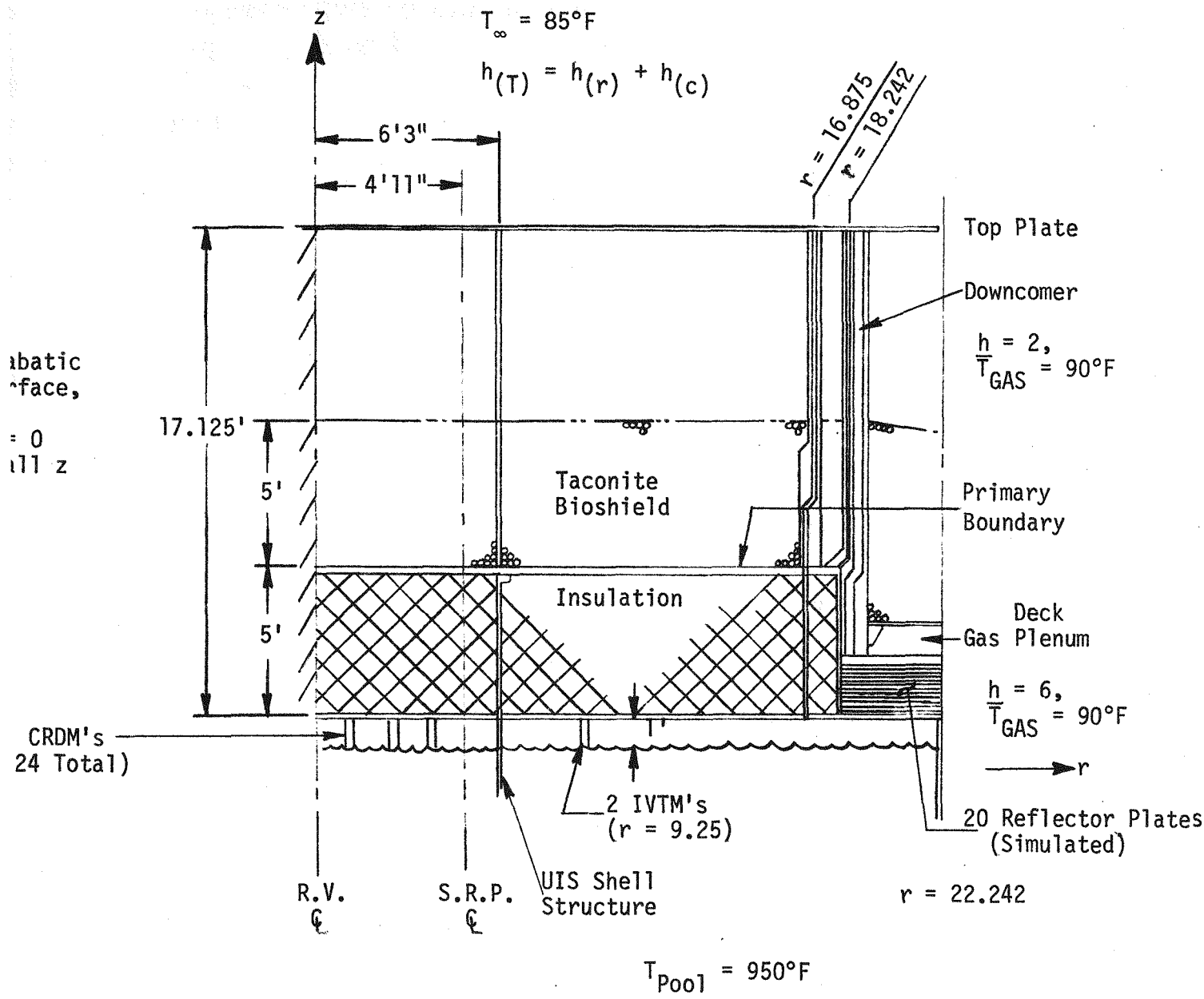

NOTE: 1) SRP/LRP Interface @ r = 16.875
2) LRP/Deck Interface @ r = 18.242

Figure B-27. LPR Rotatable Plugs Thermal Model Section - Passive Plug Cooling With Insulation

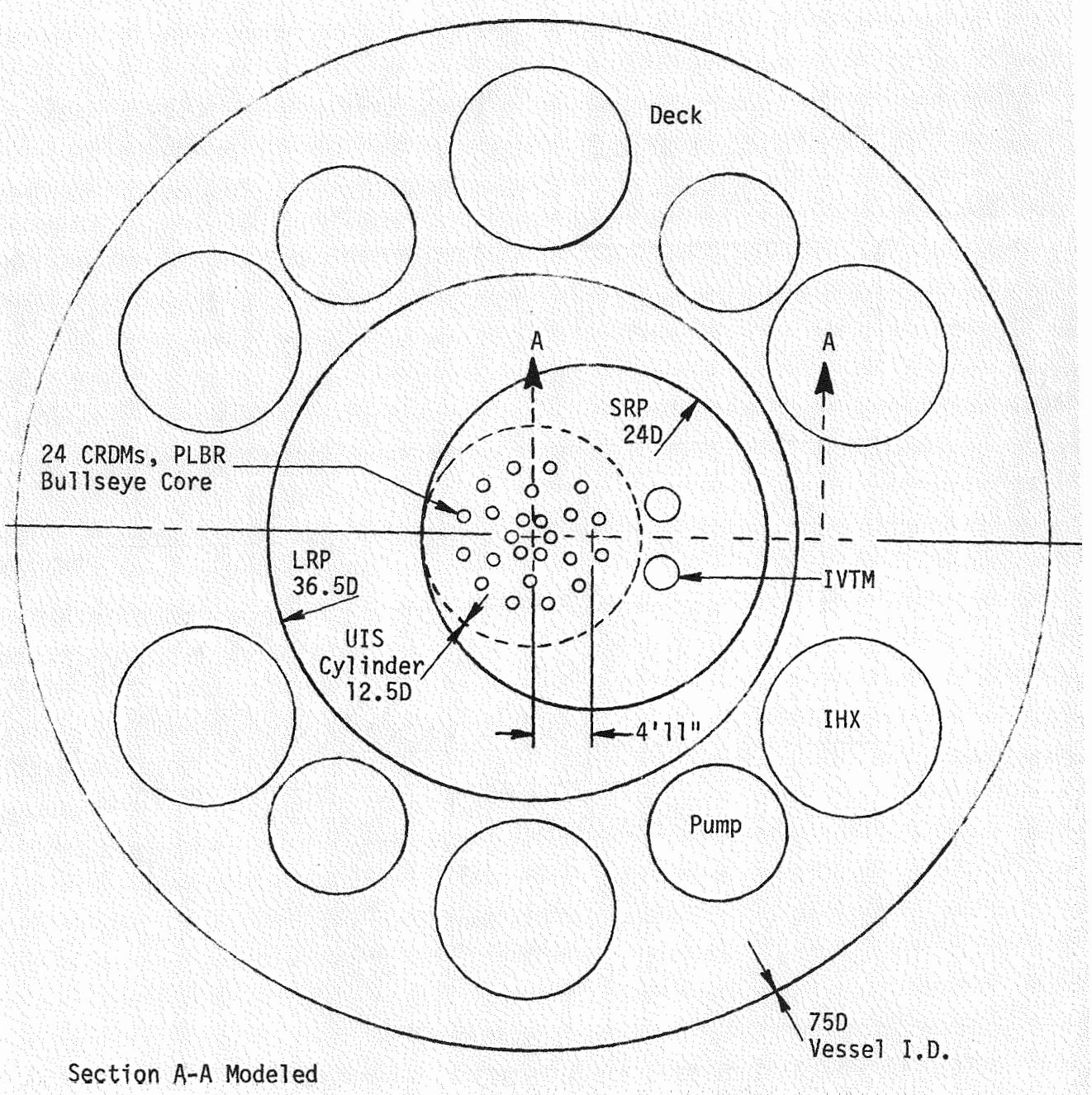

Figure B-28. Plan View of LPR Rotatable Plugs and Deck

Circumferential heat transfer effects due to the eccentric plug configuration are neglected, and a 2-D axisymmetric thermal model (ANSYS) of the region is defined (see Figure B-29). Included are all of the major penetrations in the center plug region, (i.e., the 24 CRDM's, UIS cylinder, and the 2 IVTM's). Axial conductances of these members are calculated on a per radian basis. Additional penetration heating due to the insulation attachment bolts is also simulated. The axial conduction area of the bolts is 2.2% of the total insulation area. An ANSYS verification plot of the geometry is shown in Figure B-30.

Radially, the model extends from the reactor vessel centerline 4 feet into the stationary deck. Enough of the stationary deck is included in the model to properly simulate thermal interfacing between the passively cooled plugs and the actively cooled deck. Nominally, the plugs are separated by a one inch gap which is permeated with argon cover gas. Both gaseous conduction and radiation across the gap is accounted for.

Radiation and natural convection boundary conditions are imposed on the following surfaces: (a) insulation casing facing the pool, (b) in the enclosure between the top surface of the bioshielding and the top plate, and (c) top plate surface exposed to the head access area. The temperature of the pool is $950^{o}F$ and the temperature of the ambient air in the head access area and also the containment surfaces is taken to be at $85^{o}F$. Adiabatic surfaces are assumed at the reactor vessel centerline and also at the deck cutoff at r = 22.2 feet.

At the stationary deck, forced cooling occurs in the deck gas plenum and in the downcomer supplying the plenum. The downcomer annulus is located at the inboard radius of the stationary deck. Heat transfer coefficients of 6 $BTU/hr\text{-}ft^{2}\text{-}^{o}F$ and 2 $BTU/hr\text{-}ft^{2}\text{-}^{o}F$ are applied in the plenum and the downcomer, respectively. A bulk temperature of the coolant gas of $90^{o}F$ was assumed. Nuclear heating is applied.

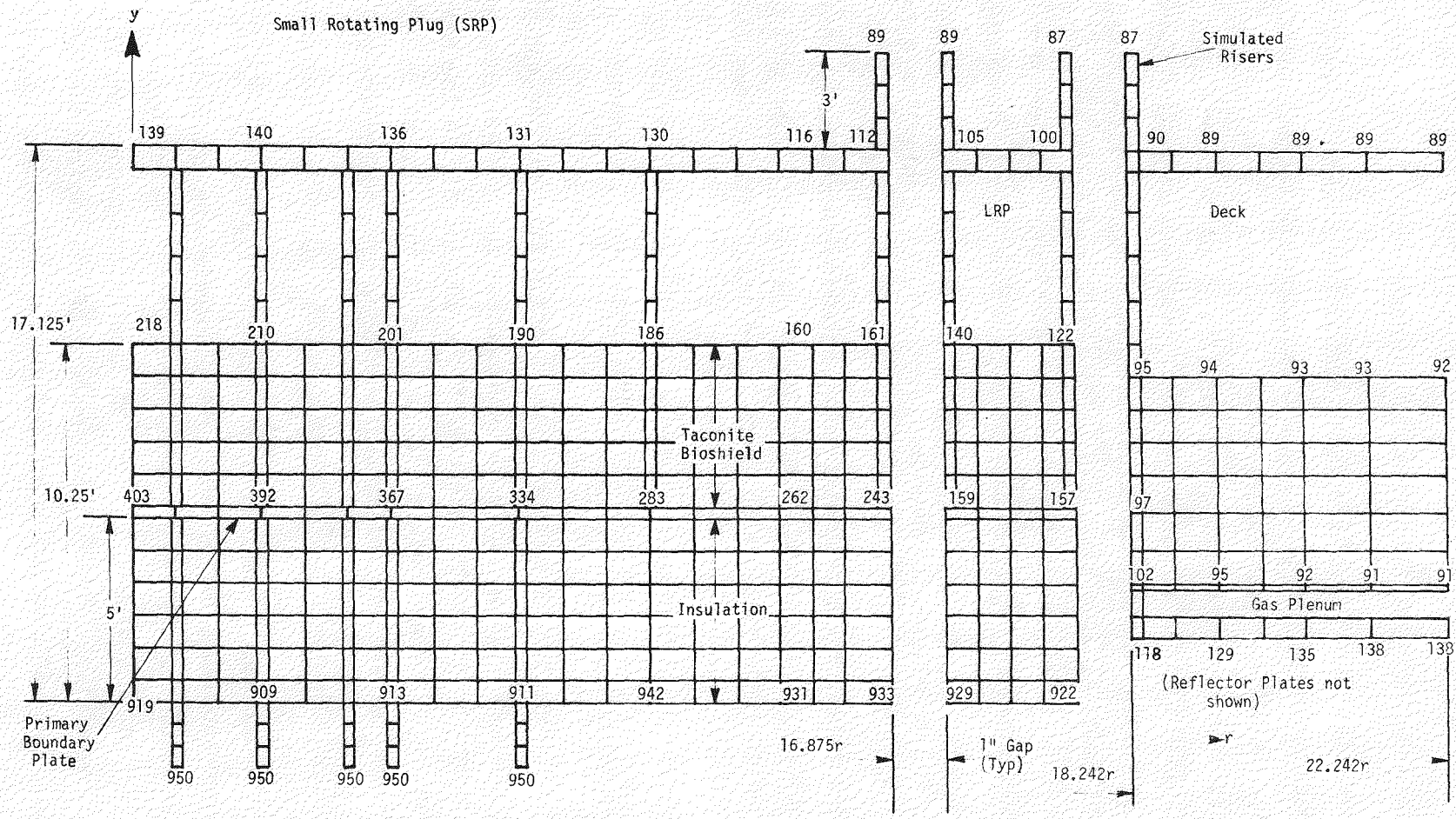

Figure B-29. ANSYS Thermal Model of LPR Rotatable Plugs - Normal Operation Steady State Temperatures Indicated

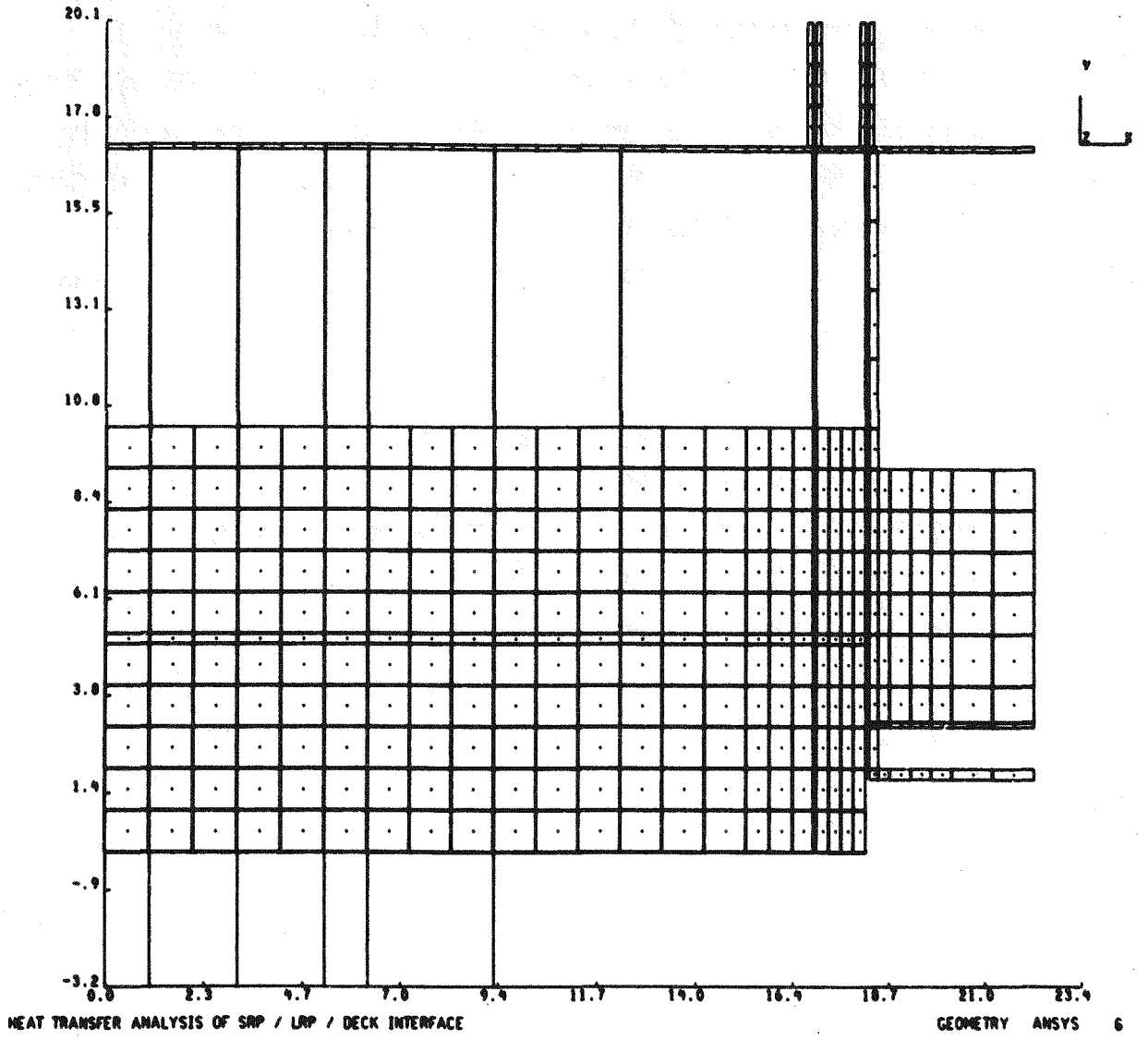

Figure B-30. ANSYS Verification Plot of 2-D Rotatable Plugs Model

B.4.1.3.2 RESULTS (COMPLEX MODEL)

Results of the analysis are presented in Figure B-29. Shown are radial temperature distributions of the primary boundary plate and the top plate of the plugs. Also shown are temperatures occurring in the stationary deck and the bottom surface of the insulation. Maximum temperatures of 403^{o}F and 140^{o}F are predicted at the primary boundary and the top plate, well above the respective limiting temperatures of 150^{o}F and 110^{o}F. These temperatures occur in the vicinity of the reactor vessel centerline, where the cluster of CRDM's and the UIS cylinder wicking to the hot pool most significantly contribute to center plug heating.

Primary boundary temperatures decrease to 243^{o}F at the interface between the small rotatable plug (SRP) and the large rotatable plug (LRP). At the LRP section, primary boundary temperatures attenuate to about 158^{o}F, due to the absence of penetrations in this region. Some cooling influence on the LRP by the adjacent stationary deck is also realized, where the deck interface temperature is at about 100^{o}F.

With respect to the allowable temperatures of the primary boundary plate and the top plate of 150^{o}F and 110^{o}F, it is concluded that the rotatable plug passive cooling scheme utilizing a thick blanket of insulation is totally impractical, since the allowable temperatures are greatly exceeded.

B.4.1.4 THERMAL PROTECTION UTILIZING REFLECTOR PLATES

B.4.1.4.1 DISCUSSION (REFLECTOR PLATES ONLY)

Thermal protection of the rotatable plug bottom surface was also analyzed using multiple horizontal reflector plates in place of the insulation examined above.

A 1-D thermal model (ANSYS) of an array of reflector plates is shown in Figure B-31. Adjacent plates are connected by radiation and conduction links. The conduction links combine effects of heat shorts through the reflector plate support columns and gaseous conduction through the argon

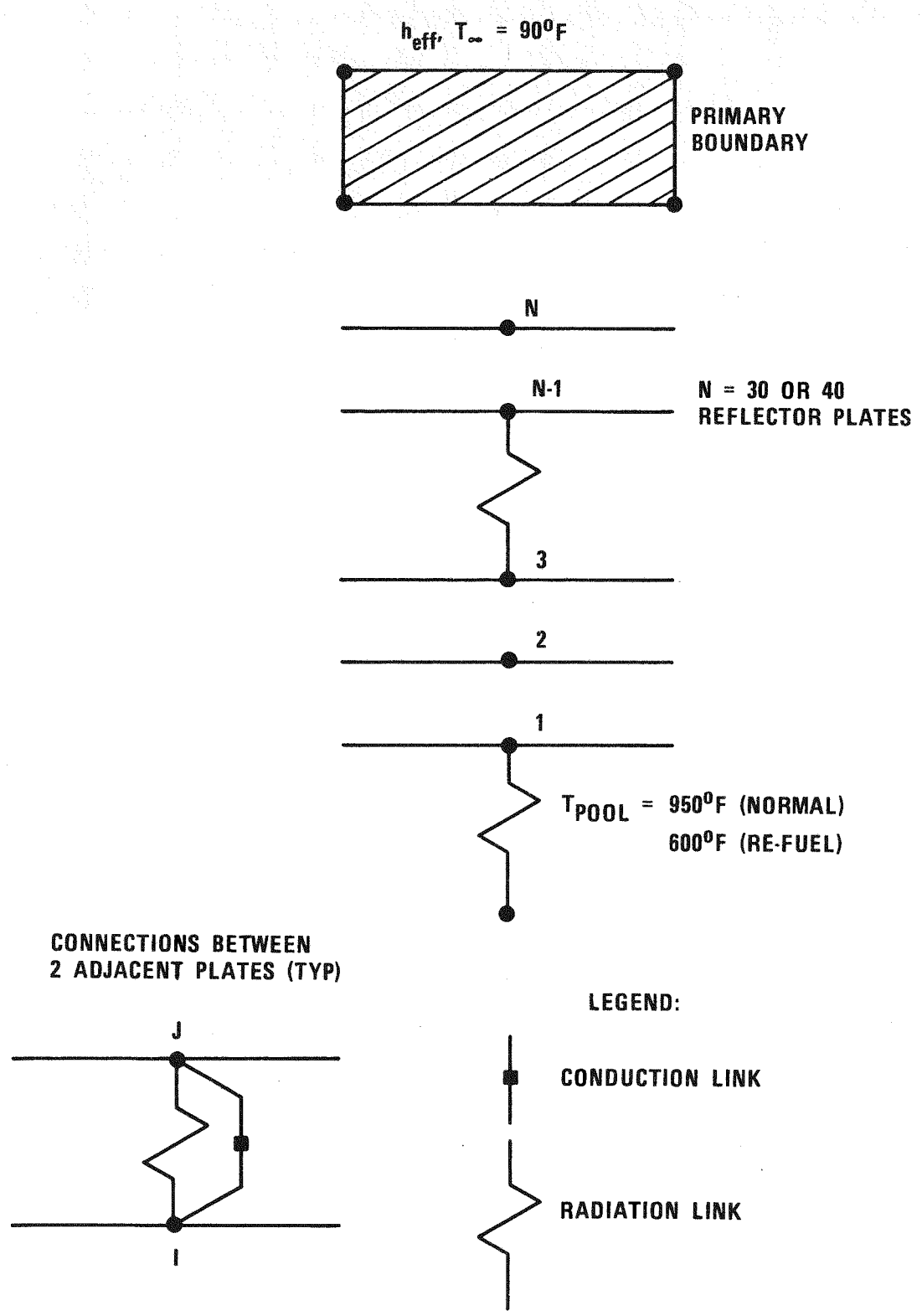

Figure B-31. Thermal Model of Reflector Plate Array

0665-97

cover gas. The plate spacing is 0.75 inches. At this spacing, and at ambient cover gas conditions during normal operation, free convection in the spaces between the plates is practically non-existent, and simple gaseous conduction occurs. Radiation and natural convection effects between the pool and the first plate are included. Penetration heating attributable to the CRDM's, UIS cylinder, and the IVTM's is not included in this analysis.

For passive cooling of the rotatable plugs, arrays consisting of 30 and 40 reflector plates are evaluated. In this case, h_{eff} represents the overall conductance through the structure to the ambient air in the head access area. A h_{eff} of 0.3 BTU/hr-ft^2^{o}F is calculated.

Estimates of structural temperatures occurring in the rotatable plugs during normal and refueling operations are summarized in Table B-11.

TABLE B-11

DECK ROTATABLE PLUG TEMPERATURES
WITH REFLECTOR PLATES ONLY

Configuration	Operating* Condition	Primary Boundary Temp. (^{o}F)	Deck Top Plate Temp. (^{o}F)	Heat Flux (BTU/hr-ft^2)
30 Plates	Normal Operation	435	181	105
	Refueling	270	136	55.6
40 Plates	Normal Operation	382	166	89.2
	Refueling	245	129	48.0

*Normal Operation: T_{Pool} = 950^{o}F

Refueling: T_{Pool} = 600^{o}F

B.4.1.4.2 RESULTS (REFLECTOR PLATES ONLY)

With respect to the top plate and the primary boundary, it is seen that temperatures well above the limiting temperature of 110°F and 150°F, respectively, exist for all cases. Further, bowing of the plugs may well occur, attributable to the substantial temperature differences between the top plate and the primary boundary. Thus, if an array of either 30 or 40 thermal reflector plates is used below the plugs, some forced cooling is required. It is also concluded that attempting to cool the structure entirely by means of reflector plates would require an inordinately large number of plates and is not practical. Effects of equipment penetration heating, which were not included, would further increase the rotatable plug temperatures.

B.4.1.5 PASSIVE VERSUS ACTIVE COOLING CONCLUSIONS

One dimensional analysis indicated that five feet of thermal insulation adequately protects the deck plug structure top plate and primary boundary bottom plate. However, penetration heating from the CRDM's, IVTM's and the UIS results in unacceptable pressure boundary and top plate average temperatures of approximately 300°F and 130°F, respectively.

Arrays of 30 and 40 thermal reflector plates (considered to be the practical limit) also proved to be totally inadequate for thermal protection of the rotatable plug structure.

It should be noted that the analyses herein are strictly applicable to the rotatable plugs. The question arises as to whether the above analyses also apply to the stationary deck structure. It is concluded that passive cooling of the stationary deck is not feasible for the following reasons:

- Source heating from the sodium pool into the stationary deck is essentially the same as that in the plug region.
- Heat flow into the deck from sources such as the IHXs is even more severe than that occurring from the equipment penetrations in the rotatable plug region.

- Additional vessel height would be required to accommodate the increased height of the insulation or thermal plate configuration.

On the basis of the above, it is concluded that insulation/thermal plates plus forced coolng is required to maintain the primary boundary at or below $150^{o}F$ and the top plate temperature at or below $110^{o}F$ for both the rotatable plug and the stationary deck structure.

B.4.2 ROTATABLE PLUGS COOLING SYSTEM

Cooling plena geometry applicable to the rotatable plugs is schematically illustrated in Figure B-32. A total of four (4) separate cooling compartments is visualized:

- two symmetric compartments in the eccentric annulus between the small (SRP) and the large (LRP) rotatable plugs
- two compartments circumscribed within the offset SRP.

A detailed analysis is done on a cooling plenum in the annulus between the SRP and the LRP. Scaling factors are applied to obtain estimates of flow requirements for the region within the SRP. As in the case of the stationary portion of the deck, an uncertainty factor of 2.0 is applied in determining system fan horsepower requirements.

B.4.2.1 ROTATABLE PLUG HEATING

The total rotatable plug heat load, summarized in Table B-12, occurs from pool and penetration heating. The nominal heat flux through the array of 30 reflector plates is 175 BUT/hr-ft^2 per Table B-2. Effects of nuclear heating are included. Based on a total rotatable plug surface area of 1046 ft^2 exposed to the hot pool, the integrated heat load is 183,000 BTU/hr. Penetration heating results from the cluster of 24 control rod drive mechanisms (CRDMs), two in vessel transfer machines (IVTMs), and the UIS cylinder. See Figures B-27 and B-28 above. A total of 62,000 BTU/hr is calculated for the penetration heating, or pool wicking effect for these components.

TABLE B-12

ROTATABLE PLUG HEAT LOAD SUMMARY

Region/Component	Q (BTU/hr)
Reflector Plates	183,000
Penetrations	62,000
Total	245,000

B.4.2.2 LARGE ROTATABLE PLUG FLOW REQUIREMENTS

As stated previously, a detailed analysis is performed on the eccentric SRP/LRP annulus, shown in Figure B-32. Following procedures documented in Section B.3.2.1, cooling requirements compatible with the rotatable plugs heat load are defined, so that the average temperature of the primary boundary plate does not exceed 150^{o}. A detailed step-by-step description is not presented as in the case of the stationary deck, since the analytical approach is straightforward; rather, summaries of results are presented.

B.4.2.2.1 DESCRIPTION OF LRP PLENUM GEOMETRY

The elevation view of Figure B-32 indicates a nominal plenum height of three inches. Circumferentially, from θ = 45 degrees to θ 180 degrees, a horizontal baffle installed three inches above the primary boundary plate is used to ensure adequate flow velocity required for good heat transfer. At the narrowed inlet, however, where the offset SRP is closest to the LRP, the plenum height is increased to one foot, with the bioshield support plate forming the upper boundary of the flow channel. The increased height ensures that flow velocities are maintained within the incompressible range. By avoiding compressible flow at the restricted inlet passage (θ = 0 to 45 degrees), uncertainties associated with higher pressure loss coefficients that would increase the cooling system fan horsepower are eliminated.

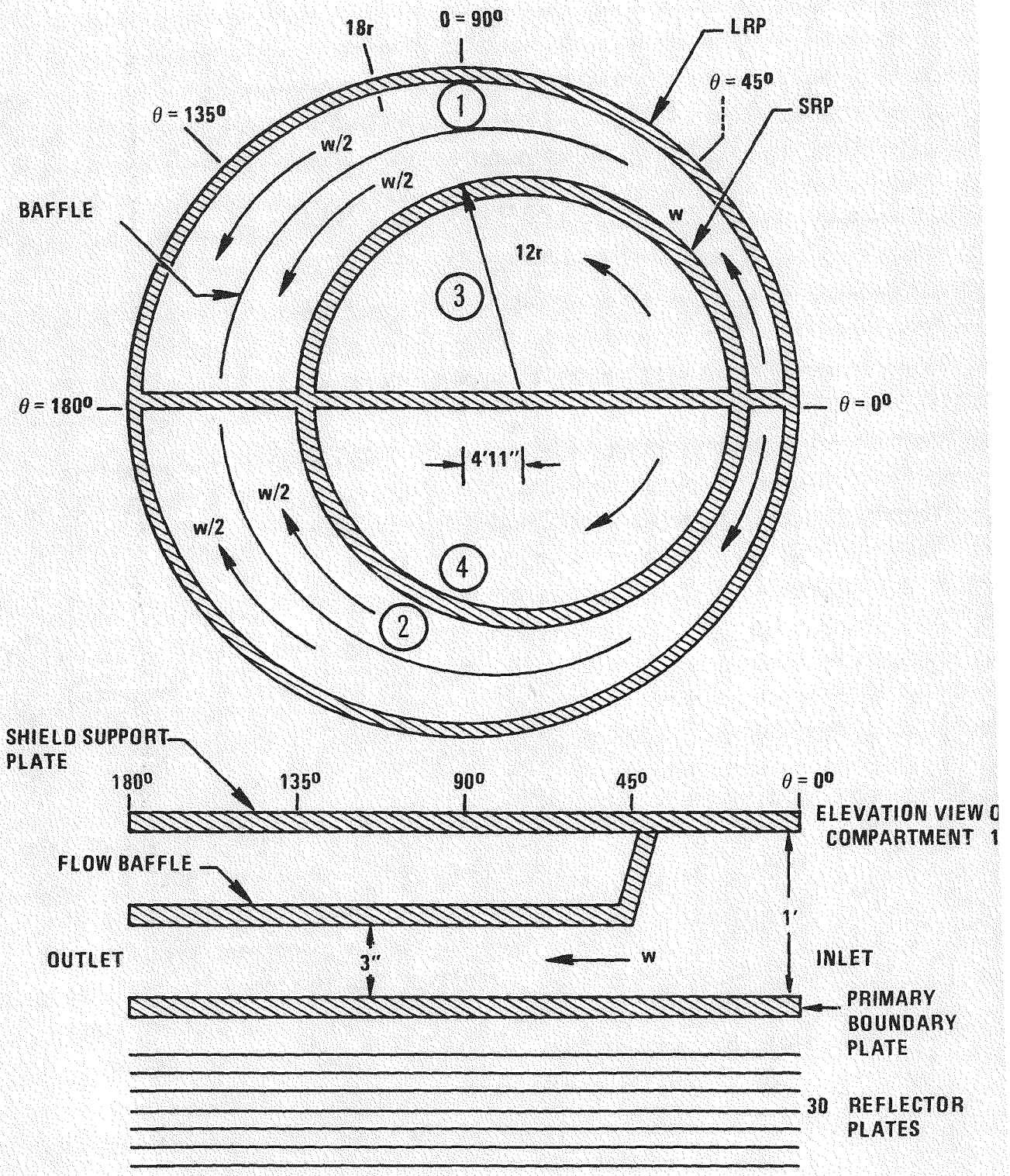

Figure B-32. Large Rotatable Plug Cooling Plena

0665-134

It is noted in Figure B-32 that vertical baffling is provided to guide the flow. This minimizes the possible occurrence of stagnation regions.

B.4.2.2.2 SELECTION OF DESIGN BASIS COOLANT FLOW

Shown in Table B-13 is a summary of calculated heat transfer coefficients versus the SRP/LRP plenum air coolant flow, at the locations shown in Figure B-32. With respect to matching a required heat transfer coefficient of 5.4 BTU/hr-ft-^{2}-^{o}F, a design flow of 4000 SCFM is selected. At this flow, the area averaged calculated heat transfer coefficient is 6.4 BTU/hr-ft^2-^{o}F. Compared to the required heat transfer coefficient, adequate heat transfer capability is ensured. Shown in Figure B-33 are plenum heat transfer coefficients and velocities at the selected flow.

TABLE B-13

SRP/LRP PLENUM CALCULATED HEAT TRANSFER COEFFICIENTS VERSUS COOLANT FLOW RATE AT VARIOUS CIRCUMFERENTIAL (θ) LOCATIONS

Flow (SCFM)	h (BTU/hr-ft^2-^{o}F) θ (degrees)* 0	45	90	135	180
2000	5.1	5.9	3.8	2.9	2.6
3000	7.2	8.2	5.2	4.0	3.8
4000	9.0	10.2	6.5	5.1	4.8
5000	10.8	12.3	7.8	6.1	5.7

*See θ locations in Figure B-32.

A summary of the SRP/LRP plenum geometry is presented in Table B-14. Plotted in Figure B-34 is the variation of the air coolant temperature rise versus flow. At 4000 SCFM, the bulk coolant temperature rise is 21^{o}F, per Figure B-34.

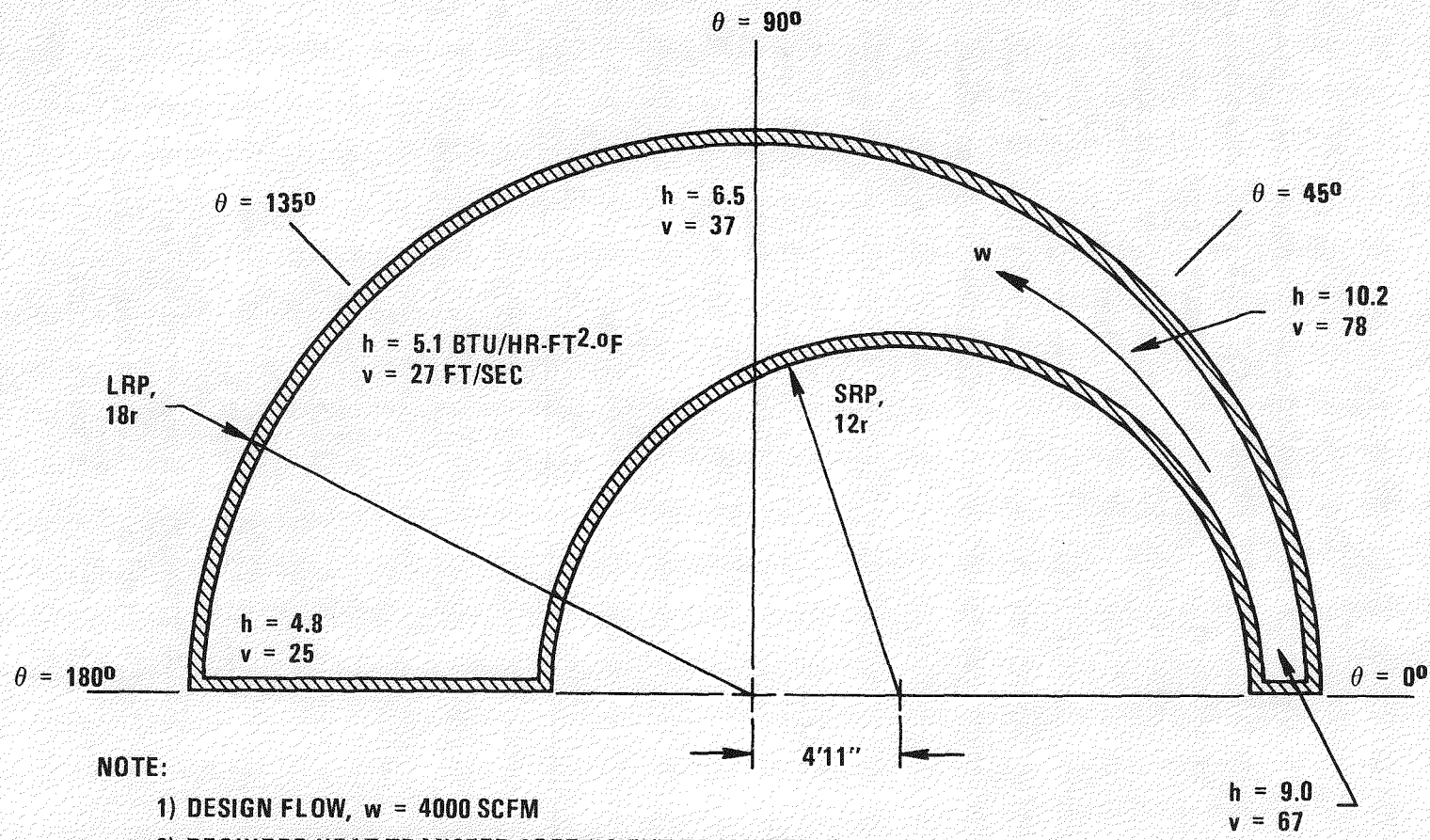

NOTE:

1) DESIGN FLOW, w = 4000 SCFM
2) REQUIRED HEAT TRANSFER COEFFICIENT TO MAINTAIN PRIMARY BOUNDARY PLATE BELOW 150°F
   $h_{REQUIRED}$ = 5.4 BTU/HR-FT^{2}-°F

Figure B-33. SRP/LRP Cooling Plenum Heat Transfer Coefficients and Velocities at Design Flow Conditions

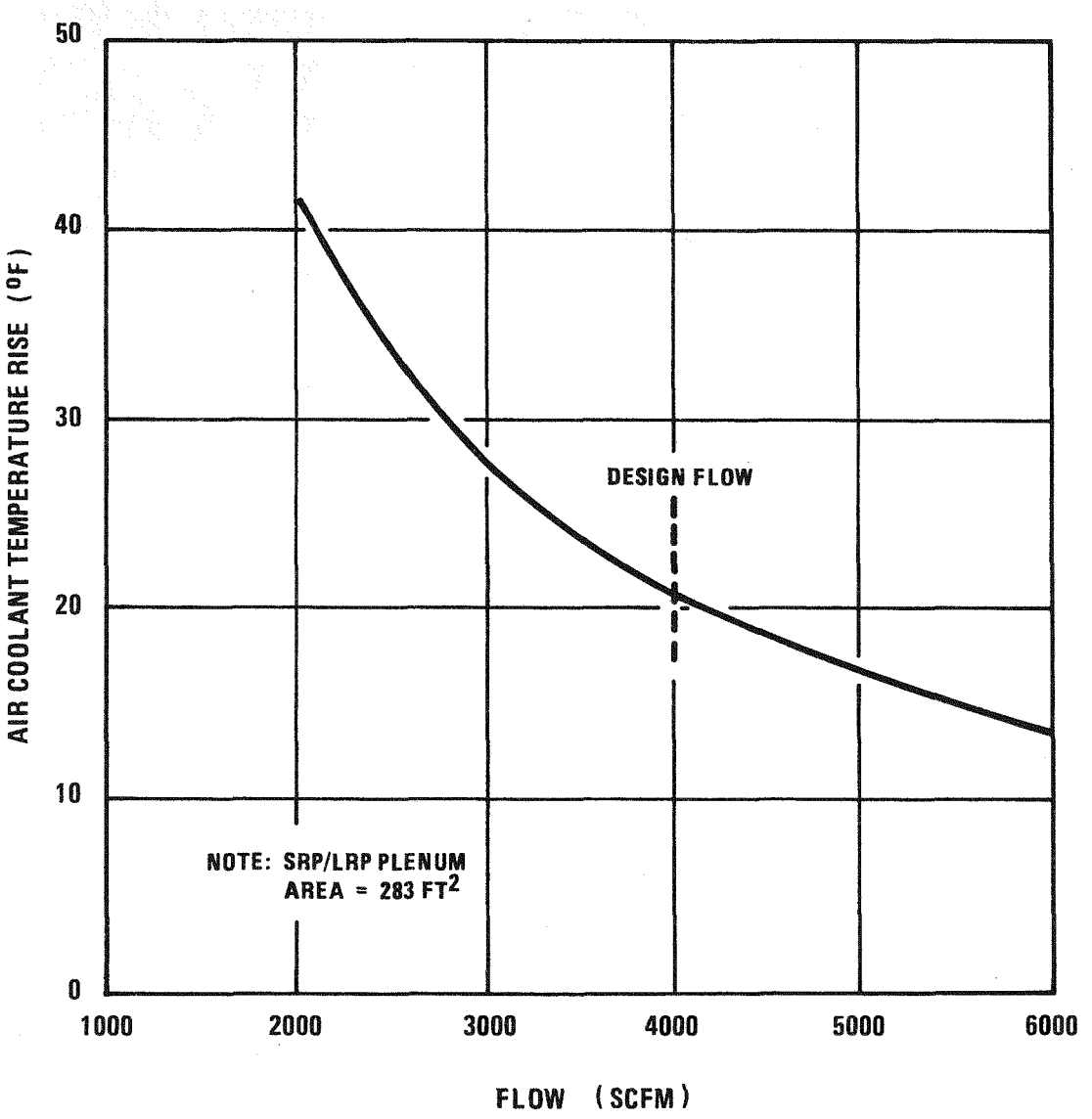

Figure B-34. SRP/LRP Plenum Air Coolant Temperature Rise Versus Coolant Flow Rate

0665-136

TABLE B-14

SRP/LRP PLENUM GEOMETRY SUMMARY

θ (degrees)	Hydraulic Diameter, D_H (feet)	Flow Area (ft^2)
0	1.0	1.0
45	0.44	0.85
90	0.47	1.8
135	0.48	2.5
180	0.48	2.7

B.4.2.2.3 COOLING OF SMALL ROTATABLE PLUG REGION

Applying area scaling factors, flow requirements for the deck region contained within the small rotatable plug are obtained. The areas of each smaller inboard SRP Plenum and each larger outboard SRP/LRP plenum are 226 and 283 square feet, respectively. Also accounting for increased penetration heating in the smaller SRP region, a scaled flow of 3700 SCFM is determined. For design purposes, however, a value of 4000 SCFM is considered. The total flow required for the four (4) rotatable plugs plena then is 16,000 SCFM.

Combined with the maximum system pressure drop of 27 inches H_2O, the theoretical horsepower is 68 H.P. Assuming an efficiency factor of 0.7, the required horsepower is 97 H.P.

B.4.2.2.4 LRP ROTATABLE PLUGS COOLING SYSTEM PARAMETER SUMMARY

A summary of the LPR rotatable plugs cooling system parameters is presented in Table B-15.

TABLE B-15

LPR ROTATABLE PLUGS-COOLING
SYSTEM PARAMETERS

Primary Boundary Plate Design Temperature	150°F
Deck Top Plate Design Temperature	110°F
Total Rotatable Plug Heat Load	245,000 BTU/hr
Design Flow Rate (Maximum)	16,000 SCFM
Air Coolant Inlet Temperature	85°F
Air Coolant Temperature Rise	21°F
Maximum System Pressure Drop	27 inches H_2O
Total Fan Horsepower (70% efficiency)	97
System Uncertainty Factor (Reflected in Fan Horsepower)	2.0

B.4.2.2.5 ROTATABLE PLUGS COOLING SYSTEM VERIFICATION

Detailed follow-up verification analyses of the rotatable plugs per the reference design utilizing 2-D or 3-D thermal models are not performed. However, based on 1-D analysis and an extrapolation of results obtained for the stationary portion of the deck (Sections B.3.3 and B.3.4), the cooling system is found to be adequate. At steady-state normal operating conditions, the average estimated temperature of the plug primary boundary is 130°F, while the top plate average temperature is 92°F. These temperatures correspond to the design basis flow of 16,000 SCFM.

In the event of a loss of air coolant, it can be deduced that a slower heatup of the plug structure and less severe overall temperature gradients occur, compared with the stationary deck. This is partially due to the fact that on a unit area basis, the thermal capacitances of the rotatable plugs

and the stationary deck are approximately equal, and would therefore respond identically to the transient. Additionally, the greater thermal capacitance associated with the 30 reflector plates of the rotatable plugs, versus the 20 plates of the stationary deck, would tend to result in a slower heatup of the plugs.

B.5 CONCLUSIONS

B.5.1 STATIONARY DECK

- At steady state normal operating conditions, deck temperatures are found to be within acceptable levels. This is true if the deck cooling system is operative at both 100% and 66.6% of the design basis flow. Since acceptable temperatures are obtained at the reduced coolant flow, it is concluded that the deck cooling flow requirements are adequate to maintain specified temperatures, and that sufficient margin against uncertainty is provided.

- In the event of a loss of air coolant accident, the slow heatup of the deck structure should pose no serious structural difficulty. The deck structure was shown good for a more severe transient in the Interim Report. However, detailed corresponding structural analyses should be performed as the design evolves.

B.5.2 ROTATABLE PLUGS

- Based on extrapolations of results obtained from analysis of the stationary deck it is concluded that the rotatable center plugs cooling system is adequate, both at steady state and transient conditions. Also, the 30 reflector plates of the rotatable plugs versus the 20 plates at the stationary deck provides moderate additional thermal protection.

APPENDIX C
VESSEL COOLING AND INTERMEDIATE PLENUM ANALYSES

C.1 INTRODUCTION

This Appendix presents the thermal and hydraulic analyses used to define the reference vessel insulation. The insulation consists of a series of thin (150 mils), concentric steel shells called "reflector plates" of different lengths which produce the desired vessel temperature distribution from the bottom of the deck to a location about 13 ft below the deck. Figure C-1 shows a longitudinal view of the reflector plates. Parameters considered in the analysis are the location of the gas dam between the reactor vessel and the guard tank, horizontal baffle height, number and lengths of reflector plates, passive and active vessel cooling and nitrogen heat transfer coefficient in the reactor cavity. A one-dimensional heat transfer scoping analysis provided the basis to select a preliminary vessel reflector plate geometry and a two-dimensional heat transfer analysis confirmed the adequacy of the vessel reflector plate geometry.

The principal function of the three intermediate plena, Figure C-2, is to insulate the lower support structure from the large hot and cold pool temperature difference. Practically all of the pool temperature difference occurs across the sodium in the intermediate plena. Knowledge of the plena spatial temperature distribution is important in the design of the components which form the boundaries of the plena. Two-dimension steady state and transient analyses are reported for the intermediate plenum. The data consists of plots of velocity distributions and temperature isotherms.

C.2 ONE-DIMENSIONAL METHOD

C.2.1 METHOD OF ANALYSIS

The selection of the number of reflector plates and their lengths to produce specified vessel axial temperature gradient is a two-dimensional heat

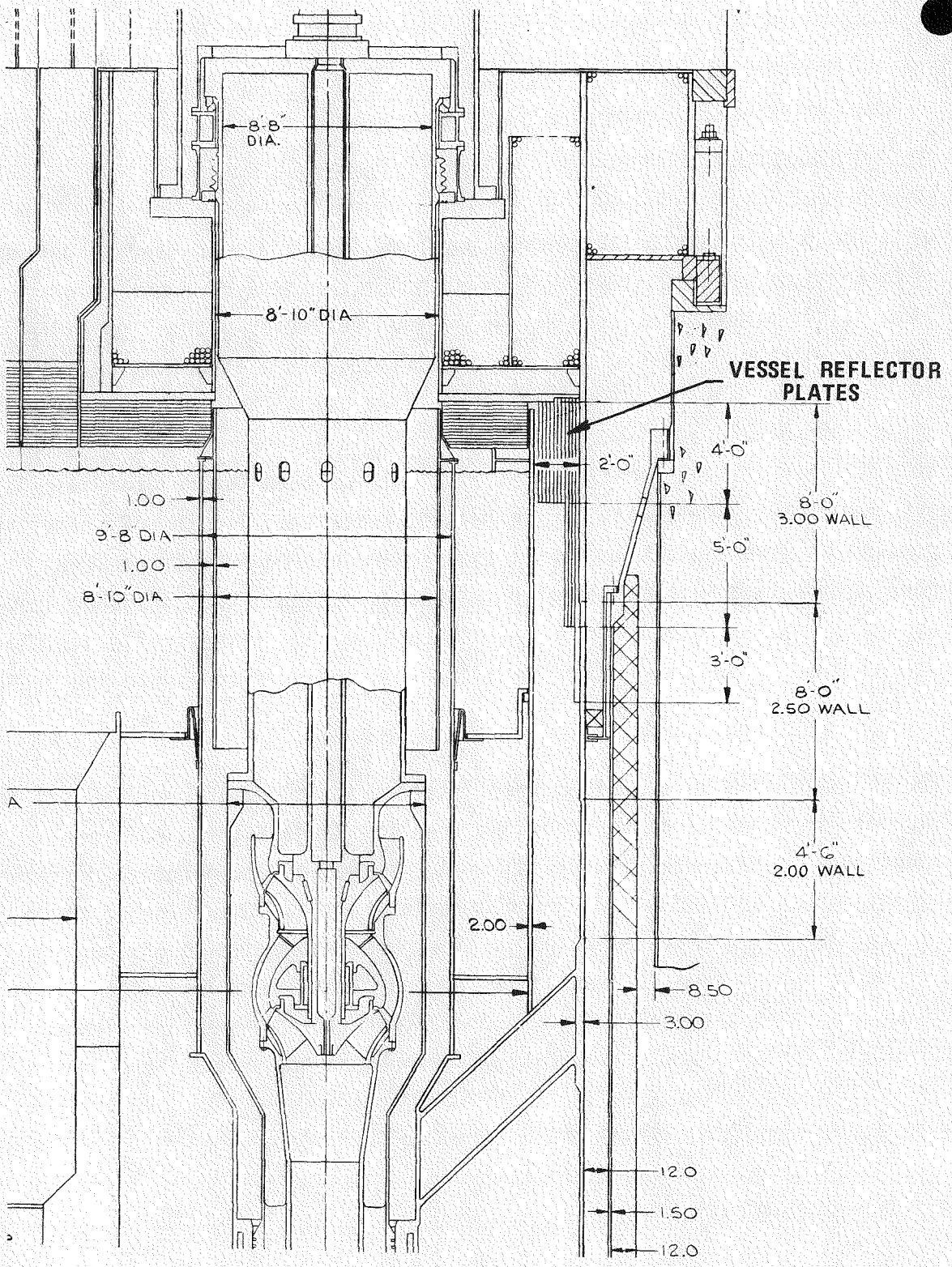

Figure C-1. Longitudinal View of Vessel Reflector Plates

0665

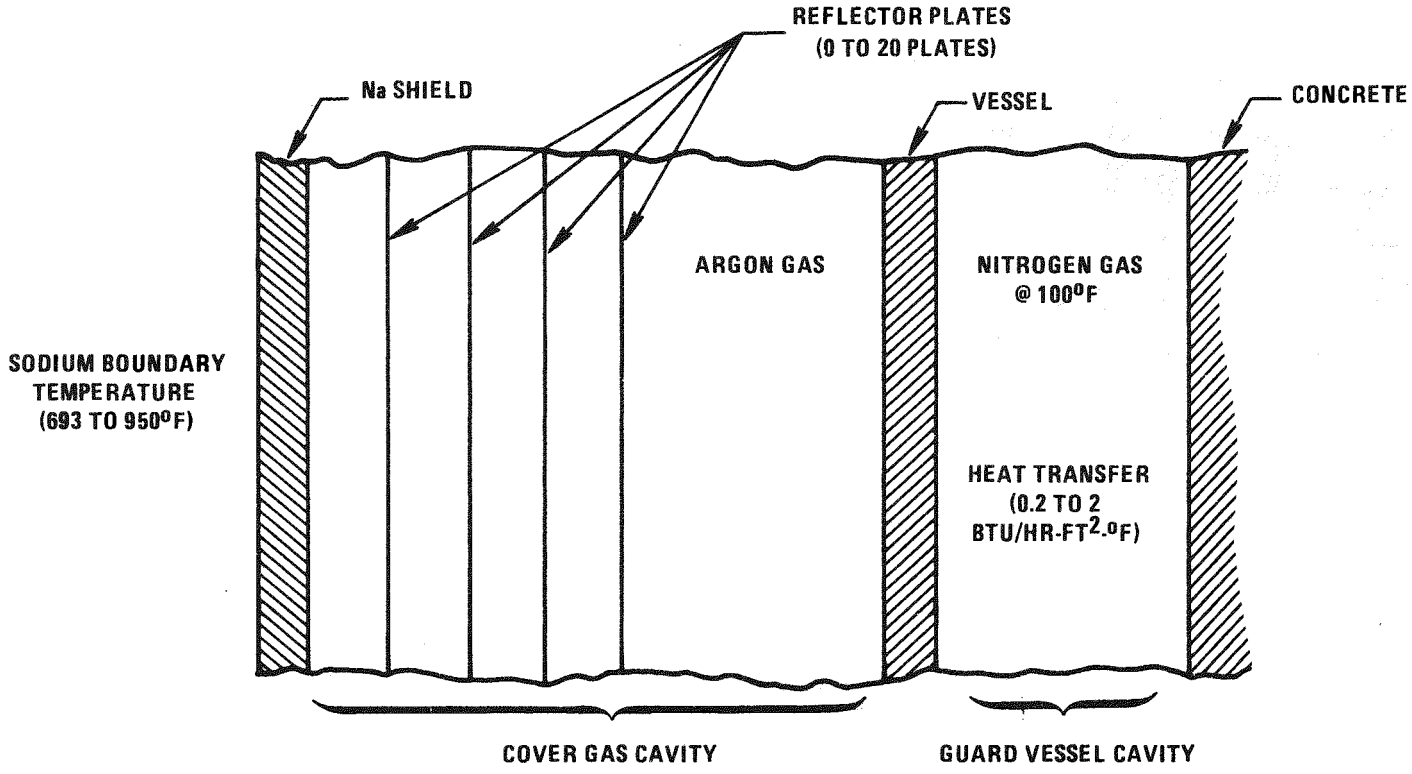

Figure C-2. One-Dimensional Vessel Cooling Geometry

transfer problem. Other factors which complicate the selection are passive or active vessel cooling, horizontal baffle elevation, and gas dam location. An active vessel cooling system physically differs from a passive vessel cooling system by the addition of a one inch steel cylinder just inside the sodium shield cylinder. The annulus formed is the cooling flow annulus in which one percent of the pump flow enters the bottom of the annulus and discharges from the top of the annulus into the hot pool.

A scoping method of analysis is developed which involves a one-dimensional heat transfer analysis to rapidly assess the axial temperature gradient considering the above variables. From this analysis, a preliminary reflector plate geometry is selected for the vessel.

C.2.1.1 MODEL

The LPR region modeled extends radially outward from the sodium shield to the reactor cavity wall. A unit axial length is chosen to provide the flexibility to simulate any axial section of the sodium shield. Figure C-3 shows the geometry analyzed by the TAP-A model, Reference C-1.

The model parameters which are varied to control the vessel temperature are:

- Sodium Shield Inner Boundary Temperature. A range of temperatures from 693°F to 950°F permits simulation of active or passive plenum separator cooling.
- Reflector Plates. The number of reflector plates is varied to obtain the desired vessel temperature.
- Reactor Cavity Heat Transfer Coefficient. The range of heat transfer coefficients considered varies from 0 to 2.0 BTU/hr-ft^2-°F. Natural, laminar, or force convection modes of heat transfer can be selected in the cavity.

The heat transfer assumptions are:

- Thermal radiation between all surfaces.
- Natural convection between vessel and reflector plate adjacent to vessel.

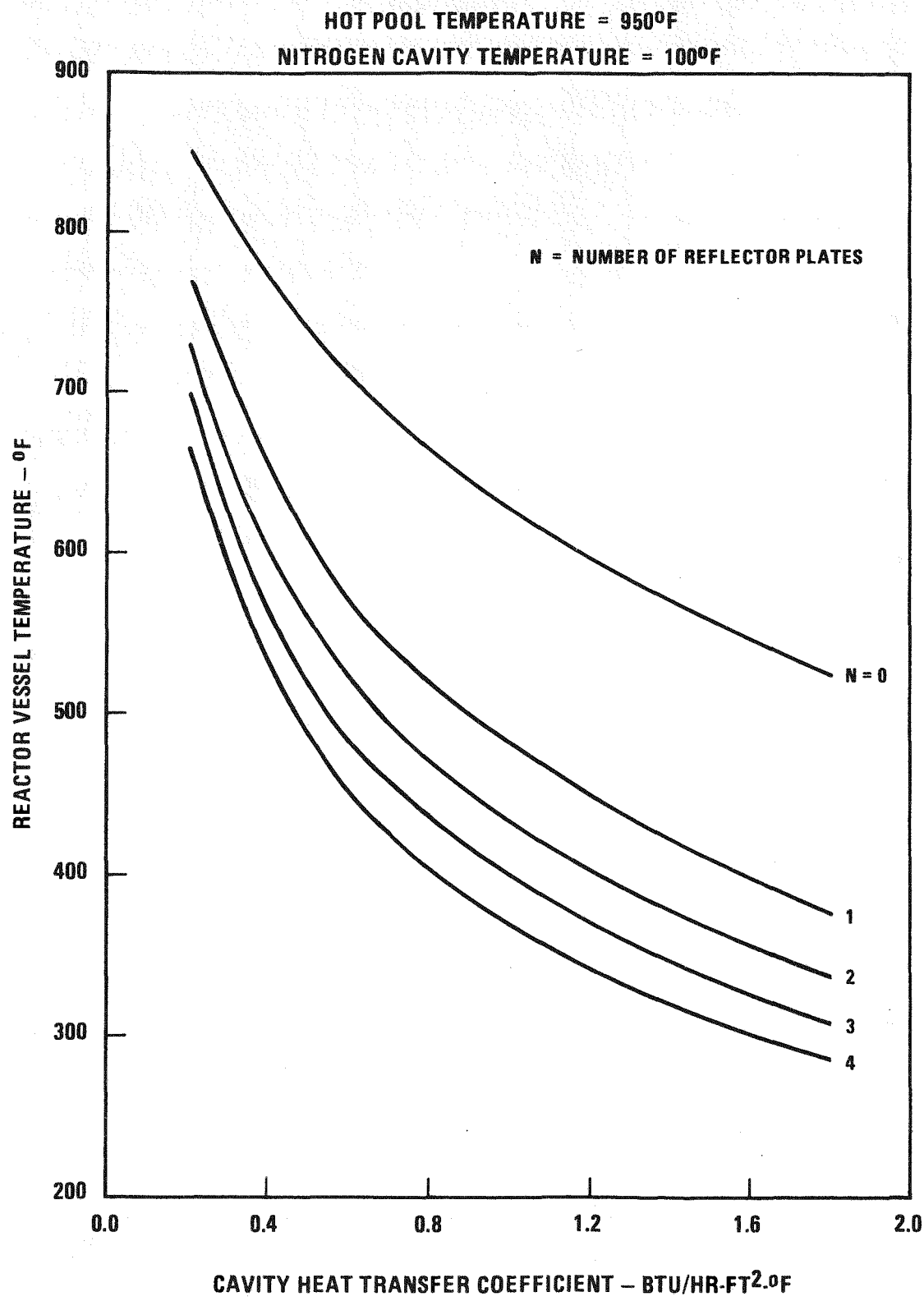

Figure C-3. One-Dimensional Vessel Analysis Results

0665-114

- o Vessel and concrete to nitrogen heat transfer coefficients are equal.
- o Concrete surface is an adiabatic boundary.
- o Mechanical spacers between vessel and reflector plates equivalent heat transfer area is 2% of the vessel heat transfer area.
- o Emissivity = 0.28

C.2.1.2 RESULTS

The reactor vessel temperature vs. cavity heat transfer coefficients for different numbers of reflector plates are shown in Figures C-4 to C-9. The results for a 950^{o}F hot pool temperature correspond to a passively cooled plenum separator, and the 693^{o}F to 747^{o}F hot pool temperatures correspond to an actively cooled plenum separator with 1% cooling flow. The 693^{o}F temperature is the inlet sodium coolant temperature and the 747^{o}F temperature is the outlet sodium coolant temperature.

C.2.1.3 AXIAL TEMPERATURE DISTRIBUTION

The procedure to estimate the axial vessel temperature distribution from the one-dimensional model is explained in the following example. First the type of plenum separator cooling is selected (for the example it is passive vessel cooling). Therefore, Figures C-4 and C-5, which have the 950^{o}F hot pool temperature, apply.

The desired axial temperature distribution is basically linear having smooth transitions at the top and bottom temperature interfaces (resembles an elongated S-shaped curve). The top of the vessel temperature equals the deck primary boundary temperature of 150^{o}F. The vessel axial temperature distribution below the gas dam equals the sodium shield axial temperature distribution. The reason for this is that the radial heat flux from the vessel below the horizontal baffle is negligible because the guard tank is heavily insulated and the gas dam prevents the natural circulation of the hot nitrogen in the guard tank/vessel annulus with the cool nitrogen from the reactor cavity. Thus, the temperature of the lower part of the vessel

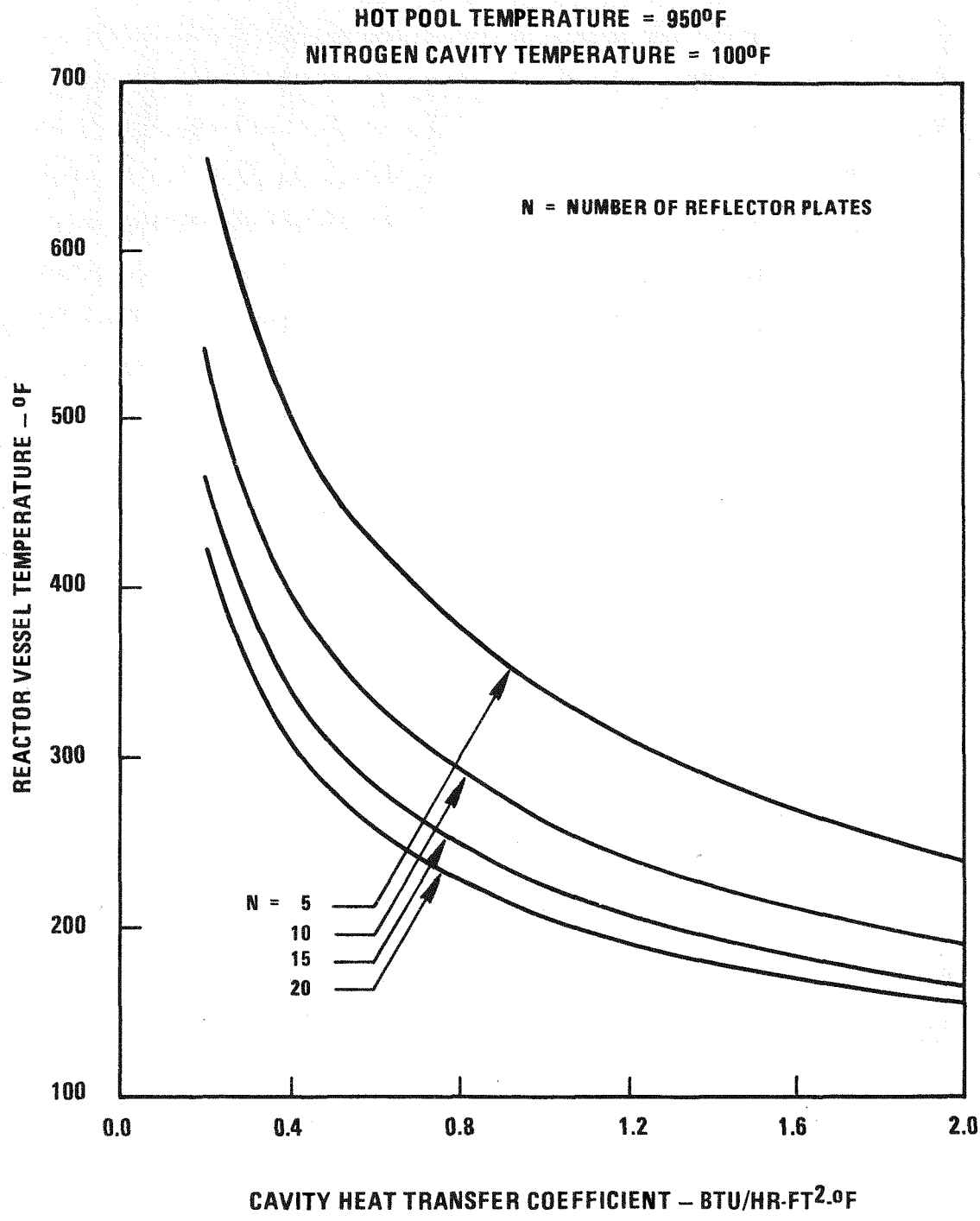

Figure C-4. One-Dimensional Vessel Analysis Results

0665-119

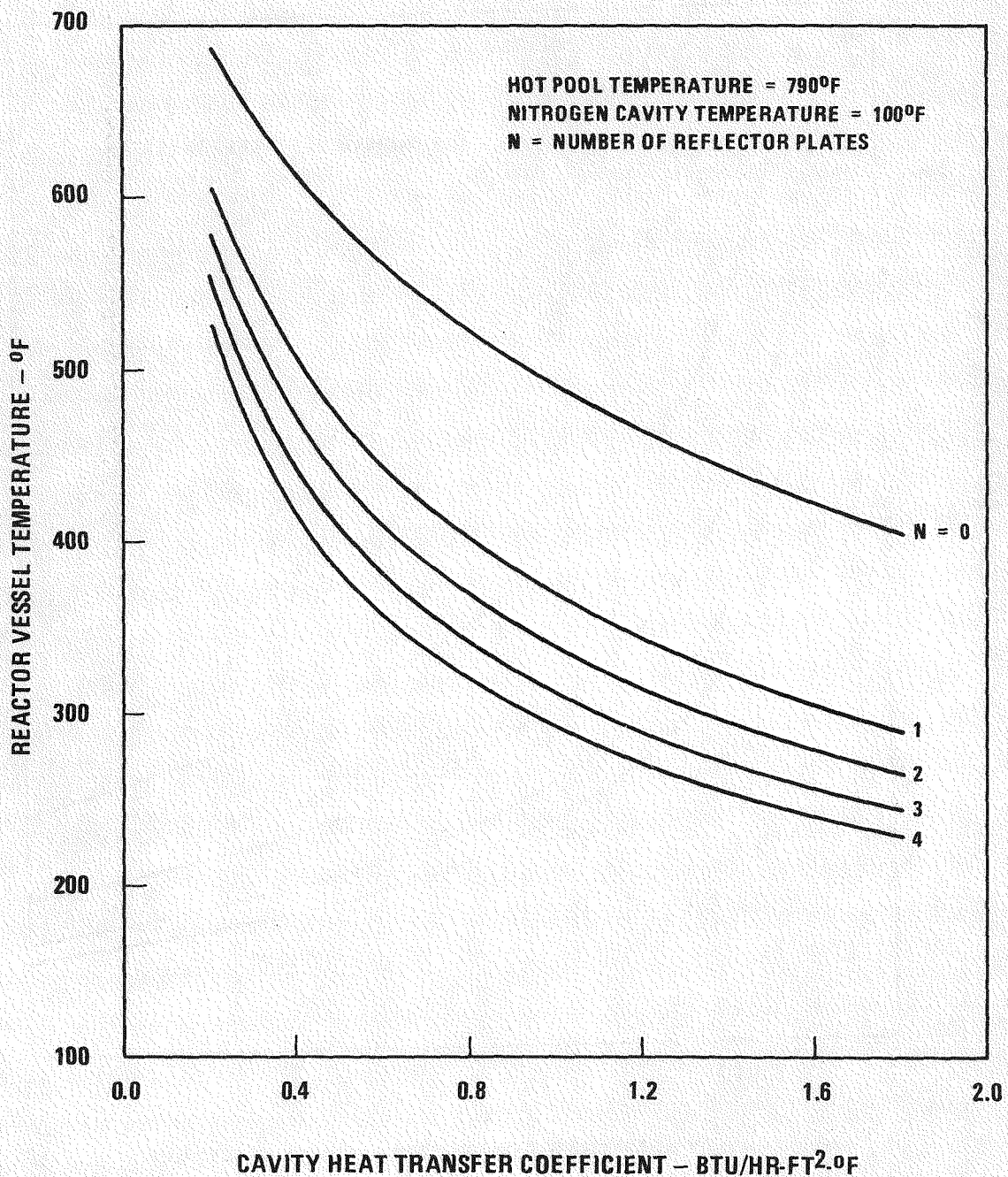

Figure C-5. One-Dimensional Vessel Analysis Results

0665-23

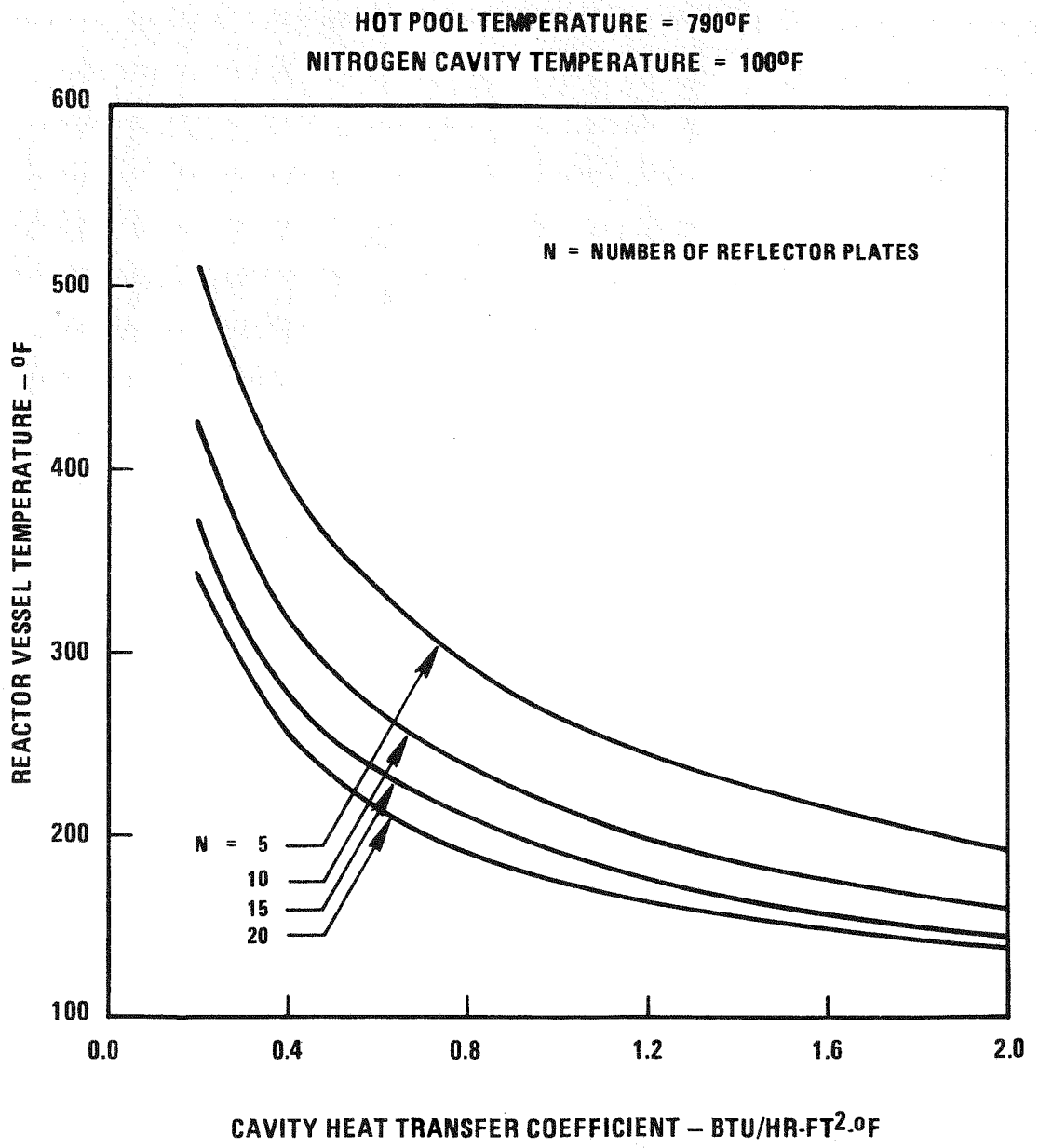

Figure C-6. One-Dimensional Vessel Analysis Results

0665-120

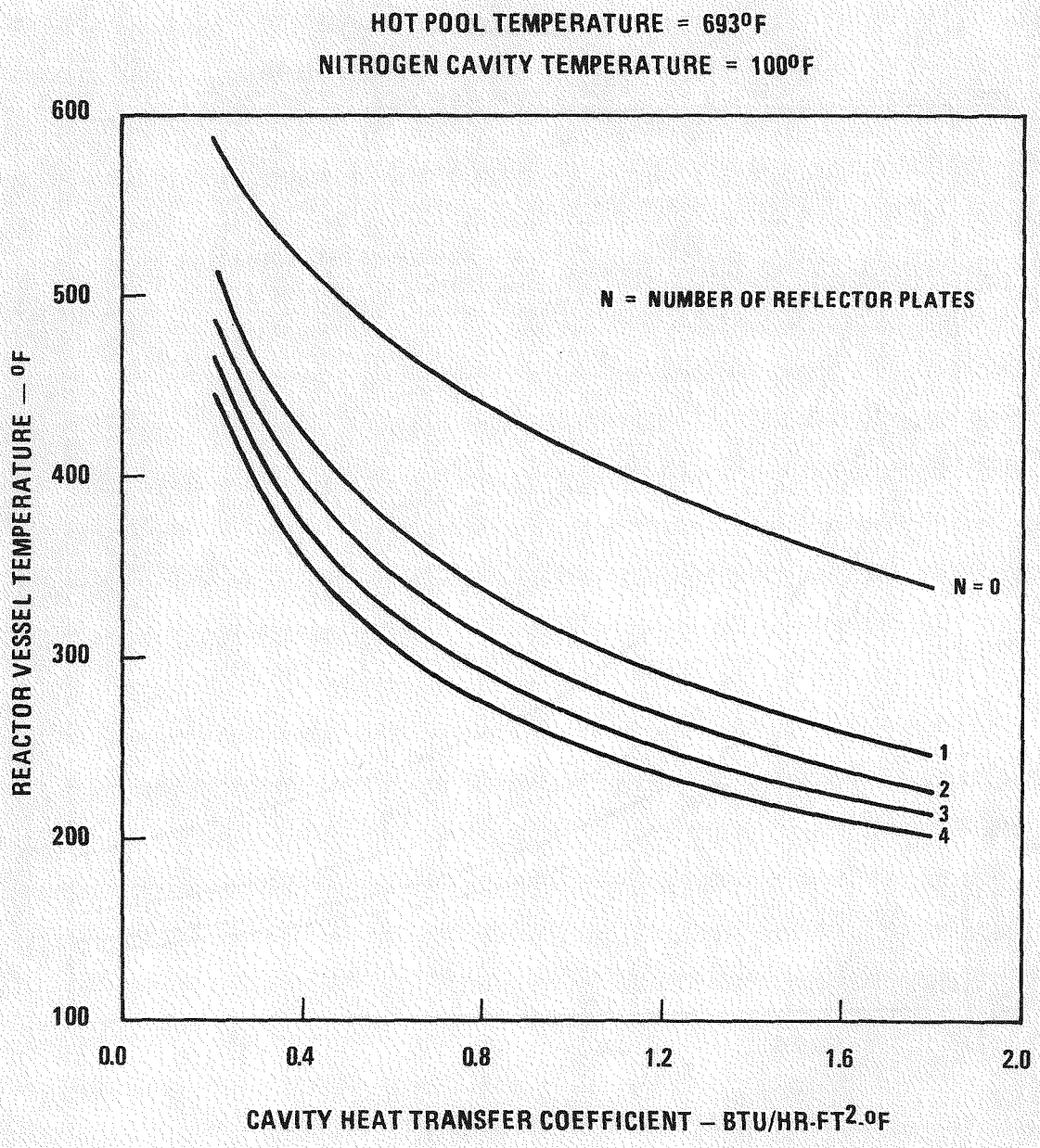

Figure C-7. One-Dimensional Vessel Analysis Results

0665-121

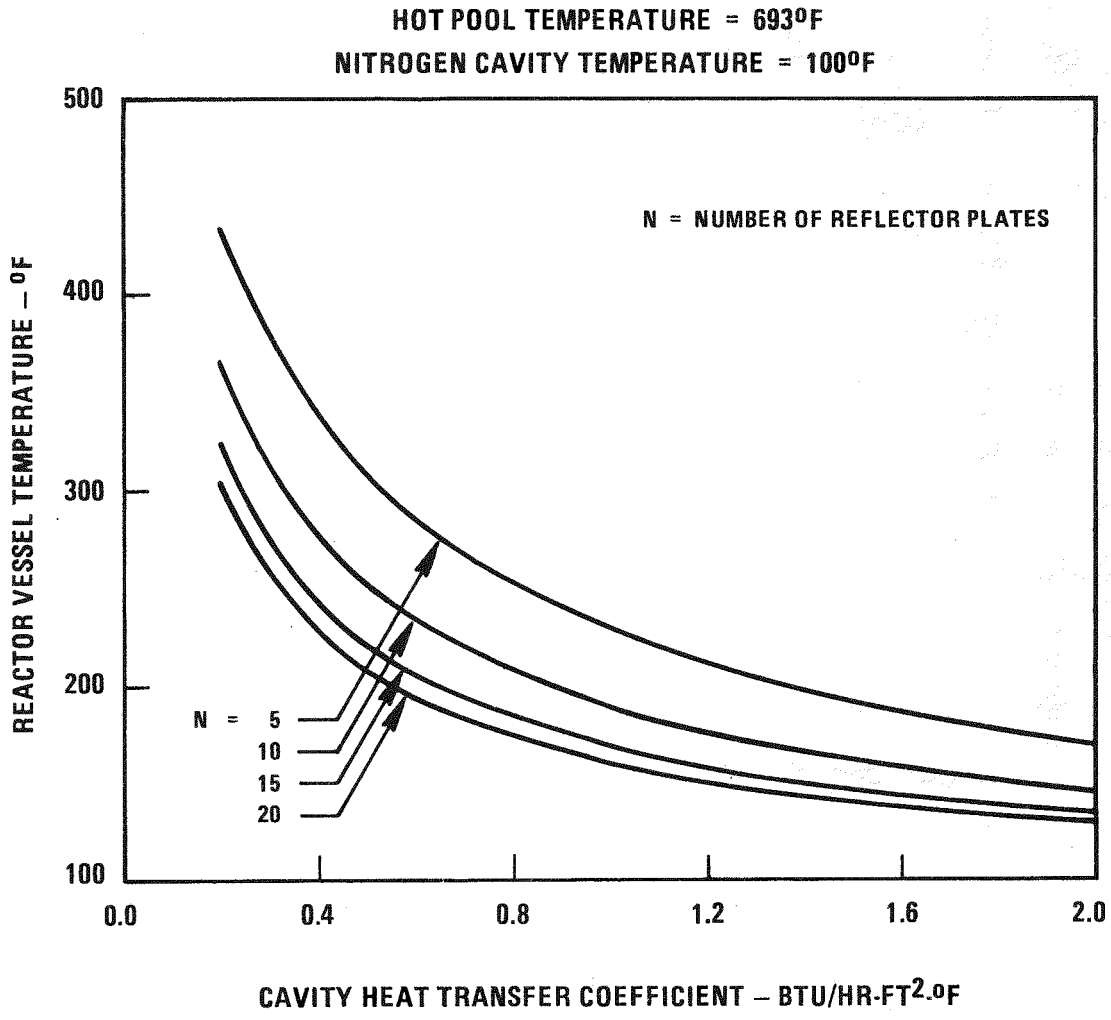

Figure C-8. One-Dimensional Vessel Analysis Results

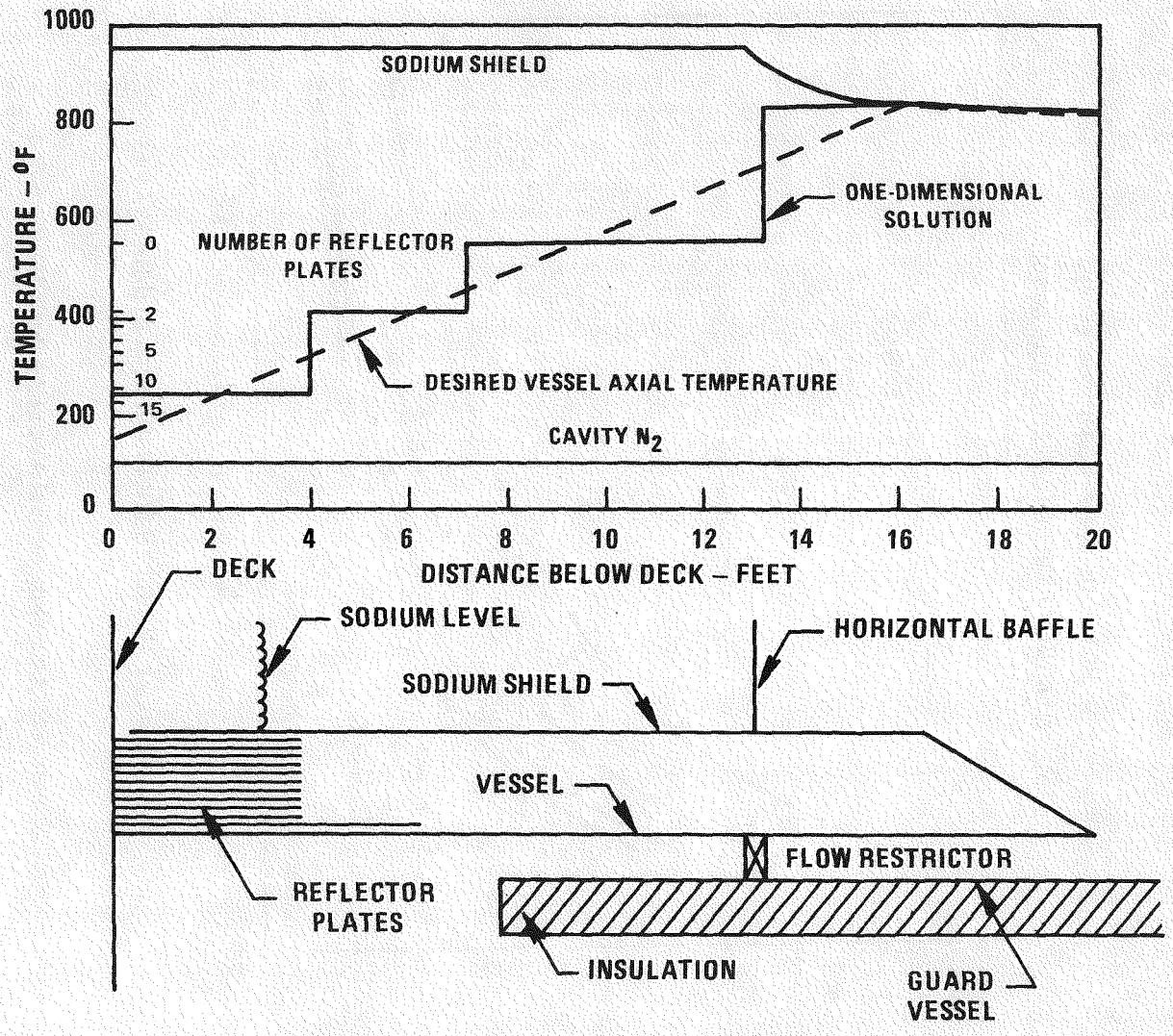

Figure C-9. One-Dimensional Vessel Temperature Distribution for Passive Vessel Cooling

equals the sodium shield temperature at the gas dam, which is 820°F. Figure C-10 shows the desired vessel temperature distribution from a maximum temperature of 820°F to a temperature of 150°F near the top of the vessel.

The next step is to select the number and lengths of reflector plates to obtain the desired vessel temperature. The selection of the number of reflector plates and their length is accomplished by placing on the temperature scale, tick marks which indicate the number of reflector plates to give that vessel temperature. Then the number of plates and length of plates are selected as a series of steps that bound the desired temperature distribution. Axial conduction in the vessel smooths out the steps and approximates the desired temperature distribution. About 11 plates are needed for the first four feet from the deck primary boundary, and one plate which extends three feet beyond these eleven.

An interesting point can be made concerning the nitrogen convection in the reactor cavity. The vessel temperature step from the maximum vessel temperature, 820°F, to the no reflector plate temperature, 550°F, is 270°F which is significant. The no reflector plate temperature is based on natural circulation in the reactor cavity. If forced convection is used in the reactor cavity, the no reflector plate temperature is reduced which results in too large a vessel temperature step. Therefore, natural convection in the reactor cavity is required and is used throughout the analysis.

C.2.2 SELECTION OF ACTIVE OR PASSIVE PLENUM SEPARATOR COOLING

The vessel temperature distributions for active and passive plenum separator cooling are shown respectively in Figures C-10 and C-11. The maximum temperature with passive cooling is 800°F, and, with active cooling, it is about 700°F. The active cooling requires a smaller number of reflector plates because of the colder sodium boundary temperature, but requires considerable design complexity to cool the vessel. However, the advantage of a lower maximum vessel temperature and a smaller number of reflector

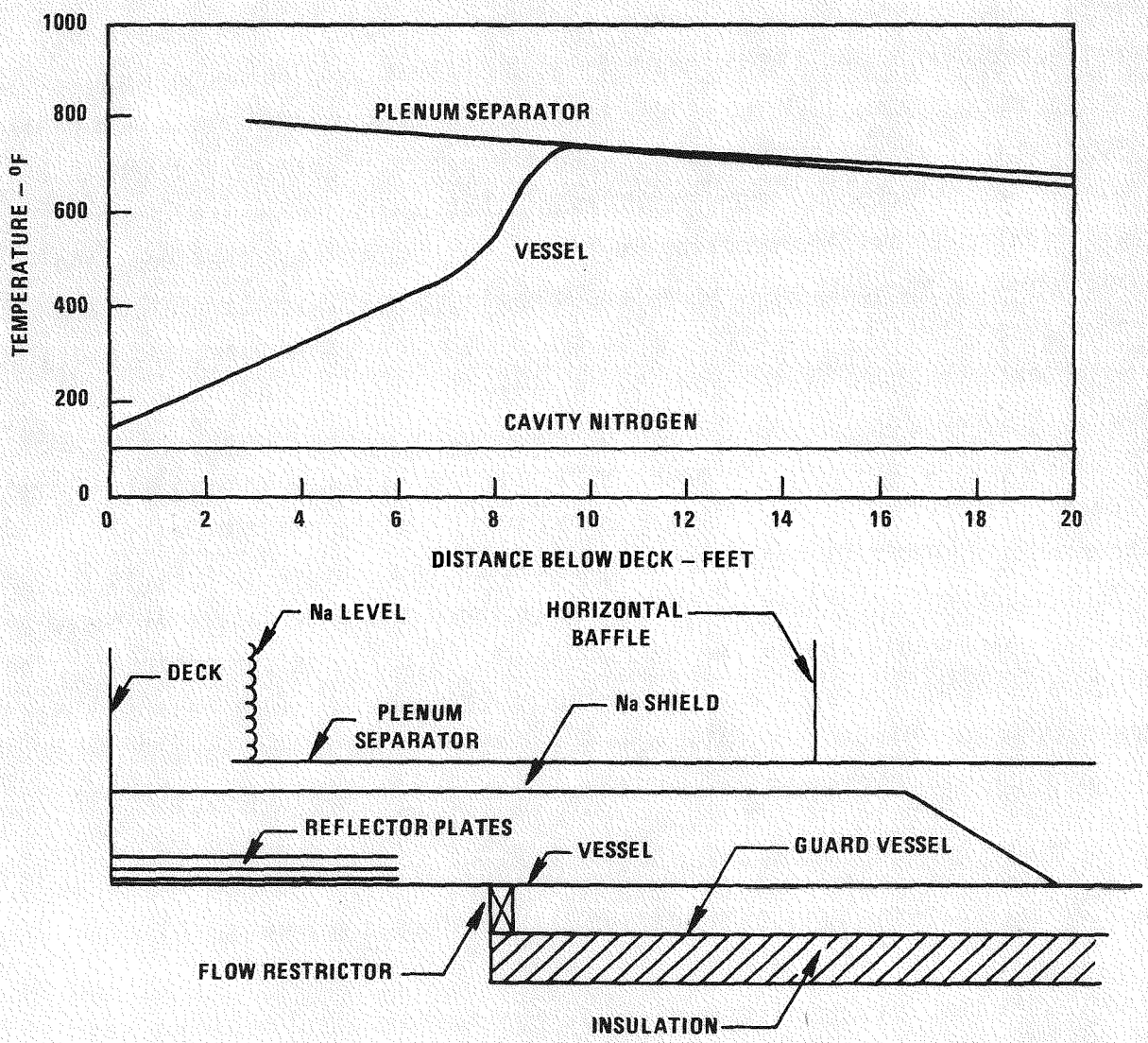

Figure C-10. One-Dimensional Vessel Temperature Distribution for Active Vessel Cooling

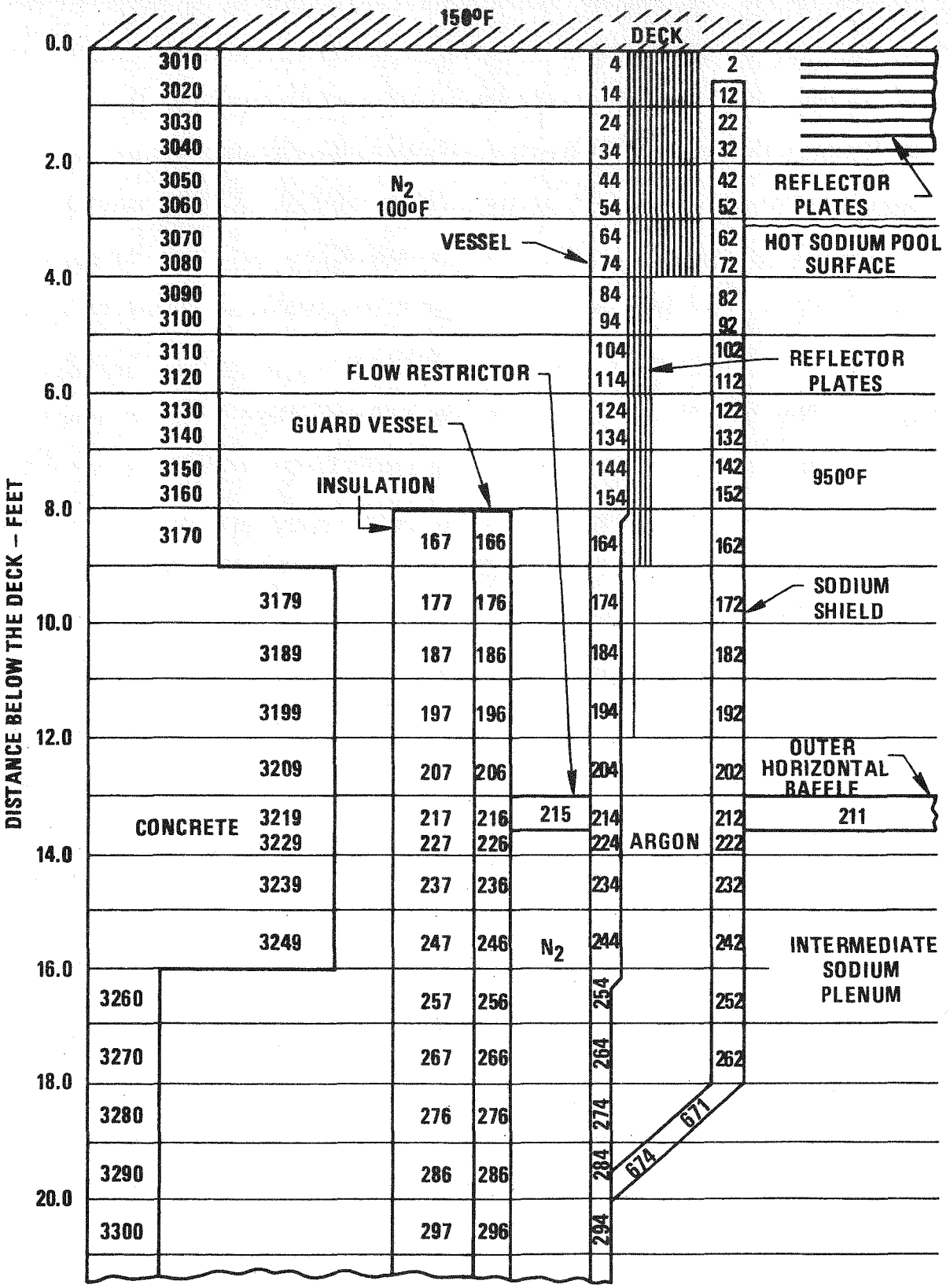

Figure C-11. TAP-A Two-Dimensional Nodal Model of the Vessel

0665-139

plates is not worth the inefficiency of a one percent active plenum separator cooling flow which must be discharged at a low temperature into the hot pool. The added design complexity is also undesirable. Therefore, passive vessel cooling is selected as the preferred cooling mode.

C.2.3 EFFECT OF HORIZONTAL BAFFLE AND GAS DAM LOCATIONS

The horizontal baffle defines the length of vessel exposed to the hot pool ($950^{o}F$). A slight reduction of the heat flux to the vessel occurs if the horizontal baffle is located close to the free sodium surface. However, the reduction in heat flux is not significant, and other factors dictate the horizontal baffle height. A small hot pool height causes high velocities over the horizontal baffles. The consequence of a high velocity is the possible formation of vortices which increase cover gas entrainment, and could possibly cause IHX flow oscillations. Also, a large intermediate plenum enclosed by a thin shell structure may have excessive flow induced vibrations. A reasonable hot pool height which mitigates these factors is judged to be about 13 ft.

The nitrogen gas dam located in the annulus between the vessel and guard tank affects the vessel temperature distribution. The gas dam minimizes the natural convection heat loss from the vessel below the dam. The dam in conjunction with the guard tank insulation, results in a negligible radial heat flux. Thus, the axial temperature of the vessel is approximately equal to the sodium shield axial temperature below the dam.

If the dam is moved above the horizontal baffle height, the vessel temperature would increase to the sodium shield hot pool temperature. This is undesirable because it increases the vessel temperature gradient. Movement of the dam down from the horizontal baffle elevation, stretches out the vessel temperature gradient. This requires longer and possibly more reflector plates to achieve the stretch out temperature gradient. Consequently, the best position for the dam is at the same elevation as the horizontal baffle.

C.3 TWO-DIMENSIONAL ANALYSIS

The one-dimensional vessel analysis is used to select a preliminary reflector plate geometry. Neglected in the analysis is vessel axial heat conduction. A two-dimensional analysis is required to assess the axial conduction before firming-up the reflector plate geometry.

C.3.1 MODEL

The section modeled for the TAP-A computer code consists of a 5 degree slice extending from the reactor deck down 22 ft toward the bottom of the vessel, and radially from the hot pool side of the sodium shield to the concrete containment wall. Figure C-12 shows an elevation view of the TAP-A nodal model.

The external thermal boundary conditions are:

- Primary boundary plate at bottom of deck is at 150°F.
- Sodium shield exposed to cover gas above the hot pool. Thermal radiation from the hot pool surface, 950°F, and from the edge of the deck reflector plates and natural convection.
- Sodium shield containing the hot pool is at 950°F.
- Sodium shield exposed to intermediate plenum varies exponentially from 950°F at the horizontal baffle to 820°F three feet below.
- All component surfaces at bottom of model have adiabitic surfaces.
- Concrete containment wall is adiabatic.
- Natural convection occurs between adjacent surfaces in the concrete cavity.
- Nitrogen at 100°F is contained in the concrete cavity.

The internal thermal boundary conditions are:

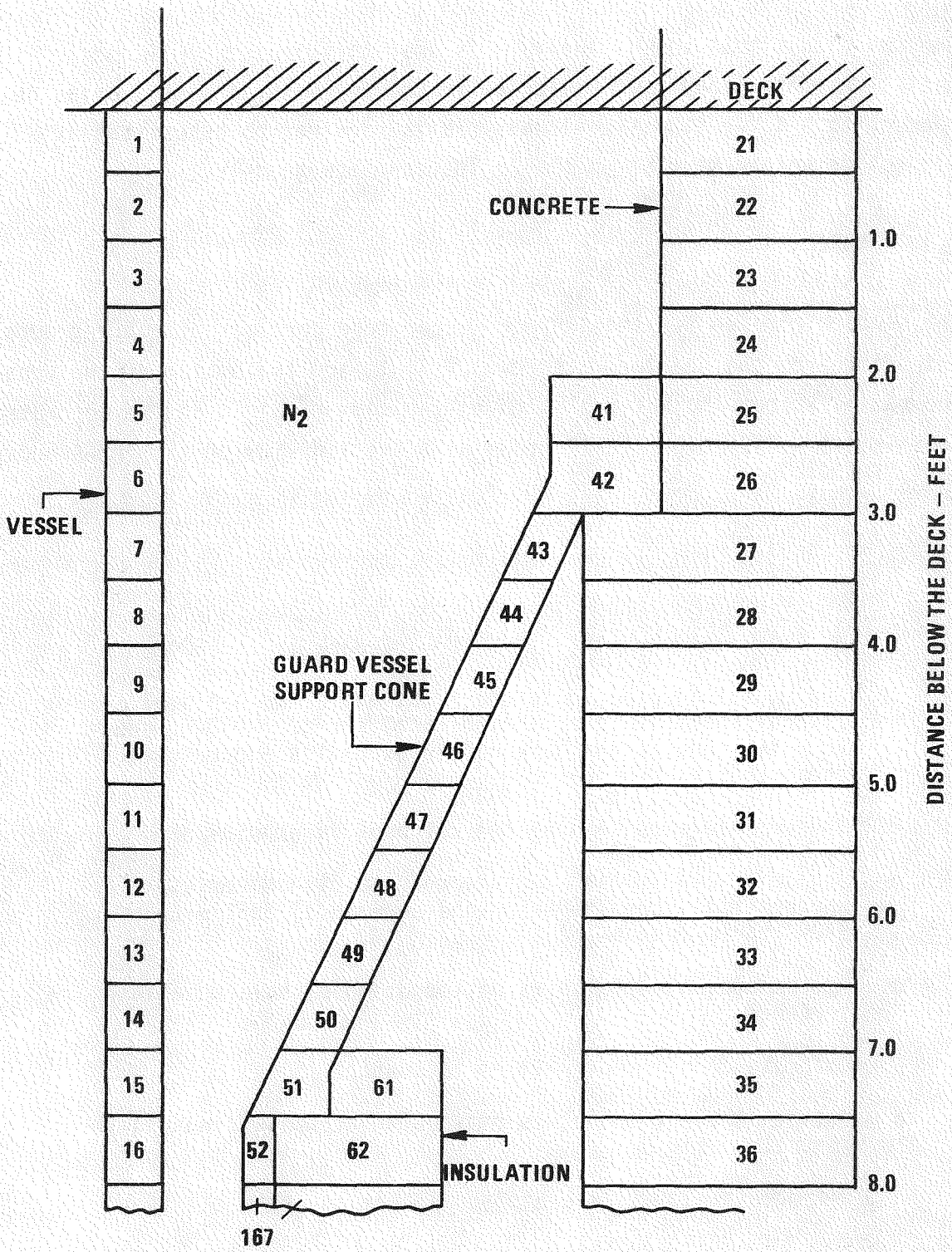

Figure C-12. TAP-A Two-Dimensional Nodal Model of the Guard Vessel Support Cone

0665-140

- o Sodium shield/vessel annulus. Argon cover gas is in the annulus and natural convection occurs between sodium shield and adjacent reflector plate and the vessel and sodium shield. Thermal radiation occurs between the vessel, reflector plates and sodium shield.

- o Axial and radial conduction occurs in all the components.

- o Guard tank/vessel annulus. Below the flow restrictor the mode of heat transfer is thermal radiation. Above the flow restrictor the modes of heat transfer are thermal radiation and natural convection.

The top cone portion of the guard tank is not modelled in the TAP-A model. When the TAP-A model was generated the reference design was not complete. The tank temperature is only slightly affected by the exclusion of the guard tank top cone. A separate TAP-A model was generated for the top cone and its nodal map is shown in Figure C-13. This model supplies the guard tank and concrete wall temperatures in the guard tank cone region.

C.3.2 COMPARISON WITH ONE-DIMENSIONAL ANALYSIS

The two-dimensional model is used to calculate the same reflector plate geometry as the one-dimensional model. Figure C-14 shows a comparison of the vessel axial temperature distribution for the one and two dimensional models. The location that has the largest difference in vessel temperature is at the deck boundary or zero vessel length. It is not surprising because the deck reflector plates acts as insulation which causes the rather flat temperature distribution over the first two feet of vessel length. Because of the deck boundary effect on vessel temperature, more and longer reflector plates are added to improve the temperature distribution.

C.3.3 SELECTION OF REFLECTOR PLATE GEOMETRY

The one-dimensional reflector plate geometry is not an optimum one as the two-dimensional model demonstrates. The one-dimensional reflector plate geometry is improved with the two dimensional model and the resultant reflector plate geometry is shown in Figure C-15. A small flattening of the

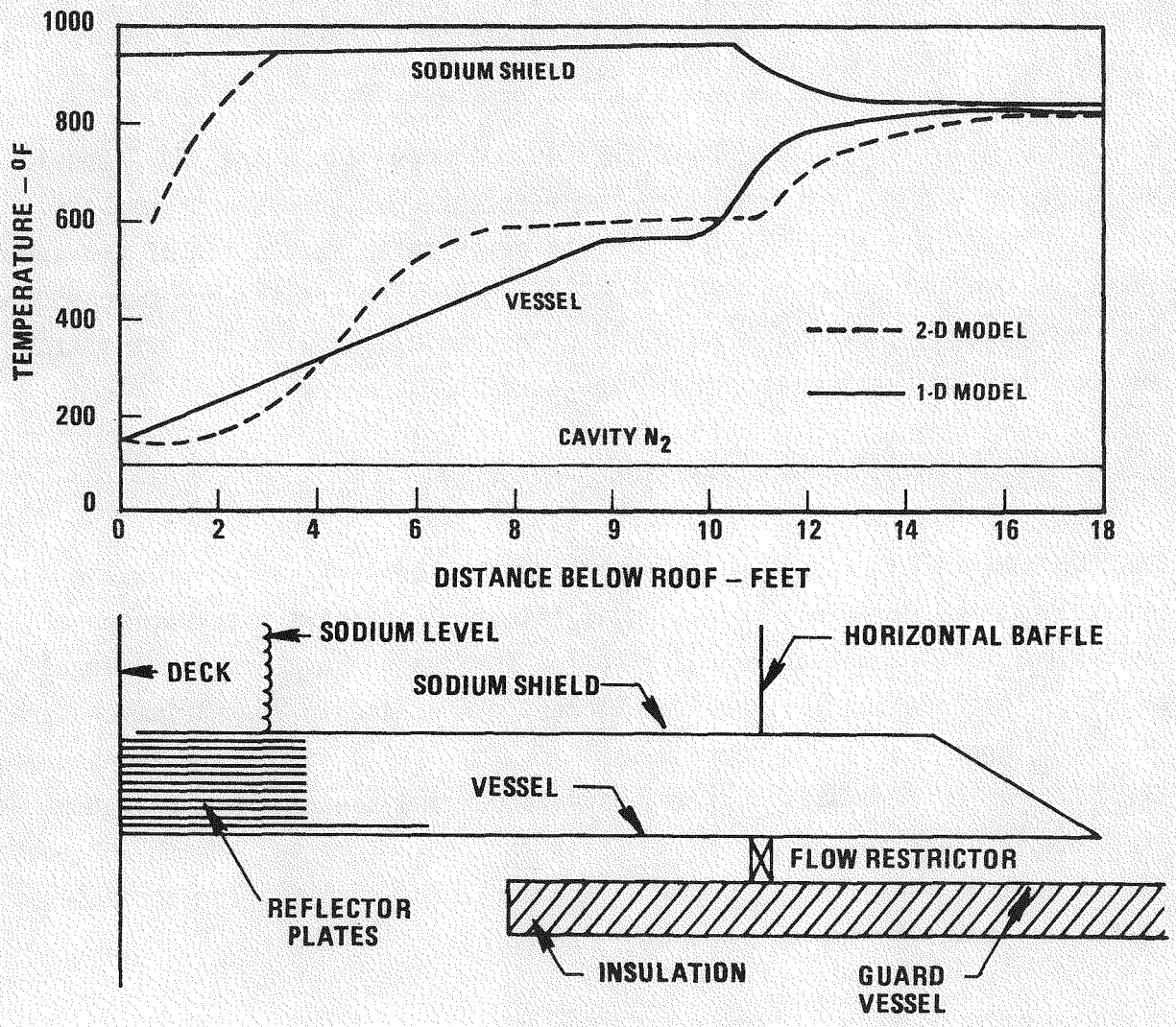

Figure C-13. Comparison of Vessel Temperatures for 1-Dimensional and 2-Dimensional Models

0665

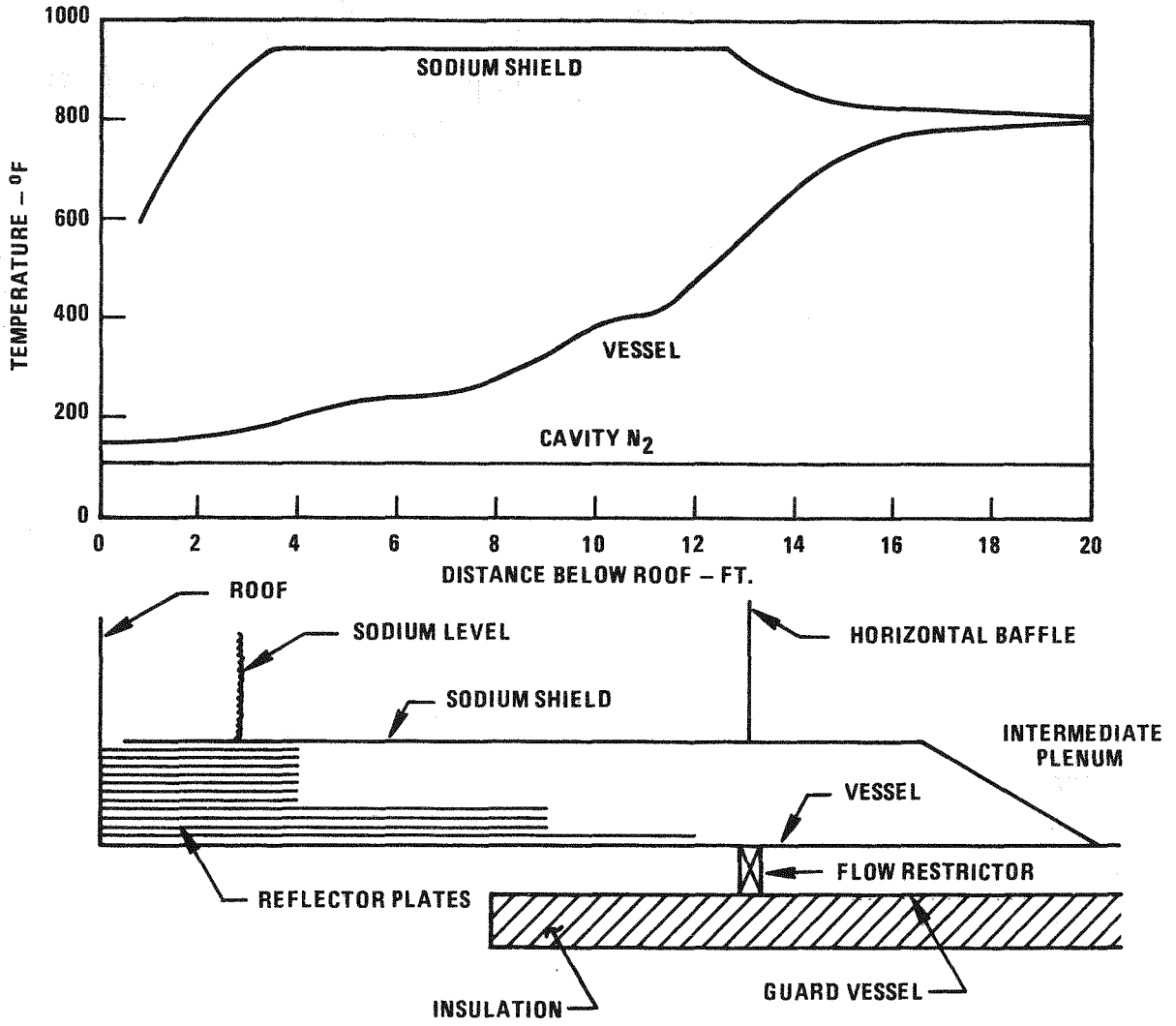

Figure C-14. Reference Vessel Design Axial Temperature Distribution

0665

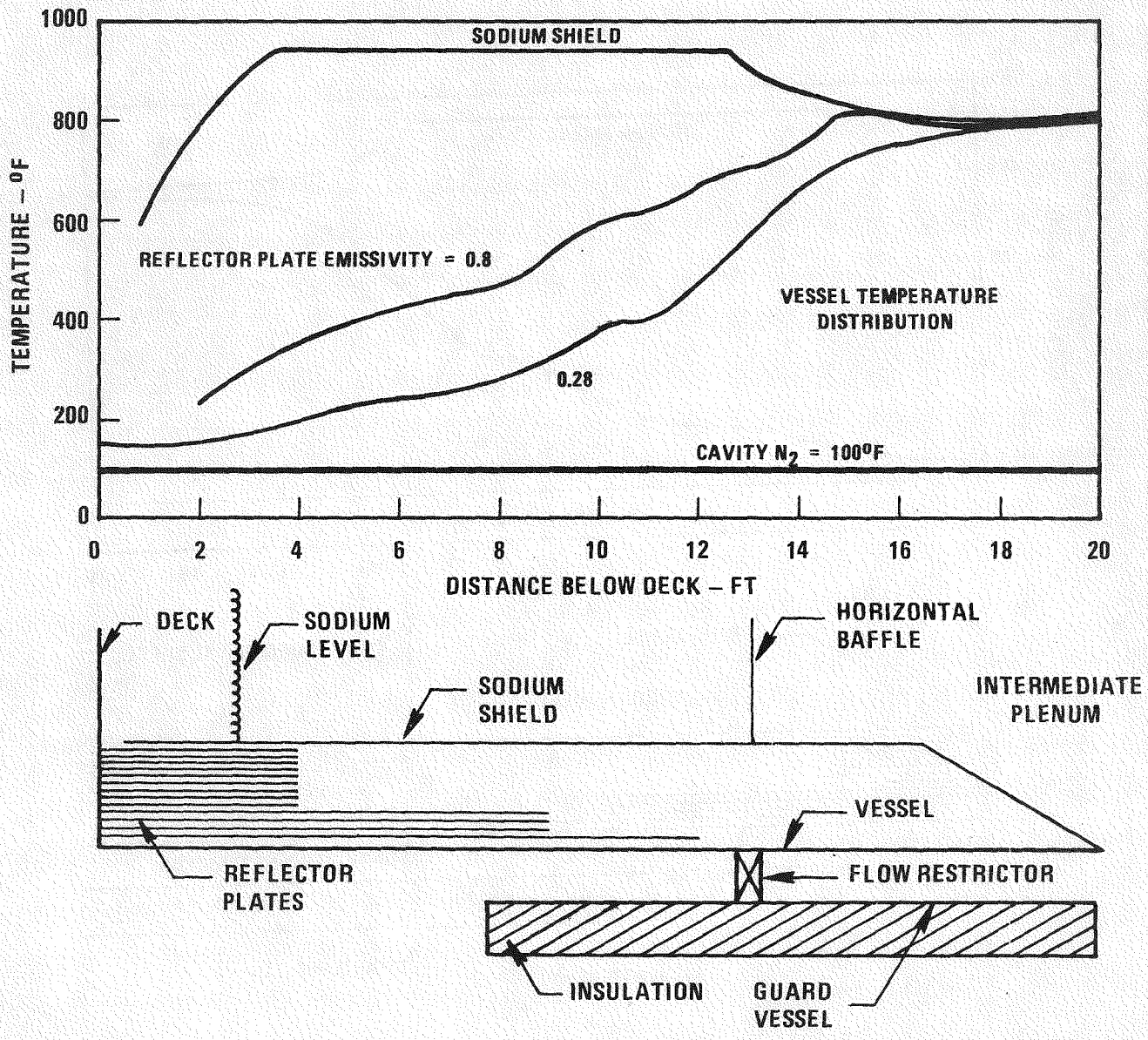

Figure C-15. Effect of Reflector Plate Emissivity on Vessel Axial Temperature Distribution

0665-138

temperature profile occurs at 10.5 ft. This can be eliminated by a small extension of the four reflector plates in the event stress analysis indicates that it is not acceptable.

To finalize the reflector plate design, all the uncertainties in the heat transfer analysis should be evaluated to assess their effect on the vessel temperature distribution. One of these, emissivity, was varied from 0.28 to 0.8. The comparison of the temperature distribution for the two emissivities is shown in Figure C-16. The higher emissivity temperature distribution is steeper but still acceptable from the thermal stress viewpoint. The other uncertainties that need to be considered are convection in the reactor cavity, convection in the vessel/sodium shield annulus, convection between reflector plates, instabilities in convection flow patterns, and intermediate plenum mixing.

A small TAP-A model, see Figure C-13, calculated the temperatures in the guard vessel cone region. These temperature data combined with the larger TAP-A model temperature data gave the axial temperatures of the vessel, guard vessel, and concrete wall as shown in Figure C-17. The maximum concrete temperature is approximately 125^{o}F, which does not exceed the design concrete temperature limit of 150^{o}F.

C.4 INTERMEDIATE PLENUM

The three annular plena above the core support structure act as a plenum separator between the hot and cold pools. These plena are shown in Figure C-12. Knowledge of the plena thermal conditions during steady state and transient operation is important because the sodium spatial temperature distribution in the plena form the temperature boundary conditions of adjoining components (such as: core support structure, lower support structure, vessel, pumps, IHXs and neutron shield).

A VARR-II, Reference C-2, 2-D transient hydrodynamic computer code which includes the effect of density variations in the sodium is used to calculate the sodium natural circulation in the intermediate plenum. The azimuthal

location of the analyzed intermediate plenum is shown in Figure C-18. The effects of pumps and IHXs are not included in the VARR-II model because it is a 2-D computer code. The model consists of 24 axial and 10 radial nodes shown in Figure C-19. This figure also gives the steady state temperature boundary conditions for the intermediate plenum. These were calculated from a conduction computer code, TAP-A, which assumes that the sodium is a solid material. Consequently, the bottom temperatures show a radial temperature variation. Because the sodium temperatures from the VARR-II model are isotherms in the radial direction, the bottom boundary temperature should have been constant. Future calculations will reflect this change. Nevertheless, the general behavior of an enclosed plenum, flow stratification, is not affected by the plenum bottom boundary temperatures.

Figure C-19 shows the intermediate plenum isotherms as calculated from VARR-II. The isotherms are constant in a radial direction which means that the plenum sodium is stratified. An axial plot of the isotherms are in Figure C-20. Since the temperature gradient is not linear from the top to bottom surface, partial mixing occurs in the plenum. Complete mixing occurs when the plenum temperature is constant throughout the plenum. Figure C-21 shows the velocity vectors for the steady state condition. The velocity cell patterns demonstrate that mixing occurs but the isotherm plot, (Figure C-19) shows that the isotherms are flat indicating that the bouyant force is important.

The transient response of the intermediate plenum to a fast flow coastdown from design flow to seven percent pony motor flow was calculated to determine how an enclosed plenum behaves during a transient. The flow in the hot pool for a coastdown transient stratifies and the transient is simulated by instantly changing the horizontal baffle temperature on top of the intermediate plenum from 950^{o}F to 670^{o}F. The plenum velocity and temperature maps are shown in Figure C-22 for transient times of 200 and 400 seconds and are shown in Figure C-23 for transient times of 600 and 800 seconds.

The sodium in the plenum remains essentially stratified during the transient. The axial temperature in the plenum can be characterized as a gradual flattening of the axial plenum temperature profile to the 670^{o}F cold and hot pool temperature.

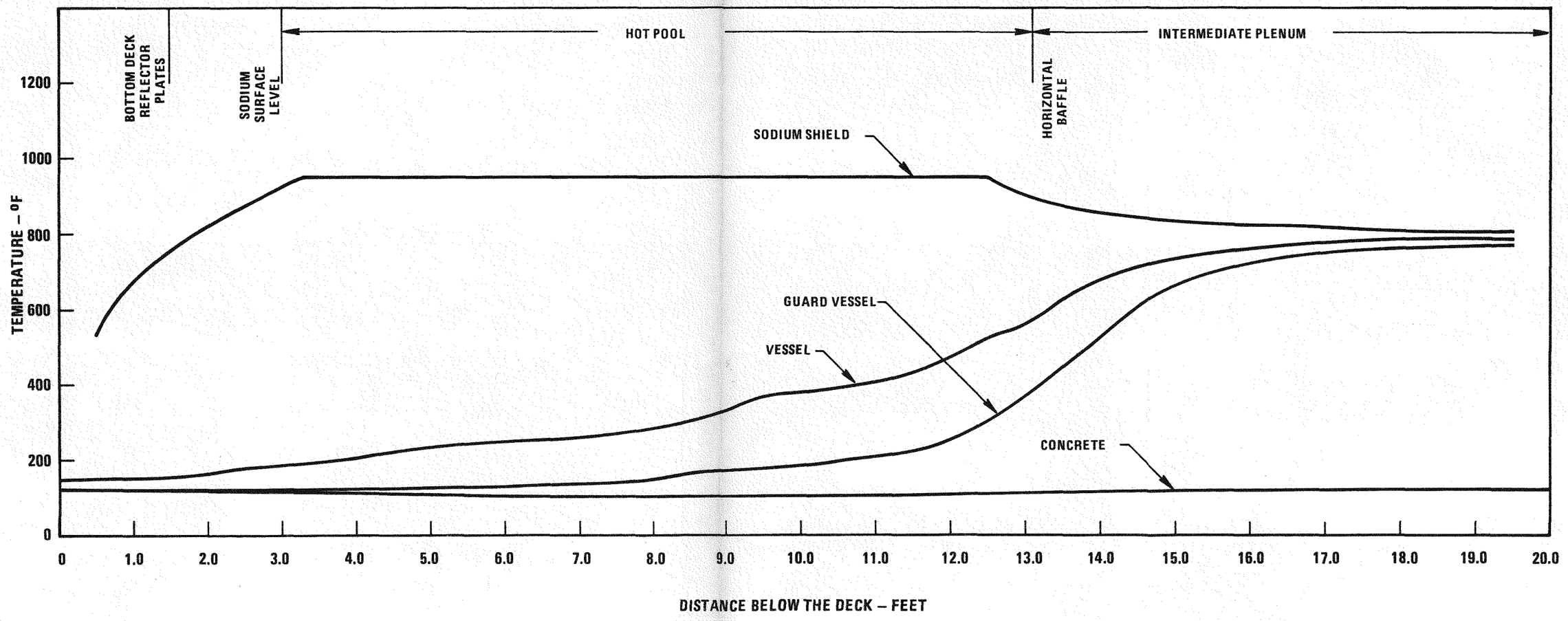

Figure C-16. Axial Temperature Distributions From TAP-A Vessel and Guard Vessel Support Cone Models.

0665-144

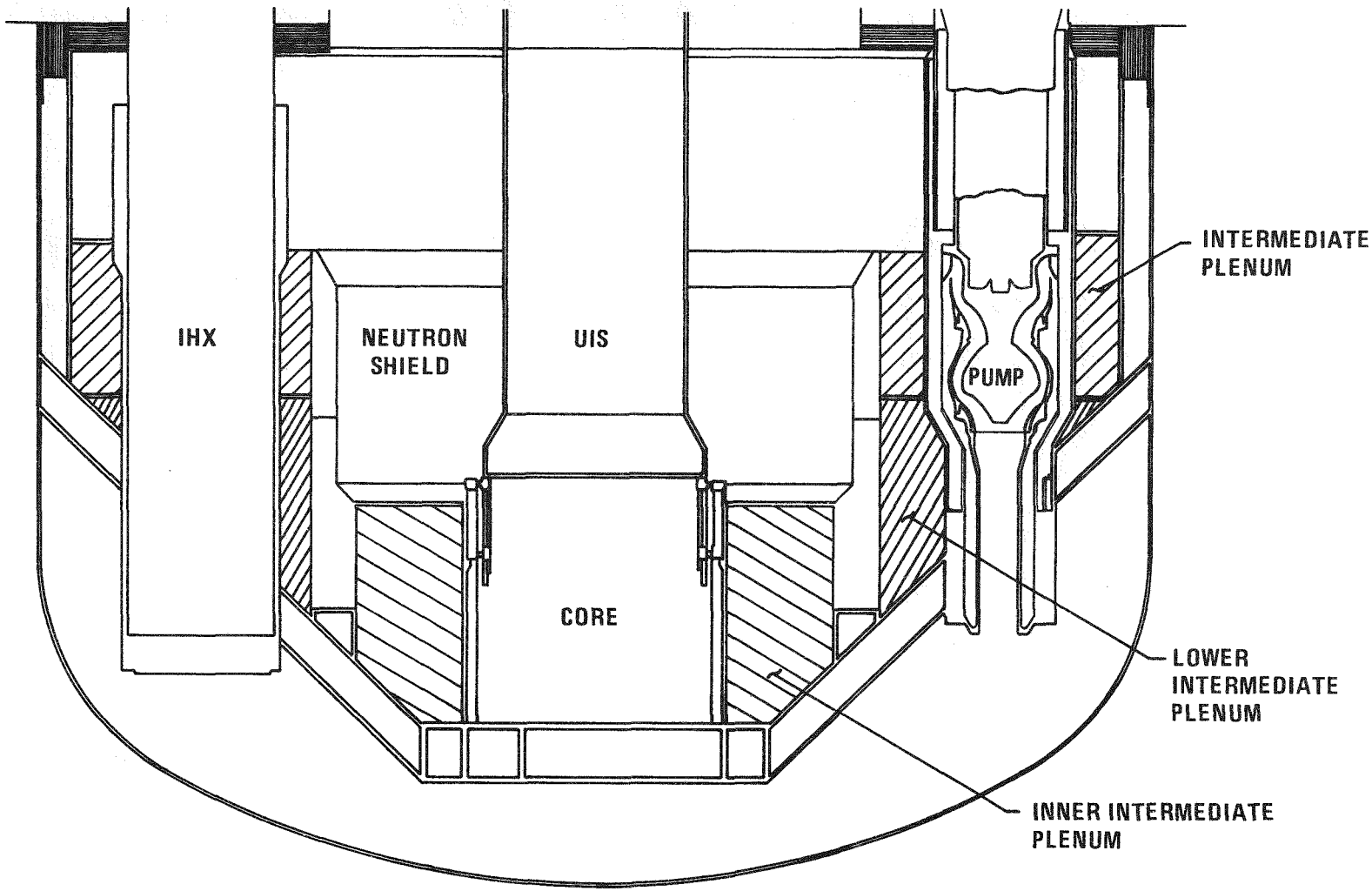

Figure C-17. LPR Three Intermediate Plena

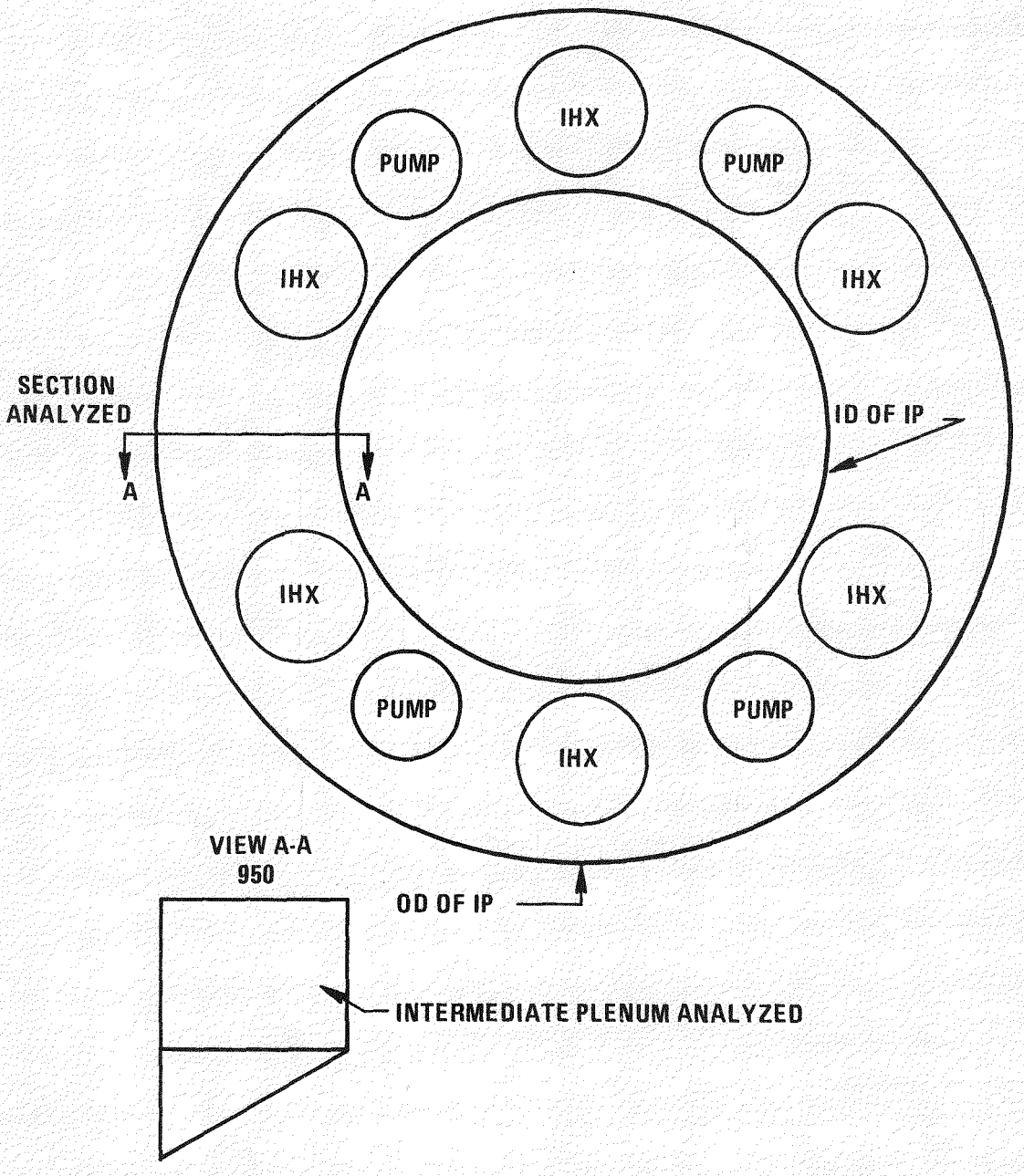

Figure C-18. Azimuthal Location of Intermediate Plenum Cross-Section Analyzed with VARR-II

0665-117

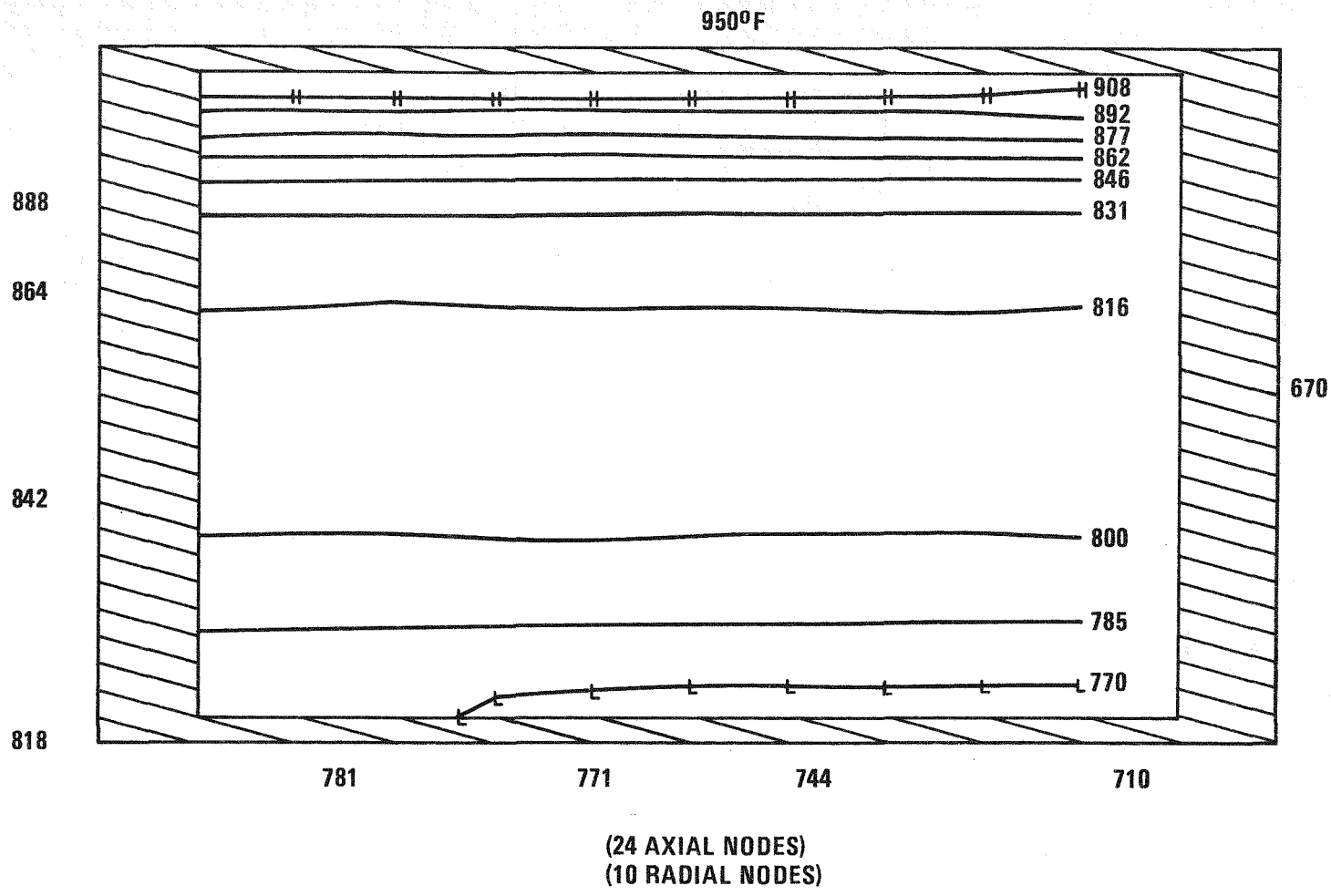

Figure C-19. Intermediate Plenum Temperature Contours Assuming No Pump or IHX Penetrations in the Plenum

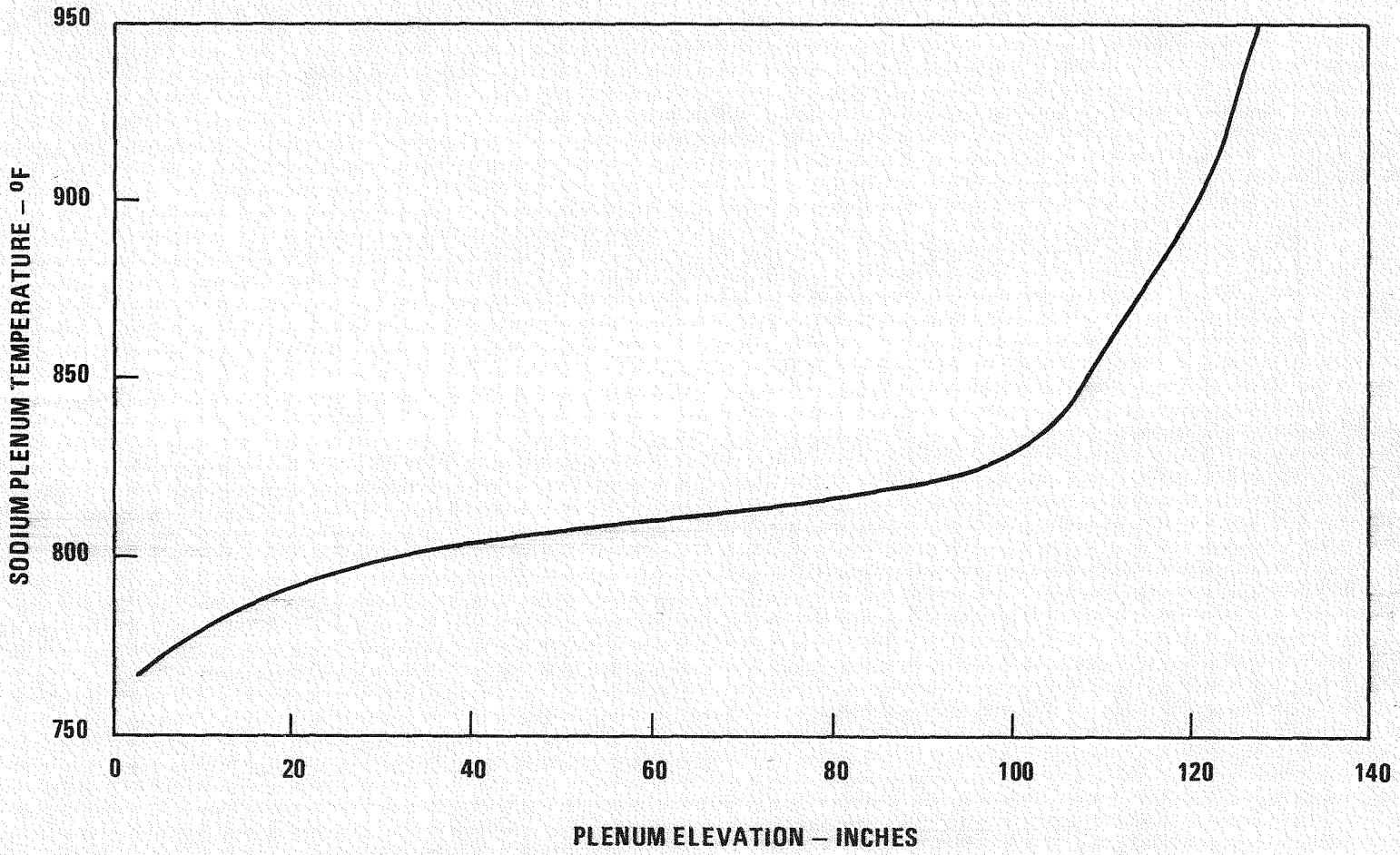

Figure C-20. VARR-II Intermediate Plenum Axial Temperature Distribution Assuming No Pump or IHX Penetrations in the Plenum

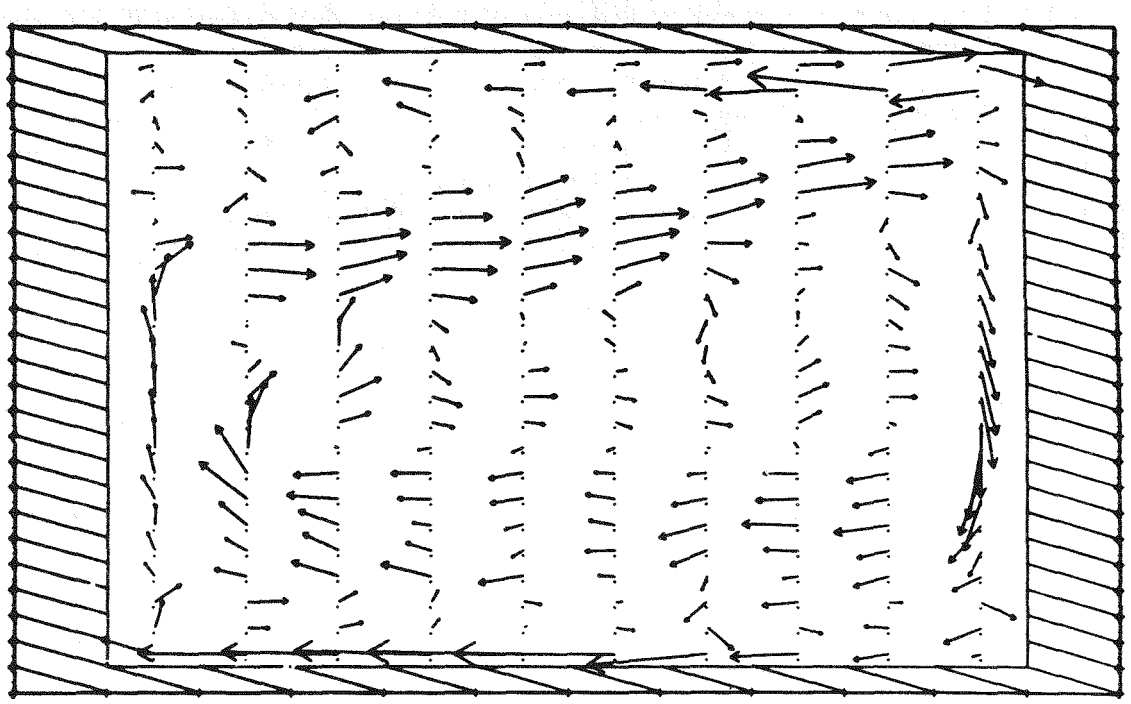

Figure C-21. Intermediate Plenum Velocity Distribution Assuming No Pump or IHX Penetrations in the Plenum

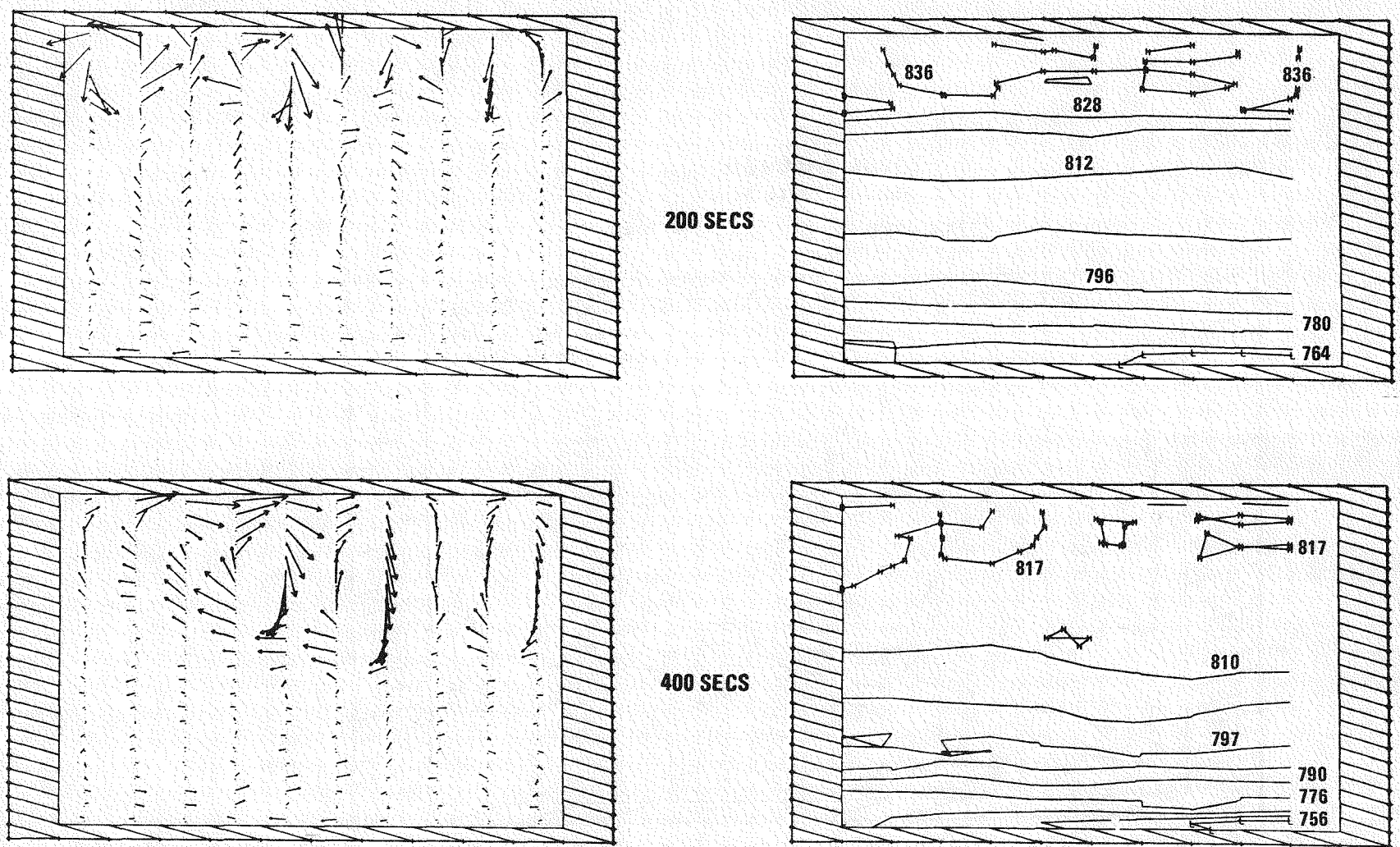

Figure C-22. Intermediate Plenum Transient Velocity and Temperature Distributions

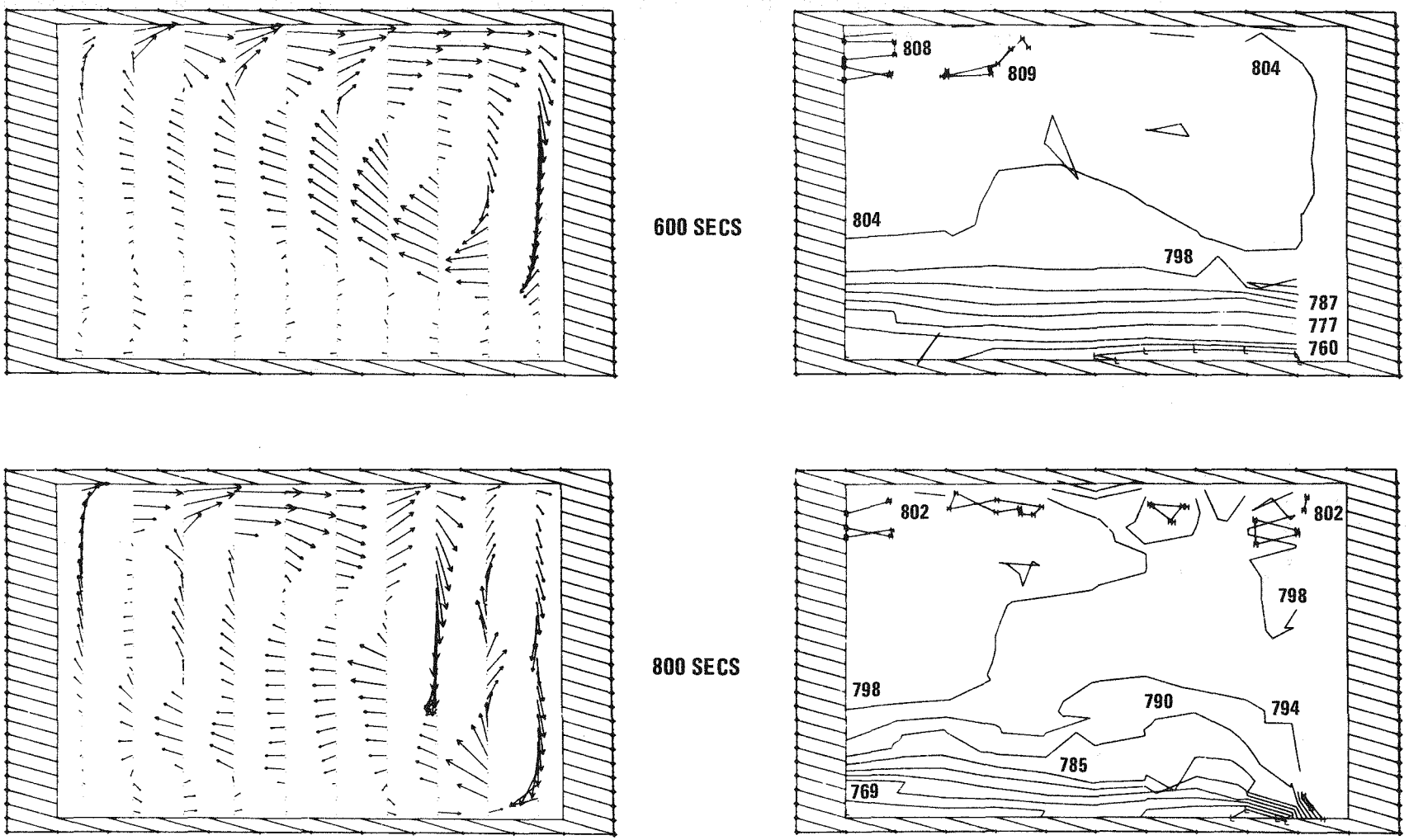

Figure C-23. Intermediate Plenum Transient Velocity and Temperature Distributions

C.4 REFERENCES

C-1 Letter, FRT-471, E. H. Novendstern, "TAP-A Heat Conduction Computer Code", May 1971.

C-2 Report, WARD-D-0106, "VARR-II A Computer Program for Calculating Time Dependent Turbulent Fluid Flows with Slight Density Variations", May 1975.

APPENDIX D
RADIATION ANALYSES

INTRODUCTION

The radiation environment influences requirements relative to visual inspection and shielding for maintenance operations. This appendix contains results of scoping analyses that were performed to determine if it is possible to visually inspect the support area of the reactor vessel after shutdown and the shielding that is required during removal of a primary cold trap from the LPR deck.

VISUAL INSPECTION OF REACTOR VESSEL

During the life of an LPR it may be desirable to periodically inspect the reactor vessel welds in the vessel support region. Analysis was performed to verify that it is feasible to have manned access for visual inspection of the reactor vessel support welds.

The analytical results indicate that, at shutdown, the reactor vessel support area radiation environment is approximately equal to 300 r/hr and decays to 2 mr/hr at 10 days after shutdown. The maximum acceptable radiation environment for visual inspection of the reactor vessel welds is 100 mr/hr and is reached approximately five days after shutdown. These results are based on extrapolation of the CRBR end of equilibrium cycle results.

SHIELDING REQUIRED TO REMOVE A PRIMARY COLD TRAP

During the life of an LPR it is necessary to remove the primary cold traps and replace them with new units. Since the gamma radiation level of the cold traps at the end of life immensely exceeds the allowable human exposure limit, an irradiated cold trap must be removed in a shielded container.

Analysis of the gamma shield requirements for a primary cold trap container was completed. The analysis is based on the following assumptions:

- 0.3% failed fuel,
- 15 year cold trap life,
- cold trap source term evaluated 10 days after shutdown,
- gamma source term distributed uniformly over a volume of 270 cubic feet.

The cold trap activity level with no shielding is 3,930 r/hr. With this radiation level an 8.0 in thick carbon steel container is needed so that the allowable human exposure limit of 200 mr/hr is not exceeded.

APPENDIX E
PERFORMANCE ANALYSIS

E.1 INTRODUCTION

The transient analysis effort for the LPR study includes the COMTRAN modeling of a pool plant (using Westinghouse strategic funds) and the subsequent analysis of the transient behavior of the LPR plant. The initial modeling changes needed prior to analyzing a pool type reactor include simple upper and lower plenum mixing models, an IHX with the primary sodium on the tube side, and changes which eliminate the appropriate piping in the primary heat transport system. The transient analysis is concerned with identifying a plant shutdown strategy which will result in acceptable conditions for the components. To assure conservative results close coordination between the modeling and transient analysis efforts establishes the limitations of the mixing models for the different shutdown strategies.

The shutdown strategies that are examined following a reactor trip include:

- Immediate Exponential Pump Coastdown
- Pump Stays at Full Flow
- Pump Stays at Full Flow, Turbine Trips
- Time Delayed Exponential Pump Coastdown
- Pump Ramp Down at 1%/second

This report discusses the modeling changes and the results of the study.

E.2 COMPUTER MODEL

The thermal transient analysis uses the COMTRAN[1] version 4.3 of the DEMO[2] computer code, developed for CRBRP. The program uses an Euler

(1) COMTRAN is a Westinghouse Proprietary computer program written in FORTRAN IV for the CDC 7600 computer.

(2) WARD-D-0005, Rev. 4, "LMFBR DEMO Plant Simulation Plant Simulation Model (DEMO).

integration method (explicit). Under normal transient conditions the reactorand protection system integrate on a 0.01 second time step and the remainder of the program integrates on a 0.05 second time step. However, to accommodate slow long-term thermal-hydraulic transients, there is a time step control which allows larger time steps.

The major component models required are the reactor vessel, hot pool, cold pool, primary and intermediate heat transport systems, the intermediate heat exchanger, and the steam generator. The heat transport loops of the plant are simulated by a two loop model; one loop, the S loop, represents a single plant loop primarily for the single loop initiated events and the second loop, the L loop, represents the remainder of the plant.

The power generation is modeled by the neutron kinetics and decay heat equations. The vessel internals are represented by models of a lower plenum, lower axial blanket, active core, upper axial blanket, inner radial blanket, outer radial blanket, and bypass channel.

The heated sodium leaves the core, traverses the hot pool and then enters the tube side of the IHX. After leaving the IHX, the sodium mixes in the cold pool and enters the primary pump. From the pump the sodium goes through the lower support structure to the core inlet. The components of this flow path represents the primary heat transport system.

The shell side of the IHX, secondary sodium containing piping, and shell side of the steam generator and the intermediate pump constitutes the intermediate heat transport system.

The representation of each water/steam system includes models of the feedwater pump, feedwater control valves, piping, and the tube side of the steam generator. The steam leaving all steam generators enters a common steam header, flows through piping to the turbine throttle valve and a steam dump valve.

Input to the program includes design data for the plant or plant functions. The design engineer selects the data to represent a desired configuration at any chosen instant of plant life. Section E.3 gives the key plant parameters used for the large pool reactor plant.

E.2.1 SIX-LOOP OPERATION

As CRBRP is only a three loop plant, modifications to the DEMO computer code are required. This was accomplished by internally increasing the computer code to handle any number of lumped loops. For this analysis, the COMTRAN code simulates up to six primary and secondary loops.

E.2.2 RADIAL PARFAIT CORE

The COMTRAN model uses four channels for the modeling of the core - these are average and hot fuel, and the average and hot radial blanket. To minimize the changes to the reactor model, the radial blanket channels were modified so that the channel previously set aside for the average radial blanket now represents the average in-core blanket and the channel that previously modeled the hot radial blanket now represents the average outer radial blanket.

The required input Doppler coefficients, sodium density coefficients, flow fractions, power fractions, and geometry are for both the inner and outer radial blanket.

E.2.3 UPPER PLENUM MIXING MODEL

The upper plenum mixing model is a simple but accurate model based on adjusting the mixing efficiency. The mixing efficiency agrees with the more detailed thermal and hydraulic computer code VARR-II. To obtain this agreement between the upper plenum mixing model used in COMTRAN and the results predicted by VARR-II, a series of plant trips were analyzed. A multiplier on the rate of temperature change leaving the reactor and entering the IHX provides agreement with VARR-II prediction. The results of this parametric study show good agreement with a multiplier of 2.0. This

multiplier is equivalent to a mixing efficiency of 50%. This factor results in conservative predictions for the full flow cases. For the exponential coastdowns, the results are not as conservative.

The plenum empirical mixing equations are given by the following energy equation,

$$\int dT = \int Wdt \cdot C(T_1 - T)$$

$$\int Wdt = \text{constant}$$

t = Time
T = Plenum Fluid Temperature
T_1 = Plenum Inlet Temperature
W = Plenum Flow
C = Mixing Constant

E.2.4 LOWER PLENUM MIXING MODEL

This model is similar to the upper plenum model. The current lower plenum mixing model assumes 50% mixing efficiency with the sodium volume of the cold pool. Improvements to this model will be developed in conjunction with the Thermal and Hydraulics Analysis group.

E.2.5 IHX

A user input option provides the ability to simulate primary sodium in the tubes and the intermediate sodium on the shell side. Changes were made internally to the computer program to accommodate this design change. Verification with steady-state design codes was performed.

E.2.6 BENSON STEAM GENERATING CYCLE

Many changes were required in the feedwater and recirculation systems to simulate the Benson steam cycle. These changes were to the STGEN portions of COMTRAN. Changes to the SODAR model, which is for severe water side transients model, are also completed.

The Benson cycle employs one steam generator unit that heats feedwater ($465^{o}F$) to superheated steam conditions ($855^{o}F$). A variable number of fixed spatial nodes can be inputed and 60 nodes are used for this analyses. Also, a multi-region model which subdivides a spatial node when a change in water side heat transfer regime occurs (ex: nucleate boiling to film boiling).

E.3 DESIGN DATA

The thermal transient analyses are performed with a plant representative of the design as of April 15, 1978 and shown in Figure E-1. The design includes the hot center pool with a radial parfait core design.

The plant has the Benson steam generation system with one duplex straight tube unit per loop. All analyses is performed from an initial power level and flow rates of 102%.

Table E-1 gives the overall plant parameters. Table E-2 gives the major reactor parameters, and Table E-3 gives the major design parameters for the IHX and the steam generator.

E.4 SHUTDOWN STRATEGIES

Five shutdown strategies for the LPR plant are identified for studying their impact on the reactor and plant system and components. The strategies are based on various primary and intermediate pump responses following the reactor scram and the dropping of plant control rods.

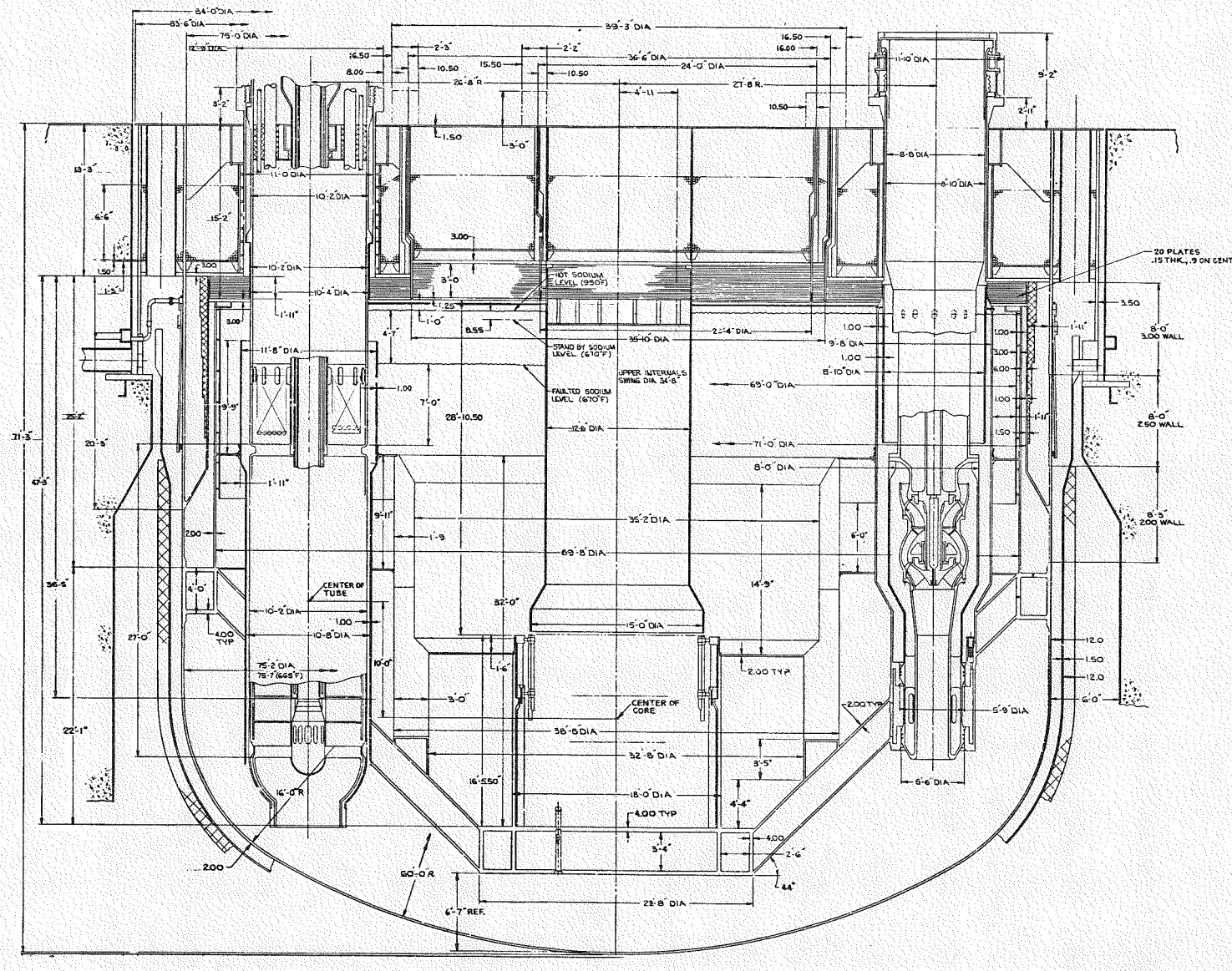

Figure E-1 LBB Plant Design – Analytical Base

TABLE E-1

OVERALL LARGE POOL REACTOR PLANT DESIGN PARAMETERS
BENSON STRAIGHT TUBE STEAM GENERATING SYSTEM
(FOR COMTRAN ANALYSES)
VERSION 4.3 (6/6/68)

Reactor Power, MWt.	2550
Number of Primary/Intermediate Heat Transport Loops	6/6*
Primary Hot Leg Temperature, ^{o}F	950
Primary Cold Leg Temperature, ^{o}F	670
Primary Loop Flow Rate, 10^6 lb/hr	17.03
Intermediate Hot Leg Temperature, ^{o}F	900
Intermediate Cold Leg Temperature, ^{o}F	605
Intermediate Loop Flow Rate, 10^6 lb/hr.	16.08
Steam Pressure at Turbine Inlet, psia	2215
Steam Temperature at Turbine Inlet, ^{o}F.	850
Steam Flow to Turbine, 10^6 lb/hr.	9.504
Feedwater (Loop) Flow Rate, 10^6 lb/hr	1.584
Steam Generator Water Inlet Temperature, ^{o}F	465
Steam Generator Steam Outlet Temperature, ^{o}F.	855
Steam Generator Inlet Pressure (Orifice), psia.	2320
Steam Generator Inlet Pressure (Active Tube), psia.	2315
Steam Generator Exit Pressure (Active Tube), psia	2300
Steam Header Pressure, psia	2285

*For initial analysis, six primary loops are used.

TABLE E-2

REACTOR PARAMETERS
(FOR COMTRAN ANALYSES)

Core Fuel	PuO_2/UO_2
Blanket Fuel	Depleted UO_2
Neutron Absorber Material	B_4C
Active Core Height, in	48
Axial Blanket Height, Each End, in	14
Fuel Assemblies (Number/Rods Per Assembly)	252/271
In-Core Blanket Assembly (Number/Rods Per Assembly)	97/127
Radial Blanket Assemblies (Number/Rods Per Assembly)	144/127
Number of Control Assemblies (Primary/Secondary)	10/8
Doppler Coefficient, Total, -T dk/dT	0.01015
Sodium Density Reactivity coefficients, Total, $/^{o}F	.496
Reactor Flow Fraction, Core/Inner Blanket/Rad.	.7272/.1618/
Blanket/Bypass	.051/.060
Power Distribution, Core/Inner Blanket/Radial Blanket	.794/.157/.049
Fuel Pin, OD, in	0.31
Pitch/Diameter Ratio	1.148
Clad Thickness, in	0.016

TABLE E-3

IHX DESIGN PARAMETERS
(FOR COMTRAN ANALYSES)

Thermal Duty, MWt	425
Number of Tubes	5460
Tube OD, in	.875
Tube Thickness, in	.785
Tube Pitch (Triangular), in	1.3125
Active Tube Length, ft	25.0

STEAM GENERATOR SYSTEM DESIGN PARAMETERS
(FOR COMTRAN ANALYSES)

Thermal Duty, MWt	425
Number of Units Per Loop	1
Number of Tubes	4200
Outer Tube OD, in	.75
Inner Tube ID, in	.406
Tube Pitch (Triangular), in	1.375
Active Tube Length, ft	66.
Shell OD, in	99
Overall Height, ft	85.

The presence of the large volumes of sodium in both the upper plenum (hot pool) and lower plenum (cold pool) significantly affects the method of shutdown as compared to methods used for loop type plants. The large volumes mitigate some thermal response.

The following sections describe five plant shutdown strategies and show the thermal behavior of various plant parameters for each strategy. The initial decay heat level for all the analyses is minimum decay heat using values associated with the CRBR AFMS core. The initial conditions for transient analysis are the structural design reactor outlet temperature of 950°F and a 280°F core ΔT. The thermal power and sodium and water flows are 102% of nominal.

E.4.1 IMMEDIATE EXPONENTIAL PUMP COASTDOWN

This shutdown strategy is a variation of that previously used for the loop type plants. Because of the reduced flow rates, the thermal responses are relatively slow. The basis for the exponential coastdown are realistic pump inertias provided by pump designers.

The reactor is tripped at T = 0 seconds. The primary and secondary sodium pumps coastdown to pony motor speed (7%), which results in a sodium flow of approximately 6.3% full flow in the primary and 6.4% full flow in the secondary loops. The primary pump reaches 7% speed at T=45 seconds, and the secondary pump at T=63 seconds. The turbine is tripped at T=2 seconds. The feedwater valve closes from fully opened to fully closed in 60 seconds. Feedwater is introduced to the startup vessel to maintain 5% flow to the steam generator. Starting five seconds after turbine trip, the evaporator inlet temperature undergoes a linear ramp from 465°F to 625°F over a 500 second period. The assumption is that a programmed live steam feedwater heater or the startup vessel can easily provide this steam generator inlet temperature increase.

Figures E-2 through E-12 show the thermal response of key parameters. Figure E-2 shows the transient response of the reactor vessel temperatures. The inlet temperature shows a very slight decrease, while the outlet

Figure E-2 Reactor Vessel Temperatures

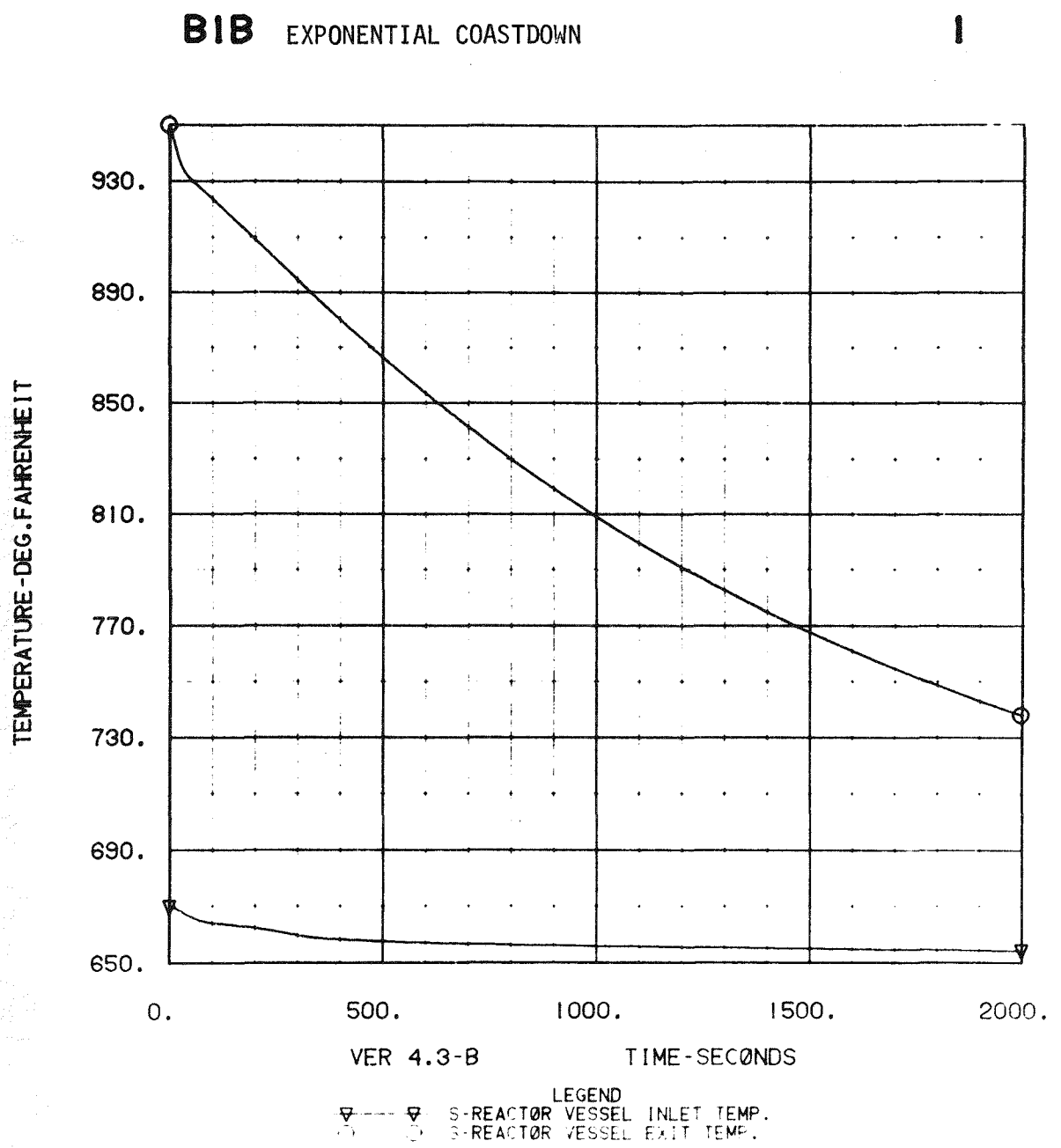

temperature decreases from 950°F to 740°F at a fairly constant rate of change. Figure E-3 shows the rapid decrease to near inlet sodium temperature conditions for the upper axial blanket outlet temperatures, the slight rise, and then the asymptotic decrease. The cold leg sodium temperatures (see Figure E-4) decrease toward the intial feedwater temperature before returning to about 650°F, above the standby feedwater temperature of 625°F. The hot leg temperatures decrease toward 740°F. The primary pump sodium temperature shows only a slight decrease (see Figure E-5) similar to that for the reactor inlet temperature. Figure E-5 also shows the secondary pump sodium temperature which shows the typical cold leg decrease, ~65°F, before it approaches 650°F. Figure E-6 shows the rapid decrease in thermal power and nuclear reactor power following the reactor trip. The reactor vessel inlet flow shows a slower decrease to ~6% flow. The sodium flow through the primary and intermediate pumps are equivalent after about 1000 seconds (see Figure E-7). However, during the initial stage the secondary flow is higher than the primary flow rate. Because of its lower pump head, the secondary pump coastdown is longer than the primary (63 seconds to 7% speed versus 45 seconds for the primary). Figure E-8 shows this slight effect.

Figures E-9 through E-12 show the steam generator response to a reactor trip. Figure E-9 shows typical hot and cold leg sodium temperatures responses. Figure E-10 shows the assumed inlet temperature response produced by the use of live steam or the startup vessel, and also the outlet steam temperature decrease with decreasing sodium temperature. Figure E-11 shows the decrease in steam generator water flow based on the use of the startup vessel. The steam pressure initially increases, see Figure E-12, before decreasing to the standby pressure of 2300 psi. The step effect is due to numerical problems in the plotting package which rounds off to four significant figures.

E.4.2 SODIUM PUMPS STAY AT FULL FLOW, NO TURBINE TRIP

This shutdown strategy, in which sodium flow is maintained at full flow results in the most rapid hot leg temperature decrease. The primary and secondary pumps remain at 100% (102% for analysis purposes) following the

Figure E-3 Reactor Core
Temperatures

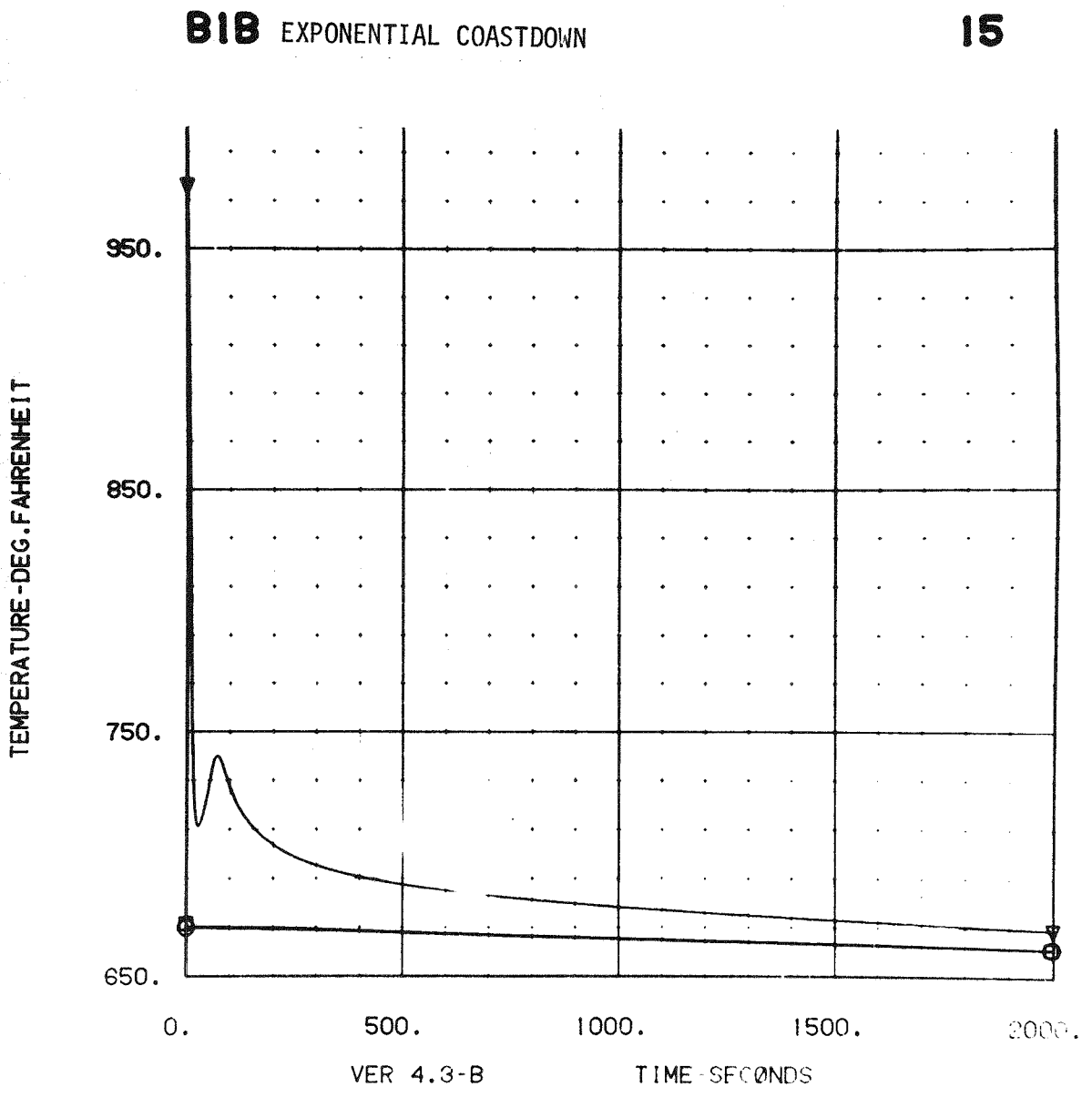

Figure E-4 Intermediate Heat Exchanger Temperatures

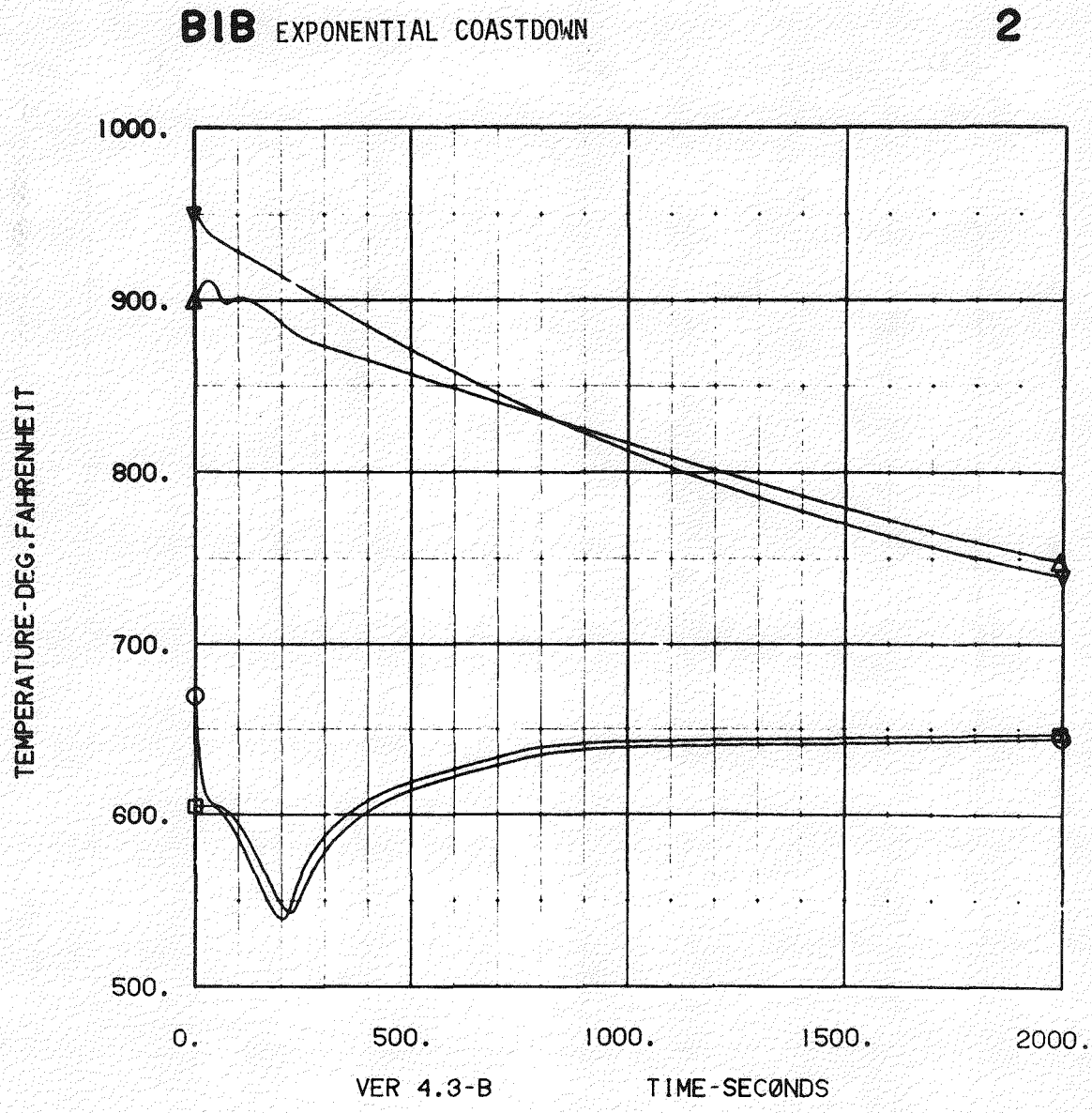

Figure E-5 Sodium Pump
Temperatures

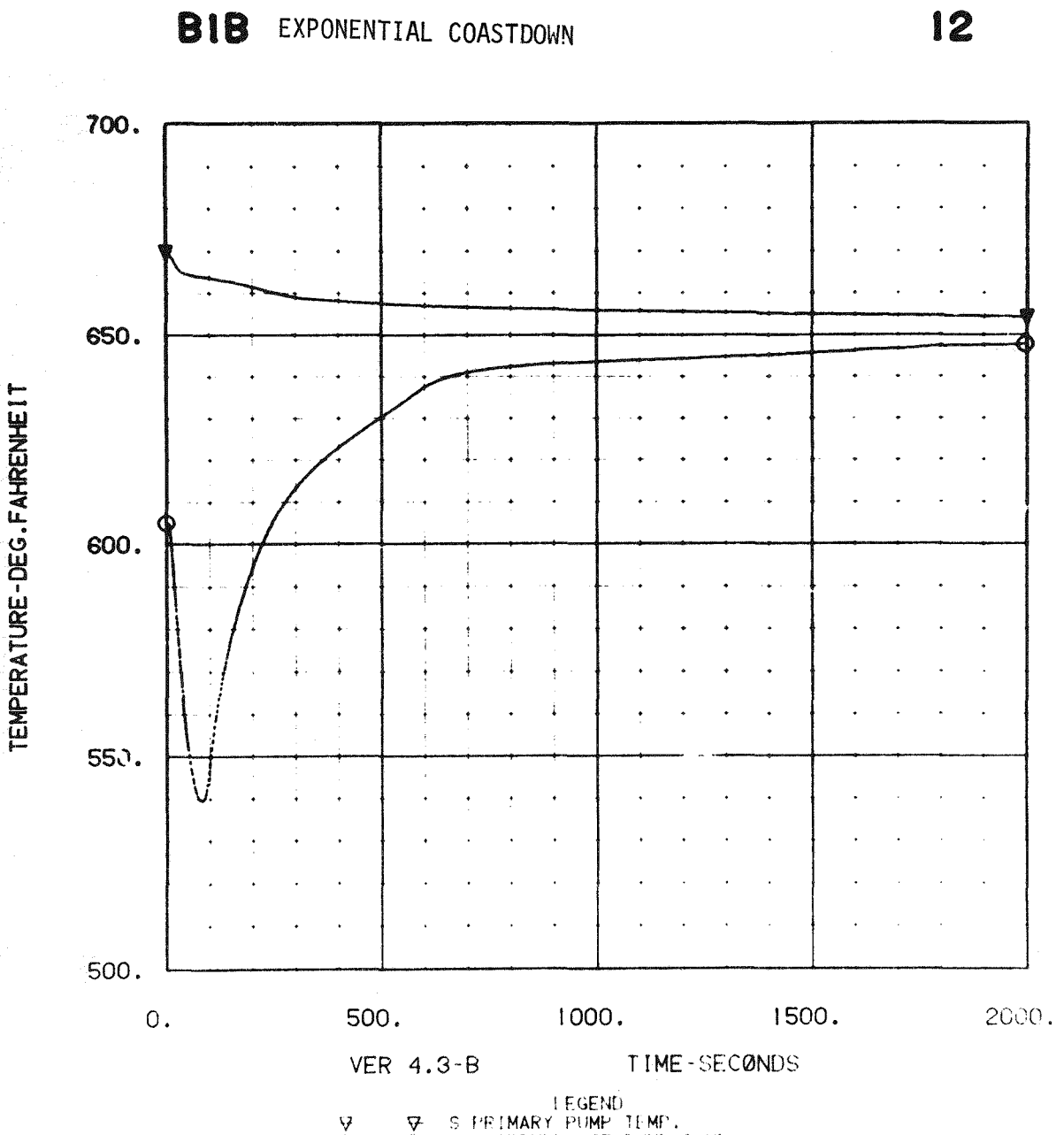

Figure E-6 Reactor Power & Flow Rate

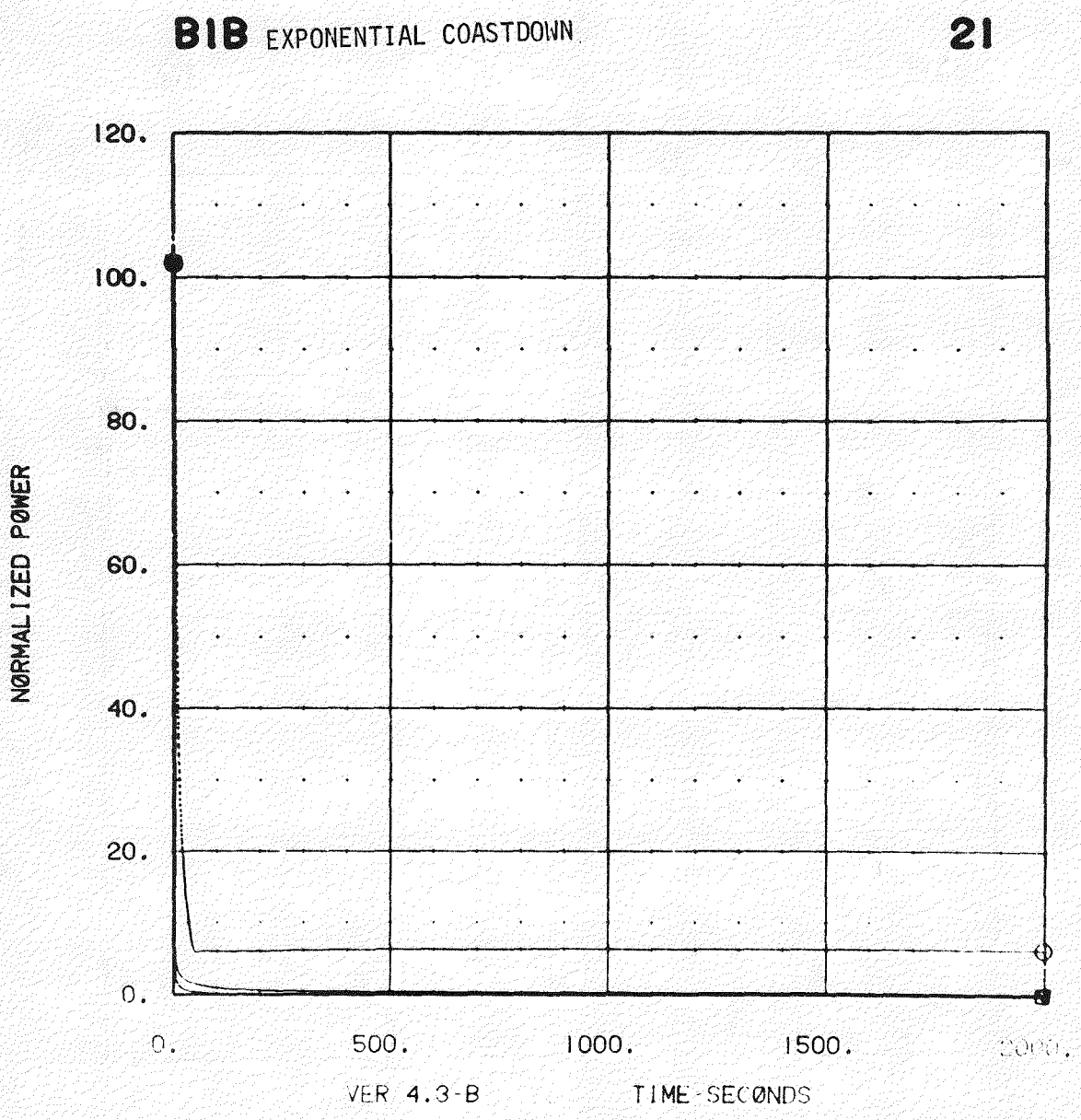

Figure E-7 Sodium Pump Flow Rates

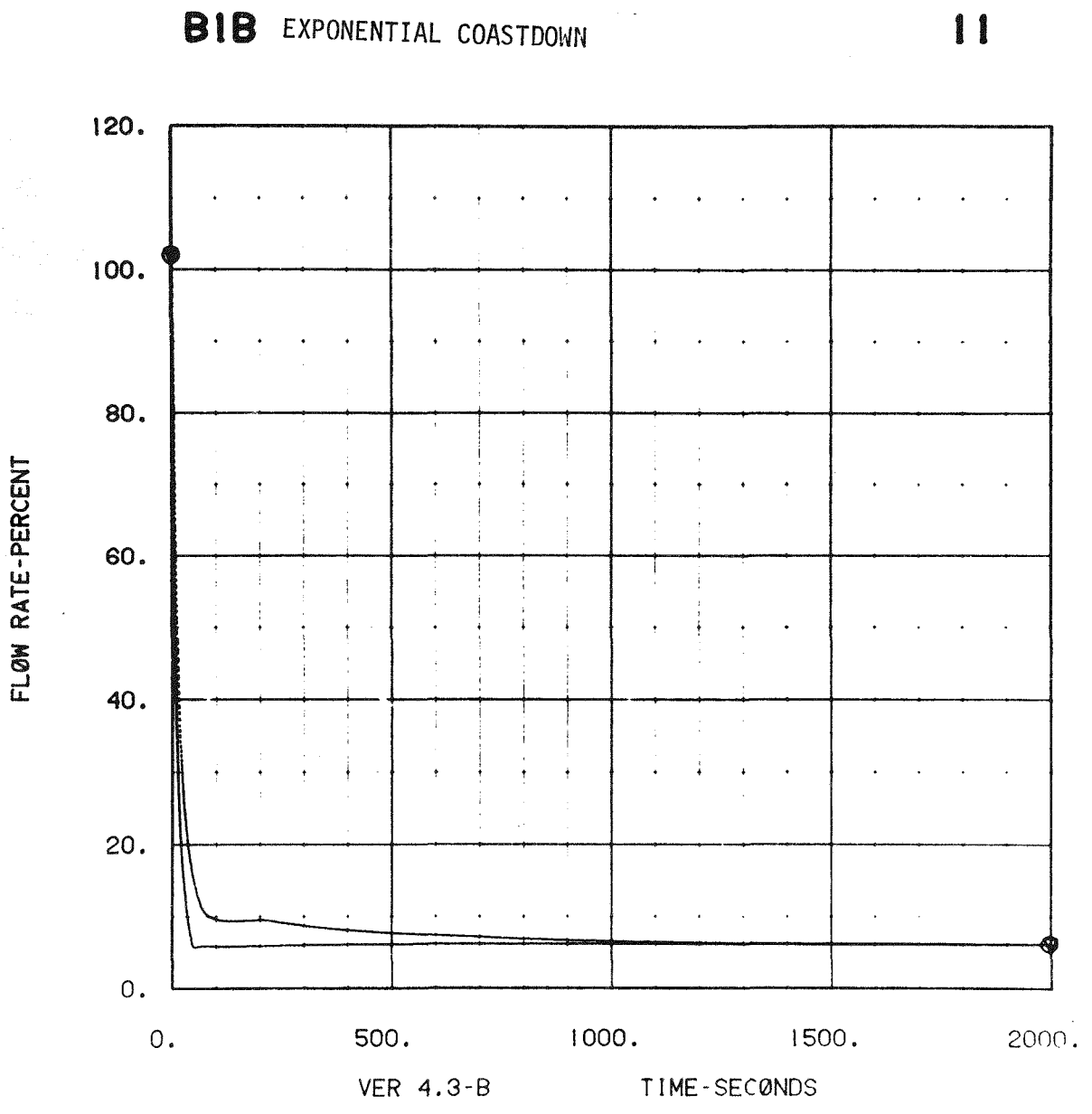

Figure E-8 Sodium Pump Speeds

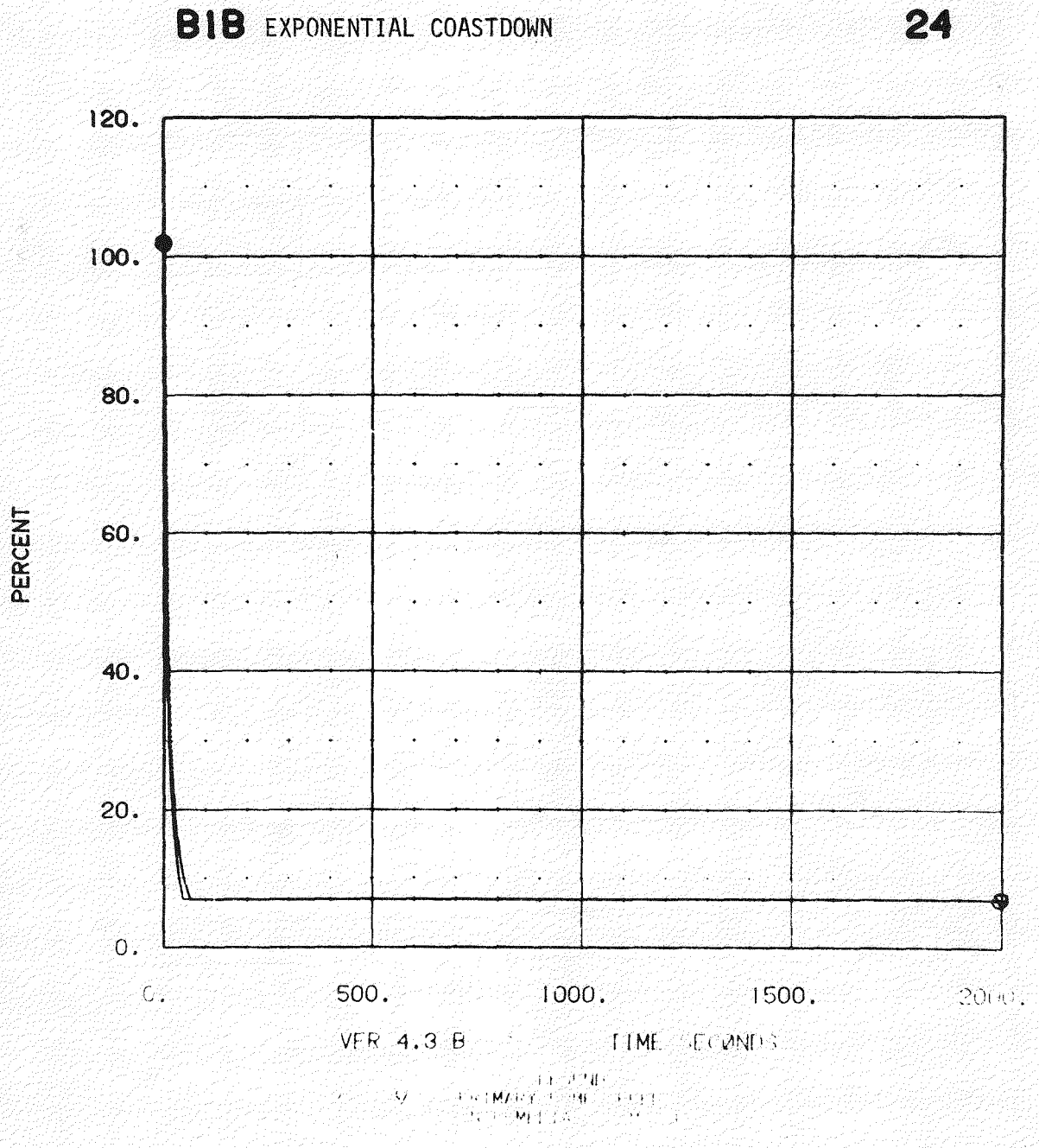

Figure E-9 Steam Generator
Sodium Temperatures

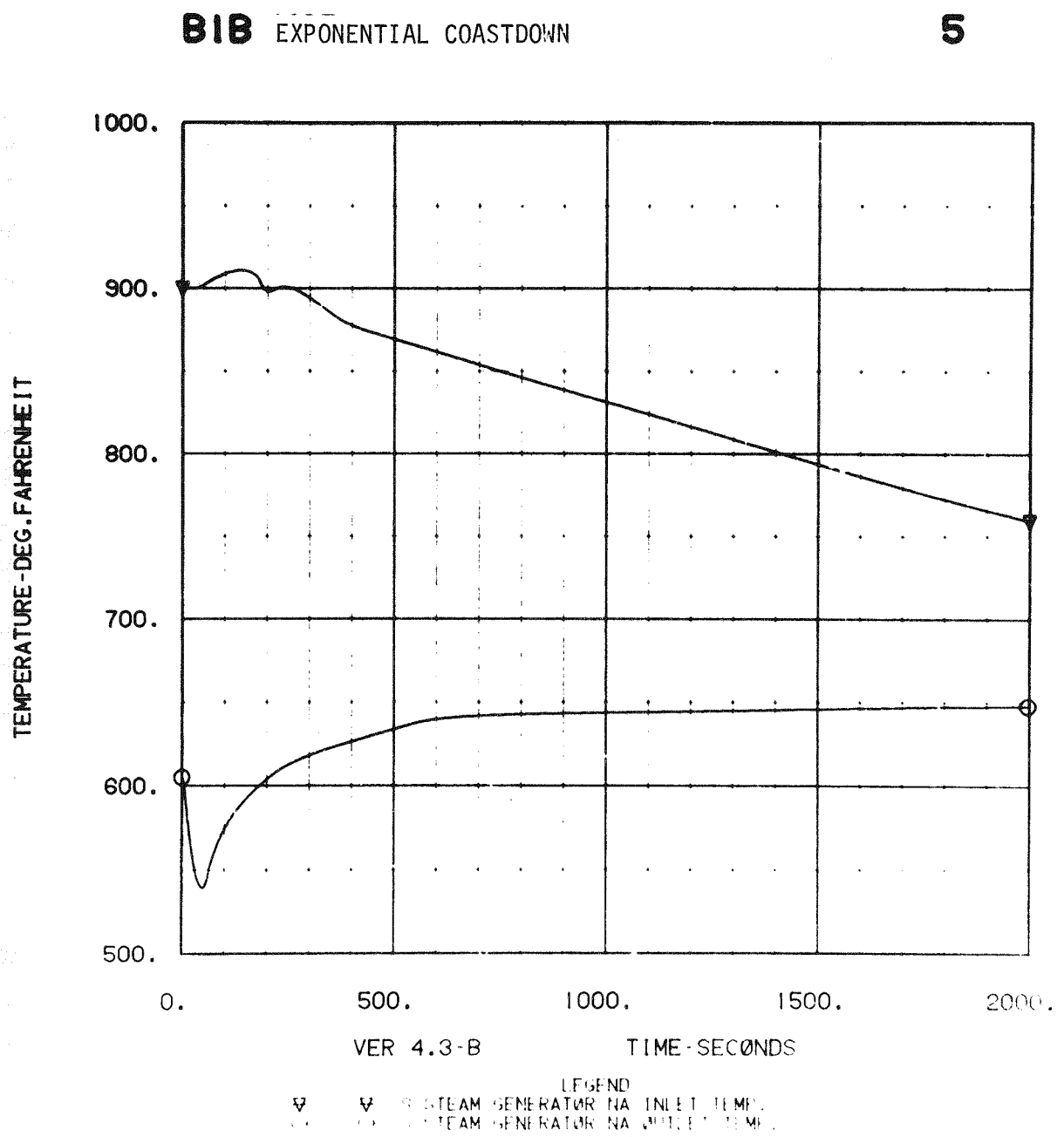

Figure E-10 Steam Generator Water Temperatures

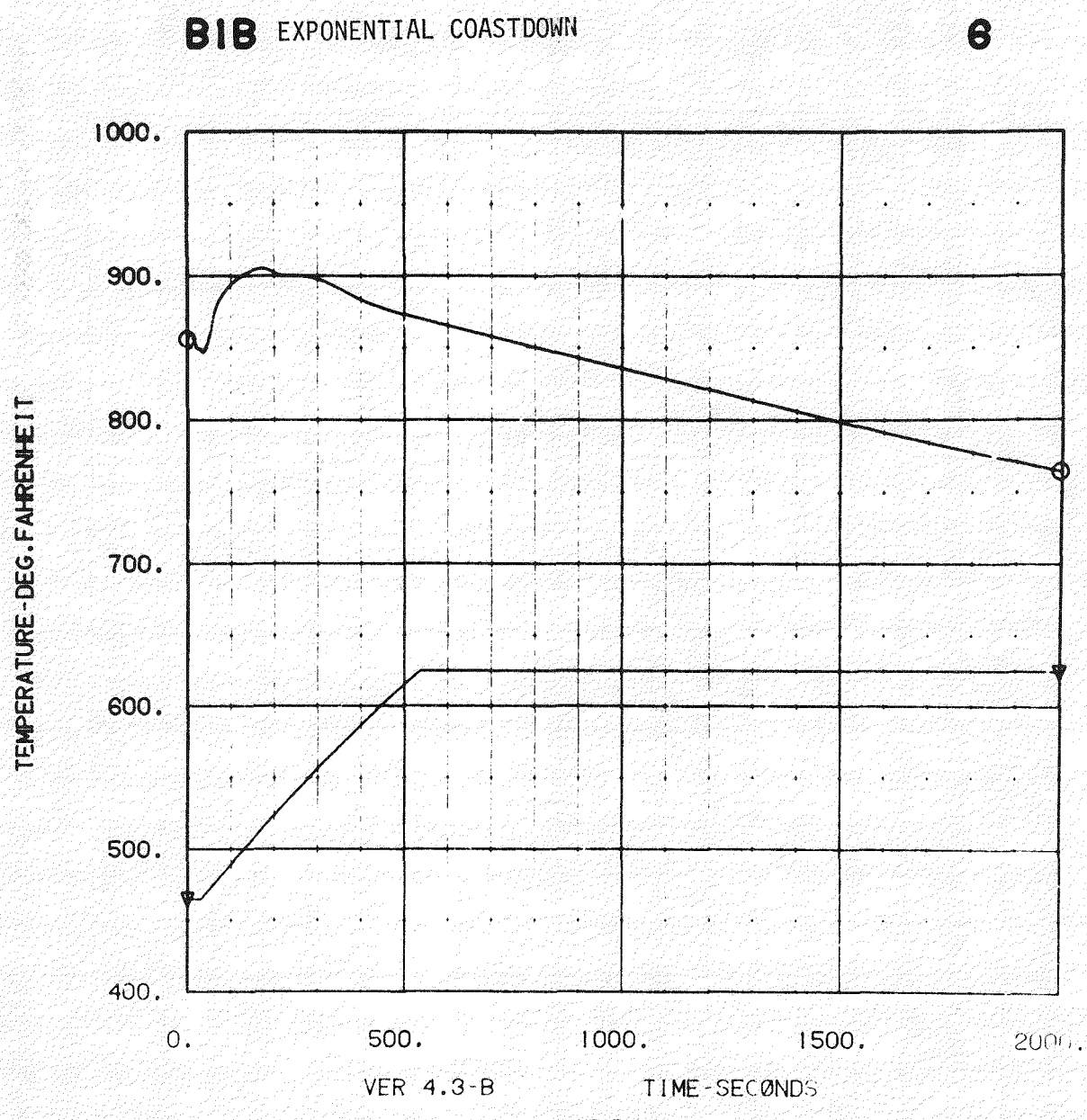

Figure E-11 Steam Generator Flow Rate

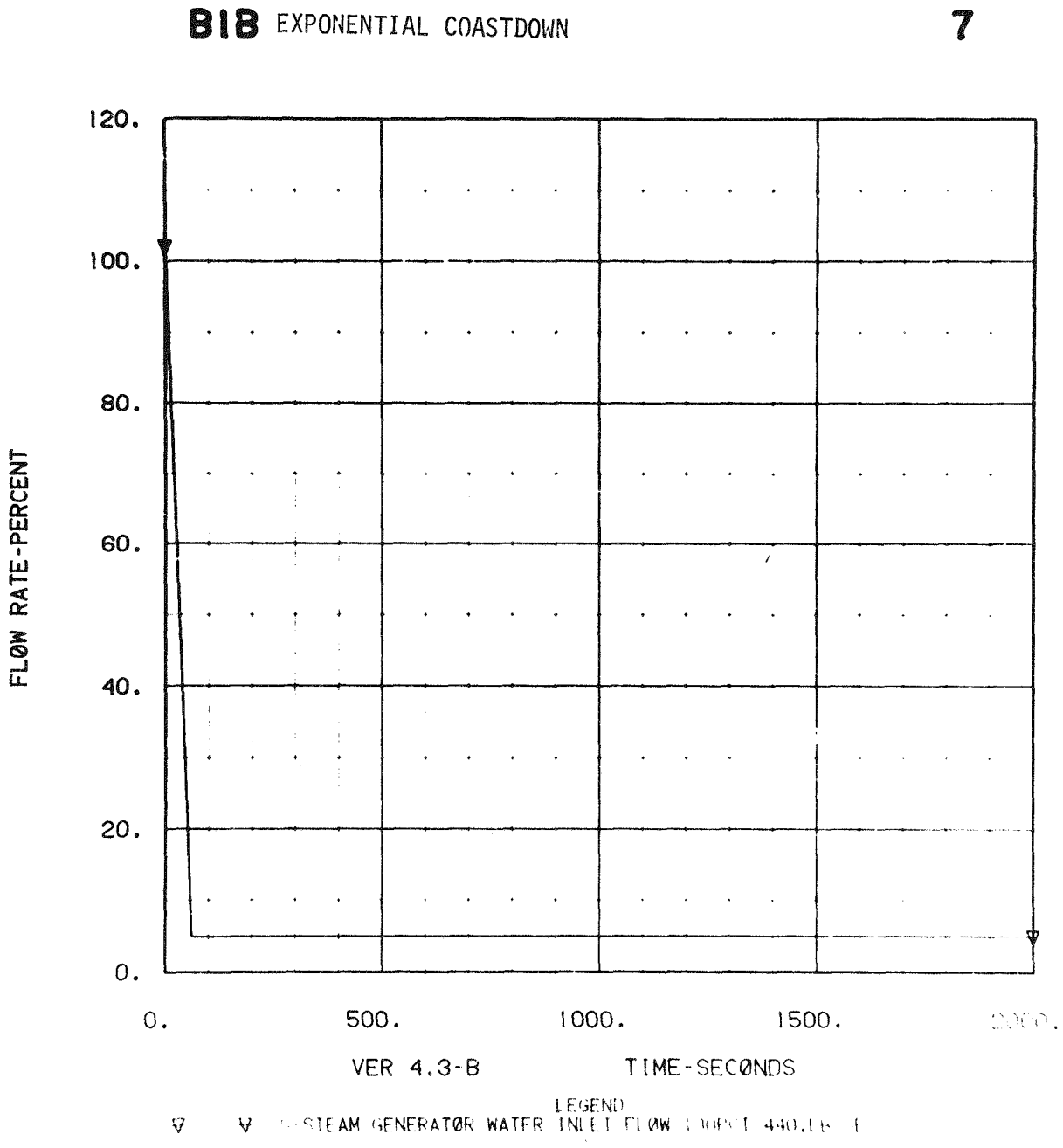

Figure E-12 Steam Generator
Pressures

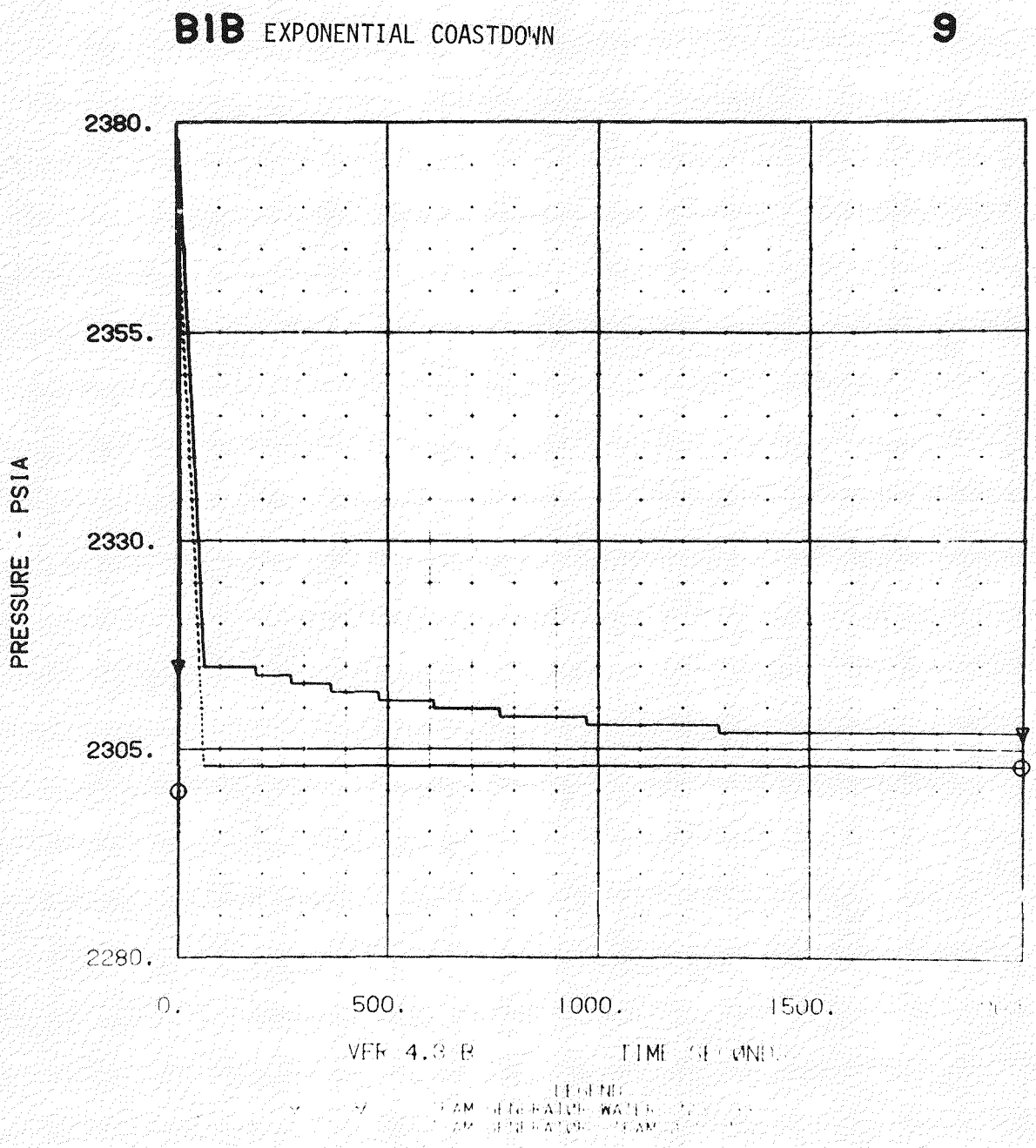

reactor trip. The turbine and water side remain on to provide an enveloping case and to determine water-side response requirements. Only 100 seconds of analysis is presented.

The reactor exit temperature (Figure E-13) for this strategy decreases at a much more rapid rate than with the exponential flow coastdown strategy. In 95 accounts the temperature drops to 770°F as opposed to about 920°F for the previous case. The cold leg temperature shows no change. The hot leg temperatures for the IHX (Figure E-15) show a similar rapid temperature decrease. The primary and secondary pump show little change in sodium temperatures (E-16). Figure E-14 shows the decrease in upper axial blanket sodium temperature. Unlike the previous case there is no turnaround between 20 and 80 seconds. Figure E-17 shows the rapid power decrease and the constant sodium flow rate. The sodium pump flow rates remain constant (see Figure E-18).

E.4.3 SODIUM PUMPS STAY AT FULL FLOW, TURBINE TRIP

This strategy is similar to that discussed in section E.4.2. However, when the steam temprature decreases to 835°F the turbine begins to trip. This 835°F corresponds to a $\pm$15°F temperature requirement requested for normal operation by the turbine manufacturer.

This signal, with an 0.5 second delay, results in the sodium pumps coasting down to 7% flow and the feedwater valve starting to close. The water side sequence is similar to the exponential flow coastdown strategy, except for the initial delay. The turbine trips at 56 seconds.

The hot pool exit temperature (Figure E-19) decreases rapidly to about 810°F at 100 seconds and than slowly decreases to 710°F at 2000 seconds. This is a less rapid drop than for the case without water side action: 770° at 85 seconds. The decrease is more than for the immediate exponential coastdown which results in a more steady drop to about 740°F at 2000 seconds. The inlet temperature responds similar to the previous cases. The upper axial blanket sodium temperature, Figure E-20, decreases

Figure E-13 Reactor Vessel Temperatures

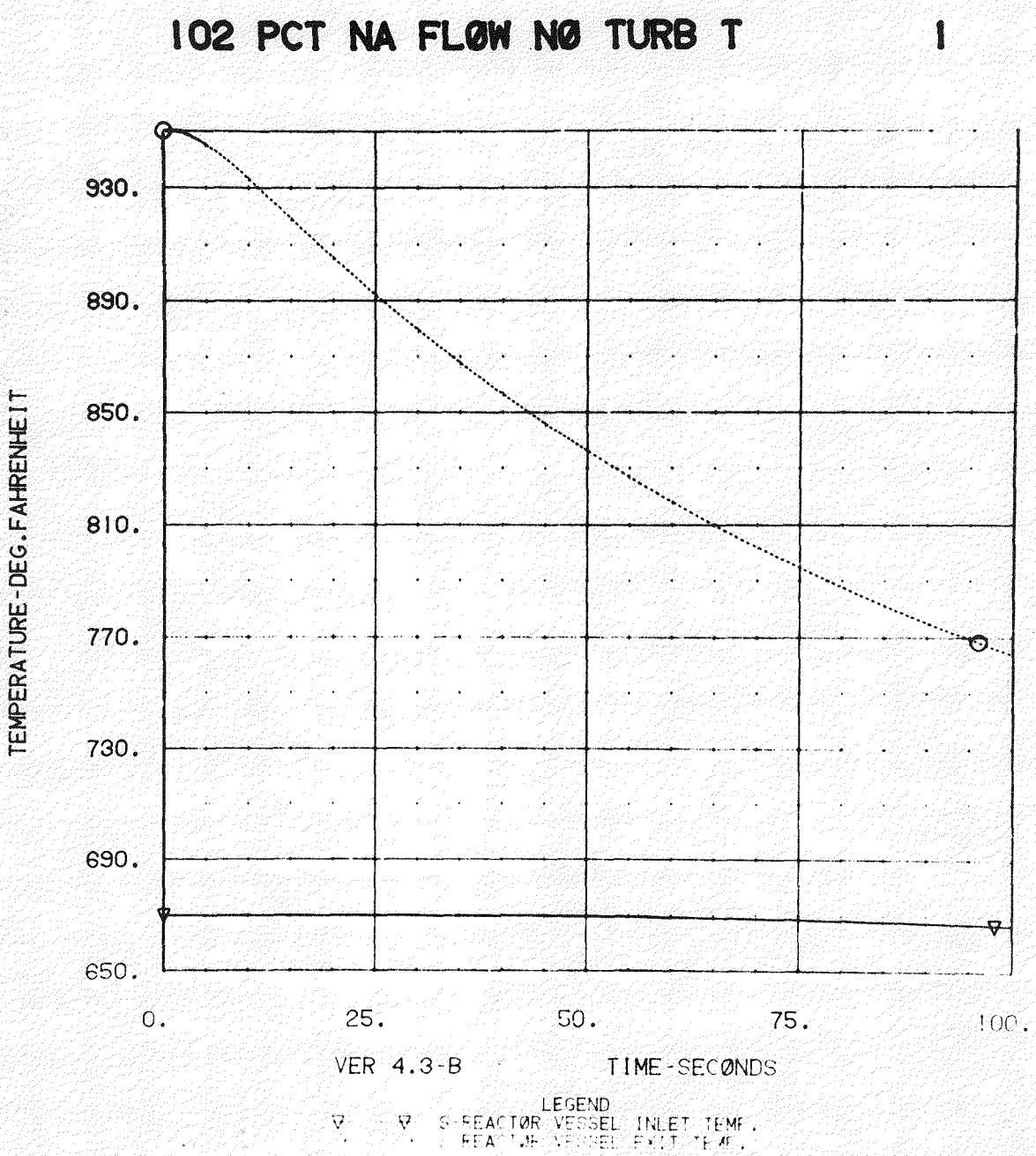

Figure E-14 Reactor Core Temperatures

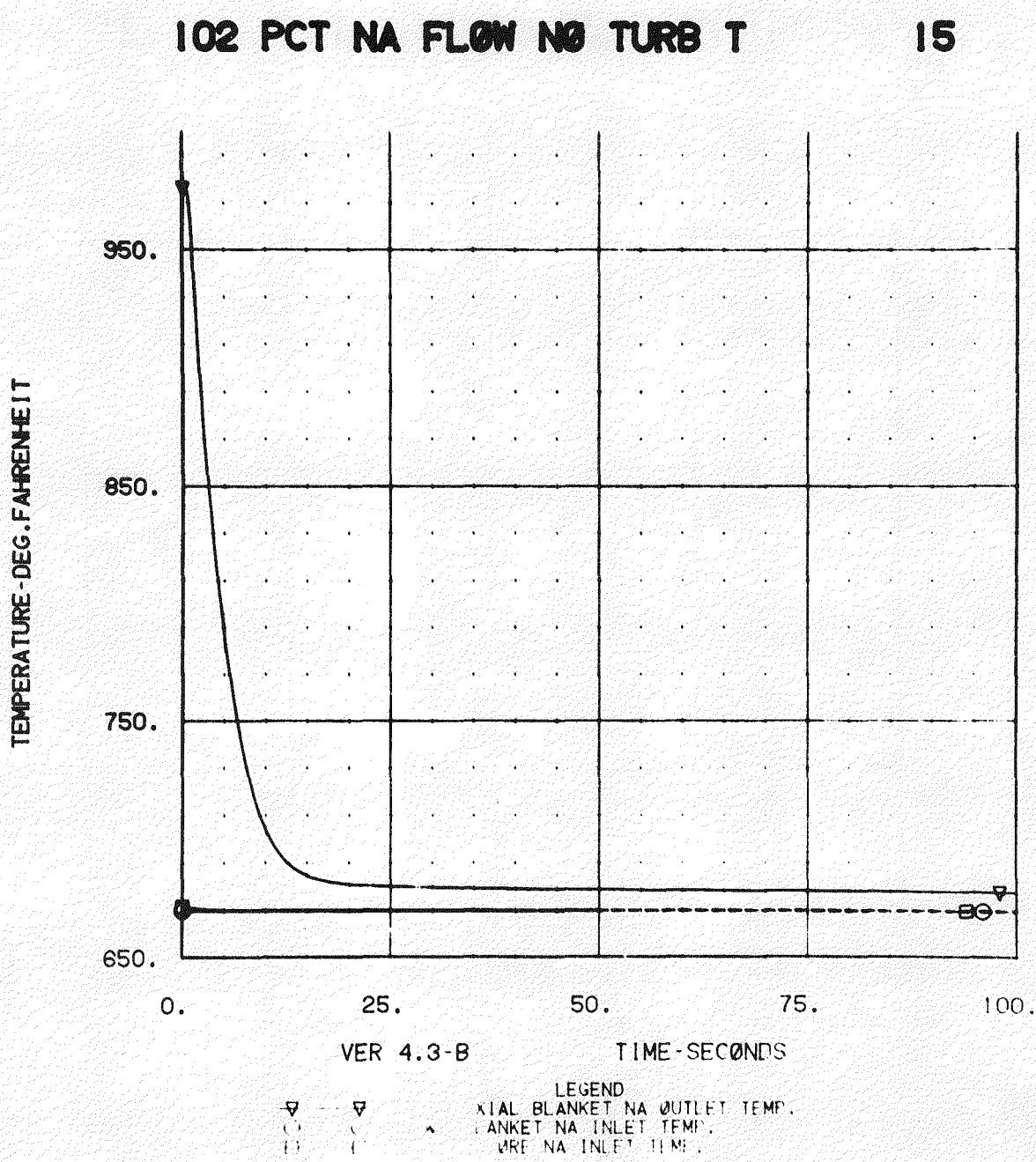

Figure E-15 Intermediate Heat Exchanger Temperatures

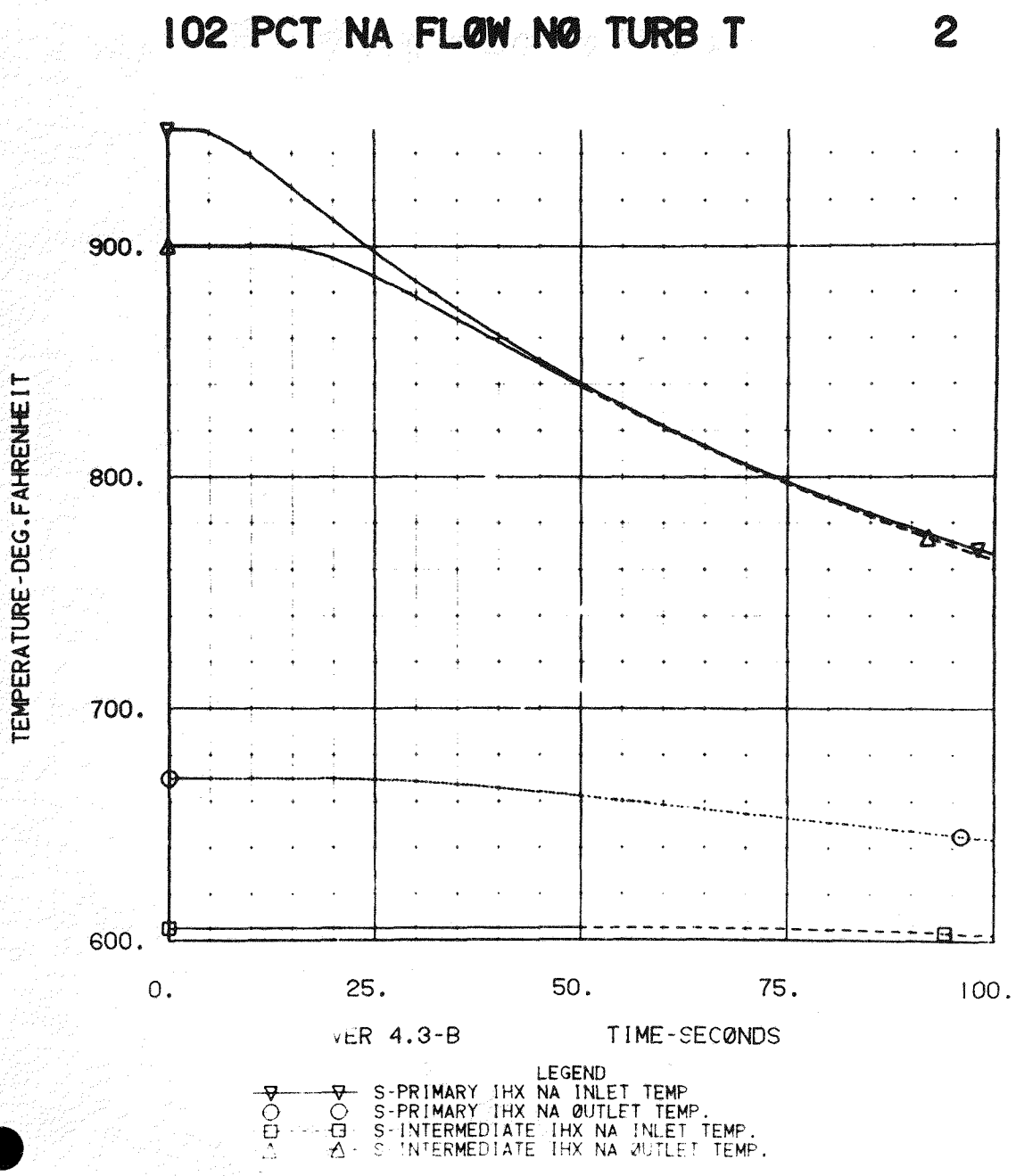

Figure E-16 Sodium Pump Temperatures

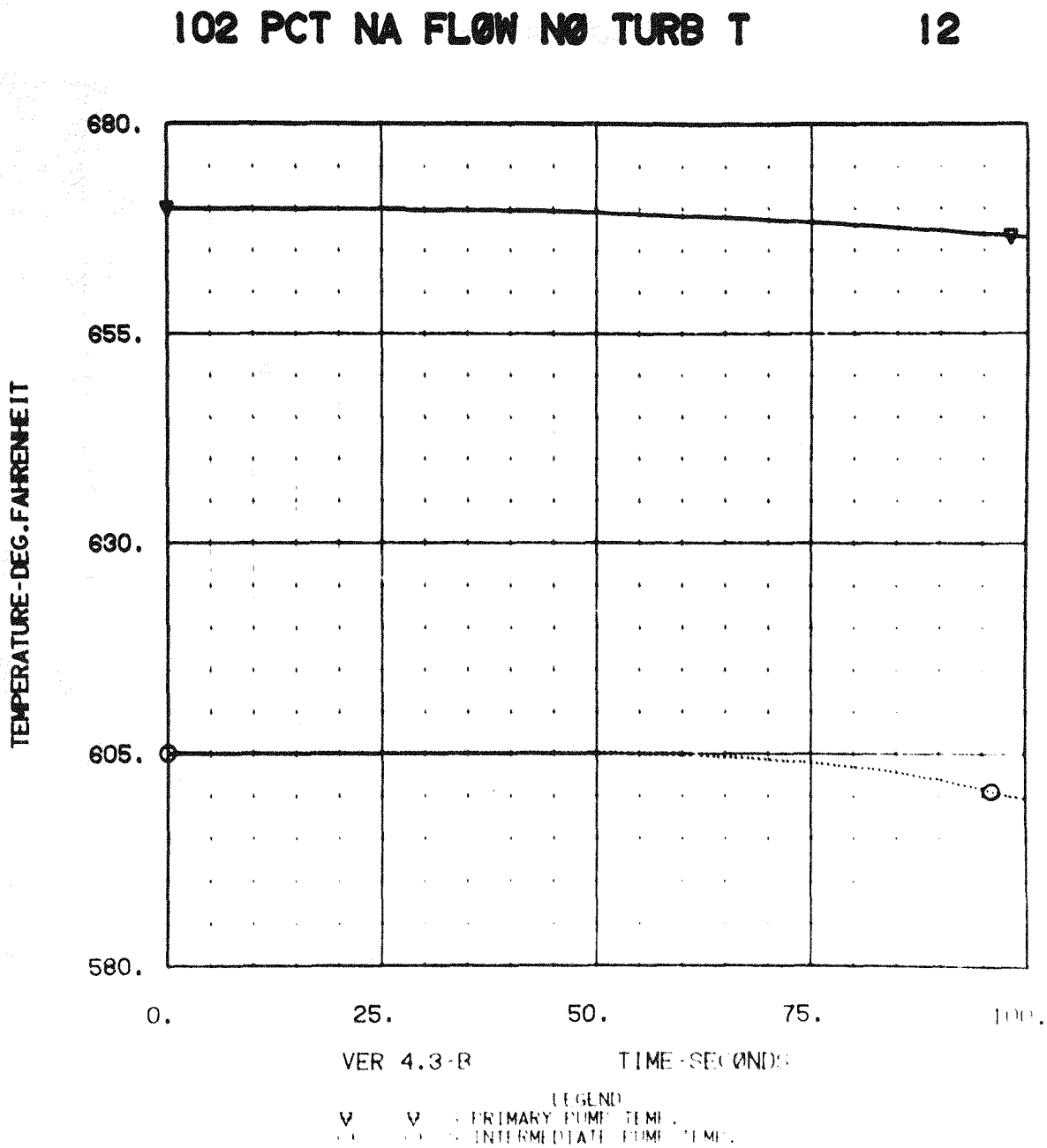

Figure E-17 Reactor Power & Flow Rate

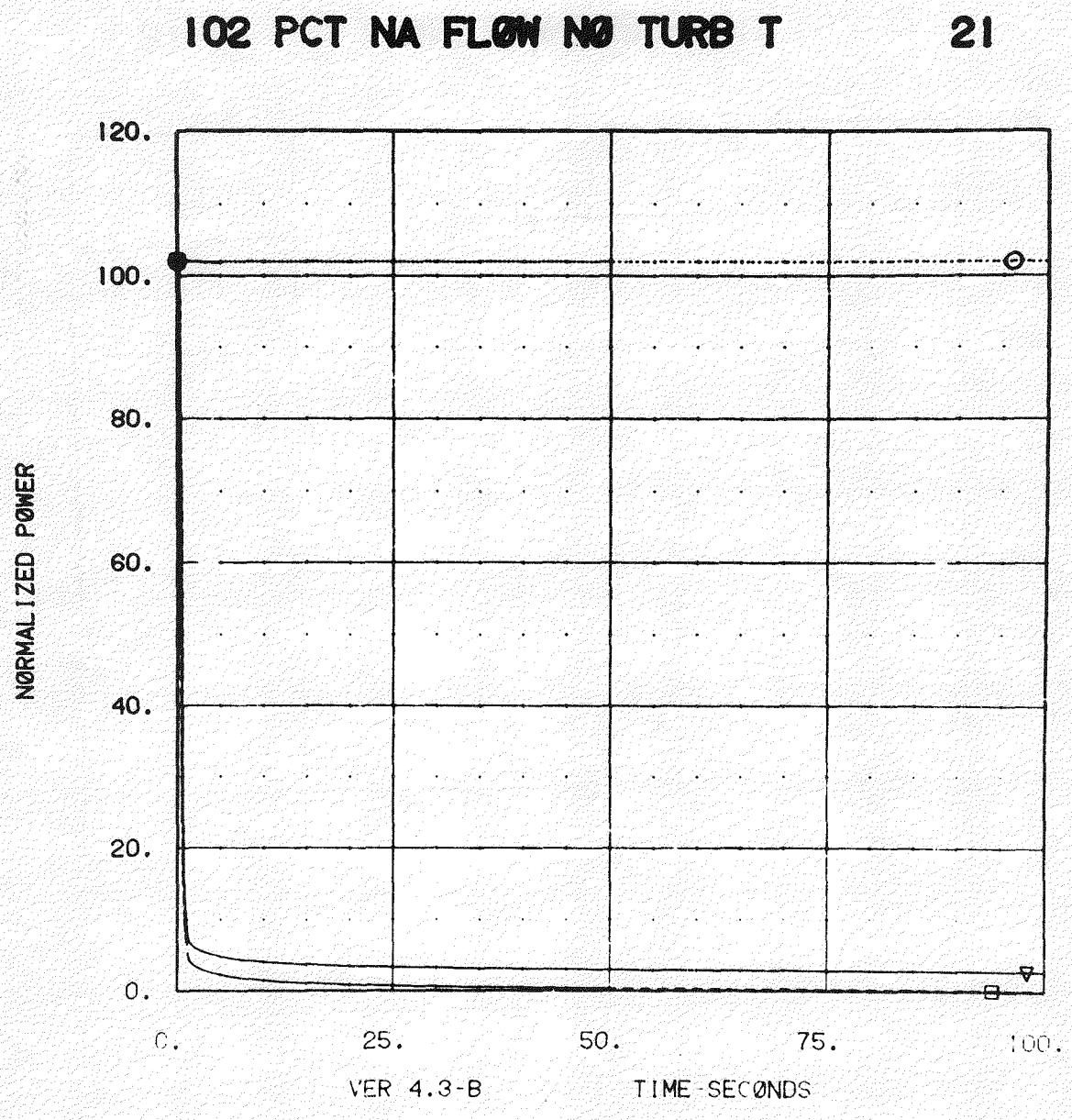

Figure E-18 Sodium Pump Flow Rates

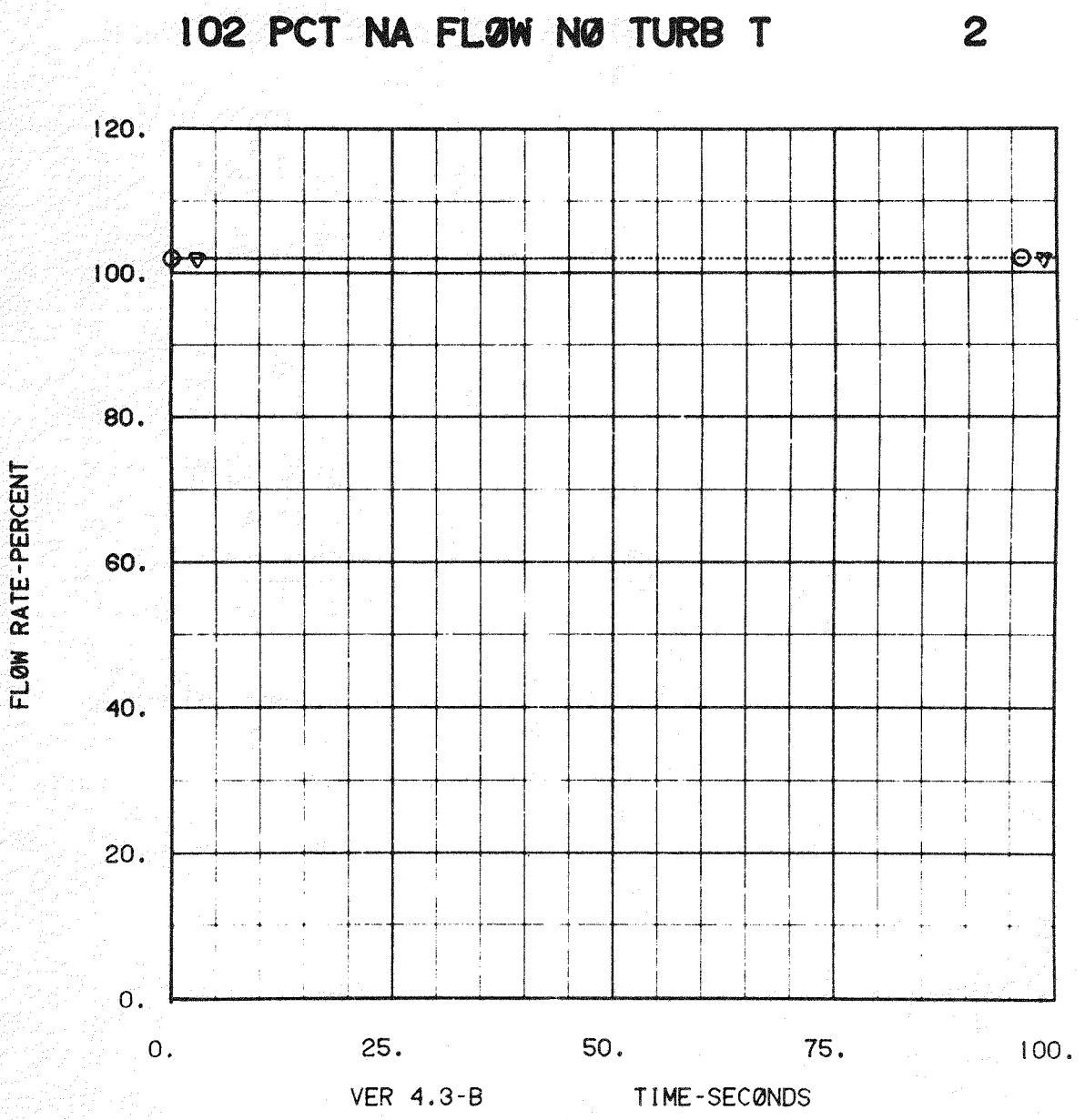

Figure E-19 Reactor Vessel Temperatures

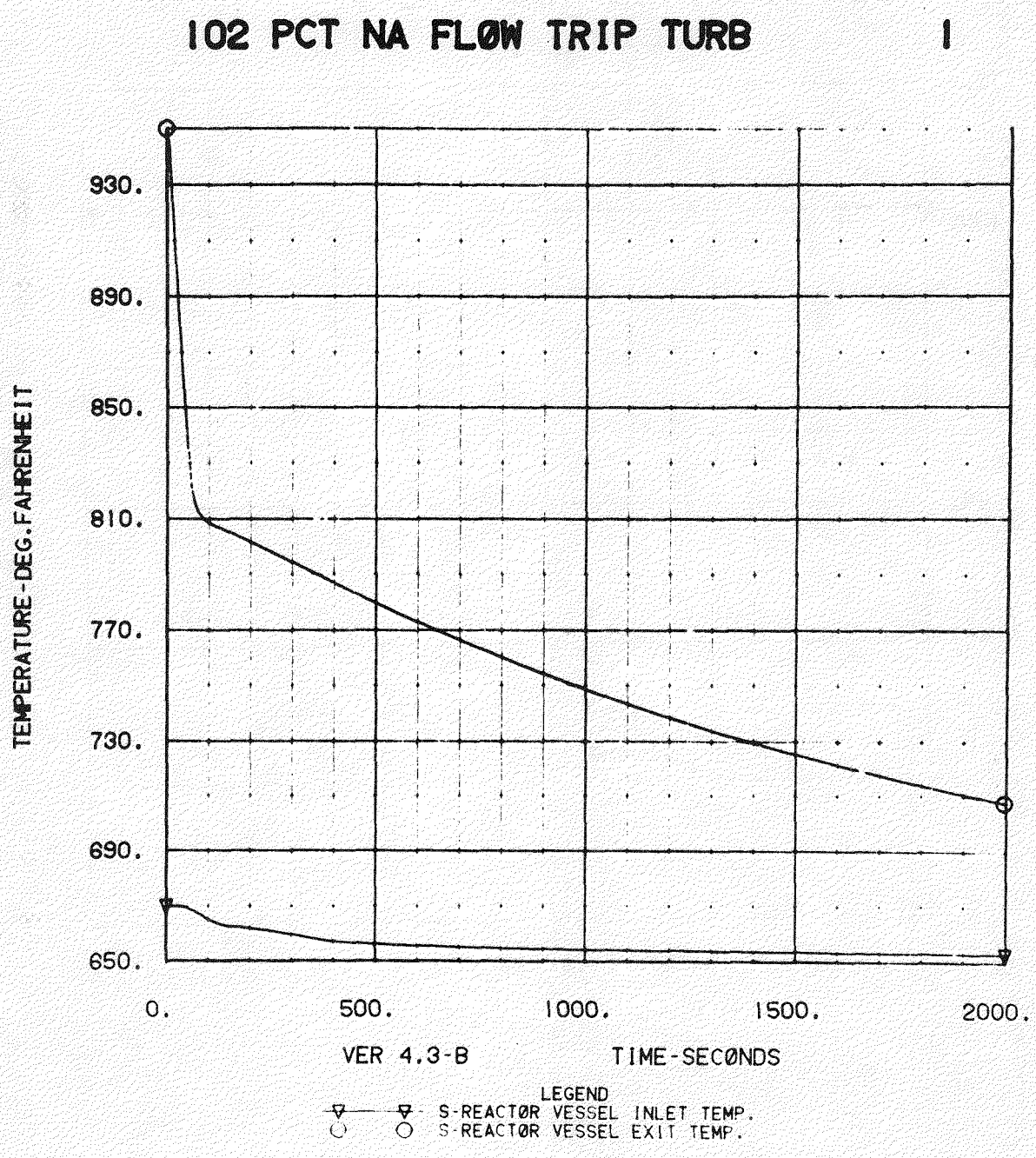

Figure E-20 Reactor Core Temperatures

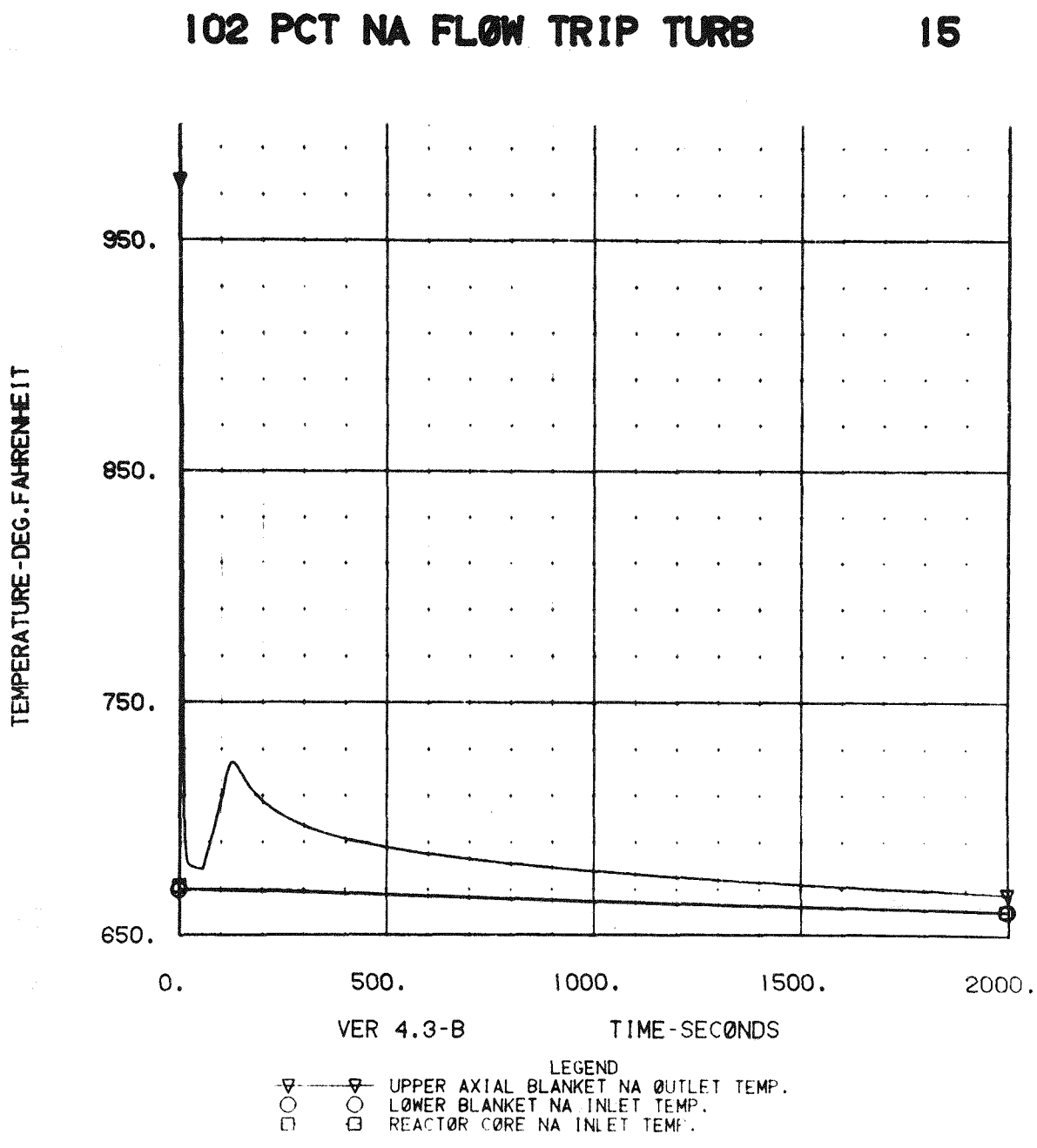

rapidly but following the water side shutdown, increases briefly before leveling off. The hot leg sodium temperature at the IHX, Figure E-21, show a corresponding temperature response as does the reactor exit. The cold leg temperatures show a delay before responding as in the exponential coastdown case. The pump temperatures (Figure E-22) show similar agreement. Figure E-23 shows the power and flow behavior and Figure E-24 shows the secondary and primary pump flows. Both graphs show the delay in the sodium coastdown to pony motor flow.

E.4.4 TIME DELAYED EXPONENTIAL COASTDOWN

At full sodium flow it takes approximately 100 seconds to change the volume of sodium in the upper plenum. A system delay of 25 seconds provide a 25% volume replacement prior to sodium pump trip. Figures E-25 through E-30 show the thermal and system response. The results show more rapid temperature decreases than the immediate exponential coastdown (E.4.1) but are less severe than for the coastdown following the turbine trip (E.4.3).

E.4.5 PUMP RAMP DOWN AT 1%/SECOND

Following a reactor trip, the primary and secondary sodium pumps are ramped down in speed at 1%/second, their normal speed control rate. At 40% speed, lower limit of control system, the pumps are tripped and coastdown to the pony motor speed of 7% using the same inertias as used for the normal exponential coastdown.

The reactor exit temperature initially decreases at about $2^{o}F$/second then slows down to less than $0.1^{o}F$/second and reaches about $720^{o}F$ at 2000 seconds (see Figure E-31). The cold leg sodium temperature decreases slowly to about $650^{o}F$. Figure E-32 shows that the upper axial blanket decreases to the sodium inlet temperature, then increases to about $730^{o}F$ before asymptotically decreasing over again toward the inlet temperature. The IHX sodium temperatures (Figure E-33) show hot leg behavior similar to the reactor exit. The cold leg temperatures decrease toward the initial feedwater temperature before they recover to $650^{o}F$, above the final

Figure E-21 Intermediate Heat
Exchanger Temperatures

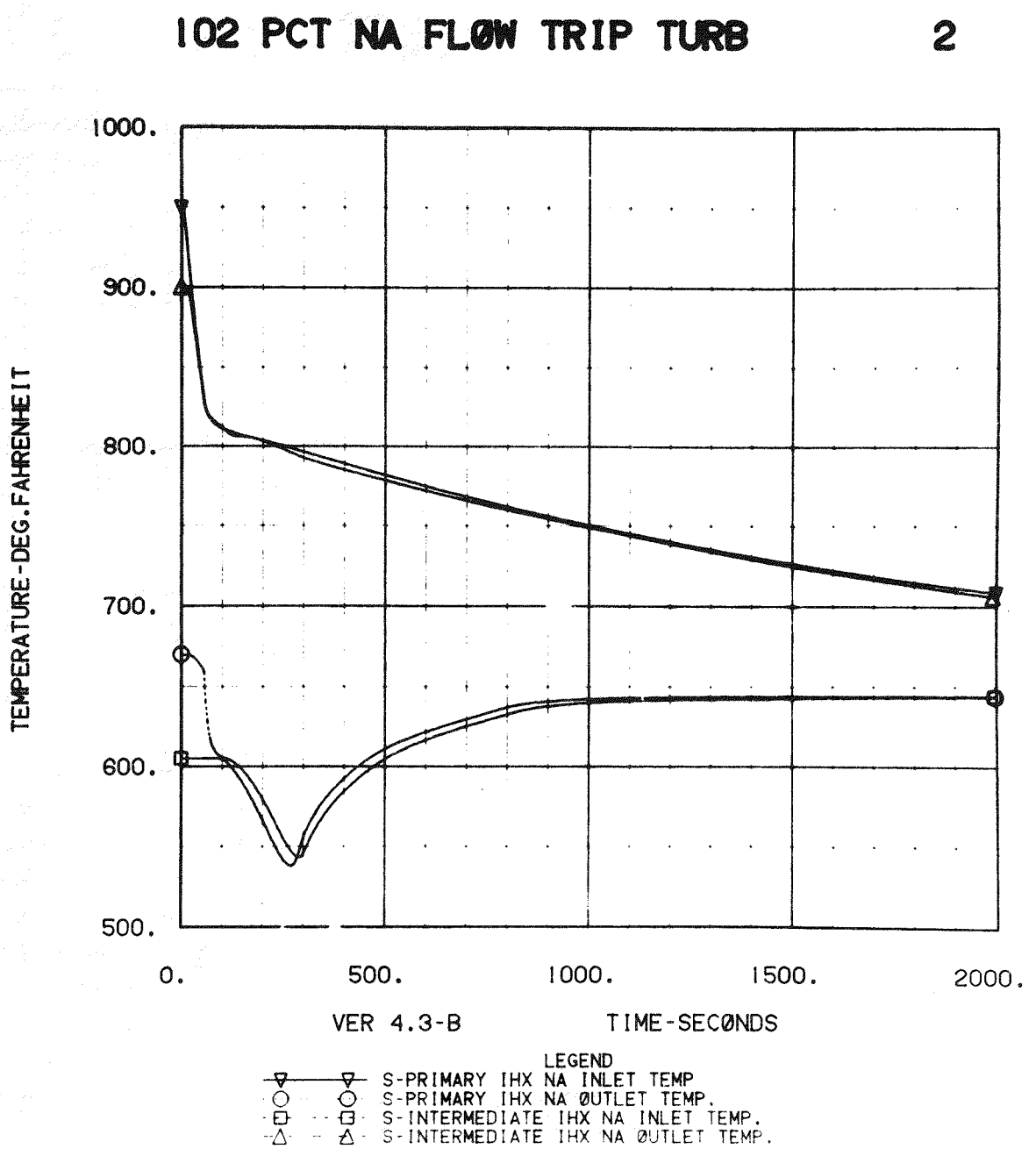

Figure E-22 Sodium Pump Temperatures

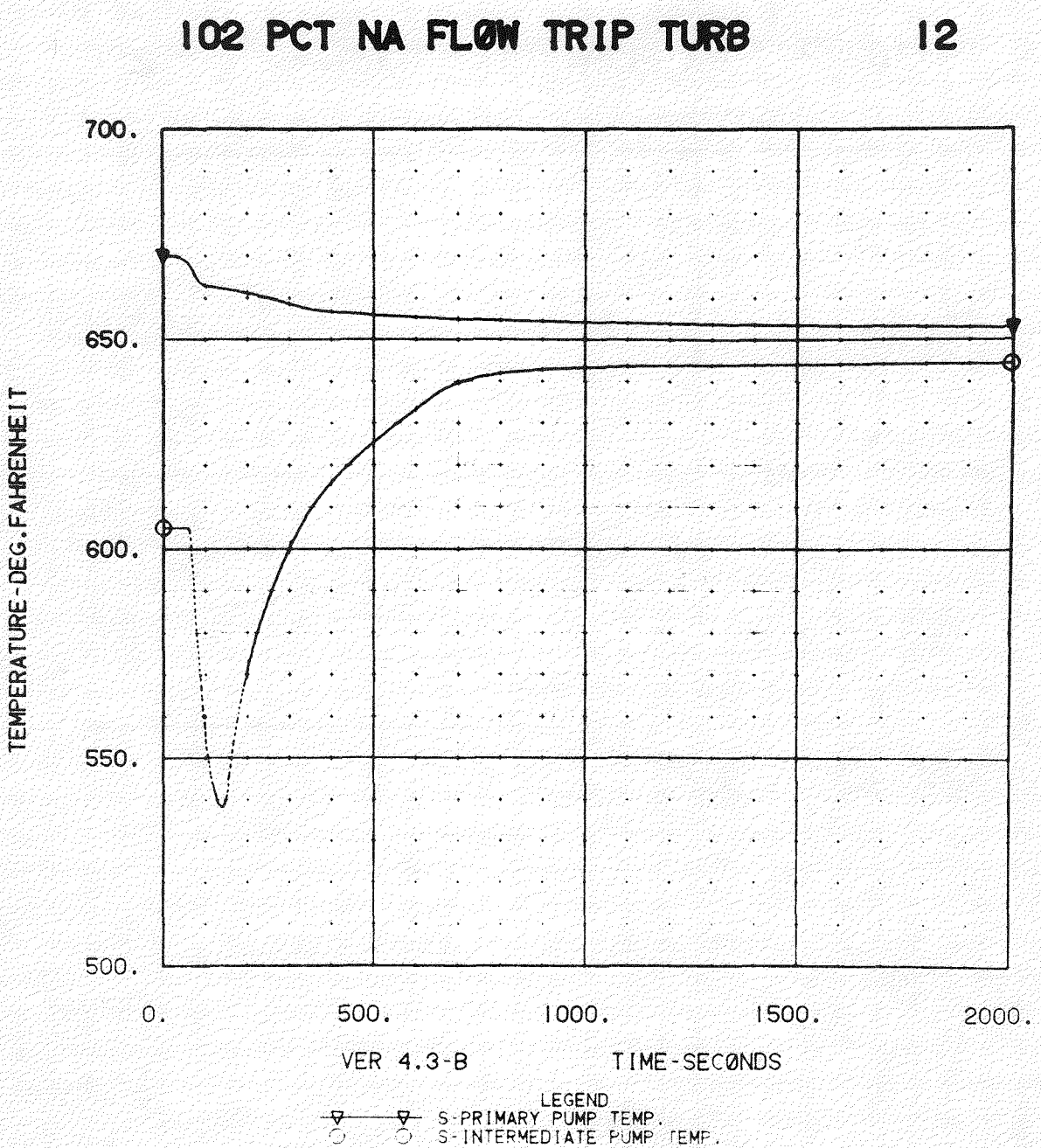

Figure E-23 Reactor Power & Flow Rate

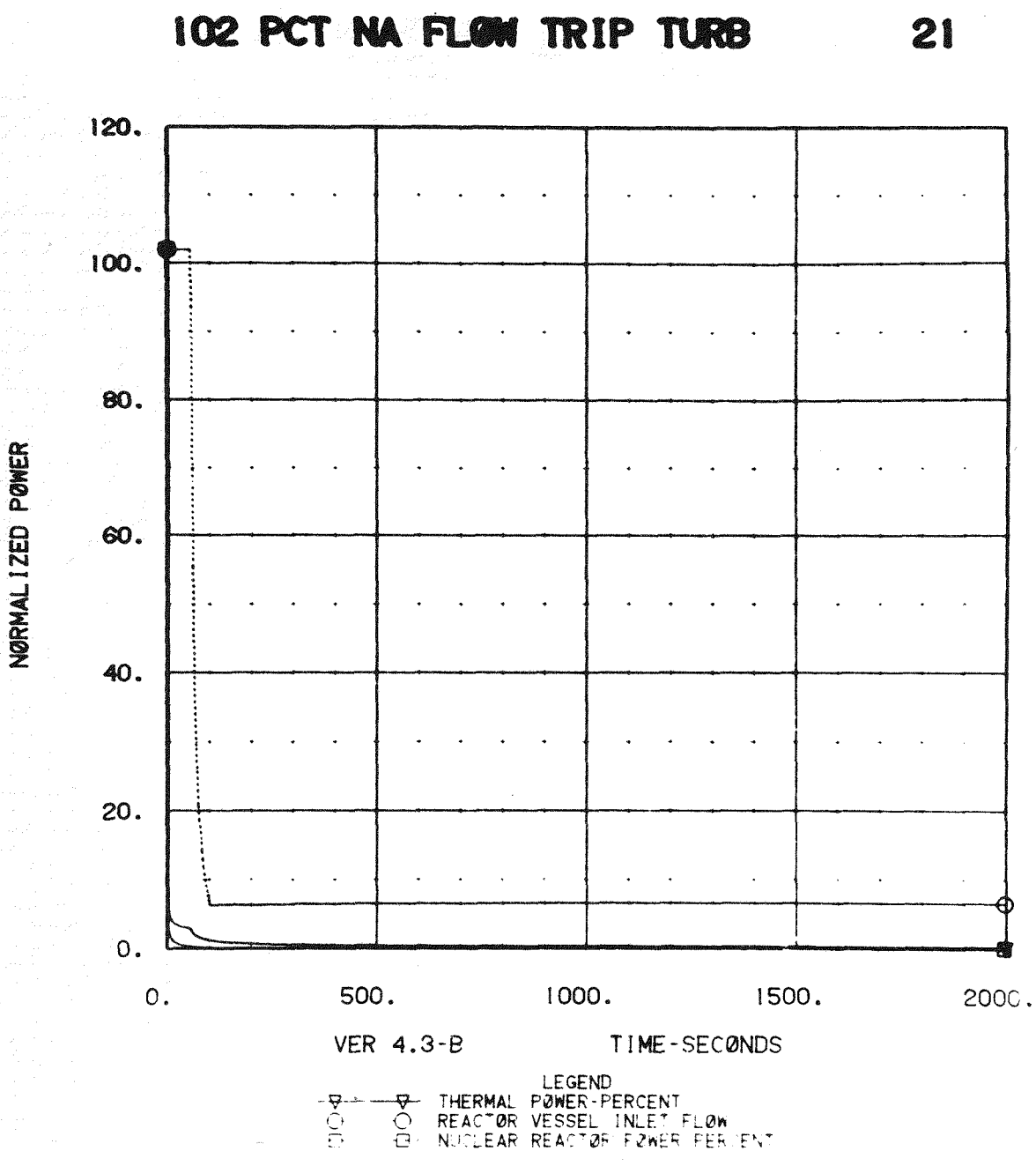

Figure E-24 Sodium Pump Flow Rates

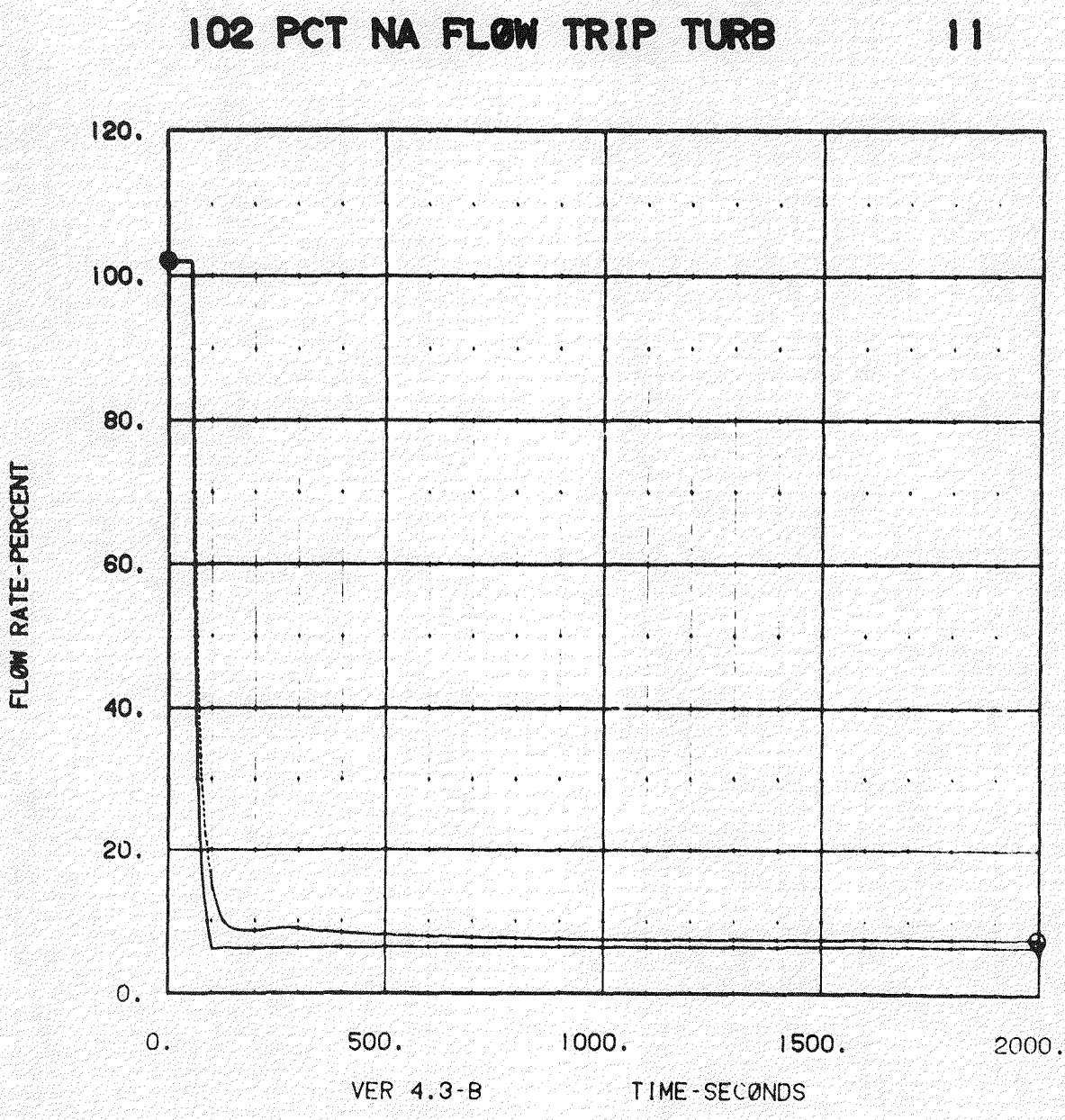

Figure E-25 Reactor Vessel Temperatures

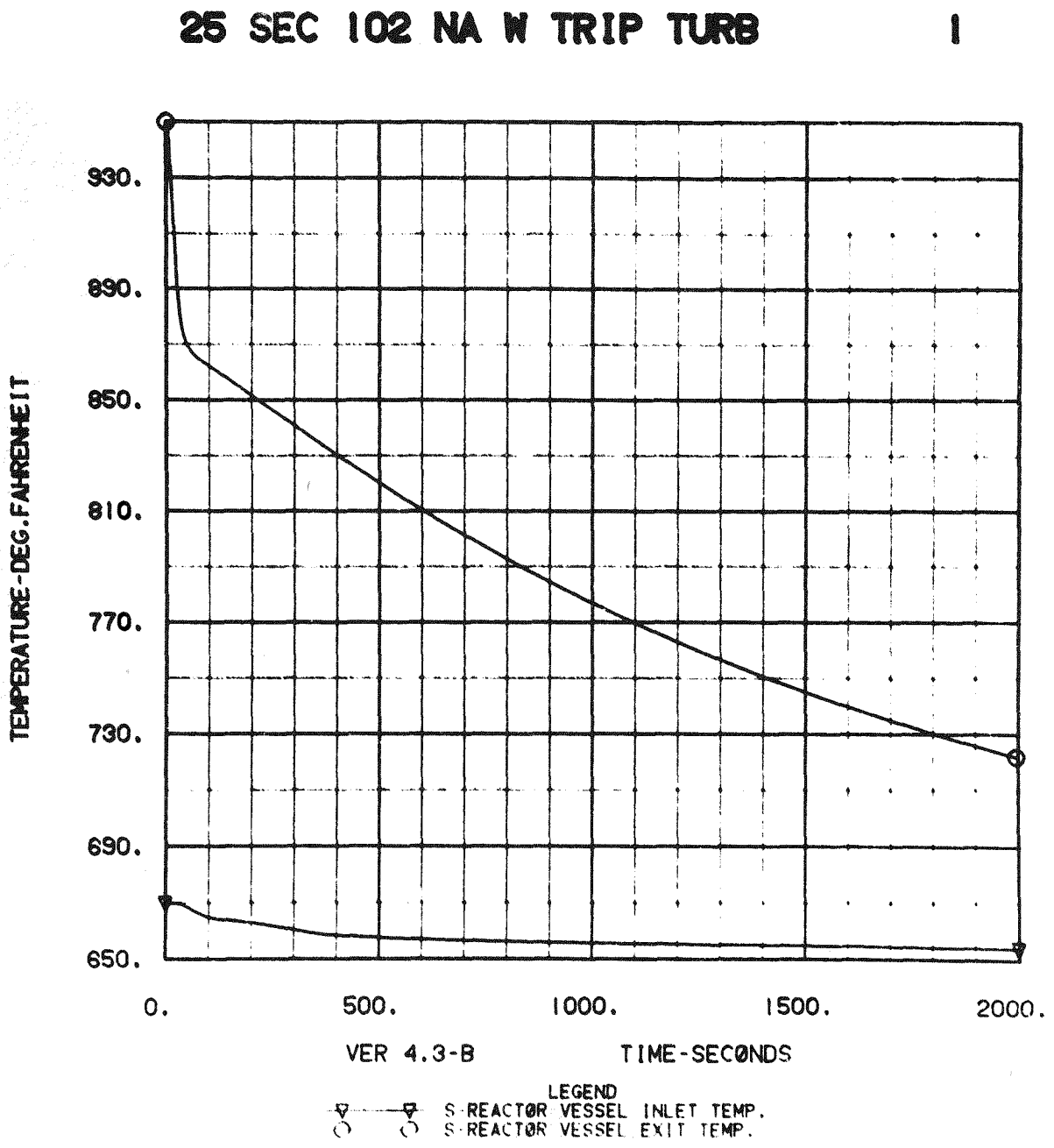

Figure E-26 Reactor Core
Temperatures

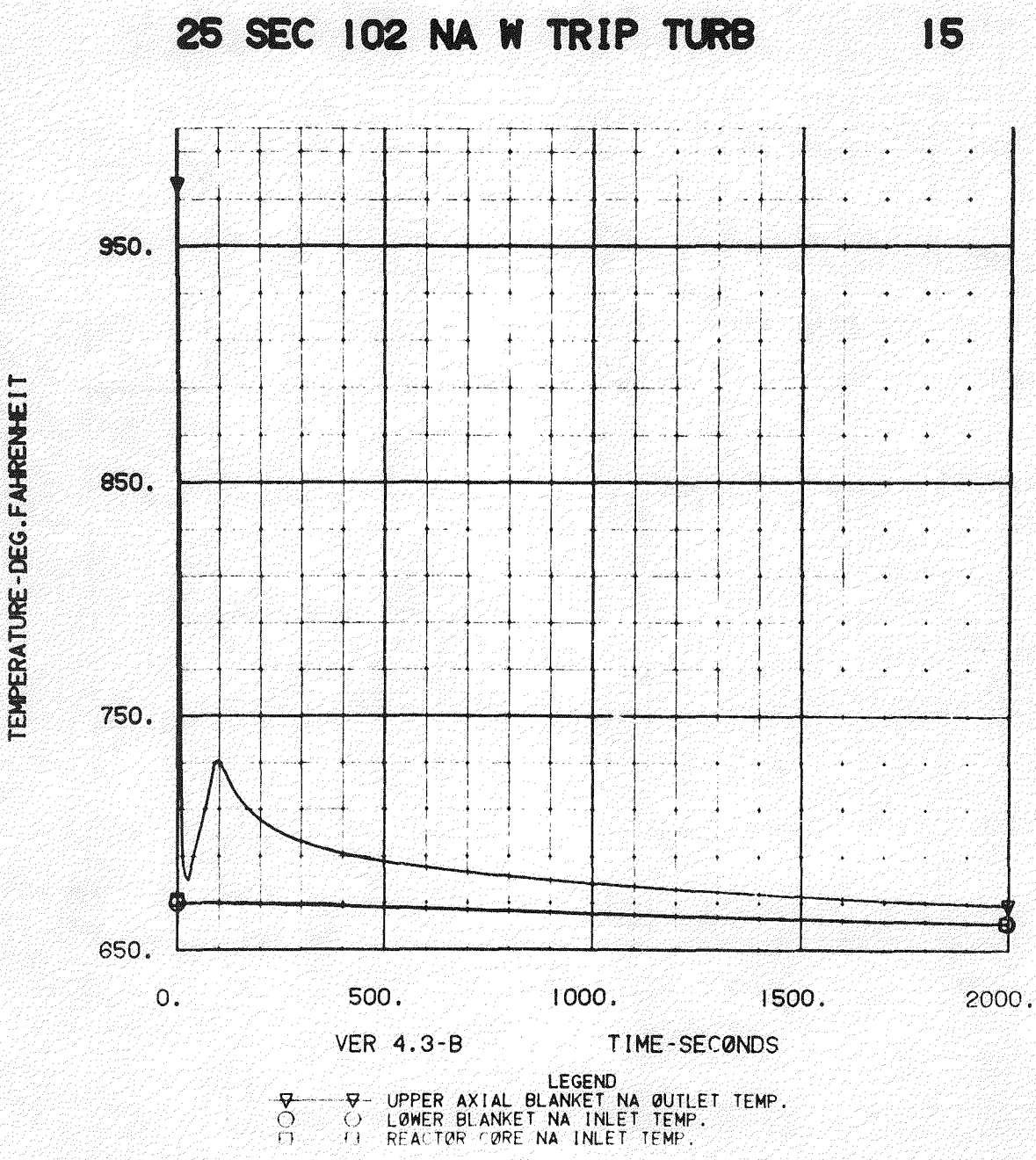

Figure E-27 Intermediate Heat
Exchanger Temperatures

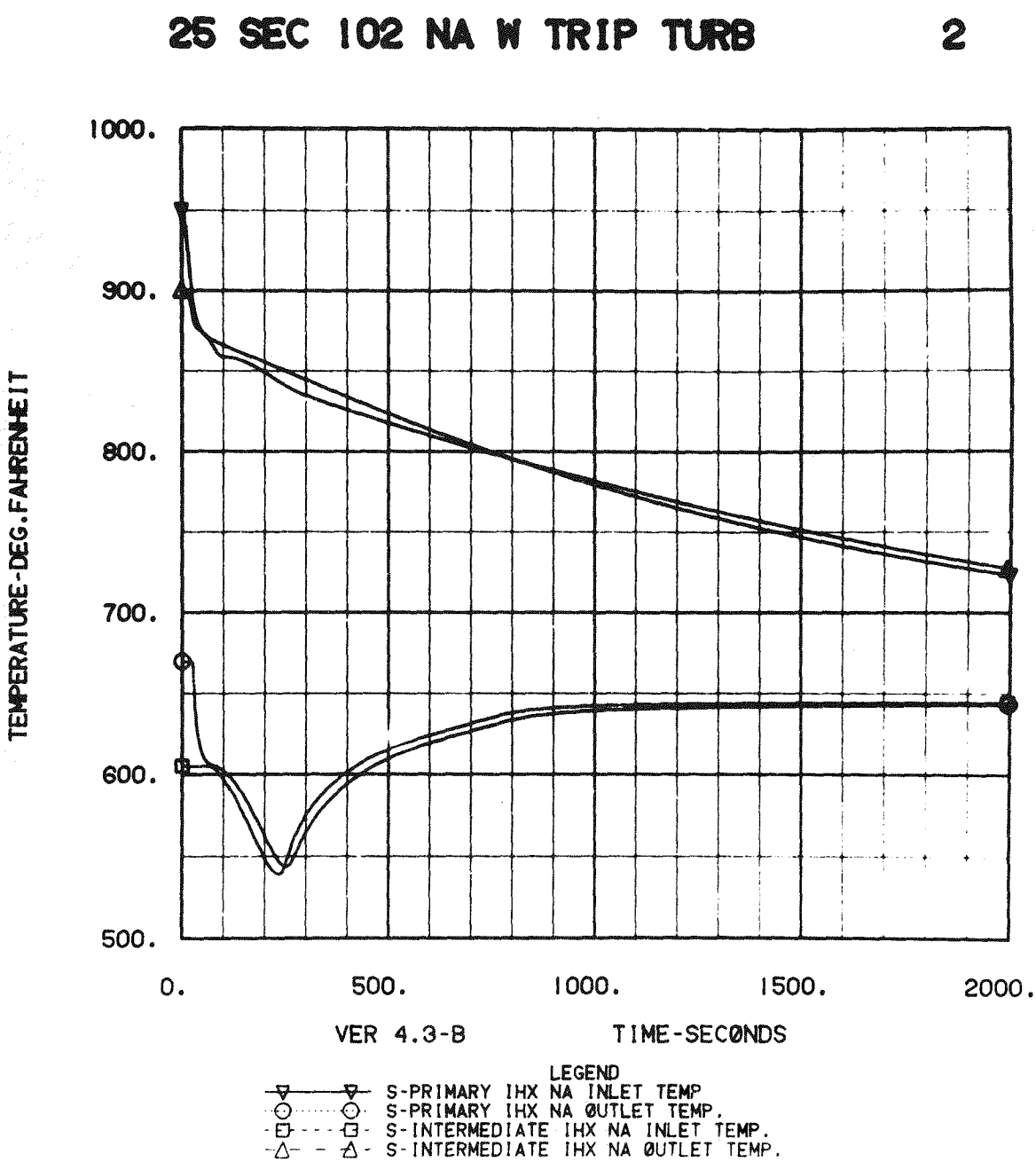

Figure E-28 Sodium Pump
Temperatures

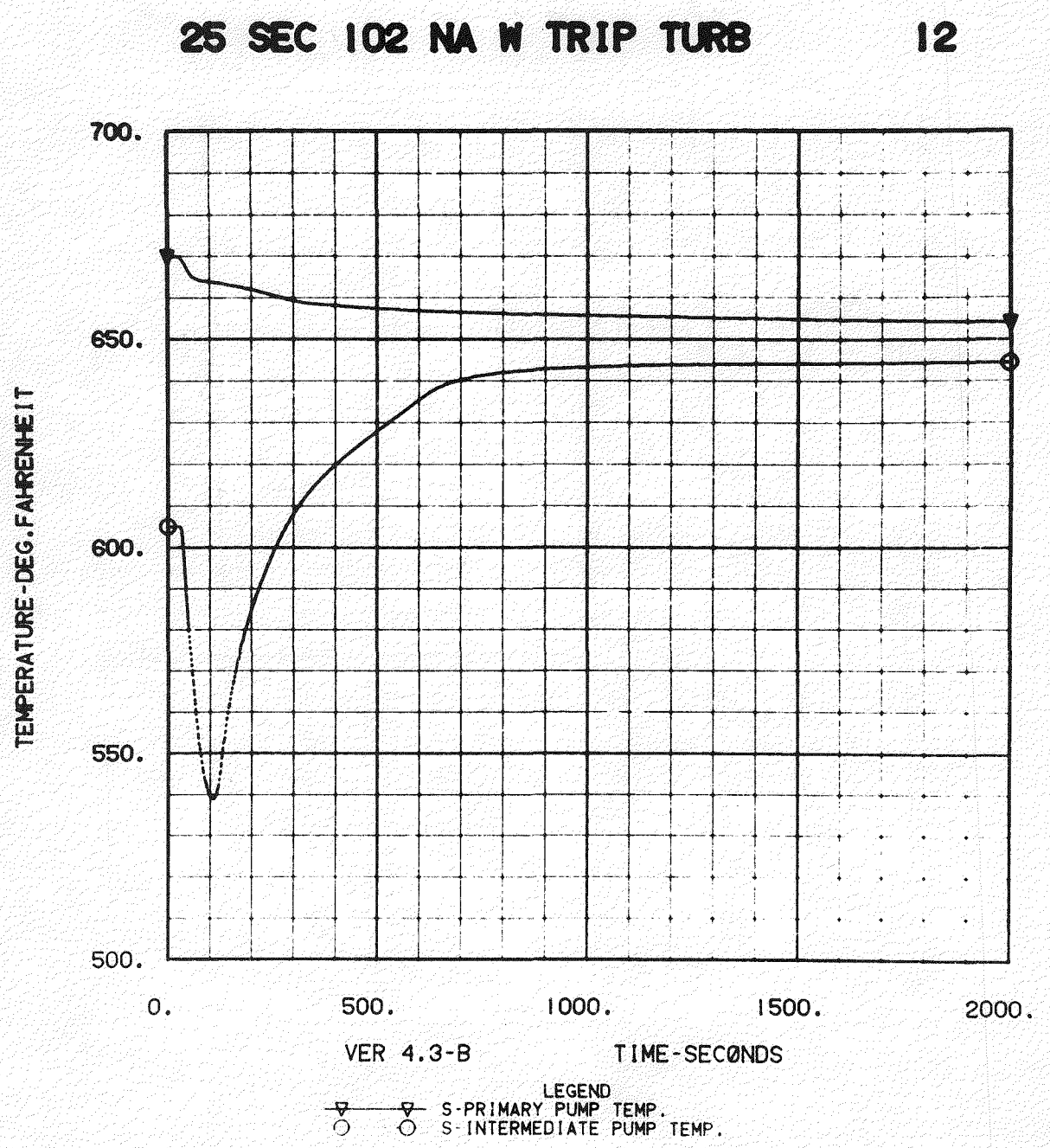

Figure E-29 Reactor Power & Flow Rate

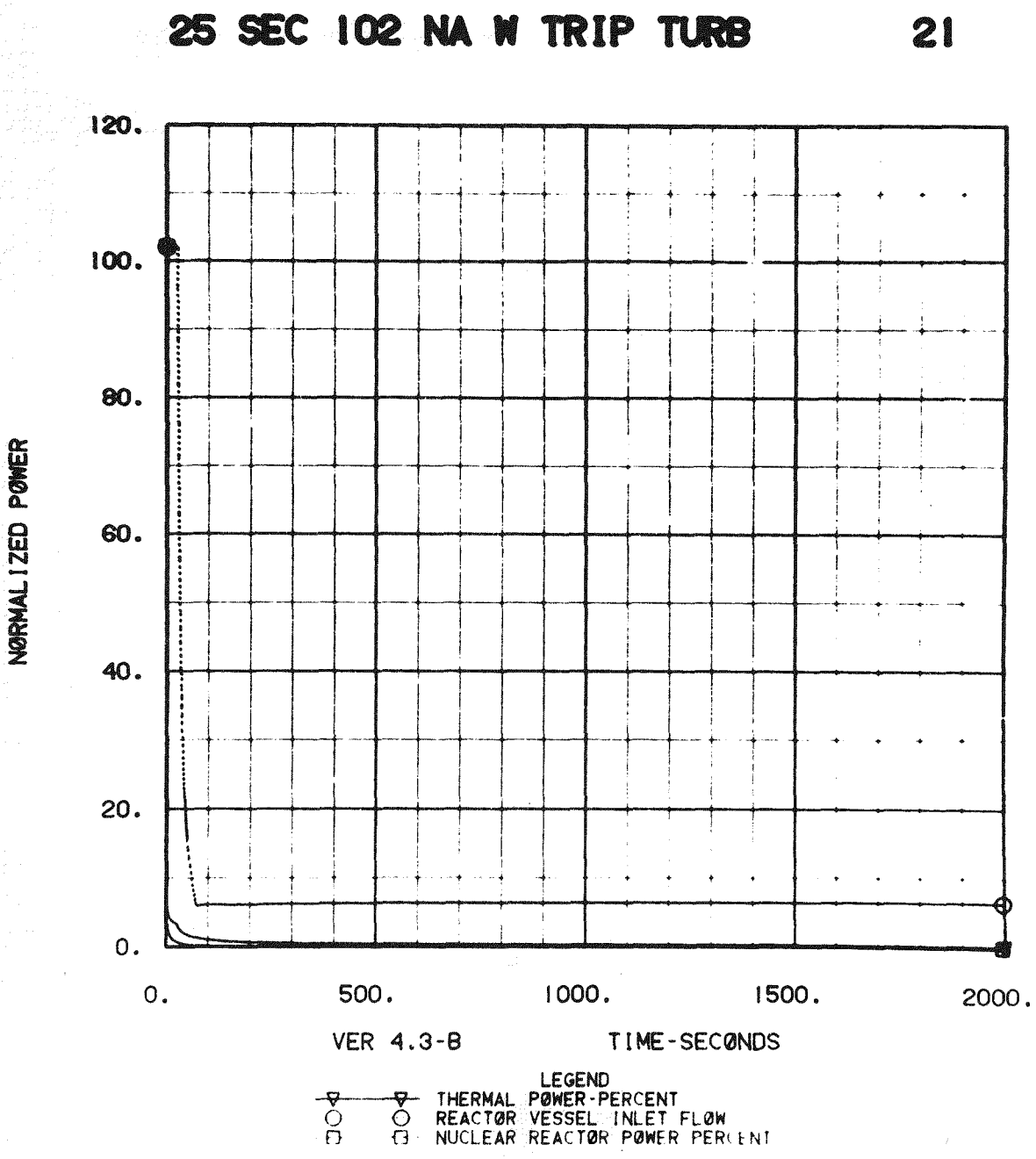

Figure E-30 Sodium Pump Flow Rates

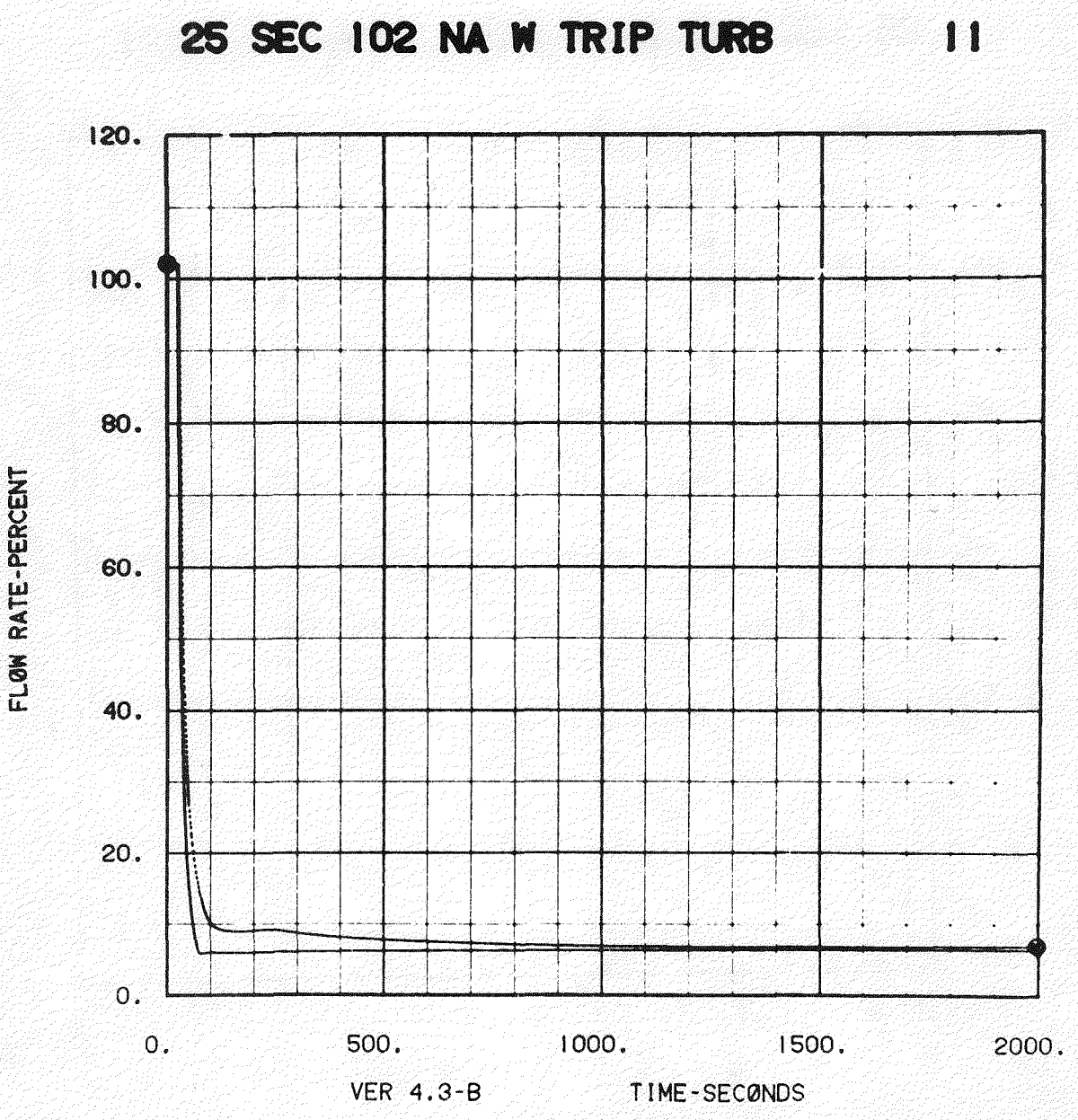

Figure E-31 Reactor Vessel Temperatures

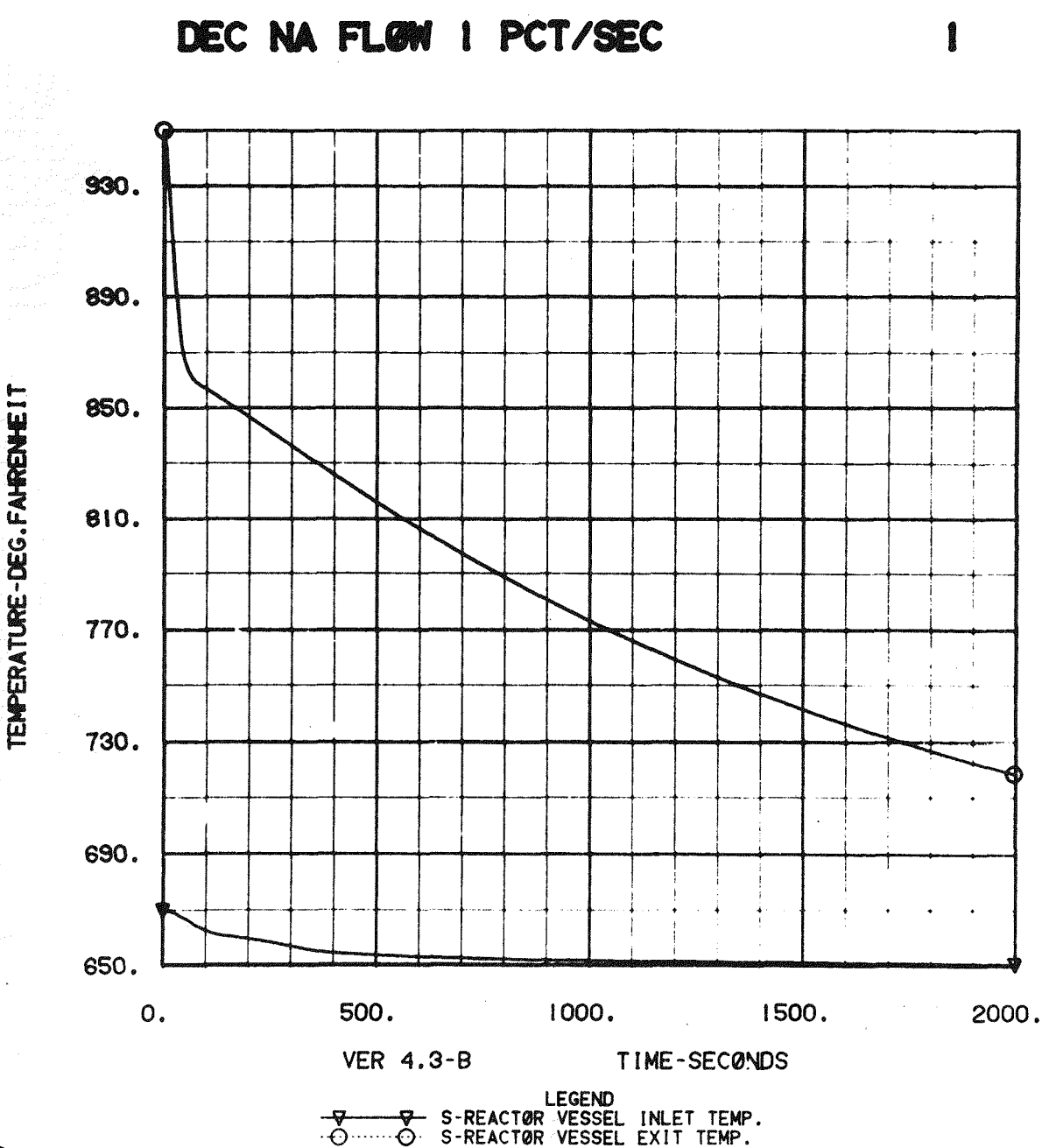

Figure E-32 Reactor Core Temperatures

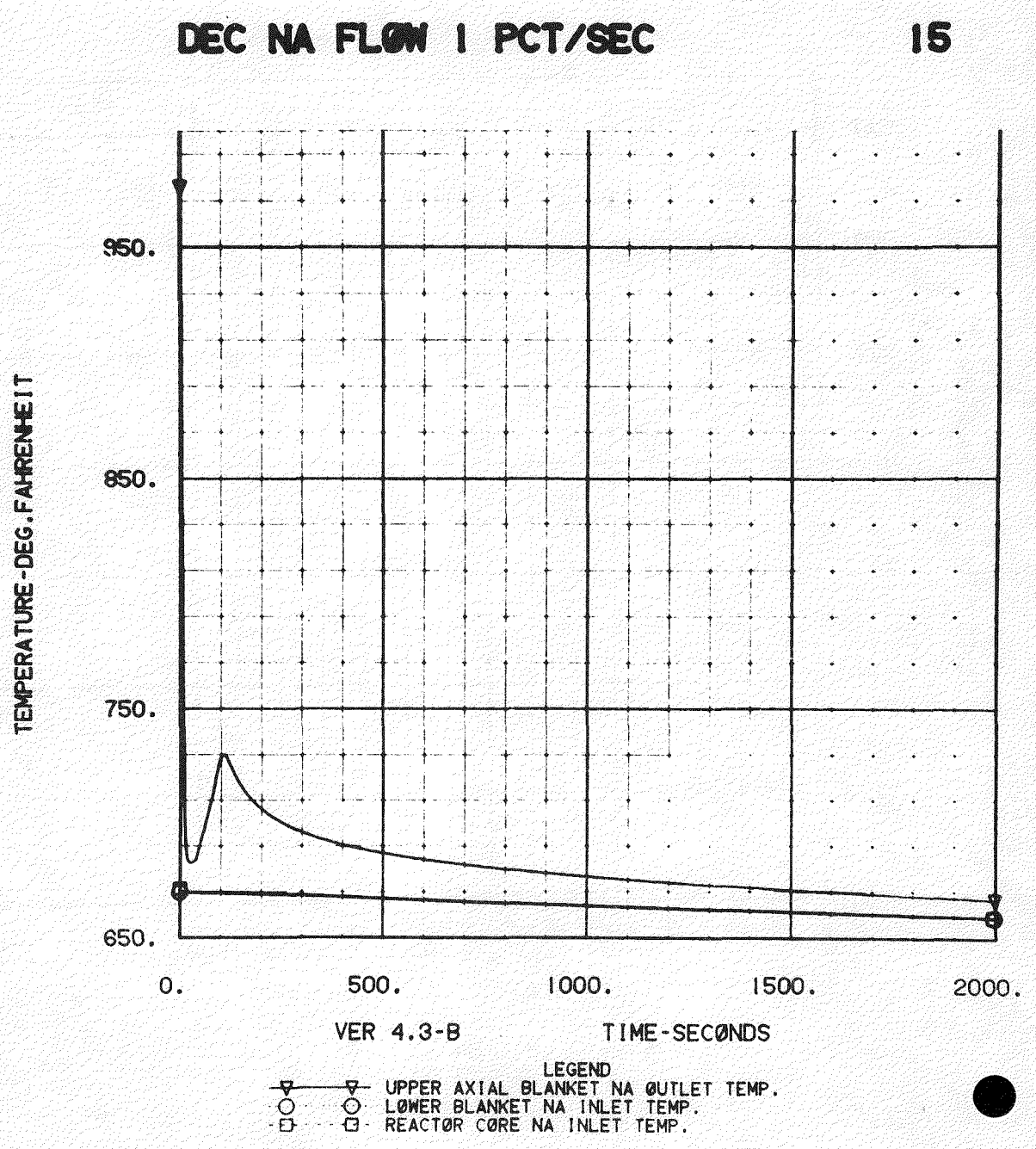

Figure E-33 Intermediate Heat
Exchanger Temperatures

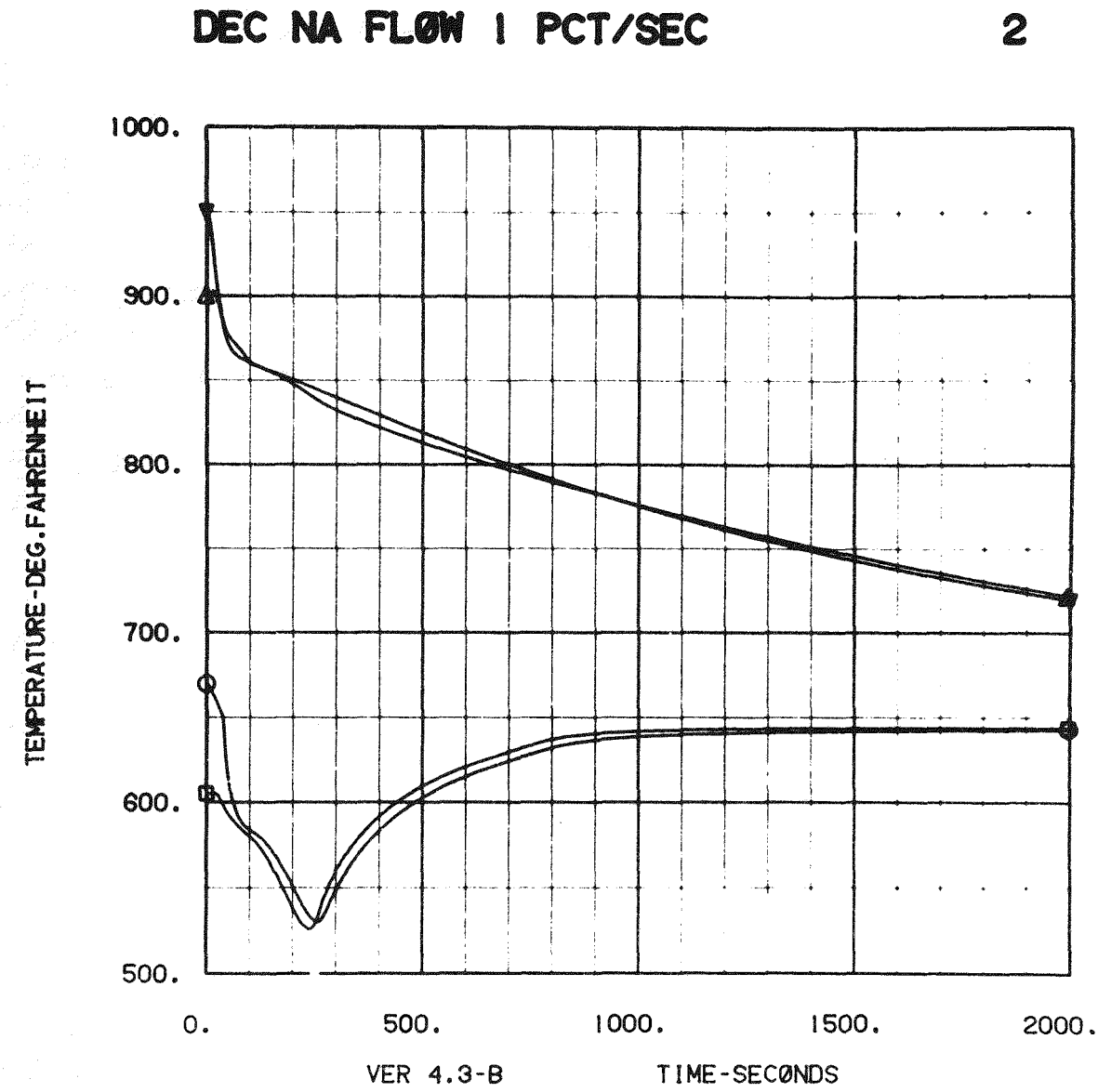

feedwater temperature. The dip is more severe than for the immediate exponential coastdown. The sodium pump temperatures (Figure E-34) are similar to the cold leg responses at the IHX. The thermal and nuclear power decrease rapidly, Figure E-35. However, the total flow curve shows the ramped down behavior prior to the exponential coastdown. The sodium pump flow rates (E-36) decrease at a slower rate until the 40% speed is obtained. The flow then decreases to pony motor flow rates.

E.4.6 CONCLUSIONS

The thermal behavior of the LPR plant for several proposed shutdown strategies is available for analyzing the thermal response of reactor and plant systems and components. Until this analysis is complete, the preferred shutdown strategy cannot be finally selected.

Figure E-34 Sodium Pump
Temperatures

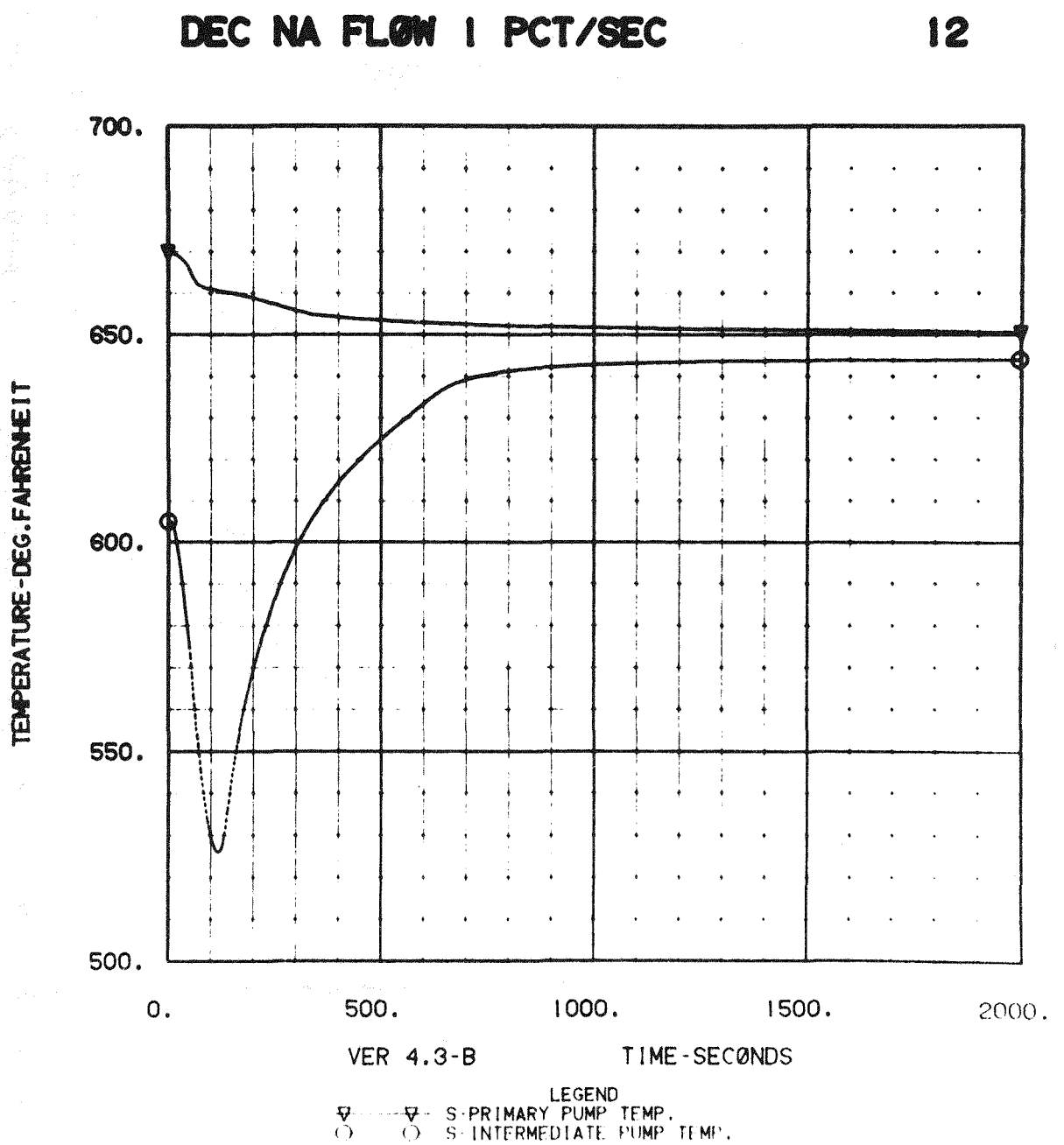

Figure E-35 Reactor Power & Flow Rate

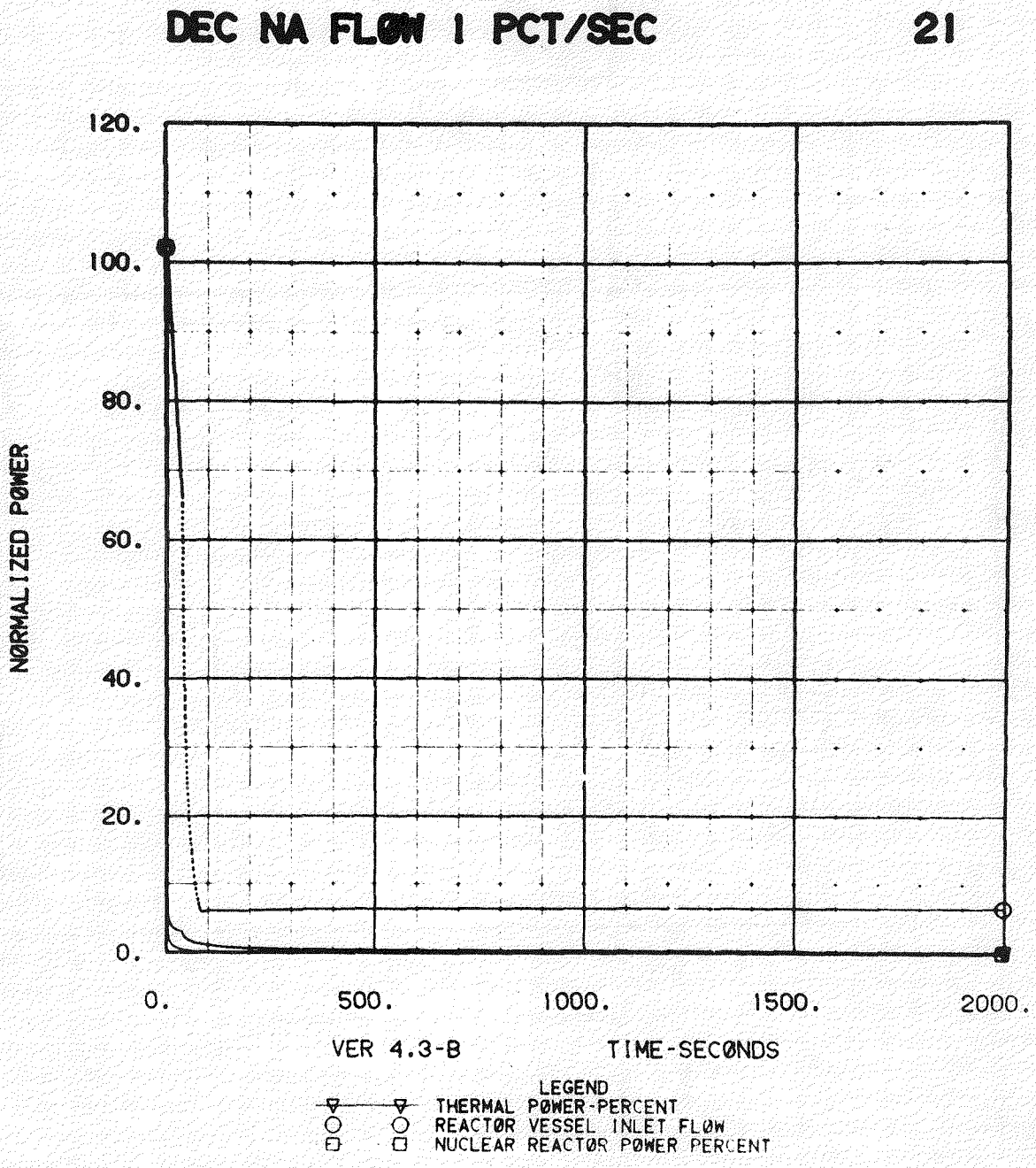

Figure E-36 Sodium Pump Flow Rates

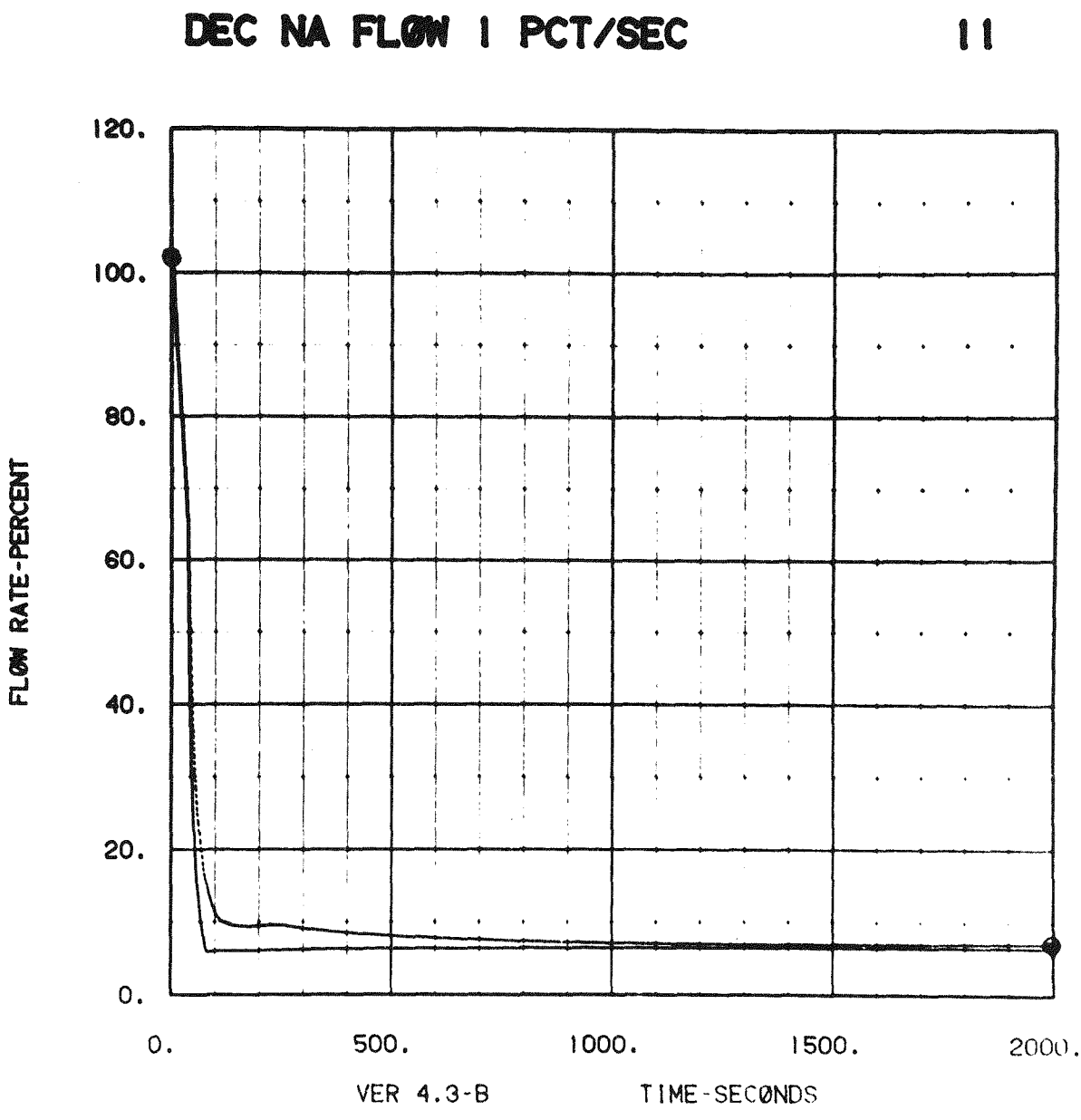

APPENDIX F
RESIDUAL HEAT REMOVAL SYSTEM DESIGN STUDY

F.1 INTRODUCTION

A design study was performed to develop a conceptual design of both an active and a passive Residual Heat Removal System (RHRS). The reference concept for the active RHRS (RHR-A) is the concept previously developed for the PLBR. The reference concept for the passive RHRS (RHR-P) was chosen as the result of a concept selection study described in Appendix K. Both systems are described in Volume 2, Section 3.2.3 of this report.

This appendix describes the work performed during the RHRS design study, which included the preliminary definition of the system heat removal capacity, the establishment of the system configuration, and the sizing of components, for both the active and the passive systems. Also included are the selection of the secondary coolant and the steady state thermal and hydraulic design analysis for the passive system.

Although the analyses done to define the required system heat removal capacity involve the calculation of bulk reactor sodium and structural temperatures as a function of time, detailed RHRS temperature and flow transient calculation were beyond the scope of this study. Also, no detailed analyses of the natural circulation conditions in the reactor during RHR-P operation were performed. These analyses are of critical importance in the design of the RHRS and should be performed as soon as the necessary analytical models are developed.

F.2 SECONDARY COOLANT SELECTION

Either sodium or NaK could be used satisfactorily as the secondary coolant for the passive Residual Heat Removal System. Table F-1 lists the

TABLE F-1

COMPARISON OF SODIUM AND Nak (78)

Property		Na		NaK (78% K eutectic)
o Melting Point		207.5°F	*	10°F
o Density (ρ) at 800°F	*	53.2 lb/ft^3		49.5 lb/ft^3
o Viscosity, μ at 800°F		1.83 x 10^4 lb/ft-sec	*	1.47 x 10^{-4} lb/ft-sec
o Conductivity, K at 800°F	*	121 x 10^{-4} $\frac{Btu}{ft\text{-}sec\text{-}^oF}$		11.9 x 10^{-4} $\frac{Btu}{ft\text{-}sec\text{-}^oF}$
o Boiling Pt	*	1616°F		1446°F
o C_p at 800°F	*	0.304 Btu/lb-°F		0.210 Btu/lb-°F
o Volumetric heat capacity ($\rho p x C_p$)	*	16.2 $\frac{BTU}{Ft^3\text{-}^oF}$		10.4 $\frac{BTU}{Ft^3\text{-}^oF}$
o Volumetric coefficient of thermal expansion ($\rho/\Delta T$)		0.0083 $\frac{lb}{ft^3\text{-}^oF}$		0.0083 $\frac{lb}{ft^3\text{-}^oF}$
o Cost		*$12.10 for 200 lbs		$13.00 for 200 lbs

*Most desirable property value

significant thermal and physical properties of sodium and the NaK (78) eutectic alloy. A comparison of these properties was made to determine which fluid would be best suited for this particular application.

Although the sodium and NaK alloys are similar, the heat transport characteristics of sodium are more attractive for a secondary coolant. As shown in Table F-1, sodium has a higher specific heat, a higher volumetric heat capacity, a higher thermal conductivity, and a higher boiling point. Because the volumetric heat capacity relates directly to the pumping power which must be expended to transport a unit of heat around the RHR-P loop, this parameter is very important in a natural circulation system in which pumping power is provided by density changes only. Sodium is about 60% better than NaKin this regard. The volumetric coefficient of thermal expansion is also an important parameter for natural circulation, but sodium and NaK are equal in this characteristic.

Both Na and NaK present a fire hazard since they readily react with water and oxygen. Perhaps the most important chemical difference between Na and NaK is their oxidation products. Sodium has two oxide forms Na_2O and Na_2O_2. The higher oxide is not found in the presence of excessive sodium and, although highly corrosive, no reaction hazard exists. With the potassium in NaK, three oxides are know; K_2O, K_2O_2, and K_2O_4. Special precautions are required with these oxides. They can exist in the presence of one another and the higher oxides or super oxides may react violently with lower oxides causing explosions. Accidents have been reported when potassium tetroxide has reacted violently with potassium. Sodium and potassium both react vigorously with carbon dioxide to form carbon monoxide and free carbon. In addition, the potassium will continue to react with carbon monoxide to form the highly explosive and unstable compound potassium carbonyl. Sodium will not form comparable explosive mixtures.

Each RHR-A loop contains approximately 470 ft^3 of coolant. With NaK 78 as the coolant, one loop would contain about 1800 lbs of K. If all of the NaK in one loop were to leak into the primary reactor sodium, the potassium

impurity concentration would increase by about 1800 ppm. This potassium could not be removed by cold trapping. Although this amount of potassium in the primary sodium would exceed the initial impurity concentration limits of the Sodium Purchase Specification (Reference 13), no unacceptable consequences of this contamination have been identified.

The most significant difference between NaK and sodium is that NaK is liquid above $10^{o}F$ while sodium is melts at $208^{o}F$. In the RHR-P application, the lower freezing point of NaK would not be particularly valuable because: (1) the NDHX must operate at ambient air temperatures below $10^{o}F$, (2) the NaK plugging temperature might be $50^{o}F$ or more above the freezing point and (3) the minimum allowable RHR-P operating temperature would be $50^{o}F$ or more above the plugging temperature (i.e., about $100^{o}F$). Thus, the RHR-P system must be provided with an external heating system whether NaK or sodium is used as coolant. If sodium is used, the heaters would be designed to maintain a minimum temperature of about $350^{o}F$ rather than $100^{o}F$, but, in a heavily insulated high temperature system, this difference is not very significant in terms of heater design.

Based on the above considerations, sodium has been selected as the RHR-P coolant for the LPR reference design. The RHR-P design could however accomodate NaK if a significant advantage should be identified during subsequent studies.

F.3 SYSTEM CAPACITY

Scoping analyses were performed to determine the required thermal capacity of the RHRS. The effect of reactor decay heat on the reactor sodium temperature with various constant heat rejection rates was determined.

F.3.1 DECAY HEAT

Figure F-1 represents the LPR total decay power as a function of the time after shutdown (TAS). The shape of this curve is based on data from Table 50 of Reference 2. A reactor thermal power level of 2900 MWt was

proportioned against this data to produce the curve of Figure F-1. A power level of 2900 MW_t was conservatively assumed to envelope all possible steam cycles. This data base is the best available and uses an approximate three sigma uncertainty factor. No additional factors have been added to Figure F-1.

F.3.2 HOT PLENUM ANALYSES

Figure F-2 shows the upper-bound reactor temperature transient for various constant heat rejection rates beginning at zero time after shutdown. The heat capacities of only the hot pool sodium and adjacent metal structures were considered in the analysis. The heat capacity of the intermediate and cold pool and any heat transfer occurring between the hot pool and the other pools were ignored. The heat rejection includes all the heat removed from the plenum and does not differentiate between heat removed by the RHR or heat lost thru the vessel wall or deck. The analysis conservatively ignores the heat removed by the IHTS and steam generator system during the pump coastdown period.

The analysis used an equation of the form $P = Ct^n$ to represent the core decay heat (P) of Figure F-1. The "t" represents time after shutdown while the C and n are unique constants for the particular decay curve shown.

The constant heat rejection rate (H) is subtracted from the decay heat equation and the difference integrated with respect to time. The result is the energy stored in the outlet plenum. The temperature rise of the outlet plenum with respect to time is a function of this stored energy and the heat capacities of the hot sodium pool.

The results are presented parametrically on Figure F-2. If a $950^{o}F$ outlet plenum temperature is assumed at the beginning of the transient, it is concluded from Figure F-2 that 25 MW heat removal is more than adequate to maintain the maximum plenum temperature below acceptable limits. As discussed below, other considerations affect this conclusion.

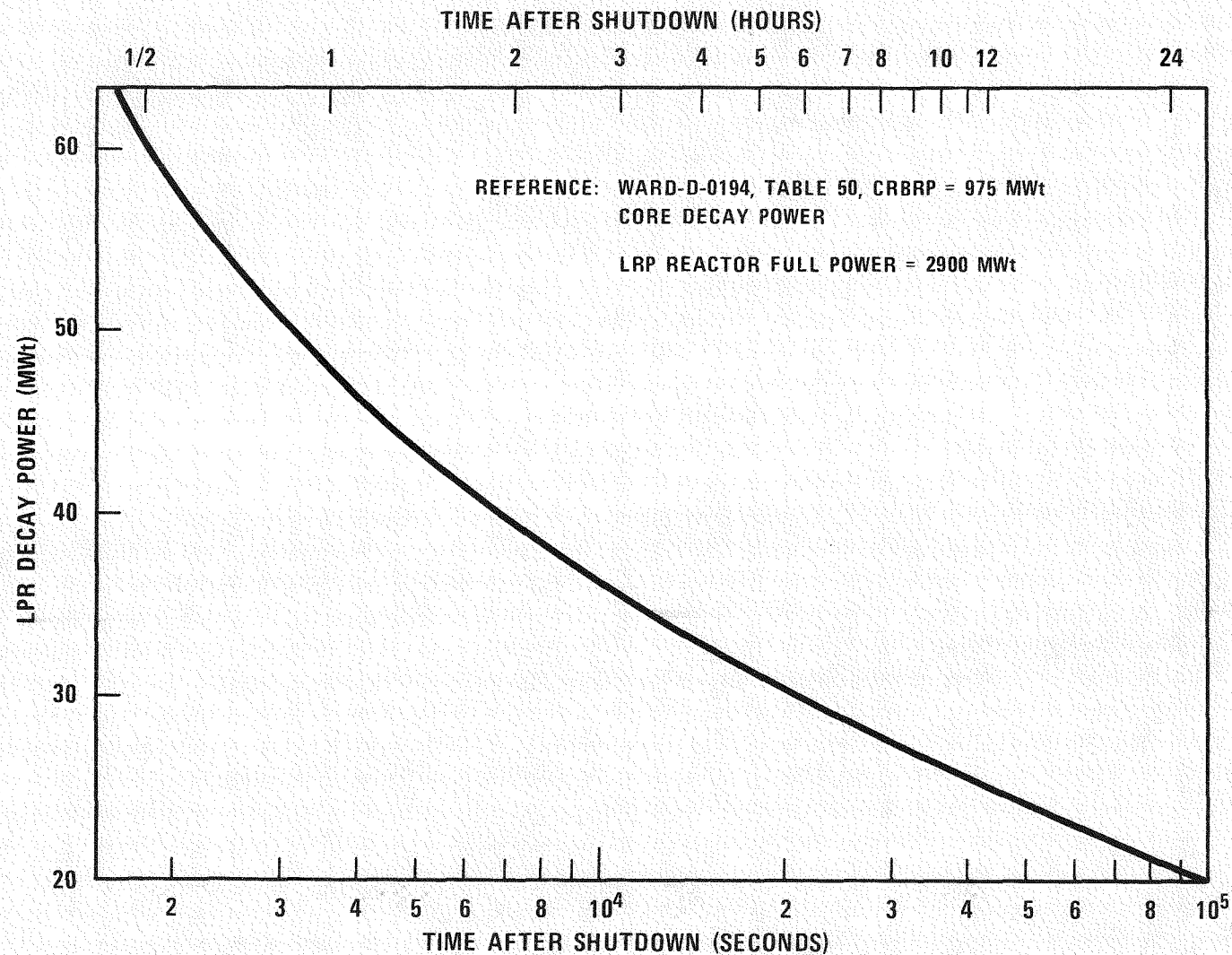

Figure F-1. Time After Shutdown Versus Total LPR Decay Power

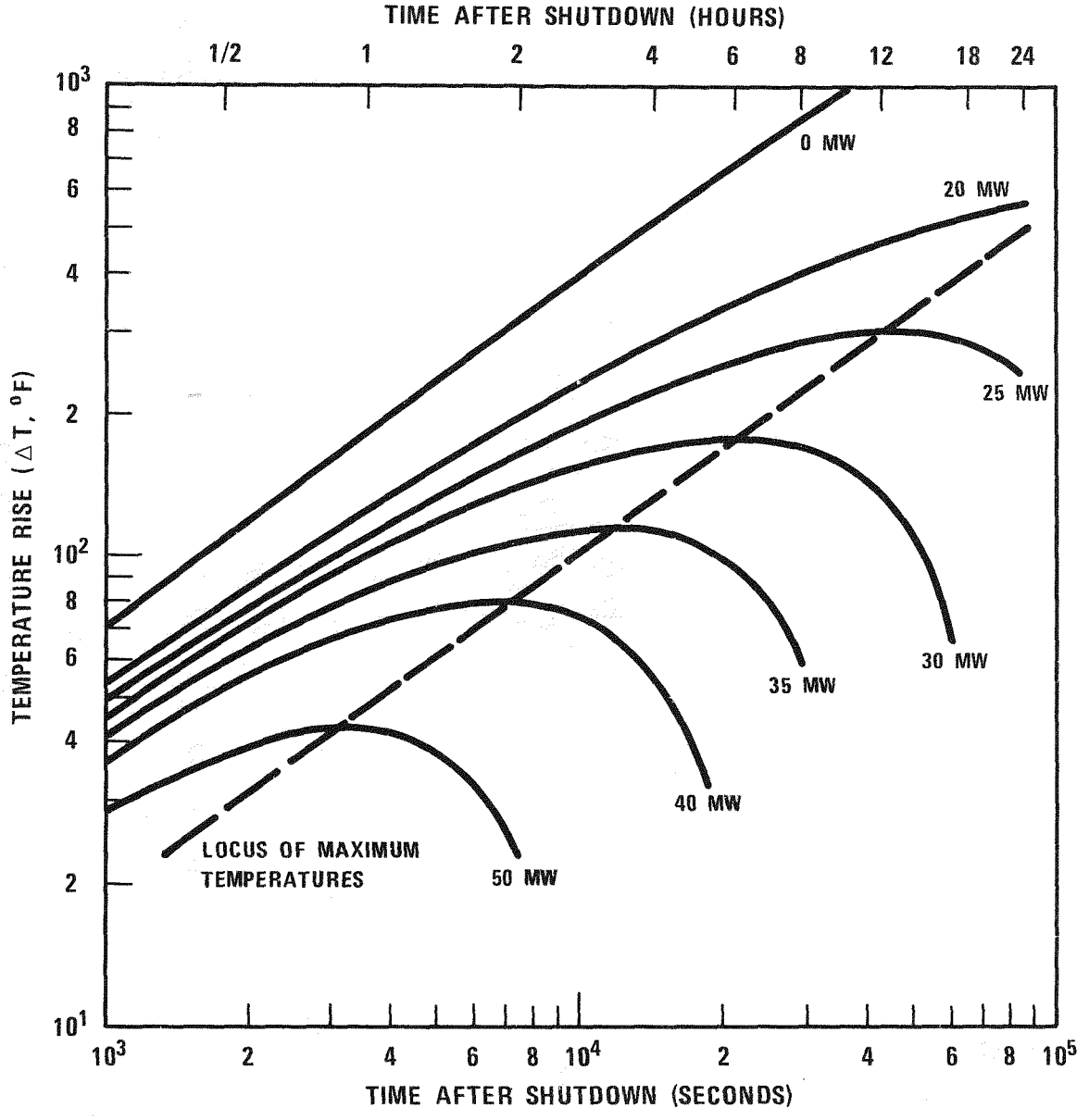

Figure F-2. Outlet Plenum Temperature Rise Versus Time After Shutdown

0665-30

F.3.3 ALL PLENUM ANALYSIS

The above analysis conservatively assumed no heat transfer or mixing between the hot plenum and the cold or intermediate plenums. The transients shown on Figure F-3 represent the other extreme and may be considered the lower bound analysis. Perfect heat transfer and/or mixing among all plenums was assumed. The analysis performed utilized the heat capacities of all of the sodium and most of the metal contained within the reactor vessel, including the vessel itself. Besides the structural and sodium heat capacity differences, an initial reactor power of 2550 MWt (corresponding to a superheated steam system) was used in this analysis instead of the 2900 MWt assumed previously.

The above changes were incorporated into the same equations used in the previous section. The temperature rise of the reactor sodium amd structure with respect to time was then determined from the stored energy and heat capacities of the system. The resulting temperature rises are represented on Figure F-3 with respect to time for various RHR heat removal rates. It is concluded that 20 MW heat removal rate is sufficient to meet the objectives using the assumptions of the all-plenum analysis.

F.3.4 DISCUSSION

Selection of the proper RHRS capacity must consider the sodium temperature rise in the inlet and outlet plenums. The normal steady state operating conditions for the LPR maintains the hot plenum at $950^{o}F$ and the cold plenum at $670^{o}F$. Any increase in temperature from the normal conditions must consider the vessel and internal structures as well as fuel cladding integrity.

Structures that are contained within the hot plenum (UIS, etc.) are able to tolerate, for short periods, temperatures in the $1200^{o}F$ to $1300^{o}F$ range without seriously affecting component life. This judgement is based upon analysis performed on similiar components in FFTF and CRBRP. A comparison of the limits of ASME Boiler and Pressure Vessel Elevated Temperature Code

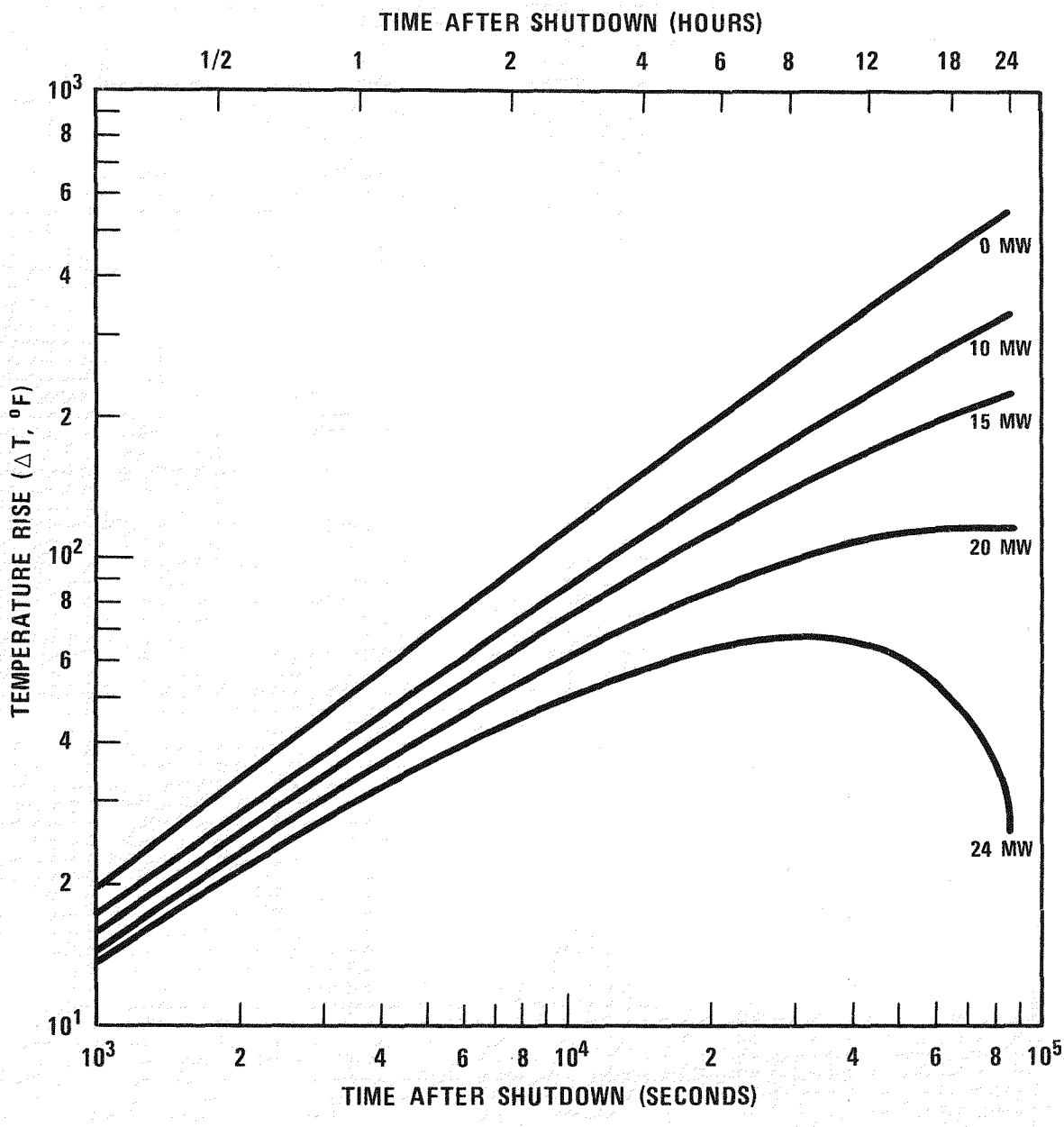

Figure F-3. LPR Sodium Temperature Rise Versus Time After Shutdown Assuming Heat Capacity of all Sodium and Metal Within Vessel is Effective.

0665-29

Case N-47 (1592-10) with the projected steady state stresses in the LPR components indicates the LPR hot pool structures can also withstand a temperature excursion of about 300^{o}F.

The high temperature rules of code case N-47 are applicable to the vessel. The core support structure which exists in the cold pool presents a different problem. High temperature rules do not exist for its analysis. it is necessary to either issue a high temperature code for temperatures above 800^{o}F or use the rules of Code Case N-47 in the interim.

Assuming that the code can be satisfied, the structural considerations remain as the problem. Time and initial stress are both considerations in addition to the temperature. Since the load on the core support, etc. are primary loads (dead weight, pressure, etc.), accumulation of creep-strain, deformation, and creep damage could be a problem. These failure modes require further analysis on a well defined design of the structure. Definition of the temperature transient is also required. In the absence of specific high temperature rules for internals, the analysis of code case N-47 is used here.

The high temperature code case N-47 reveals the importance of a low initial stress level when entering the loss of all power transient. The allowable stress intensity values (S_{mt} of code case N-47) indicates a maximum primary membrane stress of 12,200 psi is permitted at 950^{o}F. Using a steady state stress of 7000 psi (Reference Appendix A) shows sufficient margin to allow the temperature to rise in excess of 1250^{o}F assuming a time constant of 300 hours. The isochronous curves of Case N-47 for SS-304 shows that above 1150^{o}F the yield points start decreasing rapidly. A review of the isochronous stress-strain curves for SS304 to determine if the structures approach a conservatively assumed 0.1% creep strain limit (in membrane) shows a 7000 psi stress is acceptable at and below 1250^{o}F. The stress level decreases rapidly for higher tempratures. The key to having the structures take elevated temperature is to have initial primary stress levels low to prevent excessive creep strain and creep damage from occuring.

It is concluded from the above that temperatures on the cold structures in the range of 1250^{o}F would probably satisfy the reactor emergency condition limits, but it is premature to state this as a firm temperature limit. This conclusion needs to be based upon many factors not defined at this time, in particular, the primary stress of in-vessel structures needs to be known with a high confidence level. A detailed analysis must be performed that considers the permanent deformation of the structure. The entire transient effects including pump coastdown, etc. needs to be considered in detail.

A review of preliminary work on elevated temperature design rules being performed by Westinghouse on the evaluation of SS304 and SS316 confirms the above conclusions. It appears that SS304 could conservatively accept a temperature increase to 1020^{o}F for a short duration of time without doing an inelastic analysis for the type of transient predicted when the RHRS is required.

Thus, a temperature excursion of approximately 300^{o}F would be acceptable to the structures in both the hot and cold plenums of the LPR. This would allow the hot (outlet) plenum to rise to 1250^{o}F and the cold (inlet) plenum to reach about 1000^{o}F.

Another constraint on the plenum temperature rise must be considered, however, before the RHR system capacity is finally selected. The EPRI guidelines require the fuel cladding temperature not exceed 1400^{o}F. It was beyond the work scope of this RHRS task to perform the detailed core analysis necessary to determine fuel cladding temperature.

A transient analysis of an early PLBR core was performed previously (Reference 5). The three loop natural circulation event (E-14) studies, which results from loss of electric power, is analogous to the LPR situation which requires RHRS use. The study showed that after natural circulation is fully established, the cladding temperature approaches its steady state value within three minutes after shutdown. This temperature slowly decreases as the decay heat decreases with time. After shutdown, the maximum fuel cladding temperature and maximum coolant temperature at any

axial location is shown to be approximately equal due to the relatively low heat flux of the decay heat. A constant coolant inlet temperature of 650°F was assumed during the entire analysis. From this it may be concluded that any increase in the inlet temperature above its steady state design value results in a comparable increase in cladding temperature above its steady state value, after natural circulation through the core becomes fully established.

The core design study (Reference 4) performed by Westinghouse for the Prototype Large Breeder Reactor (PLBR) shows the maximum fuel assembly cladding temperatures during normal operation to be 1322°F (beginning-of-life) and 1236°F (end-of-life). The mean of these two temperatures is 1279°F. The same study shows the maximum mixed mean hot channel fuel outlet temperature to be 1170°F. This produces a hot (outlet) plenum average temperature of 950°F. It is assumed then that these same conditions will exist on the LPR core.

By changing the orificing scheme, using different flow coastdown values, revising control rod worths, taking into account LPR heat capacity effects, etc. different results can be obtained for the LPR. The above core analyses can only serve as a guide since different design criteria was used in its development. These analyses, however, are very useful since they do permit the following observations:

- Fuel cladding temperatures are strongly dependent upon inlet coolant temperatures under conditions which require the RHRS.
- Power-to-flow ratios for natural circulation thru the core appear favorable to allow cladding temperatures to operate near their normal operating temperatures assuming inlet coolant temperature is also near normal. The cladding temperature slowly decreases with time after the natural circulation is established.
- During normal steady state operation of the LPR, less temperature margin exists in the fuel cladding then in the reactor structures. Consequently, RHRS capacity is determined by fuel cladding temperatures and not plenum structural limitations. The cladding temperature limit (1400°F) is closer to the normal cladding hot channel operating temperatures (mean temperature of 1279°F) therefore allowing only a small margin (120°F) for increase of inlet (cold plenum) temperature.

- o A 1400°F cladding temperature limit is very conservative. A more practical limit would be based upon the cumulative damage to the cladding allowable failure rates, and detailed transient analysis. The relative ease of refueling should permit some cladding failure under the most improbable conditions which require RHRs use.

- o Considerable thermal and hydraulic analysis needs to be performed to fully evaluate the loss of all power events. The natural circulation phenomena through the fuel assemblies as well as the reactor vessel's internal flow paths requires both steady state and transient analysis. These analysis are needed before the RHRS size can be finalized.

It was also noted in the transient study (Reference 5) that a maximum cladding temperature of 1566°F is reached within just 108 seconds after initiation of the event. This peak temperature is due to the imbalance of the power-to-flow ratio during pump coastdown, high decay heat immediately after shutdown, and insufficient time for natural circulation to become effective. After the natural circulation flow becomes established, the cladding temperature decreases to the quasi-steady state value within three minutes after initiation of the event. This anomaly is noted since it shows 1) detailed core anlysis is required to determine cladding protection, 2) the worst temperature excursion occurs within first two minutes after shutdown before natural circulation becomes established, 3) the first several minutes after shutdown is relatively independent of the RHRS but strongly dependent upon plant hydralic parameters such as natural circulation, pump coastdown, IHX to core thermal centers, etc.

Since it was beyond the present scope of work to perform the required core analyses it was necessary to make assumptions regarding the acceptable plenum temperature increases. These assumptions were conservatively based on the knowledge gained from the analyses discussed above. Further validity of the conservatism of the conclusions reached is gained by considering the following points:

- o Loss of all emergency power is very unlikely.

- o The RHR-A and the RHR-P will probably both be at least partially operative at the same time thereby, providing about twice the required heat removal capacity. No credit is given to this in the analysis.

- It is extremely unlikely that it will be necessary to operate only one of the RHRS with loss of all power and with loss of one loop (N-1 condition). The (N-1) condition is assumed in the analysis.

- Maximum decay heat generation is assumed immediately after shutdown and at the worst time in life.

- The RHRS conceptual design is not very sensitive to the system size requirements. That is, with the size range considered (15 to 35 MW) the type of system chosen will not be impacted. Also, the physical dimensions, cost, etc., will vary by less than 30%.

Based upon all of the factors discussed above a RHRS size was selected for conceptual design purposes. The temperature rise of the inlet plenum was limited to $120^{o}F$ to meet the guideline of assuring fuel cladding below $1400^{o}F$. This is based upon the assumption that the steady state hot channel cladding temperature is $1279^{o}F$ during normal reactor operation and that an increase in inlet temperature will result in a direct increase in the cladding temperature.

F.3.4 CONCLUSIONS

The hot plenum analysis is too conservative since it does not take into account mixing and heat capacities of the other plenums. On the other hand, using the heat capacities of all the sodium and metal contained within the vessel may be optimistic. Detailed knowledge is required of plenum hydraulics, natural circulation, pump coastdown, IHX thermal inertia, structural temperature limits, etc. before the assumptions used in this analysis can be authenticated completely. These analyses serve only to scope the size of the RHR system. Figure F-3 represents the bound for the minimum (or lower) RHR size possible. The similar curve of Figure F-2 may be considered the conservative (or upper) boundary to be used for RHR sizing. Detailed thermal and hydraulic analysis of the reactor plenum is required to further refine these analyses.

Since the required analyses were not possible during this conceptual phase of work, certain assumptions are necessary. In order to determine the size of the RHR it is assumed:

- o Good heat transfer and/or mixing occurs between all plenums. Therefore, Figure F-3 is used to determine temperature increase with time of both the inlet and outlet plenums.

- o The temperature rise of the inlet plenum is limited to 120°F in order to assure fuel cladding below 1400°F.

- o Six separate but identical loops are used for each RHR. Only five of these loops are used to size the systems to account for the (N-1) condition requirements.

Based upon the above assumptions and the previous requirements, Figure F-3 shows that a 20 MWt system will meet all design objectives. Hence, the conceptual design of each RHRS will be based upon each of the six loops having the capability of removing 4 MWt of residual heat from the LPR hot (outlet) plenum.

F.4 COMPONENT SIZING

F.4.1 EQUIPMENT AND LOCATION

The RHRS is composed of two separate systems, an active system and a passive system. Each system is composed of six separate heat removal loops. A schematic of the active system is shown in Figure F-4. It utilizes an EM pump to draw sodium from the IHTS hot leg pipe, pass it thru an air blast heat exchanger and return it to the cold leg of the IHTS where it again passes thru the IHX to remove additional heat from the hot outlet plenum of the LPR.

Electrical power is required to operate the EM pump and the blowers on the air blast heat exchanger (ABHX). The trace and auxiliary heaters on either system need only to operate during standby conditions to prevent sodium freezing. Many thermocouples are used to assure proper operation.

A schematic for the passive system is shown in Figure F-5. It is designed to operate by natural circulation only, without any electric power. The coils in each IHX transmit the secondary fluid by natural convection to natural draft heat exchangers (NDHX). No power is required to operate the

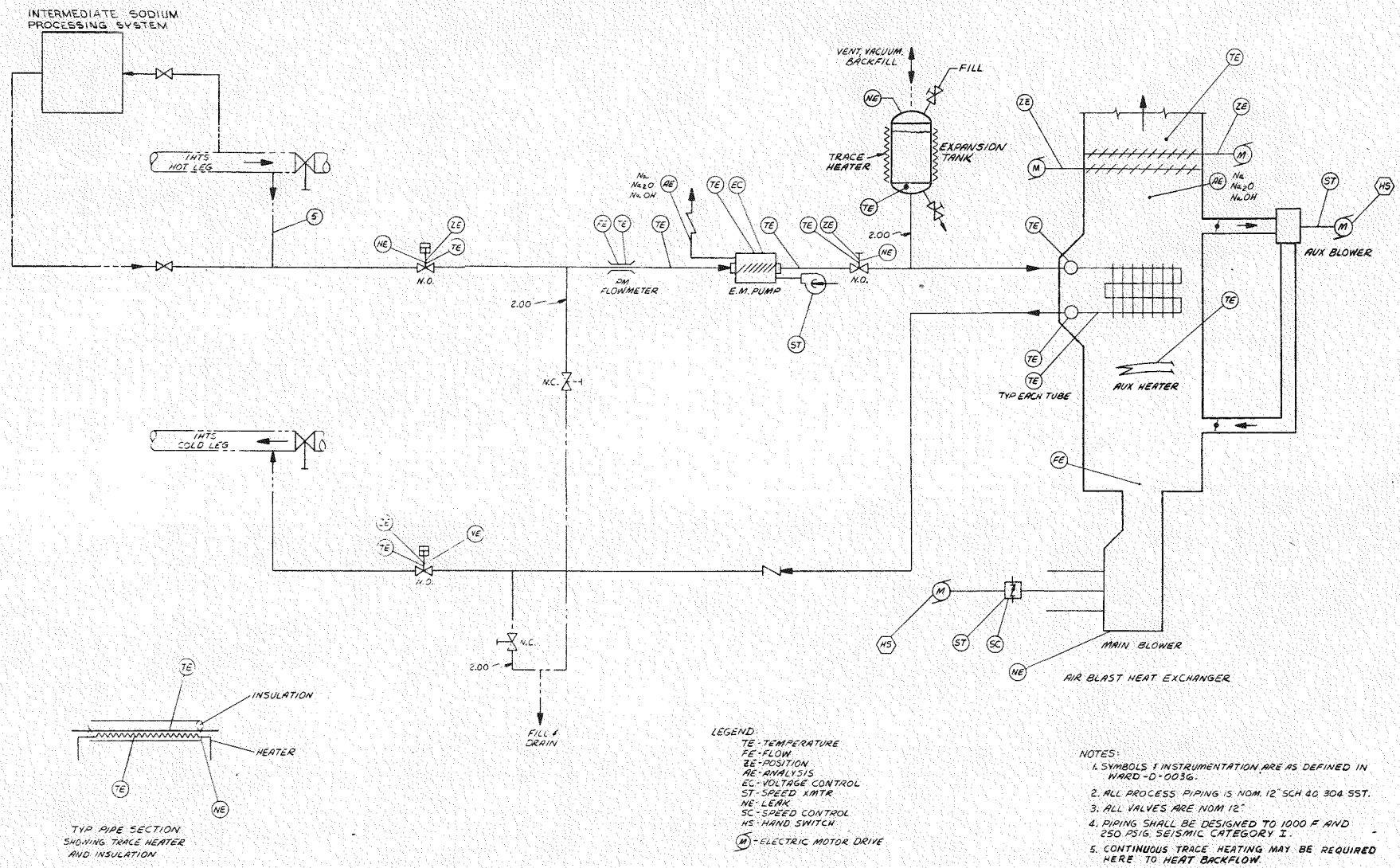

F-16

Figure F-4. RHR-A Schematic

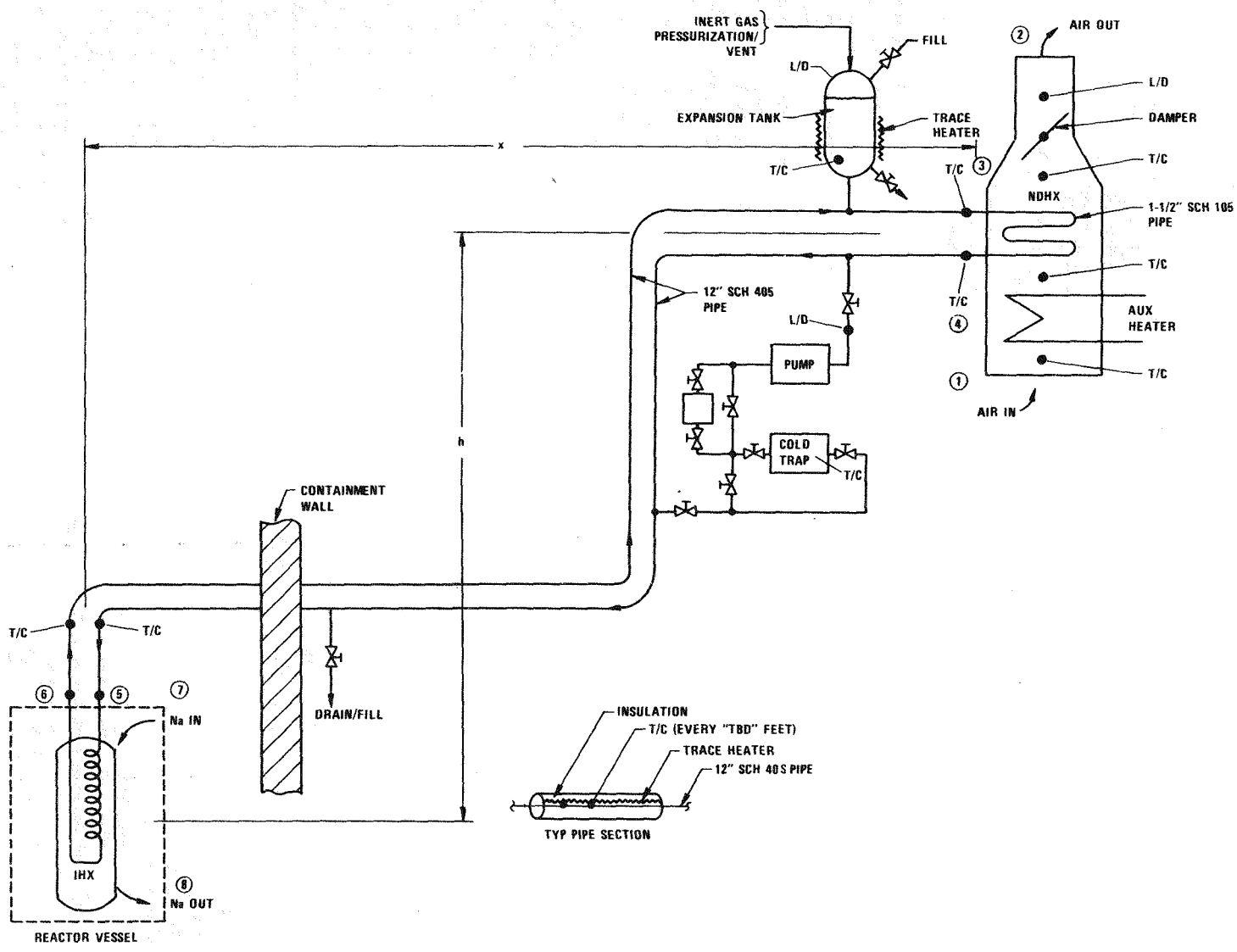

Figure F-5. RHR-P Schematic

system and no moving parts exist to hamper the startup and operation. The only moving part may be the manual damper in the stack of the NDHX used only to reduce heat loss in the standby condition. The pump, cold trap and heaters shown are used only during normal reactor operation. They are not required for use during the conditions under which RHR operation is required.

The RHRS must be protected from tornados, missiles and earthquakes. Within this constraint the RHR-A may be located anywhere a supply of air for the ABHX is available. It is advantageous however, to locate it such that natural circulation is an aid to the secondary sodium and air flow.

The RHR-P must be located with the thermal center of the NDHX far enough above the thermal center of the coils within the IHX to produce sufficient secondary flow by natural circulation. It is also necessary to position the NDHX so that sufficient stack height can be provided to induce adequate natural draft air flow.

It is the responsibility of the architect/engineer to locate the RHRS equipment. As shown in Figure F-6 and F-7, the RHRS air-cooled heat exchangers are located adjacent to the containment structure and grouped to provide three independent and physically separated safety trains. Each train consists of two active and two passive units. The passive units are located on the roof two levels above, and the active units one level above, the area where the sodium piping penetrates the containment. The concrete confinement wall has been located to provide a confinement annulus which is a continuation of the outside wall for the two electrical tunnels. The secondary sodium isolation valves, the active RHR heat exchangers, and the vertical run of piping to the RHRS units are located inside the confinement structure.

F.4.2 THERMAL AND HYDRAULIC ANALYSIS

The RHR-A system is an adaption of the PLBR Residual Heat Removal System reported in Reference 6. A complete analysis for similar design parameters

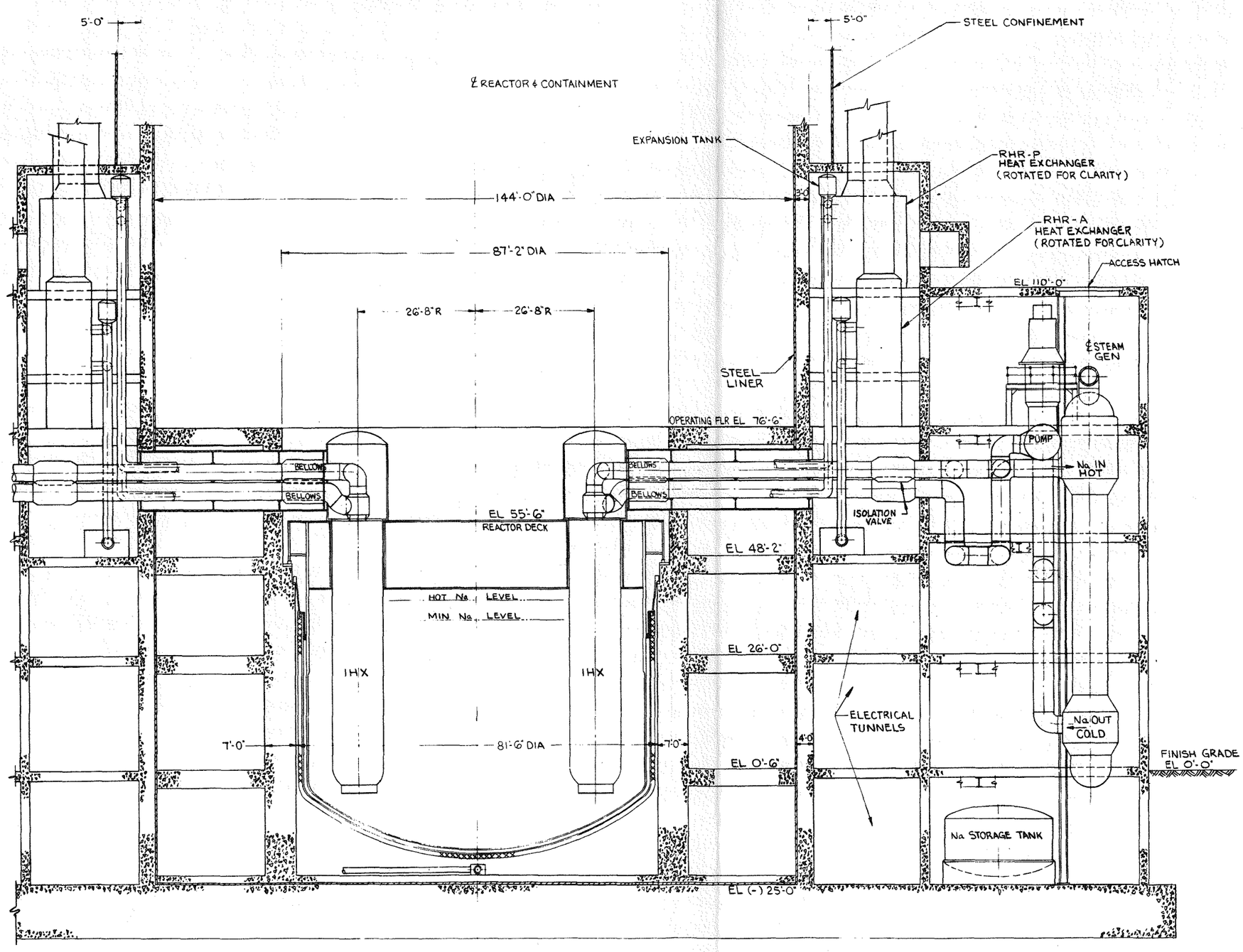

Figure F-6. RHRS Recommended Location with Plant

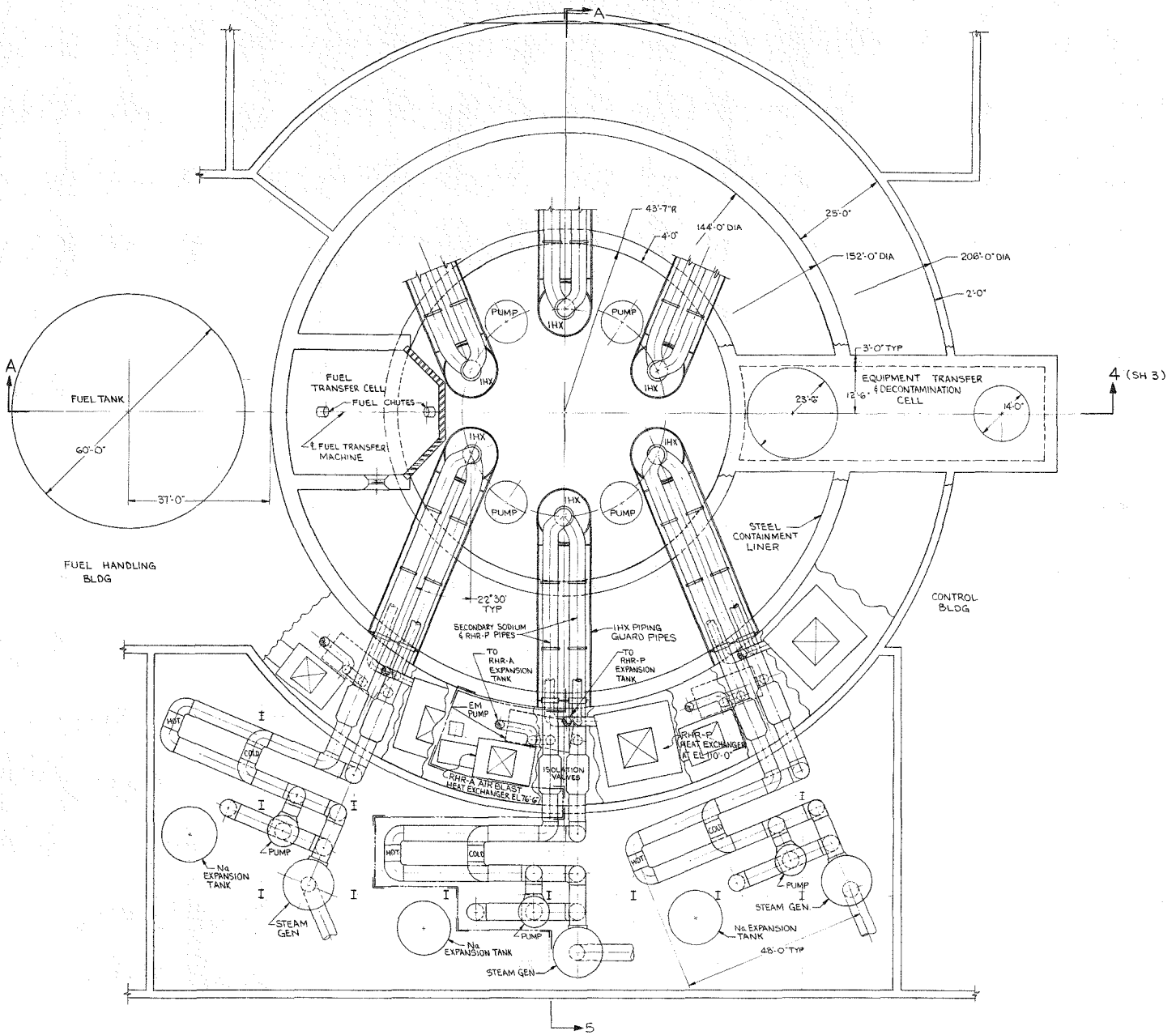

Figure F-7. RHRS Recommended Location Within Plant (Plan View)

appears in the reference and will not be repeated here. Scoping analyses have been performed on the RHR-P system and the results are presented in the following paragraphs.

F.4.2.1 COILS WITHIN IHX

The RHR-P cooling coils are located within the IHX. Because of the potential impact on the IHX design, it was necessary to arrive at a coil sizing early during the study. To ensure that the cooling coil envelope would be adequately large, and that no subsequent refinements of the RHR-P would affect the basic IHX design, conservative design parameters were assumed and used to size the coils. Design parameters assumed were as follows:

- Total decay heat of 50 MWt
- Coil power rating of 12.5 MWt (Assumed 2/3 of units will handle 100% of the load)
- Primary temperature conditions are assumed to be those at T_o(935°F inlet and 665°F outlet).
- Primary side thermal center height differential of 20 feet
- Secondary side thermal center height differential of 60 feet
- Balance of System equivalent length of pipe of 400 feet.

Subsequent to the design of the coils, design evolution of the related systems and components resulted in changes to most of these assumed parameters. The resultant changes result in relaxation of design parameters. The coil design envelope arrived at therefore is very conservative, and revision of the design to reflect finalized parameters will result in a smaller size unit, which will be similar in concept.

To size the coils initially, the available driving head for the primary temperature conditions and the available driving heads for a range of secondary coolant conditions were determined based on the assumed thermal center differential heights noted above. A series of iterative calculations

were then made to determine the reference coil design. Variables assessed with the calculations include tube size, coil arrangement geometry, secondary fluid temperatures and LMTD across the exchanger. For each specific set of conditions, required heat transfer area was estimated. A coil pressure drop has determined and compared to the available driving head. Coil tube sizes examined include 12 inch, 6 inch, 4 inch, and 3 inch. LMTDs covered by the calculations are $75^{o}F$, $100^{o}F$, and $125^{o}F$. The specific purpose of the assessment was to arrive at a natural circulation cooling heat exchanger envelope which would fit within the IHX upper plenum diameter while taking up the minimum height possible.

For the thermal analysis portion of this assessment the following correlations are employed:

The tube Side (Secondary) Heat Tranfer Coefficient is:

$$Nu = 5 + 0.025\ (Pe)^{0.8} \times f$$

based on the Subbotin correlation for liquid metal flowing inside a circular helical coil modified for flow curvature effect (Reference 11)

where:

Nu = Nusselt number = hi Di/k
hi = heat transfer coefficient based on tube inside diameter
Di = tube inside diameter
K = thermal conductivity of coolant
Pe = Peclet number
f = $(Re(Di/2R)^{2})^{0.05}$
where f is ratio of curved pipe friction factor to straight pipe friction factor, (Reference 14)
Re = Reynold Number
R = radius of curvature of helical coil

The Shell Side (Primary) Heat Transfer Coefficient is:

$$Nu = 4.03 + 0.228\ Fa_{eff}\ Fi\ Fn\ (Pe)^{0.67}$$

based on the Gilli, liquid metal flowing over helical coils (Reference 15)

where:

Nu = Nusselt Number
Pe = Peclet Number
Fa_{eff} = correction factor based on transverse pitch ratio
Fi = correction factor for tube inclination
Fn = correction factor for the number of tubes in the longitudinal direction

For the hydraulic analysis portion of this assessment the following correlations are employed:

Tube Side (Secondary) Pressure Loss (Ito correlation, Reference 14)

$$\Delta P = f_c\ LG^2/Di\rho$$

where:

L = length of helical coil
G = mass velocity
Di = tube inside diameter
ρ = density of coolant
fc = coil friction factor

$$fc = \frac{0.316\ Re(Di/\overline{D}_{He})^{2\ 0.05}}{Re^{0.25}\ F_{s2}}\ F_{s1}$$

where:

Re = Reynolds number

$\bar{D}_{He}$ = helical coil diameter

F_{s1} = Moody friction factor at actual roughness/tube ID ratio and Reynolds number

F_{s2} = Moody friction factor at roughness/tube ID ratio of 0.000001 (smooth surface) and Reynolds number

The Shell Side (Primary) Pressure Loss is:

$$\Delta P = \frac{C_i C_n f_{eff} G^2}{2\rho 85}$$

where:

C_i = correction factor for tube inclination

C_n = correction factor for number of in-line tube rows

f_{eff} = Grimison friction factor (Reference 16)

G = mass velocity

$\rho 85$ = equivalent density of fluid at temperature T85

T85 = $0.85\ T_{bulk} + 0.15\ T_{wall}$

From the results of the assessment the following coil characteristics are felt to best meet the requirements placed on it and thus are selected as the reference design:

Unit thermal capacity, MWt	12.5
Primary inlet temperature, ^{o}F	935
Primary outlet temperature, ^{o}F	665
Secondary inlet temperature, ^{o}F	510
Secondary outlet temperature, ^{o}F	835

LMTD, ^{o}F	125
Primary flowrate, lb/hr	5.19 (10^5)
Secondary flowrate, lb/hr	6.23 (10^5)
Tube diameter, in.	4.0
Tube wall, in.	0.095
Number of coils, radial/axial	6/2
Degree of turning	1299
Heat transfer area, ft^2	855
Coil height, ft	~4.5 ft

F.4.2.2 CONVECTIVE DRIVING FORCE

Sodium Side of NDHX

The RHR-P must be sized to deliver the minimum flow necessary to transfer the decay heat using only natural convection. Based upon previous discussions the following assumptions were made relative to Figure F-5:

- Eight 90° elbows exist within the IHX and NDHX
- Three 180° elbows exist with NDHX
- Total length, L, within NDHX = 88 ft. (i.e., 22 ft. per each of 4 passes)
- Total length, L, between IHX and NDHX is 400 feet
- Thirty parallel heat transfer finned tubes exist within the NDHX feeding off a common header.

The following equation can now be written for the sodium side of the NDHX.

$$\Delta P_1 = \Delta P_2 + \Delta P_3 + \Delta P_4 + \Delta P_5 + \Delta P_6 = \Delta P_{Loss}$$

where

ΔP_1 = Natural Convection Driving Force, = $h(\rho_5 - \rho_3)$
h = Distance between thermal centers
ρ = Density of fluid at specific location
ΔP_2 = Loss in IHX Coils
ΔP_3 = Loss in Straight Pipe Between IHX & NDHX
ΔP_4 = Loss in elbows Between IHX & NDHX
ΔP_5 = Loss in Straight Pipe of NDHX
ΔP_6 = Loss in elbows of NDHX

Assuming the transfer of $4MW_t$ and an inlet to outlet temperature of (835-510) = 325^oF then the minimum flow must be

$$W = \frac{q}{Cp\Delta t} = 1.359 \times 10^5 \text{ lb/hr} = 37.75 \text{ lb/sec}$$

The minimum Reynolds number calculation show that the flow is turbulent since it is in the transition region.

o ΔP_2 Calculation

The pressure loss through the IHX coils is calculated in Paragraph above as 0.3 psi. This calculation was conservatively made to transfer 12.5 MW_t per loop at a NaK flow rate of 6.23×10^5 lb/hr. The value obtained may be converted to the values used in this paragraph by ratioing the relationship

$q = W\ Cp\ \Delta T$

By letting subscript 1 refer to values calculated above for a 12.5 Mw loop and subscript 2 refer to values determined for a 4 Mw loop then the following may be calculated when $\Delta T_1 \equiv \Delta T_2$

$$\frac{W_2}{W_1} = \frac{q_2}{q_1}\frac{C_{p1}}{C_{P2}} = \left(\frac{4}{12.5}\right)\left(\frac{.212}{.309}\right) = .219$$

or $W_2 = .219\ W_1$

Now, since ΔP is proportional to W^2, then

$\Delta P_2 = P_1\ (.219) = P_1\ (.0482)$

If $\Delta P_1 = .3$ psi, then $P_2\Delta = .0145$ psi, hence the pressure loss thru the IHX coils assuming the conditions of this paragraph is $\Delta P_2 = .0145$ psi.

o Pressure Drop Calculation

The remainder of the pressure losses in the RHR-P sodium piping is determined using Darcy's equation (Reference 7, Eq 3-5) or Darcy's equation in terms of a resistance coefficient.

Thus the total pressure loss is the summation of:

$$\Delta P_{Loss} = \Delta P_2 + \Delta P_3 + \Delta P_4 + \Delta P_5 + \Delta P_6 = \Delta P_1$$

For a 12-inch schedule 40S pipe the values are:

$$\Delta P_{Loss} = (.0145) + (.03) + (.00573) + (.201) + (.0155)\ \text{psi}$$

$$\Delta P_{Loss} = .267\ \text{psi}$$

Now by equating the total pressure loss to the driving force the minimum height necessary to sustain sufficient natural circulation flow can be calculated.

Hence,

$$\Delta P_1 = \Delta P_{Loss}$$

$$h(\rho_5 - \rho_3) = \Delta P_{Loss}$$

This value obtained represents the minimum distance between thermal center of the IHX coils and the NDHX heat transfer tubes if Schedule 40S pipe is assumed.

By repeating the above calculations for various size pipes, assuming all parameters except the diameter remain the same, the following approximate values were determined:

Nominal Pipe Size	Minimum Required Thermal Center Distance
12	14.3 ft
10	16.7
8	24.9
6	64.1
5	140.6
4	402.9
3	1657.1

The current separation of the thermal centers for the RHR-P (See Figure F-6) is in excess of 80 feet. This elevation allows more than sufficient driving head for the required flow. A recommendation of the larger pipe size is advantageous during conceptual design for several reasons. First, the space envelope required is preserved. Second, flexibility in placement of the NDHX, i.e., the thermal centers, is provided. Third, margin is provided to allow for more rigorous analysis to be performed at a later date. Fourth, the cost impact is minimized, more than likely resulting in a cost reduction at a later data when better analysis is available.

Consequently, the nominal pipe size of 12 inch diameter is conservatively recommended for the conceptual design of the RHRS.

Air Side of NDHX

The natural draft heat exchanger (NDHX) must be sized to allow sufficient

air draft to transfer the prescribed amount of heat. That is, the draft created by the chimney must equal the pressure loss through the air side of the NDHX. This may be expressed mathematically as follows:

$$\Delta P_1 = \Delta P_2 + \Delta P_3 + \Delta P_4 + \Delta P_5 + \Delta P_6 + \Delta P_7$$

where:

ΔP_1 = driving draft force chimney = $h_s (P_2 - P_1)$
ΔP_2 = Inlet Loss (Ref. 8, pg. 463)
ΔP_3 = Inlet Turning Loss (negligible)

$$\Delta P_4 = \text{Tube Bundle Loss} = \frac{f G_s^2 L_p}{(5.22 \times 10^{10}) Dev\ S\phi} \left(\frac{Dev}{S_T}\right)^{0.4} \left(\frac{S_c}{S_T}\right)^{0.6}$$ (Ref. 9, Eq. 16.106)

ΔP_5 = Contraction Loss = $.0001078 K \rho v^2$
where $K = .5 (Sin\theta/2)(1-\beta)^2$ (Ref. 7, pg 3-4)

$$\Delta P_6 = \text{Stack Friction Loss} = .0942\ f\ T_g \frac{H}{D} \left(\frac{W}{100,000}\right)^2 \left(.036092 \frac{psi}{in\ M2}\right)$$
(Ref. 10, pg 5-5)

$$\Delta P_7 = \text{Exit Loss} = (.0942\ T_g/D\phi)\left(\frac{W}{100,000}\right)^2 \left(.036092 \frac{psi}{in\ H_2O}\right)$$
(Ref. 10, pg 5-5)

Assuming the transfer of $4MW_t$ to air with an inlet temperature of 100^oF and an air exit temperature of 400^oF then calculations similar to Section F.4.2.2 may be performed in terms of the stack height required. The stack height recommended for conceptual design purposes is a minimum of 40 feet.

F.4.2.3 NDHX HEAT TRANSFER COEFFICIENT

In order to determine the overall heat transfer coefficient in the NDHX it may be assumed that the heat transfer surface consist of tubes four rows deep. From Reference 7, pg. 18-102 a typical face velocity = 650 ft/min for air at 225°F is assumed. Thus, for natural convection,

$$h_c = C \frac{k}{L} \left(\frac{g\beta\Delta t L^3 \rho^2 Cp}{\mu k}\right)^d \qquad \text{(Reference 12, pg. 163, Eq. 8-6)}$$

or

$$h_c = C\, k/L(aL^3\Delta t)^d \qquad \text{(Reference 12, Eq. 8-7)}$$

where,

$h_{c_{Air}}$ = 1.99 ≴ 2.0 Btu/hr-ft^2 °F is the air side convective coefficient

Similarly, the sodium side heat transfer coefficient may be found to be,

$$h_c = .027 \frac{k}{D} \left(\frac{DV\rho}{\mu}\right)^{.8} \left(\frac{Cp\mu}{h}\right)^{1/3} \left(\frac{\mu}{\mu s}\right)^{.14} \qquad \text{(Ref. 12, pg. 138, Eq. 7-11)}$$

where

$h_{c_{Na}}$ = 7223 Btu/hr-ft^2-°F

Combining the above values to find the overall heat transfer coefficient yields.

$$U = \frac{1}{\frac{1}{h_{c_{air}}} + \frac{x}{h} + \frac{1}{h_{c_{Na}}}}$$

$$U = \frac{1}{\frac{1}{2} + \frac{.109}{11.025} + \frac{1}{7223}} \approx 2.0 \text{ Btu/hr-ft}^2\text{-°F}$$

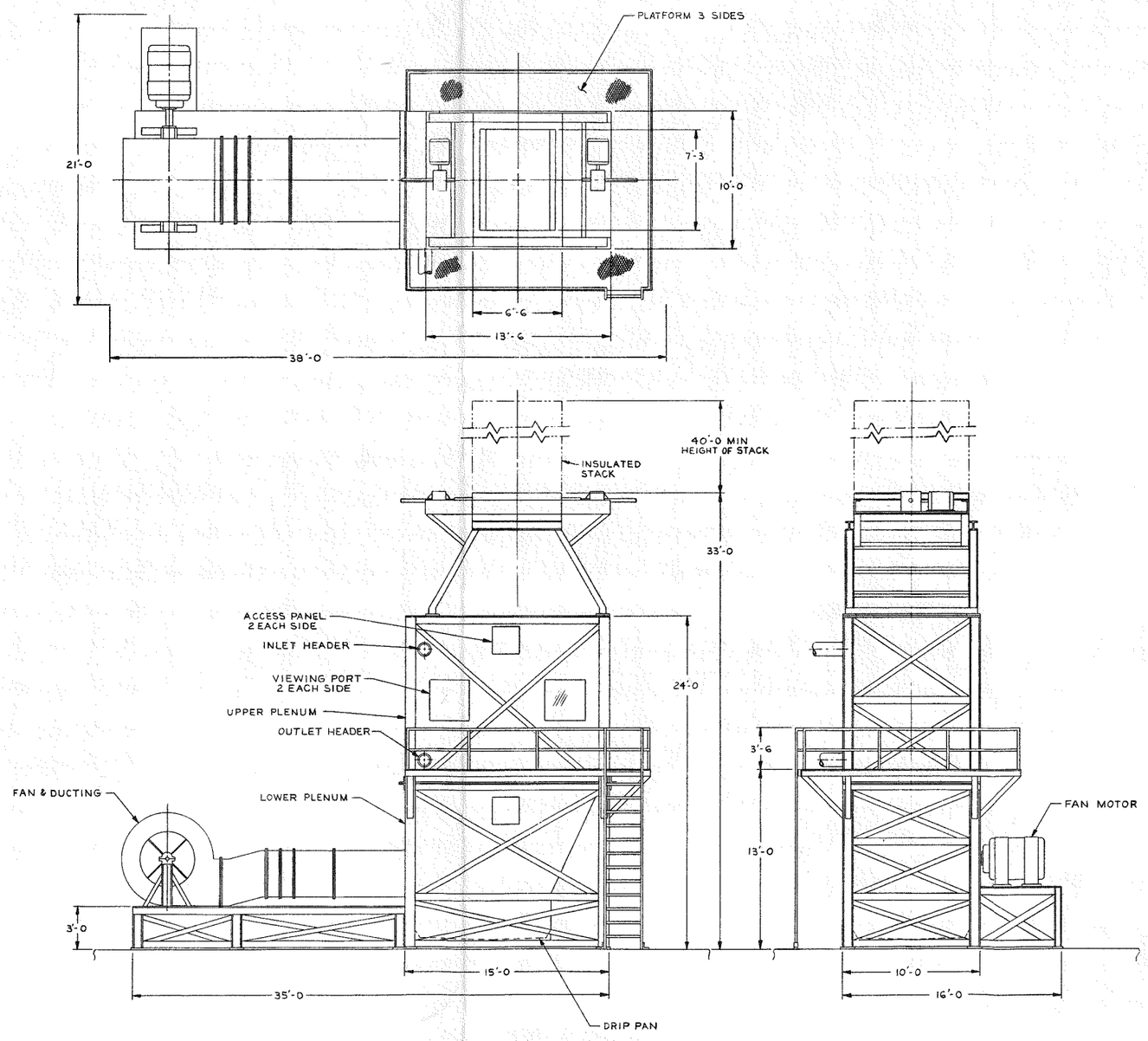

Figure F-8. Large Pool Reactor Residual Heat Removal System Air Blast Heat Exchanger.

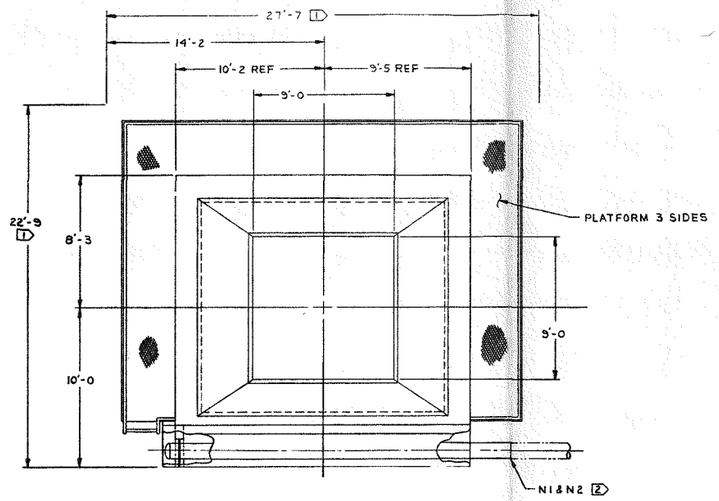

NOZZLES					
NO	DESCRIPTION	SIZE	SCHED	MATL	END PREPARATION
N1	NA INLET	12.00	40S	304SS	ANSI B16.25
N2	NA OUTLET	12.00	40S	304SS	ANSI B16.25
N3	CAPPED DRAIN	1.00	40S	304SS	ANSI B16.25

INTERFACES

1 LIMITING EQUIPMENT ENVELOPE
2 NOZZLES - SEE TABLE
3 SUPPORTS, ATTACHMENTS, & ANCHORS
4 WEIGHT, ESTIMATED: EMPTY — 50,000 LBS
FULL — 58,000 LBS
5 INSTRUMENTATION
6 ELECTRICAL LOADS
7 THERMAL INSULATION
8 HANDLING FIXTURE
9 HEAT DISSIPATION
10 ACCESS, LAYDOWN, WITHDRAWAL

NOTES

1 ALL DIMENSIONS ARE AT AMBIENT TEMPERATURES.

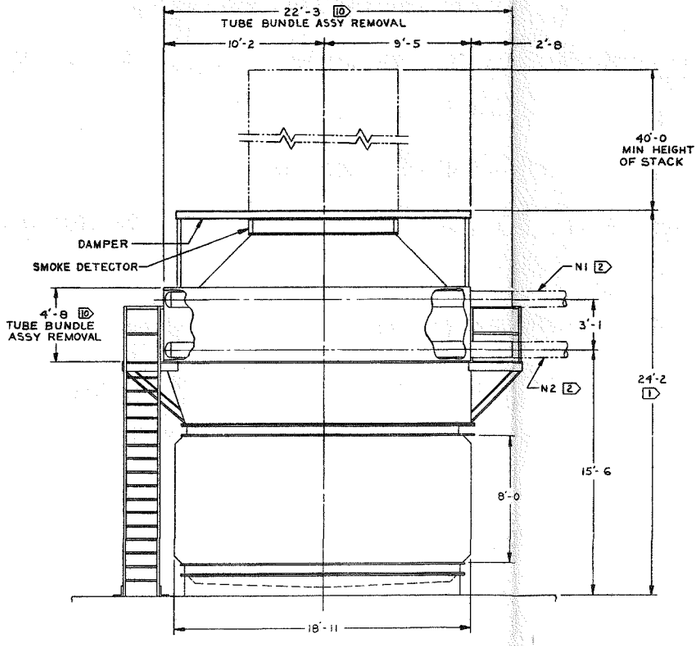

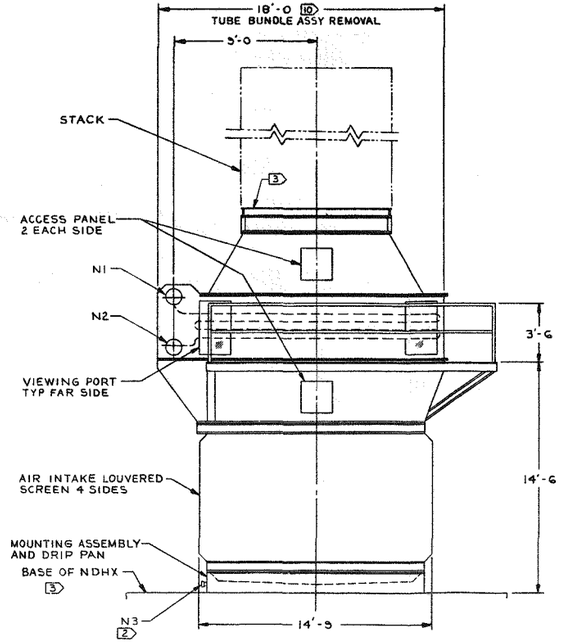

Figure F-9. Large Pool Reactor Residual Heat Removal System Natural Draft Heat Exchanger.

F.5 REFERENCES:

1. Revised Gudelines for EPRI LMFBR Pool Design, Letter from L. E. Minnick (EPRI) to J. Wett (ARD) et. al., dated 4/21/78.

2. WARD-D-0194, Table 50, CRBRP Decay Power Analysis, by R. K. Disney and C. A. McGinnis, Advanced Reactors Division, to be issued.

3. W-PO-O-12, "Monthly Progess Report for March, 1978 for Contract RP-620-26" dated 4/7/78, J. F. Wett (ARD) to G. D. Baston (EPRI).

4. WARD-353, Radial Parfait Core Design Study for EPRI Contract EY-76-C-03-1141 dated June 1977, by E. Paxson.

5. RA-77-169, Transient Analysis of PLBR Core Assemblies, dated 5/3/77, J. S. Killimayer to J. F. Wett.

6. ERDA-EPRI LMFBR Design Projects, Phase II, Final Report, Volume D1, PLBR Technical Appendix I, PLBR Residual Heat Removal System Performance Analysis, dated June 1977, by J. H. Coleman.

7. Technical Paper No. 410, Flow of Fluids Through Valves, Fittings, and Pipe, by Engineering Division of Crane Co., 16th Printing, 1976.

8. ASHRAE Handbook of Fundamentals by American Society of Heating, Refrigerating, and Air-Conditioning Engineers, Inc., New York, N.Y., 1972.

9. Process Heat Transfer, by Donald Q. Kern, McGraw-Hill Book Company, 1950.

10. Steam - Its Generation and Use, The Babcock and Wilcox Company, 37th Edition, 1955.

11. Handbook of Heat Transfer, Edited by W. M. Rohsenow and J. P. Hartnett, McGraw-Hill Book Company, 1973.

12. Introduction to Heat Trasnfer, by A. I. Brown and S. M. Marco, McGraw-Hill Book Company, 3rd Edition, 1958.

13. CRBRP Sodium Purchase Specification, by RRD dated September 1973.

14. "Friction Factors for Turbulent Flow in Curved Pipes," H. Ito, Journal of Basic Engineering, June 1956.

15. Heat Transfer and Pressure Drop for Cross Flow Through Banks of Multistart Helical Tubes with Uniform Inclinations and Uniform Longitudinal Pitches, P. V. Gilli, Nuclear Science and Engineering: 22, 298-314 (1965).

16. "Chemical Engineering Handbook," Perry, pp. 390-392.

APPENDIX G

ASSESSMENT OF PRIMARY SYSTEM FLOW AND NEUTRON FLUX MEASUREMENTS IN A LARGE POOL REACTOR PLANT

G.1 INTRODUCTION

The purpose of this study is to assess the need for primary system flow measurements and neutron flux measurements in a large pool reactor plant. This assessment begins with establishing the basic primary system monitoring requirements to satisfy the Plant Control System (PCS), the Plant Monitoring System (PMS), and the Plant Protection System (PPS). Goals throughout this study will be to determine whether the primary system flow measurements can be eliminated and to attempt to minimize the flux measurements. Once the monitoring requirements are established, the measurement methods will be evaluated to determine those necessary to meet the established requirements.

Plant duty cycle events and the addendant transient runs for the large pool reactor (LPR) have not been completed prior to this study. Reliance on foreign (PFR & PHENIX) and domestic (EBR-II) pool reactor experience and applicable events and data from the PLBR loop reactor computer runs are used as references in this study. Conservative extrapolation of this data, as applicable, is made to fit present pool reactor design guidelines and concepts.

G.2 FLOW MEASUREMENT ASSESSMENT

In order to assess the need for primary system sodium flow measurements in the large pool reactor (LPR), the basic requirements for flow measurements in the reactor and heat transport components in the pool must be addressed. Flow measurements are considered important for many reasons. These reasons can be categorized as supplying outputs to; a) the plant control system

(PCS) in order to maintain adequate flow to the core, b) the control room and data system for operator surveillance, plant status indication, reactor thermal power calculation verification, , etc., and, c) the plant protection system (PPS) in order to mitigate, through protective trip functions, the effects of plant fault events. Assessing the need for flow measurements for these functions are contained in the following paragraphs.

G.2.1 FLOW MEASUREMENT INPUT TO THE PLANT CONTROL SYSTEM

A plant control system may utilize flow measurements to insure adequate flow to maintain core temperatures, balance thermal power delivered to each IHX and IHTS, balance flow delivery from each pump (e.g., synchronize pump speed) and stabilize the system response to flow perturbations and power demand fluctuations. However, as was shown in the PLBR Phase II report for a loop plant, there are many design options and control modes for a plant control system that do not require the use of flowmeter measurements.

Consider the reactor and primary sodium coolant flow control. They can be broken down into two subsystems. A reactor control subsystem and a sodium coolant flow control subsystem.

The reactor control subsystem functions to provide control of the reactor power and temperature for all plant and reactor operations. Although the pool reactor control modes have not been established, the past reactor designs (CRBRP, PLBR) can be used as a reference. These show the reactor temperature controlled by reactor flux and the reactor flux controlled by the control rods. No flow measurements were required for this subsystem and none would be anticipated for the pool plant.

The primary sodium coolant flow control subsystem functions to provide control of sodium flow through the primary pump for all plant operations from ~10% flow to 100% flow. In contrast to the loop plant design however, the pool IHXs are decoupled from the primary pumps. In this configuration, the pump flow measurement requirements are not considered as demanding for normal plant operation. It is anticipated that a number of

adequate coolant flow control modes are available utilizing pump speed, pump outlet pressure, reactor inlet pressure and core temperature without requiring the use of flow measurements.

G.2.2 FLOW MEASUREMENTS FOR PLANT MONITORING

The measurements that fall into the category of plant monitoring would include any measurements, in addition to those required for control and PPS, deemed necessary to aid the operators in running and maintaining the plant. The additional items would include:

- Sodium level measurements in the main sodium pool required during fill and drain operations.
- Failed fuel detection and location systems.
- Shutdown flux measurements required during initial reactor fueling, refueling, startup, shutdown and other special test operations (i.e., rod drop tests, etc.)
- System and component temperature measurements during initial checkout and plant operation.
- Control rod position indicators.

No requirements have been identified that would dictate the mandatory use of flow measurements in the monitoring system.

G.2.3 FLOW MEASUREMENT INPUT TO THE PLANT PROTECTION SYSTEM

Criteria delineated in IEEE Standards 279 and 379 establish minimum requirements for safety-related functional performance and reliability of protection systems for stationary, land-based nuclear reactors producing steam for electric power generation. Because these criteria describe only minimum requirements, it is emphasized that compliance with these requirements does not necessarily fully establish the adequacy of protective system functional performance and reliability. However, omission of any of these requirements will, in most cases, be an indication of system inadequacy.

It is assumed that compliance with these requirements is sufficient to assure a licensable design for the protection system of a large scale breeder reactor of the pool concept. Examining those portions of these requirements which impact the functional design of the protection system in its response to duty cycle events will aid in determing if flowmeters are necessary. These requirements involve the number of protective functions which must respond to any given event, control and protection system interaction, and derivation of system inputs. Previous LMFBR protection system designs in this country have been conservative in their interpretation of these requirements and have perhaps established a precedence. This not withstanding, a more liberal interpretation of what constitutes adherence to the requirements should allow the design of a more streamlined protection system.

The requirements of the protection system are basic: 1) the protection system shall initiate protective action whenever a condition monitored by the system reaches a preset level; 2) any single failure within the protection system shall not prevent proper protective action at the system level when required (single failure criterion); 3) where a single random failure or credible event can cause a control system action that results in a condition requiring protective action, and, can concurrently prevent the protective action from those protection system channels designated to provide principal protection, adequate alternate protective capability shall be provided; 4) to the extent feasible and practical, protection system inputs shall be derived from signals that are direct measures of the desired variable.

The protection system in addition to the above requirements must adhere to the proposed pool concept guidelines, the electrical portion of which states for the protection system: "Two completely diverse shutdown systems are to be provided in the design including installation and operation of sensors, circuitry and drives." The analog reactor shutdown system (RSS) and digital RSS concept proposed in the PLBR design effort conforms to this guideline. However the question in point is not of architecture and equipment diversity, but of the adequacy of functional diversity. To determine the

adequacy of functional diversity, the following questions must be answered: 1) how many protective functions are required to respond to each design basis event; 2) what design basis events are to be considered; 3) what protective functions are available to respond to these events; and 4) are the requirements met when these protective functions are designed into a system?

The first question to be addressed involves the number of protective functions required for each event. The single failure criterion must be applied in this instance. If a protective function is considered as a component which is subject to a single failure whether by improper set point or some other cause, then there must be a second protective function within the protection system which provides protection for this occurrence. Here the key is "within the protection system." In the past conservatism prevailed, and the single failure criterion was applied to protective functions at the shutdown system level. However, the RSS are in fact subsystems within the protection system. Thus since two completely diverse shutdown systems are to be provided and since each is required to respond to each event as if it were the only system available, each of the two RSS must contain a protective function for any given event, and therefore compliance with the single failure criterion will be provided.

Additionally, the number of protective functions is affected by the requirement regarding control and protection system interaction. In this case if all control signals are derived from plant parameters monitored in only one of the RSS, then the protective functions provided in the redundant RSS provide compliance with the requirement. Therefore with one protective function per event in each RSS, adequate protection can be provided. It can be concluded that the number of protective functions required to comply with existing criteria is two per protection system which translates to one per RSS in LMFBRs.

The second question to be addressed is "what are the PPS design basis events involving sodium flow perturbations in the primary system to be considered?" Where the health and safety of the public is the underlying

concern, the sodium flow perturbations of consequence involve the loss of flow (LOF). However when adhering to the total plant protection concept, there is the requirement to protect major components from severe overcooling transients caused by inadvertent rapid flow increases. Table G-1 provides a preliminary listing of the anticipated Design Basis Events for the protection system involving primary system sodium flow perturbations.

Design Basis Events I, III and V require some clarification. Event I, Loss of Power, and Event III, Pump Coastdown, are quite similar except that in the latter case the pump is coasting down for some reason other than loss of power. These events, I and III, differ from V, Pump Speed Rundown, in that Event V is caused by control system action, for example, and the pump is not following its characteristic coastdown curve but is coasting down at some other rate.

The question of which protective functions are available must now be considered. COMTRAN protection system study transient runs, which were made during the PLBR loop plant design effort, cover Design Basis Events I, III and IV. These have been examined to determine what plant parameters are changing sufficiently in the time necessary to effect protective action. The following methodology was used in making this determination from the available computer run data. For the anticipated events of Table G-1 it is desirable (based on CRBRP) to limit the severity level incurred to that of an operational incident. This requires that the maximum cladding temperature of the fuel be limited to $1500^{o}F$. The response time required of the PPS is then determined as the span from the initiation of the transient to the time at which the hot channel, fuel cladding temperature reaches $1500^{o}F$. The COMTRAN model of the reactor core does not contain modeling of hot channel factors. Therefore, a conservative calculation was made to estimate the hot channel temperature. The time required to reach this temperature then served as the basis for identifying plant parameters which change a significant amount and thus might provide an input to a protective function. Figures G-1 through G-8 provide an example of the data used to develop Table G-2. For the loss of flow events studied, the loop reactor parameters which might be monitored to provide protective functions are:

TABLE G-1

PROTECTION SYSTEM DESIGN BASIS EVENTS INVOLVING
PRIMARY SYSTEM SODIUM FLOW PERTURBATIONS

Design Basis Event	Classification	RSS Protective Function	
		Analog RSS	Digital RSS
I. Loss of Power			
o 1 Primary Pump	Anticipated	Flux/$\sqrt{\text{Press.}}$	Pump Electrics
o 4 Primary Pumps	Unlikely	Flux/$\sqrt{\text{Press.}}$	Pump Electrics
o X Primary & Y Int. Pumps	TBD	Flux/$\sqrt{\text{Press.}}$	Pump Electrics
o All Primary & Int. Pumps	Anticipated	Flux/$\sqrt{\text{Press.}}$	Pump Electrics
II. Pump Speed Runout			
o 1 Primary Pump	Anticipated	TBD	Auctioneered Pump Speed Mismatch
o 4 Primary Pumps	Anticipated	TBD	Auctioneered Pump Speed Mismatch
o X Primary & Y Int. Pumps	TBD	TBD	Auctioneered Pump Speed Mismatch
o All Primary & Int. Pumps	Anticipated	TBD	TBD
III. Pump Coastdown			
o 1 Primary Pump	Anticipated	Flux/$\sqrt{\text{Press.}}$	Auctioneered Pump Speed Mismatch
IV. Pump Seizure			
o 1 Primary Pump	Unlikely	Flux/$\sqrt{\text{Press.}}$	Auctioneered Pump Speed Mismatch
V. Pump Speed Rundown			
o 1 Primary Pump	Anticipated	Flux/$\sqrt{\text{Press.}}$	Auctioneered Pump Speed Mismatch
o 4 Primary Pumps	Anticipated	Flux/$\sqrt{\text{Press.}}$	Auctioneered Pump Speed Mismatch
o X Primary & Y Int. Pumps	Unlikely	Flux/$\sqrt{\text{Press.}}$	Auctioneered Pump Speed Mismatch
o All Primary & Int. Pumps	Anticipated	Flux/$\sqrt{\text{Press.}}$	TBD

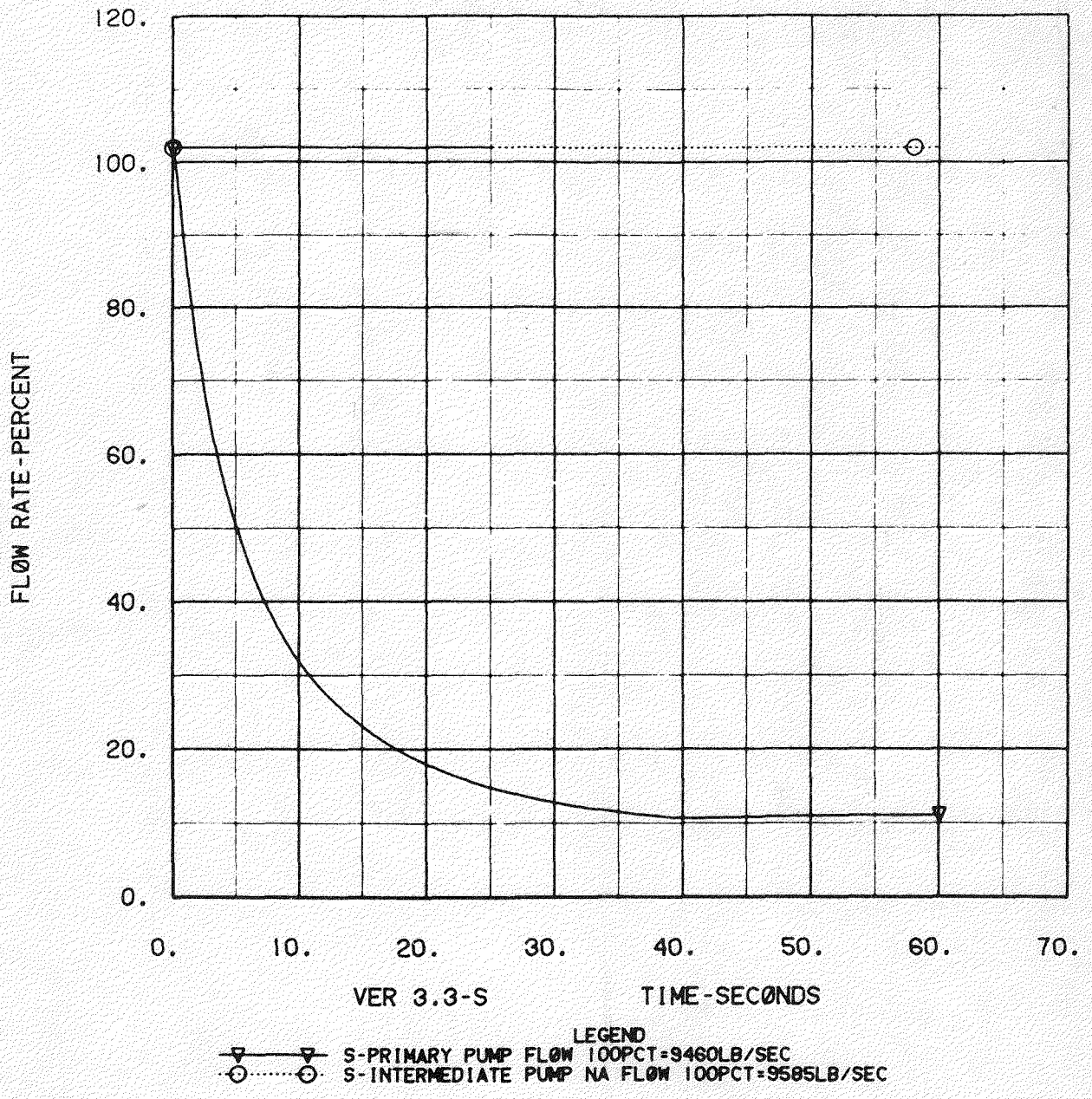

Figure G-1. PPS Study LOEP 3 Pri Pumps

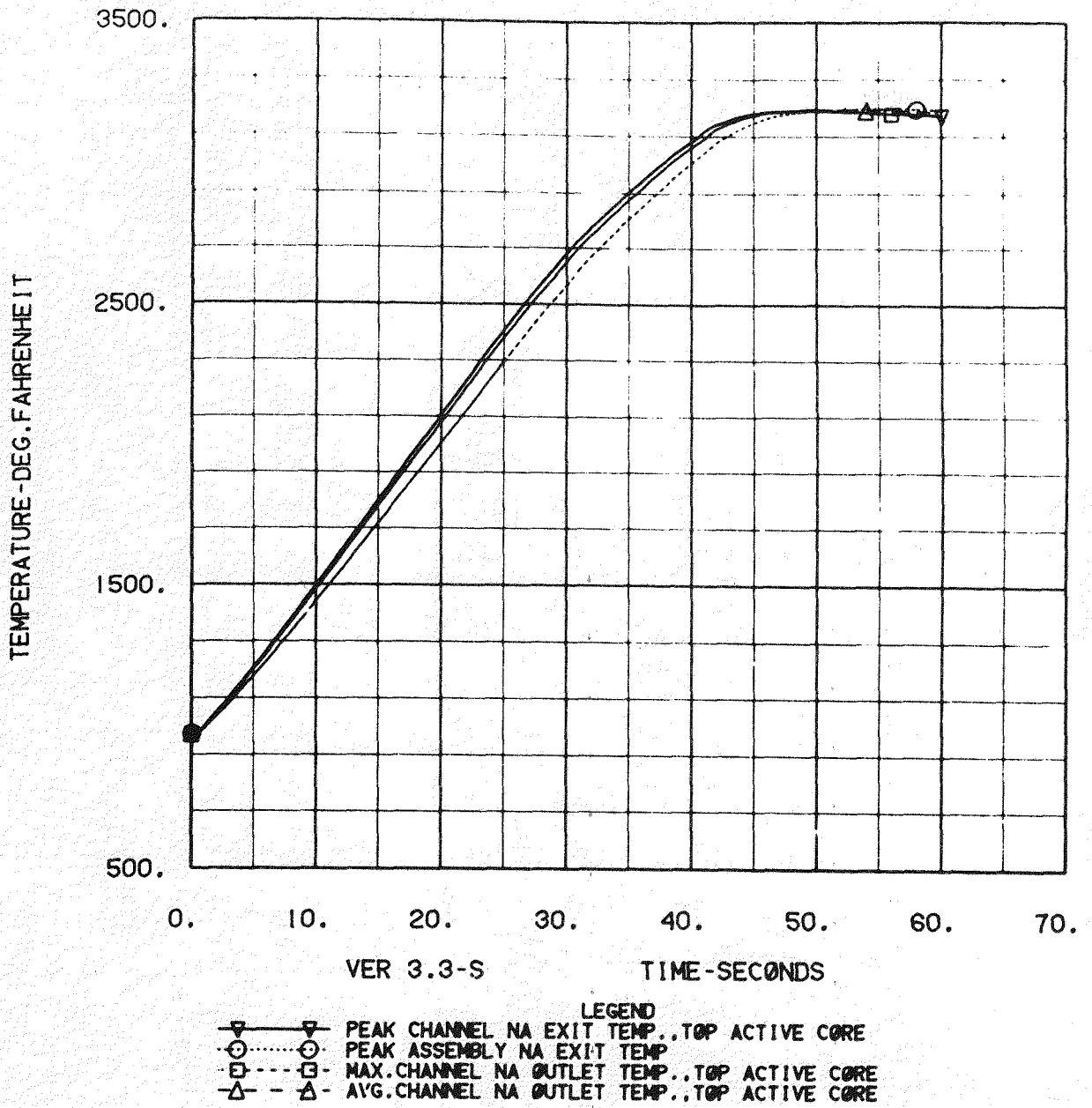

Figure G-2. PPS Study LOEP 3 Pri Pumps

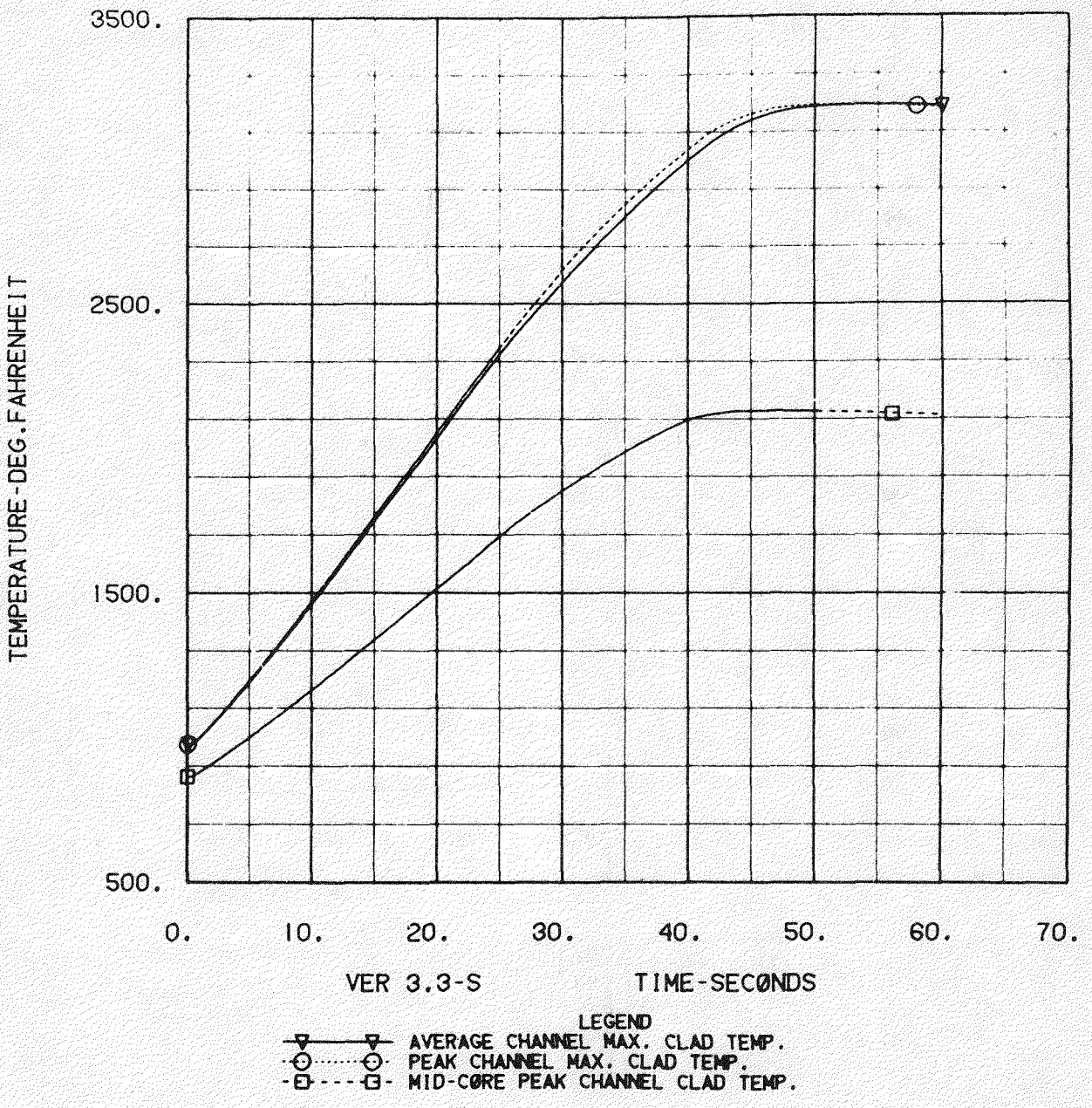

Figure G-3. PPS Study LOEP 3 Pri Pumps

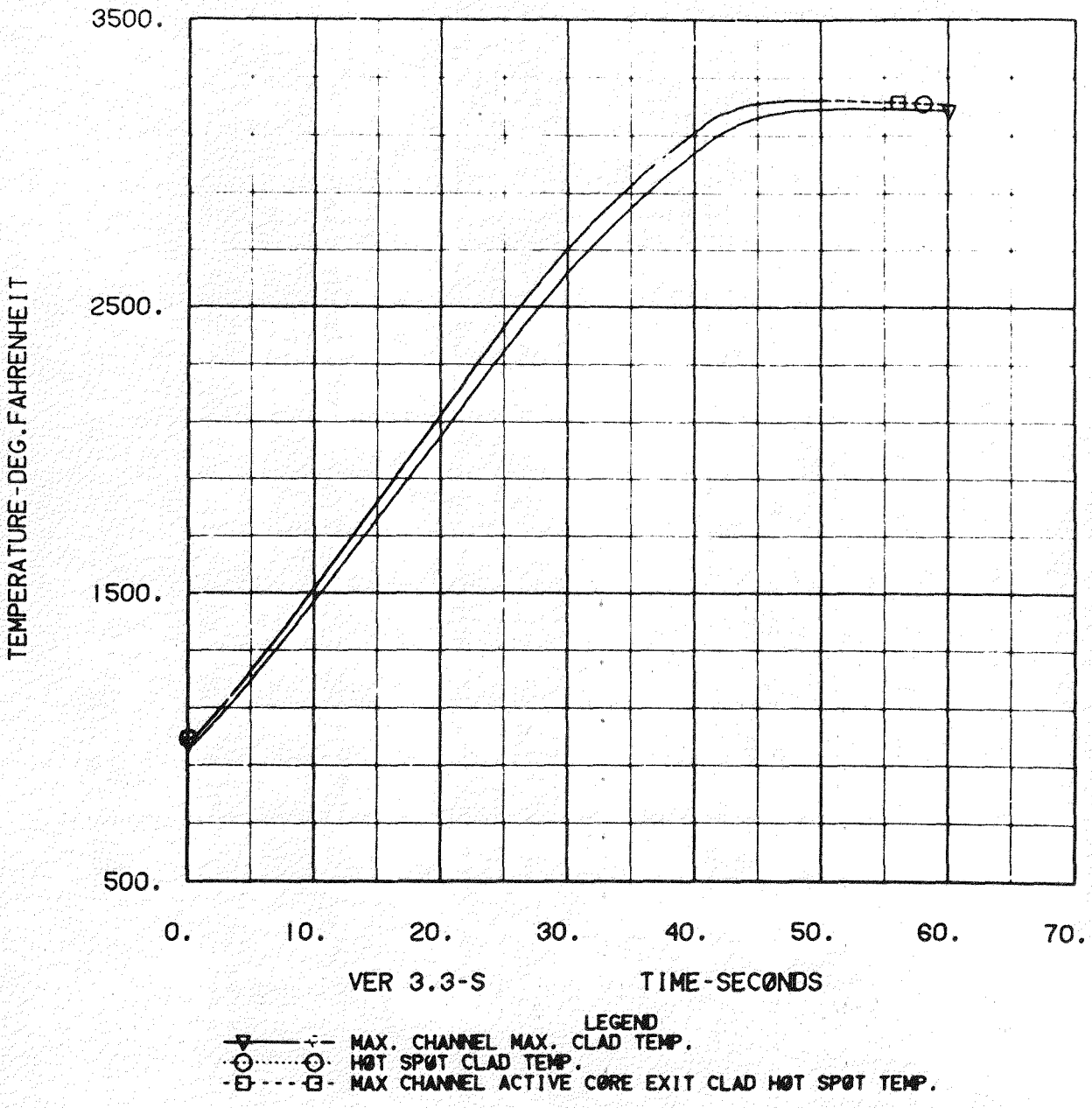

Figure G-4. PPS Study LOEP 3 Pri Pumps

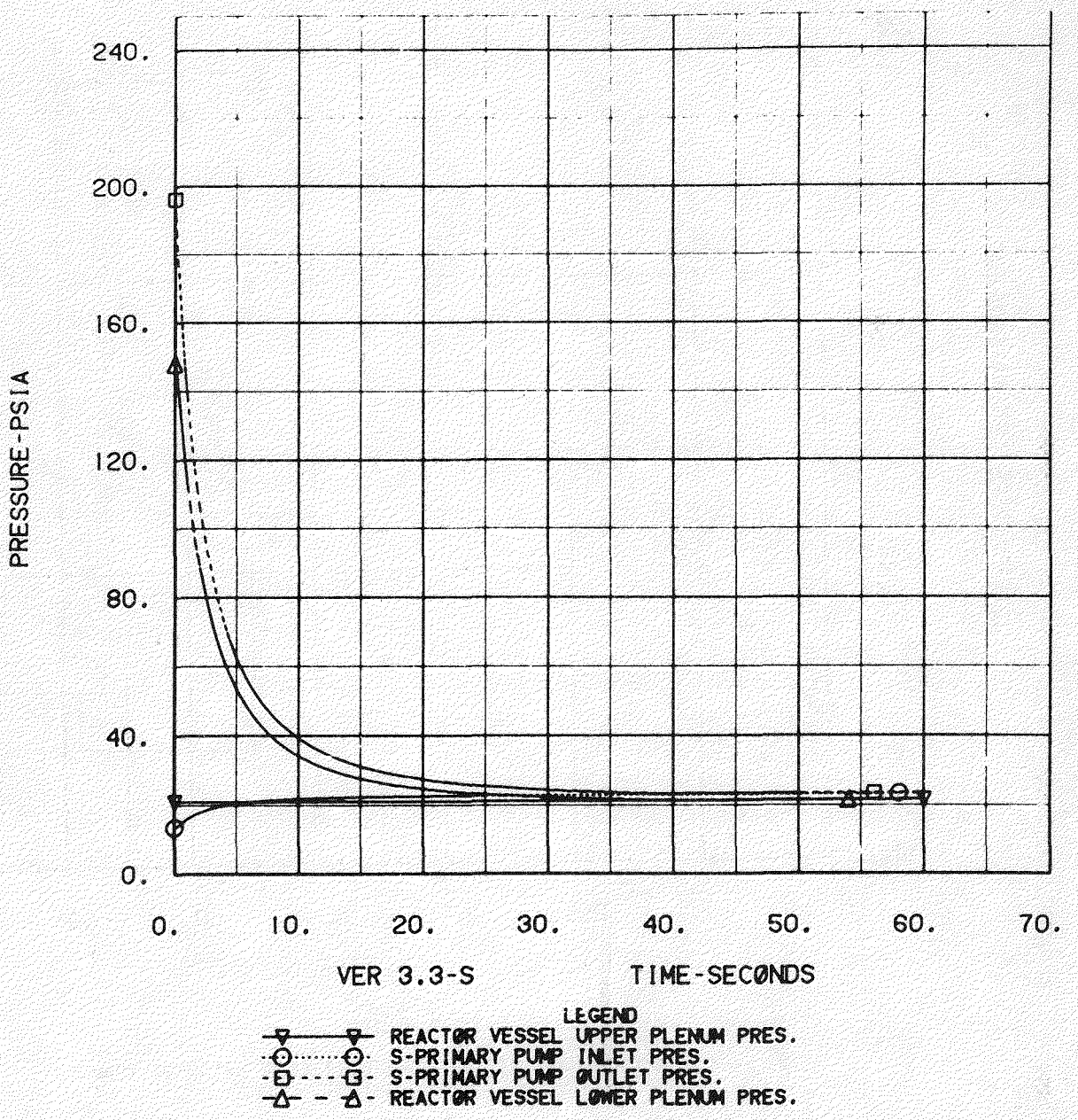

Figure G-5. PPS Study LOEP 3 Pri Pumps

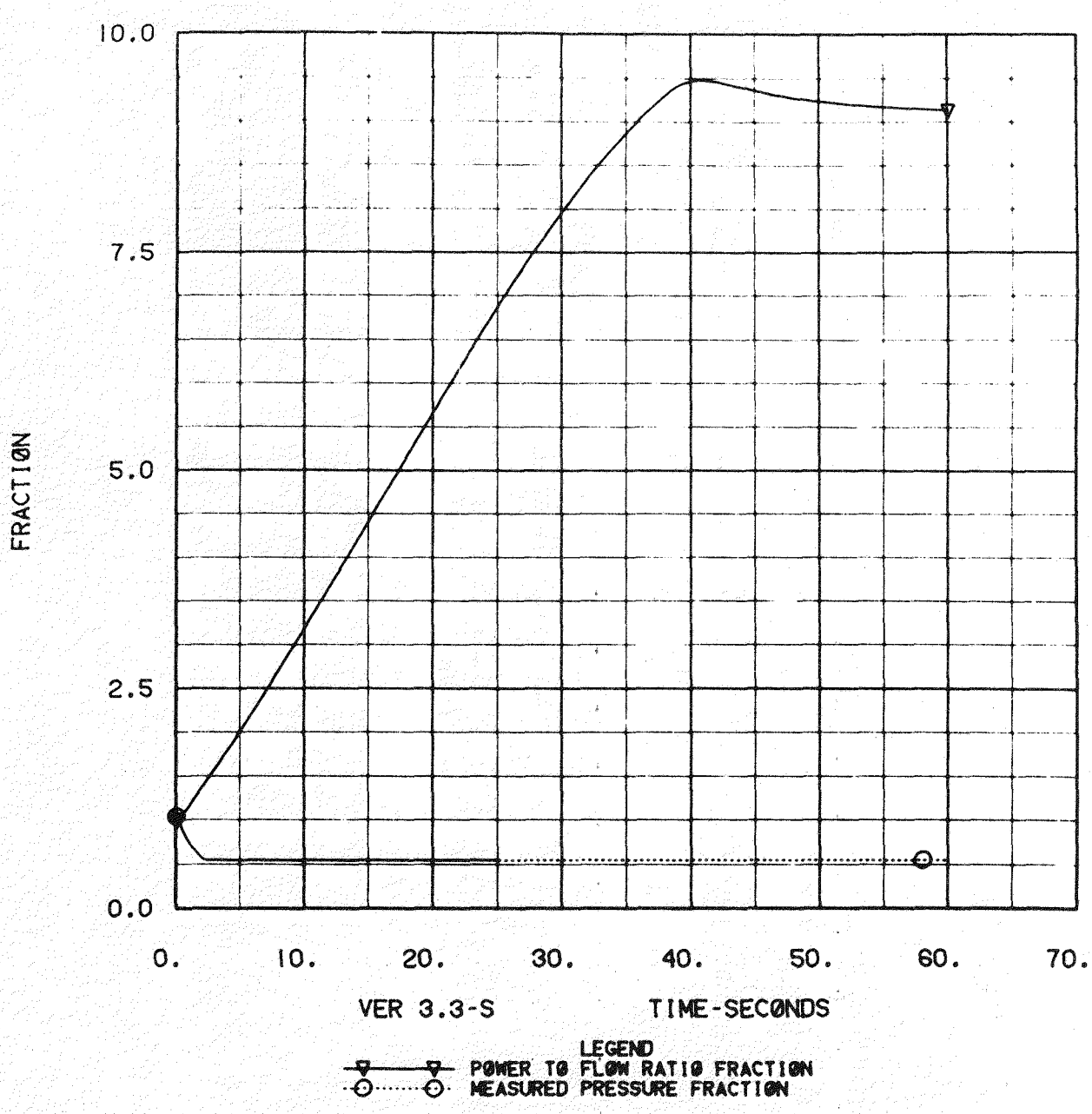

Figure G-6. PPS Study LOEP 3 Pri Pumps

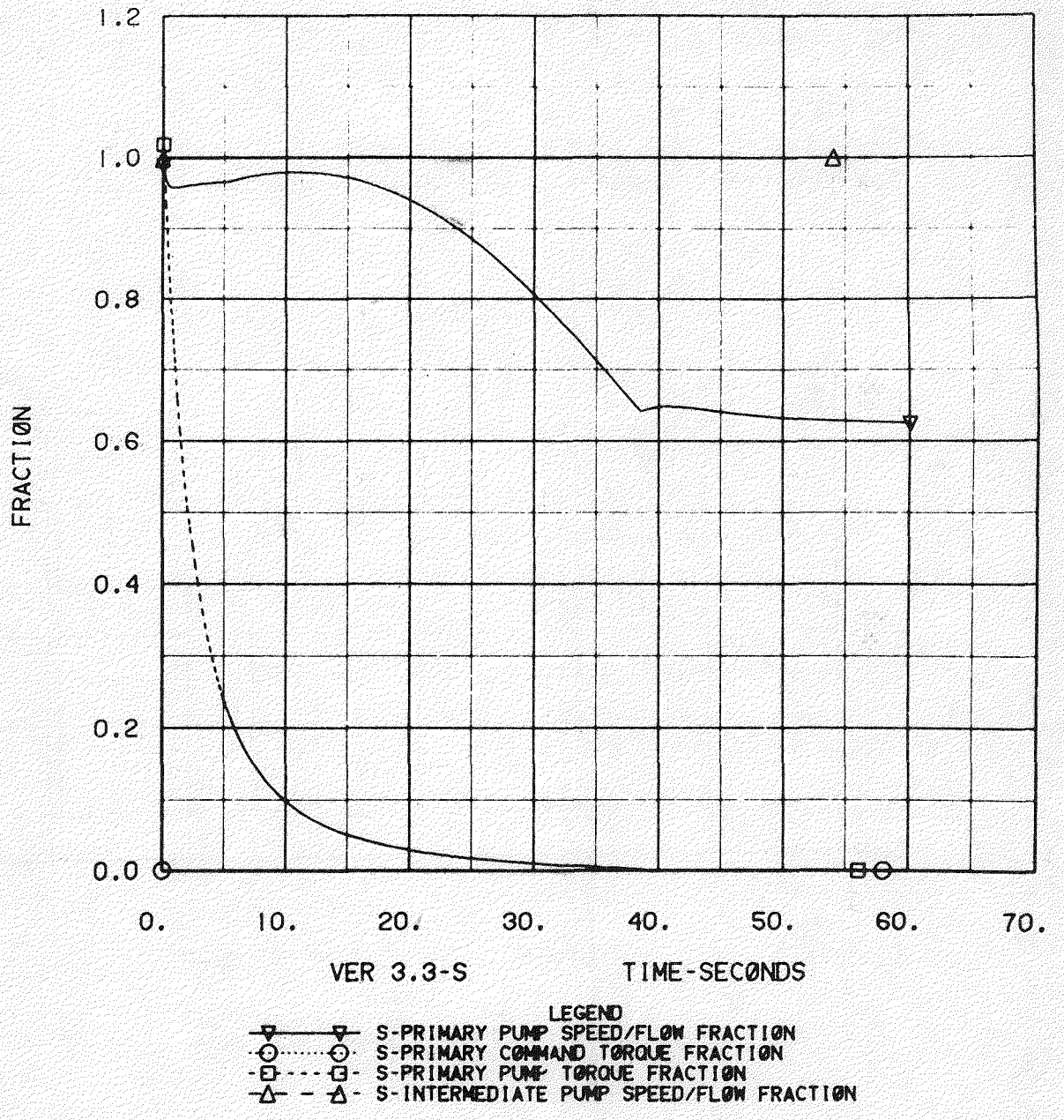

Figure G-7. PPS Study LOEP 3 Pri Pumps

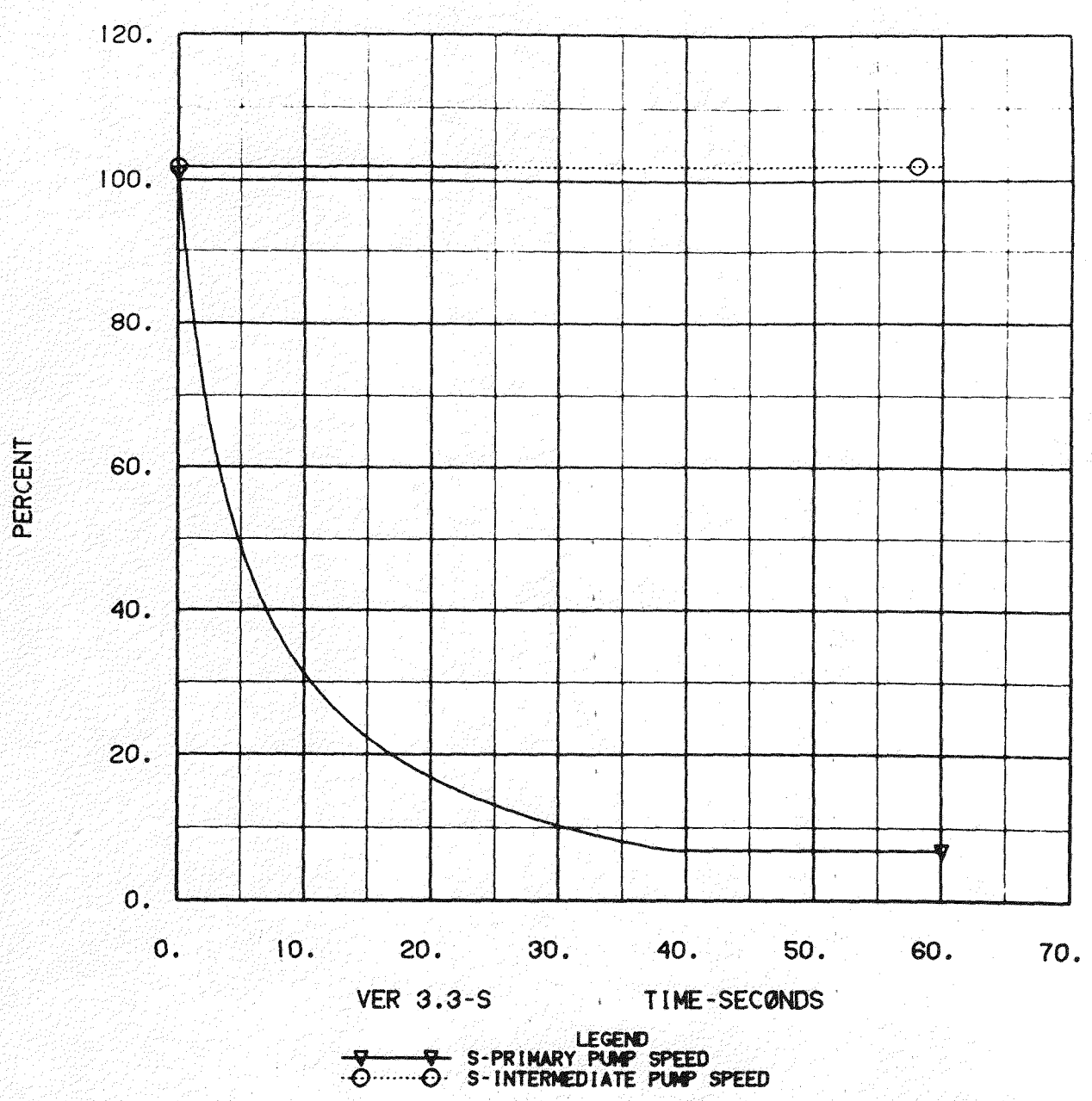

Figure G-8. PPS Study LOEP 3 Pri Pumps

TABLE G-2

LOOP TRANSIENTS SHOWING PARAMETERS WITH SIGNIFICANT VARIANCE

Event	Time** Sec	Single Loop Pri. Flow Δ%	Vessel Inlet Flow Δ%	Pri Pump Speed Δ%	Torque Δ%	Single Pri Pump Press ΔPSI	Lumped Loop Pri Pump Press ΔPSI	Lo Plenum Press ΔPSI	Core Exit Na Temp Δ°F
Seizure 1 Pri. Pump	3	-100	-30	-100	-100	-200	X	-62	+110
Coastdown 1 Pri. Pump	6	-100	-30	-50	-100	-125	-60	-63	+115
Coastdown 1 HTS Loop	6	-100	-30	-50	-100	-125	-60	-63	+115
Coastdown of All Loops	2	-26	-26	-30	-50	-93	-93	-60	+78
*LOEP 1 Pri. Pump	7	-100	X	-45	X	-125	-80	-60	+110
*LOEP 3 Pri. Pumps	3	-35	X	-40	-60	-100	X	-75	+100

*LOEP - Loss of electric power
**Time for hot channel cladding temperature to reach 1500°F

- o Pump Outlet Pressure
- o Reactor Vessel Lower Plenum Pressure
- o Pump Speed
- o Pump Electrics
- o Pump Torque
- o Sodium Flow
- o Sodium Exit Temperature at Top of Active Core

Table G-2, which is a summary of the loss of flow transients studied on the loop plant, shows the time at which the cladding temperatures reach their limits and the approximate variance of the listed parameters during this time. As an example, consider the coastdown of one primary pump event. For this event, the cladding temperature reaches its limit in 6 seconds. In this 6 seconds, the flow in a single primary loop decreases by 100%, vessel inlet flow decreases by 30%, primary pump speed and torque decrease by 50% and 100% respectively, the pressure of the pump outlet for the single loop and lumped loop decrease by 125 psi and 60 psi respectively, lower plenum pressure decreases 63 psi, and core exit sodium temperature increases by $115^{o}F$. It is important to note that the time required to effect scram is quite short in most cases, and consequently instrument response time may preclude the monitoring of some of these parameters for protective action purposes. An example of primary concern are thermocouples which monitor sodium temperature at core exit; these thermocouples would require a time response of less than two seconds.

The purpose of this study was to examine the need for primary system flow measurements with the objective of deleting requirements for such measurements in the pool reactor. An attempt was made to design a protection system which would react to the design basis events of Table G-1 without protective functions which use flow as a monitored parameter. The preliminary results of this design effort, also delineated in Table G-1, indicate that with the exception of the pump runout events, there is at least one protective function in each RSS which reacts to every design basis event. For the pump runout events it might be argued that only one function is required since this is not a safety-related event affecting the health

and safety of the public, but is of concern for plant and component protection. The protective functions listed are identical to those of the PLBR design effort with the exception of the auctioneered pump speed mismatch. This function now becomes a "complex function" involving auctioneering of pump speeds due to 4 primary and 6 intermediate pumps. In addition, hydraulics could dictate that pump speeds, at 100% condition, could vary, thus requiring normalization. Thus at this point in the analysis when considering only primary system flow perturbation, it may be possible to exclude primary flow measurements from the protection system and still conform to the requirements delineated in IEEE Standards 279 and 379.

It is now appropriate that a second classification of events be examined for their possible impact on the need for a measurement of flow. These events involve reactivity transients at less than 100% initial power conditions. These events have historically been protected against by functions which relate heat generating capacity with heat removal capacity, such as flux to flow or related parameters. Such a function is basically a neutron flux trip with a variable set point. PLBR protective functions of this type are: Flux to $\sqrt{\text{Pressure}}$, Flux to Flow, and Negative Modified Nuclear Rate (MNR). These functions along with Negative Flux to Delayed Flux provide protection for reactivity ramps and steps in the 40-100% load range.

The Phase II PLBR loop plant protective system requires measurement of primary system sodium flow as an input parameter to both the Flux to Flow and Negative MNR protective functions. Thus the deletion of flow measurements would eliminate these protective functions and leave only Flux to $\sqrt{\text{Pressure}}$ and Flux to Delayed Flux. Though no formal transient analysis of reactivity perturbation events has been performed, it appears unlikely based on CRBRP experience that these two functions alone, if separated and one placed in each RSS, could provide protection in all reactivity ramps and steps throughout the load range. Therefore it may be necessary to provide some diverse means, other than pressure, to establish a flux trip with a variable set point. One measurement which might provide this diversity is that of primary pump speed. Such a measurement once calibrated using heat balance techniques could provide an indication of flow which would be

accurate to perhaps ±5% of actual flow. This would then allow a protective function based upon flux to pump speed and reinstate the Negative MNR protective function with pump speed replacing flow as an input parameter (Table G-3). Analysis would be required to determine if protective action initiated by such functions would be adequate when accounting for inaccuracies involved in relating pump speed to flow. In this analysis, the designer would account for all normal and off-normal situations (e.g., leaks, one pump at lower speed, N-1, faulted IHX, etc.). In addition, calibration would be required for each pump (from 40% - 100% condition) for N pump and all combinations of N-1 operation.

It might be argued that a flux to speed function which provides protection against heat generating capacity exceeding heat removal capacity is in violation of the requirement that protection system inputs shall be derived from signals which are direct measures of the desired variable. However, the flux to speed function would be employed as a protective function guarding against reactivity excursion, and therefore the monitoring of flux as the prime parameter of concern could be considered as being in full compliance with the requirement. A considerable amount of effort will be required in convincing lincensing of the acceptability of this function, but if successful, the flux to pump speed protective function could provide the necessary diversity to complement the Flux to $\sqrt{\text{Pressure}}$ protective function.

The approach taken thus far has provided a preliminary protection system design, the functions of which are delineated in Tables G-1 and G-3. The preliminary design has excluded the use of primary and intermediate sodium flow measurements. This design appears promising; however, it must be emphasized that there are a number of potentially serious obstacles which must be overcome before a final decision can be made on the necessary protective functions.

As previously stated, it has been assumed in this study that the PPS Duty Cycle events for the pool LMFBR would be the same as those of the CRBRP and the PLBR loop plant. In the loop plant duty cycle events, the pipe rupture event is not included. Utilization of In-Service Inspection capabilities in

TABLE G-3

PROTECTION SYSTEM DESIGN BASIS EVENTS INVOLVING REACTIVITY PERTURBATIONS

Event	RSS Protective Functions	
	Analog RSS	Digital RSS
Positive Reactivity Ramp Insertions 40-100% Thermal Power	Flux/$\sqrt{\text{Press.}}$	Flux/Pump Speed
Positive Reactivity Step Insertions 40-100% Thermal Power	Flux/$\sqrt{\text{Press.}}$	Flux/Pump Speed
Negative Reactivity Insertions 40-100% Thermal Power	Flux Delayed Flux Negative	Modified Nuclear Rate

the design of CRBRP has played an important role in obtaining acceptance of the high integrity of primary piping. Accordingly, this acceptance has eliminated the need for considering a primary piping break as a duty cycle event for loop-type LMFBRs

The LPR, by virtue of its fundamental characteristics, has no primary piping but employs multiple coolant ducts for coolant flow from the pumps to the reactor inlet. Based on the accepted CRBRP duty cycle considerations, it is expected that as the LPR design progresses, the acceptability and the design considerations necessary to establish the same bases for eliminating the coolant inlet duct rupture event would be confirmed.

If the acceptability cannot be subsequently established, the PPS must be designed to provide adequate protection for the coolant inlet duct break event. It is anticipated that the Flux to $\sqrt{\text{Pressure}}$ protective function will provide response to duct break events in the Analog RSS; however, no function is identified in the Digital RSS which would provide coverage for this event. Without a flow measurement, it appears that the only other plant parameter capable of monitoring for protection of this event is the sodium exit temperature at the top of the active core.

A second difficulty, however, is encountered if there is an inclusion of inlet coolant duct leaks in the PPS Design Basis Events (DBEs) of the pool reactor. This is the effect of the leak on the previously proposed Flux to Pump Speed protective function in which pump speed is used as an inference of flow. The fact that leaks might be included could weaken the argument that pump speed is a good indication of flow.

There are both Primary and Intermediate HTS Pipe Leak events listed in the CRBRP PPS Design Basis Events. The PPS responds to these extremely unlikely events to preclude a loss of sodium inventory. Though in the pool plant, a duct leak between the pump and lower reactor core plenum would cause no loss of sodium, a leak certainly undermines the argument of there being a good correlation between pump speed and flow. It remains to be determined that these small duct leaks will not cause an additional uncertainty in the

correlation between pump speed and flow which would result in a flow error of greater than 5%. Such a determination must be extremely well founded if it is to be accepted. Again, a fall back position might be that the flux to pump speed protective function is used to provide protection in the event of reactivity excursions and not flow perturbations.

In conclusion, while it cannot be proven that flow measurements are an absolute must for the protection system, there is cause for concern at this time that without measurement of primary system flow the requirements of protective function redundancy and diversity may not be attainable for every design basis event. Only a complete analysis will determine if minimum protection system requirements can be met with the exclusion of primary system flow measurements. It is imperative that a well defined set of DBEs be established and agreed to by Mechanical Design and Safety and Licensing Groups, otherwise trip functions and their response times are meaningless. Transient runs must be made on a well modeled LPR which include hot channel factors if the adequacy of trip functions is to be determined with confidence.

The foregoing discussion does provide an avenue by which it appears possible to design a protection system which would not require the use of primary system flow measurements. It cannot be recommended that these flow measurements be deleted until such time that it can be proven that other protective functions exist which meet all requirements and obviate the need for protective functions based upon the measurement of flow. However, PPS design will proceed on the basis that no flow measurements are required.

G.3 NEUTRON FLUX MEASUREMENT ASSESSMENT

Core neutron flux measurements are mandatory in a nuclear power plant. These measurements provide a direct and instantaneous indication of the status of the core. As such, the flux measurements become important in the control system and reactor shutdown system because of their fast response to

core events. They are also important in the plant monitoring system because they provide the operator with instantaneous core status and changes during start-up and power operation.

G.3.1 NEUTRON FLUX INPUT TO THE PLANT CONTROL SYSTEM

Although numerous viable plant control modes involving any number of combinations of plant parameters can be selected, reactor power is considered a mandatory measured input to any nuclear power plant control system. This is evident from the fact that neutron flux (proportional to reactor power) provides the most directly measurable indication of the nuclear activity within the core. The nuclear power, being the source of the primary heat generation in the plant, therefore, becomes the obvious choice for a controlled parameter.

In a typical plant control system (as has been described in previous studies on large breeder reactors), control demands from a Supervisory Control Subsystem, are "fed forward" as inputs to various control subsystems such as a reactor control subsystem and a flow control subsystem. The reactor control subsystem, in response to the plant demands, functions to position the reactor control rods to attain the desired reactor thermal power and core outlet temperature.

Flux measurement output signals are an integral part of this control rod positioning loop. The measured flux output is compared with a flux demand establishing an error signal used to position the control rods.

Accordingly, core flux measurements provide a necessary input to the Plant Control System operation. The reactor design should provide detector locations near the core so that measurable core neutron activity as a function of power level is available.

G.3.2 NEUTRON FLUX INPUT TO THE PLANT MONITORING SYSTEM

In addition to reactor neutron flux measurements being critical inputs to the plant control and plant protection systems, they are also important for supplying reactor core status information to the reactor operators during all phases of reactor operation when fuel is in the core. During shutdown operations (initial fueling and refueling), the operator must; 1) have continuous assurance of the shutdown margin of the core, 2) be capable of detecting changes in core reactivity as a result of fuel manipulation, and, 3) be capable of observing a suitable count rate proportional to flux before rod withdrawal at startup.

During startup operations, approach to power, and shutdown, critical flux and rod worth measurements must be provided in order to characterize system performance under normal operating conditions and to develop a data log for continuing evaluation of system performance throughout reactor life. In order to ensure the minimum shutdown margin during refueling, it is essential that the following data be obtained during startup operations:

- o prompt flux response to rod drops as observed by the flux detectors
- o reactivity worths of rods from rod drops
- o reactivity worth vs rod position
- o effective coefficients of reactivity

During increase to full power and actual power operation, the operator requires core flux measurements to determine such things as the flux measurement range overlap regions, to operate control rod withdrawal bypass circuits, and to monitor reactor steady state power stability.

Core flux measurements during maintenance periods and under post-accident conditions are important since they provide assurance for the safety of the maintenance personnel as well as providing the possibility for satisfying post-accident monitoring requirements (i.e., safety of the public).

It can be concluded from the above discussion that appropriate core flux measurements are necessary for reactor monitoring and surveillance and will be provided in the design.

G.3.3 NEUTRON FLUX INPUT TO THE PPS

The only two logical measurements which can be used in PPS trip functions to guard against reactivity transients are flux and subassembly outlet temperature. For rapid reactivity transients, however, in which the fuel and cladding temperatures change very quickly, the flux measurement is the only parameter which provides adequate time response to prevent incipient fuel melting. All LMFBRs to date use a flux measurement input in their shutdown systems. Data from EBR-II, which in addition to flux related trip functions employs a subassembly outlet temperature (SOT) trip function, shows that in all cases the SOT trip is a backup to the flux trips.

Rapid reactivity transients have been included in the PPS Design Basis Events for both FFTF and CRBRP. Such events will also be included in the PPS Design Basis Events for the LPR. Therefore it is imperative that protective functions be included in each RSS which react to these events and which have an extremely fast time response. Flux monitors are the only known instruments which meet these PPS requirements. It is therefore mandatory that flux monitors be included in the PPS to provide adequate response to rapid reactivity transients.

Additionally, in order to meet the PPS requirements of redundancy and diversity, two diverse means of measuring flux must be provided. One flux monitoring technique will be used in the Analog RSS, and a second diverse means of measuring flux will be used in the Digital RSS.

G.4 FUNCTIONAL REQUIREMENTS FOR REACTOR FLUX AND PRESSURE MEASUREMENTS

The foregoing discussion has determined that instrumentation must be provided which is capable of measuring reactor flux and primary system pressure drop in the LPR. In summary the instrumentation system must provide the capability to:

- o monitor core neutron flux status during initial fueling conditions,
- o monitor core neutron flux status during refueling conditions,
- o monitor core neutron flux status from shutdown to all power levels,
- o monitor primary system pressure drop status from startup to all power and coolant flow levels.

The flux and pressure signals thus obtained will as appropriate be provided to:

- o the Plant Protection System to initiate reactor protective trips,
- o the Plant Control System for reactor and plant control,
- o the Plant Monitoring System for status display and recording.

To assure that these measurements provide the required information to the control, protection, and monitoring systems, a preliminary set of functional requirements has been identified for these measurements. These functional requirements are delineated as follows:

(Note: Priority is given to PPS requirements for those instruments providing signals to control, protection, and monitoring systems.)

- o Each instrument channel shall provide a linear analog signal proportional to the parameter being measured over the required range of measurement. An instrument channel includes the sensing element and any required conditioning devices.
- o The output of each instrument channel shall be compatible with PPS input signal requirements.
- o The functional operation of the instrumentation shall meet the performance requirements under the combined worst case variations of temperature, humidity, pressure, incident radiation, atmospheric contamination, and power supply voltage and frequency.
- o All requirements applicable to PPS equipment shall also apply to instrumentation providing input to the PPS.
- o Each instrument channel shall provide the means and capability for on-line functional performance testing of the detector and any signal conditioning.

In order to meet the measurement requirements including the separation and redundancy requirements of the PPS, the following measurements will be required:

- Four redundant measurements of reactor neutron flux must be performed by detectors installed at four appropriately spaced locations around the core and used in the Analog RSS and possibly the PCS.
- Four redundant measurements of reactor neutron flux will be performed by detectors (diverse from those used above) installed at four appropriately spaced locations around the core and used in the Digital RSS and possibly the PCS.
- Low level core flux measurements (initial core loading/refueling) will be performed by high sensitivity detectors installed at symmetrical locations around the core. (Non-PPS measurement)
- Four redundant measurements of primary coolant system and/or core pressure drop will be performed at candidate locations yet to be determined. The most likely measurement locations being studied include the core inlet pressure and the pump outlet pressure plenums.

G.5 MEASUREMENT METHODS AND LOCATIONS

In the preceding sections the measurements of the primary system pressure drop and reactor flux have been identified as being necessary in the large pool reactor design. The pressure measurement becomes a critical measurement with the proposed deletion of the primary system flowmeter. Provisions for the implementation of these measurements follows with a discussion of the measurement techniques and the sensor requirements that apply.

G.5.1 PRIMARY SYSTEM PRESSURE DROP MEASUREMENTS FOR LPR

It has previously been determined that the PPS requires primary system pressure drop measurements to provide trip initiation in response to loss of flow events. There are presently two locations under consideration to make the necessary pressure measurements, these are the core inlet plenum and the discharge side of the primary pump. Either location poses the question of how to make the measurement, with the attendant problems of how to route

sensor lines and how to replace sensors. Additionally, the total number of sensors may be affected by their location; locating sensors at the pump outlet could require four sensors per pump vice the four total sensors which would be required if they were located in the inlet plenum of the core.

Pressure measurements in CRBR have been proposed to be taken at the core inlet plenum while in FFTF they are made at the discharge side of the primary pumps. Both designs use a capillary tube type pressure sensor. This type sensor transfers fluid pressure from the high temperature sodium to a remote mounted pressure sensor transmitter via an intermediate fluid (NaK).

The only pressure measurement techniques used in a pool reactor studied thus far are those employed in Phenix. In this reactor, pressure measurements are made at the pumps and at the core inlet. Primary pressure tranducers are mounted on the pumps and monitor the flow of the pumps by measuring the differential pressure drop across an orifice installed in a by-pass line which runs between the pump outlet and a low pressure region in the vessel. Maintenance is performed on the pressure transducer by removal of the pump from the pool. To obtain the core inlet pressure a transducer is placed in the core through a fuel assembly. This is a force balance transducer of high accuracy which is used for flow calibration during startup.

Currently for the LPR it is proposed that the capillary type sensor of FFTF and CRBR be employed. For the core inlet plenum a capillary tube could be run along the lower support structure and thence up the sodium shield to the deck where the sensor would be mounted . The pressure sensor transmitter itself would then be accessible for maintenance. To measure pump discharge pressure a capillary tube could be run in the pump tank to the remote pressure sensor transmitter, again providing access for maintenance; or the transmitter could be located within the pump tank structure. Maintenance in the latter case would be performed by removal of the pump. These options plus others need to be pursued further in subsequent studies to be performed on instrumentation required for pool type LMFBRs.

It should be kept in mind that core inlet plenum pressure measurements provide an indication of total flow through the core, while pump discharge pressure measurements coupled with the use of check valves provide information on individual pump flows. Thus in keeping with PPS requirements of four separate sensors per each parameter to be measured, it may be required (as mentioned previously) to provide four sensors at each pump if the discharge pressure were to be measured. This would entail sixteen pressure transducers altogether. Measurement of core inlet plenum, since there is only one, would only require a total of four sensors to meet PPS requirements.

If the solutions to the physical problems associated with selecting pressure sensor location are equally satisfactory, the real question of concern is which location provides the required PPS response to loss of flow events, or which provides the better response and lessens the possibility of spurious PPS trips. The answers to these questions will come only through detailed transient studies of the LPR. As an example of information which must be garnered in transient analysis, it is reasonable to assume that four sensors in the core lower plenum would be preferable to sixteen sensors located at the primary pump outlet. Table G-1 indicates that the Flux/ $\sqrt{\text{Pressure}}$ protective function is being relied upon to provide Analog RSS response to loss of flow events involving the rundown of only one primary pump. In such an event, CRBR studies have shown that Flux/ $\sqrt{\text{Pressure}}$ action would act as a backup protective function and may not respond in time to limit the severity level of the event to that of an operational incident. The CRBR pressure measurement for this function is taken at the reactor inlet plenum. Such a measurement really provides reactor flow information vice the loop flow information provided by the sensor located in the pump outlet as in FFTF and proposed in PLBR. In the case of loss of a single pump, the other pumps tend to have a runout of flow and thus delay the trip provided by a reactor flow trip using lower plenum pressure as a measurement of flow. In the case of the LPR with a lower plenum pressure measurement, loss of a single pump coupled with runout flow in the remaining pumps could cause some concern. The runout flow would provide additional flow equivalent to as much as 90% total flow to the lower plenum. Thus, perhaps no reactor

trip would be required, or the trip setting of the Flux/ $\sqrt{\text{Pressure}}$ trip function may be required to be established near 90% flow conditions. This latter case would no doubt be intolerable for operational reasons. Spurious trips would be unavoidable. However, if check valves were installed in the coolant inlet ducts, pressure measurements at the pump outlets would provide a relatively fast responsing trip function which would react to the loss of a single pump.

From this example, it is easily seen that transient analyses are required prior to making a selection of the location for pressure sensors. The aforementioned sensor type, capillary tube routing, and accessibility requirements are likewise necessary information in the selection process. Subsequent effort is obviously necessary prior to making a selection on pressure sensors.

G.5.2 NEUTRON FLUX MEASUREMENTS FOR LPR

In a pool type reactor, there appears to be two options in selecting where to install neutron flux detectors. One option is to provide a location outside the vessel such as underneath the guard tank as is done on PHENIX and Super-PHENIX. The other option is to install the detectors inside a dry thimble in the sodium pool within the reactor vessel as in the British PFR design. Preliminary flux calculations were performed for various locations in the large pool reactor and underneath the guard vessel to scope acceptable locations. These preliminary calculations were based on scaling up the PLBR computer code to the LPR power level and factoring in the LPR mechanical design configuration. The flux used for shutdown was calculated by ratioing the CRBRP shutdown to full power flux and multiplying by the LPR full power flux.

The results of these calculations are tabulated on Table G-4. They indicate that the flux measurements have to be made in the sodium pool within the primary containment. Sufficient neutron flux is available for the power range detectors in the region of the inner wall of the outer neutron shield.

TABLE G-4

PLBR (POOL CONCEPT) RADIATION
ENVIRONMENT AT SELECTED FMS LOCATIONS

	FULL POWER			SHUTDOWN (T=0)		
Position	ϕ_{Th}^{Eq} (b) n/cm^2-sec	Secondary Gamma R/Hr	Na^{24} Gamma R/Hr	ϕ_{Th}^{Eq} n/cm^2-sec	Secondary Gamma R/Hr	Na^{24} Gamma R/Hr
P1	2.4×10^{8}	4.5×10^{3}	5.0×10^{4}	2.4×10^{-2}	----	5.0×10^{4}
P2	2.8×10^{3}	2.0×10^{-1}	2.1×10^{3}	2.8×10^{-7}	----	2.1×10^{3}
P3	2.0×10^{3}	1.0×10^{-1}	4.8×10^{4}	2.0×10^{-7}	----	4.8×10^{4}
P4	3.2×10^{9}	6.4×10^{4}	5.6×10^{4}	3.2×10^{-1}	----	5.6×10^{4}

(a) ϕ_{Th}^{Eq} is equivalent thermal flux based on predicted U^{235} fission rate due to neutrons of energies less than 10.0 MeV.

(b) P1 -- Inside Surface of Outer Shield
P2 -- Beneath Guard Vessel
P3 -- Outside Surface of Outer Shield
P4 -- Outside Surface of Inner Shield

For the shutdown flux detectors, sufficient neutron flux could be obtained at the outer surface of the inner shield only if a beam hole could be provided through the shield. Otherwise, the shutdown flux detectors may have to penetrate the shield sufficiently to increase the shutdown flux levels at the detector.

Access to the detector locations will be through dry wells (thimbles) installed through the deck and extending to the measurement locations. Penetration through the deck will prevent penetration of the reactor vessel wall and be outside the region of the rotating plugs. The use of the dry wells will ease the problem of installation and replacement of the detectors and protect the detectors from the radioactive sodium.

High temperature detectors and cables will be required which can operate reliably to temperatures of 850°F to 950°F and a maximum gamma flux of approximately 6×10^4 R/hr. In order to satisfy these environmental requirements, integral cable detectors will be required. High temperature fission detectors (U^{235}) will be required for the source range and wide range measurements. High temperature compensated ion chambers will be required for the power range measurements.

G.6 CONCLUSIONS

A decision to eliminate flowmeter measurements of the reactor and pump flow in the LPR, although promising, cannot be definitely stated at this time because of uncertainties still to be resolved concerning their use in the PPS. Further analyses are still required when the LPR duty cycle events and transient computer runs are available.

A preliminary protection system design has been presented that excludes the use of primary and intermediate sodium flow measurements. A number of potentially serious obstacles are presented, however, that must be overcome before a decision can be made as to its acceptability.

No mandatory requirements have been identified in the PCS or PMS to require the use of flowmeters. A number of viable reactor and primary system control modes can be designed without requiring flowmeter measurements. However, a valid calibration of pump speed vs pump flow over the operating sodium temperature range must be demonstrated.

Core neutron flux measurements are considered mandatory for use in the PCS, PMS and the PPS since they provide the most direct and instantaneous indication of the status of the core at all times.

Preliminary calculations have indicated that the neutron detectors must be located within the reactor vessel and be positioned between the inner and outer shields. The source range measurement may require detector location within the inner shield or provisions for a beam hole through the shield to the detector.

Core inlet pressure and/or pump outlet pressure drop measurements have been proposed as being critical for the PPS if primary system flowmeters are deleted.

APPENDIX H
ALTERNATE DESIGN CONSIDERATIONS

H.1 INTRODUCTION

The reference design of the LPR presented in Volumes 1 and 2 of this report represents the status of the design as of the middle of June, 1977. To complete this report by the end of July, the design was necessarily frozen just 3-1/2 months following placement of the contract between Westinghouse and EPRI. As a result, a number of design features have not been fully evaluated. Many changes are known to be desirable and others require further evaluation to confirm their potential advantages over the present configuration. This appendix discusses the following four areas of the LPR where further consideration of alternates could possibly lead to changes in the design:

- o Alternate Pump and Pump Support Designs
- o Sodium Purity and Monitoring - In-Vessel vs. Ex-Vessel
- o Component Removal for Maintenance
- o Vessel Bottom Head Configuration

H.2 ALTERNATE PUMP AND PUMP SUPPORT DESIGNS

The reference two stage pump concept for the LPR has a design operating speed of 492 rpm. The total shaft length is 552 in (46 ft) from coupling to eye of impeller, and the distance between the oil lubricated radial bearing on the top to the sodium lubricated bearing is 482 in (bearing span).

A basic concern with a shaft of this length is maintenance of an adequate margin between the lateral critical speed of the rotor, and its operating speed. A practical requirement used for preliminary shaft design is that the calculated critical speed, based on rigid bearings, shall be at least 200

percent of design speed. This results in a conservative shaft design, which meets the desired 125 percent margin between design speed and first critical speed when bearing stiffness is taken into account. Using this requirement on the LPR primary pump shaft results in a critical speed requirement on rigid supports of 16.4 hz (984 rpm).

Table H-1 gives the results of calculations using 482 in and 362 in bearing spans. The latter is assumed to be accomplished by lowering the oil bearing 60 in by redesign of the top pump support, and raising the hydraulic section 60 in. (The latter will not impact the hydraulic design.) The wall thickness of the shaft torque tube has only a slight effect on critical speed, indicating that pump drive torque and shaft manufacturability should determine the wall thickness.

The 482 in bearing span requires a torque tube diameter of 35 in with a 1 in wall thickness. Using the shorter bearing span of 362 in, a 20 in diameter torque tube with a 1 in wall thickness can be used. This demonstrates a significant payoff from shortening the bearing span. It is, however, clear that both the 35 in and 20 in diameter torque tubes can be manufactured without significant problems. There are two changes in the design which can bring about a reduced bearing span. Raising the hydraulic section of the pump approximately 5 ft can be done without reducing pump NPSH available below 50 ft. The hydraulic section had been lowered below what was hydraulically required, to obtain a more favorable thermal environment. It was found, however, that this thermal environment could be changed without jeopardizing the pumps mechanical performance. Figure H-1 shows a preferred alternate concept for the primary pump. The impeller section is raised 5 ft compared with the reference concept. Additionally a simplification of the bottom piping arrangement is made, whereby one pipe is eliminated, and the bottom part of the pump well serves the purpose of a discharge pipe. The upper piston ring seal is replaced by a bellows face seal at a higher elevation.

The upper pump support requires a spherical bearing surface to accommodate the thermal movement. The reference design locates this surface external to the pressure boundary. The configuration allows no radial motion at the level of

TABLE H-1

FIRST CRITICAL SPEED OF PRIMARY PUMP SHAFT

Bearing Span (in.)	Torque Tube Diameter (in.)	Torque Tube Wall Thickness (in.)	Critical Speed (hz)
482	28	2	12.70
482	28	1	13.10
482	28	0.75	13.24
482	28	0.50	13.36
482	30	1	14.09
482	34	1	16.04
482	35	1	16.52
362	28	1	23.27
362	26	1	21.54
362	20	1	16.40

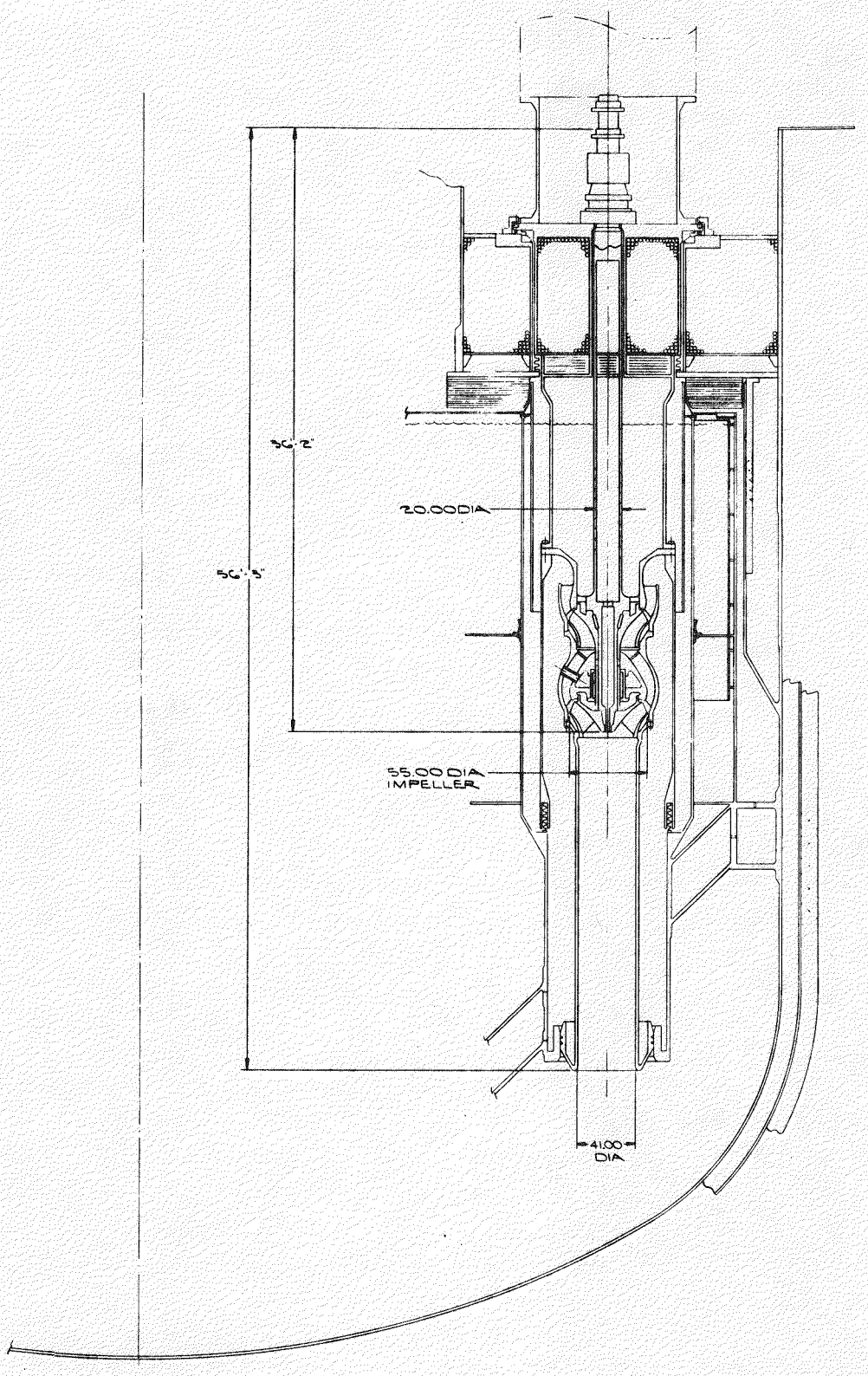

Figure H-1. Large Pool Reactor Primary System Pump Concepts

the upper seismic support. This support arrangement raises the pump flange approximately 60 in above the bottom end of the motor support. The preferred alternate design has the spherical support surfaces located within the pressure boundary, which allows the pump flange to be lowered 60 in compared with the reference design. For this reason there is a secondary bellows face seal located at the bottom of the roof penetration serving two purposes: preventing sodium vapor from reaching the lubrite spherical support surface, and preventing cellular convection of hot cover gas in the annulus between the pump shield plug and the deck. The sodium containment boundary bellows seal is located between the pump flange and support flange, and is designed to take the thermal motion of the pump. For the preferred alternate concept the motor support is mounted directly on the pump flange, which eliminates misalignment between pump and motor shafts due to thermal motions.

By reducing the shaft length approximately 10 ft between the reference and the preferred alternate designs, the torque tube diameter of the shaft can be reduced from 35 in to 20 in. This simplifies the dynamic balancing of the shaft, since the sensitivity to wall thickness variation is nearly eliminated.

A second alternate top support arrangement consists of a solid, non-compliant support, as shown in Figure H-2. This arrangement requires the high pressure sodium seals to be designed to accommodate the radial thermal motions. Discussions with EMD indicates that this approach is preferred by the pump manufacturer. EMD considers that bellows with sliding face seals can accomplish the desired seal. One question that needs to be answered before a solid support can be considered is whether the seismic requirements can be satisfied with a pump cantilevered from the roof.

H.3 SODIUM PURITY AND MONITORING -- IN-VESSEL VS. EX-VESSEL

In the LPR reference design, the primary sodium purification system (SPS) and primary sodium purity monitoring system (SPMS) are placed inside the LPR reactor vessel. The design guidelines of Appendix L require that both of these systems be located within the reactor vessel so that no primary sodium is circulated outside the primary tank. A similar design criterion is

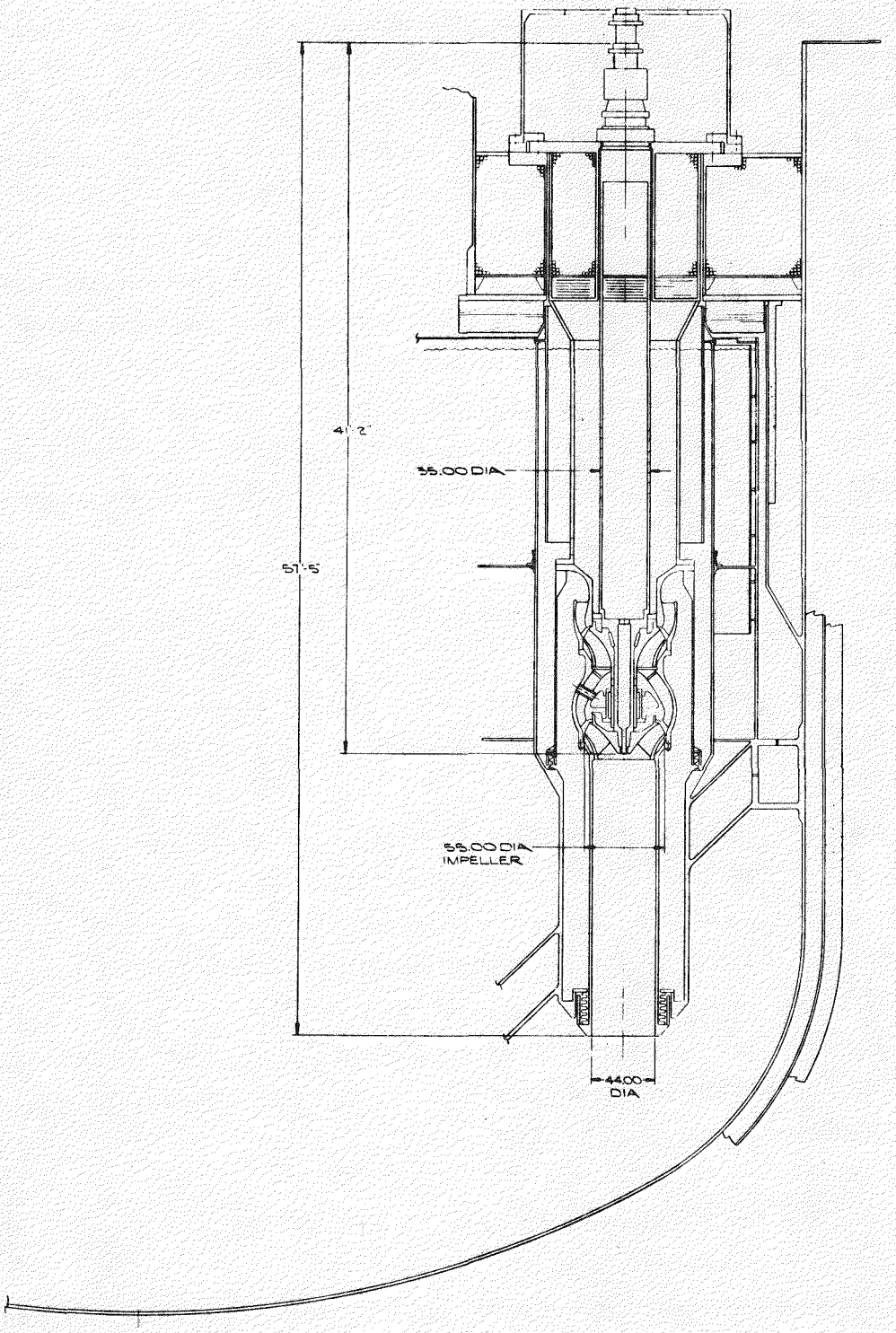

Figure H-2. Large Pool Reactor Primary System Pump Concepts

apparently being implemented in the French Super Phenix reactor now under construction. In other pool-type plants including EBR-II, Phenix, PFR and the CDFR design, the SPS is located outside of the reactor vessel in shielded cells. IN PFR, parts of the SPMS including the plugging meters and one or more impurity monitoring meters are installed inside the reactor vessel. A study was performed to compare the characteristics of the in-vessel and ex-vessel locations for these auxiliary systems.

SODIUM PURIFICATION SYSTEMS

The significant characteristics of the reference in-vessel SPS conceptual design are described in 2.3.10.1, Volume 1. The major benefits of the in-vessel concept are:

- o No primary sodium is transported out of the reactor vessel; therefore, the possibility of having a leak of radioactive sodium from the SPS to cause a fire, concrete reaction, radioactivity release, etc. is precluded.
- o Additional steel-lined, shielded, inert cells to confine the radioactive cold traps inside the containment building are not required. Inerted guard pipes surrounding the NaK cooling lines are needed, however, to protect against a NaK fire inside containment.

The benefits of having the SPS located in a separate cell as shown in Figure H-3, are as follows:

- o Maintenance operations, including the complete removal of major SPS components, can be carried out on the ex-vessel system without shutting down the reactor. Since maintenance of the in-vessel cold trap entails opening the primary coolant boundary by removal of a shield plug in the reactor deck, reactor shutdown would be necessary. Because cold trap systems have historically required relatively frequent maintenance, the availability of the plant is expected to be greater with the ex-vessel cold trap.
- o With the ex-vessel SPS located in a cell adjacent to the reactor cavity, the sodium is transported between the reactor and the SPS through small pipes (2 or 3 in) running below the deck. The reactor design is considerably simplified with the

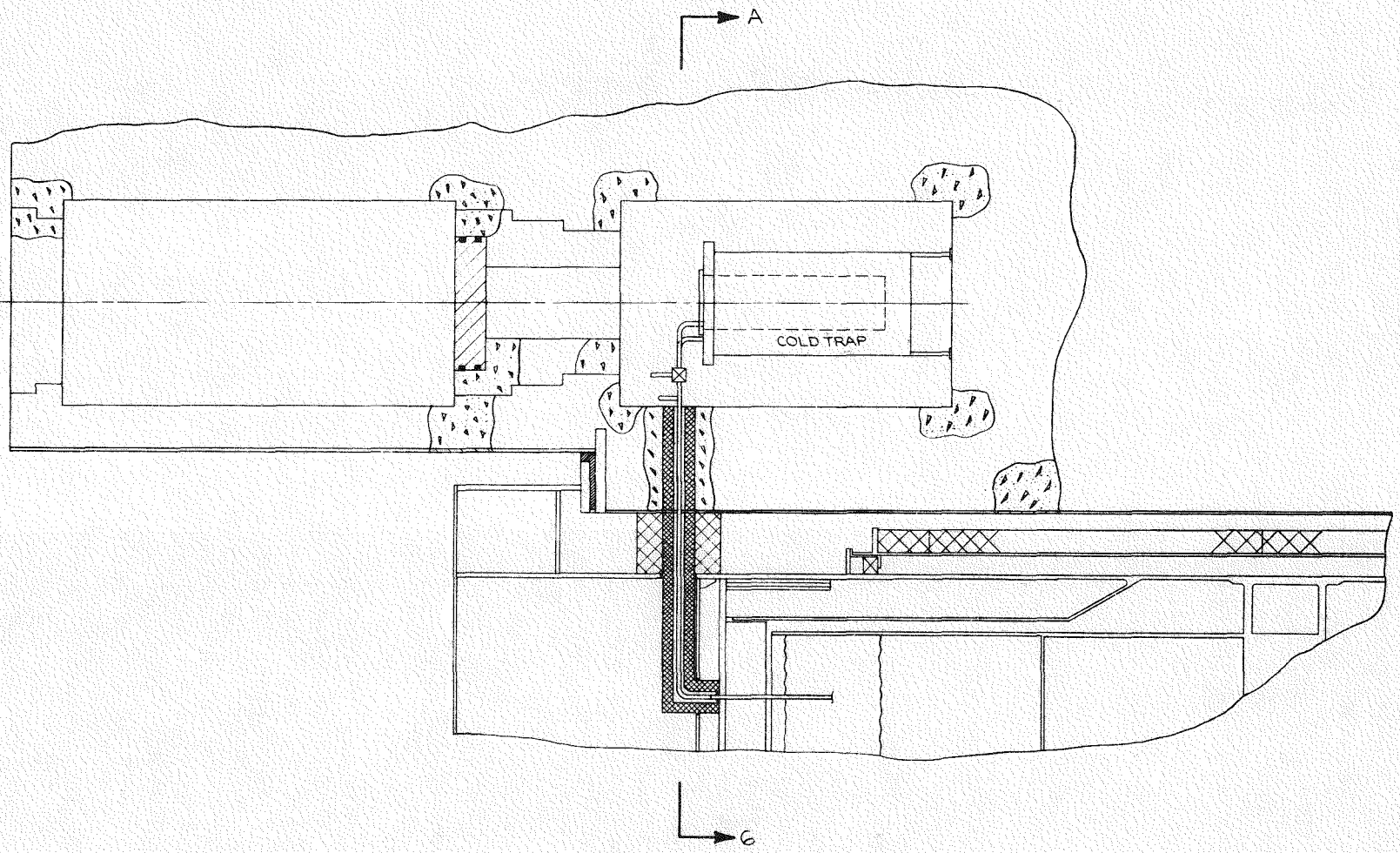

Figure H-3. Ex-Vessel Cold Trap Concept

ex-vessel concept because the large deck penetration for the SPS thimbles and the large guard pipes for the NaK coolant lines are not needed.

- No significant cold trap system component development is required for the ex-vessel concept because most equipment designed for FFTF and CRBRP can be adapted readily for use in the LPR. For the in-vessel location, the entire system must be designed for the 950°F environment of the hot pool. A small EM pump which can operate at that temperature without cooling is not commercially available in the U.S. and a development program would be required to produce an acceptable component.

- Because of the ample space available in an ex-vessel cell, inert gas cooled crystallizers can be used rather than the relatively expensive NaK cooled systems needed for the very compact in-vessel design. Also, the ex-vessel location offers the potential to use regenerable crystallizers designed to be flushed out during periods when no cold trapping is being done. With such a design, the crystallizer mesh never becomes filled with impurities and, consequently, does not need replacement during the plant lifetime.

SODIUM PURITY MONITORING SYSTEM

The significant characteristics of the reference in-vessel SPMS are described in Section 2.3.10.2, Volume 1. The major advantages of the in-vessel location for the SPMS are the same as those previously given for the SPS: (1) radioactive sodium leaks from the systems are absolutely prevented; and, (2) inert cells to confine these systems do not need to be provided.

The major advantages of having the SPMS components located in inert cells adjacent to the reactor vessel are as follows:

- Maintenance operations can be performed on the ex-vessel systems without shutting down the reactor. Thus, plant availability should be less affected by SPMS failures.

- A simple fan cooled plugging meter developed for FFTF and CRBRP can be used in the cell location. The in-vessel installation requires a somewhat more complex NaK cooled plugging meter.

- Existing FFTF/CRBRP impurity meters (oxygen, hydrogen and carbon detectors) may be used in ex-vessel cells with little or no modification. Incorporation of impurity meters into a thimble configuration for in-vessel use requires more design and testing effort and can possibly involve problems with European patents.

- With the ex-vessel concept, a reasonably large hot cell (about 1000 ft^3) is provided adjacent to the reactor for the multi-purpose sodium sampling system. A cell of this size allows the radioactive samples to be handled by simple remote manipulators controlled directly by an operator viewing through a shielded window. With the cell located in or on the reactor deck, the space is restricted and more complex remote handling and viewing equipment is probably needed.

- With the SPMS located in a cell adjacent to the SPS cell, the SPS sodium pump and piping system can be used to supply sodium to the SPMS, therefore, no separate SPMS sodium circulation system is needed.

CONCLUSIONS AND RECOMMENDATIONS

The most significant results of the location evaluation are summarized in Table H-2. The principal benefits obtained by locating the SPS and SPMS inside the reactor vessel are (1), radioactive sodium leaks from these systems are absolutely prevented, and (2), inert cells to confine these systems need not be provided. Because the in-vessel SPS uses a NaK cooling system however, the potential exists for a NaK leak inside containment and, therefore, inert guard pipes must be installed around the NaK pipes to preclude a fire. The consideration of providing additional inert cells is not extremely significant because adequate space is available in the containment building around the reactor cavity for the 6 small cells (about 1000 ft^3 per cell) needed to house the SPS and SPMS.

The most critical problems associated with the in-vessel location are: (1), the systems cannot be maintained without shutting down the reactor; (2), the design of the reactor vessel and deck is made more complicated; and (3) the designs of the SPS and SPMS are themselves more complicated.

TABLE H-2

SPS AND SPMS LOCATION EVALUATION SUMMARY

Design Consideration	In-Vessel Location	Ex-Vessel Location
1. Potential for radioactive sodium leak, fire, concrete reaction, release etc.	None	Low probability.
2. Structures inside containment.	Requires guard pipes for SPS NaK lines and two inert cells in deck for sodium samplers.	Requires 6 small inert cells adjacent to reactor cavity.
3. Maintainability	Reactor shutdown required for any maintenance.	All maintenance may be done with reactor operating.
4. Plant availability	Reference	Better than reference because of maintainability.
5. Reactor deck design	Requires 2 large deck penetrations for cold traps and 4 small penetrations for SPMS equipment. Also needs inert cells in or on deck for sodium samplers.	No deck penetrations required. Small primary sodium lines exit reactor vessel shell extension near the bottom of the deck.
6. Component development	Requires development of: 1. SPS sodium pump for 950°F service, 2. New multi-purpose sodium sampler design 3. Impurity meter designs	Can utilize FFTF and CRBRP equipment with little modification. Regenerable crystallizer concept would require development.
7. Design flexibility	Space limitations demand very compact system packaging and limit flexibility. Must use NaK as cold trap coolant.	Cells provide adequate space to allow use of: 1. Conventional equipment and arrangements 2. More bulky gas cooled cold traps. 3. Regenerable crystallizers

On the basis of this study, it is concluded that the ex-vessel location is preferred to the in-vessel location for both the SPS and the SPMS. It is recommended that EPRI consider changing the guidelines for future LPR design studies to allow the design for both of these auxiliary systems to be developed for the ex-vessel location.

H.4 COMPONENT REMOVAL FOR MAINTENANCE

The procedure for removal of major components from LPR for maintenance, involves the use of an inert transfer cask to move the components from the reactor to the Equipment Transfer Cell. Sodium removal and decontamination must be done either in the cell or in the maintenance building to make the components available for hands on maintenance. Decontamination in the cell requires that all decontamination and sodium removal processing equipment and chemicals be integral with the equipment transfer cell air-lock. As an alternate to this, it is possible to eliminate the decontamination functions from the equipment transfer cell, by retaining the component in the cask, and transporting the cask through the equipment transfer cell to a separate decontamination area remote from the reactor containment building. Both of these options are discussed in this Section.

H.4.1 DECONTAMINATION AWAY FROM THE CONTAINMENT BUILDING

By separating the decontamination bay from the equipment transfer cell, the equipment transfer cell is always maintained clean and available to handle other components, thus expediting the ingress and egress of equipment to and from the containment building. Also, the cell does not have to be sealed and inerted.

The main disadvantage of this alternative is that the size of the opening into the equipment removal room must be large enough to pass not only the component, but also the cask and a bottom closure which can be either a cover or a valve. With the present cask design, there is insufficient room to accommodate a pass through opening large enough to accomodate a gate valve without impacting the diameter of the containment building. The use

of a flapper type valve at the bottom of the cask is compatible with the current opening size; however, a higher containment is needed for the additional height of the flapper valve. The possibility exists that the cask could be closed and sealed after it is lifted from the floor valve. This approach would not require added containment height.

H.4.2 DECONTAMINATION IN THE EQUIPMENT TRANSFER CELL

If sodium removal and decontamination activities are done in the equipment transfer cell, the cell must be designed to be sealed and inerted. With this option, the component transfer casks never leave the reactor containment building. The cask is equipped with its own bottom gate valve similar to the one on the floor valve. After the component is raised up into the cask, the cask valve is closed along with the floor valve. This operation safely seals the component within the cask in an argon environment.

When the cask is positioned over the transfer hatch to the equipment transfer cell, it is mated to a floor valve attached to the hatch cover. This double valve arrangement assures that the inert atmosphere of the cell can be maintained during transfer of the component into the cell. The cell atmosphere is nitrogen, therefore the cask must first be purged of its radioactive argon and backfilled with nitrogen. Both valves are then opened and the component is lowered into the cell where sodium removal and decontamination processing are accomplished. After the component is clean, it can be handled in air and moved to any convenient shop for the required maintenance.

The advantage of this system is that no radioactive material ever leaves the reactor containment building (except for the cleaning process residue which is handled in approved waste containers). Also, the added weight of the transfer cask and related shielding does not have to be considered in cell handling operations or shipping equipment used to move the component to the maintenance facility. The basic disadvantage is that the cell design must be more complex, and cell availability may be impacted by any extensive cleaning process that may be required.

H.5 VESSEL BOTTOM HEAD CONFIGURATION

When the LPR reactor vessel was first configured, a torispherical bottom head was selected to minimize the total vessel length. At that time, the IHX configuration was unknown, and it was assumed that the IHX bottom discharge would occur at the face of the bottom tube sheet. The recent work effort has resulted in definition of the IHX, and the bottom discharge is actually six feet below the face of the tube sheet. Also, the discharge opening is reduced which results in a higher discharge velocity which will impinge on the reactor vessel. The flow streams and mixing which occur in the bottom inlet plenum are the subject of an on-going flow model test, and the results will not be available until the fourth quarter of 1978. However, it is recognized that some type of flow diverter is required at the bottom of each IHX to protect the vessel shell from sudden thermal transients, and to promote mixing in the cold plenum. The space currently provided by the vessel torispherical head is inadequate for adding any such diverter.

There are two ways in which the cold sodium plenum can be increased: 1) increase the length of the cylindrical portion of the vessel; or 2) replace the bottom head with a hemispherical head. The latter method, using a hemispherical head, is the most effective way of achieving the desired result. The increased axial length is not required out at the 75 ft diameter of the vessel, but is required at the 54 ft diameter where the IHXs are located. The hemispherical shape is more effective in providing the increased length where it is needed. Also, the hemisphere is the most efficient shape for containing a given volume; thus, its use would be expected to result in minimizing vessel weight, material requirements, and sodium inventory. Also, the tooling requirements to form a spherical shell are considerably less than that needed to form the knuckle sections of a torispherical head. It is judged that a hemispherical shell is less expensive to manufacture.

The only objection to using a hemispherical head is that the overall vessel length is greater than that of a comparable design with a torispherical head. This requires a deeper reactor cavity, higher containment building, etc.

A strict trade-off study is needed to determine the optimum shape from a total cost standpoint. Time does not permit such a study, and since both positive and negative cost differences exist, it is judged that the net delta cost change would not be significant. Thus, the next iteration on design will use a hemispherical bottom head on the vessel.

APPENDIX I

SELECTION OF REFERENCE PUMP CONCEPT FOR THE LPR

I.1 INTRODUCTION

The LPR requires four primary sodium pumps that can operate submerged in the sodium pool. A review of the current state-of-the-art for liquid metal pumps provided background information for selecting a primary pump for the LPR. Table I-1 gives the most pertinent information about the primary pumps for several operating or planned sodium reactor plants. Note however, that some of this information may not be the latest revision, and also that some values which were not directly available have been inferred. Of these pumps, the largest liquid metal pump to be built and operated is the SNR-300 Primary Pump, while the largest pump in the design stage for a committed plant is for the Super Phenix. Not shown in Table I-1 is the Large Sodium Pump under development for DOE, which will deliver 85000 gpm at 500 ft total dynamic head. This project is currently in a conceptual design phase where three pump vendors are competing with three different pump concepts: Byron Jackson - double suction, Westinghouse - two stage, and Atomics International - inducer/impeller. ARD is supporting this pump development with system requirements information. Table I-1 shows that the double suction pump design has by far been the most frequently employed concept. However, single suction/single stage, and single suction/double stage are also used.

I.2 DISCUSSION

The primary pump operating requirements used in the comparison of pump concepts are 61600 gpm at 334 ft total dynamic head. This is based on a primary pump flow of 26.5×10^6 lb/hr (106×10^6 lb/hr total for all four pumps) as required by the LPR thermal-hydraulic design conditions.

TABLE I-1

PRIMARY PUMPS-SODIUM REACTORS

Plant	Pump Design	Capacity (GPM)	Total Head (Ft)	Speed (RPM)	$NPSH_A$ (Ft)	SN (Design Pt.)	Impeller Diam. (in)	Shaft Length (Ft)	Tank Diameter (in)
FFTF	Single Suction	14500	500	1110	40	8404	36	32	80
CRBR	Double Suction	33700	458	1116	53	7375	39	21	106 (Bowl)
PLBR	Single Suction w/Inducer	76300	500	870	30	18750	52	27	100 (Bowl)
PFR	Double Suction	21120	317	960	48	5469	35	∿18	60
CDFR	Single Suction, Two Stage	40000	397	480	57	4628	61	34	81
Phenix	Double Suction	18388	250	925	47	∿7000	∿32	∿25	57
Super Phenix	Single Suction	79300	246	∿480	52	∿7000	∿63.5	∿38	98
SNR-300	Single Suction	23300	459	960	42	8780	33	23.5	75 (Bowl)
SNR-2	Double Suction								
BN-350	Double Suction	14091	361	970					
BN-600	Double Suction	42712	312	970	∿65	∿8800	∿36	∿16	∿72
LPR	Single Suction Two Stage	61600	334	492	50	6500	55	46	104

To evaluate different pump concepts, the available NPSH at the pump suction must be determined. Based on a cover gas pressure of 1 atmosphere absolute (≈41 ft of sodium) and assuming an IHX pressure drop of about 8 ft, a suction pipe entrance loss of 3 ft, and an impeller located 20 ft below the hot pool sodium level, there will be ≈50 ft of NPSH. The scoping calculations for this study were therefore based on 50 ft of available NPSH, and the results are listed in Table I-2 for several pump concepts.

The three pump concepts most seriously considered include the single stage/single suction, double suction, and two stage. Suction specific speeds (S_n)* of 10,000 to 4,600 were used in scoping calculations to cover the spectrum from a slight extrapolation of the FFTF pump (8,700) to very conservative low noise pumps (4,600). For comparison only, the scoping calculations also include an inducer pump designed for 16,000 suction specific speed. From Table I-1 it is apparent that pool type reactor plants generally utilize a lower S_n than do loop type plants. There are several reasons for this; higher NPSH is usually available in the pool, and low hydraulic noise is preferred in the pool in order to facilitate the use of noise monitoring. An additional concern is that a high level of hydraulic noise may result in high cycle fatigue damage to structural components.

It is generally recognized that a pump falls in the low noise category at suction specific speed below 6800, based primarily on the British experience. Based on the desire to use a low noise pump in the pool to minimize flow induced vibration in the closely coupled pool geometry as well as cavitation damage in the pumps, a suction specific speed of 6500 was chosen. Such a conservative number virtually eliminates the chance of any long term cavitation damage to the pump, thereby reducing the possibility of having to service the pump hydraulic section over the life of the plant.

---

* $S_n = \dfrac{n \cdot Q^{0.5}}{NPSH_A^{0.75}}$

n = pump speed, RPM
Q = flow, GPM
$NPSH_A$ = available net pump suction head, ft

TABLE I-2

RESULT FOR SCOPING CALCULATIONS
FOR PRIMARY PUMP CONCEPTS

Pump Concept	Suction Specific Speed (per inlet)	Pump Speed (RPM)	Specific Speed (N_S)	Approximate Impeller Diameter (in)	
Single Suction, Single Stage	10,000	757	2,407	50	
	8,400	497	1,580	72	$NPSH_A$ = 36 ft*
	6,500	492	1,592	75	
	4,628	350	1,114	98	
Single Suction and Inducer	16,000	1,211	3,851	35	
Double Suction, Single Stage	10,000	1,071	2,407	37	
	6,500	696	1,564	52	
	4,628	496	1,114	70	
Single Suction Two Stage	10,000	757	4,048	39	
	8,400	355	1,899	72	$NPSH_A$ = 23 ft*
	6,500	492	2,630	55	
	4,628	350	1,873	73	

*Lower $NPSH_A$ as a result of shortening the length of the pump. This was done to investigate the effect of submergence on the impeller diameter.

Table I-3 gives a comparison of operating speed and impeller size for the three most promising concepts. The single suction/single stage concept was eliminated due to the large impeller diameter required and because the pump tank would exceed the 8 ft diameter set as an upper limit space envelope. Westinghouse Electro-Mechanical Division has indicated that impellers up to 60 in in diameter can be cast within the current state-of-the-art.

TABLE I-3

	Suction Specific Speed (S_n)	Pump Speed (RPM)	Impeller Diameter (in)
Single Suction	6500	492	75
Double Suction	6500	696	52
Two Stage	6500	492	55

The table also shows that the double suction pump and the two stage pump concepts are very similar in size. The two stage pump has a significantly lower shaft speed which is an advantage in avoiding dynamics problems with the relatively long shaft required in a pool type reactor. Due to the lower operating speed of the two stage pump, the drive motor is expected to be slightly larger and more expensive, but only marginally so.

The LPR configuration has discharge and suction lines which are concentric and plug into the core support structure. To use the double suction pump results in a complicated flow path, while the two stage pump has a simple flow arrangement. Westinghouse Electro-Mechanical Division (EMD) has been consulted on the relative merits of two stage versus double suction. Their view is that a two stage pump offers a simpler hydraulic design than the double suction pump and, as a result, its use is preferred.

I.3 CONCLUSION

Both double suction and two stage pump concepts are well suited to meet the performance requirements in the pool. The two stage design, however, offers the more practical solution for the plug-in pump concept, combined with the simpler and more conservative design in hydraulics and shaft dynamics. Westinghouse ARD adopted the two stage pump as a reference concept for the Large Pool Reactor.

APPENDIX J
INTERMEDIATE HEAT EXCHANGER DESIGN STUDIES

INTRODUCTION

The Intermediate Heat Exchanger (IHX) is a key component in the pool reactor plant. Due to its geometry and size and the number of units required for such a plant, it has a significant impact on the size and geometry of the pool reactor vessel and associated structures and components. Operating characteristics and ancillary equipment for the IHX may also have an impact on the pool reactor design and operation. During the development of the IHX conceptual design described in Section 2.3.6 (Volume I), several evaluations were made on specific areas of the IHX concept. These evaluations are summarized in the following sections.

PRIMARY COOLANT FLOW PATH

The guidelines for this study established that the primary coolant flow path should be on the tube side of the IHX. Previous experience with IHX loop type concepts has been with shell side primary designs. A brief evaluation was carried out to assess the advantages and disadvantages of the tube side primary IHX concept in relation to shell side primary designs.

When considering an IHX concept for a pool type reactor, primary pressure loss is limited by hot to cold pool level difference, or allowable pressure differentials between the hot and cold plena, and becomes a major influence in selecting the concept. For pool type reactors the IHX pressure drop is generally limited to 5 psi or below with a preferable pressure drop of ~2-3 psi. When allowable component pressure drop levels are this low, selection of an IHX concept employing primary flow on the tube side becomes attractive.

In the past for loop reactors the primary sodium flow has been maintained on the shell side rather than on the tube side. Studies (by FWEC) have shown that the most economic loop type IHX design from a component standpoint is a straight tube concept with a non-removable tube bundle, and with no central downcomer. These studies have shown that a reasonably high confidence technical design can be obtained only with relatively high component ΔP's (15-25 psi range) on the shell side. These units require very good flow distribution to ensure tolerable ΔT's between tubes. The cross/counterflow distribution needed necessitates the use of distribution plates that result in high coolant pressure drops. With a non-removable tube bundle in-place maintenance procedures become necessary. A shell side primary was favored for loop type reactors because 1) it is much easier to perform in-place tube plugging and in-service inspection on an essentially non-radioactive intermediate tube side rather than a highly radioactive primary tube side and 2) in the event of a Na-H_2O reaction from a steam generator leak, it is much easier to clean up a tube side intermediate than a shell side intermediate. For pool type reactors the primary side cannot be drained, so for maintenance on the primary side, removal of the IHX from the pool becomes desirable. Also IHXs for pool type reactors often employ integral auxiliary equipment (i.e., residual heat removal coils, isolation valves) that require IHX removal from the pool for maintenance purposes. For these reasons pool type IHXs are invariable designed for removal from the pool.

Although the reasons for not employing a tube side primary IHX concept for loop reactor applications noted previously can be pertinent for pool reactors, there are modifying considerations that come into play for pool reactor applications. Shell side primary IHX concepts have been employed in EBR-II and the operating French PHENIX reactor. These IHX concepts have had acceptably low pressure drops. However as size increases it becomes progressively more difficult to achieve a combination of acceptable pressure drops, necessary flow distribution, and an economic component. The UK, on the other hand, has selected an IHX concept with primary flow on the tube side for its pool type reactors. The bases for this selection were 1) thermal response of the internals, 2) low primary side pressure drop, and 3) easier decontamination of the radioactive primary side. In order to assess the

advantages and disadvantages of primary tube or shell side concepts for IHXs for pool type reactors, a tabulation of considerations is provided along with applicable pluses and/or minuses for each concept (see Table J-1).

The general conclusion reached from this qualitative assessment is that because of certain specific characteristics which are particularly attractive for pool reactor use, the straight tube, primary tube side IHX concept appears to be the best selection for the LPR design.

INTERMEDIATE HEAT EXCHANGER PARAMETER EVALUATION

Because of its geometry and size, the IHX has a significant effect on the design and layout of the pool reactor vessel and internals. It is the largest (both in diameter and length) of all the components that penetrate the deck structure and are hung in the pool. It also has the most units (6) of any of the primary components. This then results in the IHX design having the most significant impact of any of these components on the pool reactor vessel diameter and height and the internal structure size and geometry. The geometry of the IHX is substantially effected by the heat exchanger bundle design, auxiliary equipment design, and pertinent primary system design considerations. To relate these design variables and the system requirements imposed upon the IHX with their effect on the vessel and internals design, parametric evaluations were made and layout studies performed. On the basis of these evaluations a reference IHX geometry was chosen.

TUBE BUNDLE SIZING

A series of parametric tube bundle sizings were made for the IHX based on the reference pool reactor plant thermal design conditions. These parametric evaluations were performed employing the IHX sizing model of the PLANO* computer code. This code is a program for the optimization of a sodium cooled fast breeder reactor plant. The parameters assessed included the following:

*PLANO: A Computer Code for the Optimization of a Sodium Cooled Fast Breeder Reactor Power System, J. D. Mangus and G. R. Marlatt, WARD-102, July, 1969 (Westinghouse Proprietary Class II).

TABLE J-1 TUBE/SHELL SIDE PRIMARY COMPARISON FOR POOL IHXs

Consideration	Tube Side Primary	Shell Side Primary
1) Hydraulics	o Low ΔP (~2-3 psi) and good flow distribution easy to achieve. o Intermediate flow is on high ΔP shell side; no limitation on ΔP on intermediate side.	o Low confidence for acceptable combination of low ΔP, necessary flow distribution and desired geometry for straight tube concept. o For bent tube concept, low ΔP less sensative to flow maldistribution; achievable but difficult to fabricate.
2) Structural and Geometry	o Maximum flexibility on selecting tube bundle geometry. o Shell thicker as design must consider sodium/water reaction. o Lower max. bundle elevation as upper tube sheet must be below minimum sodium level. Natural circulation cooling considerations.	o Straight tube designs have significant geometry restrictions placed on bundle. o Geometry restrictions eased with bent tube designs.
3) Decay Heat Removal	o Natural clear space available above tube sheet for decay heat cooling coils. o Placement of decay heat cooling coils above tube sheet results in lower max. bundle elevation further below minimum sodium level.	o Location of decay heat removal coils more difficult Most potential locations result in increased unit diameter.
4) Scale-Up Potential	o Small effect of geometry on ΔP permits flexibility in designing optimum bundle and results in minimum impact on scaling plant design.	o Difficult to extrapolate straight tube concepts to large sizes and still meet hydraulic requirements. o Bent tube designs can be extrapolated and still meet hydraulic design objectives but are difficult to fabricate.
5) Maintenance	o Easier to decontaminate deposited active corrosion and fission products (important to a removable unit).	o Can perform in-place tube plugging and inspection. (Since pool IHXs are removable, this becomes less important than for a non-removable loop type IHX bundle) o Easier to clean up sodium water reaction products carried into an IHX in event of a sodium-water reaction resulting from a steam generator leak.

TABLE J-1 TUBE/SHELL SIDE PRIMARY COMPARISON FOR POOL IHXs (Continued)

Consideration	Tube Side Primary	Shell Side Primary
6) Thermal	o Accomodates tube bundle thermal differences and response. o Thicker shell more sensitive to thermal transients.	o Bent tubes may be required to accomodate tube bundle thermal differences in desired size range.
7) Cost	o Heavier shell is more costly. o Concepts envisioned with no heads would result in reduced costs. o Flexibility in design geometry due to hydraulic advantages tend to lower costs.	o Bent tube concept more costly than straight tube (bent tube may be required to meet thermal/hydraulic requirements). o Thinner shell less costly. o Formed heads for intermediate side result in added costs. o Geometry effects of hydraulic requirements tend to increase costs.

- o Tubing diameter
- o Tube bundle diameter
- o Tube bundle length
- o Tube bundle pressure drop
- o Number of tubes
- o Heat transfer surface area

The results of the analysis is illustrated in Figures J-1 through 4. Figure J-1 shows the interaction between tube bundle diameter and tube bundle length for different tube sizes. Figure J-2 illustrates primary pressure drop as a function of tube bundle lengths for different tube sizes. Employing the pressure drop information, the range of tube bundle geometries with primary pressure drops within the specified IHX pressure drop allotment (3 psi) were determined. These geometries were then employed in the assessment of the impact of the IHX on the reactor vessel and internals design. Figures J-3 and J-4 present the effect of tube bundle length upon 1) the number of tubes in the bundle and 2) the resulting heat transfer surface area for the bundle, respectively, for different tube diameters. These latter two figures illustrate economic considerations for the tube bundle as represented by the number of tubes to be installed and the heat transfer area required for the bundle.

REFERENCE GEOMETRY SELECTION

Employing the tube bundle parametric information discussed above, IHX space envelopes were developed along with system or component related location requirements. The space envelopes and location requirements were used to assess impact of the IHX on the pool reactor vessel and internal structures. The various IHX envelopes were examined to determine effect on resulting pool vessel diameter and height, deck structure layout, internal structure layout, etc. Factors that went into establishing the IHX envelopes and location requirements are as follows:

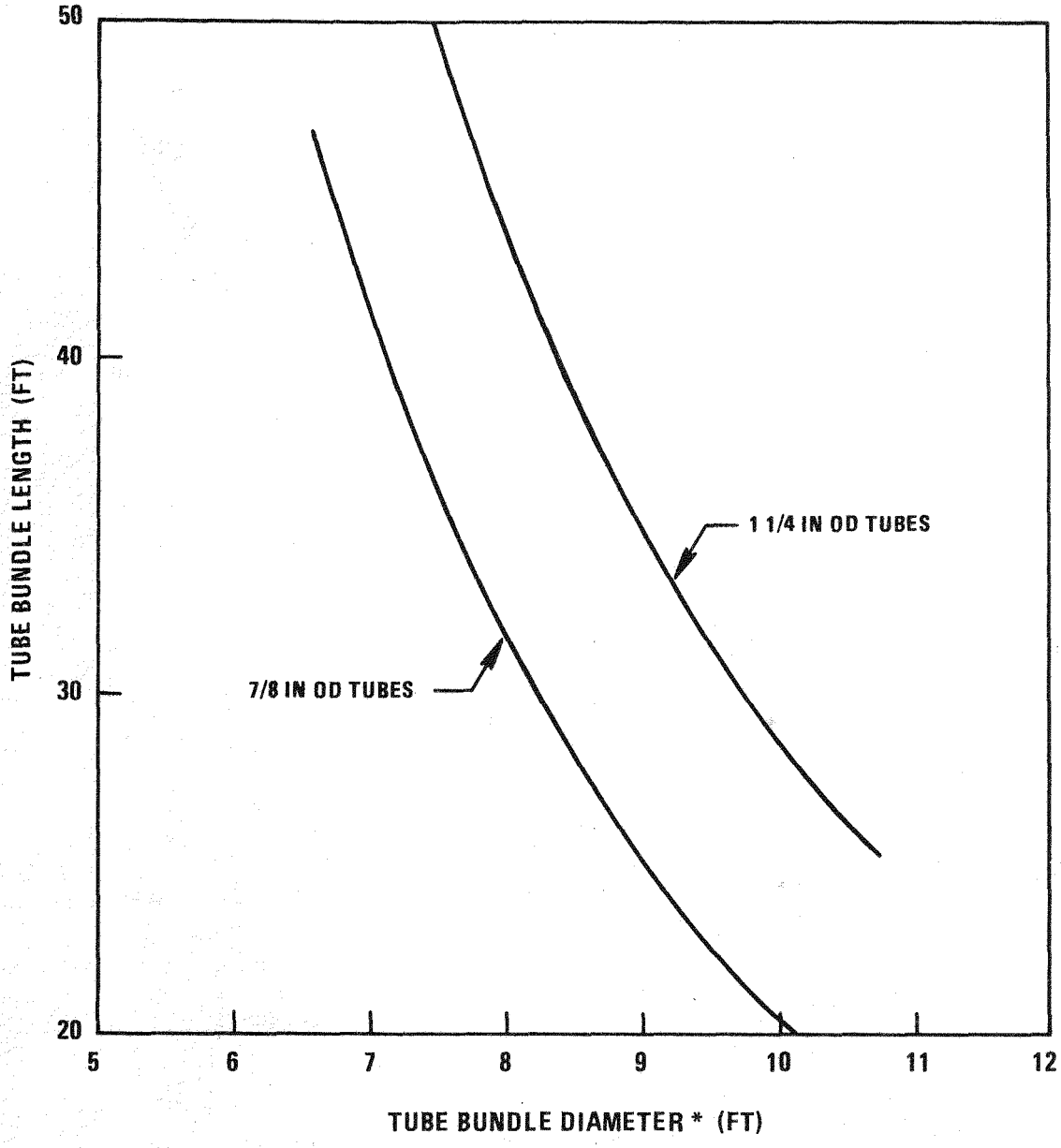

Figure J-1. Tube Bundle Geometry LPR Thermal and Hydraulic Design Conditions

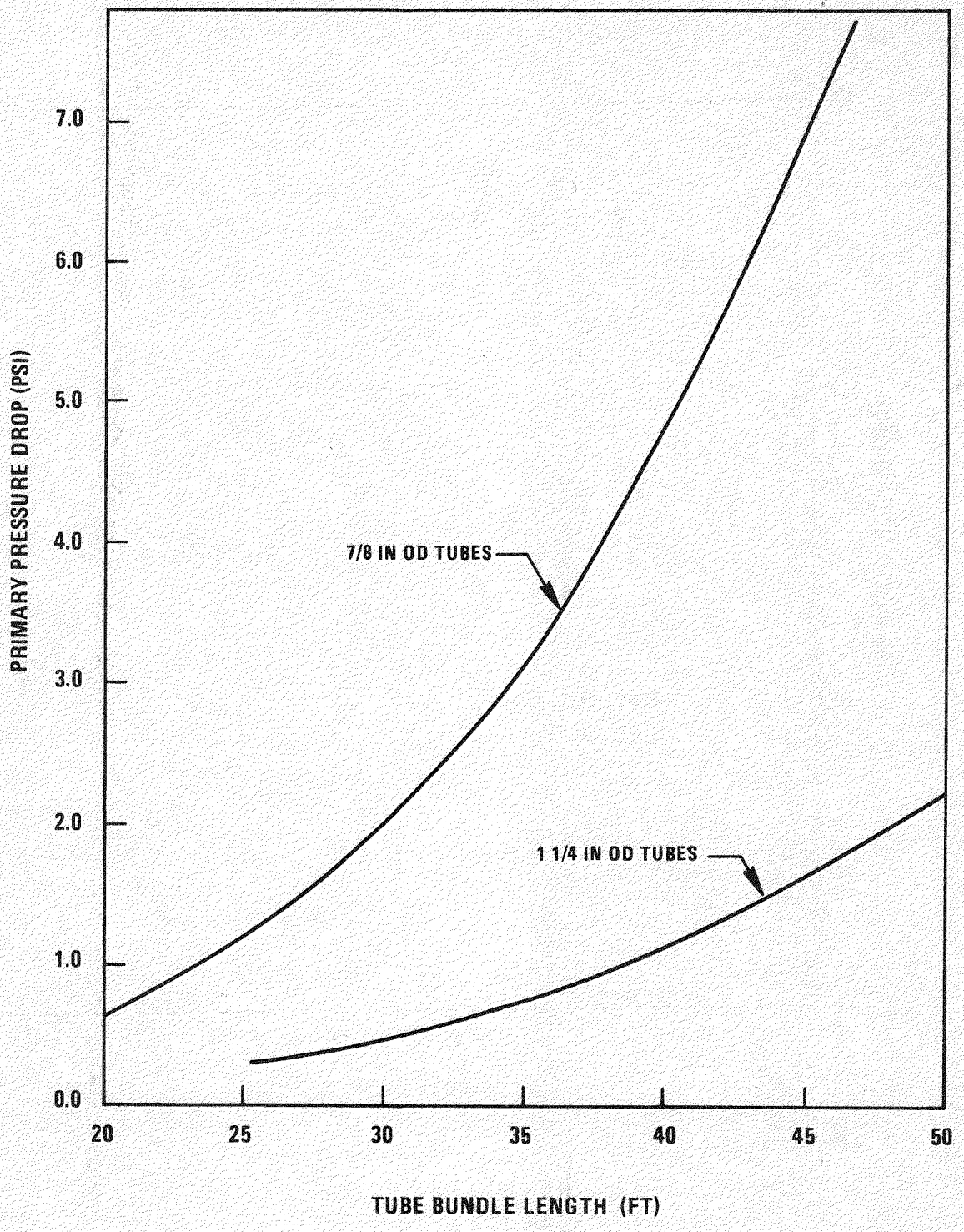

Figure J-2. Tube Bundle Pressure Drop LPR Thermal and Hydraulic Conditions

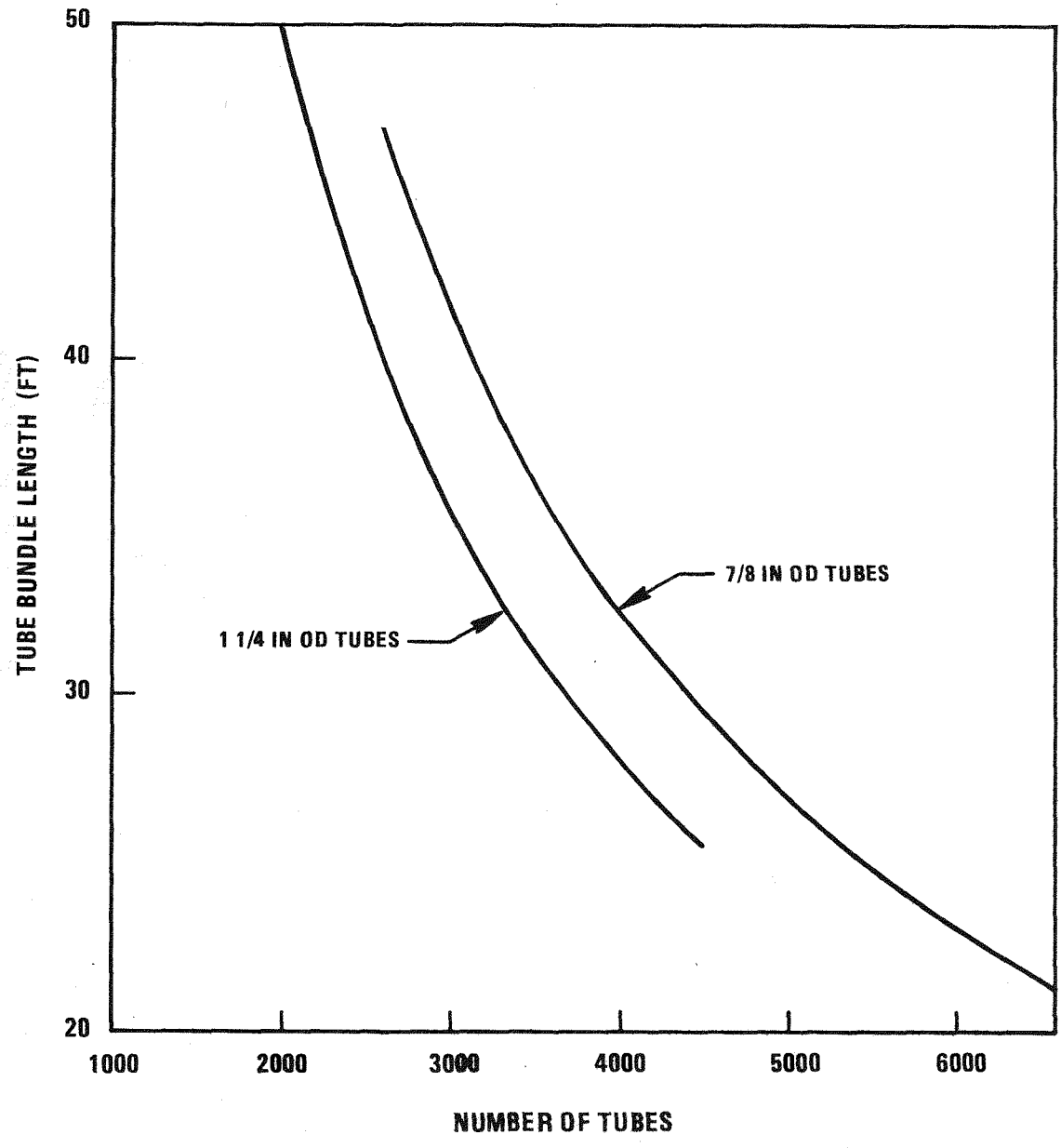

Figure J-3. Number of Tubes LPR Thermal and Hydraulic Design Conditions

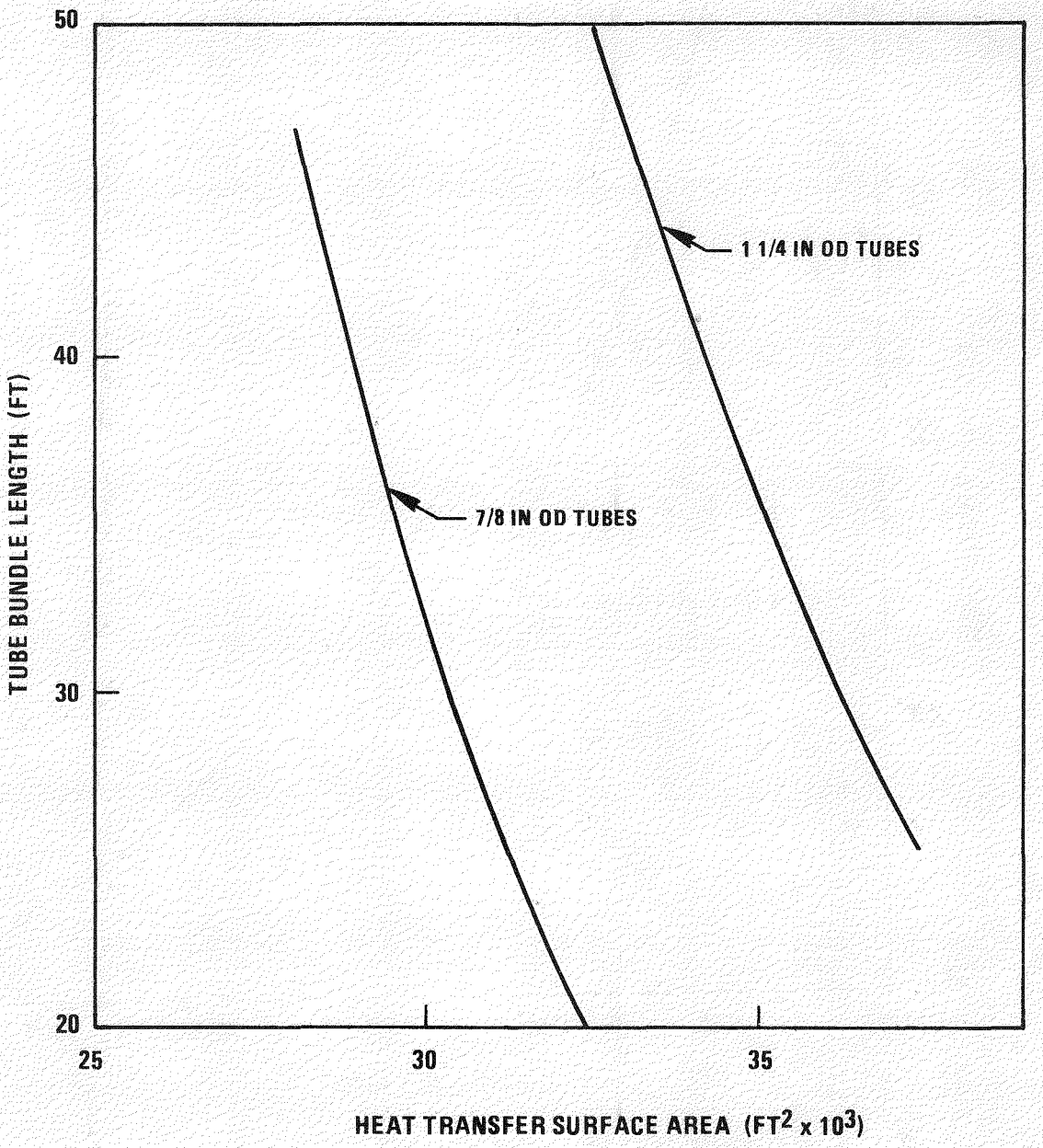

Figure J-4. Tube Bundle Heat Transfer Area LPR Thermal and Hydraulic Design Conditions

- Height allowance for tube sheets.
- Diametrical allowances for baffling and shell walls.
- Height allowance for primary outlet plenum and nozzle. This took into consideration minimizing pressure drop while providing for both tube bundle/shell differential expansion and IHX support at the lower end.
- Height allowance for clearance between primary outlet nozzle and the vessel wall. This is to minimize impingement and its effect on the vessel wall.
- Height allowance for the Passive Residual Heat Removal System (RHR-P) cooling coils in the upper plenum along with flow distribution space. The evaluation to determine the RHR-P cooling coil envelope is discussed in the Residual Heat Removal System Design Study (Ref. Appendix F, Vol. 3). These coils were designed to minimize the height of their envelope.
- Height allowances for cover gas space, thermal baffling, and shielding.
- Location of the IHX to allow for an adequate IHX/Reactor core thermal center differential elevation. Immediately following coast down of the pumps during a loss of power event and scram, the thermal center of the IHX is near the midpoint of the tube bundle. To ensure initiation of natural convection cooling prior to assumption of cooling duty by the RHR-P cooling coils, which are located fairly high in the IHX above the upper tube sheet, sufficient differential elevation must be provided between the core thermal center and the IHX thermal center to provide the necessary natural convection driving head.
- Location of the RHR-P cooling coils to ensure cooling capability under all possible events. To ensure this, the RHR-P cooling coils and the primary coolant inlet ports to the IHX must be located below the faulted sodium level. Then with a faulted level condition the primary coolant path will still be complete.

As a result of the assessment of the IHX envelope relative to the reactor vessel and internal structures, a reference IHX geometry was selected, which is reflected in the design descriptions of the Intermediate Heat Exchangers (Ref. 2.3.6, Vol. 1). The reference tube bundle is 27 ft long from tube sheet to tubesheet limits with a 25 ft long active tube length. 5480 tubes, 0.975 in OD with 0.045 in thick walls, are located on a 1.3125 in triangular

pitch, producing a maximum tube envelope of 9 ft 1 in in diameter. The intermediate coolant downcomer has a 24 in OD and the return annulus has a 36 in OD. The tube bundle shell has an outer diameter of 9 ft 11 in The thermal center of the tube bundle is located so that there is differential elevation of 10 ft between it and the thermal center of the core. The lower IHX plenum and primary outlet nozzle extend six feet beyond the lower tube sheet with the nozzle terminated approximately seven feet from the lower vessel wall. The RHR-P coil is five feet in overall height and is located within the support cylinder approximately one foot below the faulted sodium level and one foot above the upper tube sheet. The ouside diameter of the support cylinder is 10 ft 2 in and the primary coolant entrance ports that penetrate it are located below the faulted sodium level, which is 4 ft 7 in below the normal hot sodium level. The overall IHX length (nozzle to nozzle), which results when all considerations have been incorporated, is 63 ft 7 in, with 44 ft 7 in extending below the normal hot level of the pool. The IHX penetrates the deck through an 11 ft diameter hole. The mounting flange outer diameter is 12 ft 9 in. There is a high level of confidence that, when a more detailed IHX design is developed for the pool reactor plant, the reference envelope will be adequate for the design.

OUTLET NOZZLE EVALUATION

The reference primary outlet nozzle concept is necked down somewhat from the outlet plenum diameter. This reduction in diameter permits the use of a smaller sized expansion bellows. Yet, as presently conceived, this has small effect on the overall unit pressure drop, which is well within the design allotment of 3 psi. With the present design there is some concern with impingement of the primary flow stream exiting from this nozzle on the vessel wall, especially in relation to the effect of transients imposed by the impinging stream. The possibility of employing a flow diverter, which would direct the primary outlet stream into the lower plenum region and prevent direct impingement on the vessel wall, is being considered. It would be desirable from a space standpoint for the primary outlet nozzle and the diverter to be a smaller diameter than the present 66 in diameter nozzle. A reduction in the size of the nozzle would also have the added

benefit of reducing the expansion bellows from its present size. A preliminary hydraulic assessment was made of reduced nozzle diameters along with added diverters. Examination of the layout of the nozzle/diverter arrangements was also made to determine any effect on the vessel structure. The results indicated that a nozzle reduction to a ~40 in diameter, along with the addition of a diverter, could be made while still maintaining the IHX primary side pressure drop within its design pressure drop allotment. The layout evaluation showed that an increase in vessel length of 1 to 2 ft would probably be required to accommodate the revised concept. A decision on implementing this proposed revision has been deferred pending detailed hydraulic analysis of the lower plenum region and the proposed diverters.

IHX VALVE ASSESSMENT

From operational and availability considerations, it is desirable to be able to isolate the primary coolant flow from the IHX in each circuit. This will permit shutdown of the corresponding intermediate loop for maintenance operations, while still being able to maintain flow through the reactor core with the remaining loops. In order to select a reference concept for the IHX, a review was made of the following potential methods for isolation:

- Gas valve
- Butterfly valve
- Rotational sleeve valve
- Sliding sleeve valve

A brief summary of the considerations examined for each of these methods follows:

GAS VALVE

The initial impression of this concept is that it is very simple. A cylindrical bell is provided outside of the upper portion of the IHX, extending from the bottom of the deck structure down to an elevation below

the primary inlet ports (see Figure J-5a). Cover gas is introduced into the bell until it forces the sodium level within the bell down to a point where it is below the inlet ports. This concept will be leak tight. It will however, give on/off duty only and does not have the potential for even rough throttling capability that some of the other methods could have.

The gas controls required to implement this concept are relatively simple with a feed/bleed gas control arrangement being satisfactory. Sodium level can be determined by pressure indication of the gas within the bell. However, it probably would be very desirable to have a level indicator to measure actual sodium level within the bell. This would require penetrating the plug and upper plenum region of each of the 6 IHX units with such an instrument. The pressure requirement for operating the gas valve is approximately 3 psig.

In addition to extending down to a point below the primary inlet ports for shut off purposes, two phenomena necessitate extension of the bell further down below this point to prevent possible discharge of significant quantities of gas into the upper plenum region. These are as follows:

- During operation with an activated gas valve, the level within the primary side of the IHX will be depressed a distance equivalent to the pressure differential. If pump shutdown should occur, loss of the pressure differential will cause this depressed sodium level to rise and in turn the level in the bell annulus will be displaced downward. Allowance for this displacement would be required.

- The pool sodium will shrink during transient events. Allowance for the pool level change which reflects this shrinkage would be required.

It has been estimated that the bell should extend approximately 13 ft below the normal sodium level to ensure satisfactory operation.

A concern with this concept is the potential for gas collection within the bell during normal operation. Although not easily quantified, collection of entrained or released dissolved cover gas within IHXs has always been a

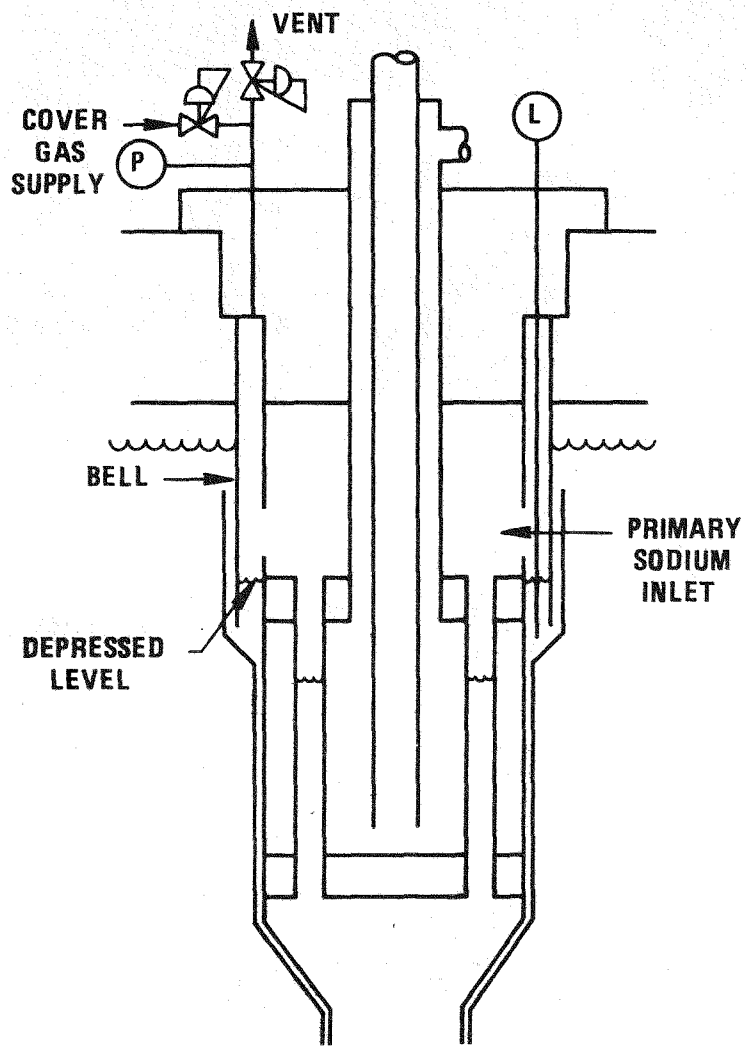

a) GAS VALVE

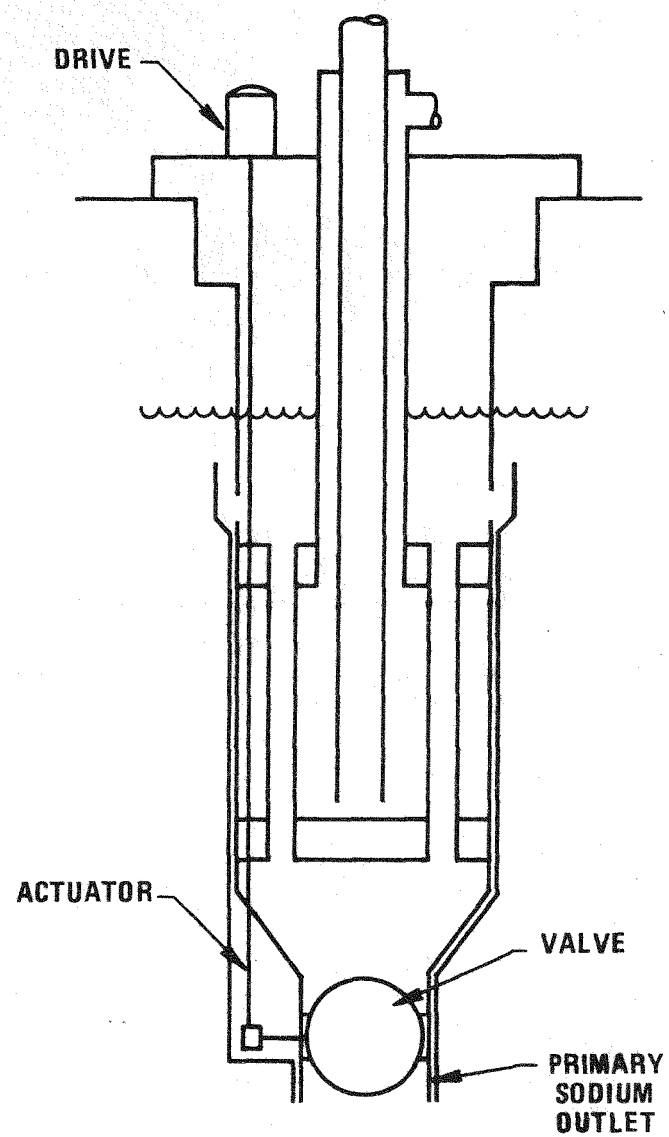

b) BUTTERFLY VALVE

Figure J-5.

significant concern. Employment of the bell structure for a gas valve results in the potential for trapping gases that may be evolved and released within the IHXs.

The present reference concept does not employ a shroud hanging from the deck structure that could be modified to make a bell. Presently there is a standpipe supported from the lower support structure. This standpipe is to ensure flow sweeping of the hot pool so there will be no stagnation within the pool. Even with the addition of the bell, the standpipe would still be required. With the addition of a bell structure within the standpipe, the flow path for primary coolant becomes very complex. This becomes of special concern when considering the natural convection cooling mode of operation.

It was concluded from the assessment that the gas valve should not be selected as the reference IHX valve concept.

BUTTERFLY VALVE

The UK has considered a butterfly valve as a possible alternative valve concept for CFR. In their design this valve is located in the primary outlet plenum of the IHX. Examination of this concept results in the conclusion that, taking the design of the upper portion of the LPR IHX as the present reference concept, the only practical location for this valve would be in the IHX lower plenum (see Figure J-5b). This places the operating mechanism in the cold pool region, however, it also dictates that an actuator ~70 ft long be employed in order to reach from the top of the unit to the lower plenum region. This also means providing ways to accommodate the actuator. This would probably have to be done in one of the baffled regions. Locating the valve in the lower plenum region will result in an increase in length of the IHX with resultant impact on the vessel height. Finally, this type valve is generally not noted for tight sealing and therefore leakage could be a problem. It was concluded that this valve should not be selected for the reference IHX valve concept.

SLEEVE VALVE

The UK and the French both employ this concept. It is generally composed of a concentric cylinder that can be moved to block the primary entrance ports on either the outside or the inside of the inlet cylindrical structure. Either vertical or rotational motion concepts can be envisioned (see Figures J-6a and b).

Rotational Motion Valve

This concept would require a gearing arrangement the approximate size of the hanging support cylinder. This mechanism would probably have to operate under sodium and would be space consuming in the inlet plenum region. However, the most difficult aspect of this concept would be sealing. It is difficult to envision how sealing would be implemented for either inlet flow ports or flow distribution orifices. It was concluded that this valve concept should not be selected for the reference IHX concept.

Vertical Motion Valve

All existing plants that employ IHX shutoff valves use this basic concept, although the specific design approaches vary. The primary differences generally come about due to the method of sealing that is employed.

The UK design employs piston rings on the sleeve, which seal to the IHX support cylinder above and below the entrance ports when the valve is in the closed position. The French design appears to employ a combination of ring and face seals for its upper and lower sealing locations. Several methods of sealing were reviewed for applicability to this basic valve concept. These included the following:

1. Piston ring seals
2. C-seals

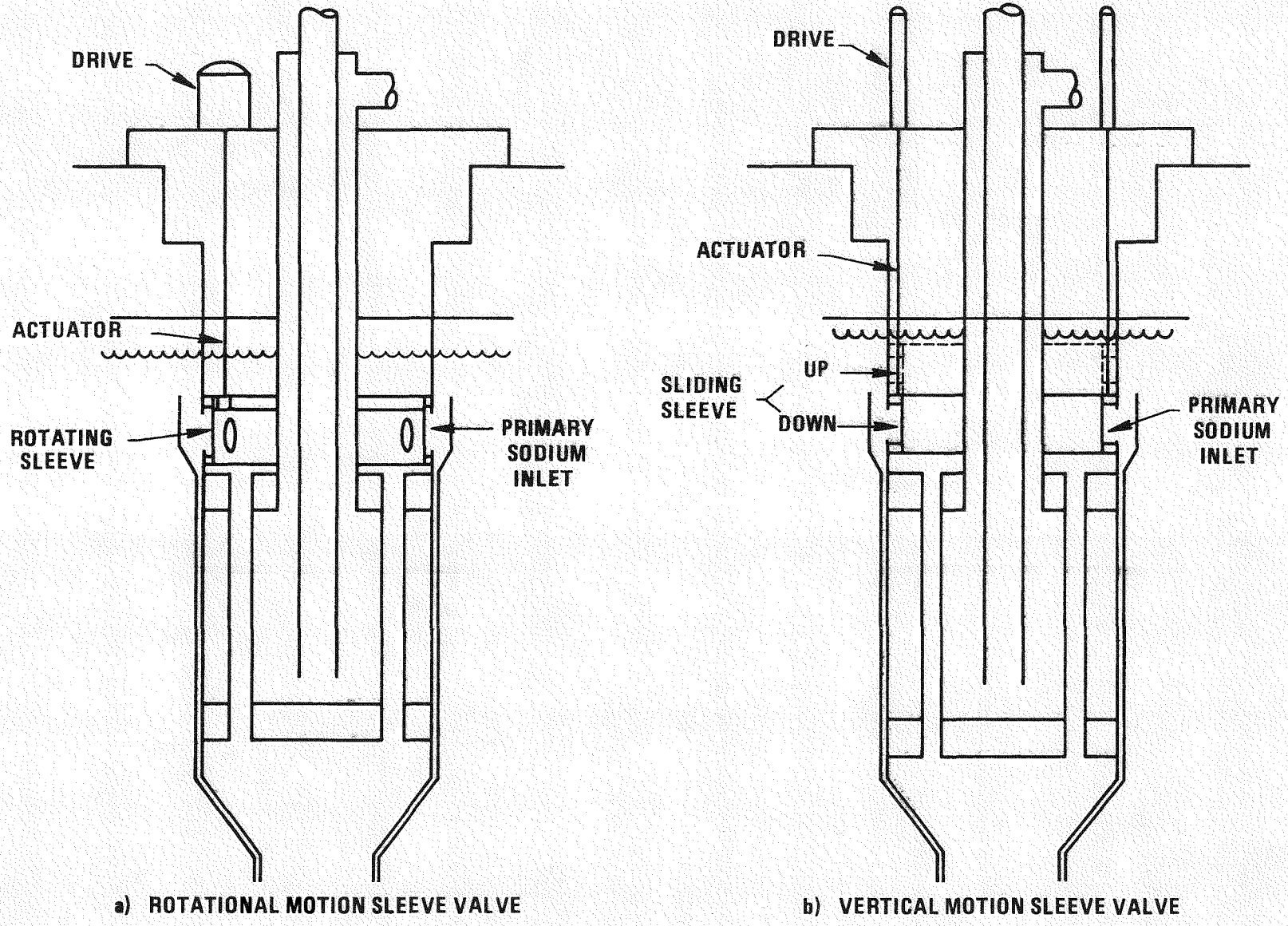
DRIVE
ACTUATOR
ROTATING SLEEVE
PRIMARY SODIUM INLET
a) ROTATIONAL MOTION SLEEVE VALVE
DRIVE
ACTUATOR
SLIDING SLEEVE
UP
DOWN
PRIMARY SODIUM INLET
b) VERTICAL MOTION SLEEVE VALVE

Figure J-6.

3. Spring seals
4. Bellows type face seal
5. Spring type face seal

Face seal concepts were felt to be sensitive to misalignment and thermal distortions. The noted face seal concepts included means for adding flexibility to adjust for misalignments or distortions.

These face seal concepts were more complex in design and required more space in the reference IHX concept. They also necessitated either supplemental ring seals at the upper portion of the inlet or the valve cylinders had to be extended above the sodium level. The piston ring, C-seals and spring seals were much simpler in concept. Although the C-seals and the spring seals both seem to have some promise, the piston ring seal was selected for the reference sealing method for the valve, due to the most experience having been had with it. The basic sleeve valve concept with the piston ring seals was then selected as reference concept for the pool reactor IHX, due to its simplicity, anticipated ease of operation, and minimal space requirements.

COMBINATION SHUTOFF VALVE AND IHX FLOW PLUG

A variation on the basic sleeve valve that was also considered, was a combination valve/flow plug. In this concept the valve would act as a shutoff valve when the IHX was in position in the pool, and would act as a flow plug or block if an IHX should have to be removed from the pool. To perform these duties, the cylindrical sleeve of the valve would have to be located outside of the shell. This would cause an increase in the size of the penetration through the deck structure and necessitate a plug-in-plug design, since the valve would have to be removed separately from the IHX. After examining this concept it was concluded that in order to operate the reactor with an IHX removed, the lower end of the IHX standpipe would also have to be blocked to prevent either 1) unwanted circulation into the empty IHX cavity from the plenum below, or 2) draw down in the empty IHX cavity

due to the loss of the IHX flow resistance. It was then concluded that a maintenance plug with a dummy IHX shell, that would fit into and seal the IHX standpipe, would be a more desirable concept. This maintenance plug would fit into the same deck penetration as the IHX and would block flow at both the top and bottom plenums. One such reusable plug per plant, or perhaps one available from a central service facility should be satisfactory for this function.

REFERENCES

1. Final Report Commercial Breeder Intermediate Heat Exchanger (IHX), FWC/FWEC/ND-75/52, Nov. 7, 1975.

2. Interim Report Commercial IHX Follow-on Study, FWC/FWEC/ND-76/141 May 7, 1976.

3. Redirected Work Final Report Commercial IHX Follow-on Study, FWC/FWEC/ND-76/40, July 30, 1976.

4. Final Report Commercial IHX Study, FWC/FWEC/ND-76/58, November 30, 1976.

5. Prototype Fast Reactor Heat Transport System, D. Tayler IAEA-SM-130/57 IAEA Symposium on Sodium Cooled Fast Reactor Engineering, Monaco, March 23-27, 1970.

6. Operation of PFR and the Influence, Upon the Design of CFR-I, A. D. Evens and W. Macrae, International Nuclear Industries Fair, Basel Switzerland, Oct. 7-11, 1975.

7. US/UK Breeder Reactor Component Design Meeting, Germantown Md., October 25-28, 1977.

APPENDIX K

PASSIVE RESIDUAL HEAT REMOVAL SYSTEM CONCEPT SELECTION

K.1 INTRODUCTION

The EPRI guidelines (Appendix L) require that both an active and a passive Residual Heat Removal System (RHRS) be provided in the LPR design. For the active RHRS, the concept previously developed for the PLBR was selected as the reference concept. A study was performed to select a passive RHRS (RHR-P) reference concept. The results of this passive system concept relation study are presented in this Appendix.

K.2 CONCEPTS

Numerous passive concepts were identified which could remove residual heat from the reactor vessel, however, most were discarded because they were deemed impractical or they failed to meet the important design guidelines. The three concepts which were judged to be the most promising after the initial screening process are shown in Figure K-1. Each of the concepts consists of: (1) a residual heat exchanger (RHX) located in the reactor vessel to accept heat from the primary sodium, (2) a natural draft heat exchanger (NDHX) located outside containment to reject heat to the atmosphere and (3) coolant piping to transport heat from the RHX to the NDHX by natural convection. The basic difference among the concepts is the placement of the RHXs within the reactor vessel.

In Concept A, the RHXs are placed inside the IHX, above the top tube sheet. During RHR-P operation, primary sodium flows by natural circulation from the hot pool into the IHX, over the RHX coils, into and through the IHX tubes to the cold pool, into the pump inlet and through the pump to the reactor inlet plenum, through the reactor core and back into the hot pool. This concept is similar to that used by the United Kingdom in PFR and CDFR.

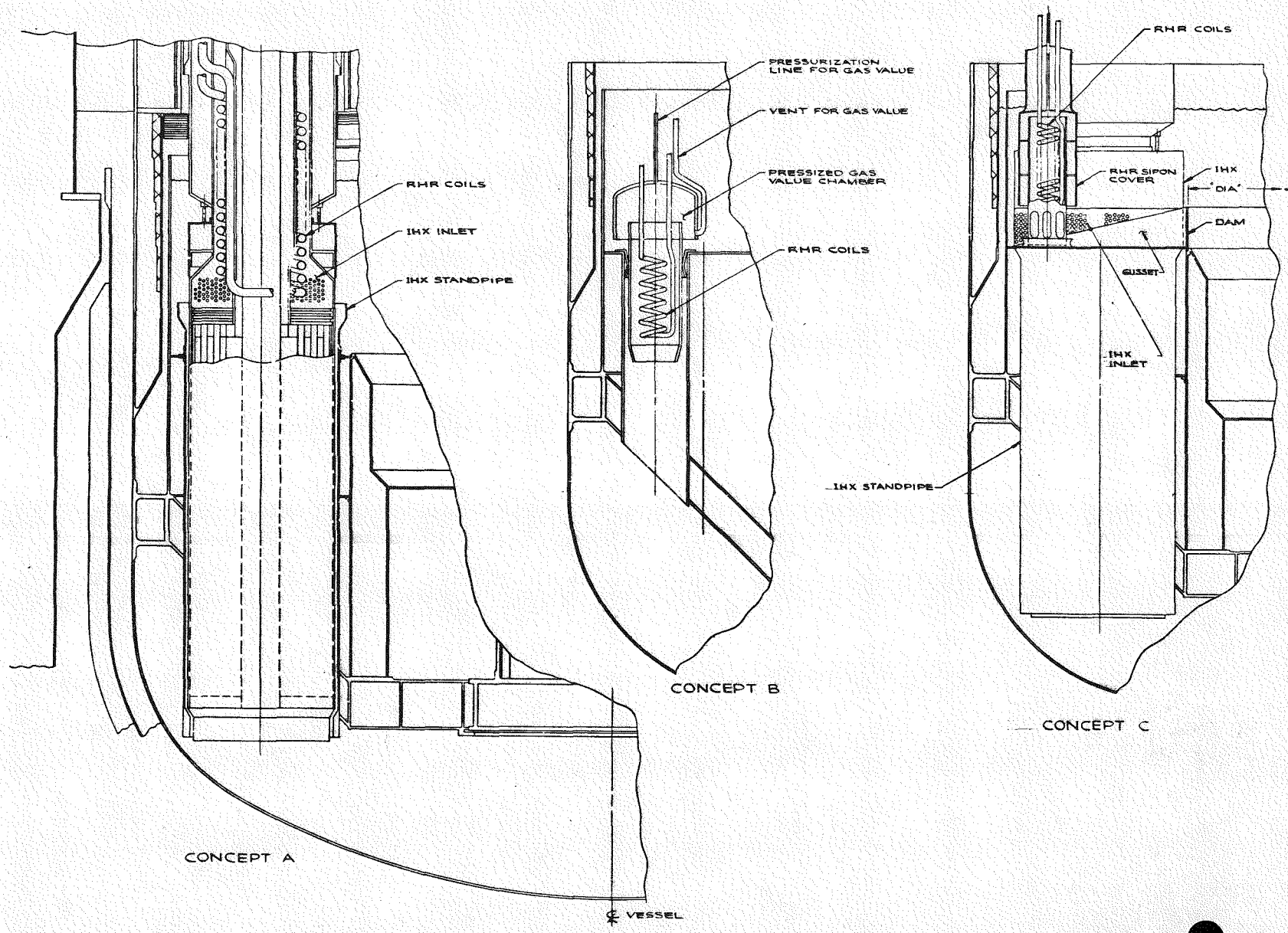

Figure K-1. Residual Heat Removal System Concept Selection

In Concept B, the RHXs are independent of the IHXs and are located in separate standpipes between the hot and cold pools. During RHR-P operation, primary sodium flows from the hot pool, into the RHX inlet, through the RHX tubes and into the cold pool to continue the flow circuit.

Concept C utilizes RHXs located in the hot pool having no standpipe connection to the cold pool. A dam-like structure is provided to enable the cooled sodium to flow in a stratified layer from an RHX outlet to an IHX inlet. The IHXs then serve as a conduit to carry the cooled sodium down into the cold pool to continue to flow circuit. After preliminary study, this concept was dropped from further consideration because the basic feasibility of the RHX to IHX stratified layer flow scheme was in doubt.

K.3 EVALUATION

After a preliminary study, it was concluded the RHR Concepts A and B are the only concepts having a reasonable potential for providing acceptable performance and for meeting the EPRI guidelines. The most significant characteristics of these two concepts were compared qualitatively and, on the basis of this comparison, it was concluded that Concept A should be adopted as the reference concept. The most significant points of comparison are discussed below:

- o Flow Continuity

  In Concept A, the primary sodium flow path is the same during RHR-P operation as it is during normal reactor operation. This means that, following a loss of electrical power, a continuous transition can be made from the forced circulation conditions which exist during the pump coastdown, to the natural circulation conditions which develop after the pumps stop. In Concept B, a new primary sodium flow pattern must be set in motion as the RHXs begin to take over the cooling function from the IHXs. Since it is obviously easier to continue an existing pattern of fluid motion than it is to change or initiate a new pattern, Concept A has a clear superiority in this regard.

- o Flow Resistance

  In Concept A, the IHX tubes serve as the conduit to carry the sodium flow from the RHX to the cold pool. In Concept B, the RHX standpipes perform this function. Since the cross section area of the more than

30,000 tubes in the 6 IHXs is many times greater than that which could practically be provided in a reasonable number (3 to 6) of separate RHX standpipes, Concept A offers a lower flow resistance for natural circulation.

- o Thermal Center Separation

  The forces tending to provide natural circulation are proportional to the vertical distance between the heat source and the heat sink. Because the RHX coil in Concept A can be very large in diameter (as large as the IHX) and short in height, the thermal center can be placed higher with respect to the core than in Concept B, which must use a smaller diameter and therefore longer RHX configuration. The higher RHX thermal center gives Concept A an advantage over Concept B with regard to natural circulation flow.

- o Analytical Modeling

  The dynamic behavior of the RHR and reactor flow must be analytically predictable with a high level of confidence to provide assurance to regulatory authorities that the plant meets safety requirements. It is expected that the dynamic behavior of Concept A will be significantly less difficult to predict accurately than that of Concept B in which the transition from forced to natural circulation involves stopping one flow circuit and starting another.

- o Independence and Diversity

  Concept B provides the most diversity from the normal reactor heat transport system because, once natural circulation is established through the RHX and standpipes, the IHXs are no longer needed as flow conduits to the cold pool.

  This does not appear to be an important advantage because no design basis event has been identified which could credibly block a significant fraction of the over 30,000 IHX tubes available to carry natural circulation flow to the cold pool.

- o Passiveness

  Because the Concept B RHX provides a direct flow path between the hot and cold pools, a device is required to block the flow of sodium from the hot pool to the cold pool during normal reactor operation. This device could be either a mechanical valve or a trapped gas bubble. In either case, some external automatic action is required to initiate RHR operation; therefore, Concept B does not meet the passiveness requirement of the EPRI guidelines.

- o Experience

  In the UK, a Concept A type RHRS is used in PFR and is being incorporated into the CDFR design. Operation of the PFR system has been successfully demonstrated under natural circulation conditions. A Concept B RHRS has not been used previously.

- o Reactor Design

  In Concept B, the RHXs require individual reactor deck penetrations and standpipes passing through the intermediate plenum. A larger reactor vessel diameter may also be required. Separate guard pipes are required above the deck to confine the RHR coolant piping.

  In Concept A, the RHXs have no significant inpact on reactor design and the coolant lines are run in the same guard pipes provided for the IHTS piping.

- o IHX Design

  To provide space inside the IHX for the Concept A RHX unit, the IHX tube bundle must be made about 5 ft shorter than it could otherwise be. Shortening the IHX tubes by this amount (i.e., from 30 ft to 25 ft), requires that the diameter be increased about 1 ft to maintain the necessary heat transfer area.

  The presence of the RHX unit increases the primary side pressure drop slightly but not enough to have design significance.

- o Maintainability

  In Concept A, the entire IHX must be removed to perform maintenance on the RHX unit. In Concept B, the individual RHX unit could be removed without disturbing any of the other reactor components. Because of the relative ease of RHX maintenance, Concept B would probably provide somewhat better plant availability.

K.4 CONCLUSION

The results of the concept selection study show that Concept A is the best Passive Residual Heat Removal System concept available. The most significant advantage of this concept is that the design of the reactor internals and deck are much simplified by having the RHXs located inside the IHXs rather than in separate standpipes. The most significant disadvantage of this concept is that the design of the IHX is made more complex and the diameter is increased by about 1 ft. The main advantage of Concept B is that a RHX located in a separate standpipe could be removed for maintenance more easily than one located inside an IHX.

The fact that Concept B requires an active flow control device is a significant disadvantage and a violation of the EPRI guidelines, although such a device could probably be made fail-safe for the loss of power situation.

Based on the evaluations which were made, it is recommended that the Concept A RHRS be selected as the reference concept and be incorporated into the LPR reference design.

APPENDIX L

GUIDELINES FOR EPRI LMFBR POOL DESIGN

The purpose of these guidelines is to reduce the time and effort devoted to consideration of alternative approaches during Phase "A". This will allow the effort to be concentrated on the critical engineering aspects of the pool concept in order to establish fundamental viability and in order to provide the basis for an EPRI determination of the relative design, construction, and operational characteristics of pool and loop LMFBR designs.

It is intended that Phase A design guidelines will continue on into Phase B work unless good reasons develop which merit a change in guidelines. If such justification does arise, the contractors are to bring it to the attention of the Sponsor's Project Manager and modified criteria and approach may be worked out by the Project Office and the contractor.

The primary aspects of pool design to be investigated are the primary tank and its support, the deck and plugs, and the primary tank internals. A preponderance of effort is to be devoted to a thorough understanding and to specific design drawings demonstrating reasonable engineering solutions of these three areas. It is recognized and, indeed, emphasized that many aspects of plant design must be considered in the course of such investigations.

The design guidelines are divided into three categories. Category I are those which are now established for use in Phase A. Category II lists those guidelines which are not completely finalized but must be settled very soon. The contractors are to decide on the approach that appears to them to be best and let the P.O. know within three weeks of receiving this document. The P.O. will then work with the contractors to finalize these guidelines. Category III are guidelines that need to be settled as soon as practicable but are not urgent because they have little influence on Phase A work but will be needed for Phase B and beyond.

I. CATEGORY I

1.	Plant Rating	1000 MWe Gross
2.	Sodium Reheat	None
3.	Mixed Mean (Thermal-Hydraulic) Reactor Outlet Temperature	875°F
4.	Reactor ΔT	200°F
5.	Concept	"Hot Pool"
6.	Steam Cycle	Saturated, 1000 psig, at Turbine Throttle
7.	Economic and Site Parameters	See Attachments A & B
8.	Safety Approach	See Attachment C
9.	Site Suitability Source Term	See Attachment D
10.	Operational Mode	Base Loaded

11. Reactor Core - It is recognized that core design and fuel cycle cannot be finally established until an acceptable approach from the viewpoint of proliferation and diversion are developed by other parallel efforts. The core concept to be assumed as the reference for the Phase A work is as follows: To minimize HCDA energy characteristics, a heterogeneous "bullseye" core will be used, as shown in Sketch 1. (The details of the bullseye core will be developed in later phases of this work. The assumptions on which Sketch 1 is based are described in Attachment G). The work of Phase A should be based on whole-core (batch) refueling, with the additional requirement that the capability for annual refueling shall be retained.

12. Primary Pumps and Valves

There shall be four mechanical primary pumps of minimum diameter practicable for the total assembly including drive and shield plug.

The assembly shall provide for a check valve or a shutoff valve that can be removed with the pump for any repair that might become necessary. If N-1 operation can be accomplished safely without a valve between each primary pump and the core inlet plenum, then these valves would not be required.

Both the pump and valve should be designed with the goal of not needing maintenance for the life of the plant. The valve must be of a very simple design with inherently high reliability.

The pump shall have a fixed support in the deck.

The drive assembly shall be removable without interrupting the function of the cover gas seal. The pump assembly shall be removable in an inerted silo. Flanges or other fastening and sealing surfaces are to be provided for the silo or other type removal device. Bags are considered impractical for such large heavy devices as the pumps because they would be subject to damage and resulting leaks.

Motor bearing and any shaft seal lubrication must be such that leakage into the sodium cannot occur. The arrangement used on the B-J pumps at EBR-II is a reasonable example.

13. Lower Support Grid and Inlet Plenums (Flow Control to Core and Blanket Assemblies)

There shall be two inlet plenums; one high pressure and one low pressure as discussed in the attached exerpt from "PLBR Project Office Review of Bullseye Core Studies", Attachment E.

The design shall provide a simple means for changing the split of flow between the high and low pressure plenums during the fuel cycle. Positive means shall be provided to limit the minimum flow to each plenum. The required flow split will be determined and verified by instrumentation which monitors the outlet temperatures of all core and blanket assemblies except those outer blanket assemblies not adjacent to core assemblies.

The design shall protect against a "core drop".

14. Intermediate Heat Exchangers

Use six IHX's of minimum diameter practicable consistent with other requirements such as low pressure drop and natural convection cooling. Shutoff capability shall be provided to preclude hot sodium bypass from the hot sodium zone to the cool zone if it should be necessary to operate with one of the intermediate sodium loops out of service. Assume that the reactor power would be reduced or shut down before the IHX shutoff would be accomplished.

15. Intermediate Heat Transport System

The plant design shall include six IHTS loops, each of which shall include one IHX, one mechanical pump (cold leg) and one steam generator. The design and layout of the IHTS loops shall be such that a break in the IHTS piping within containment shall not result in sodium fires or sodium concrete reactions. Shutoff valves shall be included in the IHTS. Consideration for sodium expansion and contraction on the IHX side of the valves must also be provided.

16. N-1 Loop Operation

The plant shall be capable of being operated while any single primary pump or any component of a single IHTS loop, including an IHX, is out of service.

17. Primary Tank and Guard Tank

The primary tank shall be cooled by inlet temperature sodium to attain an operating temperature closer to inlet than to outlet temperature, giving special attention to the upper portion of the tank where the inert gas covers the primary sodium and where the tank suspension is involved. Provisions should be made to allow the operator to control the temperatures of the primary tank wall from just above the sodium contact level to the support point. These temperatures must be controlable to within prescribed limits set by the design.

The tank diameter shall be minimized without excessive crowding. There shall be no penetrations of the walls of the primary or the guard tanks. All penetrations are to be through the top plugs and deck.

The primary tank shall be supported near the top. The guard tank shall be supported so as to avoid common mode failure and to avoid bumping in case of seismic accelerations.

Provisions shall be made to accommodate inspection of the outside of the primary tank and either the inside or outside of the guard tank. The primary tank surface is considered the primary coolant boundary for safety purposes.

The design of the primary and guard tanks shall provide for integrity testing when manufacturing and installation are completed. The NSSS designer should carefully define that which will be good and adequate testing to verify integrity before the primary tank is loaded with sodium.

18. Rotating Plugs and Deck

The deck and rotating plugs shall be insulated and cooled. A passive system is preferred but may not be feasible, in which case, forced circulation cooling would be needed. The structural integrity of the deck and plugs shall not require an active cooling system to be functioning at all times. The insulation must be capable of retaining a high fraction of its resistance to heat transfer throughout the 40-year life of the plant. Condensed sodium should drain back into the pool and not "short" the insulation. Insulation shall be chemically compatible (must not dissolve, swell, nor fall apart) with sodium. The same is true of all other parts and materials exposed continuously to sodium liquid or vapors.

Use of water or organic fluids incuding silicones is not acceptable in cooling systems associated with the reactor cover or rotating plugs. The possibility of contaminant solids, liquids, or vapors getting to the primary sodium must be precluded. Lubricants must be applied, in design and operation, with extreme care to preclude sodium contamination even in off-normal situations.

Provide in your design for flanges or adaptors needed for attachment and use of maintenance and removal equipment such as silos and pull pipes. For example, when a primary pump is to be removed from the primary sodium

for cleaning and repair, a silo-like device can be attached to the deck, sealed and purged with cover gas preparatory to pulling the pump. Features must be provided that will keep the system inerted during the removal and during the interim period until a pump is replaced and sealed in the deck. EBR-II experience with such devices is available.

The rotating plugs perform the important function of equipment location and accurate location of core "addresses" by the control rod drives and fuel handling devices. The design shall make provisions for any adjustments and/or calibration that will be needed for satisfactory operations. Temperature change for refueling should be minimized and thus minimize the time required to reach near equilibrium temperature conditions. The deck and plugs shall be designed to be capable of refueling within 50°F or less of 595°F sodium temperature, and 400°F sodium temperature for removal of equipment such as control rod drives, pumps, etc. Refueling near 595°F will keep all components in the cool portion of the pool, and the primary tank near normal operating temperature. This should help minimize the stress and cycling of the upper wall of the primary tank which carries the load.

Bearings for rotating plugs shall be located relative to the seals so the bearings are not exposed to sodium vapor. Vapors from bearing lubricants shall not normally have access to primary sodium. It must be impossible to spill bearing lubricant so that it could reach the annuli which are exposed to primary sodium vapor. The bearings shall be protected from debris and shall be accessible for cleaning and lubrication.

Elastomer seals should not be used where there are any possibilities of overheating, sticking or need for frequent replacement. Elastomeric gaskets or "O" rings may be used for sealing small simple plugs where low enough temperatures are assured and replacement will be easy and quick.

20. Fuel Handling

Sodium temperature in the pool during fuel handling shall be within 50°F or less of 595°F.

The fuel handling gripper shall have a positive means of determining when the gripper is firmly attached to an assembly and also when it is completely disengaged from an assembly.

There shall be a force indicator and force limiter in the push-pull device that inserts and removes fuel, blanket and removable shield pieces from their positions in the support grid.

There shall be two fuel handling mechanisms. Both in-vessel fuel handling mechanisms (IVTM) shall stay in the vessel during reactor operation and should be parked in a retracted mode to reduce activation by neutrons. Neutron shield material may be incuded if necessary to minimize activation of the parts that will need to be maintained. The activation shield probably can be used to steady the IVTM for resisting seismic forces. Removal for maintenance shall be planned and provided for in the design. Ease of cleaning after removal is also an important design criteria for this machine and its handling equipment.

Transfer of fuel and blanket assemblies from a receiving point in the primary tank to an external storage facility shall be through the fixed part of the deck. A fixed shielded cell above the deck is preferred instead of a movable ex-vessel handling machine. In any case, a large open door through the reactor containment wall must not be required for fuel handling. A reasonable sized gaslock port should accommodate transfer through the containment wall.

Preparation for fuel handling after producing power and preparation for returning to reactor operation mode after fuel handling should require a minimum of installation and removal of equipment. Equipment which normally oprates in sodium should remain in sodium when not in use.

Equipment handling, cleaning, inspection and repair provisions must be included in the detailed design criteria and implementation. When access to equipment is limited, the designs must provide for recovery from malfunctions.

Time required for fuel handling operations during reactor shutdown shall be minimized consistent with safe handling requirements.

Spent fuel assembies normally will not be stored in the primary tank. However, for special purposes, provision shall be made for temporary storage of a few spent fuel assembies within the primary tank. A maximum number of such locations shall be provided but shall not require an increase in the diameter of the primary tank or the rotating plugs.

Although very little is to be done in this area during Phase A, the spent fuel storage tank shall be located outside the containment building but not necessarily outside the confinement building. The spent fuel storage tank(s) shall be sized to contain the spent fuel from a batch refueling plus the off-load of an entire core for maintenance.

21. Reactor Containment Building

A circular containment building incorporated in a containment/confinement scheme shall be provided to conform to the Phase I and Phase II Project Office guidance on common site characteristics, Attachment A and site suitability source term, Attachment D.

The containment shall be designed for tornado, missiles, and earthquake requirements. The pressure containment capability of such a design shall be calculated. This pressure shall be identified as to how it was determined. There will be no hypothetical fire or other unfounded basis for building design pressure.

Removal and handling of major components such as an IHX tube bundle, primary pump and valve assembly, or upper internals structure, shall be considered in planning the circular containment building size and layout. During removal from the building, it is preferred that these components with their handling silos be maintained in the vertical position.

An auxiliary tank for draining the full inventory of primary sodium is not required in the containment building. Provisions for draining, via a syphon, to a location outside the containment building and detailed plans and space for the drain tank(s) should be provided.

22. Cold Trap, Plugging Meter and Sodium Sampling

There shall be no radio-active primary sodium circulated outside the primary tank. The cleanup system for the primary sodium shall be located in the primary tank. Leakage of coolant for the cold trap and the plugging meter shall not contaminate the primary sodium.

The plugging meters for primary sodium shall be located in the primary tank. The meters shall normally give continuous indication but short outages will not require reactor shutdown. The plugging meter assemblies shall be individually removable for repair using pull pipes or other specially designed devices to effect removal and replacement without contamination of cover gas.

Primary sodium shall circulate through sampling stations within the primary tank to obtain mixing thus assuring a representative sample which is removed via purged locks. This assembly shall be removable for repair.

23. Emergency Heat Removal

Diverse and redundant systems are required for emergency shutdown heat rejection. One such type of system shall remove heat directly from the primary sodium and promote the needed convective circulation through the reactor. This shall be a passive system on the primary, secondary, and air sides. The secondary fluid, probably Nak, shall circulate outside the primary tank leaving the primary sodium in the primary tank. The secondary fluid shall be cooled by convective air flow. The only thing not passive shall be the dampers or other devices needed to preclude major heat loss during normal power production. These dampers or devices must be highly reliable and testable while operating at power.

The required number of these passive systems is three or more (N). Failure of one of these systems, leaving N-1 still operative shall provide for sufficient cooling to hold the cladding maximum temperature at 1400°F or less without any other cooling. In the absence of sufficient detail to determine fuel cladding maximum temperature, assume a limit of 1350°F maximum temperature of the sodium leaving the top of the core or blanket assemblies. Temperature limitations of the primary tank wall shall be considered and provisions made to assure that safe* limits are not exceeded. The IHX's heat transfer surfaces themselves are not acceptable to meet the requirements for the passive system.

*The temperature limits may result in faulted design conditions if only natural air convection cooling is available indefinitely at the air cooled heat exchangers. This design condition is based on the assumption that within four hours, the active system can be made available, and the tank wall temperature will thus be maintained below the emergency design limit.

The above will meet the reuqirement for redundancy of the one type system. Diversity must be accomplished by other redundant systems also having three or more separate loops (N) to meet the requirements of 10 CFR 50 Appendix A. These, too, must be sufficient to assure safe limits for the primary tank wall and to limit the maximum temperature of the cladding to 1400°F or less, with no help from other systems, when one of the N active loops is out of service. These are not required to be totally passive but must be operable with the loss of all off-site power.

24. Shutdown Systems

Two completely diverse shutdown systems are to be provided in the design including installation and operation of sensors, circuitry, drives, latches and rods. One of these systems shall have the added feature of self-actuation so as to maintain a coolable geometry in case of transient undercooling. This self-actuation is to be independent of all external circuitry and equipment, and independent of motion of the head, where control rod drives are mounted, relative to the core. Detailed work on these shutdown systems will be deferred until Phase B.

25. Steam Generators

Although there will be no work on steam generators in Phase A, the following assumptions are made. The plant design shall include six evaporators of the double tube, double tubesheet (or equivalent) type. Double tubesheets or equivalent shall be employed on both ends. The recirculation ratio shall be 6:1; blowdown shall be conservatively established to avoid corrosion.

These evaporators shall have a leak detection and alarm system with sensors or sampling devices between the tubesheets (or equivalent). The system shall detect water and/or sodium leakage anywhere along the tubes or at the tubesheet welds.

The sodium flowing from each evaporator shall be monitored for hydrogen to obtain early indication and alarm if sodium-water reaction is initiated. Minimize sodium valves in the detector systems. These detector systems shall provide recall information to tell which indicator sensed the leak first, to enable the operator to tell which evaporator has the leak.

The intermediate sodium surge tank and relief system shall provide relief of pressure increases caused by limited sodium-water reactions resulting in slow pressure rises. These surge tanks should be located near the steam generators and give as much moderation of pressure surges as practicable.

26. Maintenance Provisions

Maintenance plans and facilities must be provided for replacement or repair of an IHX, a primary coolant pump, and the upper internals structure. The maintenance facility should be located outside the reactor containment building and should include areas for cleaning,

examination and repair. Careful safety considerations are required due to hydrogen that may evolve from reacting sodium, and the flammability of cleaning solvents such as alcohol.

II. CATEGORY II

1. There are a number of places where differential expansion must be accommodated in a careful and reliable manner; for example, the primary coolant pumps. Fixed mounting of the pumps in the deck requires that reasonably good seals be devised to allow the core support, plenums and flow manifolds to expand horizontally relative to the fixed center line of the pumps. Expansion loops don't seem to offer the best solution. A sliding seal, actuated by pressure difference, acting against a horizontal surface of a flow manifold looks to be a good possibility for a successful approach. Other innovations may prove to be feasible and reliable. If a bellows is used to compensate for vertical differential expansion, from the pump support to the bottom of the pump and valve assembly, it shall be replaceable and removable with the pump. Stability under flow induced vibrations and low stresses under seismic loads must be achieved and will be a factor in the approach to accommodation of differential expansion.

2. Neutron Shielding

The need for neutron shielding must be examined critically. The criteria are:

a. to avoid excessive activation of intermdiate sodium and components that may need maintenance,

b. utilize the effects of the large amounts of sodium to the fullest to reduce the need for steel shielding to attenuate the neutron currents coming from the core and blankets,

c. review the amount of steel shielding estimated at the top of the reference core assemblies and adjust as necessary,

d. consider the core restraint system when the neutron shield around the core and blankets is designed,

e. those neutron shield pieces, arund the core, that will sustain sufficient damage to require that the pieces be replaced every few years, must be accessible for removal by the IVTM but this number must be no larger than necessary because plug diameters and other costly items are influenced,

f. support of the neutron shield and movement of sodium in that space must be carefully considered in the design of the core support and plenums structure. Cooling of the shield pieces must be considered but the steel can run hot and forced convection probably will be minimal or zero. The nonreplaceable neutron shield assembly will constitute an important part of the barriers between hot and cooler sodium, careful design will help reduce heat flow between the hot and cool sodium pools.

3. Insulation of Deck and Rotating Plugs

While the specific insulation scheme and materials for the deck and plugs are at present an open question, this is a major problem that requires intensive study on a first priority basis. An efficient insulation is needed to allow a major vertical portion of the deck to be a cool structure and keep the overall deck thickness and heat losses within reasonable limits (because this will be a large cost factor). Details of support and penetrations must be a part of any practical insulation scheme. At locations where cool surfaces are exposed to sodium vapor (and aerosol), careful consideration must be given to the possible deposition of sodium by condensation and/or accumulation of solid phase frost. This consideration must include careful attention to convection currents and edge effects where insulation is used. The designer should be able to illustrate by fundamental principles and logical arguments that buildup of sodium or oxide, transported from the bulk hot sodium, will not impair the function of insulation and parts sensitive to temperature or temperature differences.

4. Thermal Barriers Between Hot and Cool Sodium

Finding a truly practical design approach for the barriers which separate the hot and cool sodium pools is an urgent, high priority task. Details of support and fastenings are particularly important. Forces tending to "oil can" the large sheets must receive careful attention. The barriers must function satisfactorily for the life of the plant without any maintenance.

Thermal convection currents tending to heat or cool the surfaces of the barriers should be kept as low as practicable. If gas separated sheets are utilized, possibilities of leaks, diffusion, absorption of gas and other perturbations must be carefully considered. Heat transferred across the barriers is not a true loss but must be kept as low as practicable.

5. Approach to Design of the Deck

The deck will be a structural support for accurately locating many components. The thick slab of steel shown in some concepts in Phase II work does not appear to be economical nor practical. A bridge structure made up of weldment subassemblies is probably a good approach to take. Give careful consideration to the use of removable shielding such as shot that can be added after the weldment subassemblies are in place. This should facilitate lifts, handling and transport. Also, if the shot or other gamma shield were to ever need to be removed for repair of gas leaks or any such problems, removal and replacement would be possible. Use concrete only where the use serves a purpose and the disadvantages are carefully reviewed before the selection is made.

Careful attention should be given early in the design to: the specific scheme for fastening and supporting the heavily loaded tank, location and movement of cables relative to the deck and plugs, cooling ducts and emergency cooling pipe runs.

Stress in the deck structure should be very conservative. Any tendency for crack propagation in the stressed skin must not be tolerated.

The deck design is a critical item in Phase A and must receive attention as early as possible.

6. Rotating Plugs and Fuel Handling

The diameters of the rotating plugs are to be minimized consistent with reasonable spacing for operations and maintenance. The three plug system may not be the most desirable. The rotating plugs concept should be reviewed.

Pantographs are not considered an acceptable approach. Straight-pull grippers (for in-vessel fuel handling machine) have advantages; however, an offset gripper can be used to reduce the size of the rotating plugs. Also, an offset transfer arm may be used if the extra motion is justified by net system advantages such as smaller rotating plugs and smaller primary tank. EBR-II experience with a transfer arm is available.

Some LMFBRs have been successfully operated without using steps in the rotating plugs. That is, the annuli between the deck and the rotating plugs are straight up and down with no steps or shelves upon which condensed sodium, oxide, and frost can collect. Such no-step annuli should be included in the PLBR design. It may be necessary to place shielding rings on top to eliminate streaming. Utilizing these straight vertical annuli, make provision in the design for cleaning the annuli if it were necessary.

7. IHX

Capability to operate with a cluster of plugged tubes is not mandatory. An IHX concept having primary coolant flow through the tubes is to be the reference design. This offers the possibility of minimizing cross flow pressure drop and maldistribution at the inlet and outlet.

The design concept should be as small in diameter as practical without sacrificing low pressure drop and needed natural convection of the primary sodium.

Careful attention must be given to mounting, installation in the barrier assembly between hot and cool sodium pool, flow and temperature distribution, resistance to seismic forces and sodium sloshing, provisions for attaching equipment for removal of the tube bundle without exposing sodium to air, and avoiding flow induced vibrations.

8. Support of Large Loads Inside the Primary Tank

The supports of the core, blankets, neutron shields, flow manifolds, etc., inside the main reactor vessel (primary pool tank) probably are different in the pool as compared to a loop-type plant. Early in Phase A a practical design concept must be defined (shown in a layout drawing) to

illustrate how the primary tank, support structures (internal to the tank), flow manifolds and plenums, primary pumps, etc., all relate to one another in a consistently practical manner.

III. CATEGORY III

1. Rotating Plugs, Deck and Ex-Vessel Fuel Handling

The heavy metal (Sn/Bi) dipseal is one method that may be used for sealing rotating plugs during the rotating mode. During the reactor-operating mode, sodium vapor should not reach such a dipseal. Attachment F illustrates one such method. The Sn/Bi dipseal must be accessible for cleaning while the rotating plugs are in the non-rotating mode. Gaskets or "O" rings must be replaceable. Any seals and bearing scheme proposed must be very carefully reviewed for reliability and cost of maintaining same.

The problem with sodium vapor escaping through the opening in the deck during refueling (from the primary tank into the inerted cell), above the deck, that receives the cooling coil around the outside of the duct which forms the removal passage. Circulating chilled nitrogen in such a coil will cause sodium vapor to condense on the duct inside wall and run back into the primary tank. This will reduce the amount of sodium that would otherwise migrate into the cell while the port is open to the primary sodium. It may be necessary to have cooling coils in the atmosphere near the wall of the inerted cell above the port. Such cooling would serve to further reduce the amount of sodium in the gas atmosphere clear enough to see through. Dripping sodium from the fuel handling can still be a problem with which to contend.

Handling, storing and shipping spent fuel after it leaves the primary tank, must be planned carefully (mostly in Phase B) to minimize the motions (separate operations) required and to minimize the facilities needed to accomplish the objective of safe and economical disposal of the spent fuel and blankets. These facilities and equipment must provide for sufficient cooling and shielding during all operations, including situations where a fuel assembly inadvertently stops (sticks, etc.) in transfer mode. Cleaning, servicing, and repair of bearings, mechanisms, drives, seals, etc., must be anticipated in the design of the equipment and facilities. Methods of recovery from malfunctions must be considered in arriving at the detailed design criteria.

The manner in which spent fuel is to be handled and stored prior to shipment off-site requires a critical evaluation. The pros and cons of storage in sodium versus cleaning and storage in water should be reviewed carefully. There is a strong incentive for cleaning and storing in water prior to shipment based on the following considerations, viz., shipping spent fuel in water will be easier to accomplish than shipping in sodium - and may indeed be preferable from a safety/licensing point of view; under-water storage and its associated cleaning system(s) will prove to be less costly and easier than under-sodium storage and its associated auxiliaries; and the potential for sodium fires will be reduced.

EBR-II experience in washing driver fuel (sodium bonded metal alloy) and experimental mixed oxide fuel when it leaves the fuel unloading machine should be reviewed. If residual NaOH is considered to be a problem, the use of boric acid in the storage tank should be considered.

In any event, the selection of the appropriate scheme for PLBR will require a careful examination of the advantages and disadvantages associated with the two concepts. The cost impact in terms of building size, space allocation, systems and components; fire prevention; servicing of equipment exposed to sodium; the treatment and disposal of radwaste generated in the cleaning process; heating and cooling loads and the potential safety/licensing aspects associated with fuel handling, storage and shipping offsite must be considered in this evaluation.

ATTACHMENT "B"

ECONOMIC GUIDELINES

The economic parameters herein are to be used for "base case" results. Other values may be used provided they are identified and the results compared with the base case.

The values below are, for the most part, identical to those used for Phases I and II. Changes are highlighted by asterisks.

PROJECT SCHEDULE

PLBR	Start Engineering	1/1/79
	Utility Operation	1/1/87*

INFLATION

Time Reference Point	1/1/77*
Annual Rate	6%

LEVEL ANNUAL REVENUE REQUIREMENTS

Book Life	30 yrs.
Levelization Period	16 yrs.
Non-Depreciating	15.56% per yr.
With Depreciation, Taxes, and Insurance	14.64% per yr.

INTEREST RATE FOR PRESENT WORTH EVALUATION

10.24% per yr.

INTEREST DURING CONSTRUCTION

9% per yr.
simple interest

PLANT LOADING SCHEDULE

	PLBR
1st Year	55%
2nd Year	75%
Thereafter	80%

VALUE OF INCREMENTAL CAPACITY

$325/kw*

REPLACEMENT ENERGY COST

27 mills/kwh*

VALUE OF ONE DAY'S OUTAGE (24 hrs.)*

	Maintenance	Forced
Replacement Energy	$500,000	$500,000

URANIUM COST vs. AVAILABILITY

As shown in Figure 1 of "Breeder Reactor Economics"

SEPARATIVE WORK $/SWU - (.34 X Cost of U_3O_8) + $64

FUEL ISOTOPICS

Plutonium	Pu-238	1%
	239	60%
	240	22%
	241	13%
	242	4%
Depleted U	U-235	0.25%

Pu PROCESSING LOSSES (for calculating Breeding Ratio and Fuel Cycle Cost)

Fabrication	0.5%*
Recovery	0.5%

Pu VALUE 40% of value of U-235

FUEL TRANSPORTATION, RECOVERY, AND WASTE STORAGE $200/kg Mixed Oxide

OUT-OF-CORE FUEL CYCLE TIME

Fabrication - 4 months
Recovery - 6 months

ATTACHMENT "C"

PLBR DESIGN SAFETY APPROACH

The PLBR will achieve and demonstrate a level of safety comparable to that of current generation LWRs. In accomplishing this, the following principles will be observed:

(1) A spectrum of conditions will be defined and categorized (i.e., normal, upset, emergency, and faulted conditions) and capability will be provided in the design to limit the consequences of these conditions to levels consistent with the categorization. Definition of transients, and general safety design criteria will be based on consideration of LWR practice, modified to reflect LMFBR characteristics. Significant departures from LWR practice (e.g., treatment of piping integrity, in-service inspection) will be clearly identified and justified by the contractors and formal agreement reached with the EPRI Project Office.

(2) It will be shown that disruption of the core would involve sequences of postulated successive failures beyond those postulated for establishing the design basis for protective systems and engineered safety features. Therefore, core disruption will clearly be in Class 9 per the accident categorization in the proposed Annex to Appendix D, 10CFR50. Among the means to achieve this are as follows:

   (a) provision of at least two independent, diverse, and functionally redundant reactor shutdown systems to assure that the reactor power level will be quickly and reliably reduced whenever plant conditions require such action.

   (b) provision of at least two independent, diverse and functionally redundant shutdown heat removal systems.

   (c) provision of instrumentation to detect subassembly faults as necessary to prevent significant propagation.

   (d) provision of a heat transport system of very high integrity, and assurance that this level of integrity is maintained.

   (e) provision of means to protect the containment system from the effects of releases of sodium from the main heat transport system equipment, and from the effects of all other design base events.

   (f) documentation of a detailed, systematic and disciplined search for potential initiating events which could lead to extended overpower or undercooling, or autocatalytic conditions. State-of-the-art failure analysis methods (e.g., FMEA, fault trees, common mode failure analysis, etc.) will be fully utilized in the search.

(3) It will be shown that the incremental environmental risk from Class 9 accidents is extremely low, and does not appreciably add to the overall plant risk which is balanced against the benefits in the environmental evaluation. Among the means to achieve this are as follows:

(a) a risk assessment will be performed, consistent with the data base and achievable technology available at the time of ER preparation. The development effort necessary to ensure that the technology is adequate will be identified to the ERDA base program as high priority.

(b) it will be shown that Class 9 accidents, particularly those considered least improbable do not bring abut major step increases in consequences. Included in this evaluation will be the effects of considerations such as inherent containment capabilities and evacuation times for local populations.

(c) it is anticipated that the PLBR, as conservatively designed to accommodate the consequences of all events within the design basis, will have inherent capabilities to mitigate the consequences of core disruption. Such inherent structural and thermal (i.e., debris retention) capabilities will be evaluated and reported as such. It is also recognized that, historically, consideration has been given to providing safety factors or margins to enhance the demonstrability of acceptable risk from Class 9 accidents. Examples of these include head hold-down devices, rotating plug keys, materials choices (e.g., containment concrete), vessel support system dynamic load capability requirements, clearance requirements, etc. Such safety factors or margins might be incorporated in cases where it is judged that significant risk reduction could be achieved in a substantially cost beneficial manner and without significant performance penalties. This judgment may be reached on the basis of engineering judgment and experience with analysis of Class 9 accidents in the past. Any such safety factors or margins presently in the design or proposed for incorporation should be so identified and provided to the Project Office for review.

(4) Certain design features have been identified which may have an apparent potential to reduce accident probabilities or consequences and enhance the overall safety of PLBR. The teams will actively consider each of these items and document the tradeoff rationale leading to their incorporation or exclusion. These features are:

(a) a radial parfait-type core configuration to reduce or eliminate the energetics in the postulated accidents.

(b) a self-actuated shut-down system for accomplishing scram under accident-initiation conditions.

(c) extended pump coast-down or flowering core for delaying the on-set of Na boiling in the loss of flow situation.

(d) a design of the control rod system to reduce the TOP reactivity addition rate due to control rod withdrawal.

(e) a passive diverse decay heat removal system.

(f) a design of the core restraint system precluding large additions of reactivity due to postulated compaction.

Any future additions to this list will be clearly so identified.

ATTACHMENT "D"

SITE SUITABILITY SOURCE TERM

Background

The PLBR is being designed in a very conservative manner to ensure that under all reasonably conceivable conditions, essentially no hazard to the public will exist. A spectrum of transients is established for the design basis and the release of radioactive material as a result of any event within the design basis is kept to exceedingly small levels. However, notwithstanding the fact that no substantial release of radioactive material would ever be expected, the siting policy of NRC, as set forth in part in 10CFR100, requires the assumption of a fission product release from the core for use in evaluating the adequacy of the exclusion radius, low population zone and population center distance. It is instructive to consider the NRC policy for LWRs in this area to gain insight into the degree of conservatism in that policy. The PLBR project intends to provide a comparable degree of margin and conservatism in the source term to be proposed to NRC in compliance with 10CFR100. It is not considered necessary to quantify the conservatism in the LWR practice. Rather, comparability will be established, and the margin provided in the PLBR design and source term will be defined to provide perspective on and support for the proposed PLBR source term.

Current practice for LWRs (as reflected in Reg. Guides 1.3 and 1.4) is to assume the release of radioactive material far in excess of that which would be calculated on an extremely conservative basis for the most severe design basis event. In fact, the historical development of this release is tied to a substantial meltdown of the core, despite the fact that LWRs are required to demonstrate that core meltdown will not result from any design basis event. PLBR will also demonstrate that core meltdown will not result from any design basis event. The LWR assumption required by NRC is that 25% of the iodine and 100% of the noble gas in the equilibrium core is immediately available for leakage from the reactor containment.

In 10CFR100, unique or unusual features of a reactor which bear significantly on the probability or consequences of a release of radioactivity are stated to be among the factors to be considered in the site evluation. It is the Project's intent to include consideration of such factors, along with the perspective provided by LWR practice, in developing a source term for PLBR. The consideration should include, for example, different coolant physical properties (e.g., lack of a means, such as blowdown, to rapidly remove sodium from the reactor vessel), different colant chemical properties (e.g., sodium/iodine intereaction properties), and different quantities, physical forms and locations of radioactive materials, including fission products and plutonium.

The precise definition of, and the basis for, the site suitability source term to be ultimately proposed to NRC for use in fulfillment of regulations in 10CFR100 is, at present, indeterminate. Efforts in Phases 2 and 3 will be focused on defining the source term and its basis and on proceeding with containment design on what is judged to be an appropriately conservative basis.

Direction

Consistent with the foregoing, the following actions are to be taken:

(1) Continue to assure that the release of radioactivity to containment as a result of events within the design basis spectrum is maintained at exceedingly low levels (i.e., essentially zero).

(2) Examine in detail the key features of PLBR which have an impact on the source term definition and are different from LWRs, in order to determine release assumptions which would be consistent with maintaining a level of conservatism for PLBR comparable to that currently employed for LWRs. The relative likelihood of release of radioactive materials in each of the categories (i.e., noble gases, halogens, etc.) and the relative ability of PLBR materials and features to mitigate the transport of the radioactive materials should be assessed. This assessment should include, but not necessarily be limited to, the factors mentioned above. Consideration should also be given to the NRC staff position on iodine attenuation in pressure suppression pools, (see Reg. Guide 1.3, p. 1.3-2, section C.1.f.) and the considerable body of data in this area, to assess the impact of this position on the PLBR source term.

(3) Develop sufficient information to provide strong assurance that releases from reasonably conceivable events beyond the design basis are very low, and to establish the probabilities of these various events beyond the design basis for comparison with the probabilities of limiting design basis events. This activity should include surveys of locations of radioactive material in containment, potential mechanisms for release, and identification of key controlling physical processes.

(4) Define and recommend to the Project Office any development efforts required to verify key conclusions of the above activities.

(5) Proceed with containment design on the following basis:

Source term:	100% noble gases
	5% halogens
	1% other fission products
	0.1% plutonium

The percentages refer to equilibrium cycle core inventories. The quantities are assumed to be instantaneously available for leakage from containment. The dose guidelines to be used are:

Whole Body	20 rem
Thyroid	150 rem
Bone	75 rem
Lung	37.5 rem

It is our judgment that designing for this source term is an adequately conservative basis for proceeding in Phases 2 and 3, and provides sufficient margin to allow for the uncertainties in the source term to be proposed in the PSAR. It is expected that this source term will require a dual containment or containment/confinement (e.g., similar to LWR designs at sites with poor dispersion characteristics), or the equivalent. If this is not the case, the Project Office should be so advised.

(6) Based on all of the above, recommend a source term and basis to be used in the PSAR.

After comparability with the degree of conservatism in LWR practice has been established and after the margins in the interim PLBR source term are clearly defined, consideration may be given, at that point in time, to reducing the degree of conservatism in the containment design.

ATTACHMENT "E"

EXCERPT FROM "PLBR" PROJECT OFFICE REVIEW OF BULLSEYE CORE STUDIES"

Power density shifts during a burn cycle is inherent with having blanket assemblies adjacent to fuel, both at the internal blanket and radial blanket locations but constant flow in each assembly during the cycle period is not inherent. It is apparent that the flow split between fuel and blanket regions must be changed during the cycle. This can be done fairly easily by feeding the fuel and blanket from two separate inlet plenums.

The low pressure plenum feeding the blanket assemblies would have a small share of the total flow at the beginning of life. This share would be increased as the cycle progresses. The design criteria would be to keep the outlet temperature as close as practicable to the mixed mean sodium outlet temperature. This would tend to keep the power to flow ratio fairly well matched. This would reduce the large differences between clad temperatures, allowing a reduction in the maximum temperatures and making a more conservative operation. The blankets should be slightly over cooled to assure incoherence.

The attached sketch illustrates schematically how the required change in flow during the cycles might be accomplished. The control valve would be such that neither flow could be reduced below a certain safe minimum. The control valve would be adjusted by observing outlet thermocouples in the outlet of each assembly. Instead of orificing inside the assemblies, a la CRBR design, the orificing would be accomplished in the inlet holes in the walls of the lower pole pieces of the assemblies. A stepped grid could be used, a la EBR-II design, to give a different orificing for each hexagonal ring location. If it is necessary to have different orificing for assemblies in the same ring, the lower pole piece holes can be two or even three different designs. Each different hole arrangement would have its unique discriminator to avoid putting an assembly in the wrong position. Even with this added complexity the number of different discriminators and assembly orificies would be less than the current CRBR and PLBR uniform core designs; even though effectively many more orificing zones would be accomplished.

The disadvantage of having the low pressure plenum below the high pressure plenum may be slightly longer assemblies and a deeper R.V. The low pressure plenum need not be as deep as the high pressure plenum. There may be better ways of accomplishing the controllable flow split between the blanket and fuel zones. Attachments I and II illustrate an alternate scheme with shorter assemblies.

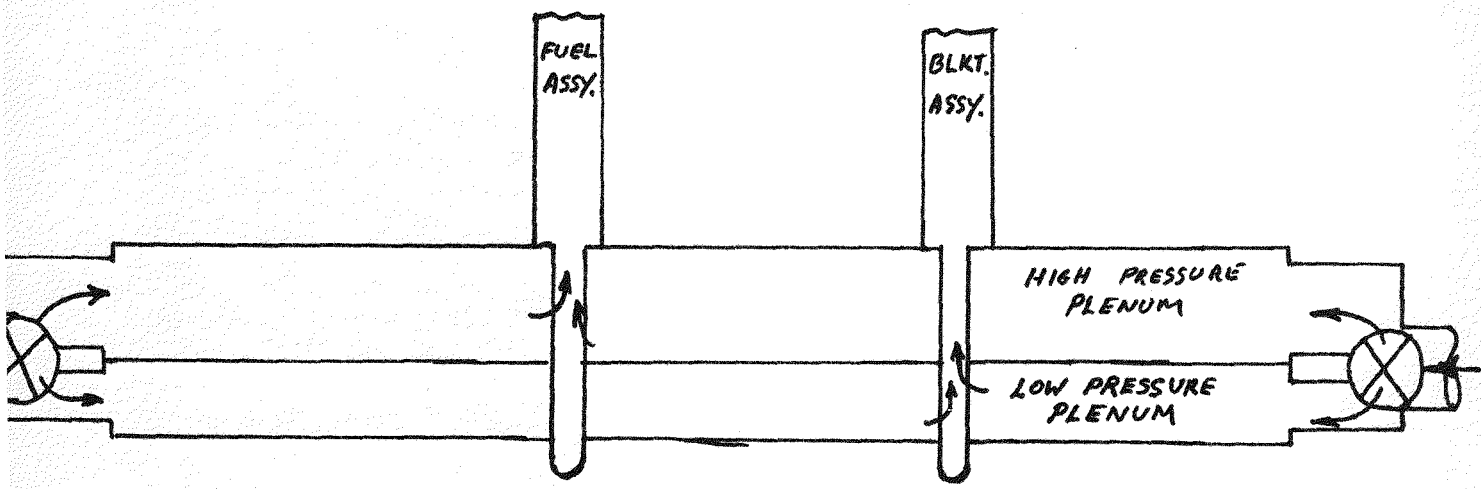

ATTACHMENT "F"

A SEAL AND BEARING ARRANGEMENT FOR ROTATING PLUGS

The experience at EBR-II with seals and bearings for the rotating plugs is both positive and negative. Taking advantage of this experience and learning from the negative portion, a satisfactory seal and bearing arrangement can be designed. The following do's and don'ts are based on that experience.

(1) The Sn/Bi dip seal must be completely accessible from both sides for cleaning without rotating the plugs.

(2) There should be a passive seal that closes off sodium vapor from the dip seal while the reactor is operating. That is, the dip seal should do the sealing when the plugs are to be rotated but not during reactor operation when the plugs are stationary.

(3) The annuli between plugs should be cleanable at critical points to avoid compaction of sodium frost and oxides where such compaction would inhibit rotation.

(4) Bearings should be located relative to the seals so the bearings are not exposed to sodium vapor.

(5) The bearings shall be protected from debris and shall be accessible for cleaning and lubrication.

(6) It must be essentially impossible to spill bearing lubricant so that it could reach the annuli which are exposed to primary sodium vapor.

The following sketch illustrates a design that complies with the do's and don'ts. When the reactor is operating and the plant is producing power, bolts "c" are loose and ring (1) rests on a sealing gasket on shoulder "A" of the support, sealing out air and avoiding any loss of cover gas from above the molten sodium. When the reactor is shut down and the plug is to be rotated, bolts "c" are tightened and ring (1) lifts to take the dead weight load on the bearing and result in a slight clearance at shoulder "A". The heavy metal, Sn/Bi, in the seal trough is molten and the dip ring, which is welded to ring (2), effects a seal during rotation. Details are discussed below.

e round-rotating-shield plug and plate are the upper shield and (with the seal parts) form the closure head of the reactor vessel. The "shear keys" are segments of a ring which is placed in the groove in the inside of the support wall. These shear keys will resist any tendency for the shield to raise if an upward force of more than one g were to occur. The "support" is the support deck flange where the rotating plug is the largest plug making up the rotating part of the head. If there is more than one plug, eccentrically placed one inside another, then the outer plug becomes the support for the inner plug. The sealing parts would be the same for both cases.

During reactor operation the gasket on shoulder "A" seals the sodium vapor and isolates that vapor from the heavy metal in the seal trough, thus there is no tendency for sodium to condense in the seal trough. Also, during reactor operation the heavy metal is frozen and chemical reaction with air at the surface is very low. The bearing is not subjected to sodium vapor in either the reactor operating mode nor the refueling mode.

Ring (3) is segmented. The segments are bolted together so they function as one ring when the load is carried by the bearing. In the reactor operating mode, bolts "c" are loosened and the seal is made at the gasket on shoulder "A". This allows the segmented ring (3) to be removed one segment at a time. The bolts holding ring (2) and its dip ring can then be removed so the heavy metal, and any dross that has formed, can be cleaned out and replaced with fresh heavy metal. The heavy metal has to be melted to allow the removal of the dip ring. The electrical heaters are not shown in the sketch. Thermocouples also are installed to sense the temperature, to tell when the heavy metal is frozen or molten. Both the electrical heaters and the thermocouples are replaceable when ring (3) is removed.

Access passages are provided in the plug, shield plate, and support for vacuuming oxide and snow from the closer fitting areas such as around the shear key. These passages are not shown in the two dimensional sketch because to do so would complicate the illustration. Vacuuming will be done only when the reactor is shutdown and the sodium temperature is lowered to a reasonable margin above freezing. The vacuum passages normally will be

sealed with plugs at the outside to avoid any air seeping into the cover gas space. Vacuum cleaning will be accomplished on a routine maintenance basis. This will avoid buildup and subsequent packing of the oxide and snow. Holes drilled through the stationary parts will allow vacuuming of a complete circle as the rotating part is moved past that hole.

A gasket for shoulder "A" is illustrated in the second sketch which is attached. Different commercially available gaskets such as metal "O" rings could be used. That illustrated in the sketch is just one type of gasket that will give the characteristics that are required. The gasket shown in the sketch has an inner ring and an outer ring that are the same thickness but are thinner than the chevrons in their free, unloaded position. The chevrons are made of thin ribbons of resilient material such as Inconel 750 separated by an asbestos packing material. When the gasket is loaded and functioning as a seal, the chevrons are compressed. Compression is limited by the flat inner and outer rings which form pads that carry the excess load and avoid crushing the chevrons.

When the gasket on shoulder "A" has to be replaced, which it may every few years, rings (3), (2) and (1) can be removed giving access for replacement of that gasket. This would have to be done after the reactor has been shut down (probably for refueling) for a period sufficiently long for the sodium 24 activity to decay about 6 days. The temperature of the sodium in the reactor vessel would be lowered to minimize diffusion of sodium vapors up the open annulus. Also, before the seal is broken, the cover gas would be monitored to be sure that the cleanup system had eliminated radioactivity from the argon cover gas. Once bolts "b" are removed, the rotating shield plug rests on shoulder "B" thus minimizing the escape of cover gas up the annulus. The cover gas pressure would be maintained slightly above the ambient air pressure above the plug.

When bolts "c" are tightened to raise the plug to rotating position, it is necessary to load the bolts fairly uniformly. This can be done inexpensively and rapidly with adjustable torque impact wrenches. Use 6 or 8 wrenches simultaneously, equally spaced around the circle. Set them to slip when they have snugged up and begun to load the bolts. Move from one

set of bolts to another tightening like you would any large flange. Take up the load a little at a time until the head is slightly raised off the passive seal at shoulder "A".

REVISED

ATTACHMENT "G"

CORE ASSUMPTIONS FOR PHASE "A"

The details given in this entire table are not optimized and are expected to be changed eventually within the space envelope defined by this table. As explained previously, the purpose of the data in this table is to give a reference that will enable the contractors to lay out comprehensive concepts of core/blanket related features and assemblies without waiting to optimize a core design.

FUEL ELEMENT	MM	INCHES
Tube O.D.	7.2	0.280±.001
Tube Wall Thickness	0.34	.013±.001
Wire Wrap Diameter over fuel length*	1.2	.046
Active Fuel Height	1060	41.73
Initial Gap, Tube I.D. Minus Pellet Diameter		0.006
Smear Density, % of Theoretical	88	
Lower Plenum Height	950	37.4
Lower Axial Blanket	360	14.17
Upper Axial Blanket	360	14.17
Upper Steel Shielding**	650	25.59

FUEL ASSEMBLY	MM	INCHES
Number of Fuel Elements per Assembly	271	
Dimension Across Flats Inside Duct	141	5.551
Wall Thickness (Slotted above Core), Hex. Duct	2.5	0.098-0.100
Dimensions Across Flats Outside of Duct	146	5.750
Interassembly Gap	7.5	0.295
Approximate Height from Seat to Top**	4600	181

*Diameter of the wrap wire may be larger above and below and fueled length where swelling will be much reduced. This will contribute to a lower pressure drop for the fuel assemblies and reduce the required pump head and pumping power.

**The steel shield may be in the assembly rather than in the elements. Minimize pressure drop. The amount of steel shielding at the top of the core is a Category II item and must be worked out as soon as possible. The primary sodium outside the core and blanket must be included in calculations to determine steel shield reuirement to avoid activation of intermediat4e sodium and removable hardware lthat could require maintenance work.

Approximate Heights:		
Bottom Steel Shielding	200	7.87
Bottom Plenum	950	37.4
Lower Axial Blanket	360	14.17
Active Core	1060	41.73
Upper Axial Blanket	360	14.17
Upper Plenum	550	21.65
Upper Steel Shielding**	650	25.59
Handling Socket	180	7.09
Miscellaneous	290	11.42
Lower Pole Piece, Seat to Bottom of Assembly	Design to Suit Plenums	

Note 1: Roll chevron grooves in duct wall, if needed, to tighten tube bundle in hexagonal duct at appropriate elevations above and below the active fuel (in the axial blanket and plenum zones). Chevrons to protrude inward.

Note 2: Seriously consider lower pole pieces and orificing of the type illustrated in Attachment E or the type used in Phenix.

Note 3: Balance pressure across duct wall at fuel elevations as much as practicable.

INTERNAL AND FIRST ROW RADIAL BLANKET ASSEMBLIES	MM	INCHES
Number of Rods per Assembly	91	
Tube O.D.	14.2	0.56
Tube Wall Thickness	0.4	0.016
Smear Density of Rods, % Theoretical	90	
Depleted Urania U-235 Content	0.0025	
Hexagonal Duct Outside Flats	146	5.750
Duct Wall Thickness	1.9	0.075
Height of Blanket Material	1800	70.87
Interassembly Gap	7.5	0.295

OUTER ROW OF RADIAL BLANKET ASSEMBLIES	MM	INCHES
Number of Rods per Assembly	37	
O.D. of Tubes	22.6	0.89
Thickness of Tube Wall	0.5	0.020
Other Parameters Same as Internal Blankets		

Note 4: All fuel assemblies, blanket assemblies and removable shield assemblies to be the same height from seat to top. The lower pole pieces from seat to bottom are to be determined by the support grids and inlet plenum details.

VOLUME FRACTIONS

Fuel Module:	Volume %
Fuel	38.17
Steel	16.89
Sodium Inside Duct	30.24
Sodium Outside Duct	9.52
Internal & 1st Row Radial Blanket Module	
Fertile Material	56.64
Steel	12.67
Sodium Inside Duct	14.86
Sodium Outside Duct	9.52
Outer Row Radial Blanket Moudle	
Fertile Material	59.68
Steel	11.04
Sodium Inside Duct	13.12
Sodium Outside Duct	9.52
Control Rod Modules	
B_4C	52.4
Steel	12.3
Sodium	35.3

See sketch for core and blanket arrangement.

ATTACHMENT "A"

ERDA/EPRI SITE CHARACTERISTICS FOR PLBR PLANT STUDY (Rev. 0, 1/26/76)

ITEM/PARAMETER		ASSUMPTIONS OF VALUES/APPROACHES		NOTES/CLARIFICATIONS	
1.	Demography/Geography				
1.1	Site Boundary and/or Exclusion Radius	1.1	0.4 miles (640 meters)	1.1	0.4 Miles Corresponds to X/Q 0 0-2 hr. Given in 3.1.1
1.2	LPZ Radius	1.2	3 miles (4830 meters)	1.2	See X/Q Values Corresponding to 3 Miles in 3.1.1
1.3	Population Center Radius	1.3	5 miles	1.3	General Note: Assumptions for 1.1, 1.2 and 1.3 Are in Accordance with Draft of Regulatory Guide 4.7
1.4	Population Distribution	1.4	See Attachment 1 - (Fig. 2.1-2 "Average Population Density in Annular AReas around Lake Sites (Land Only) Year 2000"	1.4	Reference for Attachment 1 - Stone & Webster's PWR Standard Plant Safety Analysis Report SWESSAR-P1
1.5	Adjacent Facilities and Hazard Relationship to Plant	1.5	All Routes Carrying Explosives Are Outsdie Limits of Regulatory Guide 1.91 and No Industrial or Military Facility is Located Near Enough the Plant to Pose Commercial or Military Airport Nor Below An Aircraft Corridor	1.5	All Industrial, Military and Transportation Potentially Hazardous Facilities Are Outside the Limits Prescribed in Regulatory Guide 4.7 (Draft)
1.6	Transportation Facilities; Capacity for Shop Fabricated Component Delivery	1.6	A Railroad Siding is Provided to the Plant. The Nearest Navigable Waterway is 50 Miles from the Site and Access Roads Allow the Use of Multi-wheeled Transporters		
2.	Geology/Seismology				
2.1	SSE Horizontal	2.1	0.30g. For Vertical g, Use Regulatory Guide 1.6 Assumptions	2.1	It is Believed that 90% of Probable Sites Should Fall Within the .30g Value
2.2	OBE Horizontal	2.2	0.15g (1/2 SSE); For Vertical g, Use Regulatory Guide 1.6 Assumptions		
2.3	Ground Response Spectra	2.3	Use Regulatory Guide 1.6 Assumptions		

ITEM/PARAMETER	ASSUMPTIONS OF VALUES/APPROACHES	NOTES/CLARIFICATIONS
2.4 Foundation Material	2.4 Reference Founding Conditions	
2.4.1 Type	2.4.1 Soft Rock	
2.4.2 Strength	2.4.2 16,000 PSF*	
2.4.3 Damping	2.4.3 Subgrade Material Damping: OBE=4%; SSE=7% 1	
2.4.4 "S" Wave Velocity	2.4.4 2,000 fps	
2.5 Location of Nearest Surface Capable of Faulting for 1000 ft.	2.5 The Site Is Located More Than 5 Miles from a Surface That Is Capable of Faulting Greater Than 1000 Feet in Length	2.5 Site Satisfies REstrictions Given in Draft of Regulatory Guide 4.7 for Surface Faults Location Relative to Plant.
3. Meteorology/Climatology		
3.1 Diffusion Conditions	0.4 Mile Exclusion Rad. / 3 Mile Outer LPZ	
	0-2 hr / 0-8 hr / 8-24 hr / 1-4 day / 4-30 day 1	
3.1.1 X/Q Accident	3.1.1 X/Q Sec/M^3* $2X10^{-3}$ / $2.5X10^{-5}$ / $1.5X10^{-5}$ / $3X10^{-6}$	3.1.1 Reference: Westinghouse RESAR-41, Amendment 3, Dated July 1974. Using 90% of Data Points in Curves of Sec. 2.3, and the Times and Distances Indicated
3.1.2 X/Q Average Annual	3.1.2 X/Q Sec/M^3 Average Annual at 3 Miles = $1X10^{-6}$	3.1.2 Reference: Stone & Wesbster's SWESSAR Figure 2.35-8. Using Upper 95 Percentile CHI/Q Value of 42 Nuclear Plants Data Curve and for a Distance of 3 Miles.
3.2 Precipitation		
3.2.1 Duration	3.2.1 4 Inches per Hour	
3.2.2 Frequency	3.2.2 Return Period of Once in 50 Years	
3.3 Snow and Ice Load	3.3 For Non-Safety Structures Use 40 PSF For Safety-Related Structures Use 65 PSF and for Saturated Snow Pack Conditions on Flat Roofs, Increase to 70 PSF.	3.3 For Safety-Related Structures Data Source from Recommendations of Wash. 1361 (Jan. 1975)
3.4 Wind Load and Height	3.4 For Safety-Related Structures, Use 120 mph at a Height of 30 Feet above the Ground.	3.4 Reference: ANSI-A-58.1-1972

*The $\frac{X}{Q}$ values do include a wind meander factor which might be allowed by NRC; they are, therefore, conservatively high by a factor 10 to 20%.

ITEM/PARAMETER	ASSUMPTIONS OF VALUES/APPROACHES	NOTES/CLARIFICATIONS
3.5 Temperature and Humidity (W. B. and D. B ^{o}F)	3.5 Design Temperature ^{o}F Dry Bulb ^{o}F Wet Bulb	
-Maximum	Maximum 100 80	
-Minimum	Minimum -25 --	
3.6 Cooling Tower Design Basis	3.6 Design for 95^{o}F Maximum Cooling Tower Water Outlet Temperature with 80^{o}F W. B. (1% Design Point). For the PLBR Plant Study to Avoid Inappropriate Optimization of the Plant Heat Sink System with Assumed Seasonal Site Data Use, the Following Design Point Values: 1. Cooling Tower Design Point: As Stated above and Assume a Mechanical Draft Cooling Tower with both T-G Building and Cooling Tower at Same Grade. 2. Condenser Design Point: 2.5"Hg Abs. Back Pressure at T-G Rated Load (T-G Should also be Rated at 2.5"Hg (Abs.) and a Circulating Water Temperature Rise of 27^{o}F.	3.6 Main Condenser Cooling Tower Design Bases. For Safety-Related Ultimate Heat Sink (If Required) Design Bases Use the Following as Meeting Requirements of Regulatory Guide 1.27: 1 Maximum Average D.B. ^{o}F / Maximum Average W.B. ^{o}F / Maximum Average R.H.% / Maximum Average Wind Speed MPH Worst 30-Days: 85 / 77 / 70 / 30 Worst 1-Day: 85 / 80 / 80 / 40
4. Tornado Loading Region	4. Use Regulatory Guide 1.76, Region I Design Basis Tornado	
4.1 Characteristics:	4.1 Use Region I, Design Basis Tornado Characteristics from Regulatory Guide 1.76 Which Are:	
4.1.1 Maximum Wind Speed	4.1.1 360 mph	
4.1.2 Rotational Speed	4.1.2 290 mph	
4.1.3 Maximum Translational Speed	4.1.3 70 mph	
4.1.4 Minimum Translational Speed	4.1.4 5 mph	
4.1.5 Radius of Maximum Rotational Speed	4.1.5 150 feet	
4.1.6 Pressure Drop	4.1.6 3.0 psi	
4.1.7 Rate of Pressure Drop	4.1.7 2.0 psi/sec	

ITEM/PARAMETER		ASSUMPTIONS OF VALUES/APPROACHES		NOTES/CLARIFICATIONS
4.2	Tornado Missiles	4.2	Fraction of total tornado velocity	4.2 Based on NRC Standard Review Plan, Section 3.5.1.4
	-Weight	A. Wood plank, 4 in. x 12 in. x 12 ft., weight 200 lb.	0.8	
	-Dimensions	B. Steel pipe, 3 in. diameter, schedule 40, 10 ft long, weight 78 lb.	0.4	
	-Velocity Horizontal Vertical	C. Steel rod, 1 in. diameter x 3 ft long, weight 8 lb.	0.6	
		D. Steel pipe, 6 in. diameter, schedule 40, 15 ft long, weight 285 lb.	0.4	
	-Impact Height	E. Steel pipe, 12 in. diameter, schedule 40, 15 ft long, weight 743 lb.	0.4	
		F. Utility pole, 13-1/2 in. diameter, 35 ft long, weight 1490 lb.	0.4	
		G. Automobile, frontal area 20 ft^2, weight 4000 lb.	0.2	
		These missiles are considered to be capable of striking in all directions. Missiles A, B, C, D, and E are to be considered at all elevations and missiles F and G at elevations up to 30 feet above all grade levels within 1/2 mile* of the facility structures.		

(Assume topography within 1/2 mile of site is essentially flat.) 1

ITEM/PARAMETER	ASSUMPTIONS OF VALUES/APPROACHES	NOTES/CLARIFICATIONS
5. Hydrology		
5.1 Elevation of Plant Grade Relative to Ground Water Table	5.1 Plant Grade 10 Feet Above Water Table Elevation	
5.2 Elevation of Plant Grade Relative to Water Levels Resulting From PMF	5.2 Flood Protection Is Required to Plant Grade Elevation	5.2 Flood Protection Facilities, Which Might Be Required to Keep PMF at or Below Plant Grade Elevation, Are Not to Be Included in This Study.
5.3 Source of Water for: -Plant Make-Up -Cooling Tower Make-Up -Emergency Cooling Water System Make-Up	5.3 Source of Water for All Plant Water Make-Up Will Be of a Quality Equivalent to That from Lake Michigan. 1 Typical Water Quality Values Are (in Mg/l)*: 1. PH, 7.3-8.2 2. T. Alk., 118-132 3. T. Hardness, 120-144 4. Cl, 7.5-12 5. Sulfate 18-28 6. TDS, 164-278 7. TSS, 10-110 8. Total PO_4, .02-.04 9. Na, 5.0-10.0 10. Ca, 31-48	5.3 Plant Will Utilize Wet Cooling Towers for Main Condenser Circulating and Non-Class I Plant Service Water Heat Sink

*Detailed design/optimization studies of plant water treating systems are not to be made for these assumed values. 1

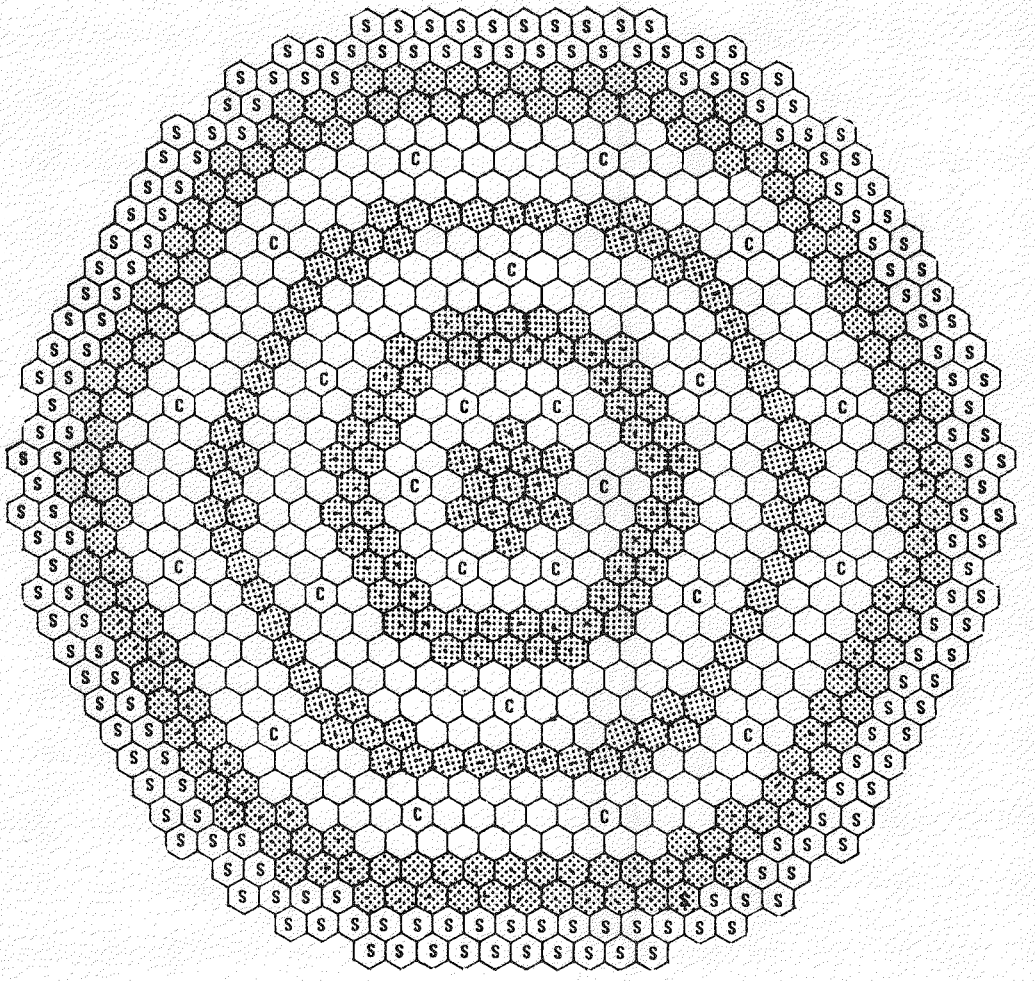

= BLANKET ASSEMBLY NUMBER OF INNER Bs = 145
NUMBER OF OUTER Bs = 162

= FUEL ASSEMBLY NUMBER = 360

= REMOVABLE SHIELD NUMBER = 180

= CONTROL ROD ASSEMBLY NUMBER = 24

PLBR Bullseye Core

0309-271

APPENDIX M

SELECTION OF INERT GAS CONTAINER FOR LIQUID METAL CONTAINING PIPE

M.1 GUIDELINES

The "Guidelines for EPRI LMFBR Design", Appendix L, state the following:

> ..."The design and layout of the IHTS loops shall be such that a break in the IHTS piping within containment shall not result in sodium fires or sodium-concrete reactions."...

It is assumed the intent of the guideline is prevention of liquid metal fires and protection of concrete, and it is extended to apply to the NaK lines within containment.

M.2 BASIC CONCEPT

The concept of providing an inert gas inside a container surrounding the liquid metal containing pipes was selected as the most practical means to prevent a liquid metal spill from contacting concrete or from becoming a hazardous fire.

M.3 CONCEPT VARIATIONS STUDIED

Study was done on three container concepts for the liquid metal containing pipes leading from the IHX and the cold traps. They are schematically shown in Figures M-1, M-2 and M-3. Figure M-1 shows four arrangements of one of the three concepts. In each arrangement, each liquid metal containing pipe is contained in its own individual guard pipe. Since the guard pipe must be removable to permit inspection of the liquid metal containing pipe, it is made

in either a "telescoping" or "clamshell" configuration. The insulation is placed either inside or outside the guard pipe, and accordingly, the guard pipe will be either cold or hot.

Figure M-2 shows an arrangement in which a group of liquid metal containing pipes (secondary sodium containing and RHR-P) from each IHX share a common guard pipe about 13.5 ft in diameter. The common guard pipe is large enough to allow personnel entry for inspection. Insulation and heat tracing is placed on each individual pipe as required and therefore the inert atmosphere inside the guard pipe is at about room temperature. Typical sections through pipe hangers and snubbers for this arrangement are shown in Figure M-4.

Figure M-3 describes a possible arrangement of liquid metal containing pipes within an inerted steel lined cell, similar to the HTS cells used in loop-type LMFBRs.

M.4 CONCEPT SELECTION SUMMARY

Early in the design phase, it became necessary to choose a reference concept to permit continuation of design work. All concepts were evaluated using cost, producibility, inspectability, maintainability and safety as criteria.

The results of a cost comparison did not provide a definitive basis for the choice. The cost differences were so small that they could easily disappear, if all concepts were designed in more and equal detail.

All concepts appear to be producible, and the relative difficulty appears to lead to equal relative cost. Therefore, producibility was not a deciding factor.

The concepts appear to be nearly equal from the safety standpoint. All adequately provide an inert atmosphere surrounding the liquid metal containing pipes within containment. However, the common guard pipe has a small advantage in safety.

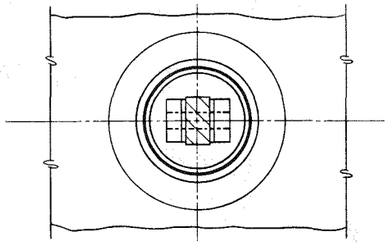

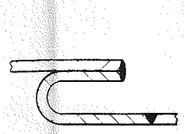

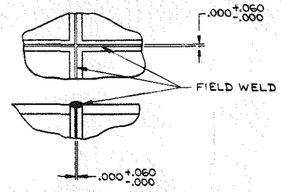

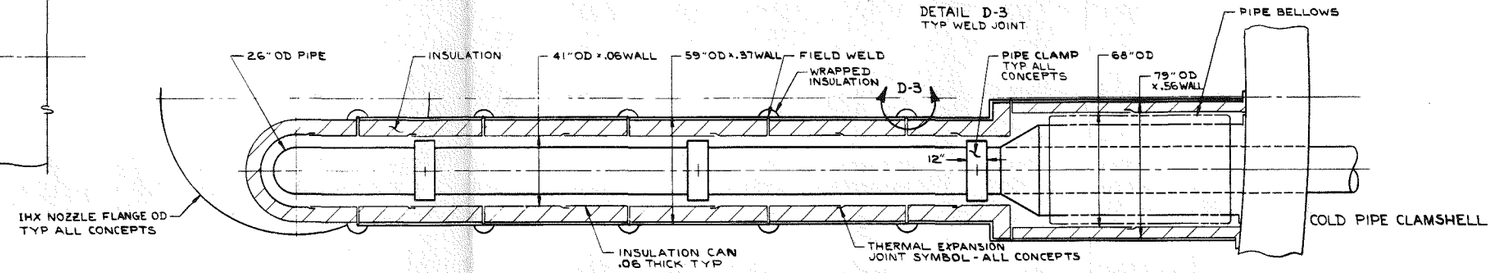

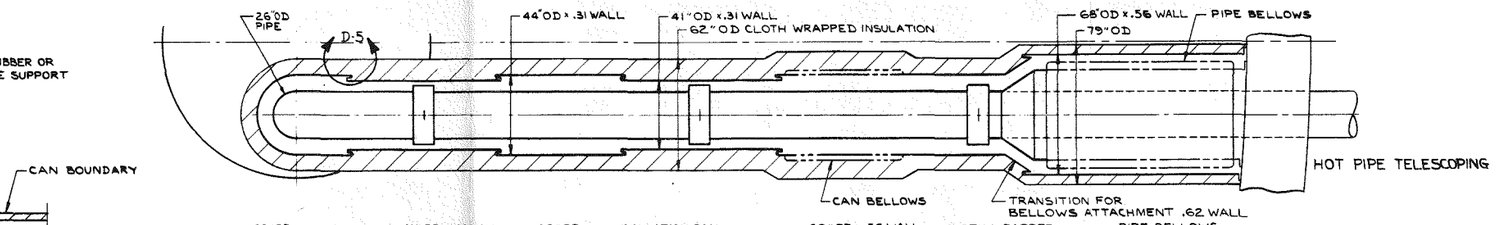

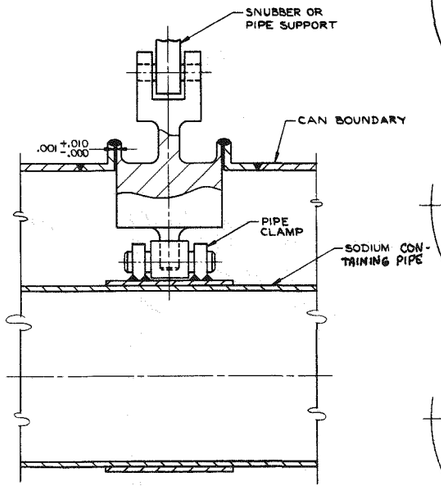

SECTION B-7
TYP PIPE CLAMP PENETRATION
3 REQUIRED AT EACH CLAMP
SCALE: NONE

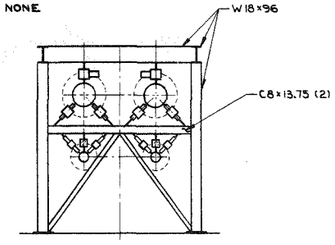

SECTION A-7
TYP ALL CONCEPTS

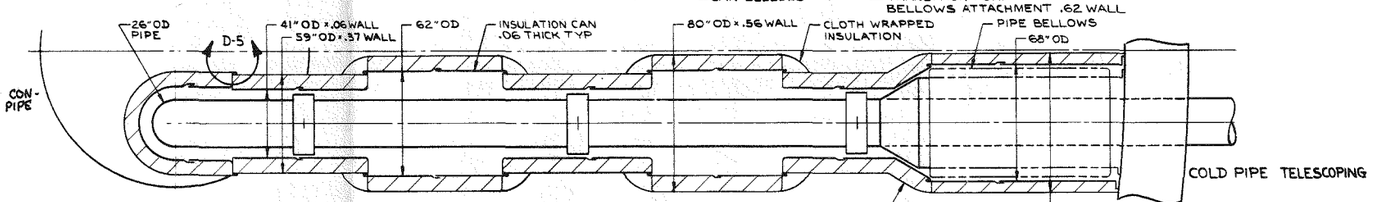

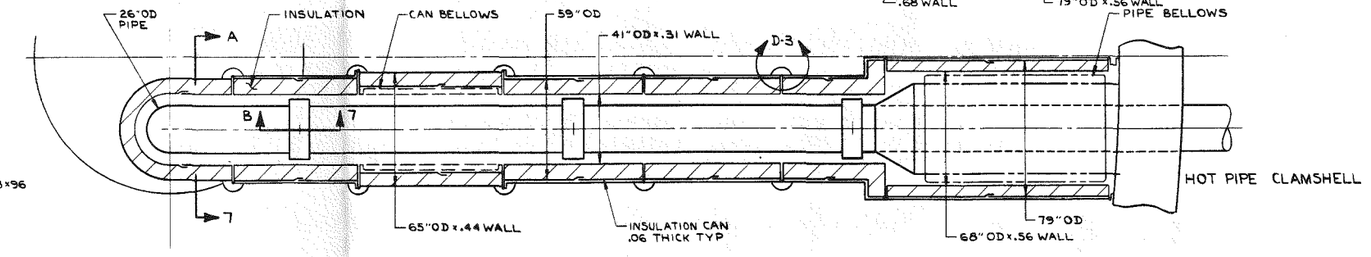

Figure M-1. Individual Guard Pipe Concept

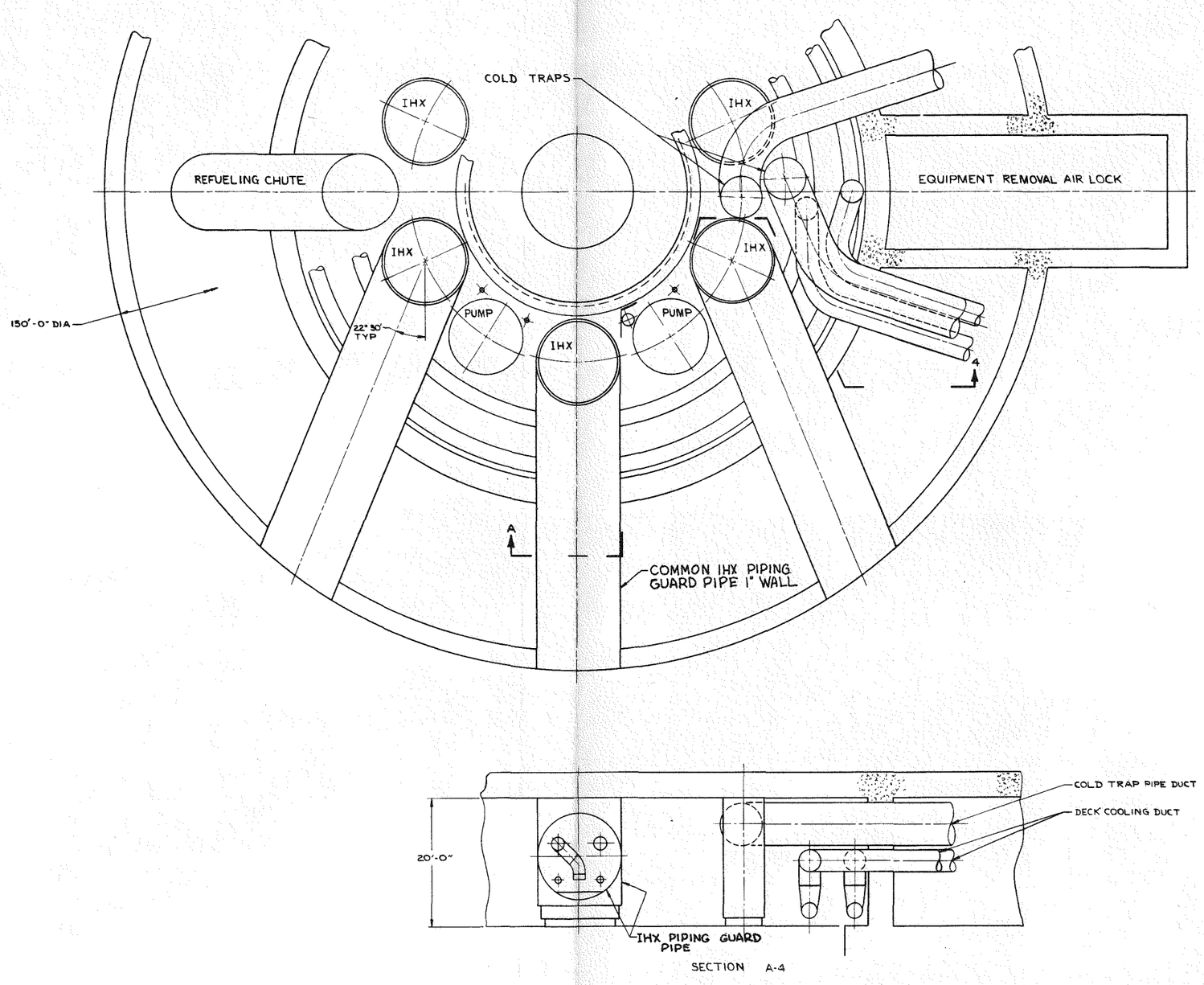

Figure M-2. Common Guard Pipe Concept

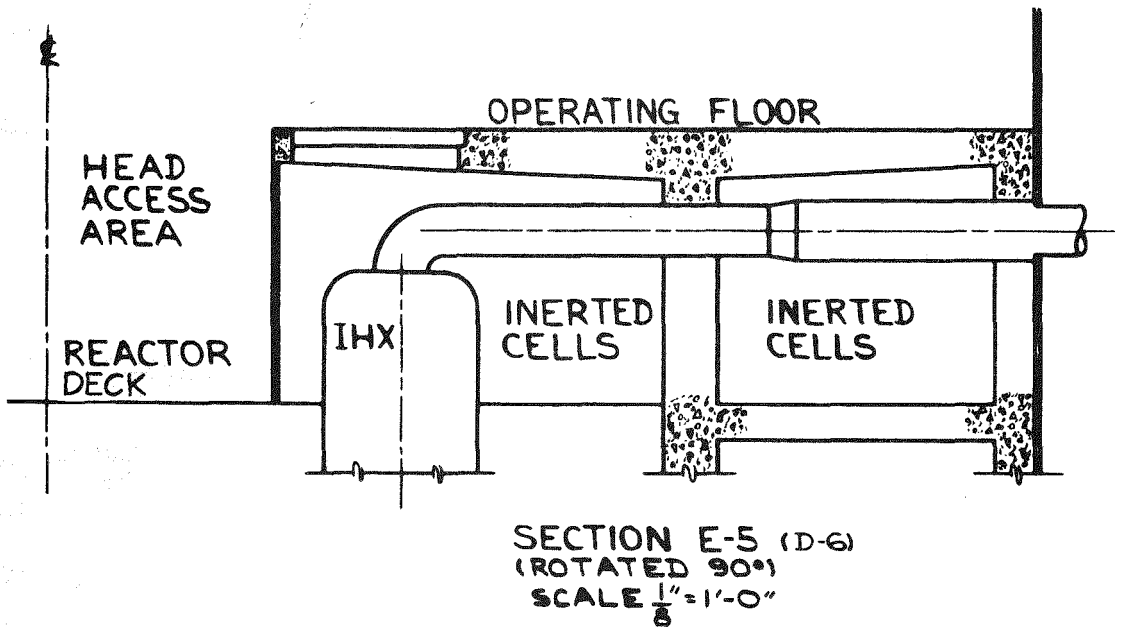

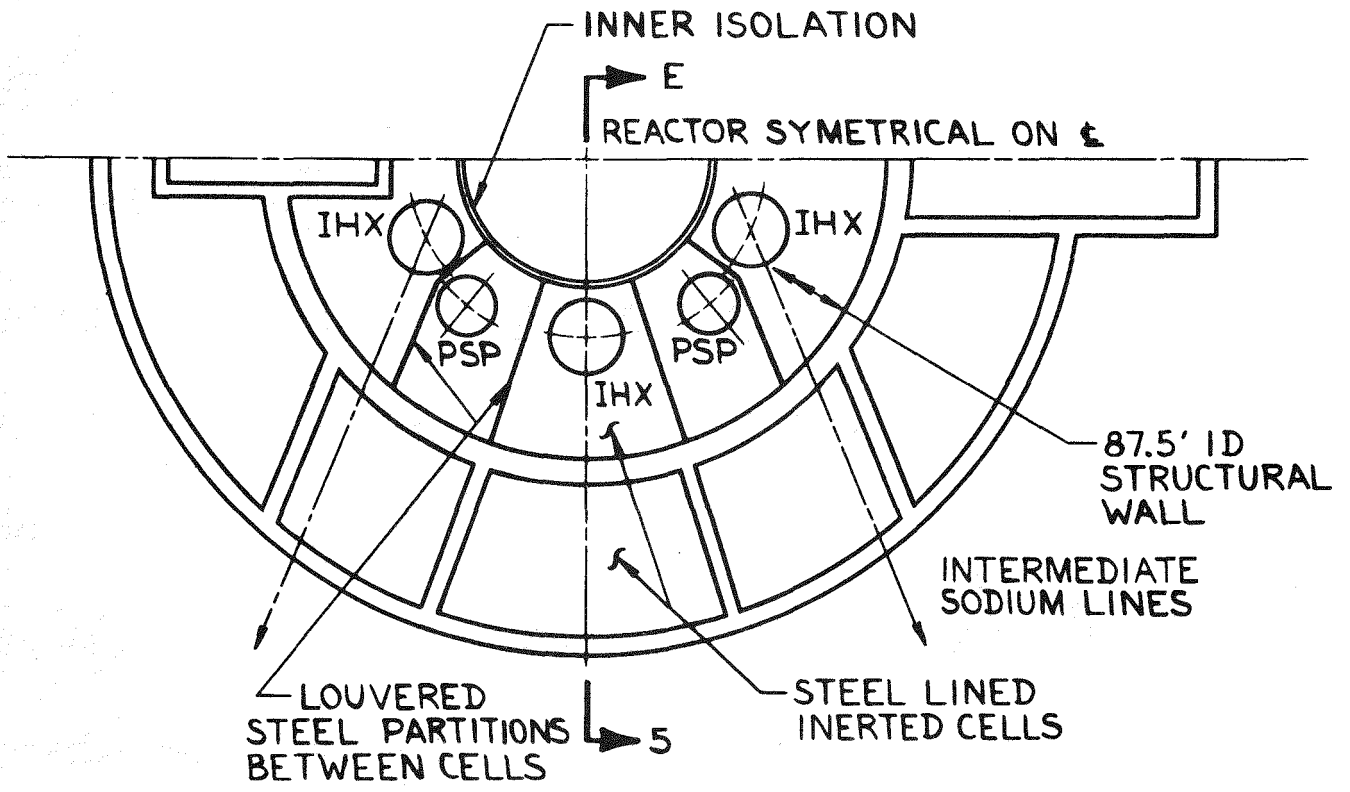

Figure M-3. Inert Cell Concept

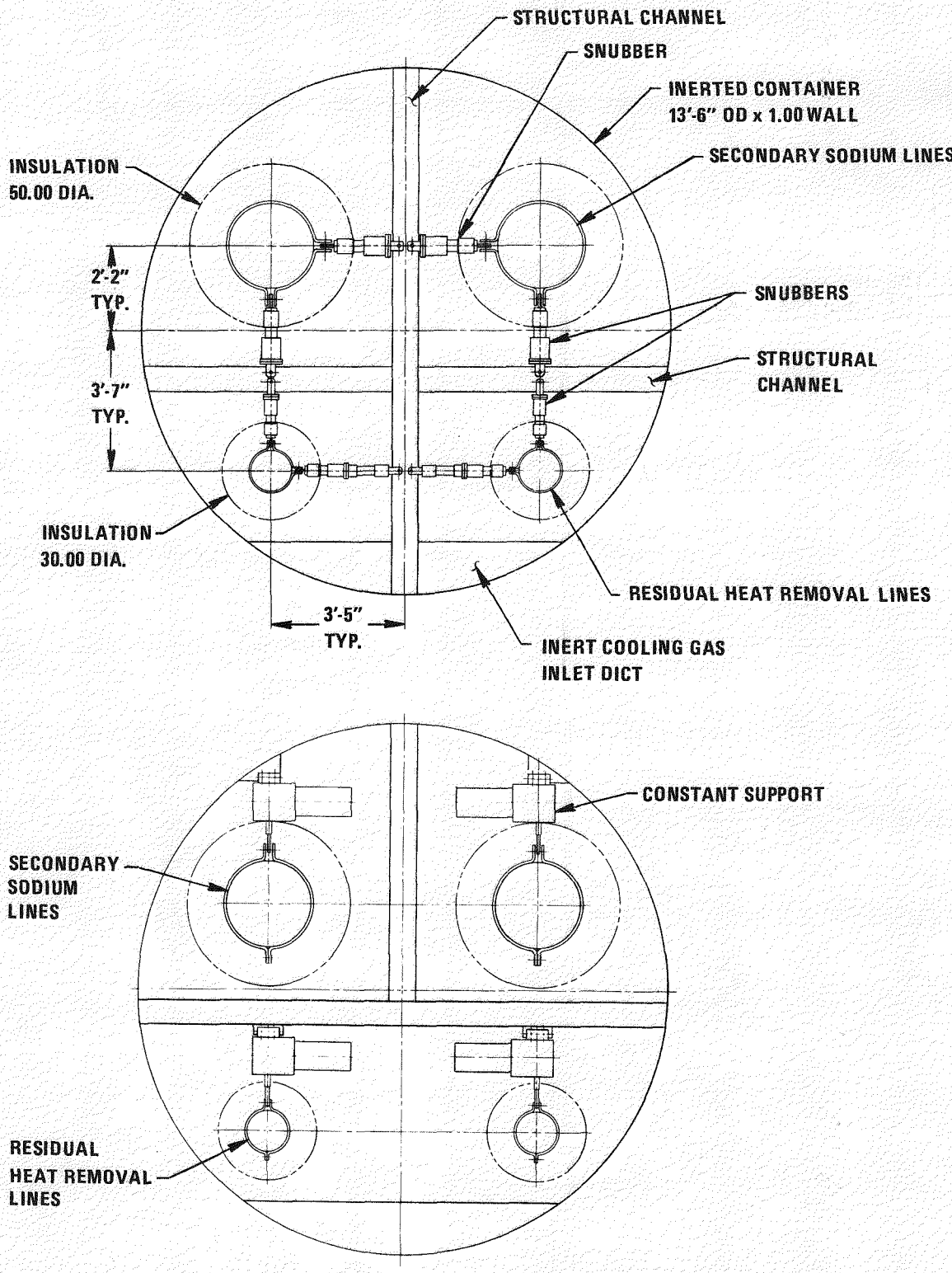

Figure M-4. Pipe Hangers and Snubbers

From the inspectability and maintainability standpoints, the common guard pipe appears to have advantages, and because of these advantages and safety, it was chosen as the reference concept.

The consideration given each criterion in the selection process is discussed in the paragraphs which follow.

M.5 EVALUATION DETAILS

M.5.1 COST AND PRODUCIBILITY

The cost comparison considered only features causing the concepts to have differing costs. The results of the comparison are summarized in Table M-1.

Many features considered in the Table M-1 comparison appear to have equal costs for two or more of the concepts. If costs were lowest, or equal and lowest, no dollar estimate was entered in the table; instead the word "base" was entered to show that the feature has been considered.

As may be seen from the table, costs are nearly the same. If the concepts were all designed in detail, the cost differences could easily disappear, or on the other hand, they could increase. It was concluded that cost should not affect the concept choice.

M.5.2 INSPECTABILITY AND MAINTAINABILITY

A basic requirement on the design of the system providing protection from leaks in the liquid metal containing piping is that it provide ample access to the pipe and pipe supports for inspection and maintenance. The frequency of inspection of welds, hangers, snubbers, heat tracing, etc. is going to be determined by the ASME Code or other regulation. We assume that inspection will not be very frequent, however, it should be feasible. Maintenance, such as repair of a leak or replacement of a faulty snubber or hanger, should be possible without causing a major disturbance to plant operation.

TABLE M-1

COST COMPARISON SUMMARY

Cost Elements	Lined Cell	Common Guard Pipe	Hot Pipe Telescoping	INDIVIDUAL CANS: Cold Pipe Telescoping	INDIVIDUAL CANS: Hot Pipe Clamshell	INDIVIDUAL CANS: Cold Pipe Clamshell
Pipe Clamp Penetrations	Base	Base	$106,700	$106,700	$106,700	$106,700
Hangers & Snubbers	Base	Base	Base	Base	Base	Base
Support Steel	$28,600	Base	28,600	28,600	28,600	28,600
Interior Support Steel	Base	Base	Base	Base	Base	Base
Extra Bellows	Base	Base	234,000	Base	276,000	Base
Guard Pipes						
1) Wt., lbs	Base	545,300 @ $3/lb	142,000 @ $8/lb	327,700 @ $4/lb	161,600 @ $8/lb	236,900 @ $5.50/lb
2) Internal Inlet Duct, lbs	Base	34,600 @ $2/lb	Base	Base	Base	Base
3) Large Bellows & Inst.	Base	133,200	Base	Base	Base	Base
TOTAL COST (1+2+3)	Base	1,838,300	1,136,000	1,310,800	1,292,800	1,302,950
Inert Gas Piping	Base	12,000	44,880	44,800	44,800	44,800
Add'l. Conc. Walls	37,300	Base	Base	Base	Base	Base
Steel Lining for Cells, lbs	501,400 @ $3/lb					
	1,504,200	Base	Base	Base	Base	Base
Louvered Stl. Part.	225,600	Base	Base	Base	Base	Base
Inert Gas Cost	41,400	3,300	Base	Base	Base	Base
Lin. Ft. Inst. Weld	Base	Base	1,620	1,750	3,200	3,040
Installation Weld Cost	Base	Base	24,390	26,300	48,000	45,600
TOTAL	$1,837,100	$1,853,600	$1,574,570	$1,517,200	$1,752,100	$1,528,650
Diff. from Cheapest	319,900	336,400	57,370	Base	234,900	11,450

Simple study of Figures M-1 and M-2 leads to the conclusion that inspection or repair operations of a pipe leak in the individual guard pipe concepts would be more difficiult than the same operations done on the common guard pipe concept, because the individual guard pipe joint must be cut away and rewelded, while the common guard pipe is not disturbed.

Study of Figure M-3 led to the conclusion that the difficulty of inspection and repair operations for the lined cell concept would be slightly less than that of the common guard pipe concept, because of better access available once an air atmosphere is achieved. However, a far greater number of pipe hangers and snubbers would be normally inaccessible in an inert environment.

M.5.3 SAFETY

The individual guard pipe and the common guard pipe concepts do not appear to have significant safety problems. However, the lined cell concept does appear to have some safety disadvantages. In case of a sodium spill, pressurization of the reactor cavity, due to sodium/oxygen reaction, could occur, if the seal separating the cavity from the inerted cells malfunctions. Any pressurization of the cavity volume outside the guard vessel or the primary vessel is considered undesirable. At any rate, such a design would require the cavity seal to have a very high reliability.

The common guard pipe has an advantage in that it has the minimum footage of liquid metal pipe functionally within containment.

APPENDIX N

INSULATION AND INSULATION SUPPORT FOR LPR DECK AND ROTATABLE PLUGS

N.1 INSULATION

In the first phase of the Westinghouse Large Pool Reactor (LPR) study, research was conducted to determine the most suitable insulation materials for use both inside and outside the reactor vessel. The results of this phase of study are given in the "Westinghouse Large Pool Reactor Interim Report", Volume 1, dated January, 1978. They show that the materials selected for in-reactor use at that time were stainless steel encased honeycomb for in-sodium use and canned laminated stainless steel foil for use in the cover gas regions which include the deck and rotating plug insulation.

Subsequently, a comparison study was conducted to determine the merit of using a series of horizontal thermal shields in lieu of the canned foil insulation under the deck. This study is based on an actively cooled deck, lower plate (pressure boundary) temperature of 150^{o}F maximum, and a maximum heat flux of 300 BTU/sq ft-hr through the bottom plate. Another assumption used is that there is a maximum of 2.5% thermal shorts through the insulation caused by the insulation support system. The results of the comparison study show that each of the following three systems perform satisfactorily:

- Twenty (20) thermal shield plates, 0.15 in thick, 0.90 in on center.
- Six inches of canned metallic foil insulation.
- Fifteen (15) thermal shield plates plus two inches of canned insulation.

The twenty plate thermal shield system is selected over the other two systems for incorporation into the LPR reference design. The basic criterion determining the selection is reliability. Cost, fabricability (which relates to cost), and ease of installation are also considered, but no appreciable difference is found among the three systems when comparisons are made on the bases of these criteria. It is felt that a certain degree of degradation of the canned foil insulation can result in the forty year life of the plant. Fifty percent is selected as a conservative value for such a possibility necessitating the use of twice the required thickness of canned insulation as dictated by the analysis. This means that where six inches of insulation does the job, twelve inches is installed to account for degradation due to can rupture or other failures.

The comparison study indicates that some shortening of the vessel could be gained with the use of an all canned insulation system because of the smaller envelope required as compared to the all shield plate system, or the combination shield plate/canned insulation system. However, the lower vessel and component costs resulting from the reduced length are offset by the higher cost of the canned insulation.

Because thermal shield plates are presently being used as an acceptable means of insulating the covers of reactor vessels and liquid sodium test vessels, confidence in their use for the LPR deck and plug insulating system is higher than for other as yet unproven systems. The only cause for reduction in the effectiveness of the plate insulation system appears to be possible bridging of the plates by condensed sodium vapor. A test program must be undertaken to determine the seriousness and frequency of such an occurrence. The tests will also be used to arrive at a configuration to eliminate or minimize the occurrence and to develop a procedure for recovery should elimination of the problem prove to be impractical. However, it does appear that methods of recovery from bridging are far more attainable than recovery from ruptured, and possibly sodium saturated, insulation cans. On this basis, the plate insulation is deemed to be more reliable than canned insulation, justifying its selection for use in the LPR.

N.2 INSULATION SUPPORT SYSTEM

Having made the selection of an insulation system, concept studies of insulation support systems were undertaken. Although no final decision or selection of such a system has been made pending stress analysis, the concepts derived from the study appear to be viable.

The problems associated with the design of the thermal shield support system are, 1) accommodating the thermal gradient of ~700°F which the stack of plates experiences during reactor operation, 2) designing for seismic loads, particularly since the insulation is hung from the deck, and 3) minimization of thermal shorts which reduce the efficiency of the insulation system.

In preparing concepts of the insulation support system, attempts are made to provide a means of modularizing the plate stacks and their supports to allow shop fabrication and assembly and easy installation on the deck and plugs. The plate area is kept as large as practicable to minimize fabrication costs. Whereas previous designs of similar systems work around the problem of differential expansion due to the thermal gradient by suspending a stack of plates by a single rod penetrating their centers of area, the support systems reported herein use multiple support points for the plates. The single support system necessitates the use of rather small plates (maximum dimension 2 ft x 2 ft), but by going to four or five support points plate size can be increased to ~5 ft x 5 ft, an increase in plate area (and therefore a reduction in the number of plates to be fabricated) by a factor of 6-1/4.

One method of insulation support, Figure N-1, considers using a steel box structure to support the plates. The sides of the box are perforated to reduce their area by 50% thereby reducing the heat flow. Cylindrical spacers made of honeycomb are used to separate the plates and are felt to contribute a minimum of additional conductance. The box structure itself, if constructed of 3/16 in stainless steel gives a thermal short value of 1.25% of the total module area when plates with 25 sq ft of area are used. This is well below the value used in the insulation analysis. However, stress analysis may show that the thermal gradient is too severe for this rigid structure.

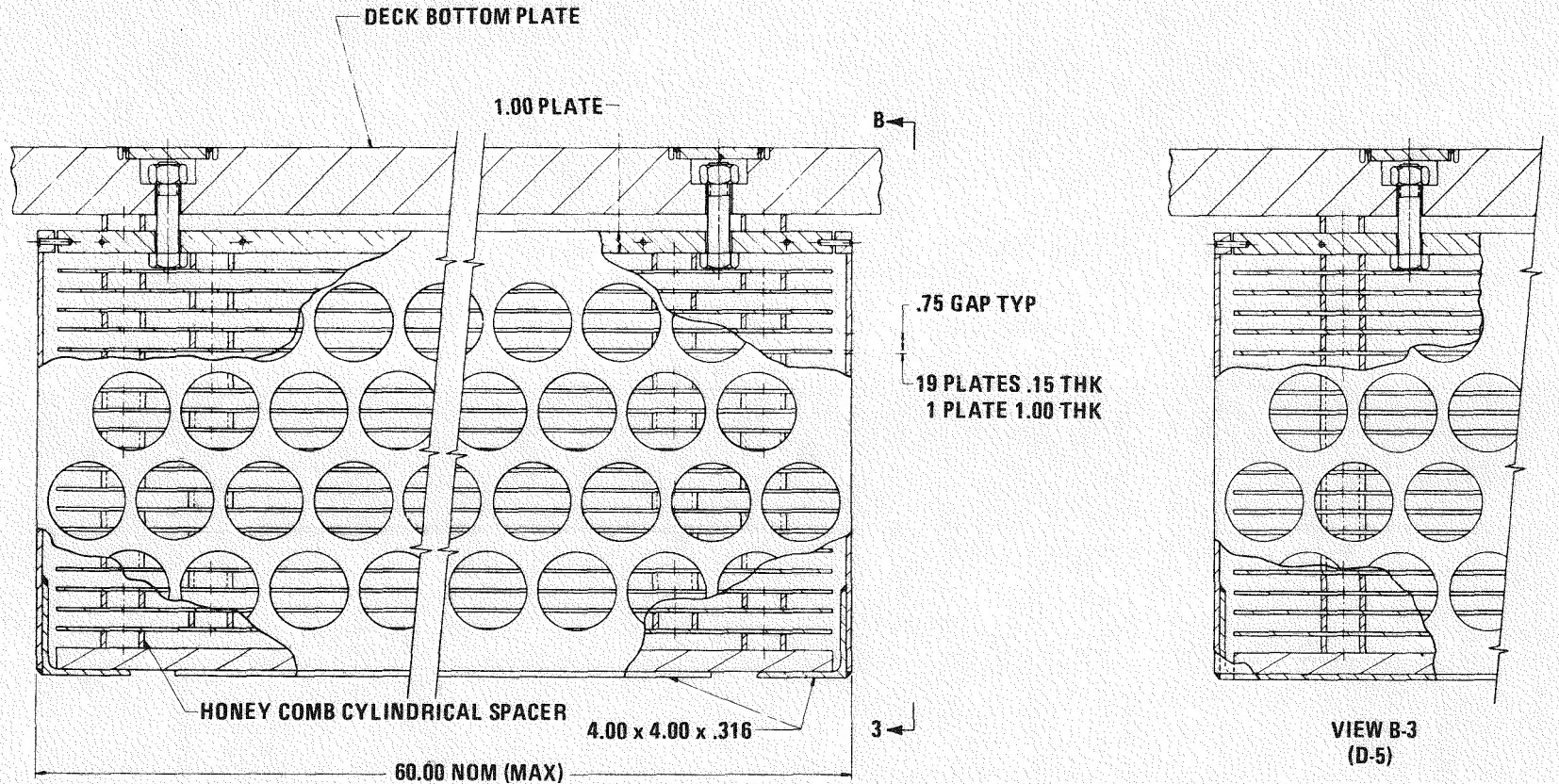

Figure N-1. Thermal Baffle System Using Box Support

As in all concepts reported herein, a feature not shown in the figures is that the plates will be provided with a slight bend to allow sodium condensation to roll off.

Figure N-2 shows a concept that uses an angle frame in lieu of the perforated box to support the plates. Horizontal triangular webs welded to the interior of the angle legs serve as shelves on which the plates are supported. Diagonal bracing is added to provide rigidity, but the structure may be found to be adequate without them. This structure gives an even lower thermal short value of 0.38%.

A chain support system, Figure N-3, is also feasible. It has two advantages over the other systems. First it has the lowest thermal short value <0.1% and secondly, it has an extremely low frequency, thereby rendering it insensitive to seismic loading, whereas all the other concepts must be designed for seismic events.

A final concept, Figure N-4, substitutes hollow hanger rods for the chains. The rods although not as flexible as the chain, are still less rigid than the box and frame structures (concepts 1 & 2) and should prove to be suitable under seismic conditions. The thermal short value of the rod support system is 0.4% - again lower than the value used in the thermal analysis of the insulation system.

The insulation system and methods of support described herein are applicable to the fixed portion of the reactor deck. A similar system is used to insulate the rotating plugs; however, a larger number of reflector plates are used to reduce the heat load and to increase the length of the thermal gradient in the upper internals structure which is rigidly attached to the small rotating plug.

In summary, four concepts for supporting reflector plate insulation are shown. All appear to be workable. A selection will be made in the future based on the results of structural analytical work.

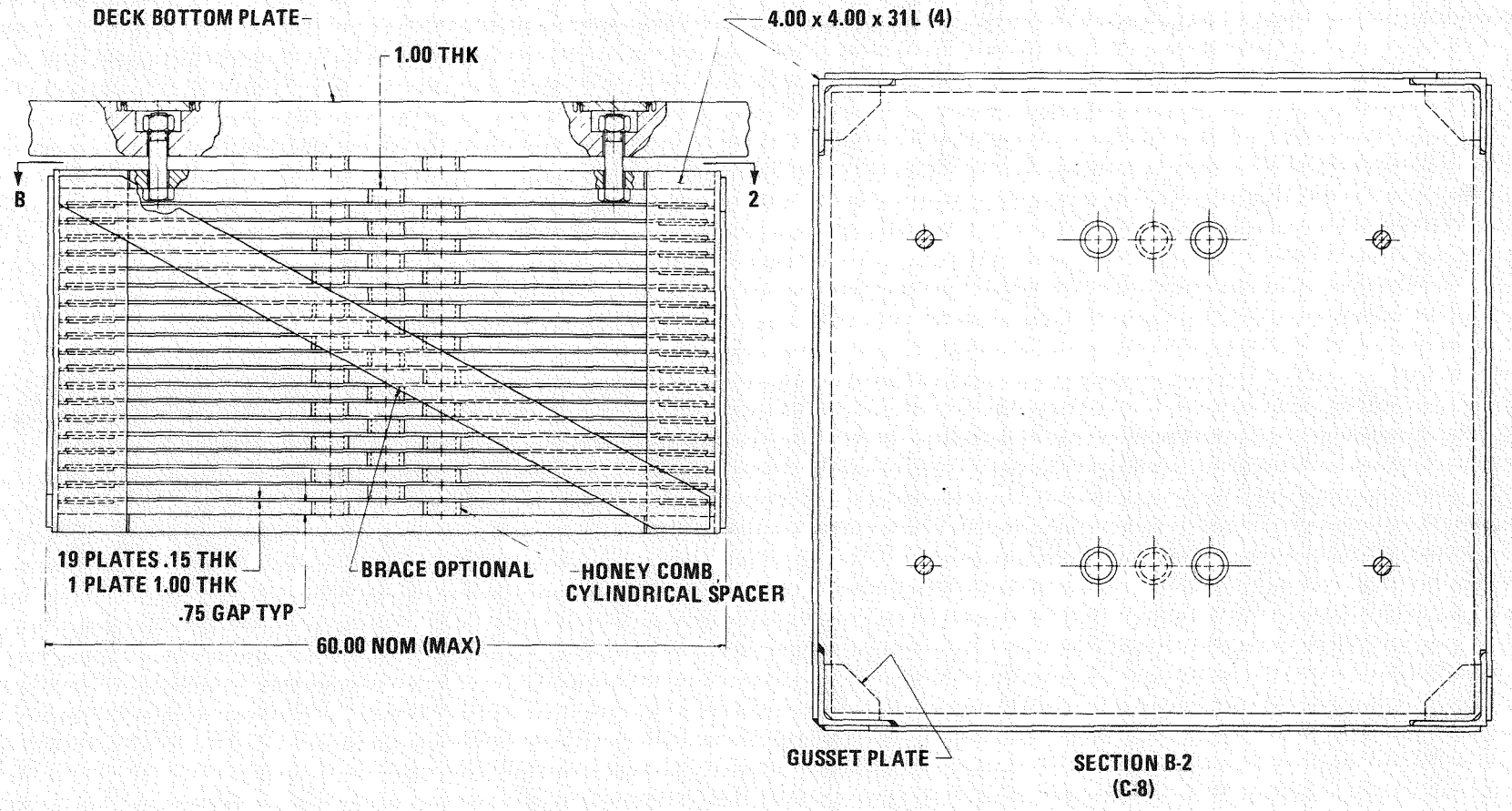

Figure N-2. Thermal Baffle System Using Frame Support

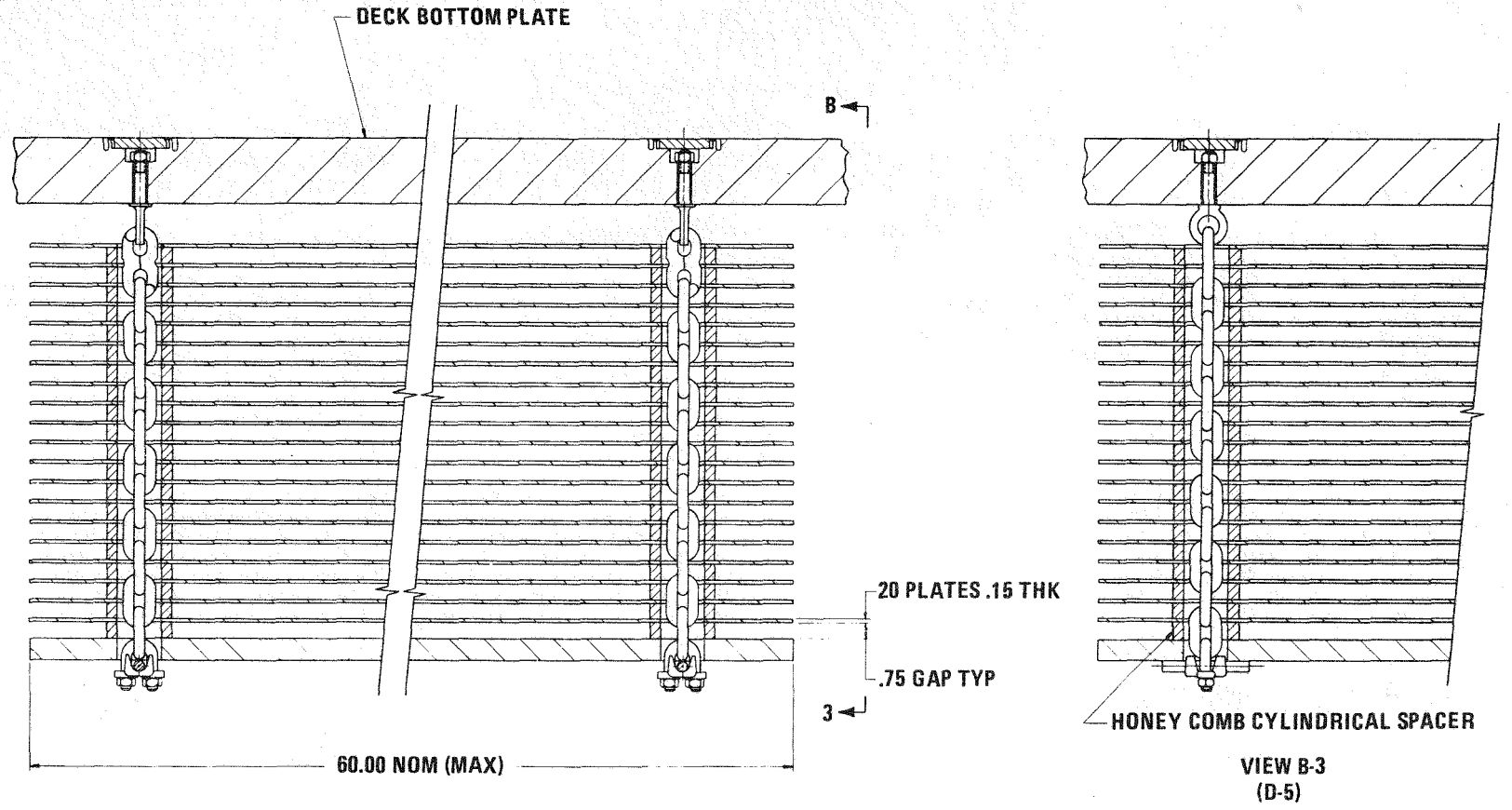

Figure N-3. Thermal Baffle System Using Chain Support

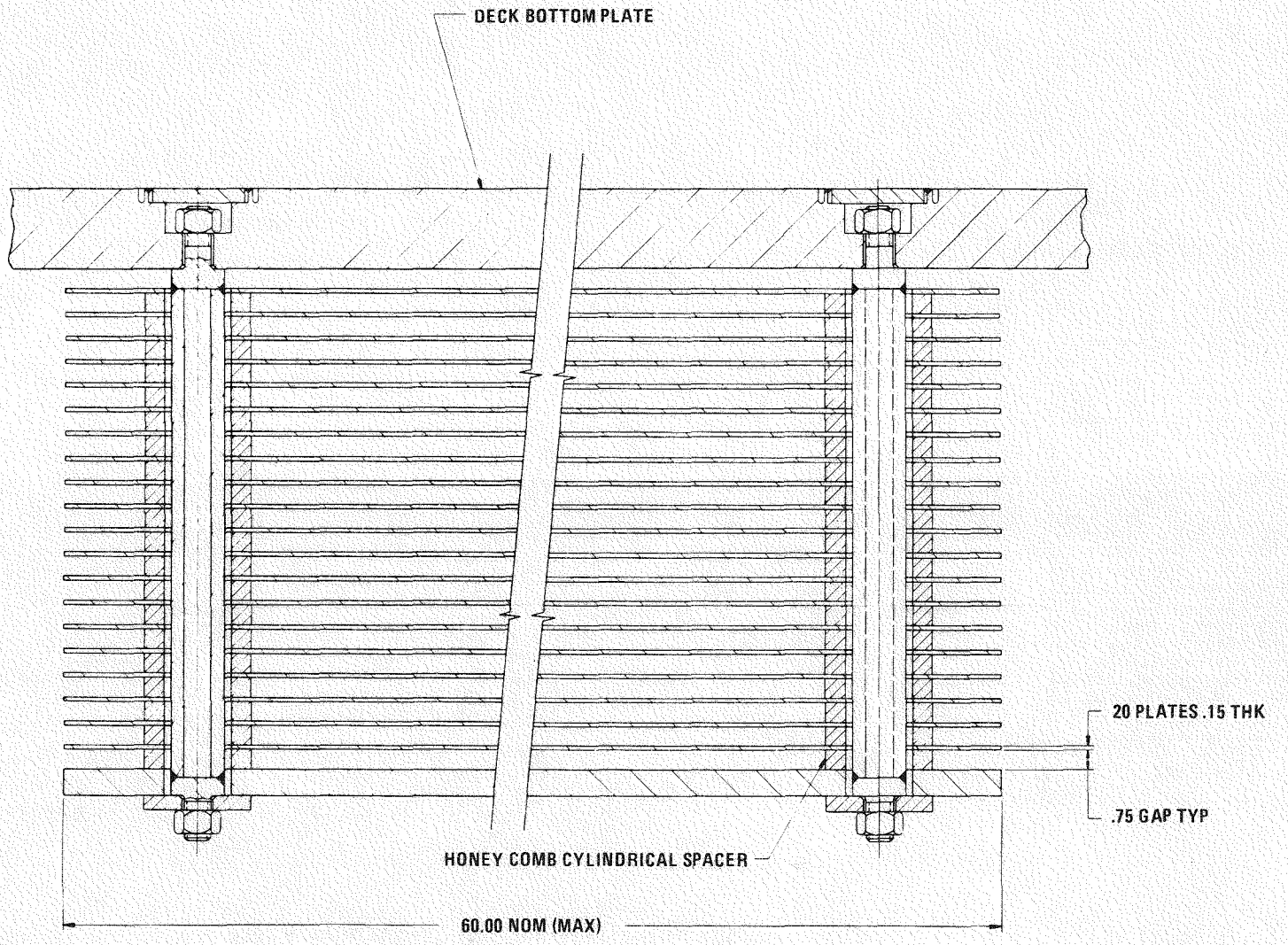

Figure N-4. Thermal Baffle System Using Rod Supports

APPENDIX O
SELECTION OF AIR AS A DECK COOLANT

The deck and rotatable plugs of the Large Pool Reactor are insulated from the hot sodium pool, and actively cooled by a gas cooling system. Sufficient insulation is provided below the primary boundary of the deck to limit the heat flow through the boundary to a maximum of 300 Btu/hr-ft^2. Gas is passed over the top surface of the primary boundary to remove this heat and thus maintain the maximum temperature of the bottom of the deck at 150^{o}F.

Four different gases were considered as possible coolants: nitrogen, argon, and helium because they are inert and therefore compatible with sodium; and air because the need to use an inert gas is not an obviously mandatory requirement. Any of the compatible gases would require that the cooling system be a closed loop system in which the coolant gas is continuously recirculated and cooled. The use of air permits consideration of an open system, where the heated air is discharged directly to the atmosphere. The physical properties of the gases in question are given in Table O-1. Based on the specific heats alone, helium would appear to be the first choice as a coolant. However, helium is also the least dense gas and, at the low pressures considered, requires a large flow rate to obtain a given heat

TABLE O-1

Gas	Air	N_2	Argon	Helium
Specific Heat (Btu/lb-^{o}F)	.241	.247	.124	1.250
Specific Gravity (Relative to Air)	1	.967	1.379	.138

removal rate for a given ΔT. Argon is the most dense gas, but it also has the lowest specific heat. By taking the product of the specific heats and the specific gravities and normalizing to helium, the four gases can be arranged in the following numerical rating for effective heat removal, for equal volume flow rates:

Argon	.993
Helium	1.00
Nitrogen	1.38
Air	1.40

Argon and helium are essentially equal in their ability to remove heat in an active cooling system. Nitrogen and air are also about equal.

Given that air is the most effective coolant, the feasibility of using air directly in contact with the primary boundary was addressed. Containment Systems Safety Engineering reviewed the deck cooling system on the basis of using air as the coolant. They identified two safety concerns: 1), in the unlikely event that a leak should develop in the primary boundary which is being cooled by the air, could air leak into the cover gas region and react with the sodium aerosol which could, in turn, impair the normal function and operation of the reactor; and 2), could the cover gas system be over pressurized by intercommunication with the cooling system through a defect in the primary boundary.

Both of these concerns are eliminated by maintaining the cooling gas plenum pressure slightly below the cover gas pressure. This is easily achieved with a system which uses suction fans to draw air through the deck, rather than blowers which force air through the deck. Since the cover gas plenum and the coolant gas plenum are both maintained at a pressure of a few inches of water the positive pressure gradient from cover gas to cooling gas would be very small and have a negligible effect on the release of cover gas through any defect.

The use of air as a coolant offers a number of system simplifications and economic advantages over inert gases. Air is the easiest gas to handle; system leakages are permissible; standard controls and equipment exist; and the supply is unlimited.

Since an active cooling system is required for the rotating plugs, the use of air offers other simplifications relative to the use of other cooling gases. By using containment air as the source of cooling, the entire cooling system

can be mounted on the rotating plugs with only the cabling for the fans crossing the plug parting lines. If an inert gas is used as the coolant, then either flexible gas supply and return ducts must be used, or the entire closed circulation systems must be self-contained on each plug. If this latter alternative were followed, then the heat load to containment air would be the same as when the coolant air is exhausted directly to containment.

The use of air for the stationary deck also eliminates a considerable amount of distribution piping since the air can be drawn directly from containment. This eliminates an inlet distribution manifold.

AIR ACTIVATION

Air is subject to activation by the neutron flux existing above the sodium pool during full power operation. Activation of air in the deck structure was predicted using neturon flux characteristics and spectra calculated for the in-vessel regions of the Fast Test Reactor (FTR).

In the deck cooling region, the activating flux intensity is primarily a function of pool depth and the thickness of the steel shield located between the pool and the cooling area. Total reactor power is not a consideration because, as long as the fuel material is a mixed oxide, the average power density is no more than that for the FTR core.

In the FTR, a total neutron flux of 10^8 nv is predicted for a sodium pool depth of 16 ft above the top of the fuel assemblies. The characteristic attenuation of neturons in the pool is a reduction in flux by a factor of 10 for every three feet of sodium. Therefore at the top of a 28' deep pool, the total neutron flux is 10^4 nv. The presence of 7.5 in of stainless steel further reduces the flux to a value of 3.4×10^2 nv in the deck cooling area.

The residence time in the neutron flux is approximated by the volume ratio $V_{\text{flux region}}/V_{\text{containment}}$. The volumes used were 47 ft^3 for each of the 12 compartments being cooled and $V_{\text{containment}} = 1.8 \times 10^6$ ft^3.

The spectrum of neutrons is fairly hard because low energy neutrons will be removed by capture in the 7.5 in of steel. The spectrum in the FTR radial shielding, E $\sim$ 0.13 MeV, was chosen to represent the cooling area spectrum for all nuclides except argon. Because argon activation rates were available from FTR cover gas activation analyses, these rates were used by scaling the neutron flux levels.

In the case of short-lived nuclides, concentrations in containment were calculated by equating production rates with decay rates. For long-lived nuclides, concentrations were calculated at one year and 30 year intervals, with no credit taken for losses, purification or reactor duty cycle. In all cases, complete mixing in containment was assumed.

Containment concentrations of nuclides produced by neutron activation of deck cooling air are given in Table O-2. The maximum permissable concentration values for 168 hour exposure in air were used to evaluate the overall results after one year and 30 years of operation. In both cases, the total MPC fraction is less than 6×10^{-6}, which is well below the permissible total of one.

RADIOLYTIC PRODUCT FORMATION

A study was performed to determine the radiolytic products formed in the deck cooling air and the effect of these products on system design. Of the products formed radiolytically, two were found which are potential problems. The two are ozone (O_3) and nitric acid (HNO_3). Both can be biologically toxic and nitric acid can also corrode carbon steel.

When containment building air is used as the deck coolant, the peak allowable ozone level, 0.1 ppm, is achieved within the containment building after 16 days of reactor operation. The calculated nitric acid level is 1.1 ppm in the containment building after one year of operation. Although the ozone level reaches the allowable limit in 16 days, the limit is based on 40 hours/week occupancy. The solution to this problem, and the one chosen in the reference design, is to provide a containment building purge. This limits the buildup

of both ozone and nitric acid within the containment building by means of continuous dilution. The corrosion rate of deck steel by nitric acid, being four grams in forty years, is not a problem.

CONCLUSION

The review of possible gases for use as a deck coolant indicates that air offers significant system and economic advantages over other possible gases. Furthermore, the use of air does not limit the safety or ability to license the LPR.

TABLE O-2

CONCENTRATIONS OF AIR ACTIVATION PRODUCTS IN LRP CONTAINMENT

Reaction	Product Nuclide	Half Life	MPC_a^{168} Ci/m^3	Concentrations, Ci/m^3 1 year	30 years
$^{14}N(n,p)^{14}C$	^{14}C	5770 y	1×10^{-6}	3.4×10^{-16}	1.0×10^{-14}
$^{15}N(n,\gamma)^{16}N$	^{16}N	7.14 s	1×10^{-10}	4.8×10^{-16}	4.8×10^{-16}
$^{16}O(n,p)^{16}N$	^{16}N	7.14 s	1×10^{-10}		
$^{18}O(n,\gamma)^{19}O$	^{19}O	29.4 s	1×10^{-10}	7.1×10^{-19}	7.1×10^{-19}
$^{17}O(n,p)^{17}N$	^{17}N	4.14 s	1×10^{-10}	7.3×10^{-23}	7.3×10^{-23}
$^{17}O(n,\alpha)^{14}C$	^{14}C	5770 y	1×10^{-6}	1.7×10^{-20}	5.1×10^{-19}
$^{16}O(n,2n)^{15}O$	^{15}O	118 s	1×10^{-10}	7.8×10^{-20}	7.8×10^{-20}
$^{14}N(n,2n)^{13}N$	^{13}N	10.05 m	1×10^{-10}	1.7×10^{-18}	1.7×10^{-18}
$^{14}N(n,t)^{12}C$	^{3}H	10 y	2×10^{-6}	$2.1\ 10^{-18}$	6.4×10^{-17}
$^{40}Ar(n,\gamma)^{41}Ar$	^{41}Ar	109 m	4×10^{-7}	2.8×10^{-13}	2.8×10^{-13}
	Total MPC_a^{168} Fraction			5.53×10^{-6}	5.54×10^{-6}

APPENDIX P
TWO PLENA CORE INLET

From the start of a fuel cycle to the end of the cycle in a 1000 MWe radial parfait core design with batch refueling, the power fraction of the fuel regions typically reduces from approximately 0.92 to 0.79 and the power fraction of the blanket regions increases from approximately 0.07 to 0.21. These values are obtained from the core analysis results reported in the PLBR Phase II final report, dated June 1977. The bullseye core in the LPR has similar values. The fuel reduces from 0.89 to 0.83 and the blanket increases from 0.11 to 0.17. These values are reported in the AI final report, EPRI NP-645, Dated April 1978. During the fuel cycle with a fixed orifice arrangement, this change in power fraction causes changes in the reactor mixed mean core outlet temperature. Initially the blanket assemblies are overcooled resulting in a lower outlet temperature. This temperature difference between the blanket and fuel assemblies changes during the fuel cycle. At the end of the fuel cycle the fuel regions are overcooled. The result is a continuous difference in outlet temperature that leads to potential stripping problems. Other than understanding that this change in mixed mean outlet temperature results in a loss of efficiency and leads to potential striping problems, a total evaluation of the thermal effects on the upper internals and other LPR components has not been completed.

In FFTF and CRBR the upper internals were designed to accept the possible striping and stratification phenomena of this outlet temperature variation. Designing for the temperature variation has added considerable complexity and cost to the FFTF and CRBR upper internals. Because of this complexity and cost, it is very desirable to ameliorate this temperature variation in the LPR design.

One method of compensating for the change in power fractions in the fuel and blanket regions is to provide a method of flow control that can be varied during the fuel cycle. Since no core design work was included in the LPR

phase A extended effort, it is assumed based on the power fractions from both of the above cores, that initially the flow through the fuel regions is 90% and the flow through the blanket regions is 8%. The remaining 2% is channeled up through the control rod and shield assemblies. By the end of life the fuel flow is 80% and the required blanket flow 18%. Flow control to accommodate this change in flow distribution can be provided with a two plena system that includes some valve system to vary the flow to the plena during the fuel cycle. Five two plena concepts were investigated. Each adds some complexity to the LPR design.

The first concept, as shown in Figure P-1, utilizes a throttle valve, pipe and flow meter arrangement that provides low pressure coolant to a plenum below the high pressure plenum similar to the EBR-II design. In this concept the valve and flowmeter are located above the conical structure. Eight penetrations are required in the conical structure for the low pressure coolant lines and four in the deck structure for the valve actuators. The coolant lines (low temperature) must be insulated since they pass through the high temperature plenum. It is conceivable in this arrangement that maintenance could be performed on the valve through a plug in the deck structure. Figure P-2, shows the valve and flowmeter below the conical structure. In this arrangement, four penetrations are required in the conical structure and four in the deck structure for the valve actuating mechanisms. Removal of a valve and/or flowmeter for maintenance is extremely difficult due to their location.

The second concept, Figure P-3, includes a throttle valve and flowmeter inside the low pressure distribution ring. This arrangement provides a flow path directly from the high pressure region to the low pressure region without long pipe runs. Since the valve is inside the core support structure, access to the valve for maintenance is next to impossible. In this concept an actuating mechanism is located in the rotating plug of the deck structure. The mechanism has to be removed during refueling operations and engages the throttle valve shaft only when the plug is in a specific parked position. Figure P-4 shows a shaft and gear box arrangement that allows the actuating

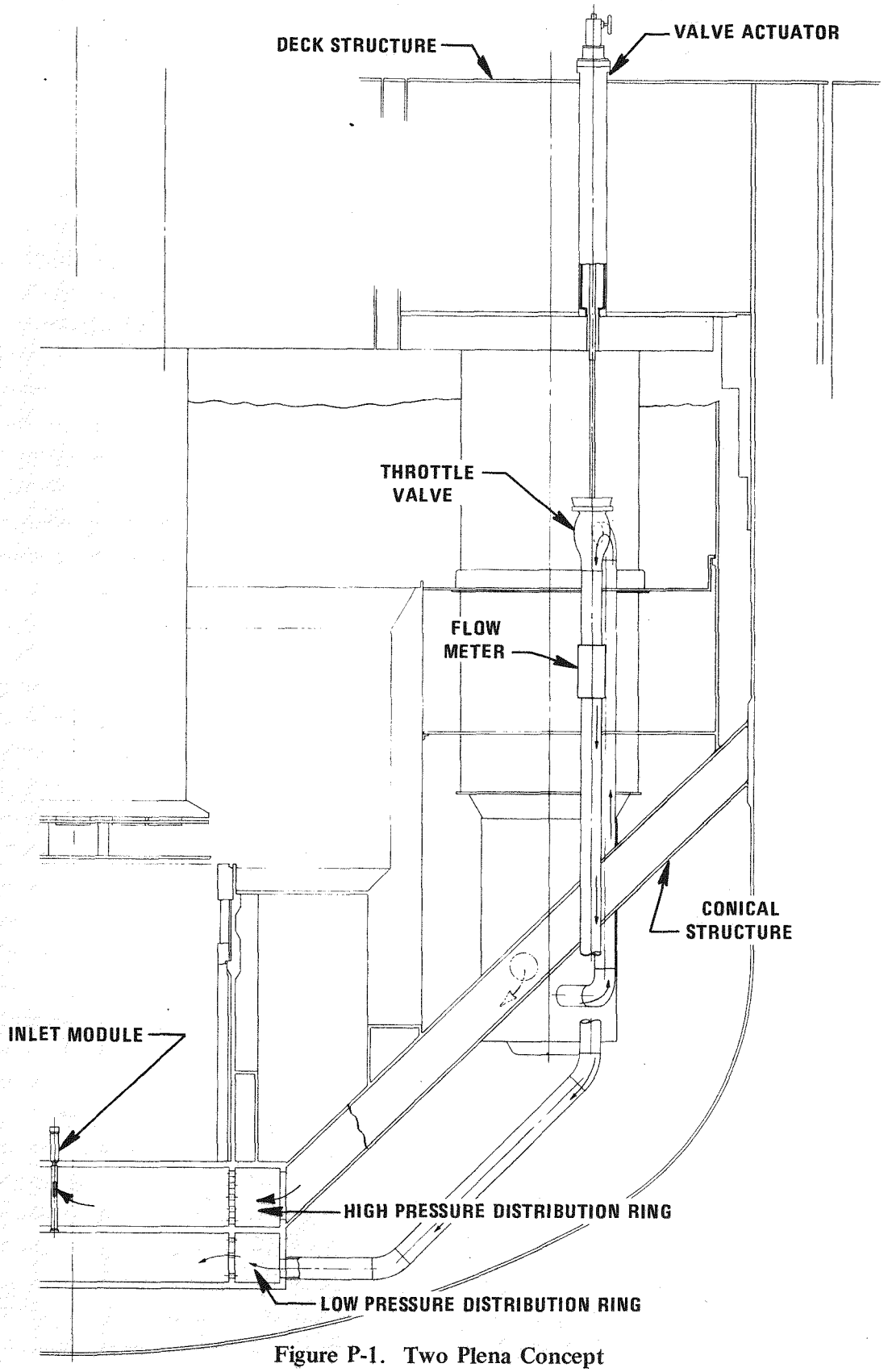

Figure P-1. Two Plena Concept

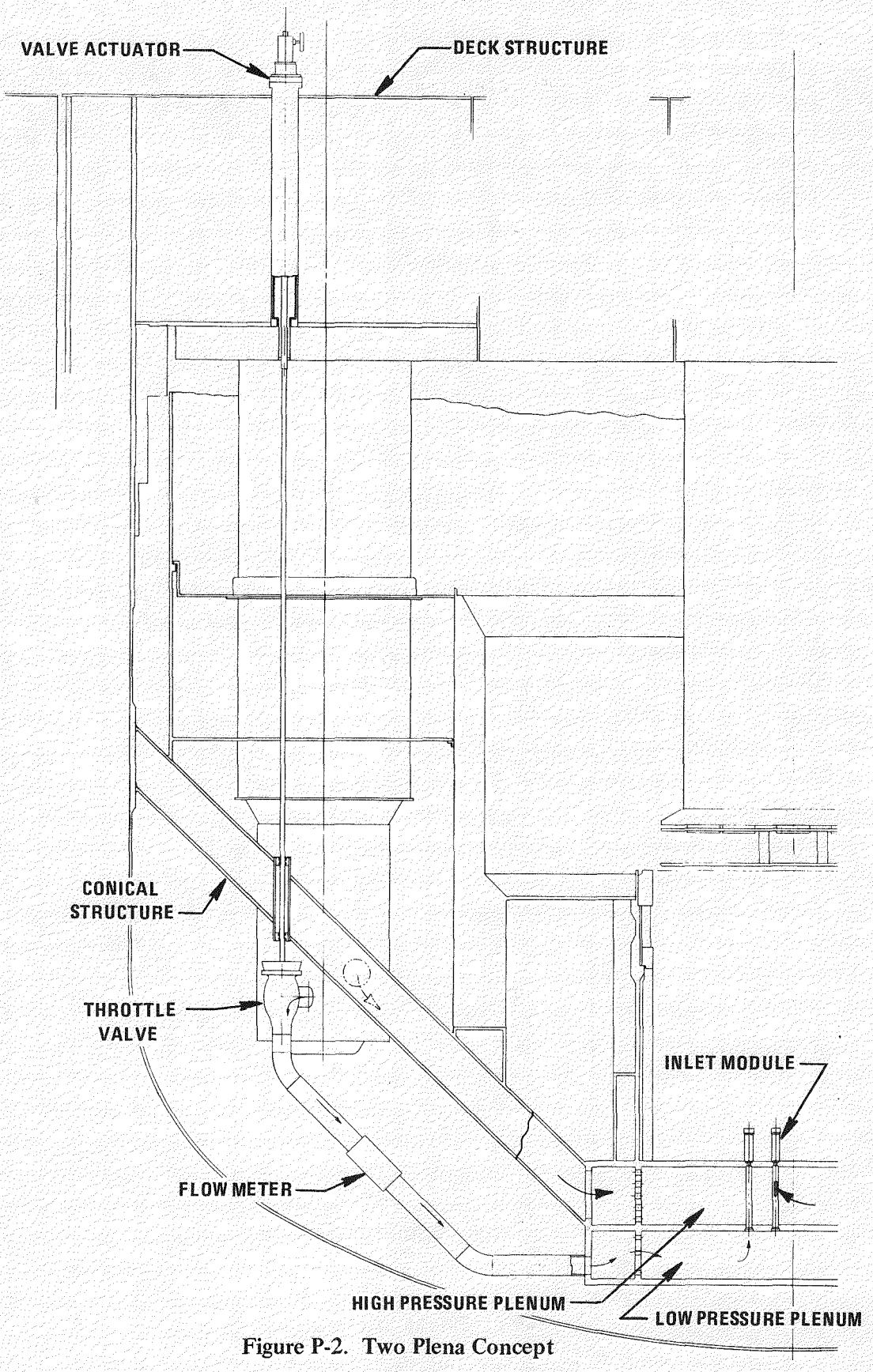

Figure P-2. Two Plena Concept

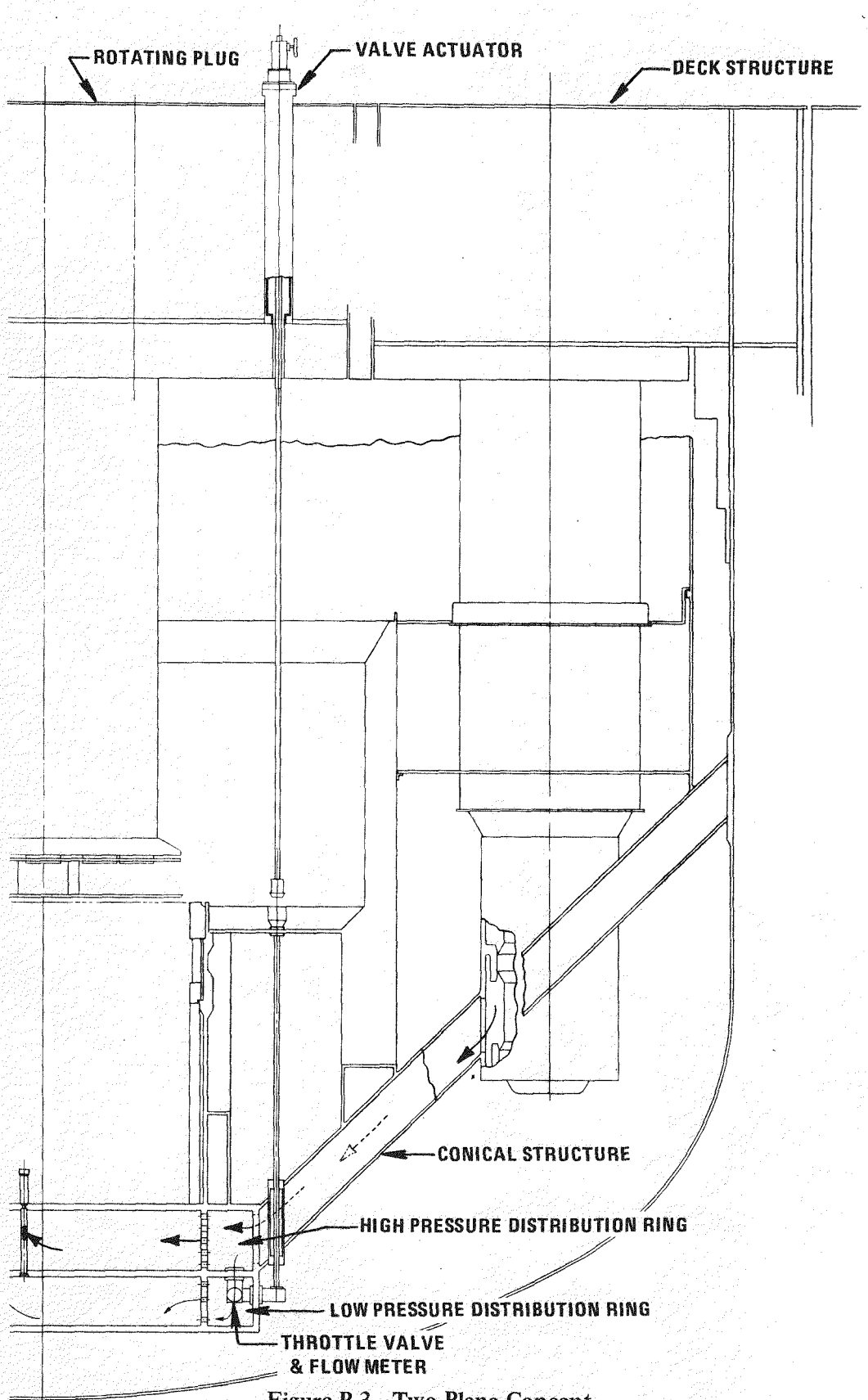

Figure P-3. Two Plena Concept

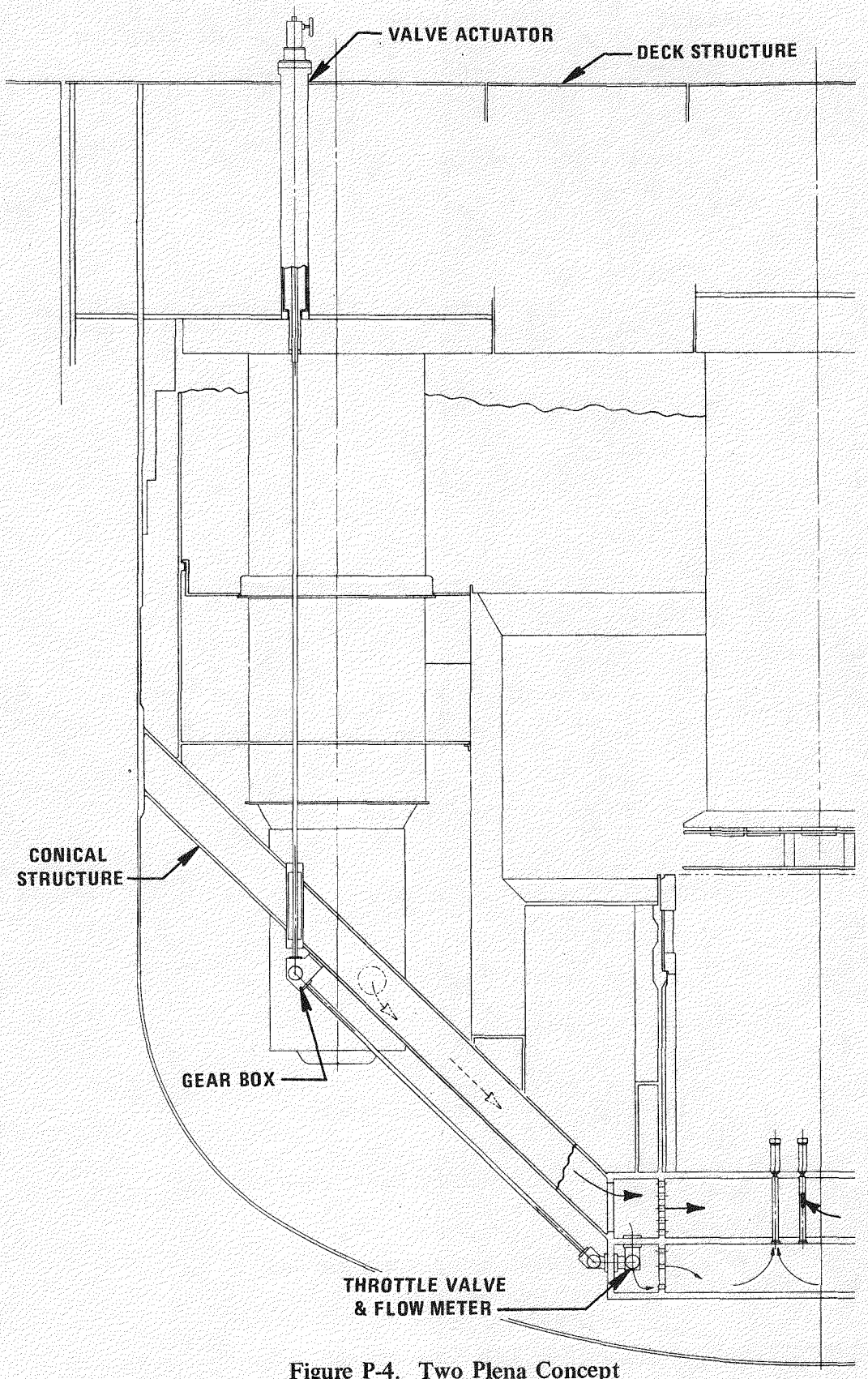

Figure P-4. Two Plena Concept

chanism to be positioned in the stationary region of the deck structure. This arrangement allows the valve to be adjusted at anytime. Both arrangements require penetrations in the conical structure and deck structure.

The third concept, Figure P-5, includes removable shield assemblies in the core periphery that provide orificed flow from the high to the low pressure plenum. The flow is controlled by the number of orificed shield assemblies installed in the core. This method doesn't require valves, pipes, or penetrations in the conical structure or the deck structure, but provides for flow adjustment only during shutdown conditions.

The fourth concept, Figure P-6 consists of utilizing six primary pumps - four high pressure and two low pressure. The low pressure pumps have the capability of supplying approximately 8 to 18 percent of the core flow to the blanket regions and the high pressure pumps are adjusted to supply the remainder to the fuel, control rod and shield regions.

In the final concept, a valve is included in the discharge chamber of the primary pump as shown in Figure P-7. A fixed orifice is located on each side of the valve to provide 8% of the flow. The value can be adjusted to provide from 0 to 10% additional flow so that the orifices combined with the valve provide 8 to 18% of the total flow. A valve actuating shaft passes up through the pump to an actuator located at the top of the pump. Seals are required where the shaft and low pressure pipe penetrate the pump pressure boundaries. A bellows-type-face seal arrangement is shown between the valve in the pump discharge chamber and the pipe leading to the low pressure plenum. A seal of this type is required at this interface to compensate for tolerances and relative motion between the two seal surfaces during change in reactor temperatures. The low pressure pipe penetrates the conical structure and is welded to the upper and lower cone. Expansion loops are included in the pipes below and above the conical structure to minimize the stresses in the pipe.

The valve and orifices in this concept can be removed with the pump if maintenance is required. The flow can be varied without shutting down the ctor. The low pressure coolant pipes probably would not require insulation

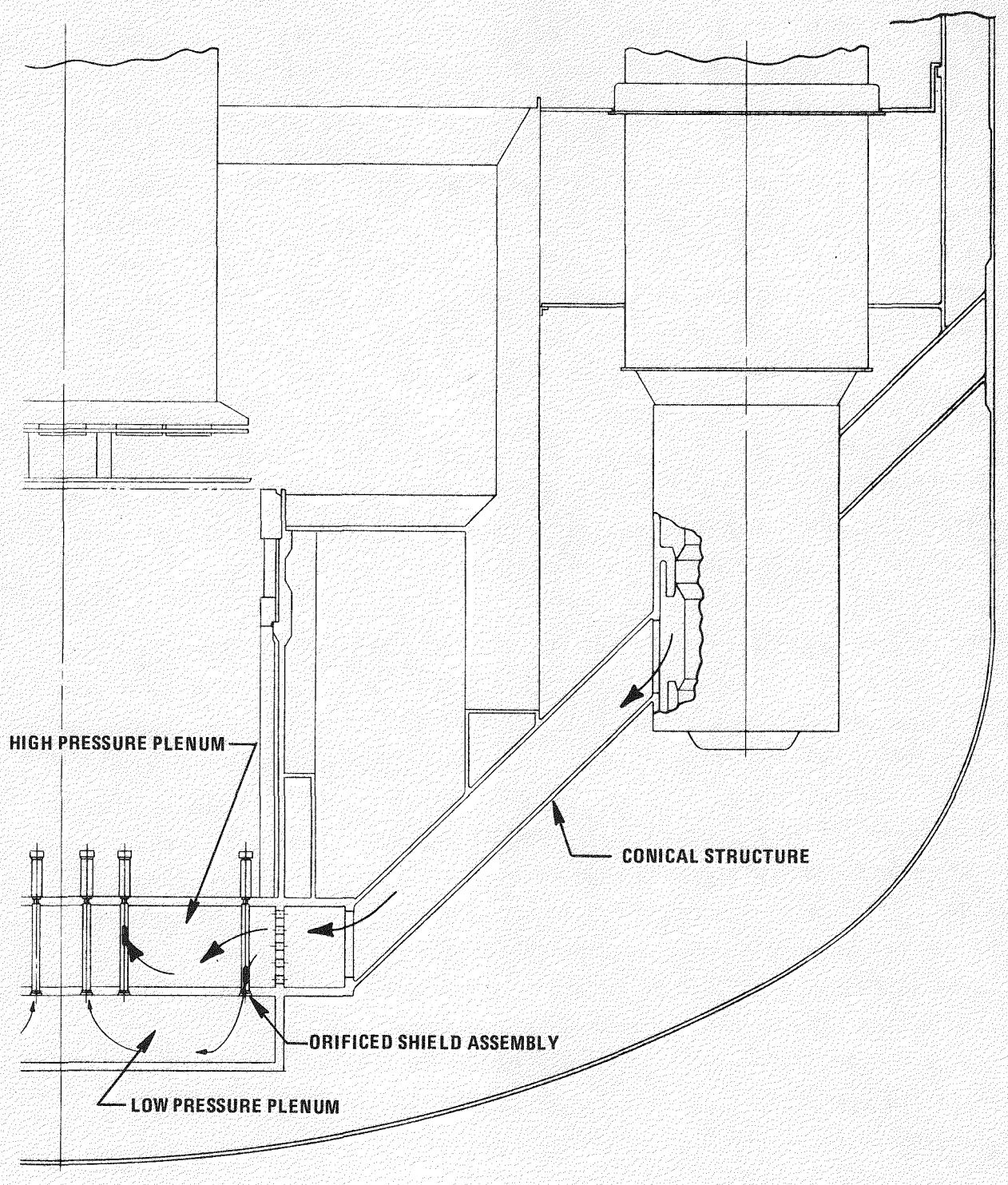

Figure P-5. Two Plena Concept

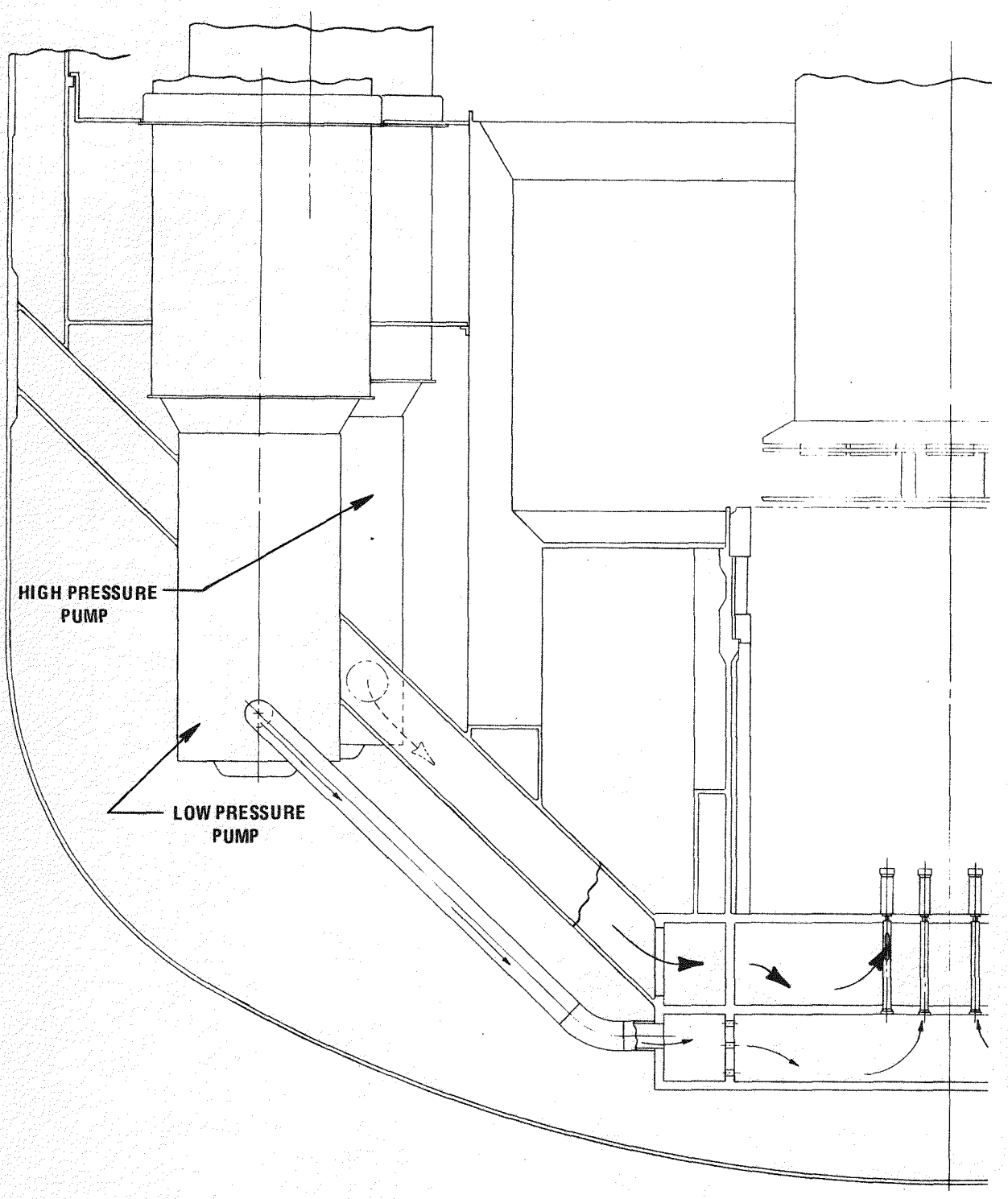

Figure P-6. Two Plena concept

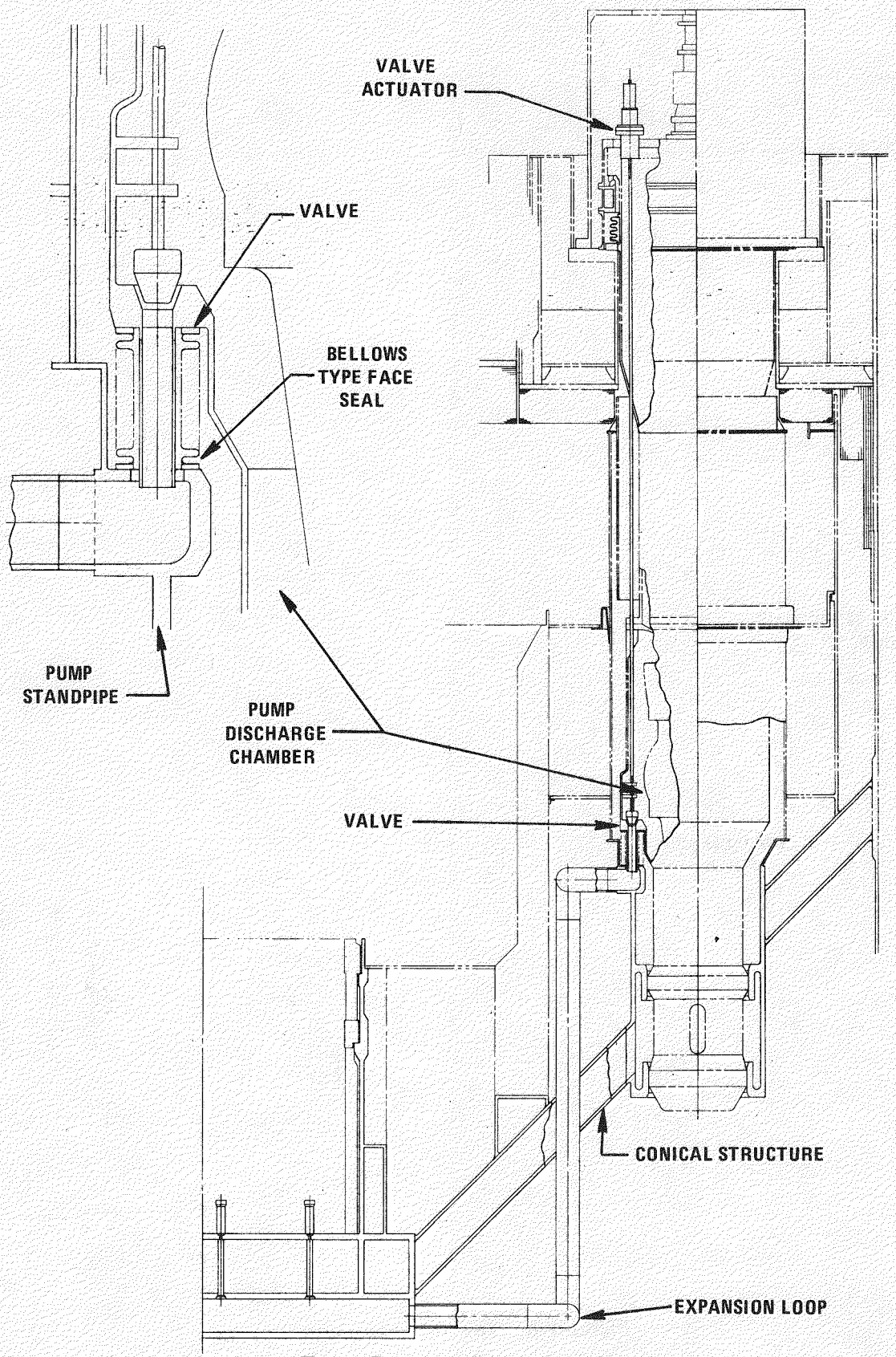

Figure P-7. Two Plena Concept

since they are located in the intermediate and cold plena below the horizontal baffles. The only identifiable major disadvantage to this concept, other than adding complexity and cost to the reactor, is the reliability of the seal required between the pump discharge chamber and the low pressure pipe.

In concepts one and two, the coolant flow through the fuel and blanket regions is verified by employing flow meters and core temperature instrumentation. In the remaining three concepts, the flow is verified by core temperature instrumentation only. It is believed that, of the concepts investigated, the final concept with the valve in the pump is the most desirable.

It is important to understand that with the limited amount of core design and thermal/hydraulic analyses completed, it is difficult to assess the value of any two plena core inlet concept. It has not been determined that there definietly are striping or stratification problems in the LPR due to variation in core outlet temperature. If the variation in outlet temperature does cause a design problem, it is not evident that a two plena core inlet system is the solution to the problem. A logical approach is to examine in detail the potential problems associated with a variation in core outlet temperature and then investigate several possible solutions, if it is determined that a problem exists. This course of action can only be completed in conjunction with intensive core design and thermal/hydraulics analyses.

APPENDIX Q
REACTOR UPPER INTERNALS STRUCTURE REMOVAL

A study was undertaken to determine the optimum upper internals structure removal configuration. Removal from the reactor could be required for periodic inspection and possible maintenance. Two basic removal configurations were examined.

- Removal of the upper internals structure as a unit through the rotatable plug to which it is attached, i.e., separately mounted UIS.
- Removal of the upper internals structure along with the rotatable plug to which it is attached, i.e., permanently mounted UIS.

Figure Q-1 and Table Q-1 indicate that for a two plug refueling system the large rotatable plug diameter increases from 36 ft 3 in for a permanently mounted UIS to 40 ft 9 in for a separately mounted UIS. Similarly for a three-plug refueling system, Figure Q-2 indicates that the large rotatable plug diameter increases from 33 ft 10 in, for a permanently mounted UIS, to 41 ft 8 in for a separately mounted UIS.

The diameter penalty to the large rotatable plug, for the separately mounted UIS structure, occurs for the following reasons.

1. A flared or skirted UIS (which minimizes plug sizes) is not possible since the UIS must be capable of being removed through the small (or intermediate) rotatable plug.
2. An additional shielding step (and set down ledge) is required on the UIS plug thereby increasing the diameter of both the small and large rotatable plugs.
3. There is a structural penalty to the small plug due to the loss of stiffness caused by the UIS plug penetration.

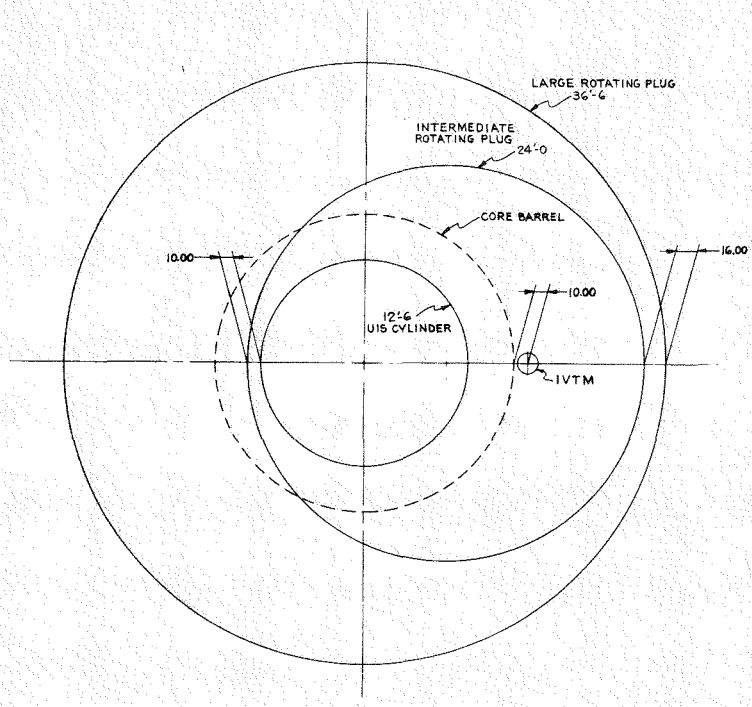

2 PLUG NON REMOVABLE UIS

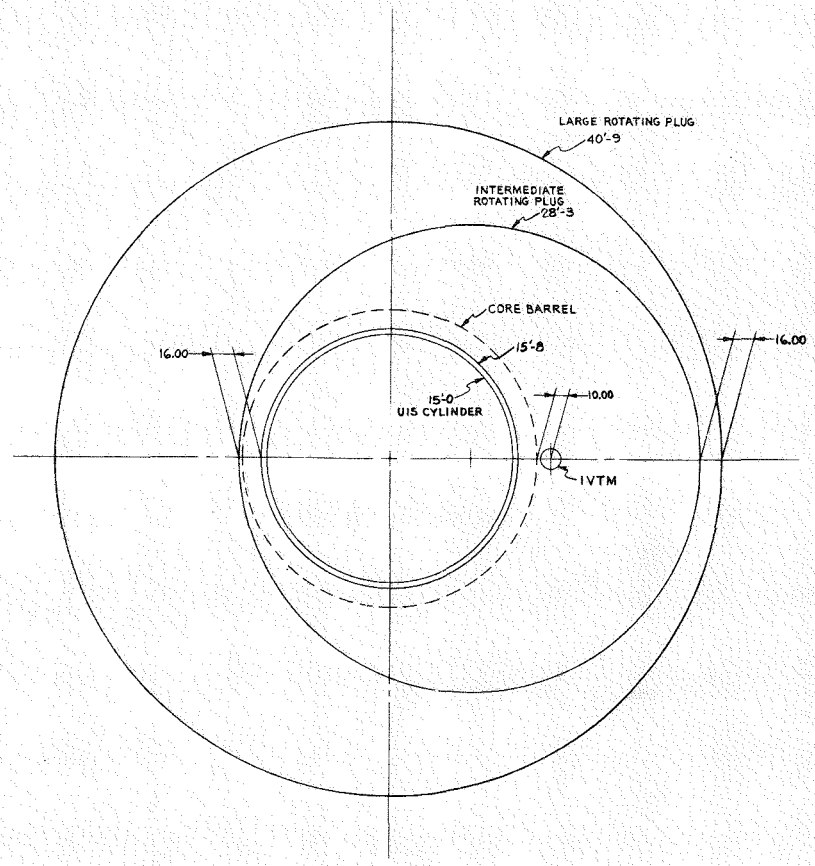

2 PLUG REMOVABLE UIS

Figure Q-1. Two Plug System

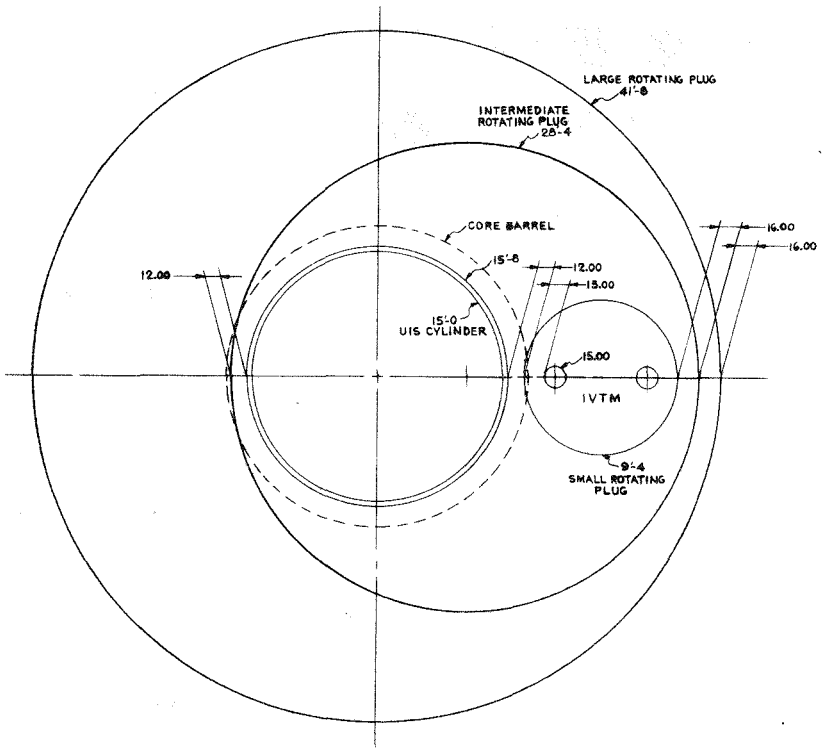

3 PLUG REMOVABLE UIS

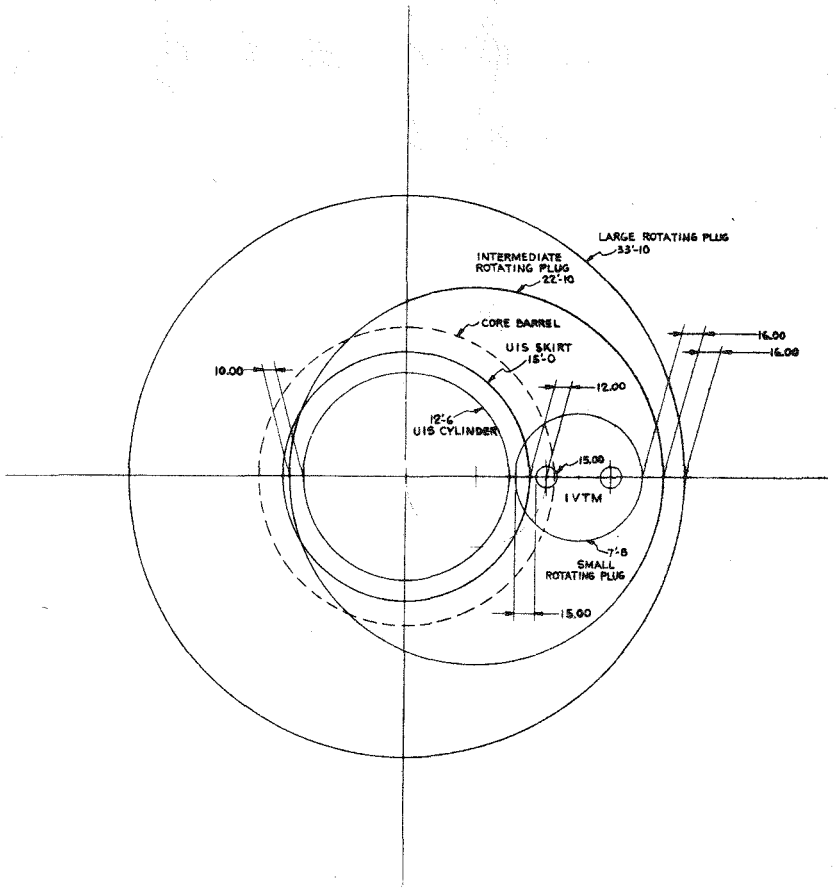

3 PLUG NON REMOVABLE UIS

Figure Q-2. Three Plug System

The conclusion from Table Q-1 is that an Upper Internals Structure that is removable for inspection through a rotatable plug cannot be accommodated without a penalty to rotatable plug (and reactor vessel) size. For this reason removal of the UIS/rotatable plug combination was investigated.

The UIS can be inspected and repaired by placing it within the containment building equipment transfer cell. Figures Q-3 and Q-4 show plan and elevation views of the UIS and UIS/plug combination within the transfer cell. Concept 1 shows that the UIS alone is able to pass into (and through) the transfer cell with no penalty to containment building size or cell width. Concept 2 shows that it is feasible for the UIS/plug combination to pass into (and through) the transfer cell at the expense of cell width and containment building diameter. Concept 3 allows top side set down of the UIS/plug combination with no effect on transfer cell width or containment building diameter. Concept 4 allows the UIS only to be positioned completely within the transfer cell. This provides full access to the UIS for inspection and maintenance with only a minor penalty to transfer cell width and no penalty to containment building diameter.

Concept 4 is the reference concept because it fulfills the UIS inspectability and maintainability requirements with minimum structural impact to cells and buildings and with no impact to the reactor, deck, and rotatable plug systems.

It should be noted that subsequent to the above study the reference large rotatable plug size increased from 33 ft 10 in as indicated in Table Q-1 to 35 ft 10 in as a result of a normal design iteration. This change does not impact the conclusions of the above work.

TABLE Q-1

LARGE ROTATABLE PLUG DIAMETERS

	Separately Mounted UIS	Permanetly Mounted UIS
2 Plug System	40'-9"	36'-6"
3 Plug System	41'-8"	33'-10"

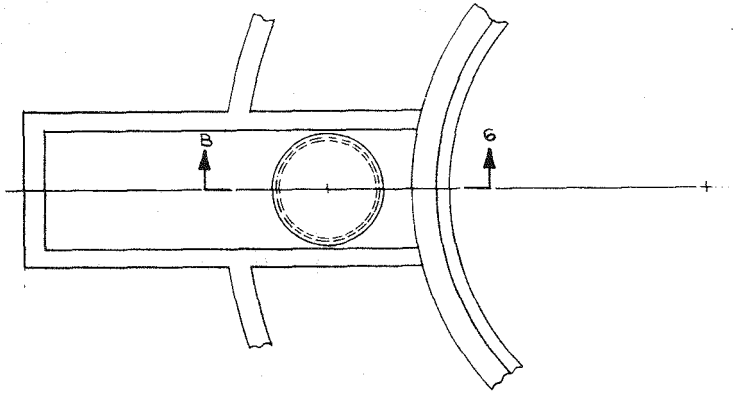

CONCEPT-1

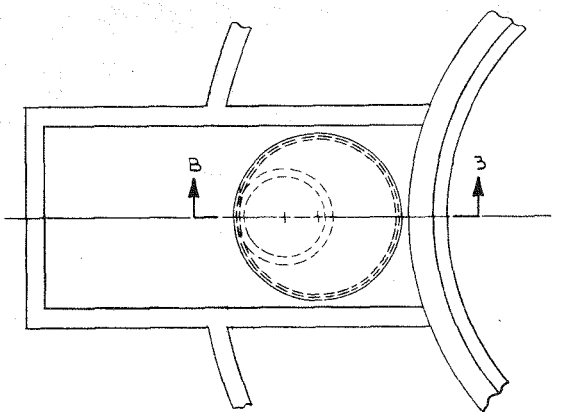

CONCEPT-2

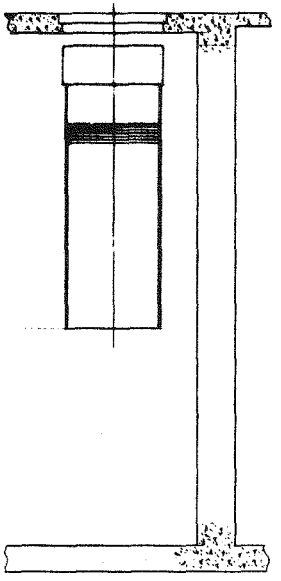

SECTION B-6
(D-7)

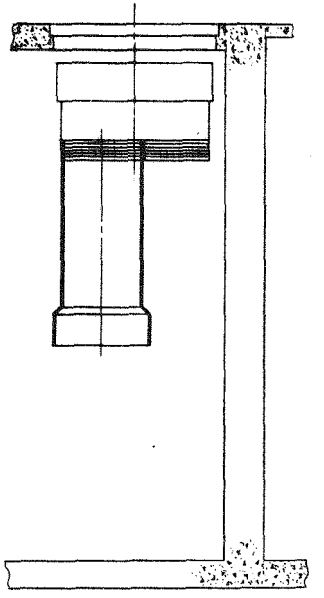

SECTION B-3
(D-3)

Figure Q-3. Transfer Cell Concepts

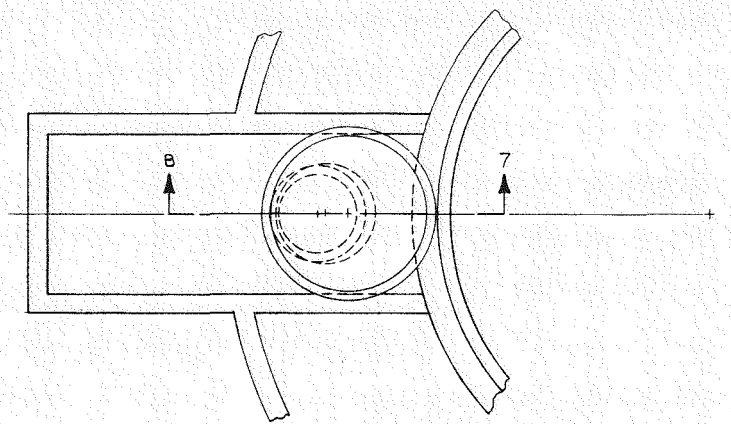

CONCEPT-3

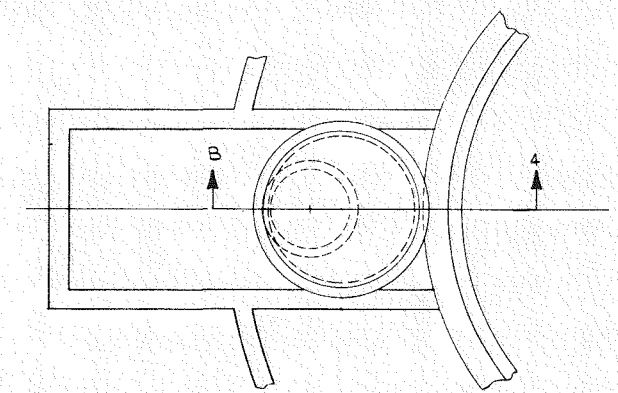

CONCEPT-4

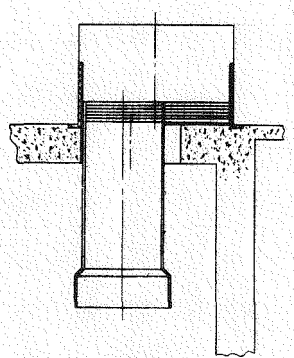

SECTION B-7
(D-7)

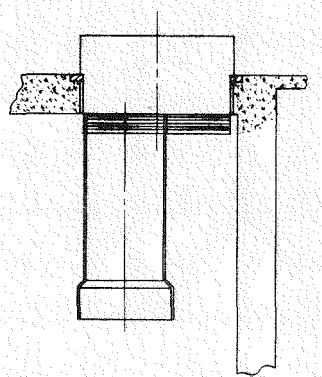

SECTION B-4
(D-4)

Figure Q-4. Transfer Cell Concepts

APPENDIX R

INSPECTION OF COMPONENTS IN A POOL TYPE REACTOR VESSEL FOR MAINTENANCE AND PERFORMANCE ASSESSMENT

R.1 GENERAL GUIDELINES FOR MAINTENANCE AND PERFORMANCE ASSESSMENT EXAMINATIONS

The following general guidelines are given for the design of pool type reactor components to accommodate monitoring and examinations, primarily for maintenance and performance assessment purposes.

- Examination should not require complete core unloading.
- All portions of non-removable structures which experience stress levels at least ten percent lower than the highest known stress (under actual operating conditions) in the structure may be exempted from examination IF that portion of the structure with the highest known stress is examined, and no condition indicating degradation is found.
- Provisions for examination of any reactor internal structure in situ shall not complicate the design, or result in any reduction in overall reliability as a result of a probable failure.
- Components that can be removed shall be modular in design to facilitate removal, handling and repair.
- Independent components shall not require removal because of an instrument failure or the need to replace an instrument.
- Removal of a component not designed for normal replacement shall not necessitate modification of the completed containment building.
- Replacement of a component shall not require in-vessel welding qualification.
- Examinations shall not require removal of sodium from the reactor.

- The need for permanent or temporary shielding for examination and removal of components shall be minimized.

R.2 COMPONENT EXAMINATION CHARACTERISTICS

The following sections contain listings of monitoring and examination techniques for the various components that could be used to comply with the guidelines given in Section R.1.

R.2.1 MAIN COOLANT PUMPS (and valves if used)

- Monitors: Motor current, motor voltage, shaft speed, noise, flow rate, orientation change.
- Examination: None in place.
- Removability: Drive motor in air. Modular pump body in inerted silo.
- Spares: TBD.

R.2.2 IHX

- Monitors: Noise, secondary Na temperature, strain gage at support, secondary Na level, primary to secondary Na leak detectors.
- Examination: None in place.
- Removability: Modular IHX in inerted silo.
- Spares: TBD.

R.2.3 COLD TRAPS, LIQUID LEVEL MONITORS, SODIUM SAMPLING STATION, COVER GAS NOZZLES, SODIUM FILL NOZZLES

- Monitors: Functional performance, leak detectors, noise.
- Examination: External visual examination; No internal examination
- Removability: Modular removal into inerted cask.
- Spares: TBD.

R.2.4 LOW LEVEL FLUX MONITOR (LLFM) TUBES

- o Monitors: Functional performance, leak detector, sticking monitors.
- o Examination: Internal boroscope if not breached. None, in place, if breached.
- o Removability: Yes, with difficulty, into inerted silo.
- o Spares: TBD.

R.2.5 REFUELING CHUTE AND TRANSPORTER

- o Monitors: Functional performance, cell temperature, motor current.
- o Examination: Remote visual examination of transporter. Under Sodium Viewer (USV) of chute for general condition.
- o Removability: Transporter into inert cell. Chute is not removable, but could have removable liner.
- o Spares: Spare chute installed (optional).

R.2.6 UPPER INTERNALS STRUCTURE (UIS) AND CONTROL ROD SYSTEM

R.2.6.1 CONTROL ROD DRIVE MECHANISM

- o Monitors: Functional performance, motor current, leak detection.
- o Examination: External visual examination; no internal examination, in place.
- o Removability: Motor in air; Mechanism in air.
- o Spares: TBD.

R.2.6.2 CONTROL ROD DRIVELINE

- o Monitors: Functional performance; scram times.
- o Examination: None, in place.
- o Removability: Yes, into inerted silo.
- o Spares: TBD.

R.2.6.3 CONTROL ROD GUIDE TUBES

- o Monitors: Condition of driveline during external visual examination; function performance.
- o Examination: USV for general condition, plug gages.
- o Removability: Yes, into inerted silo.
- o Spares: TBD.

R.2.6.4 MAIN SUPPORT STRUCTURE

- o Monitors: Forces to move during refueling operation.
- o Examination: USV of external surface for general condition.
- o Removability: Yes, with attached rotating plug;
- o Spares: No.

R.2.7 LOWER INTERNALS STRUCTURE

R.2.7.1 HORIZONTAL BAFFLES

- o Monitors: None.
- o Examination: USV of top surface for general condition.
- o Removability: No.
- o Spares: No.

R.2.7.2 PUMP AND IHX STANDPIPES

- o Monitors: None.
- o Examination: USV for general condition (through roof ports; and through pump and IHX ports when these components are removed).
- o Removability: No.
- o Spares: No.

R.2.7.3 PLENUM SEPARATOR

- o Monitors: Vessel wall temperature.
- o Examination: USV for general condition (through roof ports, and through IHX ports when IHX is removed).
- o Removability: No.
- o Spares: No.

R.2.7.4 CORE COMPONENT RECEPTACLES

- o Monitors: Refueling loads.
- o Examination: Core components for evidence of malfunction. USV for general condition.
- o Removability: Yes - through roof port into inerted cask.
- o Spares: TBD.

R.2.7.5 PUMP PLUG-IN SEAL SURFACES

- o Monitors: None.
- o Examination: USV for general condition (through pump port when pump is removed).
- o Removability: No. However, removable inserts are optional.
- o Spares: TBD.

R.2.7.6 MAIN CORE SUPPORT STRUCTURE

- o Monitors: Possible leak test of special trigger region.
- o Examination: USV for general condition of underside through pump or IHX ports. USV for general condition of upper side of structures, within core barrel, with some or all of core assemblies removed. USV entry through roof ports. USV for general condition of inside surface of fixed radial shield and core restraint hardware. USV and/or displacement examination of special trigger region.
- o Removability: No.
- o Spares: None.

R.2.8 VESSEL BOTTOM PLENUM

- o Monitors: Leak detection; examination of selected removed core components for evidence of wear or loose material presence.
- o Examination: USV for general loose material detection. (Entry through pump or IHX ports.) Sweep arm and vacuum equipment to detect and recover loose material. (Entry through pump or IHX ports.)
- o Removability: No.
- o Spares: N/A.

APPENDIX S
UPPER INTERNALS/REFUELING CHUTE INTERFERENCE STUDY

S.1 INTRODUCTION

The subject of this study is whether to tolerate a rotable plug refueling system which has the potential for Upper Internals Structure/Refueling Chute interference, even though such interference may be avoided by programming the plug control system, or to totally eliminate such a possibility altogether. The potential for interference usually occurs with a double rotable plug system when attempts are made to minimize the reactor vessel diameter. The potential is easily avoided when a three plug system is used. The type of refueling machine used, offset arm or straight pull, is also a factor effecting the possibility of interference, because an offset arm machine provides a range of reach afforded by a straight-pull machine mounted eccentrically in a rotable plug.

S.2 DISCUSSION

Many options are open to the refueling system designer in selecting features of the system. These include, but are not limited to, such things as type of in-vessel transfer machine (straight-pull, offset arm, pantograph), type of vessel deck (rotating plugs, fixed head, removable plug), and whether to refuel through the fixed portion of the deck or through a port in a rotating plug. The option also exists of using a fixed position ex-vessel transfer machine or a mobile, shielded cask. All these options, and others, provide numerous combinations of features which, when selected, determine the refueling system configuration. Many technical papers and reports have been written on this broader aspect of refueling system design. This report discusses only the subject of designing the system to assure no possibility of interference between the UIS and the refueling chute vs. preparing a design in which this potential exists, but precautionary systems are built in to avoid such interference.

To begin with, certain criteria have been established for the refueling system of the Large Pool Reactor (LPR). They are:

- It will use rotatable plugs for positioning the in-vessel transfer machine.
- It will use a straight-pull in-vessel transfer machine.
- It will use a fixed position ex-vessel transfer machine.
- It will transfer fuel through the fixed portion of the deck.
- It will not use a split upper internals structure.
- Fuel assemblies will not be double handled.

Once having had these criteria established a vessel layout is prepared. The primary concern here is the vessel size. Attempts are made to keep the vessel diameter as small as is practicable. The refueling system arrangement bears heavily in determining vessel size. When the refueling system arrangement is incorporated into the vessel layout, attempts are made to incorporate a two-plug system rather than a three-plug system, for no other reason than to reduce the number of drive systems and otherwise simplify the design.

In a two plug system the smaller of the two plugs supports the upper internals and the in-vessel transfer machine and it, in turn, is supported eccentrically from the larger plug. The eccentricity of the smaller plug is determined by taking half the distance from the core center to the in-vessel fuel transfer station. (The in-vessel transfer machine is located over the in-vessel transfer station when the reactor is operating and the UIS is in position over the core.) It is important then, that the in-vessel transfer station be kept as close to the core barrel as possible, because for every ft further away the transfer station is moved, the plug diameters and the vessel diameter are increased by two feet. However, the penalty for adhering to this rule is that when the smaller plug is rotated 180^{o}, the upper internals structure interferes with the fuel transfer chute which feeds the in-vessel transfer station. This can be seen in Figure S-1 where the swing of the upper internals is shown by the dotted line.

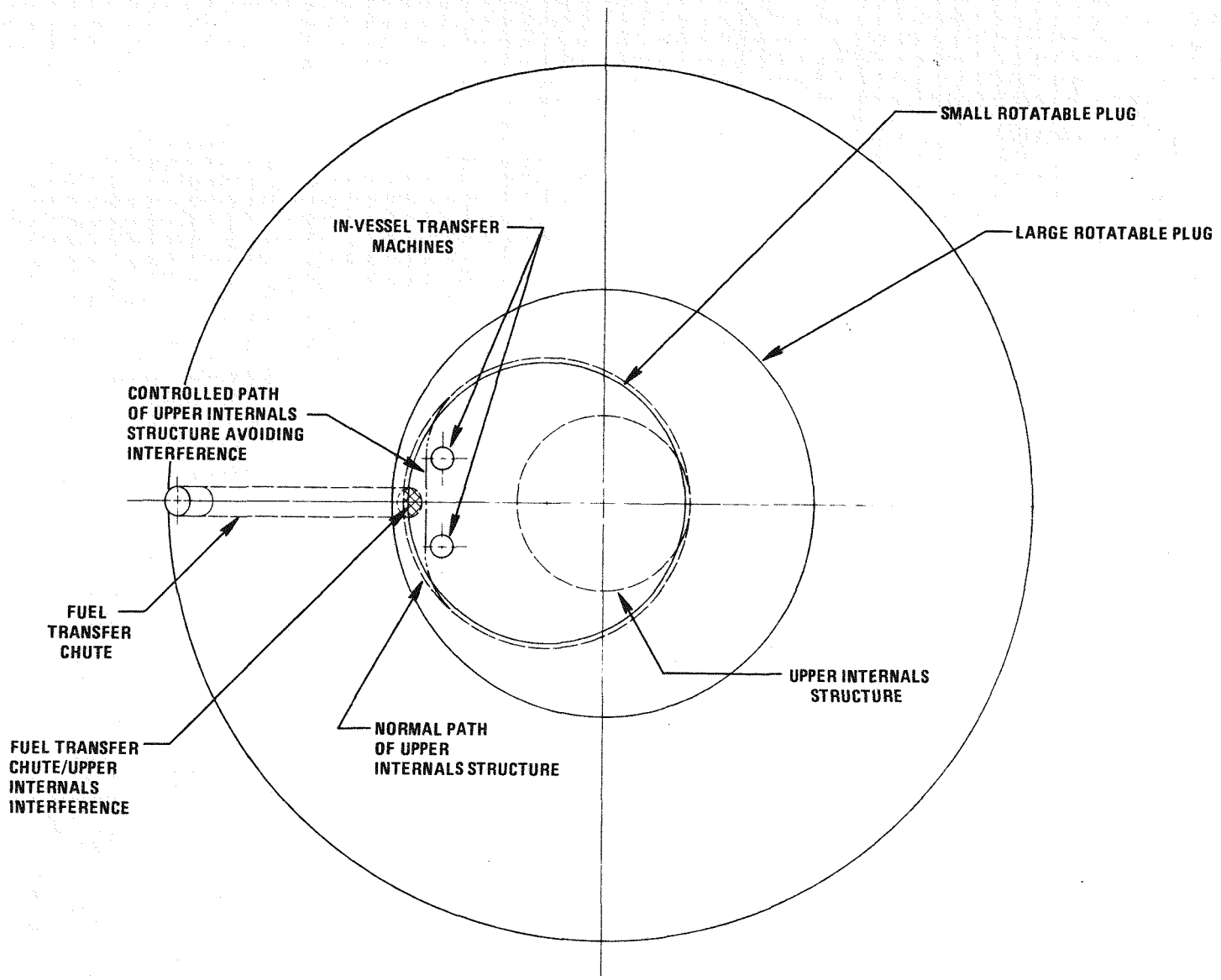

Figure S-1. Path of Upper Internals Structure Using a Two Plug Refueling System

This interference may be eliminated by fixing the computer program which commands plug rotation. Such a fix would limit the smaller plug's rotation while the larger plug is within a given range of angular attitudes giving a path of swing of the UIS as shown by the phantom line in Figure S-1.

This is not felt to be an acceptable solution because situations arise in the life of the plant where computer programs are changed by new personnel whose intent it is to "simplify" operations, or programs are overridden by manual input to overcome some problem. Personnel are not always aware of the ramifications of such changes, or, if aware, may somehow overlook them. If that were to happen with the system just described a serious accident could occur causing extensive down time for repair.

Such a situation can be completely avoided by adding a third rotatable plug which is mounted eccentrically in the smaller of the other two plugs. This third plug supports the in-vessel transfer machine which is mounted eccentrically within it. It is this eccentricity of the transfer machine within the third plug which allows the in-vessel transfer station to be placed further from the core without imposing a penalty on plug and vessel diameters and, as such, keep the fuel transfer chute clear of the swing of the upper internals structure as shown in Figure S-2.

S.3 CONCLUSION

A three plug system of refueling is chosen over a two plug system because it provides a configuration which absolutely precludes physical interference between the upper internals structure and the fuel transfer chute. Means may be provided to give the same results using a two-plug system, but this demands a larger vessel. Attempting to preclude this interference by placing restrictions in the plug drive and control systems is felt to be unacceptable for the reason that it is not a foolproof method, which, if tampered with could cause extensive damage.

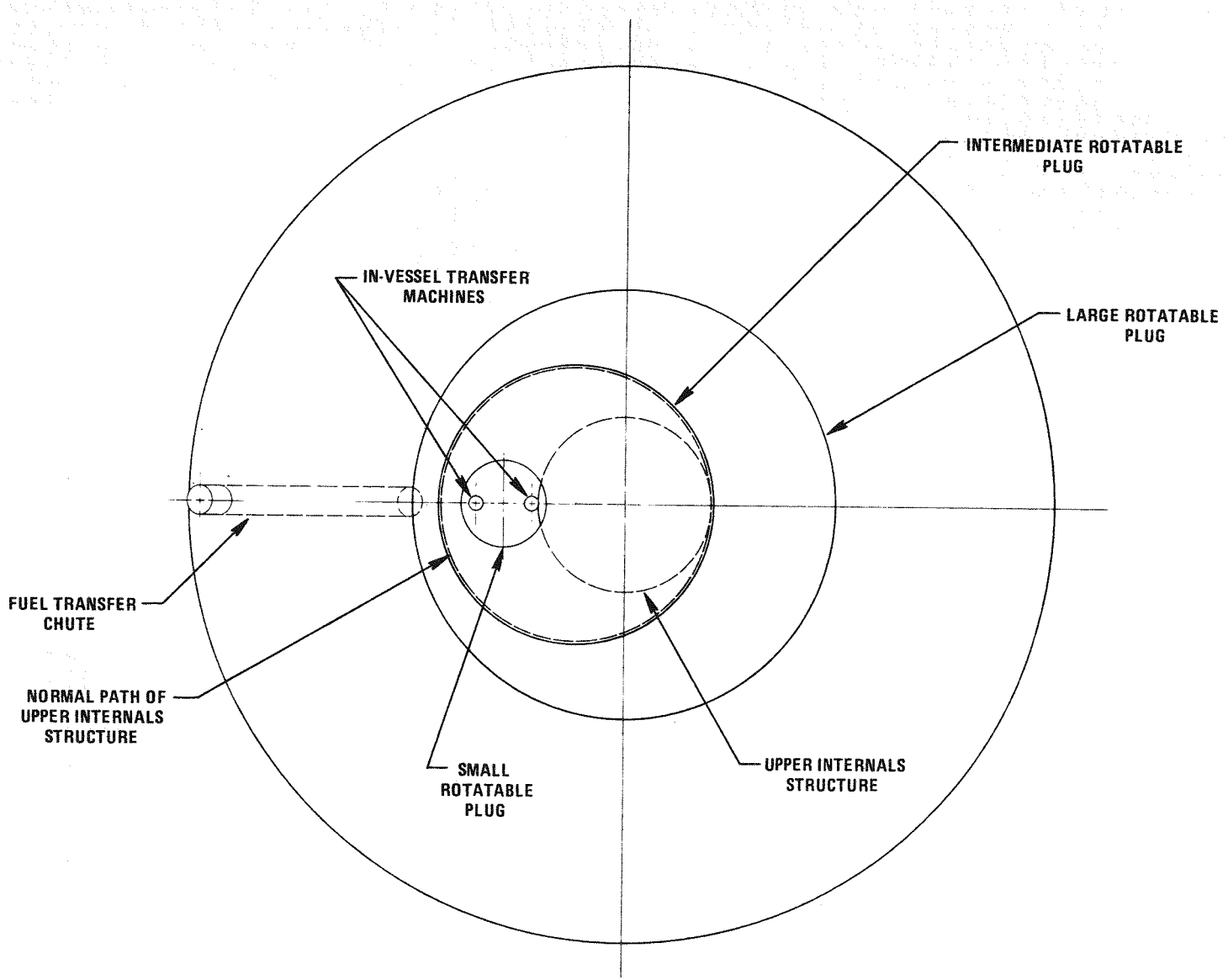

Figure S-2. Path of Upper Internals Structure Using a Three Plug Refueling System